Model-based Analysis of Solar and Heat Pump Systems for the Energy Supply of Residential Buildings

Dissertation

zur Erlangung des Grades

des Doktors der Ingenieurwissenschaften

der Naturwissenschaftlich-Technischen Fakultät
der Universität des Saarlandes

von

Danny Jonas

Saarbrücken
2023

Tag des Kolloquiums:	25.08.2023
Dekan:	Prof. Dr. rer. nat. Ludger Santen
Berichterstatter:	Prof. Dr.-Ing. Georg Frey Prof. Dr. rer. nat. Marc Deissenroth-Uhrig Prof. Dr.-Ing. Paul Motzki
Vorsitz:	Prof. Dr.-Ing. Matthias Nienhaus
Akad. Mitarbeiter:	Dr.-Ing. Marcel Otto

To my family

Acknowledgements

The completion of this PhD thesis would not have been possible without the support of several people. I would like to take this opportunity to express my gratitude and appreciation to all of them.

First of all, I would like to thank my doctoral advisor, Prof. Dr.-Ing. Georg Frey, for the opportunity to work in his research group at the Chair of Automation and Energy Systems at Saarland University and for his trust and encouragement during these years. He not only gave me guidance and scientific suggestions, but also supported me at all times in pursuing my research interests.

I would like to thank Prof. Dr. rer. nat. Marc Deissenroth-Uhrig and Prof. Dr.-Ing. Paul Motzki for their willingness to review the thesis. I would also like to thank Prof. Dr.-Ing. Matthias Nienhaus for taking over the chairmanship and Dr.-Ing. Marcel Otto for completing the examination board.

My special thanks go to my former colleagues and the complete stuff of the Chair of Automation and Energy Systems at Saarland University for their support, fruitful discussions, motivation and friendship. I would also like to thank all students who contributed to the success of this work.

I warmly thank Danjana Theis and Josef Meiers for proofreading the manuscript, their suggestions for improvement and their friendly support and helpfulness even beyond the work on the thesis.

My very special thanks go to my parents, my family and my friends who have always supported me and accompanied me on my life's journey. Especially to those who did not live to see the completion of this work. I miss you.

Finally and foremost, I would like to dedicate this work to my wife Sophie and my beloved son Fynn. Without you, this work would not have been possible. Thank you for your smiles and giggles that always built me up, the encouragement when I doubted and finally your love. I love you so much.

Saarbrücken, August 2023 *Danny Jonas*

Abstract

ENGLISH The building sector has been identified as one of the key sectors to reduce CO_2 emissions. A very promising concept for the efficient energy supply of residential buildings with high amounts of renewable energies in compliance with the EU Energy Performance of Buildings Directive is the combination of solar and heat pump systems. Due to the variety of possible system combinations and boundary conditions, the model-based analysis is a common method for comparison of different systems. The objective of this work is to close the gap of widely ranged and comparable studies with consideration of both thermal and electrical energy supply of buildings including energy storages by the systematic model-based analysis of different system concepts with regard to efficiency, environmental impact and economic aspects for different climates and types of single-family houses using the simulation environment TRNSYS. The results demonstrate that solar and heat pump systems, especially equipped with PV or PVT technologies and battery storages, are an efficient solution to achieve high CO_2 emissions savings up to 71 % in moderate climate and to fulfill the requirements of nearly zero energy buildings. In addition, the results point out the need for cost reductions and subsidies as well as carbon prices to enhance the economic efficiency of the systems. Furthermore, the developed model libraries will allow for further investigations by other works.

DEUTSCH Der Gebäudesektor wurde als ein Schlüsselsektor zur Reduzierung von CO_2-Emissionen identifiziert. Ein vielversprechendes Konzept für die effiziente Energieversorgung von Wohngebäuden mit hohem Anteil an erneuerbaren Energien im Einklang mit der EU-Gebäuderichtlinie sind solare Wärmepumpensysteme. Aufgrund der Vielzahl möglicher Systemkombinationen und Randbedingungen ist die modellbasierte Analyse eine übliche Methode zum Vergleich verschiedener Systeme. Ziel dieser Arbeit ist es, die Lücke umfassender und vergleichbarer Studien unter Berücksichtigung der thermischen und elektrischen Energieversorgung von Gebäuden einschließlich Energiespeicher durch die systematische modellbasierte Analyse verschiedener Systemkonzepte hinsichtlich Effizienz, Umweltauswirkungen und ökonomischen Aspekten für unterschiedliche Klimazonen und Typen von Einfamilienhäusern unter Verwendung der Simulationsumgebung TRNSYS zu schließen. Die Ergebnisse zeigen, dass solare Wärmepumpensysteme, insbesondere ausgestattet mit PV- oder PVT-Technologien und Batteriespeichern, eine effiziente Lösung sind, um hohe CO_2-Emissionseinsparungen von bis zu 71 % in gemäßigtem Klima zu erzielen und die Anforderungen von Niedrigstenergiegebäuden zu erfüllen. Des Weiteren zeigen die Ergebnisse die Notwendigkeit von Kostensenkungen, Subventionen sowie CO_2-Bepreisung, um die Wirtschaftlichkeit der Systeme zu steigern. Die entwickelten Modellbibliotheken werden zudem weitere Untersuchungen durch andere Arbeiten ermöglichen.

Contents

Nomenclature and List of Abbreviations

Roman Symbols

A	Area	m^2
a	Model parameter a for irradiance dependence of PV efficiency calculation	m^2/W
b	Model parameter b for irradiance dependence of PV efficiency calculation	-
b_0	Constant for incidence angle modifier IAM	-
bp	Model parameter for the compressor model of a heat pump	-
bq	Model parameter for the condenser model of a heat pump	-
C	Costs	€
C_{bat}	Battery storage capacity	kWh
c	Model parameter c for irradiance dependence of PV efficiency calculation	-
c_1	Heat loss coefficient of a solar collector	W/m^2K
c_2	Temperature dependence of the heat loss coefficient of a solar collector	W/m^2K^2
c_3	Wind speed dependence of the heat loss coefficient of a solar collector	J/m^3K
c_4	Sky temperature dependence of long wave radiation exchange of a solar collector	-
c_5	Effective thermal capacity of a solar collector	J/m^2K
c_6	Wind speed dependence of the zero loss efficiency of a solar collector	s/m
c_7	Wind speed dependence of long wave radiation exchange of a solar collector	W/m^2K^4
c_8	Radiation losses of a solar collector	W/m^2K^4
c_{CO_2}	Carbon price	€/t CO_2eq
c_{eff}	Effective thermal capacity of a solar collector	J/m^2K
c_{el}	Electricity price / tariff	€/kWh
c_{fuel}	Fuel price	€/kWh

c_{gas}	Gas price	€/kWh
c_{oil}	Oil price	€/kWh
c_p	Specific heat capacity	kJ/kgK
COP	Coefficient of performance	-
d	Price increase rate	-
E	Energy	kWh, kWh/m²a
E_{L}	Long wave irradiance	W/m²
E_λ	Spectral irradiance	W/m²nm
EP	Energy performance indicator	kWh/m²a
EP_{CO_2}	CO_2 emissions indicator	kg CO_2eq/m²a
EP_{pe}	Primary energy indicator	kWh_{pe}/m²a
F	Fuel costs	€
F'	Collector efficiency factor	-
f	Factor, fraction	-
f_{CO_2}	CO_2 emission coefficient	g CO_2eq/kWh
f_{pe}	Primary energy factor	-
f_{sav}	Fractional (energy) savings	-
$FSOC$	Fractional state of charge	-
G	(Global) solar irradiance	W/m²
G''	Net irradiance	W/m²
h	Altitude, height	m
h	Specific enthalpy	kJ/kg
I	Current	A
I	Yearly irradiation	kWh/m²a
I_0	Investment costs	€
i	Inflation rate	-
K	Incidence angle modifier (IAM)	-
l	Length	m
$LCOE$	Levelized cost of electricity	€/kWh
$LCOEn$	Levelized cost of energy	€/kWh
$LCOH$	Levelized cost of heat	€/kWh
M	Maintenance costs	€
$\dot{m}$	Mass flow rate	kg/h, kg/s
m_{CO_2}	CO_2 emissions	g CO_2eq/a
MAE	Mean absolute error of power output	W
n	Number	-
nRMSE	Normalized root mean square error of power output	-
O	Operation costs	€
P_{el}	Electrical power	W, kW
p	Pressure	bar
p_{abs}	Absolute pressure of the ambient air	Pa
p_{el}	Specific electrical power	W/m², kW/m²
PR	Performance ratio	-
$\dot{Q}$	Heat flow	W, kW
Q	Heat, thermal energy	kWh
$\dot{q}$	Specific heat flow	W/m²

q	Specific heat, specific thermal energy	kJ/kg
q_{th}	Specific thermal yield	kWh/m^{2}a
r	Discount rate	-
RER	Renewable energy ratio	-
RH	Relative humidity	%
RMSE	Root mean square error of power output	W
S_0	Subsidies and incentives	€
SCR	Self-consumption rate	-
SPF	Seasonal performance factor	-
SSR	Self-sufficiency rate	-
T	Temperature	K
T	Time period of analysis	a
t	Time	a, s
U	Internal energy	kWh
U	Voltage	V
U_0	Heat loss coefficient of a PV module	W/m^{2}K
U_1	Wind dependent heat loss coefficient of a PV module	Ws/m^{3}K
U_{PVT}	Internal heat transfer coefficient from PV cell to fluid	W/m^{2}K
u	Velocity, wind speed	m/s
UA	UA-value, heat transfer / loss rate	W/K
UR	Utilization ratio	-
V	Volume	l, m^3
W_{el}	Electrical energy	kWh
$\dot{W}_{\mathrm{t}}$	Technical power	W, kW
w_{el}	Specific electrical yield	kWh/m^{2}a
w_{t}	Specific technical work	kJ/kg

Greek Symbols

α	Absorptance	-
β	Power temperature coefficient of PV cells	%/K
η	Efficiency	-
η_0	Zero loss collector efficiency	-
θ	Angle of incidence	°
ϑ	Temperature	°C
λ	Wavelength	nm
σ	Stefan-Boltzmann constant $((5.67040 \pm 0.00004) \times 10^{-8}\,\mathrm{W/m^2K^4})$	W/m^{2}K^4
τ	Transmittance	-
$\tau\alpha$	Transmittance-absorptance product	-

Subscripts and Superscripts

abs	absorber
AC	Alternating Current

airflow	airflow
amb	ambient
AW	Air/Water
b	beam
bat	battery storage
BHE	Borehole Heat Exchanger
buffer	buffer storage
bui	building
BW	Brine/Water
c	cold
Carnot	Carnot
cell	cell
CO_2	Carbon dioxide
coll	collector
comp	compressor
cond	condenser
cooling	cooling
covered	covered
ctr	controller
D	Design
d	diffuse
del	delivered
DHW	Domestic Hot Water
EH	Electric Heating
el	electrical
evap	evaporator
exp	exported
feedin	feed-in
FPC	Flat-Plate Collector
fuel	fuel
G	Irradiance
gains	gains
gas	gas
grid	grid
ground	ground
h	hot
heating	heating
hh	household
HP	Heat Pump
HS	Heating Season
HX	Heat exchanger
IAM	Incidence Angle Modifier
ice	ice storage
in	inlet
int	internal
lat	latent
liquid	liquid
load	load

loc	location
loss	loss
m	mean
max	maximum
meas	measured
mech	mechanical
min	minimum
n	normalized
net	net
nom	nominal
nren	non-renewable
off	off
oil	oil
on	on
out	outlet
parallel	parallel
pe	primary energy
pen	penalty
prot	protection
pu	pump
PV	Photovoltaic
PVT	Photovoltaic-Thermal
r	refrigerant
rad	radiative
real	real
ref	reference
ren	renewable
room	room
S	South
sav	savings
SC	Solar Circuit
self	self-consumption
set	set point
SH	Space Heating
SHP	Solar Heat Pump
SHP+	Solar Heat Pump plus energy distribution system
sim	simulated
sol	solar
solid	solid
source	source
T	Temperature
t	time
th	thermal
tot	total
trans	transmission
use	use
useful	useful

w	water
WISC	Wind and/or Infrared Sensitive Collector

Abbreviations

AC	Alternating Current
ASHP	Air Source Heat Pump
AW	Air/Water
BEMS	Building Energy Management System
BHE	Borehole Heat Exchanger
BOS	Balance Of the System
BW	Brine/Water
CEN	Comité Européen de Normalisation
CPC	Compound Parabolic Collector
DC	Direct Current
DHW	Domestic Hot Water
EBC	Energy in Buildings and Communities programme
EMS	Energy Management System
EPB	Energy Performance of new and existing Buildings
EPBD	Energy Performance of Buildings Directive
EPDM	Ethyl Propylene Dien Monomers
ETC	Evacuated Tube Collector
ETS	Emission Trading Scheme
EU	European Union
EVA	Ethylene Vinyl Acetate
FMI	Functional Mockup Interface
FPC	Flat-Plate Collector
FSOC	Fractional State Of Charge
GHG	Greenhouse Gas
GPS	Generalized Pattern Search
GSHP	Ground Source Heat Pump
GUI	Graphical User Interface
HJ	Hooke-Jeeves
HPP	Heat Pump Programme
IAM	Incidence Angle Modifier
IEA	International Energy Agency
IPCC	Intergovernmental Panel on Climate Change
IQR	Interquartile Range
KPI	Key Performance Indicator
LCOE	Levelized Cost of Electricity
LCOEn	Levelized Cost of Energy
LCOH	Levelized Cost of Heat
MAE	Mean Absolute Error
MLR	Multiple Linear Regression
MPPT	Maximum Power Point Tracker
MV	Mixing Valve

nRMSE	normalized Root Mean Square Error
nZEB	nearly Zero Energy Building
P	Parallel
PE	Polyethylene
PP	Polypropylene
PSO	Particle Swarm Optimization
PV	Photovoltaic
PVT	Photovoltaic-Thermal
R	Regeneration
RBC	Rule-Based Control / Controller
RER	Renewable Energy Ratio
RMSE	Root Mean Square Error
S	Serial
SASHP	Solar thermal and Air Source Heat Pump
SCR	Self-Consumption Rate
SFH	Single-Family House
SG	Smart Grid
SGSHP	Solar thermal and Ground Source Heat Pump
SH	Space Heating
SHC	Solar Heating and Cooling programme
SHP	Solar Heat Pump
SISHP	Solar thermal and Ice storage Source Heat Pump
SPF	Seasonal Performance Factor
SSR	Self-Sufficiency Rate
STC	Standard Test Conditions
STHP	Solar Thermal Heat Pump
SV	Switching Valve
VAT	Value Added Tax
WISC	Wind and/or Infrared Sensitive Collector
ZEB	Zero Energy Building

Chapter 1

Introduction

1.1 Background and Motivation

Efficiency and sustainability of energy systems gain in importance due to the growing efforts being made in the field of climate protection. In 2018, the Intergovernmental Panel on Climate Change (IPCC) announced in its special report on the impacts of global warming of 1.5 °C above pre-industrial levels and related global greenhouse gas (GHG) emission pathways that "*human activities are estimated to have caused approximately 1.0 °C global warming above pre-industrial levels*" and "*global warming is likely to reach 1.5 °C between 2030 and 2052 if it continues to increase at the current rate*" [IPCC, 2018]. Furthermore, the IPCC identified robust differences in regional climate characteristics (like mean temperature, hot extremes, heavy precipitation or droughts), global mean sea level rise, impacts on biodiversity and ecosystems (including species loss and extinction), increases in ocean temperature as well as climate-related risks to health, livelihoods, food security, water supply, human security and economic growth between global warming of 1.5 °C and 2 °C. For limiting the global warming within the modeled pathways to below 1.5 °C, the global net anthropogenic carbon dioxide (CO_2) emissions have to be reduced by about 45 % from 2010 levels by 2030, reaching net zero around 2050. In order to meet this objective, rapid and far-reaching transitions, especially in the energy sector, are mandatory which imply extensive emission reductions in all sectors, a wide portfolio of mitigation options and a significant upscaling of investments in those options [IPCC, 2018].

In 2015, the United Nations decided within the Paris Agreement, which follows the Kyoto Protocol, to pursue efforts to limit the temperature increase to 1.5 °C above pre-industrial level [United Nations, 2015]. On the European level, the European Union (EU) key targets on climate change and energy included initially 20 % decrease of GHG emissions by 2020, at least 40 % by 2030 and as longer-term objective around 80 % to 95 % by 2050 compared with 1990. In addition, the EU targets implied a 20 % amount of total energy consumption from renewable energy by 2020 (at least 27 % for 2030) and 20 % increase in energy efficiency by 2020 (at least 27 % for 2030) [European Commission, 2019]. In 2016, the EU increased the ambition of these targets to a 32 % share of renewable energy and at least a 32.5 %

improvement in energy efficiency (compared to a business-as-usual scenario for 2030) by 2030. This was followed in 2018 by the objective to be climate-neutral by 2050 as vision for a long-term EU strategy for reducing GHG emissions, which is also part of the European Green Deal presented in 2019 [European Commission, 2020a]. As part of the European Green Deal, the EU goes even further with the 2030 objectives and proposed in September 2020 (with agreement in April 2021) to raise the 2030 targets to at least 55 % decrease of GHG emissions [European Commission, 2021a]. In July 2021, the European Commission adopted a package of proposals, called *Fit for 55* package, to make the EU's climate, energy, land use, transport and taxation policies fit to meet the increased GHG emissions reduction objectives [European Commission, 2021c,b]. The Europe 2020 indicators from 2018 showed an EU GHG emissions reduction of 23.2 % and a share of renewable energy of 18.0 % for the EU gross final energy consumption. Regarding the energy efficiency objective, the EU has also made progress, although the trend reversed after 2014 [Eurostat, 2020b]. According to preliminary data, the EU GHG emissions decreased by 10 % from 2019 to 2020 and the EU achieved all 2020 targets. Nevertheless, the large decline was strongly related to the Covid-19 pandemic and thus additional efforts have to be made as proposed in the Fit for 55 package to achieve the ambitious 2030 targets [European Environment Agency, 2021].

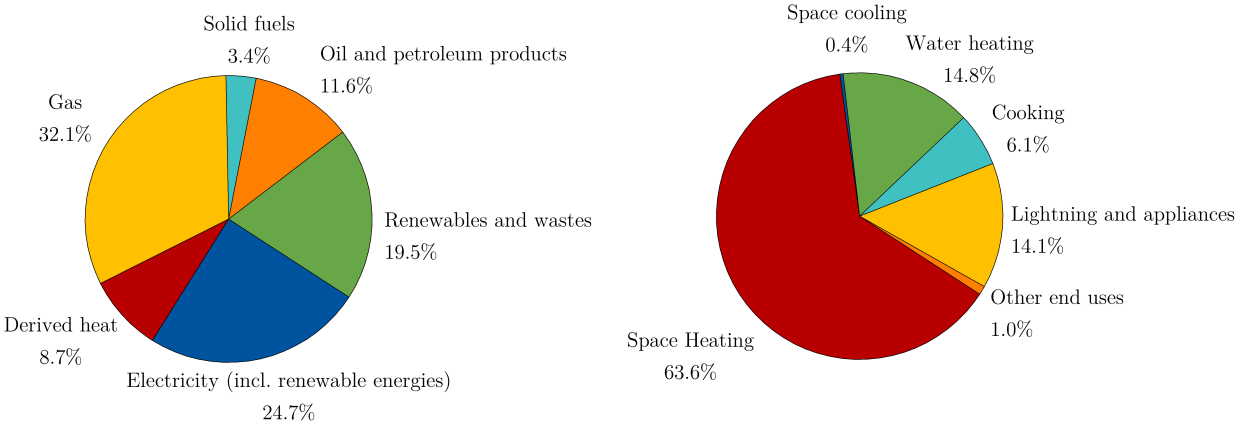

(a) Final energy consumption by energy carrier **(b)** Final energy consumption by type of end-use

Figure 1.1: Final energy consumption of the EU residential sector by energy carrier and type of end-use in 2018 [Eurostat, 2020a].

The building sector, which is responsible for nearly 40 % of total energy consumption and 36 % of CO_2 emissions in the EU, has been identified as one of the key sectors to achieve the EU's 2020 targets and, furthermore, the longer term objectives of climate protection and thus the transition to a climate-neutral society [European Commission, 2013, 2020b]. In 2018, the residential sector on its own represented 26 % of the final energy consumption in the EU. Figure 1.1 shows the final energy consumption of the EU residential sector by energy carrier and type of end-use in 2018. Currently, most of the EU final energy consumption in the residential sector is covered by gas with a share of around 32 % in 2018. At this, 94 % of the gas consumption can be allocated to space heating (SH) and water heating, which represented around 78 % of the final energy consumption of the EU residential sector in 2018 [Eurostat, 2020a]. With 52 %, the main part of the building's energy consumption for space heating and water heating is covered by conventional heating systems with gas and

oil as energy carrier and around 24 % by renewable energies. In a nutshell, these figures clarify why the transformation of the residential energy sector requires the improving of energy efficiency of buildings by renovation of the existing building stock and especially the replacement of conventional heating systems by heating systems with high amounts of renewable energies.

As main legislative instrument at EU level for improving the energy efficiency of buildings, the EU Energy Performance of Buildings Directive (EPBD) introduced nearly zero energy buildings (nZEB) with very high energy performance and a nearly zero or very low amount of energy required, which "*should be covered by energy from renewable sources, including energy from renewable sources produced on-site or nearby*" [European Parliament, 2010] as standard for all new buildings by 2021. In 2018, an amended version of the EPBD was adopted, which even goes one step further by rating the smart readiness of buildings. In this context, a smart readiness factor was introduced which "*should be used to measure the capacity of buildings to use information and communication technologies and electronic systems to adapt the operation of buildings to the needs of the occupants and the grid and to improve the energy efficiency and overall performance of buildings*" [European Parliament, 2018]. This also illustrates that energy systems for buildings have not only to be reliable, economic and efficient, but also sustainable and smart. In its net zero by 2050 roadmap, the International Energy Agency (IEA) further proposes to introduce zero-carbon-ready buildings as new building standard for all new buildings by 2030 and for retrofits of most existing buildings by 2050. A zero-carbon-ready building is mainly defined as highly energy efficient building that "*either uses renewable energy directly, or uses an energy supply that will be fully decarbonised by 2050, such as electricity or district heat*" [IEA, 2021]. In other words, this means that all zero-carbon-ready buildings will become zero-carbon buildings by 2050, without further changes to the building or its equipment [IEA, 2021].

A path to follow at the design stage of a building to achieve low-energy and low-carbon buildings introduced by the IEA can be divided in three steps (cf. Figure 1.2) [IEA, 2013]:

- Energy Sufficiency
- Energy Efficiency
- Renewable Energy.

Energy Sufficiency means reduction of energy needs of buildings and mainly comprises a set of non-technological solutions related to the design of a building and its daily management and operation like building's orientation, use of daylight and natural shading, volume and ratio of glazed areas of the building or indoor temperature setpoints. *Energy Efficiency* can be reached by the reduction of energy consumption and thus by the improvement of the building envelope (through insulation and air tightness), which reduces the heating or cooling energy demand, the use of efficient heating, cooling and hot water technologies like heat pumps and the use of efficient ventilation technologies and appliances. *Renewable Energy* generated by the building itself (e.g. solar energy) or nearby can then be used to supply thermal and/or electrical energy to systems for space heating or cooling and water heating as well as to cover the household electricity demand and consequently to reduce the CO_2 emissions of the building [IEA, 2013]. To fulfill the requirements of the EPBD, and with regard to smart grids and the volatility of renewable energies, an additional fourth step *Smartness and Flexibility* could be introduced, or it could be seen as part of energy efficiency and using renewable energy. The IEA's Energy in Buildings and Communities

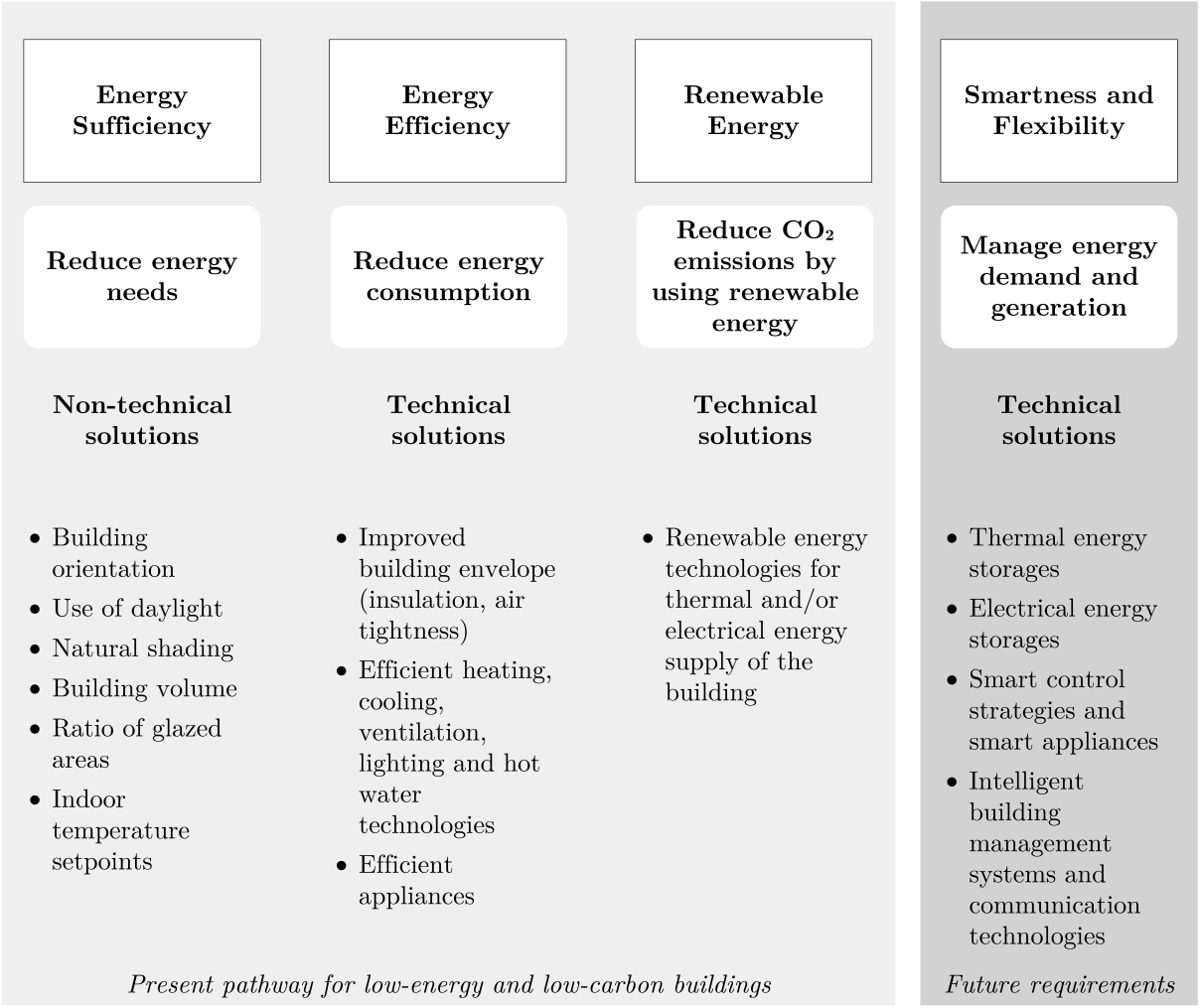

Figure 1.2: Pathway for building design.

Programme (EBC) Annex 67 defines the energy flexibility of a building as the "*ability to manage its demand and generation according to local climate conditions, user needs, and grid requirements*" [IEA, 2019]. According to IEA EBC Annex 67 energy flexibility of buildings "*will thus allow for demand side management / load control and thereby demand response based on the requirements of the surrounding grids*" [IEA, 2019]. Energy flexibility of buildings can mainly be reached by a combination of energy storage (active or passive) to shift the energy use or generation and smart control strategies including smart appliances. At this, smart control can be simple like a heat pump switched off to a defined period, more complex like rule-based control with several constraints or advanced like model-based control including e.g. forecasts of weather, occupancy behavior or energy prices [IEA, 2019]. Furthermore, energy flexibility of buildings requires innovations in intelligent overall building management systems (BMS) and appropriate communication technologies.

A very promising concept for the efficient and smart energy supply of residential buildings with high amounts of renewable energies and high energy flexibility in compliance with the EPBD is the combination of solar and heat pump (SHP) systems. At this, the notion SHP system comprises all combinations of heat pumps and solar energy systems for application in residential buildings, including photovoltaic (PV) and solar thermal systems as well as hybrid or combined PV and solar thermal energy technologies (cf. Figure 1.3). Within

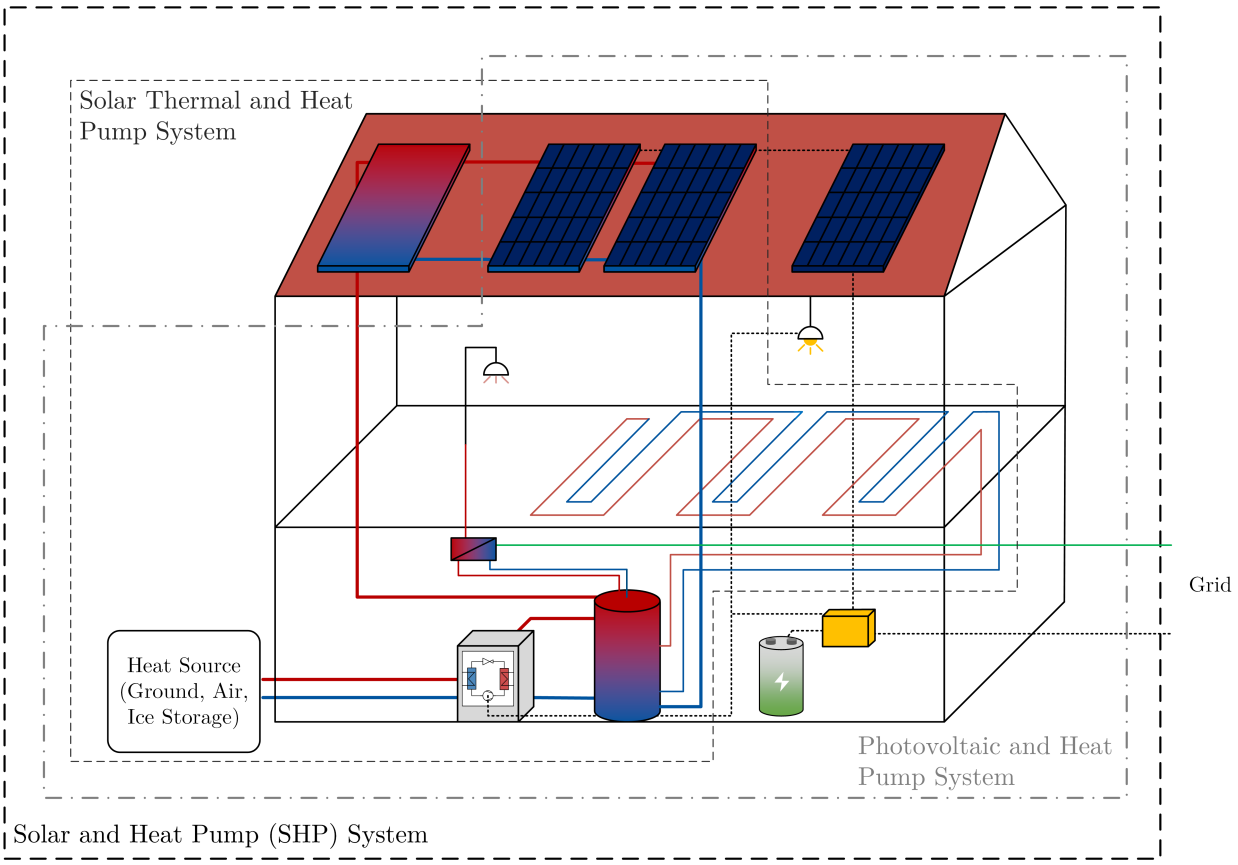

Figure 1.3: Solar and heat pump system.

these concepts, solar thermal systems are used to deliver heat (directly or on the source side of the heat pump) to the system while PV systems provide electricity to the system or building (household electricity). For heating applications, the heat pump is used to supply the space heating and/or the domestic hot water (DHW) system (or a thermal storage) with heat and is usually implemented as ground source heat pump (GSHP) or air source heat pump (ASHP) but also other concepts are used like solar only systems with latent heat storage and brine/water heat pump or water source heat pumps. At this, heat pumps and innovative technologies like photovoltaic-thermal (PVT) collectors support the possibility of linking heat and electricity in the energy generation as well as the energy consumption of a building, which is becoming increasingly important with regard to the required energy flexibility of buildings. Furthermore, the interaction of heat pumps with smart grids is supported by technologies like the Smart Grid-Ready (SG-Ready) interface that can be used to provide energy flexibility by different predefined operating modes of heat pumps. In addition, SHP systems can include thermal as well as electrical storage systems and thus support the decentralized thermal and electrical storage capacity of a building.

With regard to the increasing complexity of SHP systems and its importance in future energy systems, the optimized design and control of such systems is mandatory and thus systematic analyses and comparisons of different system designs and control strategies are necessary. Due to the variety of possible system combinations and boundary conditions (e.g. climate or considered building type), the model-based analysis is a common method for comparison of different systems and determination of most useful concepts depending on different evaluation criteria. Due to the extensive, well validated and accepted model

libraries for building energy systems and building simulation, the simulation environment TRNSYS [TRNSYS, 2020] is often used for system modeling and simulation of SHP systems. Most of the mentioned works in the following section also used TRNSYS as simulation environment which clarifies that it is the common tool in this research area. For this reason and due to the great flexibility of the software, TRNSYS is also used in this work for the system modeling and simulation.

1.2 Related Work and Research Gap

In recent years, a lot of research has been carried out for SHP systems, primarily on special topics of thermal system combinations. A comprehensive overview of earlier simulation studies on **solar thermal and heat pump systems** within the IEA Solar Heating and Cooling Programme (SHC) Task 44 / Heat Pump Programme (HPP) Annex 38 was given by Haller et al. [2014a] and Hadorn [2015]. The authors presented summaries of simulations which were performed by different authors and different simulation platforms within the framework of the IEA SHC Task 44 / HPP Annex 38 using predefined boundary conditions like climate data or heat loads for space heating and domestic hot water preparation of different single-family houses (new, renovated and non-renovated buildings). But even if these boundary conditions were used, the simulation results are not comparable in detail as different simulation parameters and conditions were used for the solar thermal and heat pump systems itself, e.g. different performance data of the heat pumps and solar thermal collectors, different assumptions on the hydraulic components (e.g. electricity consumption of pumps or hydraulic integration) or the system control. For example, Carbonell et al. [2014a] analyzed the influence of direct use of solar heat in GSHP and ASHP systems for different types of buildings and climates by simulation using different heat pumps with different performance data and efficiency in case of resizing the systems for different locations and buildings. By contrast, Poppi et al. [2016] analyzed the influence of component size on electricity demand for ASHP and GSHP systems combined with solar thermal collectors for the climates of Zurich and Carcassonne by the use of scale factors. However, the analysis was limited to renovated and non-renovated buildings. New buildings as well as cold climates like Helsinki were not considered in the study. Regarding GSHP systems with use of solar heat for regeneration of the ground heat source, especially the work of Kjellsson [2009] and Bertram [2015] should be mentioned. Kjellsson [2009] studied the combination of flat-plate solar thermal collectors with GSHPs, whereas Bertram [2015] concentrated on the integration of uncovered solar thermal collectors in heat pump systems with vertical ground heat exchanger. Furthermore, Trinkl [2006] and Faßnacht [2015] investigated the combination of solar thermal and heat pump systems with latent heat (ice) storage on the source side of the heat pump. Both works offered optimizations of the specific system concepts and special topics like control strategy or component development but no comparisons with other solar thermal and heat pump system concepts. So far, comparatively few studies like Haller et al. [2014a] or Lerch et al. [2015] compared such system concepts with other solar thermal and heat pump concepts. In a nutshell, as mentioned in Poppi et al. [2016], a lot of research has been carried out for solar thermal and heat pump systems, but there are no structured studies beside Poppi et al. [2016] that include GSHP and ASHP concepts with direct use of solar heat for a wide range of boundary conditions. As Poppi et al. [2016] concentrated on these concepts for renovated and non-renovated buildings for the climates of Zurich and Carcassonne, a comparison for new buildings and the consideration of cold climates is still

missing. Furthermore, little attention has been paid to compare those systems with solar thermal and heat pump systems with latent heat storage or heat pump only as well as conventional heating systems for a wide range of boundary conditions with uniform efficiency parameters and assumptions on the main components of the systems.

Within the field of combined **photovoltaic and heat pump systems**, especially the work of Fischer [2017] and Von Appen [2018] should be mentioned. Fischer [2017] offered a study on the integration of heat pumps into smart grids regarding system design, controls and operation on different system boundary levels, whereas Von Appen [2018] analyzed the sizing and operation of residential PV systems in combination with battery storage systems and heat pumps from a household investors and distribution network operators perspective in Germany. Furthermore, many authors like Facci et al. [2019], Battaglia et al. [2017], Thür et al. [2018] or Bee [2019] have studied specific topics of PV and heat pump systems. Facci et al. [2019] compared different PV and ASHP system concepts including heating and cooling of an apartment building. Battaglia et al. [2017] presented different system designs and control options using thermal or battery storages in SHP systems with PV, whereas another concept for the storage of PV energy within buildings is presented in Thür et al. [2018] by overheating the building itself. In addition, Bee [2019] studied different aspects like the relationships between building, heating system and boundary conditions or the control strategies on the ability of heat pump systems to increase self-consumption of PV electricity with special focus on ASHP systems. Nevertheless, a structured comparison of different combinations of PV and heat pump technologies with and without electrical energy storages for a wide range of boundary conditions regarding different types of single-family houses with uniform efficiency parameters and assumptions on the main system components is still missing.

Regarding **solar and heat pump systems** in general, Thygesen [2016] carried out a study on the combination of a GSHP with PV and/or a solar thermal system for a specific use case of a nZEB (single-family house) in Sweden considering heating applications and household electricity including the analysis of two storage concepts for PV (with battery storage or thermal storage with electrical heater). An energetic and financial evaluation of a PV and air/air heat pump system in comparison with different water/air heat pump systems using solar thermal or PVT collectors as heat source including a coupled system with solar thermal collectors and PV as well as concepts with battery storages was presented by Bellos et al. [2016] for the warm climate of Athens. In addition, techno-economic comparisons between combinations of PV or PVT with GSHPs for multi-family houses were given by Sommerfeldt and Madani [2018, 2019] for the cold climate of Sweden. Furthermore, Poppi [2017] carried out a study on solar thermal as well as PV systems in combination with heat pumps for heating applications. The author did a literature based economic analysis and performed system simulations with special focus on a reference solar thermal and heat pump system with ASHP. Additionally, the work presented investigations on special system improvements like vapor injection cycle or the use of variable speed compressors for the specific ASHP reference system. As a conclusion, the author recommended that more techno-economic studies of solar PV and hybrid solar thermal / PV systems in combination with heat pumps are required and as the results were only for a limited range of variation in heat loads and system configurations, extended work for other heat loads as well as system configurations is needed [Poppi, 2017]. Moreover, in Poppi et al. [2018] the authors mentioned that there are no consistent boundaries or approaches regarding different studies which make comparisons between systems difficult or impossible. In a recent systematic review of ASHP systems in combination with solar thermal, PV and PVT, Wang et al. [2020]

figured out that there is a lack of standardized indicators to evaluate the system performance and only few papers take into account environmental and economic aspects. Furthermore, the authors recommended the development of a common simulation tool [Wang et al., 2020].

Within other works, SHP systems were often used as application case for other investigations like the control strategy for low exergy residential buildings [Goffin, 2014], the optimization of the combination of active and passive building components in refurbishment projects to allow for net-zero emission architecture [Ritter, 2012] or the thermal management of PVT collectors [Lämmle, 2018].

Regarding the related works, typically a certain system concept and specific aspects for fixed or slightly variable boundary conditions are taken into account but rarely widespread system comparisons are done. Furthermore, especially different possibilities of thermal combinations of solar and heat pump technologies or the combination with PV as driving energy for the heat pump were investigated but comparatively few studies have compared or combined those systems. In contrast, this work has the objective to close this gap by considering SHP concepts with integration of solar thermal and PV as well as hybrid concepts or combinations for a wide range of SHP system concepts and applications in residential buildings (single-family houses). To sum up, due to the variety of SHP system concepts and the gap of widely ranged and comparable studies on different SHP concepts, especially with consideration of both thermal and electrical energy supply of buildings including thermal and electrical energy storages, the objective of this work is the systematic model-based analysis of different SHP system concepts with regard to system performance / efficiency, environmental impact and economic aspects using consistent performance data of the SHP system components as well as consistent boundary conditions like climates (cold, moderate and warm) or types of residential buildings (new, renovated and non-renovated single-family houses) including heat load (space heating and domestic hot water preparation) and household electricity demand. Consequently, this work is mainly assigned to the design steps *Energy Efficiency* and *Renewable Energy* regarding the pathway for building design from Section 1.1. Furthermore, the development of SHP model libraries in the context of this work will allow for further investigations on the *Smartness and Flexibility* of future buildings by other works.

1.3 Methodological Approach of Model-Based System Analysis

The methodological approach of *model-based system analysis* used for the research investigations in this work is shown in Figure 1.4. The first step can be summarized as *theoretical and conceptual work* including the selection of SHP system concepts which should be analyzed, the definition of objectives and key performance indicators (KPI) to quantify the objectives achievements and the general SHP system design. This is followed by the *modeling* which comprises the component modeling (especially different building types including thermal and electrical loads, heat pumps, solar thermal collectors, PV or PVT, thermal and electrical storages or ground heat exchangers), its parameterization and finally the composition of the component models to SHP system models including the system control. To consider the state of the art in modeling of energy systems for buildings and to make the research results comparable to other works, the models are based on earlier, established works or standards if existing. If completely new models of components have to be developed, the developed

models are validated with measurements of real components (e.g. for PVT collectors). For a better consideration of real systems and its behavior, component models are parameterized by standardized, validated parameter sets (literature based) or data from manufacturers (directly as parameter or via parameter identification). For new models and components without available valid parameter sets (like PVT), tests with real systems are needed. At this, measurement data is used for parameter identification of the component models and the parameter identification procedure is developed. The last step of this approach includes the *system analysis* based on the developed models, starting with system design analysis and ending up with case studies and system optimization, e.g. potential improvement analysis by use of different PVT collector technologies.

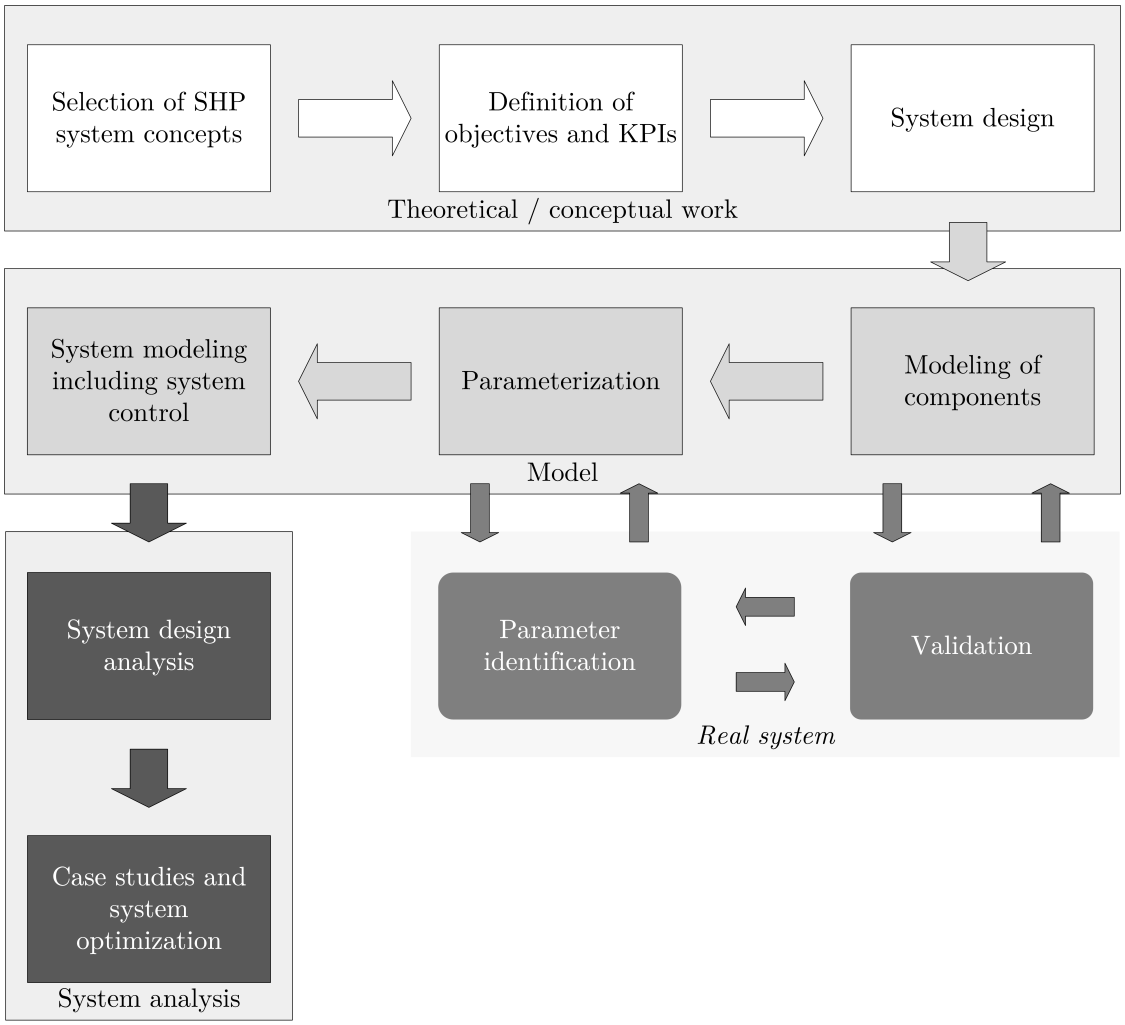

Figure 1.4: Methodological Approach.

1.4 Research Objectives and Thesis Structure/Approach

The research of this work can be divided into four main research topics. The subject of research topic 1 is the analysis and development of **new methods/approaches for SHP systems** (combined thermal and electrical) and give answers to the questions:

- *Which SHP system combinations exist and how can these systems be classified and described? Are further developments for system description needed?*
- *How can SHP systems and buildings with SHP systems be analyzed and rated (in general and in the context of nZEBs)? What KPIs exist? Do the KPIs fit the needs or is further KPI development needed?*
- *Which systems should be analyzed in this work?*

Research topic 2 goes on to the detailed **system modeling** and provide insights into:

- *How can SHP systems be modeled and what models already exist? Are new model developments needed?*
- *How can new models be validated and how can parameters of new models be identified for system analysis?*

Within research topic 3 a detailed **analysis of different concepts regarding the system design** is carried out to answer the research questions:

- *Which SHP system combination or technology is suitable for which application, considering different KPIs?*
- *Can SHP systems and solar technologies significantly reduce the CO_2 emissions of a building?*
- *Are SHP systems economically efficient?*
- *What are the benefits of hybrid systems and components (PVT)?*

Research topic 4 represent **case studies on different topics and optimizations** of SHP systems to show further system optimization potentials and investigation possibilities offered by the use of the developed models:

- *How does the system sizing influence the performance of SHP systems?*
- *Can the system performance be improved by choosing the PVT collector technology depending on the application?*
- *Can new buildings with SHP systems fulfill the requirements of nZEBs?*
- *How do subsidies and carbon prices influence the economic efficiency of SHP systems?*

The thesis approach is summarized in Figure 1.5 including the assignment of the research topics to the chapters of the thesis. **Chapter 2** introduces the reader to the basics of solar thermal, PV and heat pump technologies as well as whole SHP systems with special focus on the energy supply of buildings and thus presents the necessary background information to understand the research work performed within this thesis. Therefore, Chapter 2 also includes a general introduction in energy performance of residential buildings, especially in the context of nZEBs. In addition, this chapter describes the SHP system concepts that are analyzed in this work in detail. Finally, KPIs for SHP system analysis and its further development are presented.

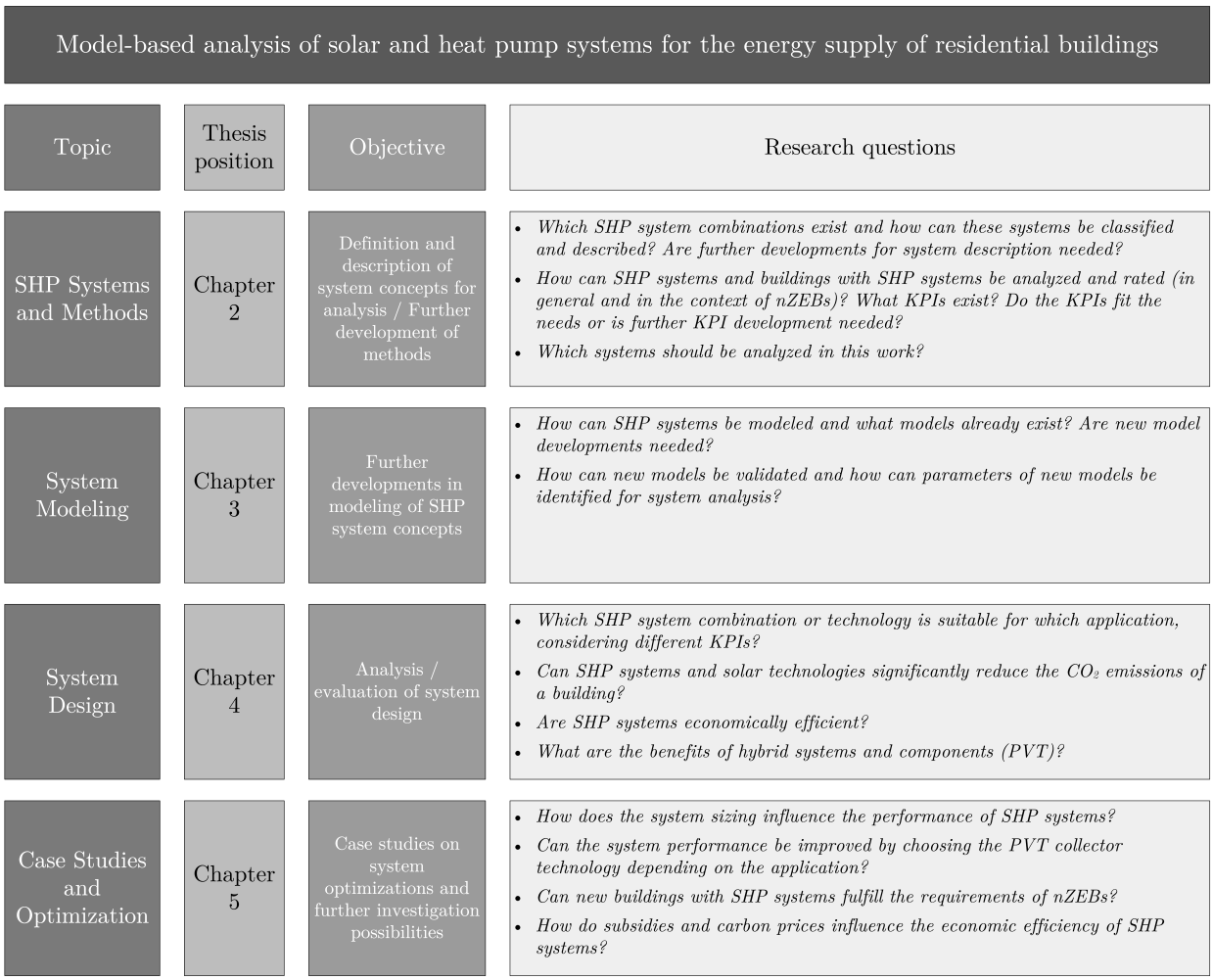

Figure 1.5: Thesis approach.

Chapter 3 then moves on to describe the detailed model development of SHP system concepts. Starting with a general introduction to the model design in TRNSYS, this chapter includes the building modeling, the modeling of thermal and electrical system components as well as the SHP system modeling and the explanation of implemented control strategies. This also contains the description of general boundary conditions (like climate properties), the parameterization of SHP component models (like heat pumps, solar thermal and PVT collectors, PV modules, thermal and electrical energy storages) including model parameter identification procedures and validation for new component models.

Based on the SHP system modeling and the previously defined KPIs, **Chapter 4** provides an analysis of the SHP system design regarding different evaluation criteria like performance and efficiency, environmental impact and economic aspects by the comparison of different system concepts. The performed system simulations are explained in detail including the used boundary conditions. For a better readability, the chapter is structured by the different evaluation criteria including summaries for each KPI and a final discussion on the results.

Chapter 5 then goes on to discuss the potential of SHP systems and special topics by analysis of simulation case studies. This includes case studies on system sizing and potential benefits by the use of different PVT collector technologies depending on the application in SHP systems. Furthermore, this chapter provides a case study on SHP systems in the context of nZEBs and an economic efficiency analysis of SHP systems with consideration of

subsidies and carbon prices.

Finally, **Chapter 6** summarizes the performed evaluations and offers conclusions on the use of SHP systems for the energy supply of residential buildings. In addition, this chapter gives an outlook on further works with special focus on the further use of the developed models.

Chapter 2

Solar and Heat Pump Systems for Residential Buildings

This chapter presents an overview of solar and heat pump systems for the energy supply of residential buildings with special focus on system concepts considered in the model-based analysis of this work. Beginning with an introduction to the energy performance of residential buildings, especially in the context of nearly zero energy buildings, and a general definition and classification of solar and heat pump systems, the fundamentals of the individual technologies like heat pumps, solar thermal, photovoltaic and photovoltaic-thermal systems are explained. This is followed by an introduction to solar and heat pump system concepts including different combinations of the previously described heat pump and solar energy technologies. Furthermore, this chapter includes the description of the basic operation and design of the solar and heat pump system concepts that are analyzed in this work and their evaluation by different performance figures regarding system performance and efficiency, environmental impact as well as economic aspects.

2.1 Energy Performance of Residential Buildings

Regarding the energy performance of residential buildings, a large variation of energy standards and definitions exists, especially in different national regulations. Furthermore, within these national regulations different calculation methods are defined. Hence, it is important to define the main energy terms, balances and boundaries in the context of residential buildings used in this work. The energy balance of residential buildings with consideration of different system boundaries as proposed in Kurnitski et al. [2011a,b]; Kurnitski [2013a,b] is illustrated with some minor adaptions in Figure 2.1. Regarding different boundaries and flow directions, energy is divided into energy demand, net energy demand, total energy use, delivered energy, net delivered energy and exported energy. In the following sections the different types of energy with respect to the different system boundaries and its calculation are described in detail. Furthermore, Section 2.1.3 has a special focus on energy performance

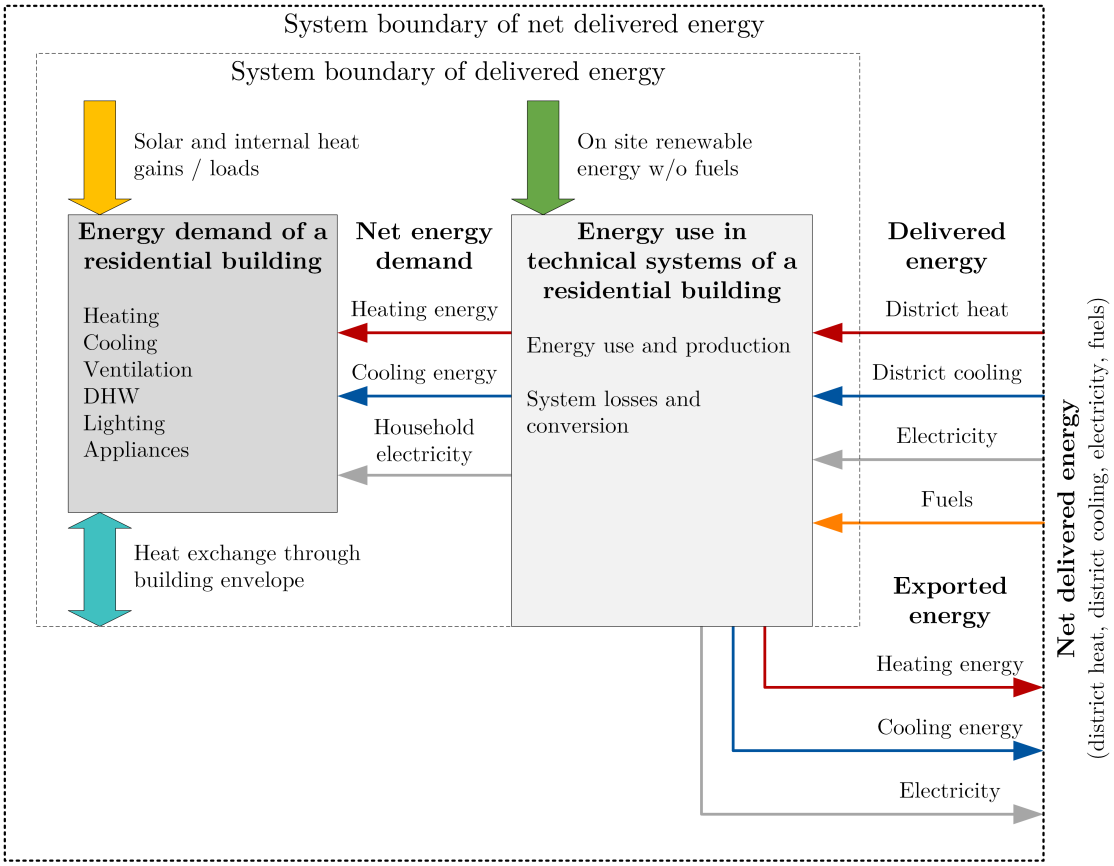

Figure 2.1: Energy balances and system boundaries for energy performance calculations of residential buildings. Adapted from Kurnitski et al. [2011a,b]; Kurnitski [2013a,b].

definitions and calculations for nZEBs in compliance with the EU EPBD.

2.1.1 Energy Demand

The *energy demand* (or energy need) of a residential building is separated in energy demand for heating, cooling, ventilation, domestic hot water, lighting and appliances. Taking the example of energy demand for heating, the energy demand represents the energy which is needed to maintain indoor climate conditions in consequence of heat exchange (thermal losses) through the building envelope. At this, the energy demand is reduced by solar and internal heat gains and the *net energy demand* is the remaining energy demand after the reduction by energy gains. In case of energy for heating, this remaining part of energy demand - the *net heating energy demand* - is usually simplified referred to as *heating energy demand*. The net energy demand of a residential building E_{bui} can be calculated with:

$$E_{\mathrm{bui}} = E_{\mathrm{bui,heating}} + E_{\mathrm{bui,cooling}} + E_{\mathrm{bui,el,hh}}, \tag{2.1}$$

where $E_{\mathrm{bui,heating}}$ is the net energy demand for heating including domestic hot water preparation, $E_{\mathrm{bui,cooling}}$ is the net energy demand for cooling and $E_{\mathrm{bui,el,hh}}$ is the net energy demand for household electricity of the building. Within this work, the cooling of buildings is not considered and, furthermore, the driving energy demand for mechanical ventilation is ne-

glected. Consequently, the net energy demand of residential buildings considered in this work can be simplified and divided into

a. energy demand for space heating Q_{SH} and domestic hot water preparation Q_{DHW} and

b. household electricity demand $W_{\mathrm{el,hh}}$ (lighting and appliances),

and thus the net energy demand of a residential building can be described with:

$$E_{\mathrm{bui}} = Q_{\mathrm{SH}} + Q_{\mathrm{DHW}} + W_{\mathrm{el,hh}} \tag{2.2}$$

or as net energy demand indicator with the useful floor area $A_{\mathrm{bui,net}}$ of the building:

$$EP_{\mathrm{bui}} = \frac{E_{\mathrm{bui}}}{A_{\mathrm{bui,net}}}. \tag{2.3}$$

The net heating energy demand of a building is usually calculated as annual value, or monthly values for a more detailed analysis, and is referred to as *annual heat load*. The amount of annual heat load for space heating depends mainly on the thermal behavior of the building whereas the annual heat load for domestic hot water preparation especially depends on the user behavior and the number of residents. Regarding the space heat load, it is important to define the detailed thermal energy balance of a residential building with its different heat flows and losses. In general, the thermal energy balance of a building considers all heat flows through the building envelope and all heat gains and loads within the building envelope. Usually, the domestic hot water preparation and the heating system itself are not considered within the building envelope as heating systems are often placed in the basement and thus do not belong to the heated part of residential buildings. Consequently, losses of the heating system itself including thermal losses of domestic hot water preparation or thermal storages are often not considered in the thermal energy balance of a building. These assumptions are also made in this work and, thus, the space heat load includes losses of the heat transfer in the room, but no losses of the heat distribution, storage or generation in the building. Subsequently, the space heat load is equal to the supplied space heat to the rooms in the building (including heat transfer losses). Under these conditions, the thermal energy balance of a residential building can be defined with (cf. Figure 2.2):

$$\mathrm{d}U_{\mathrm{bui}} = Q_{\mathrm{loss,trans}} + Q_{\mathrm{loss,airflow}} + Q_{\mathrm{loss,ground}} + Q_{\mathrm{SH}} + Q_{\mathrm{gains,int}} + Q_{\mathrm{gains,sol}}, \tag{2.4}$$

where $\mathrm{d}U_{\mathrm{bui}}$ is the change of internal energy in the building, $Q_{\mathrm{loss,trans}}$ are heat transmission losses through the building envelope (without ground losses), $Q_{\mathrm{loss,airflow}}$ are airflow heat losses (by infiltration and ventilation), $Q_{\mathrm{loss,ground}}$ are heat transmission losses to the ground, Q_{SH} is the supplied space heat (equal to the space heat load), $Q_{\mathrm{gains,int}}$ are internal heat gains (e.g. by persons, equipment) and $Q_{\mathrm{gains,sol}}$ are solar heat gains.

Regarding the annual energy balance of a building, the change of internal energy in the building is usually assumed to be zero and thus Equation 2.4 can be simplified to:

$$0 = Q_{\mathrm{loss,trans}} + Q_{\mathrm{loss,airflow}} + Q_{\mathrm{loss,ground}} + Q_{\mathrm{SH}} + Q_{\mathrm{gains,int}} + Q_{\mathrm{gains,sol}}. \tag{2.5}$$

The net annual heating energy demand of a residential building $E_{\mathrm{bui,heating}}$ includes the annual heat load for space heating Q_{SH} and the annual heat load for domestic hot water

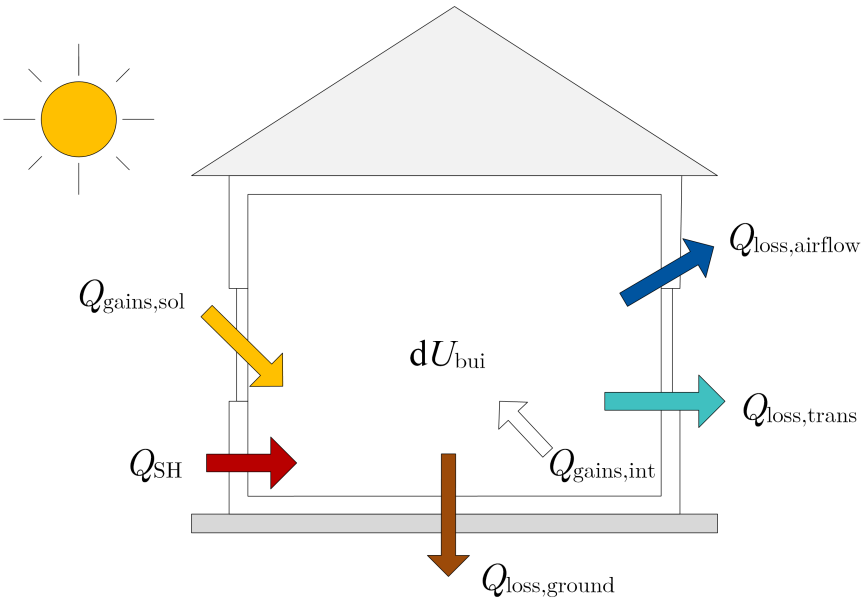

Figure 2.2: Thermal energy balance of a building.

preparation Q_{DHW} and can be calculated with:

$$E_{\text{bui,heating}} = Q_{\text{SH}} + Q_{\text{DHW}} \tag{2.6}$$

or as net annual heating energy demand indicator with the useful floor area of the building:

$$EP_{\text{bui,heating}} = \frac{E_{\text{bui,heating}}}{A_{\text{bui,net}}}. \tag{2.7}$$

2.1.2 Energy Use, Delivered and Exported Energy

For the covering of the building net energy demand, technical systems are required such as, for example, space heating circuits, heating devices, thermal or electrical storages. As these systems have different energy conversion, transfer or storage losses, the *energy use* of a building is higher than the energy demand of the building. For the provision of the energy use of the building, on-site renewable energy can be used or energy must be purchased. Regarding the energy purchase, the *delivered energy* $E_{\text{bui,del}}$ through the system boundary is divided into district heat, district cooling, electricity or fuels. Furthermore, the technical building energy system can export energy ($E_{\text{bui,exp}}$) through the system boundary like solar energy from on-site PV systems which is fed into the electricity grid. At this, the *exported energy* is divided into heating energy, cooling energy and electricity. The *total energy use* of a building $E_{\text{bui,use}}$ can be defined with:

$$E_{\text{bui,use}} = E_{\text{bui,del}} + E_{\text{bui,ren,self}} \tag{2.8}$$

and the *net total energy use* of a building $E_{\text{bui,use,net}}$ with:

$$E_{\text{bui,use,net}} = (E_{\text{bui,del}} - E_{\text{bui,exp}}) + E_{\text{bui,ren,self}}, \tag{2.9}$$

where $E_{\text{bui,ren,self}}$ is the self-consumed on-site renewable energy without fuels. At this, *total* means that self-consumed on-site renewable energy is included and the term *net* is used as subscript to express that the exported energy is considered to compensate the delivered energy. In addition to the used definition in this work, the total energy use can be divided into electricity and thermal energy use [Kurnitski, 2013a,b]. As cooling of residential buildings is not considered and, furthermore, district heating is also not within the research focus of this work, the delivered energy to the building can be calculated with the delivered fuel energy $E_{\text{bui,fuel}}$ and electrical energy from the grid $W_{\text{el,grid}}$:

$$E_{\text{bui,del}} = E_{\text{bui,fuel}} + W_{\text{el,grid}} \tag{2.10}$$

or as delivered energy indicator with the useful floor area of the building:

$$EP_{\text{bui,del}} = \frac{E_{\text{bui,del}}}{A_{\text{bui,net}}}. \tag{2.11}$$

The exported energy of the building can be calculated with the grid feed-in $W_{\text{el,feedin}}$:

$$E_{\text{bui,exp}} = W_{\text{el,feedin}}. \tag{2.12}$$

Furthermore, the *net delivered energy* can be calculated with:

$$E_{\text{bui,del,net}} = E_{\text{bui,del}} - E_{\text{bui,exp}}, \tag{2.13}$$

which can be transformed with Equation 2.10 and Equation 2.12 to:

$$E_{\text{bui,del,net}} = E_{\text{bui,fuel}} + W_{\text{el,grid}} - W_{\text{el,feedin}} \tag{2.14}$$

or as net delivered energy indicator with the useful floor area of the building:

$$EP_{\text{bui,del,net}} = \frac{E_{\text{bui,del,net}}}{A_{\text{bui,net}}}. \tag{2.15}$$

2.1.3 Nearly Zero Energy Buildings and Performance Indicators of Residential Buildings

Within the recast of the EU EPBD from 2010, the term *nearly zero energy buildings* (nZEB) is introduced as standard that is required for all new buildings in the EU by 2021. A nZEB is defined as building with a very high energy performance and nearly zero or very low amount of energy required, which should be covered by energy from renewable sources produced on-site or nearby [European Parliament, 2010]. Each member state of the EU shall detail the nZEB definitions, considering national, regional or local conditions, and define a numerical indicator of primary energy use expressed in kWh/m^2 per year [D'Agostino and Mazzarella, 2019]. Furthermore, the primary energy factors used for the determination of primary energy use may be based on national or regional yearly average values and may take into account relevant European standards [European Parliament, 2010]. As a result, the definition of a nZEB is not uniform and standardized as every member state has its own regulations how the nZEB standard can be fulfilled. However, the European Commission gave mandate to the European Committee for Standardization (CEN) to formulate standards to support the member states in the transposition of the EPBD into national application [Zirngibl, 2014].

This results in a set of energy performance of new and existing buildings (EPB) standards like ISO 52000-1:2017 [ISO 52000-1, 2017] that establishes a systematic, comprehensive and modular structure for assessing the EPB in a holistic way. An overview of the progress of the nZEB implementation in Europe and a comparison of definitions is given by D'Agostino and Mazzarella [2019].

Due to the different definitions of the nZEB standard, it is requisite to further clarify the used definitions in the context of nZEBs in this work. As nearby renewable energy production is no research subject in this work, the following definitions are limited to on-site renewable energies. The CEN defines *on-site* as the premises and the parcel of land on which the building is located and the building itself [ISO 52000-1, 2017]. Regarding the term *primary energy*, it should be distinguished between:

- primary energy: renewable or non-renewable energy which has not undergone any conversion or transformation process and
- final energy: energy which reaches the final consumer's door after conversion or transformation processes.

Furthermore, if renewable and non-renewable primary energy are taken into account it is referred to as total primary energy. Considering the recommendations of the European Commission in European Commission [2016], it is mandatory to evaluate the energy needs, the primary energy use, the on-site renewable sources as well as the net primary energy of a building in the context of nZEBs. At this, the primary energy is not further specified as renewable, non-renewable or total primary energy. According to the EPBD, all components of the energy use of a building are mandatory except the energy use of appliances which may or may not be included in the indicators [Kurnitski, 2013b]. Within this work, the appliances are included and, as mentioned in Section 2.1.1, are summarized with the energy demand for lighting to the household electricity demand.

Adapting an extended rating procedure incorporating the energy needs presented by Zirngibl [2014] and the methodical proposal in ISO 52000-1 [2017], the following indicators are proposed to evaluate a building regarding the nZEB standard:

- Net energy demand of a building: indicator for the energy needs (cf. Section 2.1.1)
- Total primary energy use of a building: indicator for the performance of the technical building systems
- Non-renewable primary energy use of a building: indicator for on-site renewable energy sources without compensation by exporting energy
- Net non-renewable primary energy use of a building: indicator for on-site renewable energy sources with compensation by exporting energy.

Regarding the pathways of building design from Section 1.1, the net energy demand of a building is mainly assigned to the assessment of the design step *Energy Sufficiency*, the total primary energy use of a building to *Energy Efficiency* and the non-renewable primary energy use and net non-renewable primary energy use of a building to *Renewable Energy*. Within this work, the net energy demand of the building is given by predefined single-family house standards and household electricity profiles resulting in different net heating energy demands and household electricity demands depending on the considered climate. Furthermore, it

is assumed that the defined new buildings in this work fulfill the requirements of the net energy demand for the considered locations as the buildings represent new buildings with very high energy standard.

The *total primary energy use* of a building $E_{\mathrm{pe,bui,tot}}$ can be defined as:

$$E_{\mathrm{pe,bui,tot}} = \sum_i \left(E_{\mathrm{bui,del},i}\ f_{\mathrm{pe,del,tot},i}\right) + \sum_i \left(E_{\mathrm{bui,ren,self},i}\ f_{\mathrm{pe,ren,self,tot},i}\right), \tag{2.16}$$

where $E_{\mathrm{bui,del},i}$ is the delivered energy for energy carrier i, $f_{\mathrm{pe,del,tot},i}$ is the total (renewable and non-renewable) primary energy factor for the delivered energy carrier i, $E_{\mathrm{bui,ren,self},i}$ is the self-consumed on-site renewable energy for energy carrier i and $f_{\mathrm{pe,ren,self,tot},i}$ is the total primary energy factor of the self-consumed on-site renewable energy for energy carrier i. As the total primary energy factor of the self-consumed on-site renewable energy for energy carrier i is usually 1, Equation 2.16 can be simplified to:

$$E_{\mathrm{pe,bui,tot}} = \sum_i \left(E_{\mathrm{bui,del},i}\ f_{\mathrm{pe,del,tot},i}\right) + \sum_i E_{\mathrm{bui,ren,self},i}. \tag{2.17}$$

The total primary energy use indicator $EP_{\mathrm{pe,bui,tot}}$ can then be calculated with the useful floor area of the building:

$$EP_{\mathrm{pe,bui,tot}} = \frac{E_{\mathrm{pe,bui,tot}}}{A_{\mathrm{bui,net}}}. \tag{2.18}$$

The *non-renewable primary energy use* $E_{\mathrm{pe,bui,nren}}$ of a building can be defined as:

$$E_{\mathrm{pe,bui,nren}} = \sum_i \left(E_{\mathrm{bui,del},i}\ f_{\mathrm{pe,del,nren},i}\right) + \sum_i \left(E_{\mathrm{bui,ren,self},i}\ f_{\mathrm{pe,ren,self,nren},i}\right), \tag{2.19}$$

where $f_{\mathrm{pe,del,nren},i}$ is the non-renewable primary energy factor for the delivered energy carrier i and $f_{\mathrm{pe,ren,self,nren},i}$ is the non-renewable primary energy factor of the self-consumed on-site renewable energy for energy carrier i. As the non-renewable primary energy factor of the self-consumed on-site renewable energy for energy carrier i is usually 0, Equation 2.19 can be simplified to:

$$E_{\mathrm{pe,bui,nren}} = \sum_i \left(E_{\mathrm{bui,del},i}\ f_{\mathrm{pe,del,nren},i}\right). \tag{2.20}$$

The non-renewable primary energy use indicator $EP_{\mathrm{pe,bui,nren}}$ can then be calculated with the useful floor area of the building:

$$EP_{\mathrm{pe,bui,nren}} = \frac{E_{\mathrm{pe,bui,nren}}}{A_{\mathrm{bui,net}}}. \tag{2.21}$$

The *net non-renewable primary energy use* indicator is typically the final numerical indicator to determine whether a building fulfill the requirements of a nZEB and sums up all non-renewable delivered and exported energy of a building into a single indicator. Following the calculation principles presented in Kurnitski [2013b], the net non-renewable primary energy use of a building $E_{\mathrm{pe,bui,nren,net}}$ is calculated from all delivered and exported energy

with:

$$E_{\text{pe,bui,nren,net}} = \sum_i \left(E_{\text{bui,del},i}\ f_{\text{pe,del,nren},i}\right) - \sum_i \left(E_{\text{bui,exp},i}\ f_{\text{pe,exp,nren},i}\right), \tag{2.22}$$

where $E_{\text{bui,exp},i}$ is the exported energy for energy carrier i and $f_{\text{pe,exp,nren},i}$ is the non-renewable primary energy factor of the delivered energy compensated by the exported energy for energy carrier i which is by default equal to the factor of the delivered energy (substitution value approach) if not nationally defined in other way. The net non-renewable primary energy use indicator $EP_{\text{pe,bui,nren,net}}$ can then be calculated with the useful floor area of the building [Kurnitski, 2013b]:

$$EP_{\text{pe,bui,nren,net}} = \frac{E_{\text{pe,bui,nren,net}}}{A_{\text{bui,net}}}. \tag{2.23}$$

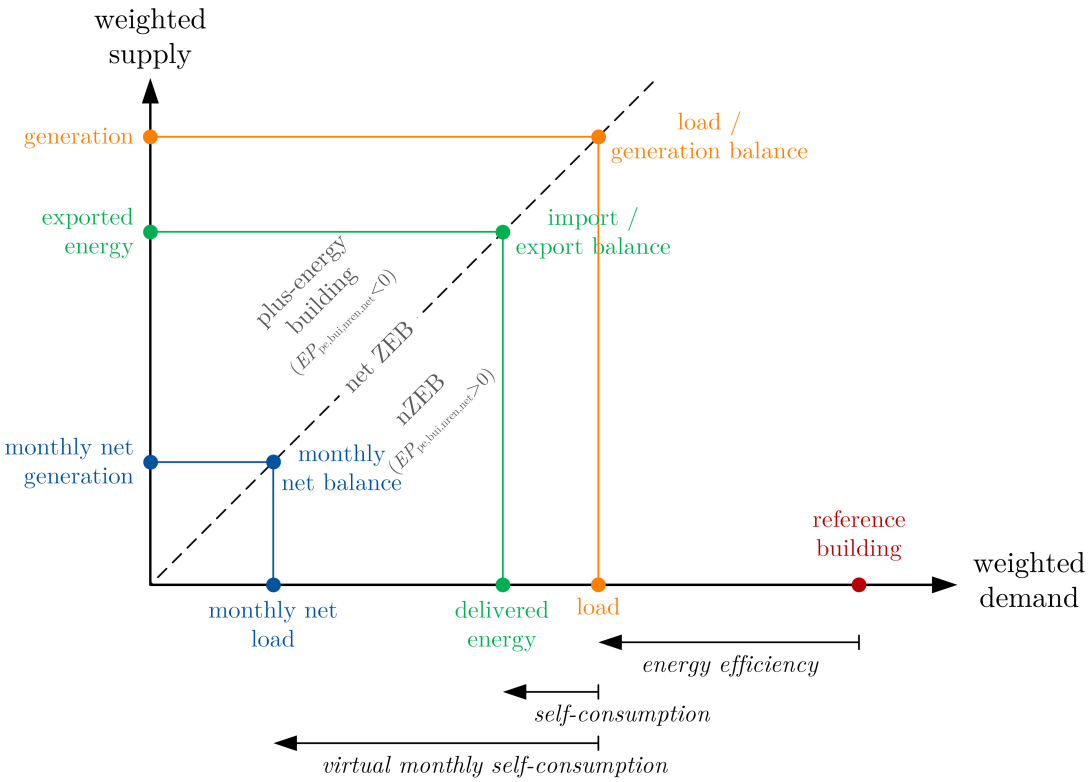

Figure 2.3: Different types of energy balances of a building in the context of nZEBs. Adapted from Sartori et al. [2012]; Voss et al. [2012].

According to Kurnitski [2013b], a *net zero energy building* (net ZEB) has an exact annual net non-renewable primary energy indicator of $0\,\text{kWh}_{\text{pe}}/\text{m}^2\text{a}$ whereas a *nearly zero energy building* (nZEB) has a technically and reasonably achievable use of $> 0\,\text{kWh}_{\text{pe}}/\text{m}^2\text{a}$ but no more than a national limit value, which should be achieved with a combination of best practice energy efficiency measures and renewable energy technologies. If the net non-renewable primary energy indicator is lower than zero, the building can be classified as *plus-energy building* [Kurnitski, 2013a]. This definition refers to an annual primary energy balance calculated from delivered and exported energy as shown in Figure 2.3 (import/export balance) and described with Equation 2.22. Depending on the application, it could be necessary

to use the load/generation balance between on-site generation and energy demand of the building, e.g. in the design phase if no data on the time dependent load and generation profiles is available [Voss et al., 2012]. The load/generation balance considers the building independently from a grid and thus the generated energy, whether self-consumed or not, does not affect the efficiency of the building. In contrast, the import/export balance is seen in connection with the grid and the self-consumption reduces the amount of exchanged energy and improves the efficiency of the system *building-grid* [Sartori et al., 2012]. Furthermore, a monthly virtual net balance that quantifies the monthly residuals between on-site generation and load can be used to characterize the seasonal mismatch between generation and load [Voss et al., 2012]. Within this work, the import/export balance is suitable as the model-based system analysis gives detailed information on the time dependent generation and load data and thus the imported and exported energy can be calculated. Starting from a reference building which is built according to the minimum requirements of a national building code or an existing building prior to renovation, the pathway to a net or nearly ZEB is given by the balance of reduction of energy demand (energy efficiency, x-axis in Figure 2.3) and energy generation (y-axis in Figure 2.3) to get enough credits to achieve the balance [Sartori et al., 2012]. Due to the technical limitations, solar thermal energy is typically consumed entirely on-site and thus solar thermal energy is sometimes treated as energy efficiency (demand reduction) technology (energy efficiency path in Figure 2.3) [Voss et al., 2012]. Within this work, solar thermal as well as other self-consumed renewable energy are treated as self-consumption to reduce the load (self-consumption path in Figure 2.3) and thus contribute to the on-site renewable energy sources of a building.

Using only the net non-renewable primary energy use indicator to characterize a building as nZEB can provoke misleading results as it is not really able to assess the quality of building energy performance. As a result, the nZEB standard could also be reached by buildings with high energy demand and low efficiency as the energy demand can be compensated by a high energy generation. Furthermore, the indicator gives no evidence on the used renewable energy sources. Hence, as mentioned before, it is mandatory to evaluate the net energy demand, the total primary energy use and the non-renewable primary energy use indicators in addition to the net non-renewable primary energy use indicator of a building. At this, the European Commission gives benchmarks for some of those indicators regarding different climate zones. An extraction of the relevant values for this work (single-family houses in cold, moderate and warm climates) with adaption as basic maximum values for the net non-renewable primary energy use indicator $EP^{\max}_{\text{pe,bui,nren,net}}$ and the total primary energy use indicator $EP^{\max}_{\text{pe,bui,tot}}$ to achieve the nZEB standard is summarized in Table 2.1.

Table 2.1: Numerical benchmarks for nZEB primary energy use of single-family houses depending on different European climates adapted and extended from European Commission [2016].

	Warm climate (Mediterranean)	Moderate climate (Oceanic)	Cold climate (Nordic)
	Maximum values in $\text{kWh}_{\text{pe}}/\text{m}^2\text{a}$		
$EP^{\max}_{\text{pe,bui,tot}}$	50 – 65	50 – 65	65 – 90
$EP^{\max}_{\text{pe,bui,nren}}$	25 – 40	32.5 – 47.5	52.5 – 77.5
$EP^{\max}_{\text{pe,bui,nren,net}}$	0 – 15	15 – 30	40 – 65

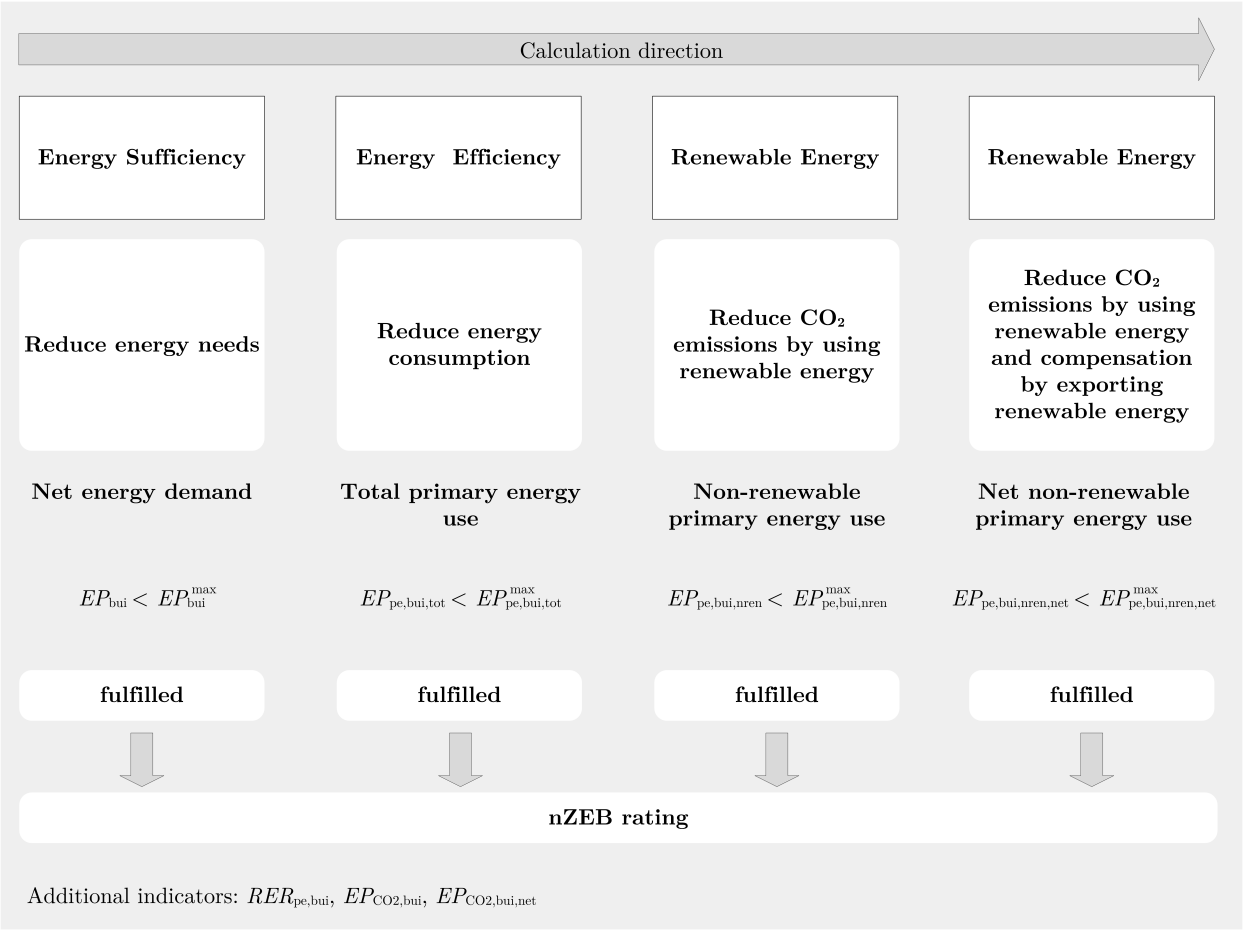

Figure 2.4: Pathway proposal for nZEB rating.

As the European Commission gives no benchmarks for the non-renewable primary energy use indicators, this work proposes that a maximum of 50 % of the difference between maximum total primary energy use and maximum net non-renewable primary energy use can be compensated by exporting energy or, in other words, 50 % of the difference between the maximum values has to be covered by renewable primary energy. The maximum non-renewable primary energy use indicators are then calculated with:

$$EP_{pe,bui,nren}^{max} = EP_{pe,bui,nren,net}^{max} + 0.5 \left(EP_{pe,bui,tot}^{max} - EP_{pe,bui,nren,net}^{max} \right) \tag{2.24}$$

and summarized in Table 2.1. The presented pathway proposal to reach nZEB standard is illustrated in Figure 2.4. As appliances are included in the nZEB indicators within this work, the presented numerical benchmarks in Table 2.1 will be increased and adapted in the following studies to indicate whether a building fulfill the requirements of a nZEB in the context of this work.

For the further evaluation of a residential building, the renewable energy ratio (RER) is an important figure for the rating of the share of renewable energy use of the building. It is complementary to the described primary energy indicators and is not directly required by EPBD [Kurnitski, 2013a]. The RER considers all renewable energy sources including, inter alia, solar thermal and PV or extracted energy from ambient used as heat source by heat pumps. As the EPBD operates with primary energy, the RER is calculated relative to all energy use in the building in terms of total primary energy and the substitution value

approach is applied. For on-site renewable energies, the total primary energy factor is 1 and the non-renewable primary energy factor is 0. The RER based on total primary energy of the building $RER_{\mathrm{pe,bui}}$ is then defined as:

$$RER_{\mathrm{pe,bui}} = \frac{\sum_i E_{\mathrm{bui,ren},i} + \sum_i \left[E_{\mathrm{bui,del},i}\left(f_{\mathrm{pe,del,tot},i} - f_{\mathrm{pe,del,nren},i}\right)\right]}{\sum_i E_{\mathrm{bui,ren},i} + \sum_i \left(E_{\mathrm{bui,del},i}\ f_{\mathrm{pe,del,tot},i}\right) - \sum_i \left(E_{\mathrm{bui,exp},i}\ f_{\mathrm{pe,exp,tot},i}\right)}, \tag{2.25}$$

where $E_{\mathrm{bui,ren},i}$ is the renewable energy produced on-site for energy carrier i and $f_{\mathrm{pe,exp,tot},i}$ is the total primary energy factor of the delivered energy compensated by the exported energy for energy carrier i which can be set equal to the factor of the delivered energy (substitution value approach) [Kurnitski, 2013b].

In addition to the primary energy, the CO_2 emissions as result of the energy use in the building $m_{\mathrm{CO_2,bui}}$ without compensation by exported energy can be calculated from the delivered energy with:

$$m_{\mathrm{CO_2,bui}} = \sum_i \left(E_{\mathrm{bui,del},i}\ f_{\mathrm{CO_2,del},i}\right) \tag{2.26}$$

and as CO_2 emissions indicator $EP_{\mathrm{CO_2,bui}}$ with the useful floor area of the building:

$$EP_{\mathrm{CO_2,bui}} = \frac{m_{\mathrm{CO_2,bui}}}{A_{\mathrm{bui,net}}}, \tag{2.27}$$

where $f_{\mathrm{CO_2,del},i}$ is the CO_2 emission coefficient for the delivered energy carrier i, or as net CO_2 emissions of the building $m_{\mathrm{CO_2,bui,net}}$ with compensation by exported energy:

$$m_{\mathrm{CO_2,bui,net}} = \sum_i \left(E_{\mathrm{bui,del},i}\ f_{\mathrm{CO_2,del},i}\right) - \sum_i \left(E_{\mathrm{bui,exp},i}\ f_{\mathrm{CO_2,exp},i}\right) \tag{2.28}$$

and as net CO_2 emissions indicator $EP_{\mathrm{CO_2,bui,net}}$:

$$EP_{\mathrm{CO_2,bui,net}} = \frac{m_{\mathrm{CO_2,bui,net}}}{A_{\mathrm{bui,net}}}, \tag{2.29}$$

where $f_{\mathrm{CO_2,exp},i}$ is the CO_2 emission coefficient for the delivered energy compensated by the exported energy carrier i which can be set equal to the coefficient of the delivered energy (substitution value approach).

2.2 Basics of Heat Pumps and Solar Energy Technologies

2.2.1 Heat Pumps

2.2.1.1 Basic Thermodynamics

In general, a heat pump is a device that transfers heat from a lower temperature level (heat source) to a higher temperature level (heat sink) using a working fluid (refrigerant) that goes through a thermodynamic cycle. According to the second law of thermodynamics, heat always flows from higher to lower temperatures unless external work is performed on the system. In other words, this process cannot run by itself and an additional driving energy is required for practical implementation. This driving energy can be provided either mechanically (compression heat pumps (electrical)) or thermally (adsorption and absorption

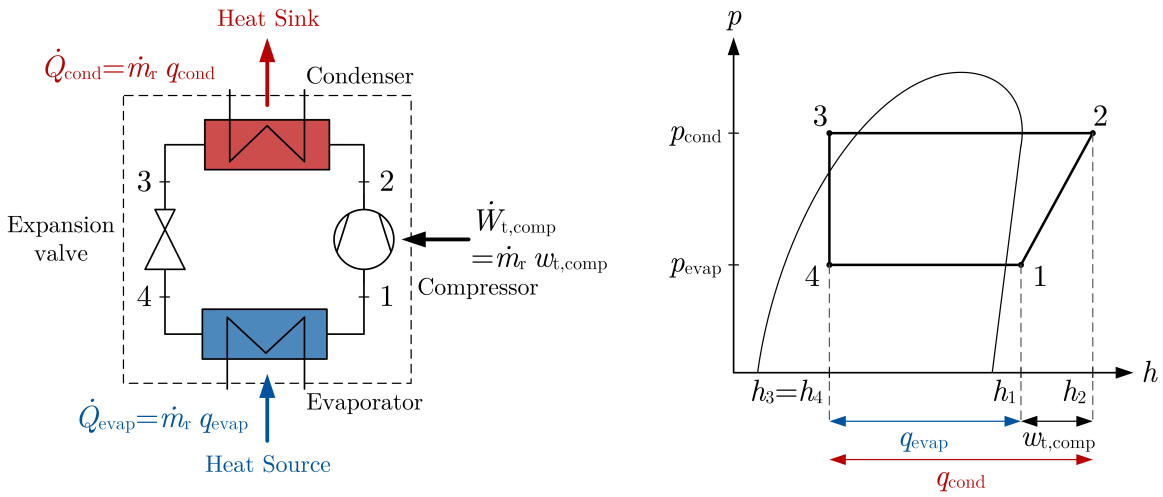

(a) Heat pump cycle **(b)** Log(p),h-diagram

Figure 2.5: Thermodynamic cycle of a heat pump process.

heat pumps). For heating and cooling applications in buildings, the most frequently used heat pumps are vapor-compression heat pumps (hereinafter referred as *heat pump*), which are also considered in this work. These heat pumps consist essentially of the four main components compressor, condenser, expansion valve and evaporator (cf. Figure 2.5a). The basic theoretical thermodynamic cycle of a heat pump is illustrated in Figure 2.5b and contains four state changes:

- 1-2: Isentropic compression
- 2-3: Isobaric condensation
- 3-4: Isenthalpic expansion
- 4-1: Isobaric evaporation.

Beginning with the process from (4) to (1), the refrigerant is evaporated and slightly overheated in the evaporator at constant pressure (p_{evap}) by the heat transfer $\dot{Q}_{evap}$ from the heat source (e.g. ambient air or the ground) at low pressure and temperature level. At this, the thermal evaporator power can be calculated with the mass flow rate of the refrigerant $\dot{m}_r$, the specific heat energy of the evaporator q_{evap} and the specific enthalpies of states (1) h_1 and (4) h_4:

$$\dot{Q}_{evap} = \dot{m}_r\ q_{evap} = \dot{m}_r\,(h_1 - h_4)\,. \tag{2.30}$$

Assuming a heat transfer without losses to the ambient, the thermal evaporator power is equal to the thermal power from the (cold) heat source $\dot{Q}_c$:

$$\dot{Q}_c = \dot{m}_c\ c_{p,c}\ \ (T_{c,in} - T_{c,out}) = \dot{Q}_{evap}, \tag{2.31}$$

where $\dot{m}_c$ is the mass flow rate of the heat source fluid, $c_{p,c}$ is the specific heat capacity of the heat source fluid, $T_{c,in}$ is the inlet temperature of the heat source fluid and $T_{c,out}$ is the outlet temperature of the heat source fluid.

The refrigerant then enters the compressor as vapor and is compressed isentropic from (1) to (2) to the condenser pressure p_{cond} with increase in temperature by the technical compressor capacity $\dot{W}_{\mathrm{t,comp}}$. At this, it is assumed that the electrical power consumption of the compressor $P_{\mathrm{el,comp}}$ is equal to the technical compressor capacity. Furthermore, this presupposes that the electrical compressor efficiency $\eta_{\mathrm{el,comp}}$ and the mechanical compressor efficiency $\eta_{\mathrm{mech,comp}}$ are without losses and thus:

$$\dot{W}_{\mathrm{t,comp}} = \eta_{\mathrm{el,comp}}\, \eta_{\mathrm{mech,comp}}\, P_{\mathrm{el,comp}} \tag{2.32}$$

can be simplified with $\eta_{\mathrm{el,comp}} = 1$ and $\eta_{\mathrm{mech,comp}} = 1$ to:

$$\dot{W}_{\mathrm{t,comp}} = P_{\mathrm{el,comp}}. \tag{2.33}$$

Consequently, the compressor power can be calculated with the mass flow rate of the refrigerant and the specific enthalpies of states (1) h_1 and (2) h_2:

$$P_{\mathrm{el,comp}} = \dot{m}_{\mathrm{r}}\, w_{\mathrm{t,comp}} = \dot{m}_{\mathrm{r}}\, (h_2 - h_1)\,, \tag{2.34}$$

where $w_{\mathrm{t,comp}}$ is the specific technical work of the compressor.

From (2) to (3) the heat flow $\dot{Q}_{\mathrm{cond}}$ is transferred at high pressure and temperature level from the hot refrigerant to a heat sink (e.g. a buffer storage, space heating or domestic hot water circuit) in the condenser. Within this process, the refrigerant condensates from a vapor to a saturated liquid at constant pressure and the refrigerant leaves the condenser. At this, the thermal condenser power $\dot{Q}_{\mathrm{cond}}$ can be calculated with the mass flow rate of the refrigerant, the specific heat energy of the condenser q_{cond} and the specific enthalpies of states (2) h_2 and (3) h_3:

$$\dot{Q}_{\mathrm{cond}} = \dot{m}_{\mathrm{r}}\, q_{\mathrm{cond}} = \dot{m}_{\mathrm{r}}\, (h_2 - h_3)\,. \tag{2.35}$$

Assuming a heat transfer without losses to the ambient, the heating power of the heat pump transferred to the (hot) heat sink $\dot{Q}_{\mathrm{h}}$ can be calculated with:

$$\dot{Q}_{\mathrm{h}} = \dot{m}_{\mathrm{h}}\, c_{p,\mathrm{h}}\, \left(T_{\mathrm{h,out}} - T_{\mathrm{h,in}}\right) = \dot{Q}_{\mathrm{cond}}, \tag{2.36}$$

where $\dot{m}_{\mathrm{h}}$ is the mass flow rate of the heat sink fluid, $c_{p,\mathrm{h}}$ is the specific heat capacity of the heat sink fluid, $T_{\mathrm{h,out}}$ is the outlet temperature of the heat sink fluid and $T_{\mathrm{h,in}}$ is the inlet temperature of the heat sink fluid. Finally, the refrigerant enters the expansion valve, is expanded from (3) to (4) at constant enthalpy to the evaporator pressure and reenters the evaporator.

Using the first law of thermodynamics, the general expression of the thermal power output of a heat pump by means of a steady-state energy balance in a thermodynamic cycle can be expressed as (cf. Figure 2.5):

$$\dot{Q}_{\mathrm{cond}} = \dot{Q}_{\mathrm{evap}} + \dot{W}_{\mathrm{t,comp}} \tag{2.37}$$

or

$$\dot{Q}_{\mathrm{h}} = \dot{Q}_{\mathrm{c}} + P_{\mathrm{el,comp}}. \tag{2.38}$$

Furthermore, the efficiency of a heat pump can be expressed in terms of the coefficient of performance COP:

$$COP = \frac{\dot{Q}_\mathrm{h}}{P_\mathrm{el,comp}}. \tag{2.39}$$

Thus, the COP is an expression for the ratio of the thermal power output (heating power) to the required compressor power of a heat pump. Consequently, the higher the COP the less driving energy is needed for the provision of the required heating power. The theoretical maximum of the COP is the Carnot efficiency of a heat pump process. The Carnot efficiency η_Carnot can be expressed as function of the temperatures of the heat sink T_h and heat source T_c with:

$$\eta_\mathrm{Carnot} = \max\left(\frac{\dot{Q}_\mathrm{h}}{P_\mathrm{el,comp}}\right) = \frac{T_\mathrm{h}}{T_\mathrm{h} - T_\mathrm{c}}. \tag{2.40}$$

The Carnot efficiency illustrates that an optimization of the operating conditions of a heat pump can be achieved by minimizing the temperature differences between heat sink and heat source as the maximum possible coefficient of performance can be increased. On the one hand, this can be achieved by lowering the required operating temperature of the heating system. Therefore, the efficiency of a heat pump system increases if it is used in low temperature heating systems like floor heating systems with low supply temperatures. On the other hand, an increase of the heat source temperature also leads to an increase of the heat pump efficiency. However, it should be noted that these are theoretical, maximum efficiencies and the physical optimum is not achieved in practical operation. Nevertheless, the previously described rules also apply in real systems.

For real applications, the COP definition often contains additional electrical power consumptions like pumps, controller or in case of ASHPs additional ventilators. At this, the COP_HP is calculated with the electrical power consumption of the whole heat pump $P_\mathrm{el,HP}$:

$$COP_\mathrm{HP} = \frac{\dot{Q}_\mathrm{h}}{P_\mathrm{el,HP}}. \tag{2.41}$$

2.2.1.2 Heat Pump Heating Systems and Heat Sources

In general, heat pump systems for residential buildings can be divided into four main categories depending on their application [Chua et al., 2010]:

- Heating-only heat pumps: providing space heating and/or domestic hot water
- Heating and cooling heat pumps: providing both space heating and cooling
- Integrated heat pump systems: providing space heating and cooling, domestic hot water and sometimes exhaust air heat recovery
- Heat pump water heaters: providing only domestic hot water.

As this work does not consider cooling of residential buildings, the following explanations are limited to heating-only heat pump systems for combined space heating and domestic hot water preparation. In addition, air heating systems and systems which use exhaust air as

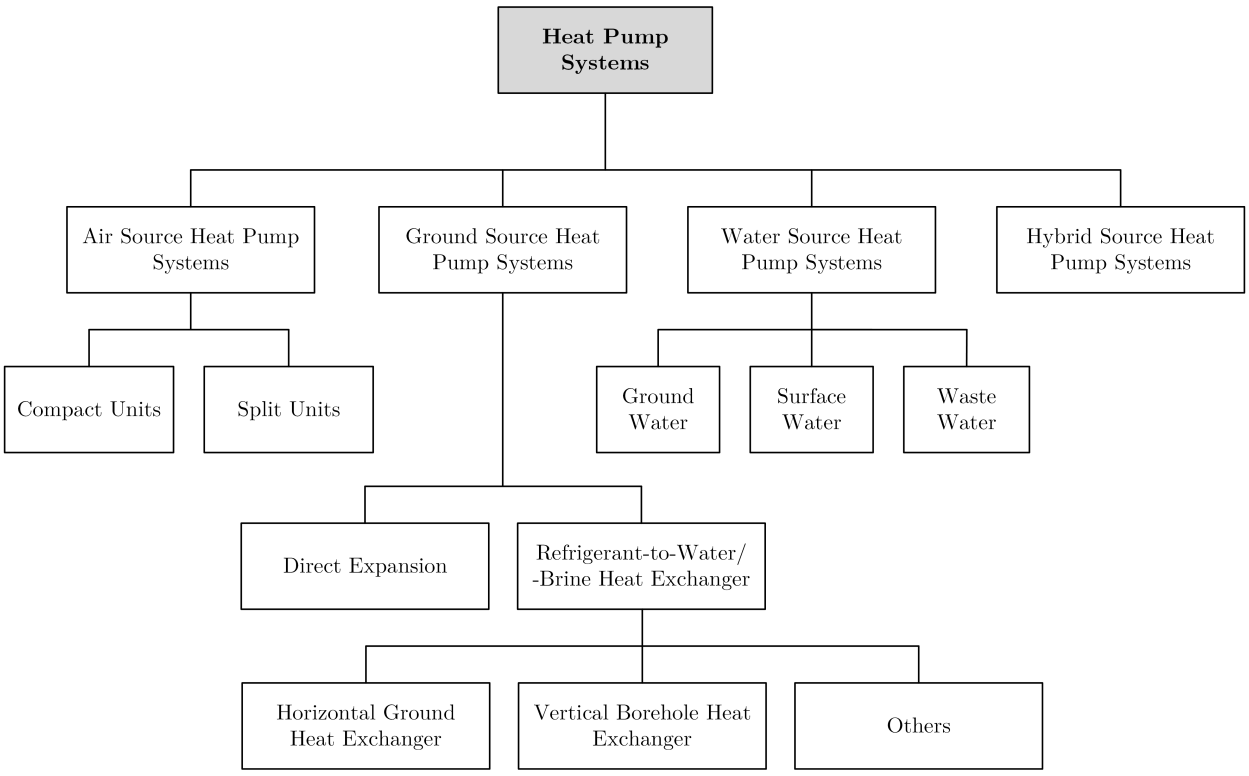

Figure 2.6: Classification of heat pump systems.

heat source are not in the research field of this work and are not considered in this section. Therefore, all systems in the following are water heating systems which uses water as energy carrier on the heat sink side of the heat pump. With the described restrictions, it is useful to further classify the heat pump heating systems depending on the heat source into ground source, air source, water source or hybrid source heat pump systems including systems with solar energy technology integration on the source side of the heat pump, cf. Figure 2.6.

Air source or air/water heat pump systems mainly use ambient air as heat source and can be divided into systems with compact units and split units. Compact units are single units that include the heat pump and the evaporator in a single housing and are designed for installation indoors or outdoors. Split units, on the other hand, consist of an indoor heat pump unit and a separated evaporator with ventilator that is usually installed outdoors [Bonin, 2015]. Water source or water/water heat pump systems can especially be divided in ground water, surface water or waste water heat pumps. Basically, GSHP systems can be divided into systems with direct expansion of the refrigerant in the heat source circuit or systems with use of refrigerant-to-water/-brine heat exchanger to separate the heat source circuit from the refrigerant circuit via heat exchanger. At this, heat pumps with refrigerant-to-brine heat exchanger for water heating systems are referred to as brine/water heat pumps. In addition, systems with separated heat source circuit can be classified in systems with horizontal ground heat exchanger, systems with vertical borehole heat exchanger (BHE) and others, e.g. systems with basket or spiral heat exchangers. GSHPs with horizontal, basket or spiral ground heat exchangers are installed close to the surface of the ground (e.g. approximately 1-2 m for horizontal ground heat exchangers) whereas vertical BHEs are normally installed with depths between 20 m and 200 m [Sarbu and Sebarchievici, 2014]. Figure 2.7 shows some typical heat sources of heat pump heating systems for residential buildings.

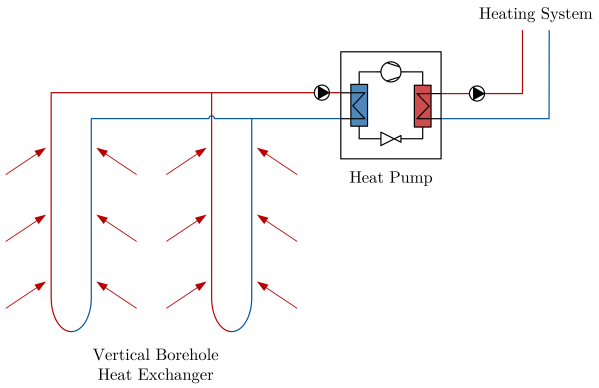

(a) Vertical borehole heat exchanger

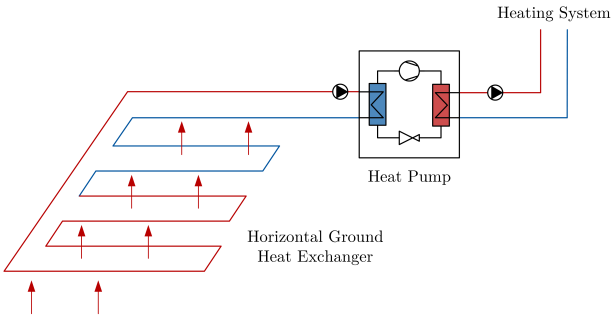

(b) Horizontal ground heat exchanger

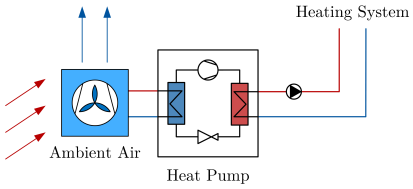

(c) Air

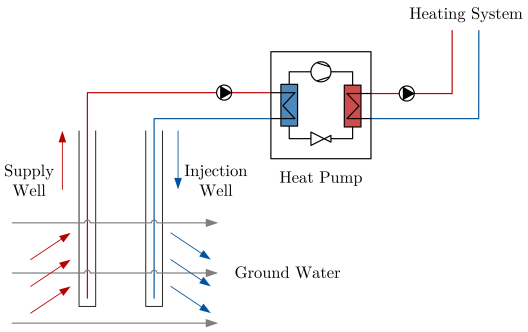

(d) Ground water

Figure 2.7: Typical heat sources of heat pumps for heating applications in residential buildings.

Regarding the design of heat pump systems, a distinction is commonly made between monovalent, monoenergetic and bivalent (parallel or alternative) system operation. In *monovalent* system concepts, the heat pump has to cover the entire heat demand of the building even on the coldest days of the year. Hence, especially ASHP systems must be able to provide the maximum heat capacity at times with lowest heat source temperatures and high heat sink temperatures which means at low efficiency. In contrast, within *bivalent* systems an additional auxiliary heater either completely takes over the heating (bivalent alternative) or is operated in addition to the heat pump (bivalent parallel) [Marguerite et al., 2019]. At this, bivalent heat pumps are often sized between 20 % to 60 % of the maximum heat load, but usually cover around 50 % to 95 % of the annual heating energy demand. The additional auxiliary heater in bivalent systems uses a different energy source or energy carrier as the heat pump, e.g. gas or oil. In contrast, within *monoenergetic* system concepts, that are often used for ASHPs, the heat pump is supported by an additional electrical heater that uses the same type of energy (electrical energy) as the heat pump [IEA HPC, 2010].

Assessing the heat pump market in Europe, heat pump sales have raised in the last years, from 2015 to 2018 by around 12 % to 13 % every year. In 2018, the installed stock of heat pumps was around 11.6 million heat pumps considering 21 European countries [EHPA, 2021]. Regarding water heating systems, ambient air and ground are the most common heat sources for heat pump installations in Europe, while others like water and exhaust air

cover only smaller market shares [Hadorn, 2015]. This is also illustrated in Figure 2.8 by the heat pump sales development of 21 European countries from 2009 to 2018. In 2018, the market share on the considered heat pump sales was 91.4 % for ASHPs (43.5 % for air/water and 47.9 % for air/air heat pump systems), while GSHPs achieved 7.8 % and others only 0.8 %. As air heating systems are not considered in this work, the following investigations of conventional heat pump systems are limited to the market-dominated heat pump water heating systems with ambient air or ground as heat source. A common and often used ground source concept is the mentioned heat pump system with vertical BHEs. Due to its better representation of geothermal energy as consequence of the deeper heat exchanger depths in the ground compared to other ground heat exchanger concepts it is chosen as representative concept for GSHPs. A comparison of the main advantages and disadvantages of GSHPs with vertical BHE and ASHPs is summarized in Table 2.2.

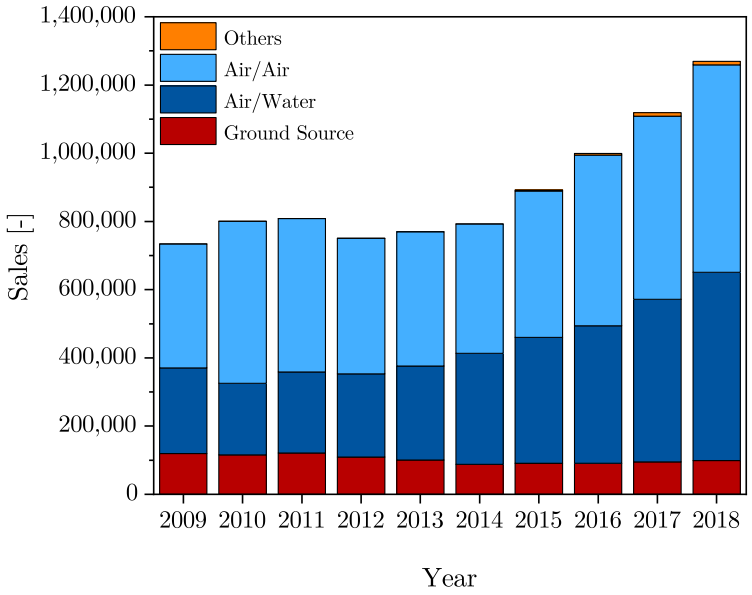

Figure 2.8: Heat pump sales development by source of 21 European countries[1] from 2009 to 2018. Data from EHPA [2021].

[1] Austria, Belgium, Czech Republic, Denmark, Estonia, Finland, France, Germany, Hungary, Ireland, Italy, Lithuania, Netherlands, Norway, Poland, Portugal, Slovakia, Spain, Sweden, Switzerland, United Kingdom.

Table 2.2: Main advantages and disadvantages of GSHP systems with vertical BHE and ASHP systems for heating applications in residential buildings.

	Advantages	Disadvantages
ASHP	- Simpler installation (no extensive earthworks) - Lower investment costs (installation and planning) - No extensive approval procedure	- High (seasonal) source temperature variation - Coldest source temperature at times of highest heat demand - Additional de-icing/-frosting energy needed for the evaporator - Higher noise emissions due to air fan operation
GSHP	- Relatively high source temperatures - Limited (seasonal) source temperature variation - No freezing of the evaporator - Efficient for heating (and cooling) applications	- High installation costs - Risk of ground freezing (if not well designed) - Extensive approval procedure - Feasibility study / soil survey required

2.2.1.3 Heat Pump System Concepts

The concept of the investigated heat pump heating system in this work, regardless of the used heat source, is shown in Figure 2.9 and consists essentially of a heat pump unit, a buffer storage tank as heat sink of the heat pump, a space heating circuit, a domestic hot water circuit with heat exchanger and additional hydraulic components (pumps, valves). The buffer storage tank is designed as combi-storage for both space heating and domestic hot

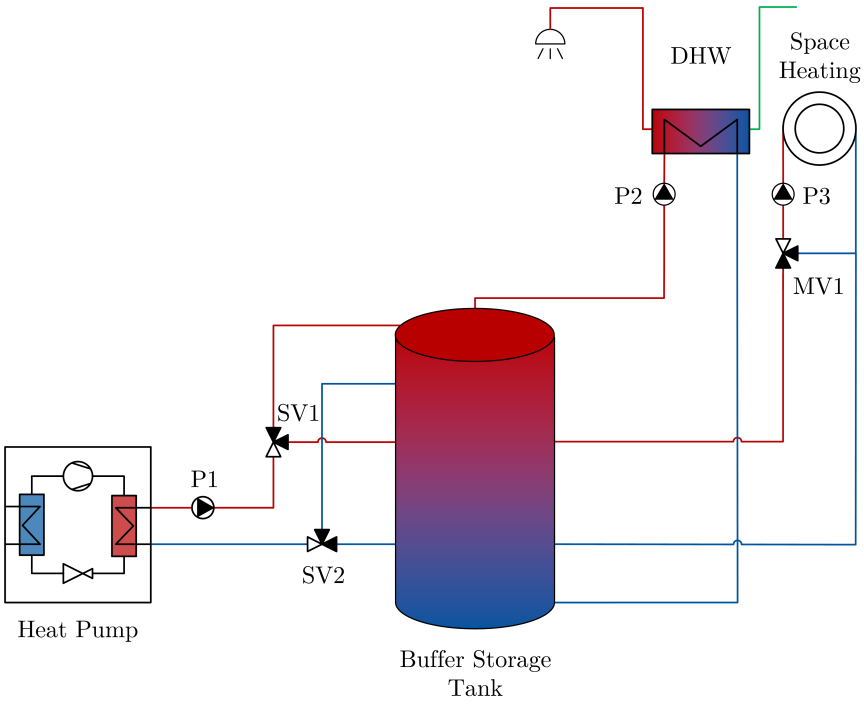

Figure 2.9: Hydraulic scheme of the heat pump heating system independent of the used heat source.

water preparation (via an external heat exchanger). The main advantages of such combi-storage concepts in comparison to systems with additional external domestic hot water storage are the reduction of complexity and the number of components of the system as well as the reduction of heat losses due to a better surface to volume ratio [Hadorn, 2015]. Furthermore, the buffer storage tank is divided in two zones. The lower/middle zone is used for the supply of the space heating circuit (SH zone) by the space heating circuit pump (P3) and the upper zone is used for the supply of the external heat exchanger for domestic hot water preparation on a higher temperature level (DHW zone) by the domestic hot water circuit pump (P2). At this, the space heating circuit is equipped with a return flow addition by a mixing valve (MV1) for temperature control of the supply temperature of the space heating circuit. The connections of the heat pump to the buffer storage are designed as four pipe connections with a three-way switching valve in the supply (SV1) and the return line (SV2), which means that the heat pump can charge the DWH zone with the storage charging pump (P1) independently from the SH zone and thus without heating up the entire storage (cf. [Poppi and Bales, 2014]). Depending on the current demands, the heat supply by the heat pump is switching to the different zones with priority on domestic hot water preparation. The purpose of this solution is to achieve better storage stratification and thus avoid storage mixing and exergy losses. It should be noted that this requires that the DWH and the SH zone do not overlap and the temperature sensor of the DHW zone for the control of domestic hot water charging is placed with sufficient distance from the SH zone [Haller et al., 2014b]. In addition, the space heating circuit is equipped with a three-way mixing valve in the supply line (MV1) to the floor or radiator heating system to regulate the supply temperature maintaining the set supply temperature by mixing colder water from the return to the supply line of the heat distribution system. The hydraulics of the considered GSHP and ASHP systems are shown in Figure 2.10. Beside of the described heat sink circuit of the heat pump, the GSHP system consists essentially of a brine/water heat pump with vertical BHE and heat source circulation pump as heat source circuit whereas the ASHP system is equipped with an ASHP unit using the ambient air as heat source. Apart from the heat source circuit of the GSHP system that uses frost protected brine, all circuits use water as heat transfer medium.

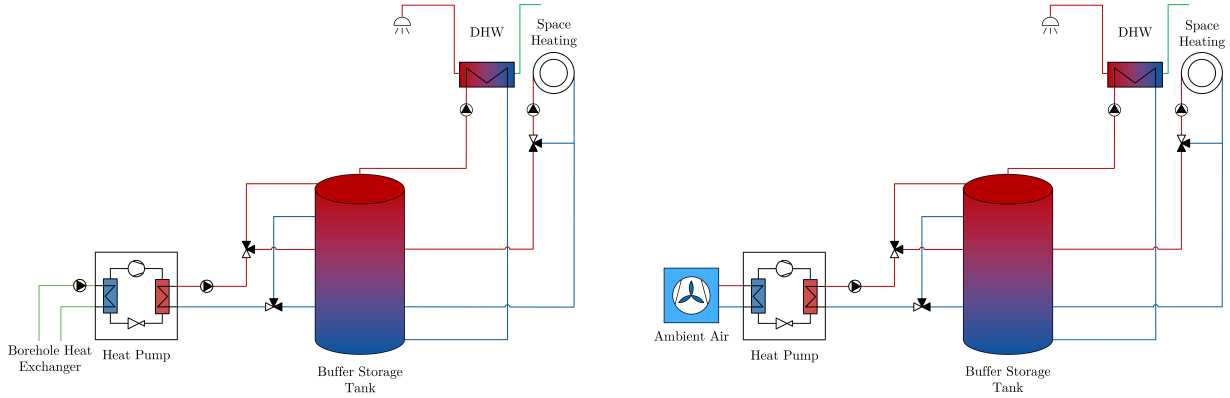

(a) GSHP **(b)** ASHP

Figure 2.10: Hydraulic schemes of the considered heat pump systems.

2.2.2 Solar Energy

Solar energy is the most abundant available energy source of all renewable sources. The annual solar radiation reaching the surface of the earth is around 3.4×10^6 EJ [Thirugnanasambandam et al., 2010]. In contrast, in 2019, the primary energy consumption worldwide was around 5.8×10^2 EJ which is equivalent to around 0.017 % of the annual solar radiation on the surface of the earth. These figures illustrate impressively the huge potential of solar energy usage for covering the global energy demand. The first known practical application of solar energy was drying for preserving food [Kalogirou, 2014]. Nowadays, solar energy is used for a multitude of applications and solar energy technologies can basically be divided in passive and active solar technologies. Passive solar technologies involve the accumulation of solar energy without transforming it into any other form, while active systems collect solar radiation and use mechanical or electrical equipment for the conversion of solar energy to heat and electricity [Kabir et al., 2018]. Regarding the energy supply of buildings, *passive solar energy* use comprises mainly the covering of heating demand by solar energy transmitting through windows or transparent thermal insulation of external walls. *Active solar energy* technologies for buildings can primarily divided in solar thermal systems to provide heat for space heating and domestic hot water preparation, PV systems to provide electricity to the building and hybrid PVT systems to provide heat and electricity (cf. Figure 2.11). Furthermore, in air-conditioned buildings, thermal cooling processes like open and closed sorption processes can be supplied by active solar components [Eicker, 2003]. In the following sections, the solar energy technologies and the necessary background with respect to the applications of solar technologies within this work are described in detail. As investigations of air-conditioning and passive solar technologies are not part of this work, this includes solar thermal, PV and PVT systems.

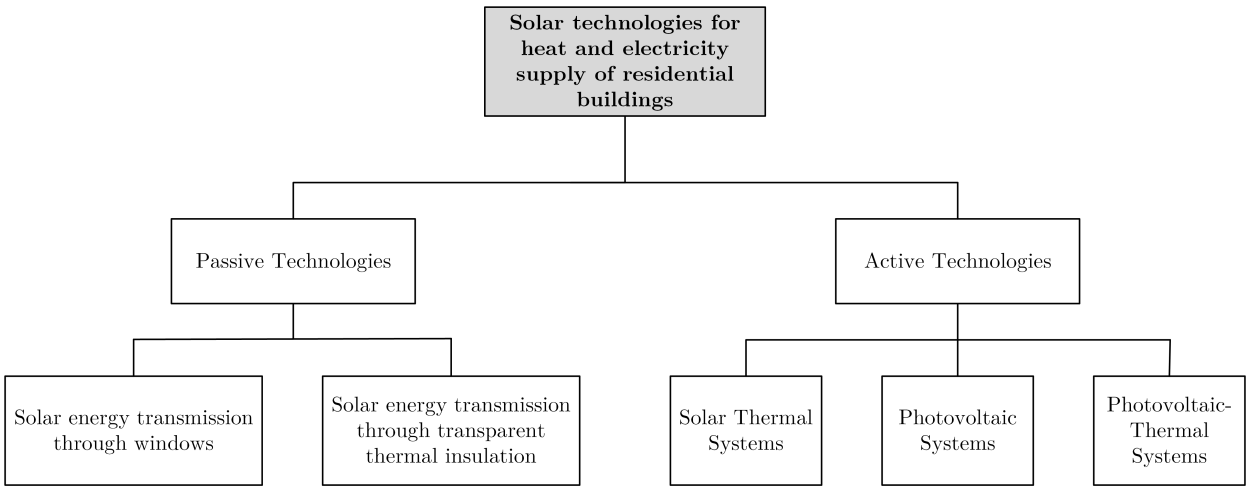

Figure 2.11: Classification of solar energy technologies for heat and electricity supply of residential buildings.

2.2.2.1 Solar Thermal Systems

A solar thermal collector is a special kind of heat exchanger that converts solar radiant energy into heat and transfers this heat to a fluid (usually air, water or oil) flowing through the collector [Duffie et al., 2020; Kalogirou, 2004]. Solar thermal collectors are used for a

variety of applications like solar water heating, space heating and cooling, solar refrigeration, industrial process heat, solar desalination or solar thermal power systems, to name the most important applications [Kalogirou, 2004]. Within this work, the focus is on solar domestic hot water and space heating systems. Regarding these applications with limitation on liquid-based collectors, stationary (without sun tracking) solar thermal collectors can be classified into wind and/or infrared sensitive collectors (WISC), flat-plate collectors (FPC), evacuated tube collectors (ETC) and compound parabolic collectors (CPC).

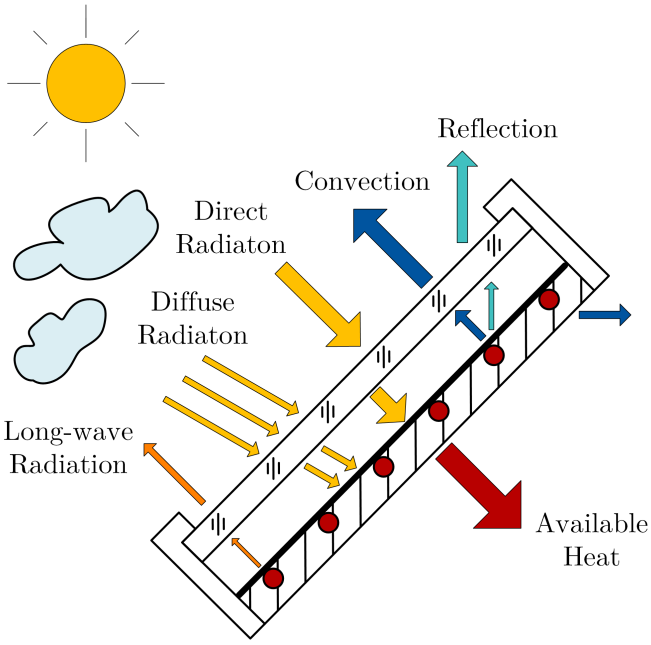

Figure 2.12: Basic principle of solar thermal collectors.

The basic principle of solar thermal collectors is shown in Figure 2.12 for the example of a FPC (see also Figure 2.14b). When solar radiation (direct and diffuse) passes through a transparent collector cover on the absorber surface, a large portion of this energy is absorbed by the plate and then transferred to the fluid. The remaining parts of the solar radiation are lost at the front glass cover, the absorber or the frame of the collector by reflection, convection and long-wave radiation. Therefore, the frame of FPC collectors and the underside of the absorber plate are well insulated to reduce convection losses. Furthermore, the transparent cover is used to reduce the convection losses through the restraint of the stagnant air layer between the absorber plate and the glass cover. In addition, the cover reduces radiation losses as it is transparent to the short-wave radiation received by the sun but it is nearly opaque to long-wave thermal radiation emitted by the absorber (greenhouse effect). Another technology that is often used for the construction of solar thermal collectors are selective coatings of the absorber that are highly absorbent to shortwave radiation by the sun but have a relatively low emittance for long-wave radiation [Kalogirou, 2004].

In steady state, the performance of solar thermal collectors is basically described by an energy balance that indicates the distribution of incident solar radiation into useful energy gain, thermal losses and optical losses [Duffie et al., 2020]. With the absorbed solar radiation $G \cdot (\tau\alpha)$ and the overall heat loss coefficient U_{loss} that represents the thermal energy loss from the collector to the surroundings by conduction, convection and long-wave radiation, the thermal power output of a solar thermal collector $\dot{Q}_{\text{th,sol}}$ with the collector area A_{coll} can

be calculated with [Kalogirou, 2014]:

$$\dot{Q}_{\mathrm{th,sol}} = A_{\mathrm{coll}} \ [G\,(\tau\alpha) - U_{\mathrm{loss}}\,(T_{\mathrm{abs}} - T_{\mathrm{amb}})] = \dot{m}\ c_p\ \ (T_{\mathrm{out}} - T_{\mathrm{in}})\,, \tag{2.42}$$

where G is the global solar irradiance in the collector plane, $\tau\alpha$ the transmittance-absorptance product, T_{abs} the mean absorber temperature of the solar thermal collector, T_{amb} the ambient temperature, $\dot{m}$ the mass flow rate of the collector fluid, c_p the specific thermal capacity of the collector fluid, T_{out} the outlet and T_{in} the inlet temperature of the collector fluid.

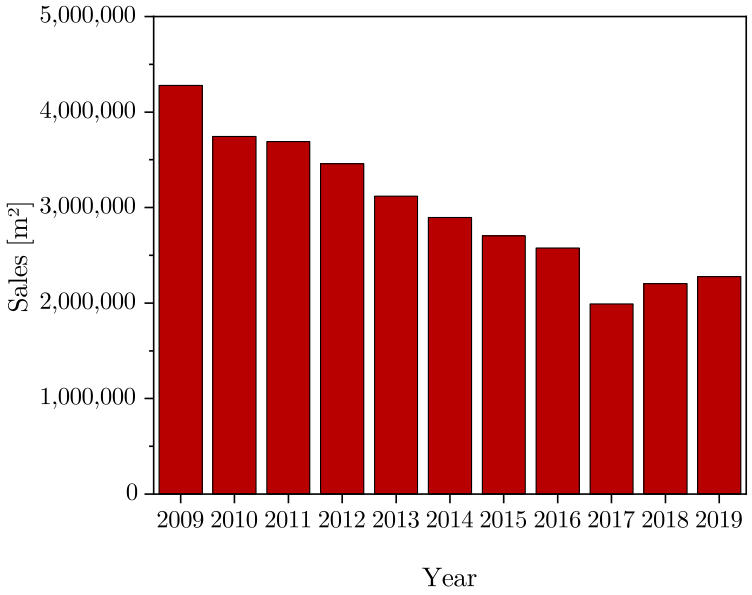

Figure 2.13: Glazed solar thermal collectors sales development of EU-27_2020, United Kingdom and Switzerland from 2009 to 2019 in m^2 collector area. Data from Solar Heat Europe [2019, 2020, 2021].

Regarding the solar thermal market in Europe, sales of glazed solar thermal collectors decreased from 2009 to 2017 by 1 % to 23 % every year (cf. Figure 2.13). Since 2018 the market grows slightly, by 11 % in 2018 and 3 % in 2019. In 2019, the installed stock of solar thermal collectors was around 52.9 million m^2 glazed collector area considering EU-27_2020, United Kingdom and Switzerland [Solar Heat Europe, 2020]. In 2018, FPCs had a market share of 90.2 %[2] for all newly installed liquid-based solar collectors in EU-27_2020, United Kingdom and Switzerland, which emphasize the importance of this solar thermal collector technology for the European market. Consequently, the focus of the investigations on solar thermal collectors within this work is on FPCs. Furthermore, as this work considers solar thermal and heat pump systems with ice storage, WISC collectors are also part of the following investigations as these solar collector types are often used for the heat supply of ice storages in SHP systems. Figure 2.14 shows the main differences in the construction of WISC and FPC collectors. WISC collectors are the simplest types of collectors and are also known as unglazed/uncovered absorbers or collectors. The non-covered black absorbers of WISC collectors are usually made of UV-resistant synthetic material like polyethylene (PE), polypropylene (PP) or ethyl propylene dien monomers (EPDM) [Eicker, 2003]. Due to its

[2]Data for EU-27_2020, United Kingdom and Switzerland calculated from Weiss and Spörk-Dür [2020].

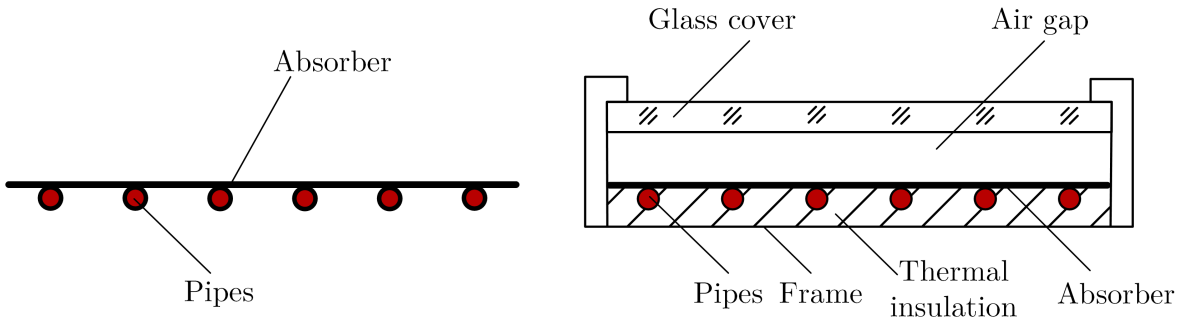

(a) WISC **(b)** FPC

Figure 2.14: Construction of solar collectors.

construction, WISC collectors have especially higher conduction losses than FPC collectors. However, higher conduction losses mean on the other hand higher heat gains in systems with operating temperatures below the ambient air and consequently WISC collectors are often used for applications with ice storages. In contrast, as described above, FPCs are equipped with technologies to limit the heat losses and, thus, are usually used for higher temperature applications like space heating and domestic hot water preparation. As the integration of solar thermal collectors in heating systems depends especially on the auxiliary heating technology and the general system design, the integration of FPCs and WISC collectors in different system concepts is described with special focus on the considered solar thermal and heat pump systems within this work in Section 2.3.1.

2.2.2.2 Photovoltaic Systems

Photovoltaic conversion is the direct conversion of short-wave solar radiation into electricity without any heat engine to interfere [Parida et al., 2011]. Solar cells consist typically of semiconductor materials and its physical principle is the photovoltaic effect. Today, the market is dominated by semiconductor solar cells based on mono- and polycrystalline silicon [Fraunhofer ISE, 2020]. Furthermore, there are also other PV cells on the market or under development like organic material-based, thin film or perovskite solar cells. As the electrical output from a single cell is small, multiple cells are connected and encapsulated (usually in ethylene vinyl acetate (EVA) film with a glass cover) to form a PV module [Kalogirou, 2014]. A number of PV modules can be connected together to a PV string to give the desired electrical power output. As the PV modules produce DC current, an electronic device called inverter is typically used to transform the DC current into AC current. In addition, a maximum power point tracker (MPPT) is used to maximize the solar power generation under varying operating conditions. The inverter, the MPPT, the mounting system of the PV modules, an optional battery storage (usually lithium-ion) with battery charger and inverter (if needed), the wiring and any other elements necessary to build a PV system are called the balance of the system (BOS) [Luque and Hegedus, 2011].

Regarding the PV market in Europe, sales of PV modules decreased after the solar boom of 2011 until 2017 by 4 % to 46 % every year, with the exception of the year 2015 (cf. Figure 2.15). Since 2018 the market regrows, by 35 % in 2018 and 88 % in 2019. In 2019, the installed capacity of PV was around 132 GW considering EU-27_2020, United Kingdom and Switzerland [IRENA, 2021]. Simultaneously, the residential battery storage market in

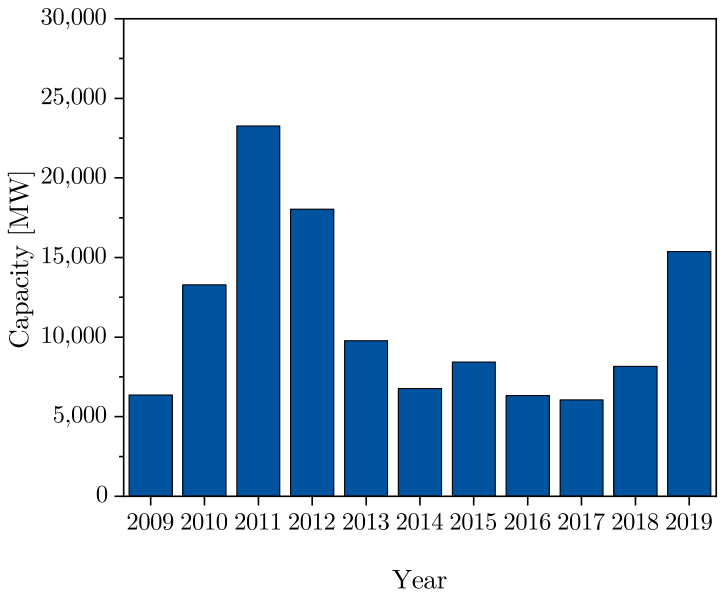

Figure 2.15: PV sales development of EU-27_2020, United Kingdom and Switzerland from 2009 to 2019 in MW newly installed PV capacity. Data from IRENA [2021].

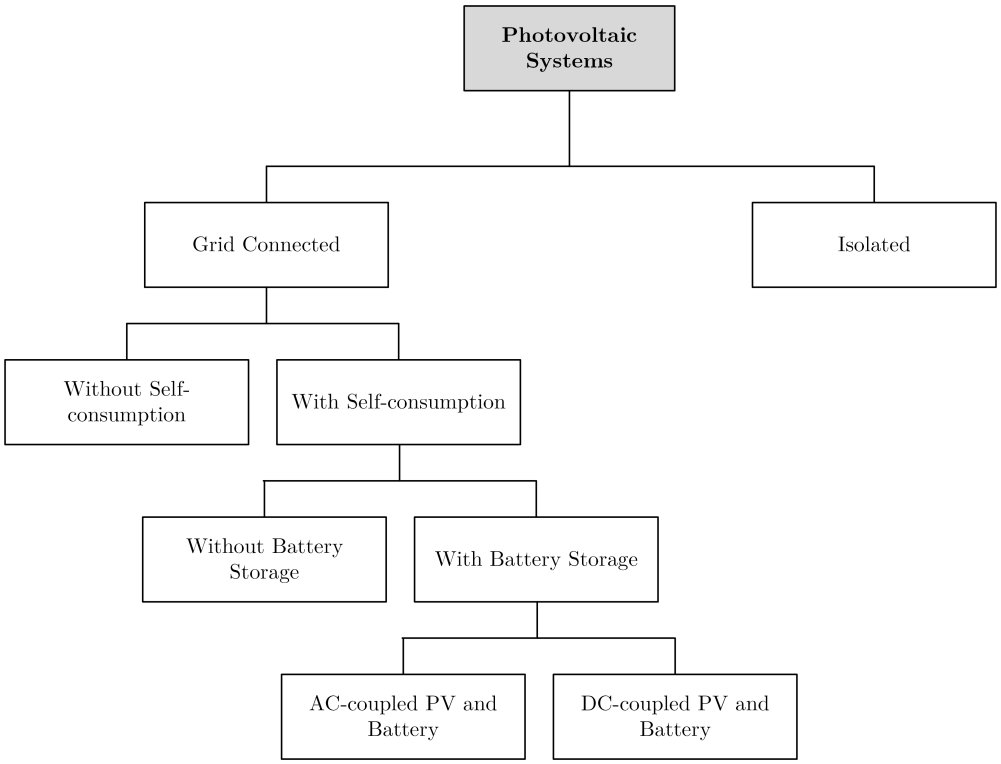

Figure 2.16: Classification of residential PV systems.

Europe grows since 2013. In 2019, the additions grew by 57 % regarding the new installations in MWh, which leads to a total installed residential storage capacity of nearly 2 GWh by the end of 2019 in Europe[3] [SolarPower Europe, 2020].

[3]It is not specified which European countries exactly are included in the data.

As shown in Figure 2.16, PV systems for residential applications can basically be divided in grid connected (on-grid) and isolated (off-grid) systems (not part of this work) [Luque and Hegedus, 2011]. The generated PV electricity in grid connected systems can either be converted to AC current and fed into the grid or used on-site for the electricity supply of the building (self-consumption). PV systems with self-consumption are classified in systems with and without battery storage. Furthermore, PV systems with battery storage can mainly be divided by the connection of the battery in DC-coupled and AC-coupled PV battery systems, as illustrated in Figure 2.17.

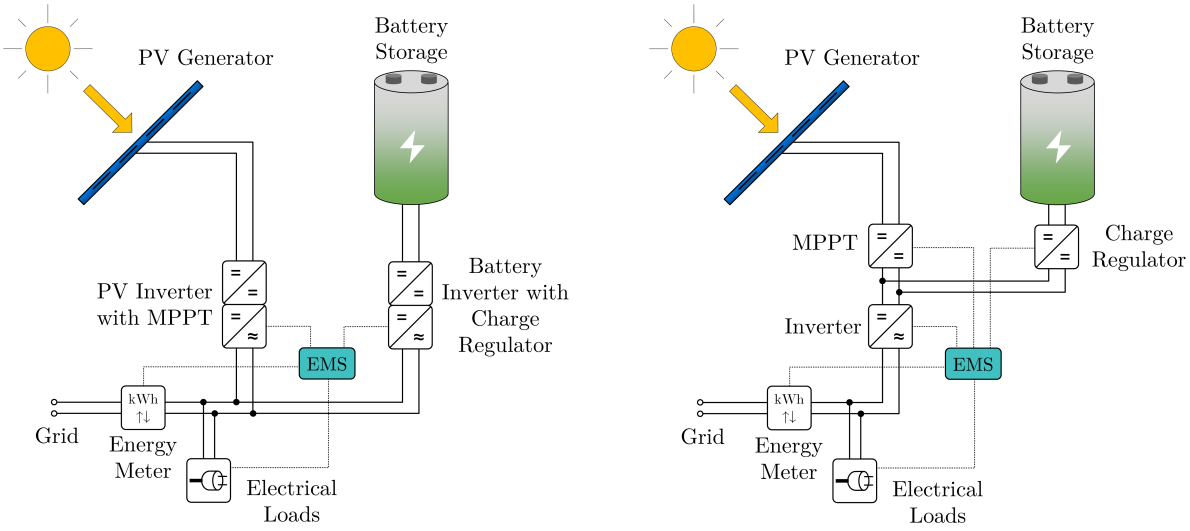

(a) AC-coupled **(b)** DC-coupled

Figure 2.17: AC-coupled and DC-coupled residential PV battery systems with simplified energy metering.

AC-coupled systems consist basically of the PV generator (PV modules), a combined PV inverter with MPPT, the battery storage, a combined battery inverter with charge regulator, an energy management system (EMS), electrical loads and energy meter. AC-coupled battery systems are connected to the AC-bus of the residential building and the PV generator via a bidirectional AC/DC converter. In contrast, within DC-coupled systems, the MPPT and the charge regulator are separated from the inverter and the battery storage is connected to the PV generator on the DC side [Weniger et al., 2014, 2016]. In both system concepts, the main purpose of the EMS is to control the energy flows in the residential PV battery system. The generated PV electricity can be used to charge the battery, supply the electrical loads or it can be fed into the grid. In addition, the battery can be discharged to cover the electrical loads or the energy for the electrical loads can be delivered by the grid. An advantage of DC-coupled systems is that there is no need for a second inverter which leads to a slight reduction of costs and conversion losses. However, DC-coupled systems require a good adjustment of the PV generator and the battery storage size and are less flexible in scaling and retrofitting. As this work considers different types of buildings including retrofitting and different types and scales of systems, the focus of the following investigations is on AC-coupled systems. An overview of the main advantages and disadvantages of AC-coupled and DC-coupled PV battery systems for residential applications is summarized in Table 2.3. The integration of AC-coupled battery systems in SHP system concepts is described in Section 2.3.2 for the considered system combinations within this work.

Table 2.3: Main advantages and disadvantages of AC-coupled and DC-coupled PV battery systems for applications in residential buildings [Graulich et al., 2018].

	Advantages	Disadvantages
AC-coupled	- High flexibility - Easy retrofitting of existing systems - Free scaling of the battery system	- Higher conversion losses - Higher space requirement - Higher investment costs due to second inverter
DC-coupled	- Lower conversion losses - Lower space requirement	- Lower flexibility - Difficult retrofitting of existing systems

2.2.2.3 Photovoltaic-Thermal Systems

PVT collectors are hybrid solutions converting solar energy in both electrical and thermal energy. At present, conventional PV modules convert around 10 % to 20 % of the incident solar radiation into electricity, whereas the remaining part is mainly dissipated into heat to the environment [Lämmle, 2018]. The main objective of PVT collectors is to use this large part of unused solar energy for thermal applications and to improve the utilization of limited roof area on buildings. The thermal coupling of solar thermal absorbers to the PV cells results in a thermal energy harvesting system for PV [Zondag, 2008]. The described operating principle and benefits are also clarified by the utilization of the solar spectrum by a PVT collector, as shown in Figure 2.18. Within this example, the unglazed PVT collector reaches an electrical peak efficiency of 15 % and a thermal peak efficiency of 61 % (at $\vartheta_{amb} = \vartheta_{m,PVT} = 25\,°C$, $G = 1\,000\,W/m^2$ and $u = 0\,m/s$). The remaining part (24 %) are optical and thermal losses [Lämmle, 2018].

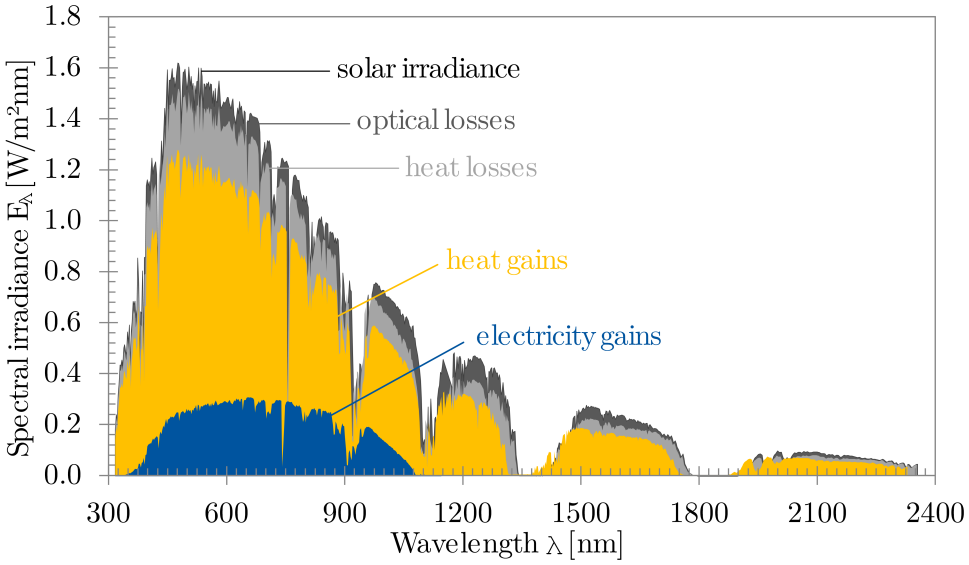

Figure 2.18: Utilization of the solar spectrum (AM1.5g) by an exemplary PVT collector. Adapted from Lämmle [2020b].

In addition, the heat transfer to a fluid leads to a cooling of the PV cells for fluid temperature conditions below the operating temperature of conventional PV modules. As the electrical efficiency of PV cells increases with decreasing cell temperature, cooling the PV

cells leads to an improvement of the electrical performance in PVT collectors [Skoplaki and Palyvos, 2009]. Depending on the PVT type and application, e.g. for the use in SHP systems for residential buildings, the use of PVT collectors can lead to a better utilization of the available roof area and finally an optimized overall solar yield.

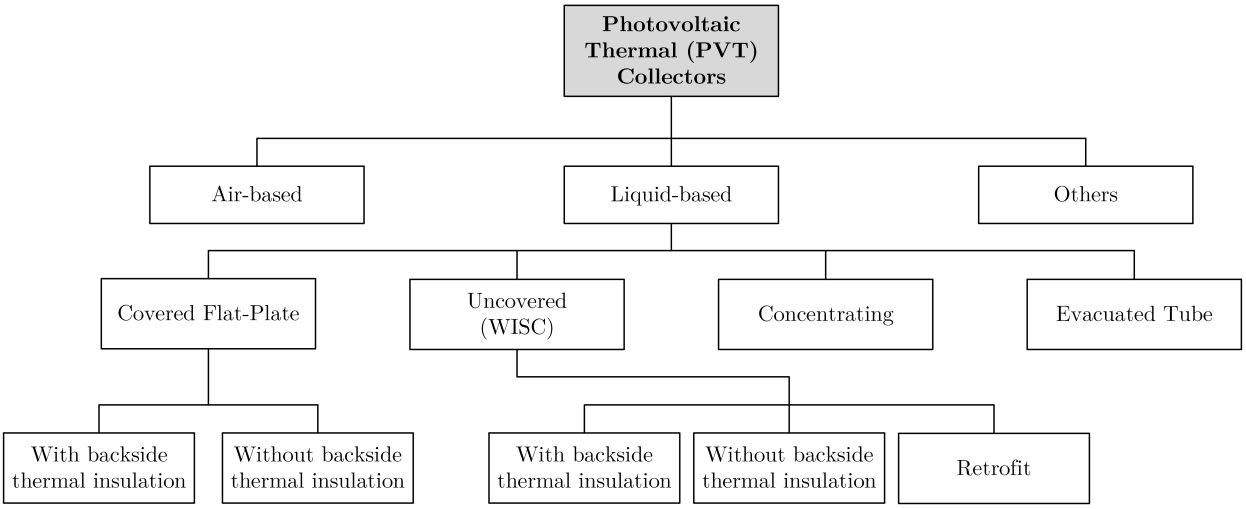

Figure 2.19: Classification of PVT collectors.

The availability of many different types of PVT collectors on the market necessitates a classification of PVT collectors based on the used technological approaches (cf. Figure 2.19). In general, PVT collectors can be classified into liquid-based PVT, air-based PVT or others, like PCM-based PVT, depending on the used heat transfer carrier medium. Regarding the design of the collector with limitation on liquid PVT collectors, PVT collectors are often classified in uncovered (WISC), covered flat-plate, concentrating or evacuated tube PVT collectors. One possibility to further distinguish between special types of WISC PVT collectors is the classification into collectors with or without backside thermal insulation and retrofit PVT collectors. Covered flat-plate PVT collectors can also be further classified into collectors with or without backside thermal insulation. A recent market survey of the IEA SHC Task 60 that represents 26 PVT collector manufacturers and system suppliers in 11 countries showed that the majority of PVT collector types on the market, especially in Europe, are liquid PVT collectors. The highest shares were achieved by WISC PVT collectors with 48 % and covered flat-plate PVT collectors with 28 % of the considered PVT collectors [Ramschak, 2020]. By the end of 2019, the total installed PVT collector area in Europe was around 675 000 m^2 (including air-based PVT)[4]. At this, the market share was 91.5 % for WISC PVT collectors and 8.3 % for covered flat-plate PVT collectors on all installed liquid-based non-concentrating PVT collectors. The small remaining proportion were evacuated tube PVT collectors.

Figure 2.20 shows the construction of a WISC PVT collector without backside thermal insulation and a covered flat-plate PVT collector with backside thermal insulation. WISC PVT collectors consist typically of a PV module (PV cells and glass cover) coupled to a heat exchanger (absorber and pipes) on the backside of the PV module and a collector frame. Some manufacturers offer heat exchangers for retrofitting of conventional PV modules to a

[4]Data for Austria, Belgium, Denmark, France, Germany, Hungary, Italy, Luxembourg, Macedonia, Netherlands, Norway, Portugal, Spain, Sweden, Switzerland and United Kingdom calculated from Weiss and Spörk-Dür [2020].

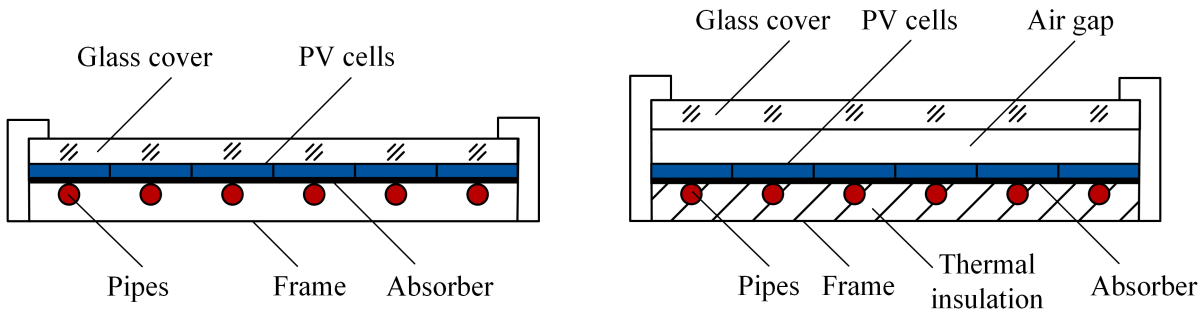

(a) WISC (uncovered) **(b)** Covered flat-plate

Figure 2.20: Construction of a WISC (uncovered) PVT collector without backside thermal insulation and a covered flat-plate PVT collector with backside thermal insulation.

retrofit PVT collector with a similar construction. At this, as for PVT collectors in general, it is essential to ensure a good and longtime thermal contact with high heat transfer coefficient between the fluid and the PV cell [Lämmle et al., 2020]. As WISC PVT collectors can only be thermally insulated at the backside of the collector, the heat losses are relatively high even for collectors with backside thermal insulation. Hence, the application of WISC PVT collectors is rather limited to low temperature systems [Lämmle, 2018]. Due to its lower operating temperatures, WISC PVT collectors are especially used on the source side of a heat pump in SHP systems or as swimming pool heating, similar to WISC solar thermal collectors. Moreover, some WISC PVT collectors provide an increased heat transfer to the ambient air for the operation as heat source of heat pumps. In contrast, covered flat-

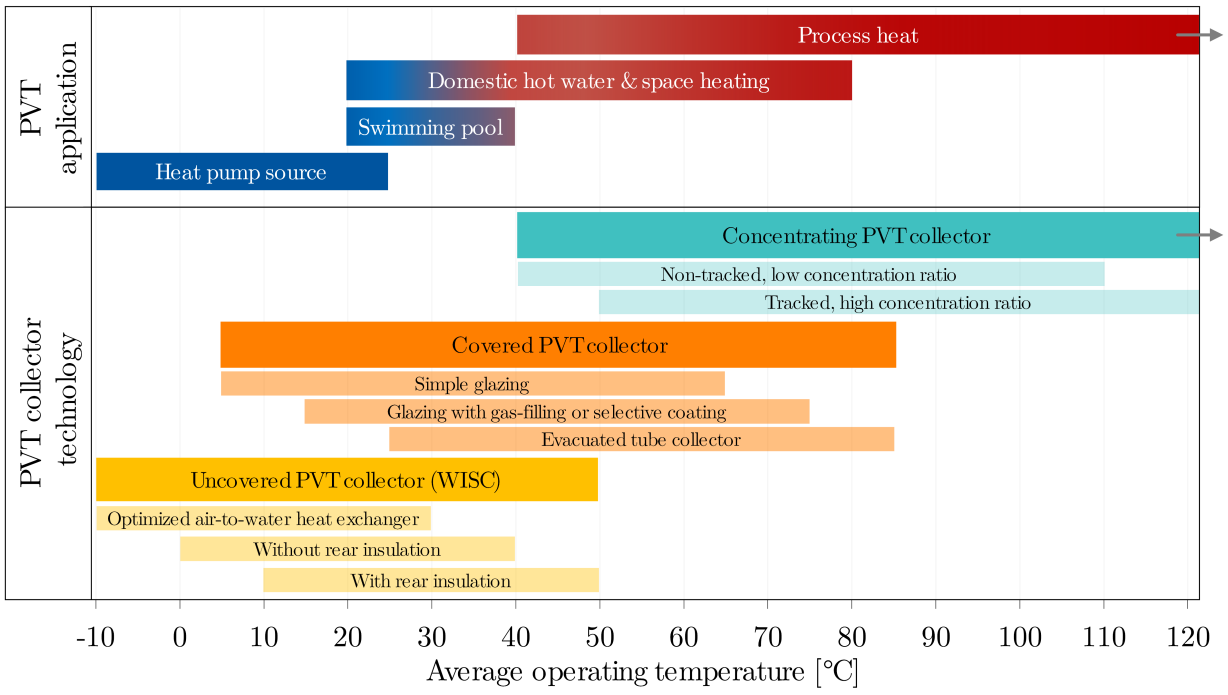

Figure 2.21: Operating temperatures and applications for different PVT collector technologies. Adapted from Lämmle [2020a].

plate PVT collectors are typically equipped with an additional insulating air layer (air gap) between the PV cells and the glass cover and a backside thermal insulation to limit the heat losses, similar to flat-plate solar thermal collectors. In addition, some covered flat-plate PVT collectors use anti-reflective coatings on the glass cover to reduce additional optical losses by the front glazing. As a result, covered flat-plate PVT collectors can reach higher operating temperatures than WISC PVT collectors and are also used for higher temperature applications like space heating and domestic hot water preparation [Lämmle et al., 2020]. A summary of the operating temperatures and applications of PVT collectors is given by Figure 2.21. Regarding the described characteristics, its high market relevance and its typical applications, the investigations in this work focus on WISC PVT collectors used on the heat source side of heat pumps and covered flat-plate PVT collectors used for the direct supply of space heating and domestic hot water systems as well as their comparison for the mentioned applications. Their integration in the different SHP system concepts considered within this work is described in Section 2.3.3.

2.3 Solar and Heat Pump Systems

A general classification of SHP systems for the energy supply of residential buildings based on solar energy conversion in thermal and electrical energy is presented in Figure 2.22. The notion *SHP system* comprises basically all combinations of heat pumps and solar energy systems, including PV (electrical energy) and solar thermal energy systems as well as hybrid or combined PV and solar thermal energy technologies. As cooling of buildings is not part of this work, solar cooling technologies are not considered in the classification. Within the mentioned system combinations, solar thermal systems are used to deliver heat (directly or on the source side of the heat pump) to the system while PV systems provide electricity to the system or building (household electricity). The heat pump is used to supply the space heating and/or the domestic hot water system (or a thermal storage) with heat. With regard to the solar energy conversion, SHP systems can be subdivided more precisely in *solar thermal and heat pump* systems (Section 2.3.1), *photovoltaic and heat pump* systems (Section 2.3.2) or *photovoltaic, solar thermal and heat pump* systems (Section 2.3.3) as thermal and electrical hybrid energy systems. At this, photovoltaic, solar thermal and heat pump systems can further be divided in *photovoltaic plus solar thermal and heat pump* systems and *photovoltaic-thermal and heat pump* systems to indicate whether the system includes only separated PV and solar thermal or hybrid PVT technologies. The following sections go on to describe SHP system concepts (with particular regard to the analyzed concepts in this work), their classifications and the state of the art for the different combinations of solar energy and heat pumps.

Due to the increasing complexity of SHP system concepts, especially within combined thermal and electrical energy systems, it is important to define a procedure to describe the composition of a SHP system and the interaction of different system components within this system concept. One possibility to describe the interaction within a SHP system is the use of block diagrams (also called *square views*) for the visualization of energy flows between the different system components as developed in IEA SHC Task 44 / HPP Annex 38 with limitation on solar thermal and heat pump systems [Frank et al., 2010; Hadorn, 2015]. In contrast, the developed approach within this work, which will be presented in the following, can be used for thermal as well as electrical system concepts, and especially the interaction of thermal and electrical parts in SHP concepts.

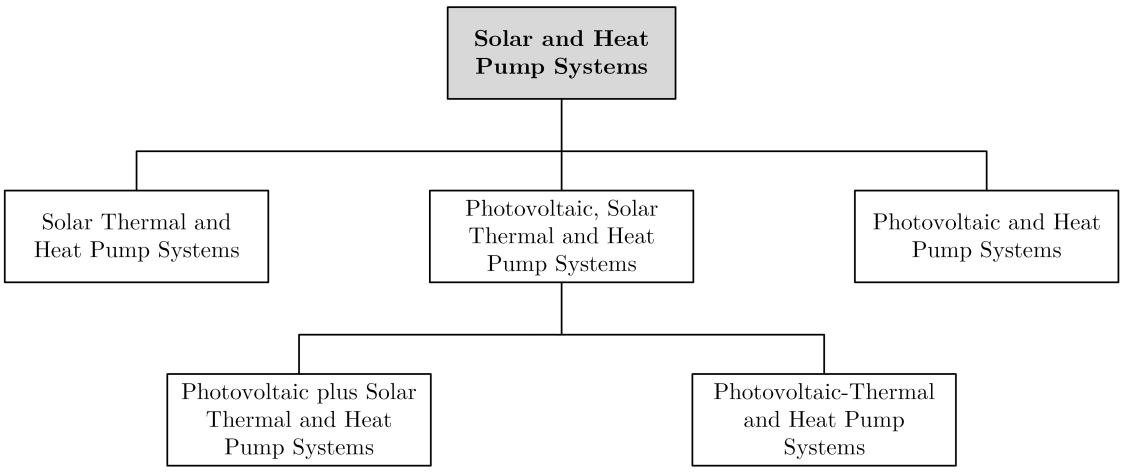

Figure 2.22: Classification of SHP systems.

The main advantage of this method is the simple and structured way to describe the functionality of a system and the interaction of its components, especially with regard to their energy flows. It allows a better comparability and fast understanding of a whole system and avoids misunderstanding of functionality. Furthermore, system developers / manufacturers can easily describe their new products and make them comparable with existing solutions and customers or engineers can identify system features and applications at a glance. Especially in complex thermal and electrical systems like SHP systems, the method shows the level of system integration of the solar energy components and whether it is part of a whole system approach or a side-by-side installation to a heat pump system without high level of integration. In addition, the method offers a possibility to define detailed system and component boundaries for the definition of KPIs that is also an important aspect to increase the comparability of systems and its analyses. The method had also been used for the representation of PVT systems within IEA SHC Task 60 and was published in Jonas [2019b].

Basically, this approach is based on the work of Frank et al. [2010] and IEA SHC Task 44 / HPP Annex 38 for solar thermal and heat pump system concepts and can be seen as an enhancement for electrical systems which were not part of the original concept. The visualization is very similar to other energy flow charts, but with fixed boundaries, positions and colors as well as defined connection line styles. In general, the system boundaries like final energy which has to be purchased, useful energy like space heating or environmental energy sources like the sun as well as different system components like a heat pump, solar collectors, PV, PVT or a storage are shown at given places and are highlighted with given colors if they exist in the system concept (cf. Figure 2.23 and Figure 2.24).

For the system components, the following given elements are defined and can be highlighted if they exist in the concept:

(1) Solar energy converters like solar thermal collectors or absorbers, PV or PVT

(2) Thermal storage on the source side of the heat pump

(3) Heat pump

(4) Backup heater like conventional boiler or heating rod

(5) Thermal storage on the sink side of the heat pump

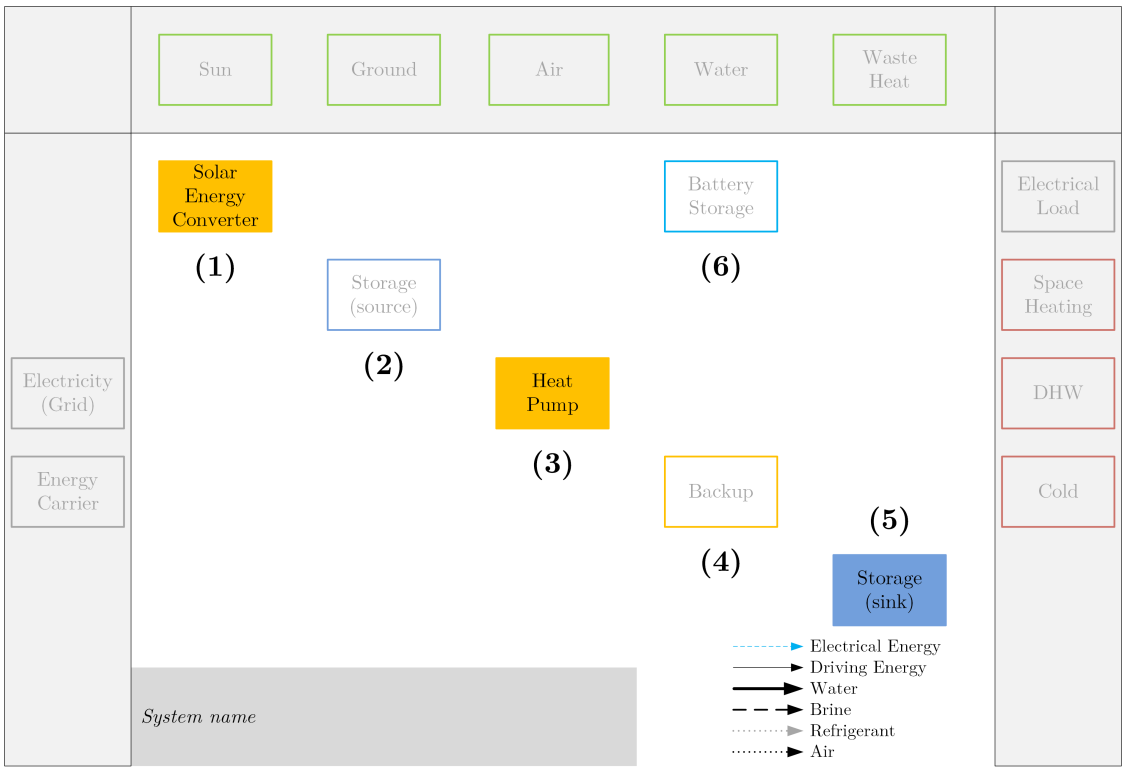

Figure 2.23: Visualization of energy flows in SHP systems. Block diagram with highlighted system components.

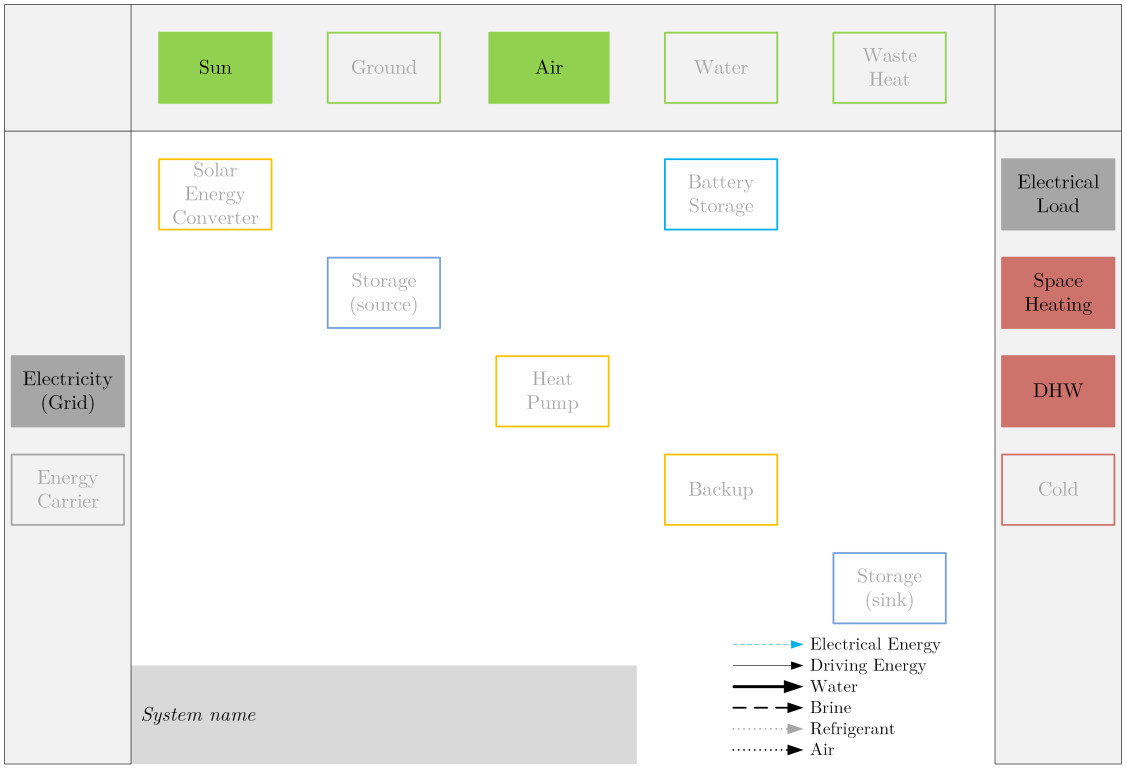

Figure 2.24: Visualization of energy flows in SHP systems. Block diagram with highlighted system boundaries.

(6) Electrical (battery) storage.

All of these components are displayed via placeholders. If a component is not used, it is also shown but without highlighting (cf. Figure 2.23). A second solar energy converter can be placed to the right of the first solar energy converters placeholder if needed, e.g. in PV plus solar thermal and heat pump systems (cf. Section 2.3.3). Furthermore, three different system boundaries are defined:

- Left boundary: *final energy*, which has to be purchased, e.g. gas or electricity (grid)
- Right boundary: *useful energy*, e.g. for domestic hot water preparation or space heating, and (final) *electrical energy consumption/load* (except the electrical energy consumption of the system), e.g. residential electricity load for lighting and appliances
- Upper boundary: *environmental energy sources*, e.g. sun, ambient air or ground.

Within the system boundaries, the different elements are also highlighted if they exist / are used in the concept (cf. Figure 2.24). To further differentiate system components and boundaries, the following colors are used:

- Energy converters: orange
- Thermal storages: blue
- Electrical storages: light blue (color also used for electrical energy flows)
- Final energy: grey
- Environmental energy: green
- Useful energy: red.

The system components are connected among themselves and with the boundaries via lines to depict the energy flows in the system. As shown in Figure 2.25, six different line styles are used for the indication of:

- different energy carrier media (water, brine, refrigerant or air),
- electrical energy or
- other driving energies (e.g. solar irradiation or gas).

For the complete description of a system concept with the presented block diagram approach, the following steps need to be performed:

1. Highlighting of existing system components
2. Highlighting of used environmental energy sources
3. Highlighting of final energy which has to be purchased
4. Highlighting of existing electrical energy consumptions and useful energy demands
5. Connection of the components of the system among themselves and with the boundaries with indication of the carrier medium / driving energy.

In the following sections, the presented system visualization approach is used to describe the different SHP system concepts considered in this work.

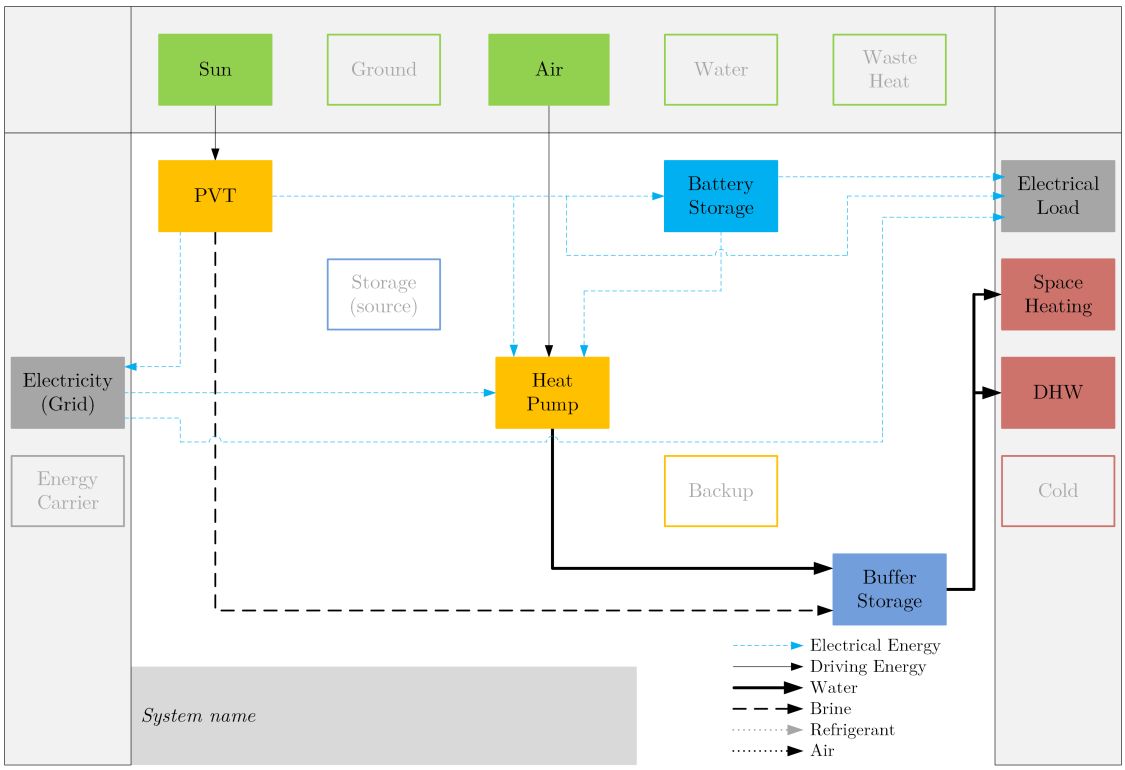

Figure 2.25: Visualization of energy flows in SHP systems. Block diagram with connections.

2.3.1 Solar Thermal and Heat Pump Systems

The combination of solar thermal systems and heat pumps focus on the efficient energy supply for space heating and domestic hot water preparation in buildings. The earliest published research work on the combination of *solar thermal and heat pump* systems started in 1955 by Sporn and Ambrose [1955]. The first research work with use of classification in series (serial) and parallel systems was carried out by Freeman et al. [1979] in 1979. During the past decade, a wide range of these hybrid heating systems entered the market. Depending on the heat source of the heat pump, solar thermal and heat pump systems can be divided in *solar thermal and ground source heat pump* (SGSHP) systems, *solar thermal and air source heat pump* (SASHP) systems, *solar thermal and ice storage source heat pump* (SISHP) systems and others, like solar thermal and water source heat pump systems, solar thermal and waste heat source heat pump systems or direct expansion solar-assisted heat pump systems. Independently of the heat source of the heat pump, the systems can be classified in *parallel*, *serial* and *regenerative* system concepts by the interaction between solar thermal system and heat pump (Figure 2.26) [Frank et al., 2010].

Parallel systems (Figure 2.26a) are systems with independent supply of useful energy for space heating and/or domestic hot water preparation by solar thermal system and heat pump, e.g. via a buffer storage tank. Serial systems (Figure 2.26b) are systems in which the solar thermal system is used as heat source for the heat pump. In these concepts the solar thermal system can either be used exclusively or as additional source and either directly or via a storage tank. Regenerative system concepts (Figure 2.26c) are systems in which the solar thermal system is used for the regeneration of the main source of the heat pump, usually the ground. Furthermore, there is the possibility to combine these system concepts

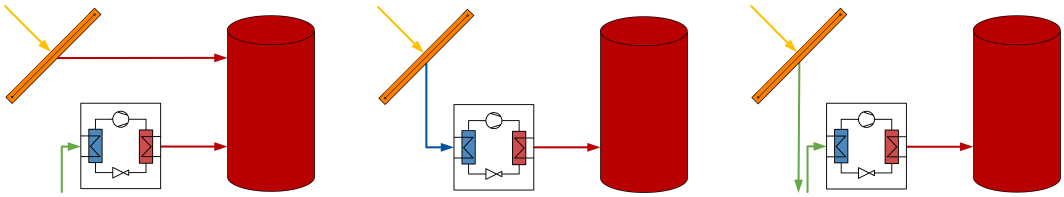

(a) Parallel **(b)** Serial **(c)** Regenerative

Figure 2.26: Overview of solar thermal and heat pump system concepts independently of the heat source.

[Frank et al., 2010; Hadorn, 2015]. The classification in parallel, serial and regenerative system concepts (or combinations) can be indicated with -P, -S and -R at the end of the abbreviation of the general solar thermal and heat pump system concept. For example, SGSHP-P means parallel combined solar thermal and ground source heat pump systems. The classification of solar thermal and heat pump systems based on the heat source and the integration of the solar thermal system is shown in Figure 2.27. All possible integrations of solar thermal systems (and their combinations) within SGSHP, SASHP and SISHP system concepts are illustrated in Table 2.4.

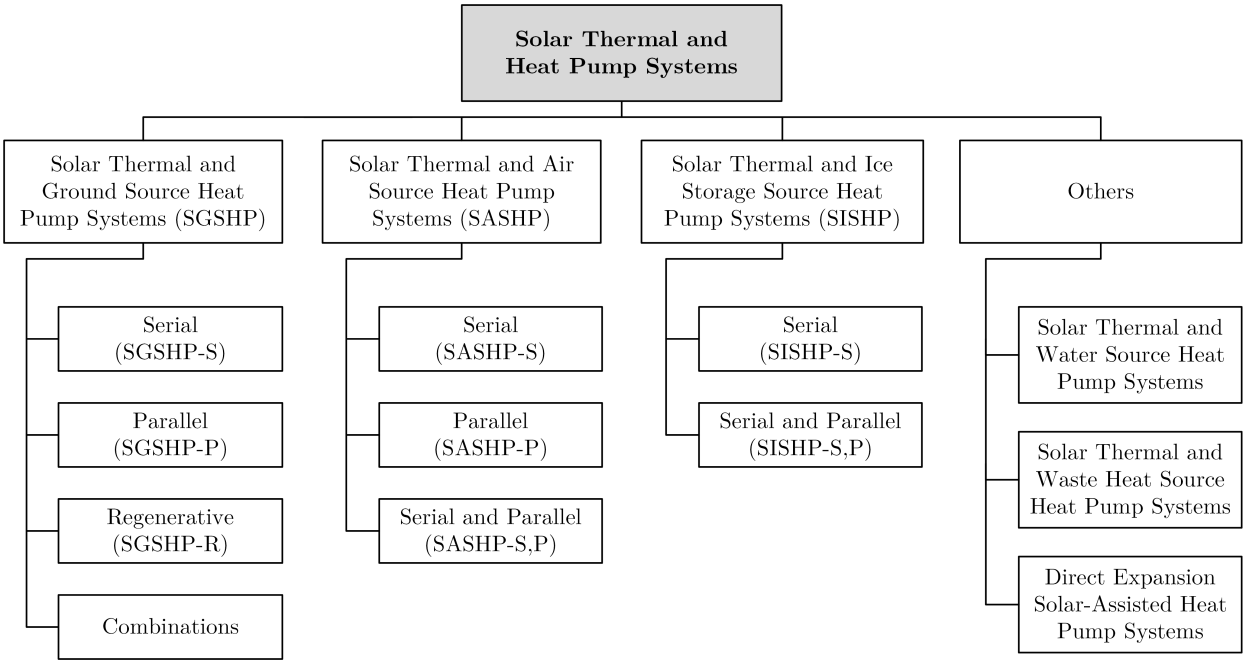

Figure 2.27: Classification of solar thermal and heat pump systems.

Table 2.4: Possible combinations of solar thermal and ground, air or ice storage source heat pump systems.

	-S	-P	-R	-S,P	-S,R	-P,R	-S,P,R
SGSHP	x	x	x	x	x	x	x
SASHP	x	x	-	x	-	-	-
SISHP	x	-	-	x	-	-	-

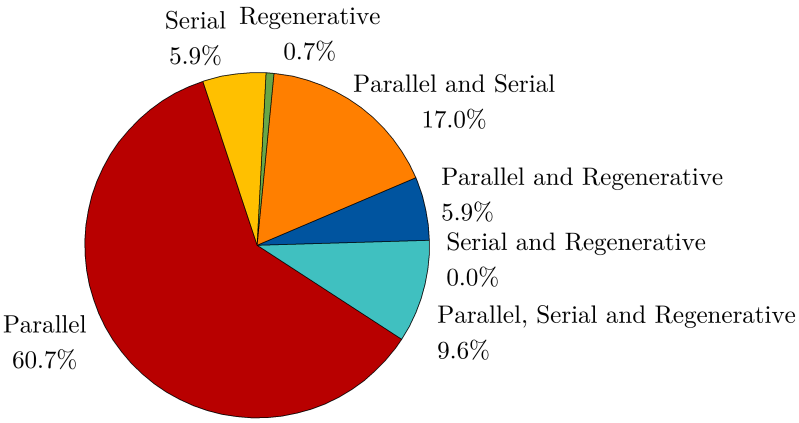

Figure 2.28: Market available system concepts by concept surveyed in 2013 by Ruschenburg et al. [2013].

A statistical analysis on market-available solar thermal and heat pump systems can be found in Hadorn [2015] and Ruschenburg et al. [2013]. As a main result, parallel systems were identified as the market-dominating system concepts with a share of around 61 % on the market available system concepts (cf. Figure 2.28) [Ruschenburg et al., 2013]. Haller et al. [2014a] compared simulation results for the performance of different system concepts, especially for a renovated building in moderate climate (Strasbourg), and identified some general findings on the direct use of solar heat in parallel solar thermal and heat pump systems:

- The main benefit of direct use of solar heat in solar thermal and heat pump systems compared to systems without use of solar energy is the increase of the performance of the overall system and thus electrical energy savings.
- The increase of the performance and the electrical energy savings mainly depends on the type of heat pump, the type and area of solar thermal collectors and the boundary conditions, especially climate and heat load.

In Hadorn [2015] the reason for the significant increase of the performance by the direct use of solar heat in SHP systems was explained by the fact that solar thermal collectors can cover a part of the heating demand with much higher ratio of heat delivered to consumed electricity (e.g. for pumps and controller) than the heat pump. Regarding the integration of solar thermal collectors in conventional heating systems, the solar collector yield and also the fuel savings decreased with increasing temperatures of the heat demand. In contrast, in SHP systems the electricity savings compared with a heat pump system without solar thermal collectors increased with increasing temperatures of the heat demand. The reason

for this is that the reduction of performance of the heat pump by increasing temperatures is higher than the reduction of solar yields.

Carbonell et al. [2014a] analyzed the influence of direct use of solar heat in GSHP and ASHP systems for different types of buildings and climates by simulation. The performance of the overall SHP system increased for both system concepts, ASHP and GSHP, by adding solar thermal collectors. In GSHP systems, the performance of the heat pump itself increased also by adding a solar thermal system due to the covering of domestic hot water loads with high temperatures and low heat pump performance by solar energy. In contrast, in most systems with ASHP, the performance of the heat pump itself decreased in comparison with ASHP systems without solar thermal collectors. On the one hand, the solar thermal system covered a part of domestic hot water loads and the ASHP worked less time with high heat sink temperatures. On the other hand, the performance of the heat pump decreased as a consequence of the covering of heat loads at times with moderately high ambient temperatures and best performance of the ASHP system, e.g. in spring, by solar energy. The decreasing effect for the ASHP performance in these periods usually dominated in comparison with the effect of increasing performance in periods with covering of high temperature demands for domestic hot water preparation by solar energy and thus the performance of the heat pump itself decreased in comparison with ASHP systems without direct use of solar energy [Carbonell et al., 2014b]. In terms of absolute electricity savings, the benefit of adding solar thermal collectors to a heat pump system increased with the electricity consumption of the reference system without solar thermal system. Therefore, ASHP systems have sometimes higher potential of electricity savings by the direct use of solar heat compared to GSHP systems [Carbonell et al., 2014a]. Nevertheless, it should be noted that the authors used different heat pumps with different performance data and efficiency in case of resizing the systems for different locations and buildings. By contrast, Poppi et al. [2016] analyzed the influence of component size on electricity demand for ASHP and GSHP systems combined with solar thermal collectors with limitation on renovated and non-renovated buildings and the climates of Zurich and Carcassonne by the use of scale factors. Regarding the influence of the collector area, the authors observed that the absolute electricity savings by adding solar thermal collectors are higher for ASHP than GSHP systems and increase with increasing collector area which is consistent to the results of Carbonell et al. [2014a].

Regarding GSHP systems with use of solar heat for regeneration of the ground heat source, especially the work of Kjellsson [2009] and Bertram [2015] should be mentioned. Kjellsson [2009] studied the combination of flat-plate solar thermal collectors with GSHPs, whereas Bertram [2015] concentrated on the integration of uncovered solar thermal collectors in heat pump systems with vertical ground heat exchanger. Both came to the conclusion that boreholes can be recharged by the solar thermal collectors, especially if neighboring boreholes are thermally influencing each other. Depending on the system, the combination also allows a ground heat exchanger shortening and to improve the performance of undersized systems. In case of FPCs, the optimal design in a new system is to use solar heat directly for domestic hot water preparation in summer and for recharging the borehole in winter periods [Kjellsson, 2009]. At this, it is important to mention that the possibility to use the solar heat directly (or via buffer storage) for space heating was not considered. Furthermore, Hadorn [2015] observed that regeneration of single boreholes has little effect on the long-term temperature level of the heat source if the boreholes are dimensioned appropriately and gave the recommendation to use solar heat first directly and only excess heat or low exergy heat (when the temperature for direct heat use cannot be reached) should be used for regeneration.

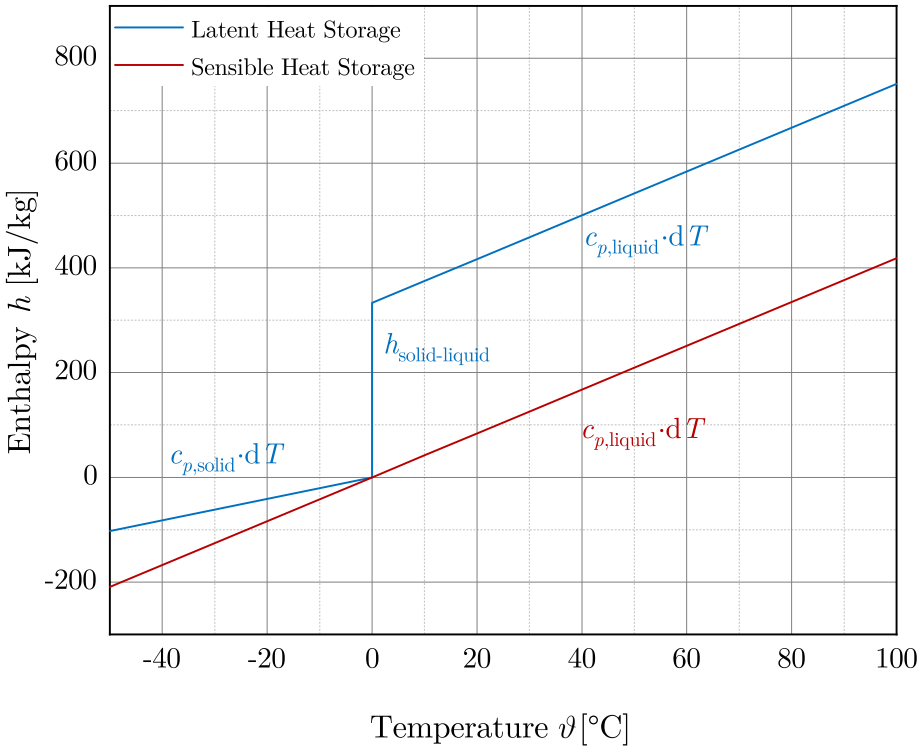

Figure 2.29: Temperature-enthalpy diagram for a sensible and a latent heat storage with the same specific heat capacity for the liquid phase. Physical properties of water are used to generate the diagram.

The combination of solar thermal system, heat pump and ice storage is usually realized as serial system concept. Within these concepts, the ice storage is used as heat source of the heat pump and is supplied with heat by the solar thermal system. In general, an ice storage is a latent heat storage that use the phase change from solid to liquid and vice versa to store and extract energy. In contrast to sensible storages of liquids like water that use only the heat capacity of the liquid ($c_{p,\text{liquid}} \cdot \mathrm{d}T$) to store energy by changing the temperature of the storage, latent heat storages like ice storages use additionally the melting enthalpy ($h_{\text{solid}-\text{liquid}}$) and partially the heat capacity of the solid ($c_{p,\text{solid}} \cdot \mathrm{d}T$) if supercooling is used to store energy (cf. Figure 2.29). As a result, the heat storage capacity of a latent heat storage with use of phase change is higher than the heat storage capacity of a sensible heat storage of a liquid with the same specific liquid heat capacity operated in the same temperature range. As the temperature does not change during the phase change of water from liquid to solid, the ice storage allows relatively constant source temperatures for a heat pump around the melting temperature of water during the freezing process if it is used in a SISHP system. In SISHP systems, the freezing is basically counteracted by energy supply of solar thermal collectors. Furthermore, ice storages (especially with high volumes) are often buried in the ground without thermal insulation and thus benefit from the ambient energy of the surrounding ground when the storage temperature is lower than the ground temperature. Due to the low temperatures of the ice storage, WISC collectors are often used for the energy supply of the ice storage as they can also be used at lower ambient temperatures with low or without solar irradiance due to their high heat gains from the ambient if the operating temperature is below the ambient temperature. During summer, the ice in the storage is usually completely melted and the storage is operated as sensible heat storage on the heat

source side of the heat pump. Furthermore, ice storages are often used as seasonal storages for solar thermal energy and ambient heat if the storage volume is adequately dimensioned [Winteler et al., 2014]. Trinkl [2006] and Faßnacht [2015] investigated the combination of solar thermal and heat pump systems with ice storage on the source side of the heat pump. Both works offered optimizations of the specific SISHP system concepts and special topics like control strategy or component development but no comparisons with other solar thermal and heat pump system concepts. Regarding the results of different simulations of solar thermal and heat pump system concepts within the IEA SHC Task 44 / HPP Annex 38, Haller et al. [2014a] came to the conclusion that solar only concepts have the advantage that no ventilated air source evaporators or ground heat exchangers are needed and that the systems can achieve similar performance as ASHP systems with direct use of solar heat or GSHP systems without solar thermal collectors. Similar results with focus on a renovated building in moderate climate were obtained in Lerch et al. [2015] comparing different solar only concepts with ASHP systems.

Due to its market dominance, the following investigations regarding the combination of solar thermal energy technologies and ground source or air source heat pump systems are restricted to parallel system concepts with FPCs. Ground regeneration is not considered as it is more beneficial if the system is not well designed (undersized boreholes) or a special attention has to be paid to shortening of the ground heat exchanger. Furthermore, this work considers solar only concepts with ice storages as alternative to system concepts with ground or air source heat pumps. To sum up, in addition to ASHP and GSHP systems and with regard to the thermal combination of solar and heat pump systems, the investigations in this work will focus mainly on the following system concepts:

a. Parallel solar thermal and ground source heat pump systems (SGSHP-P)

b. Parallel solar thermal and air source heat pump systems (SASHP-P)

c. Serial solar thermal and ice storage source heat pump systems (SISHP-S)

d. Serial solar thermal and ice storage source heat pump systems with additional parallel solar thermal collectors (SISHP-S,P).

The concept of the investigated solar thermal and heat pump systems with parallel solar thermal collector integration in this work, regardless of the used heat source, is shown in Figure 2.30. The system consists essentially of a heat pump system as described in Section 2.2.1.3 and an additional parallel solar thermal circuit that uses frost protected brine as heat transfer medium. The solar thermal circuit comprises solar thermal collectors and additional hydraulic components (pump, pipes). The solar thermal collectors are used to supply the buffer storage directly with solar thermal energy via an internal heat exchanger in the lower zone of the storage depending on the current solar thermal collector outlet temperature and the buffer storage temperature. If the outlet temperature is high enough and additional control conditions are reached, the solar circuit pump (P4) is switched on and the internal heat exchanger is supplied with solar thermal energy. This system concept with combi-storage for heating and domestic hot water preparation is based on typical market available systems and storage concepts presented and analyzed by Poppi and Bales [2014] and Haller et al. [2014b].

The considered SGSHP-P system in this work is shown in Figure 2.31a and consists of the described parallel system concept with GSHP. The SASHP-P system corresponds to the

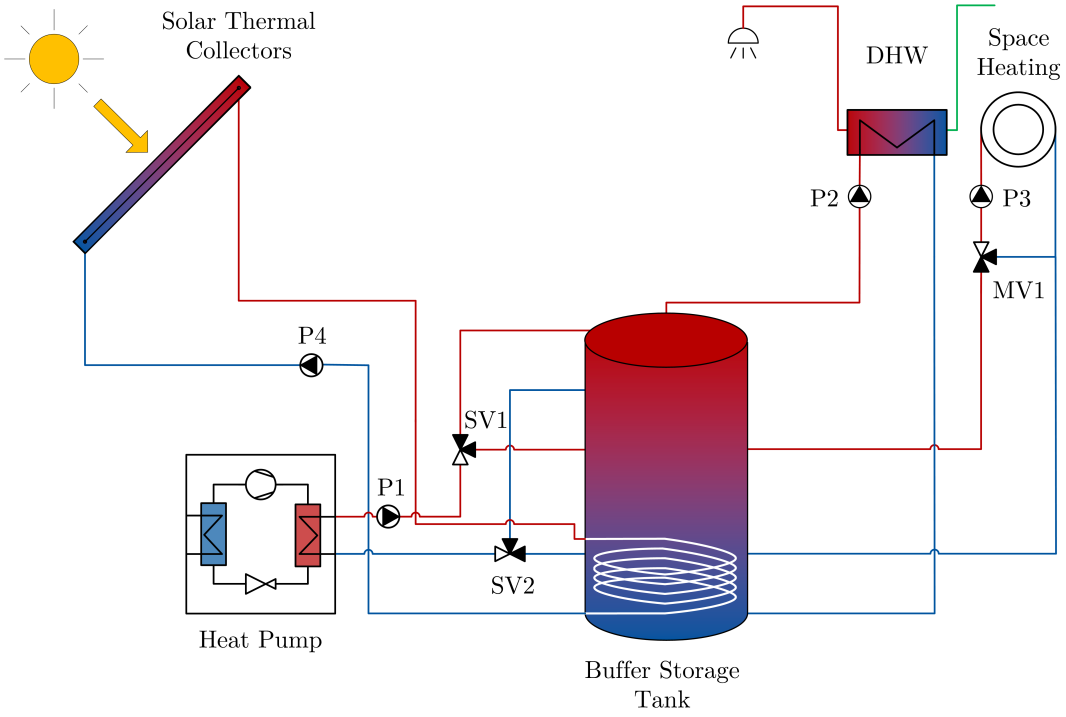

Figure 2.30: Hydraulic scheme of the solar thermal and heat pump heating system independent of the used heat source.

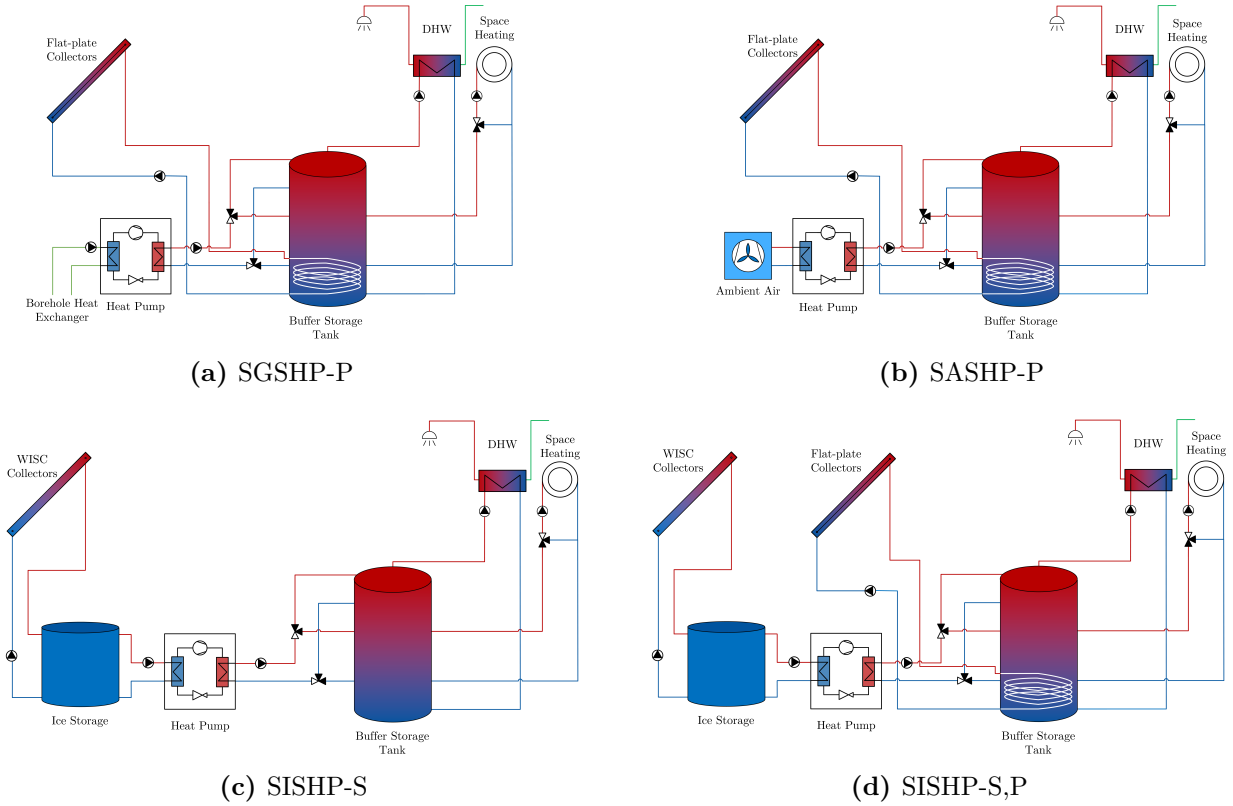

(a) SGSHP-P **(b)** SASHP-P

(c) SISHP-S **(d)** SISHP-S,P

Figure 2.31: Hydraulic schemes of the considered solar thermal and heat pump systems.

SGSHP-P system with a replacement of the GSHP by an ASHP and is shown in Figure 2.31b. At this, FPCs are used for the direct supply with solar thermal energy in both system concepts. The SISHP-S system corresponds to the GSHP system with a replacement of the heat source circuit with BHE by a heat source circuit with ice storage and solar thermal collectors in addition to the brine/water heat pump and heat sink circuit of the heat pump (cf. Figure 2.31c). The heat source circuit comprises the solar thermal source circuit, the ice storage and additional hydraulic components (pumps, pipes). WISC collectors are used to supply the ice storage with solar thermal energy if the outlet temperature of the WISC collectors is high enough and additional control conditions are reached using the solar source circuit pump. The ice storage is used as heat source of the heat pump and the heat source circulation pump to the heat pump is switched on when the heat pump is operated. The SISHP-S,P concept corresponds to the SISHP-S system with additional parallel solar thermal circuit using FPCs for the direct supply of the buffer storage tank via internal heat exchanger (cf. Figure 2.31d). Visualizations of the energy flows in the different system concepts are given in Figure 2.32, Figure 2.33, Figure 2.34 and Figure 2.35.

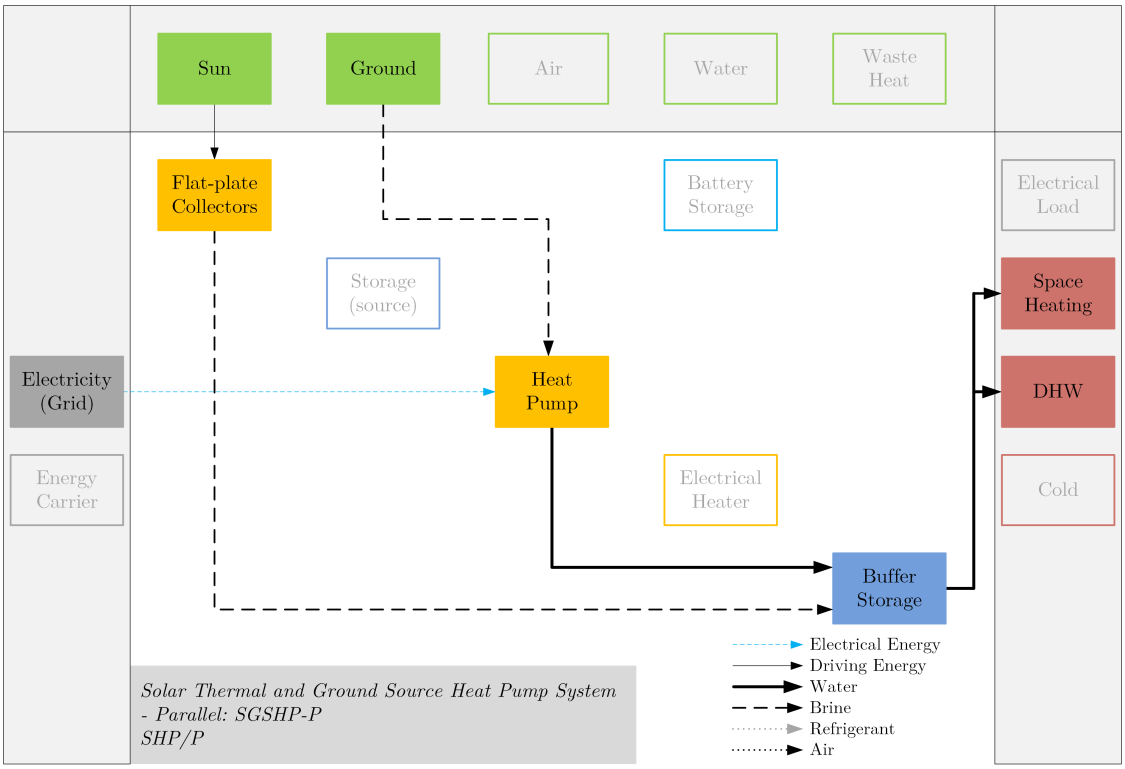

Figure 2.32: Visualization of energy flows in the considered SGSHP-P system.

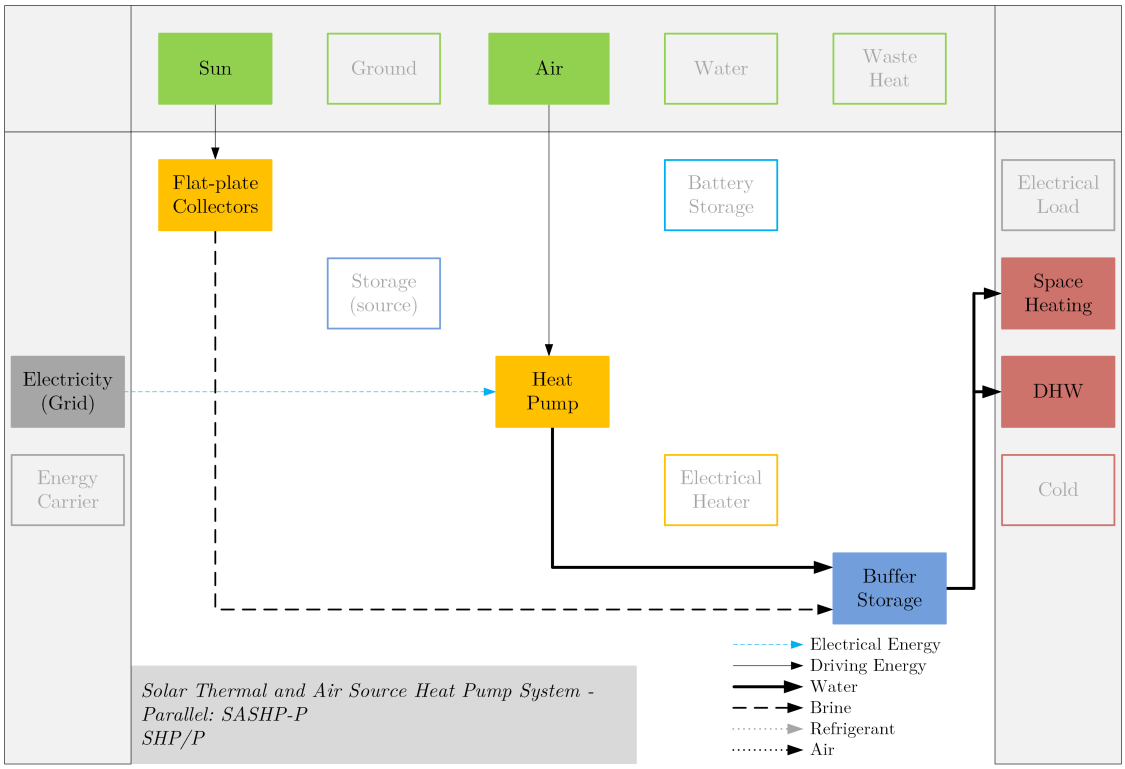

Figure 2.33: Visualization of energy flows in the considered SASHP-P system.

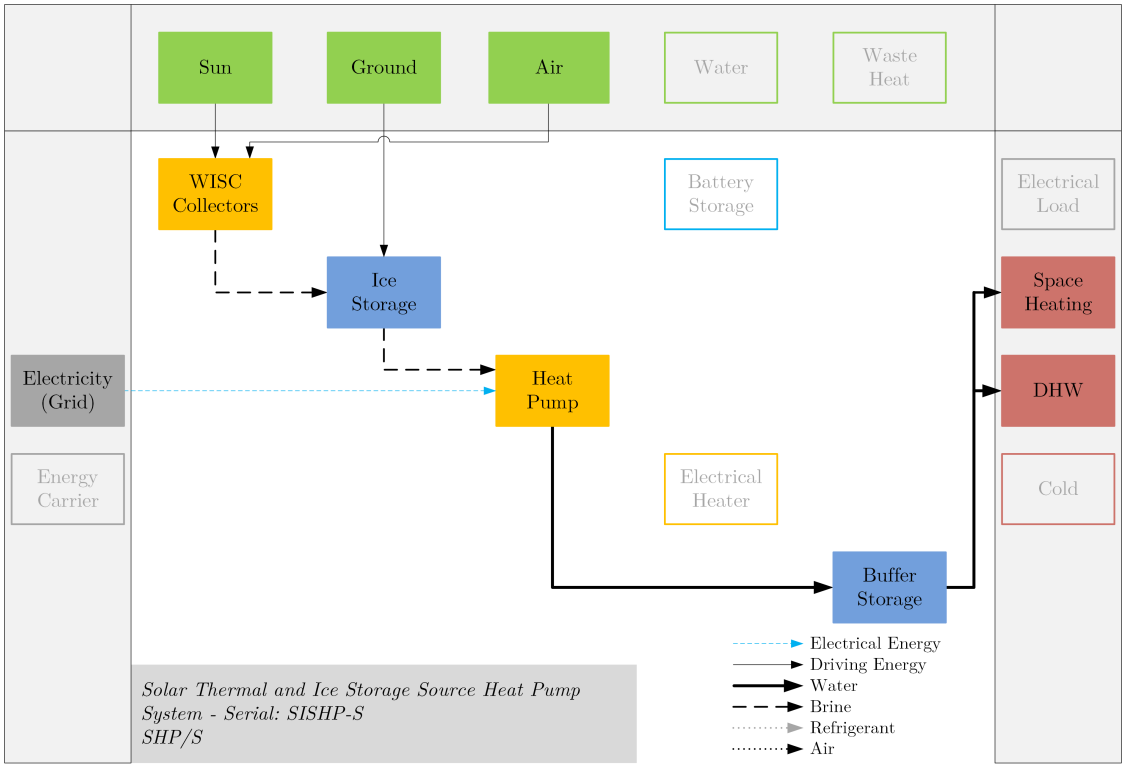

Figure 2.34: Visualization of energy flows in the considered SISHP-S system.

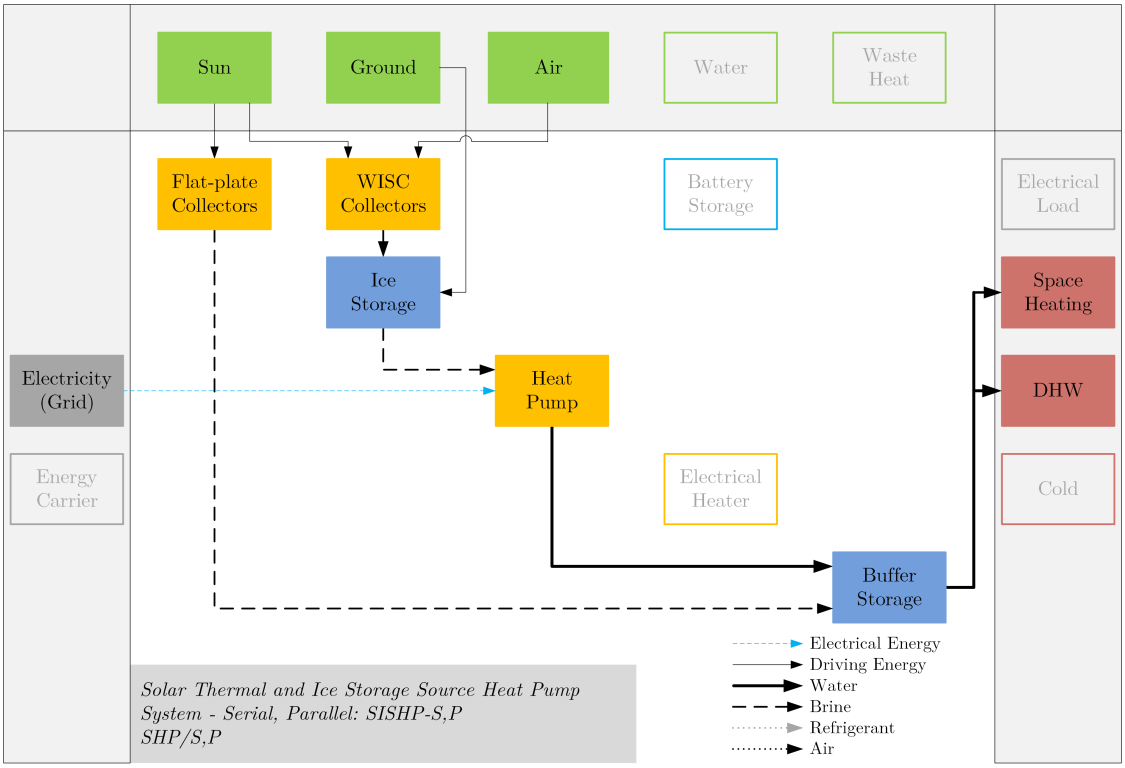

Figure 2.35: Visualization of energy flows in the considered SISHP-S,P system.

2.3.2 Photovoltaic and Heat Pump Systems

The combination of PV and heat pump systems is a promising technology for future residential energy supply systems, especially in combination with battery storages and in the context of smart grids. In general, *photovoltaic and heat pump* systems comprise all combinations of PV and heat pumps with exception of additional solar thermal system integration. Within these concepts, the PV system supplies the heat pump system with electricity. In contrast to solar thermal and heat pump systems, the combination and interaction of PV and heat pump systems are less complex in terms of system design and the systems differ especially in the combination of the used heat pump concept from Section 2.2.1.2 and the residential PV system concept from Section 2.2.2.2. In addition, a further distinction can be made whether the PV self-consumption comprises household electricity load (consumption) or not.

With regard to future residential PV systems, a case study on PV and heat pump systems from Von Appen [2018] showed that future PV systems require shifting technologies like battery storage systems and heat pumps to activate the available PV rooftop potential when feed-in tariffs significantly decrease close to zero. Furthermore, the author figured out that battery storage systems and heat pumps complement each other and the combination might offer benefits for non-modulating heat pumps. As conclusion, the author recommended a tariff or investment incentive-based framework that allows heat pumps to be an appealing economic alternative to conventional heating systems. The author summarized that this is not only essential for decentralized sector coupling and rising demand flexibility, but also for a promising business case for future residential PV systems [Von Appen, 2018; Von Appen and Braun, 2019].

Regarding different locations across Europe, Bee [2019] concluded that the capability to

consume self-produced PV energy on a yearly basis in PV and ASHP systems without any electrical storage does not significantly change for different climates and the self-consumption increases for all climates by adding a battery storage. In addition, Bee et al. [2019] observed that in warm climates, the main benefit is in the winter months as the heating demand occurs mainly during the night and it can be shifted by means of a battery storage to match the daily radiation. In contrast, in colder climates the self-consumption for PV and heat pump systems with battery storage increases especially in spring when the heating demand is still significant and the available PV energy is higher than in winter.

In addition to electrical battery storage systems, PV and heat pump systems offer the possibility to store PV energy in thermal storages. Thygesen and Karlsson [2014] analyzed two storage concepts for PV (with battery storage or thermal storage with electrical heater) for a specific use case of a nZEB (single-family house) in Sweden considering heating applications and household electricity. For the specific case, the results showed that the system with heat pump in combination with a PV system can be profitable and had high solar energy fractions and high levels of self-consumption while systems with storage were not profitable but gave higher levels of self-consumption. Within the considered system concepts, the hot water storage concept with electrical heater reached almost the same level of self-consumption as the concept with battery storage but had only half of the batteries (lead acid) levelized cost of electricity. Battaglia et al. [2017] reported that the advantage of using thermal energy storages in PV and heat pump systems in comparison to the use of battery storages are smaller investment costs while the reduction of the grid electricity purchase within the analyzed systems was higher for battery storages. At this, it should be noted that investment costs of battery storage systems have significantly decreased in recent years and thus the results may have changed in the meantime. In addition, Battaglia et al. [2017] suggested that the combination of thermal and electrical energy storages is a very promising approach as this offers the possibility to reach the same degrees of self-sufficiency with smaller battery sizes and thus smaller investment costs. Another possibility for the thermal storage of PV energy within buildings is the overheating of the building itself as analyzed in Thür et al. [2018]. However, these concepts have the disadvantage that the overheating of the room temperatures in the building directly affects the personal room comfort and thus are not favored by every occupant. Facci et al. [2019] also figured out that thermal storages can act effectively as electrical storages by the use of heat pumps and that a decoupling of heating energy generation and consumption by thermal storages has a fundamental role in optimal system operation, both in terms of energy cost savings and GHG emission reduction. Furthermore, the authors recommended that legislations should move towards promoting the self-consumption of renewable electricity.

Due to its potential and future role for residential buildings, the investigations in this work will focus mainly on the following PV and heat pump system concepts:

a. Photovoltaic and ground source heat pump systems (PV-GSHP)

b. Photovoltaic and air source heat pump systems (PV-ASHP)

with or without AC-coupled battery storage system and with PV self-consumption for the heat pump system as well as the household electricity load. The concept of the investigated PV and heat pump systems is based on a GSHP or ASHP system as described in Section 2.2.1.3 and a AC-coupled battery storage system as described in Section 2.2.2.2. The PV and heat pump system is shown regardless of the used heat source and with optional battery storage system in Figure 2.36. The generated PV electricity can be used to charge

an optional battery storage, supply the heat pump system, cover the household electricity load or it can be fed into the grid. In addition, the battery storage (if included in the system concept) can be discharged to cover the electrical loads of the heat pump system and the household electricity load or the energy for the electrical loads (heat pump system, household) can be delivered by the grid. At this, the heat pump system includes electrical loads for additional components in the heating system like controller or pumps.

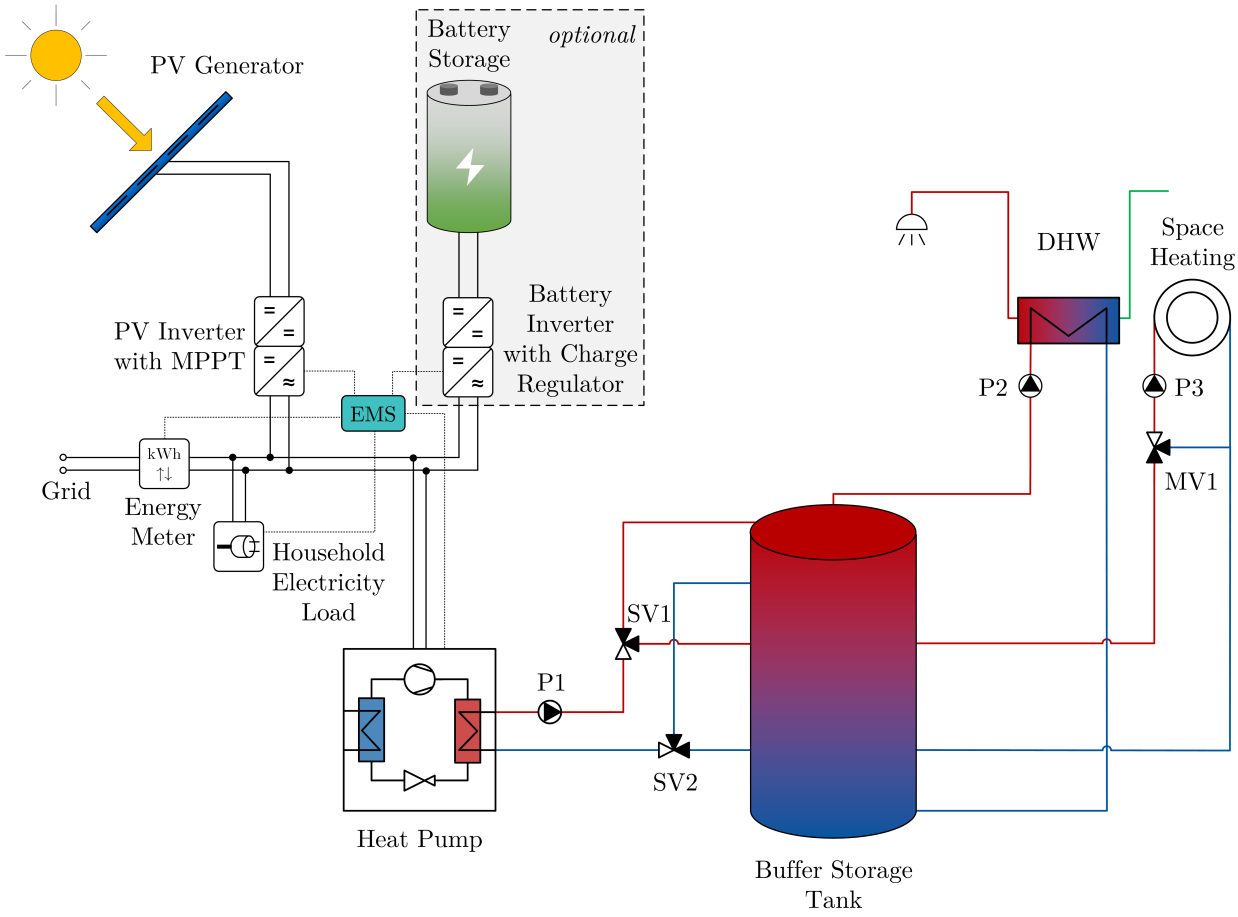

Figure 2.36: Hydraulic scheme of the PV and heat pump heating system independent of the used heat source including PV system with optional battery storage system.

Visualizations of the energy flows in the PV and heat pump system concepts are given in Figure 2.37 and Figure 2.38 for system concepts with battery storage. In system concepts without battery storages, the battery storage is removed and PV is connected directly with the heat pump and the household electricity load.

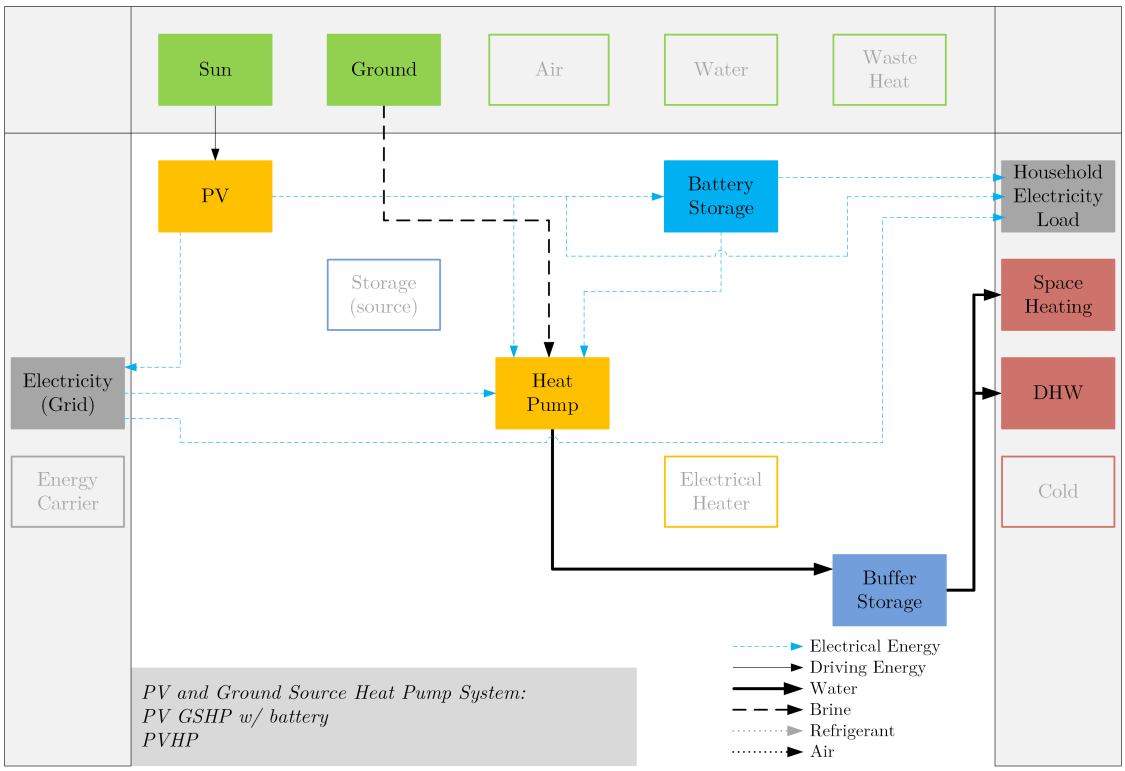

Figure 2.37: Visualization of energy flows in the considered PV-GSHP system with battery storage system.

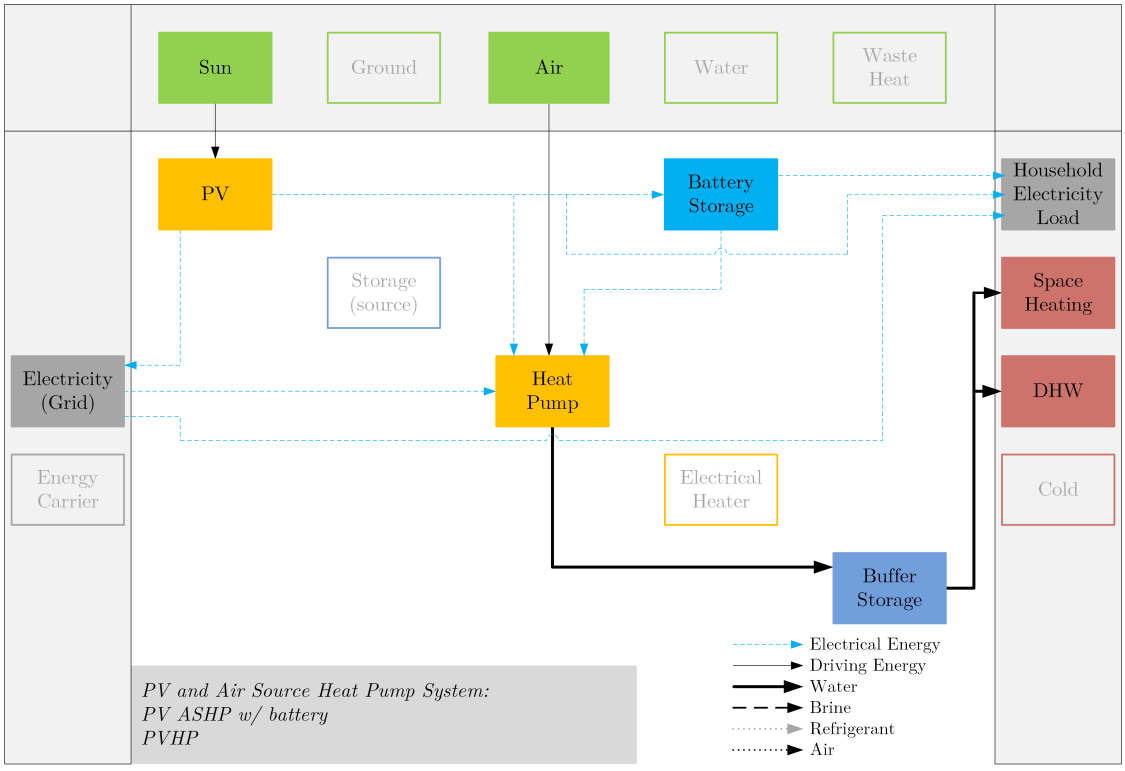

Figure 2.38: Visualization of energy flows in the considered PV-ASHP system with battery storage system.

2.3.3 Photovoltaic, Solar Thermal and Heat Pump Systems

The combination of *photovoltaic, solar thermal and heat pump* systems, also called hybrid photovoltaic / solar thermal heat pump systems, focus on the efficient thermal and electrical energy supply of buildings by solar energy technologies and is a very promising technology for future residential nearly zero energy and energy flexible buildings, especially in combination with electrical and thermal storages. In general, PV, solar thermal and heat pump systems comprise all combinations of PV, solar thermal and heat pump systems. As described in Section 2.3, the systems can be subdivided in PV plus solar thermal and heat pump systems and PVT and heat pump systems to indicate whether the system includes only separated PV and solar thermal or hybrid PVT technologies. Within PV plus solar thermal and heat pump system concepts, the PV system supplies the heat pump system with electricity whereas the solar thermal collectors supply the system with thermal energy. The systems differ especially in the combination of the used solar thermal and heat pump system concept from Section 2.3.1 and the residential PV system concept from Section 2.2.2.2. In contrast, in PVT and heat pump systems the PVT collectors supply the heat pump system with both electricity and thermal energy. PVT and heat pump system concepts also differ in particular in the combination of the used solar thermal and heat pump system concept from Section 2.3.1 and the residential PV system concept from Section 2.2.2.2 but with a replacement of the solar thermal collectors and the PV modules by PVT collectors. Furthermore, PVT and heat pump systems can be combined with PV or solar thermal systems as PV plus PVT, PVT plus solar thermal or PV plus PVT plus solar thermal and heat pump systems. In addition, a further distinction can be made for all PV, solar thermal and heat pump systems whether the PV and/or PVT self-consumption comprises household electricity load or not.

Regarding PV plus solar thermal and heat pump systems in comparison with other SHP systems, Thygesen and Karlsson [2013] carried out a study on the combination of a GSHP with PV, solar thermal or PV plus solar thermal systems for a specific use case of a nZEB (single-family house) in Sweden considering heating applications and household electricity. In comparison with PV, the authors concluded that GSHP combinations with solar thermal or PV plus solar thermal systems were not profitable and gave lower solar energy fractions for the considered use case. However, as mentioned in the previous section, investment costs have changed in recent years and thus the results may also have changed in the meantime. Furthermore, Poppi [2017] did a literature based economic analysis of PV, solar thermal and PV plus solar thermal and heat pump systems for heating applications and performed system simulations with special focus on a reference solar thermal heat pump system with ASHP. A general conclusion was that the economic performance of SHP systems depends significantly on the climate and the different assumptions concerning the costs. In addition, the author concluded that there are clear trends for decreasing payback times of SHP systems, both solar thermal and PV, with decreasing heating degree-days and with increasing solar resource. Nevertheless, the author figured out that more techno-economic studies of combinations of PV or PV and solar thermal systems with heat pump systems are required and, as the results were only obtained for a limited range of variation in heat loads and system configurations, extended work for other heat loads and system configurations is needed [Poppi, 2017]. Furthermore, Poppi et al. [2018] concluded that there are no consistent boundaries or approaches regarding different studies which make comparisons between systems difficult or impossible.

With regard to system comparisons including PVT and heat pump systems, Dott et al.

[2012] did a simulation case study on different system concepts including PV and ASHP, SASHP-P and a serial PVT and heat pump system for heating application in moderate climate without PV or PVT self-consumption. The authors concluded that SASHP-P systems have the smallest electricity consumption while serial PVT and heat pump systems used as heat source of the heat pump generate more surplus electricity than PV and ASHP systems for the specific use case. Furthermore, Sommerfeldt and Madani [2018] figured out that a benefit of adding serial PVT collectors in GSHP systems is the reducing of the borehole length with no or a limited loss of efficiency, whereas PV and GSHP systems with a fully sized borehole field have the lowest costs in case of a multi-family house in Sweden regarding a limited range of system design configurations. However, the reduction in borehole field area for a given heat pump efficiency is notable as many multi-family houses cannot use GSHPs due to a lack of drilling space and PVT and GSHP systems could open up a market currently unavailable for GSHPs and thus increase the use of renewable energies in buildings [Sommerfeldt and Madani, 2019]. Regarding PV, PVT or solar thermal and ASHP systems, Wang et al. [2020] concluded that the comparison results of different studies indicate that PV and ASHP systems have the best techno-economic performance. Furthermore, solar thermal and ASHP systems have high efficiencies, whereas PVT and ASHP systems have the highest solar energy utilization and most energy production. Nevertheless, the authors recommend that many other aspects like economics and environmental aspects have to be discussed in the future.

To sum up, the field of PV, solar thermal and heat pump systems is an ongoing research field and comparisons of different PVT, PV, solar thermal or PV plus solar thermal and heat pump system concepts especially for the heat and electricity supply of buildings are still rare, as current studies focus more on individual system concepts or specific applications (e.g. domestic hot water preparation in Martorana et al. [2021]). Consequently, as mentioned in the introduction, this work has the objective to close this research gap for typical system configurations with regard to thermal and electrical energy supply of single-family houses.

The investigations of PV plus solar thermal systems in this work focus on the combination of the chosen concepts of solar thermal and heat pump systems from Section 2.3.1 with AC-coupled PV battery storage systems as described in Section 2.2.2.2 and thus the following PV plus solar thermal and heat pump system concepts will be investigated:

a. Photovoltaic plus parallel solar thermal and ground source heat pump systems (PV-SGSHP-P)

b. Photovoltaic plus parallel solar thermal and air source heat pump systems (PV-SASHP-P)

c. Photovoltaic plus serial solar thermal and ice storage source heat pump systems (PV-SISHP-S)

d. Photovoltaic plus serial solar thermal and ice storage source heat pump systems with additional parallel solar thermal collectors (PV-SISHP-S,P)

with or without AC-coupled battery storage system and with PV self-consumption for the heat pump system as well as the household electricity load. The PV plus parallel solar thermal and heat pump system is shown regardless of the used heat source and with optional battery storage system in Figure 2.39. The functionality of the PV system part is the same as described for PV and heat pump systems in Section 2.3.2. The solar thermal and heat

pump system part is designed and operated as described in Section 2.3.1 and shown in Figure 2.31. Visualizations of the energy flows in the PV plus solar thermal and heat pump system concepts are given in Figure 2.40, Figure 2.41, Figure 2.42 and Figure 2.43 for system concepts with battery storage. In system concepts without battery storages, the battery storage is removed and PV is connected directly with the heat pump and the household electricity load.

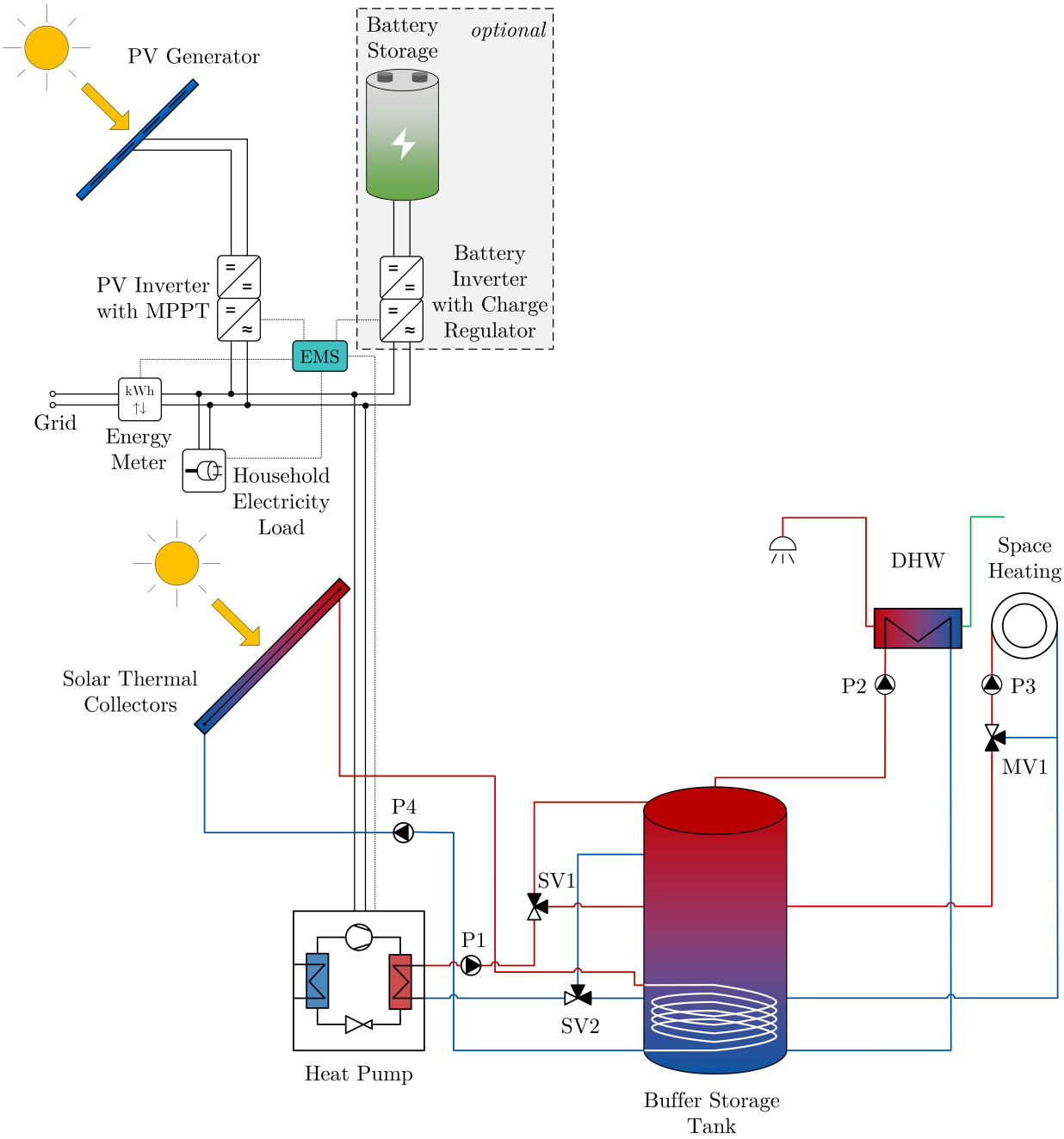

Figure 2.39: Hydraulic scheme of the PV plus parallel solar thermal and heat pump heating system independent of the used heat source including PV system with optional battery storage system.

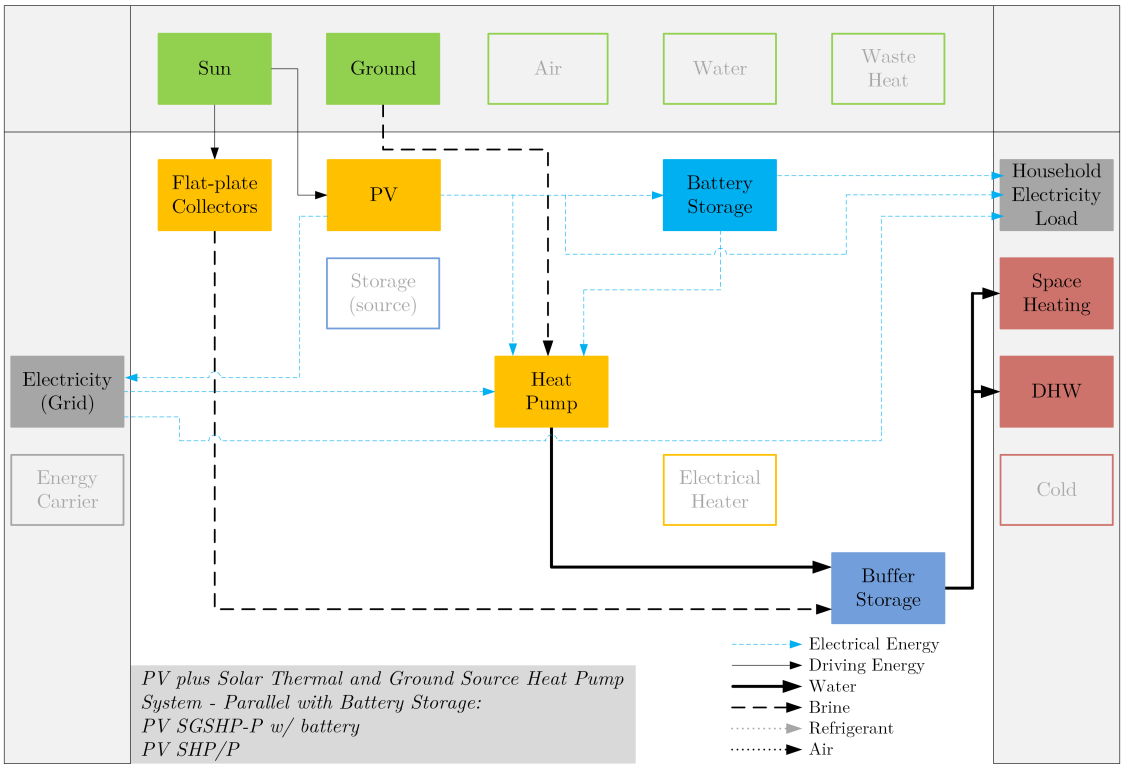

Figure 2.40: Visualization of energy flows in the considered PV-SGSHP-P system with battery storage system.

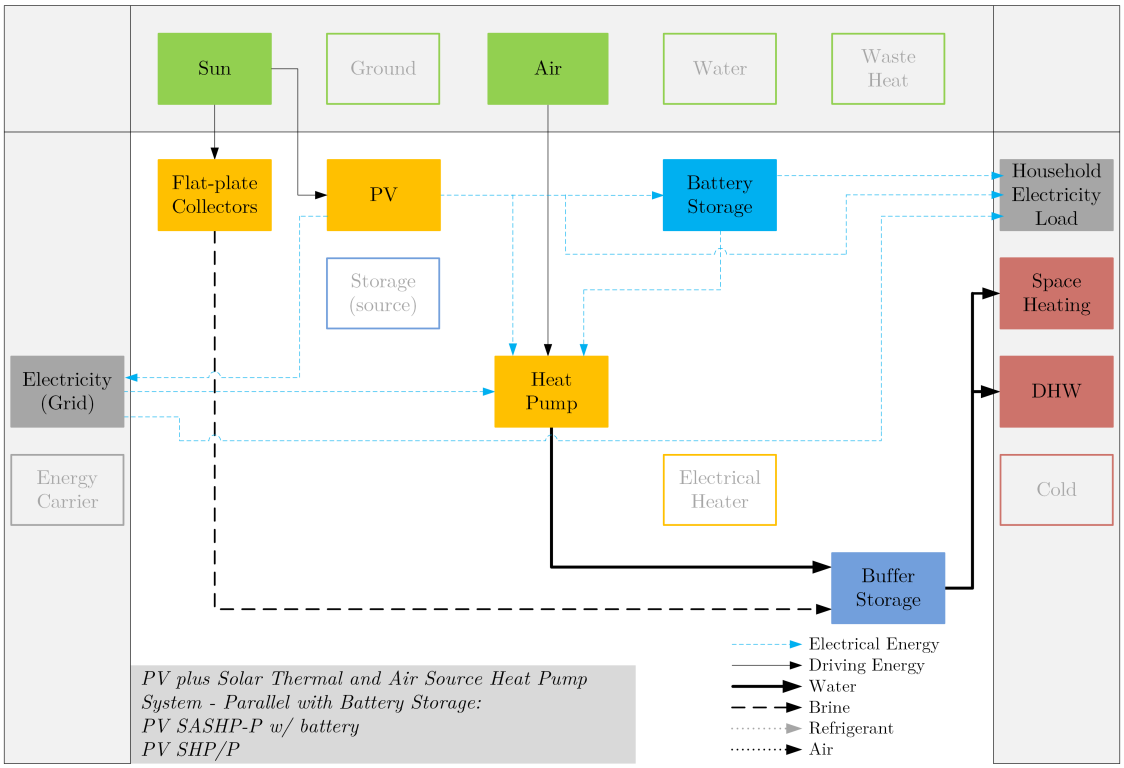

Figure 2.41: Visualization of energy flows in the considered PV-SASHP-P system with battery storage system.

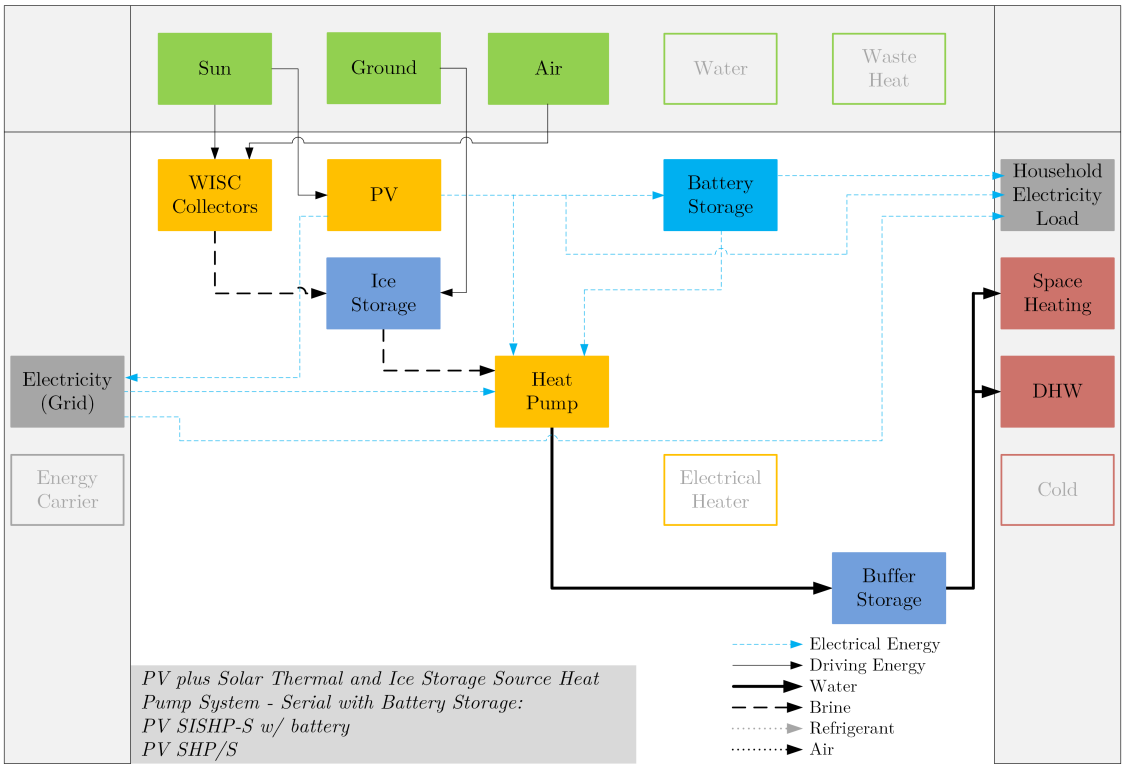

Figure 2.42: Visualization of energy flows in the considered PV-SISHP-S system with battery storage system.

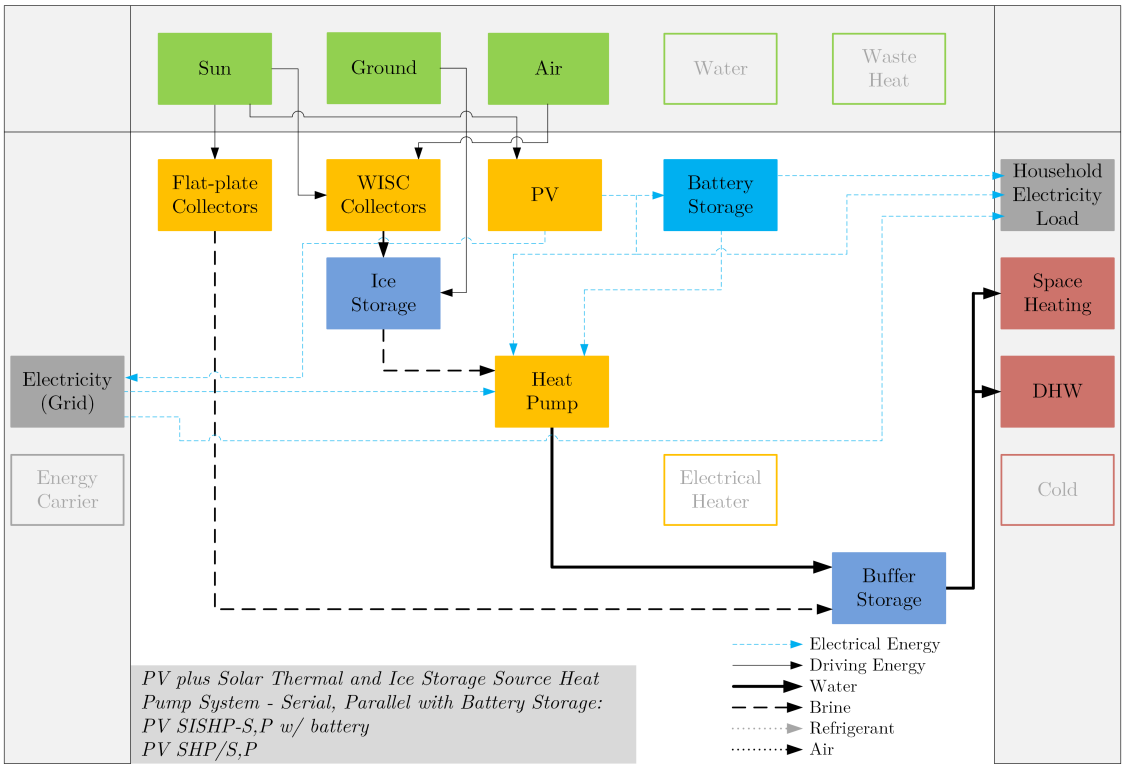

Figure 2.43: Visualization of energy flows in the considered PV-SISHP-S,P system with battery storage system.

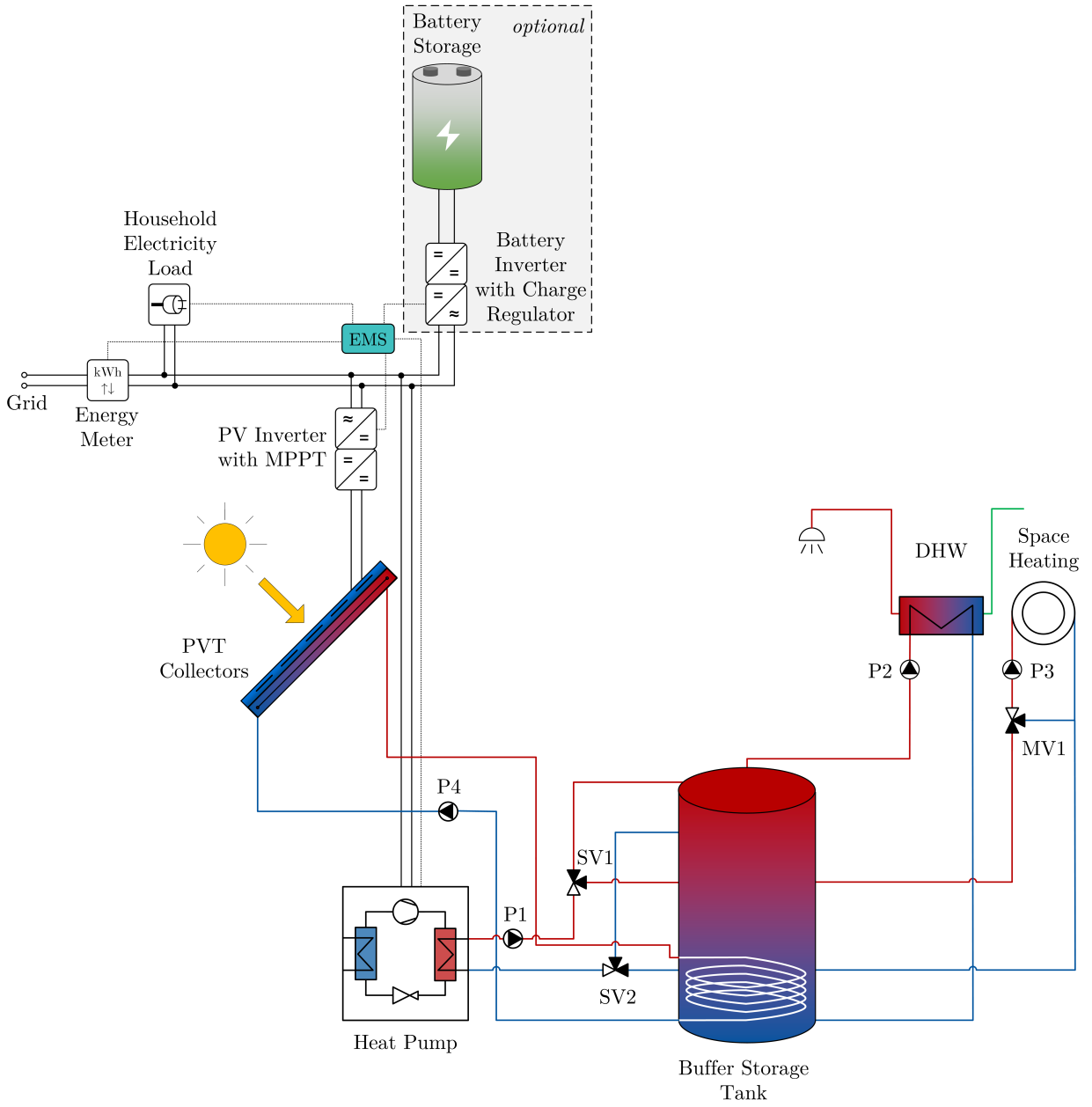

Figure 2.44: Hydraulic scheme of the PVT and heat pump heating system independent of the used heat source with optional battery storage system.

The investigations of PVT and heat pump systems in this work are also based on the combination of the chosen concepts of solar thermal and heat pump systems from Section 2.3.1 with AC-coupled PV battery storage systems as described in Section 2.2.2.2 but with a replacement of solar thermal collectors and PV modules by PVT collectors and thus the following PVT and heat pump system concepts will be investigated:

a. Parallel photovoltaic-thermal and ground source heat pump systems (PVT-SGSHP-P)

b. Parallel photovoltaic-thermal and air source heat pump systems (PVT-SASHP-P)

c. Serial photovoltaic-thermal and ice storage source heat pump systems (PVT-SISHP-S)

with or without AC-coupled battery storage system and with PVT self-consumption for the heat pump system as well as the household electricity load. The PVT and heat pump system is shown regardless of the used heat source and with optional battery storage system in Figure 2.44. The functionality of the electrical part of the PVT and heat pump system is the same as described for PV and heat pump systems in Section 2.3.2 with a replacement of PV modules by PVT collectors. The thermal part of the PVT and heat pump system is designed and operated as the SGSHP-P, SASHP-P and SISHP-S systems described in Section 2.3.1 and shown in Figure 2.31 with a replacement of the solar thermal collectors by PVT collectors. Visualizations of the energy flows in the PVT and heat pump system concepts are given in Figure 2.45, Figure 2.46 and Figure 2.47 for system concepts with battery storage. In system concepts without battery storages, the battery storage is removed and PVT is connected directly with the heat pump and the household electricity load.

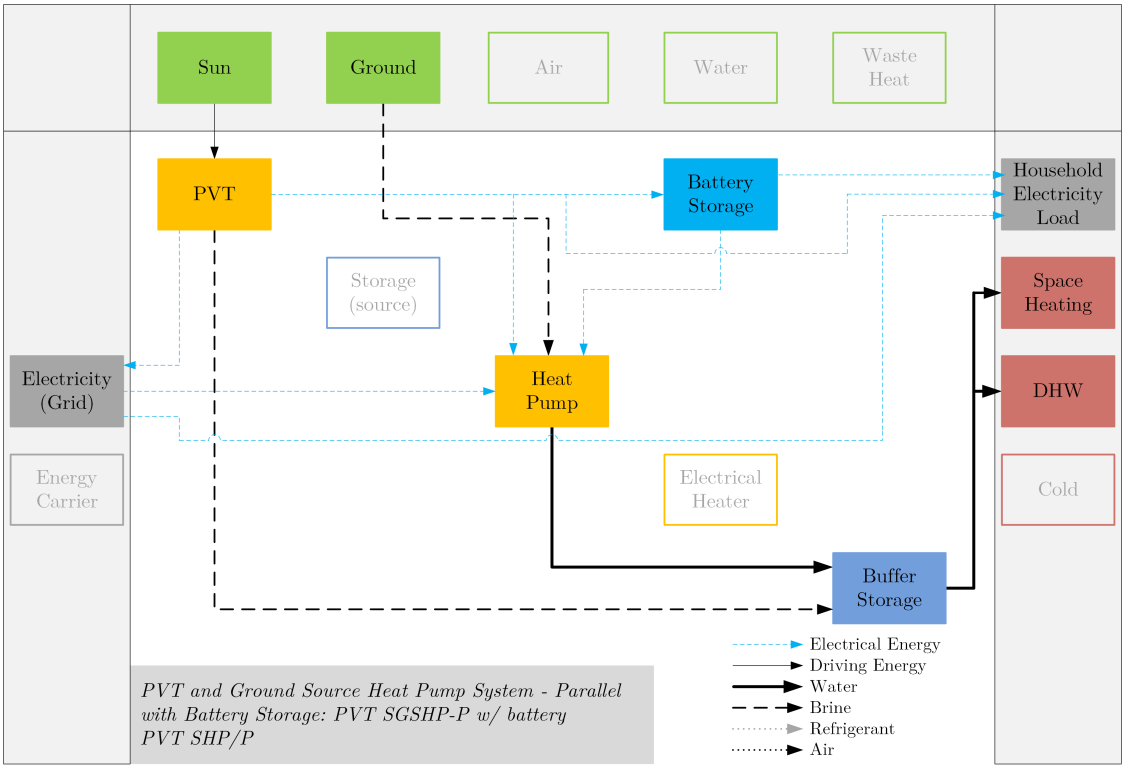

Figure 2.45: Visualization of energy flows in the considered PVT-SGSHP-P system with battery storage system.

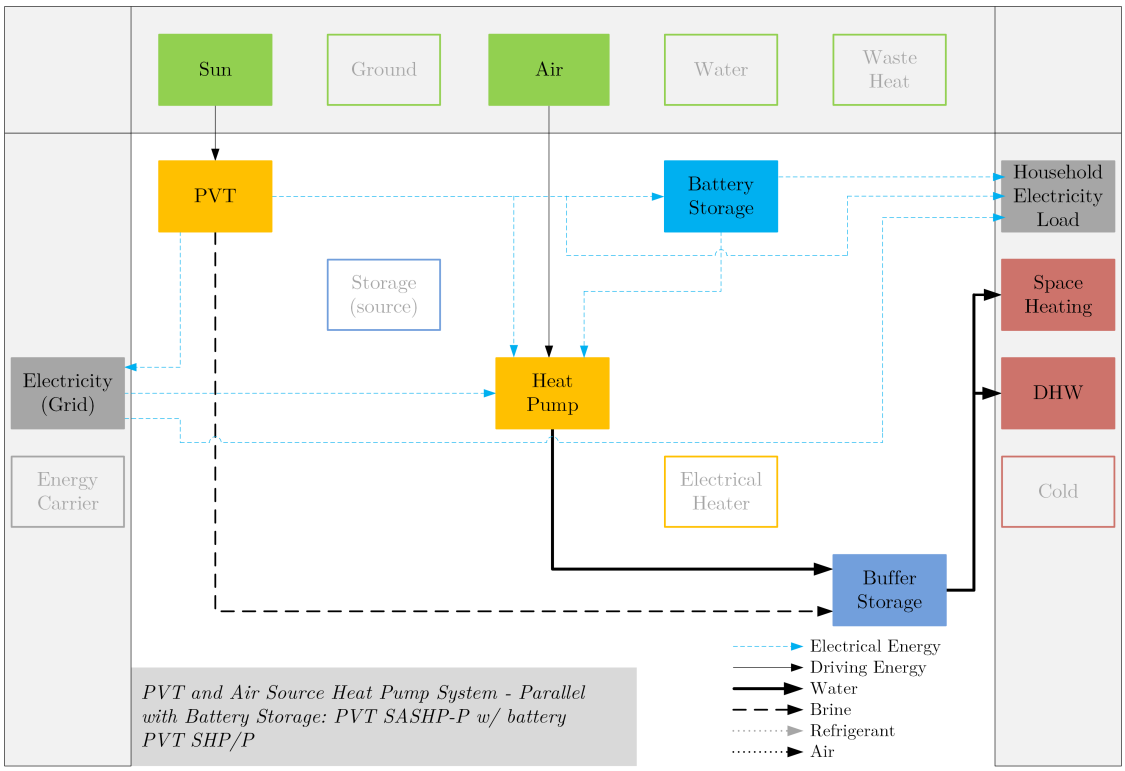

Figure 2.46: Visualization of energy flows in the considered PVT-SASHP-P system with battery storage system.

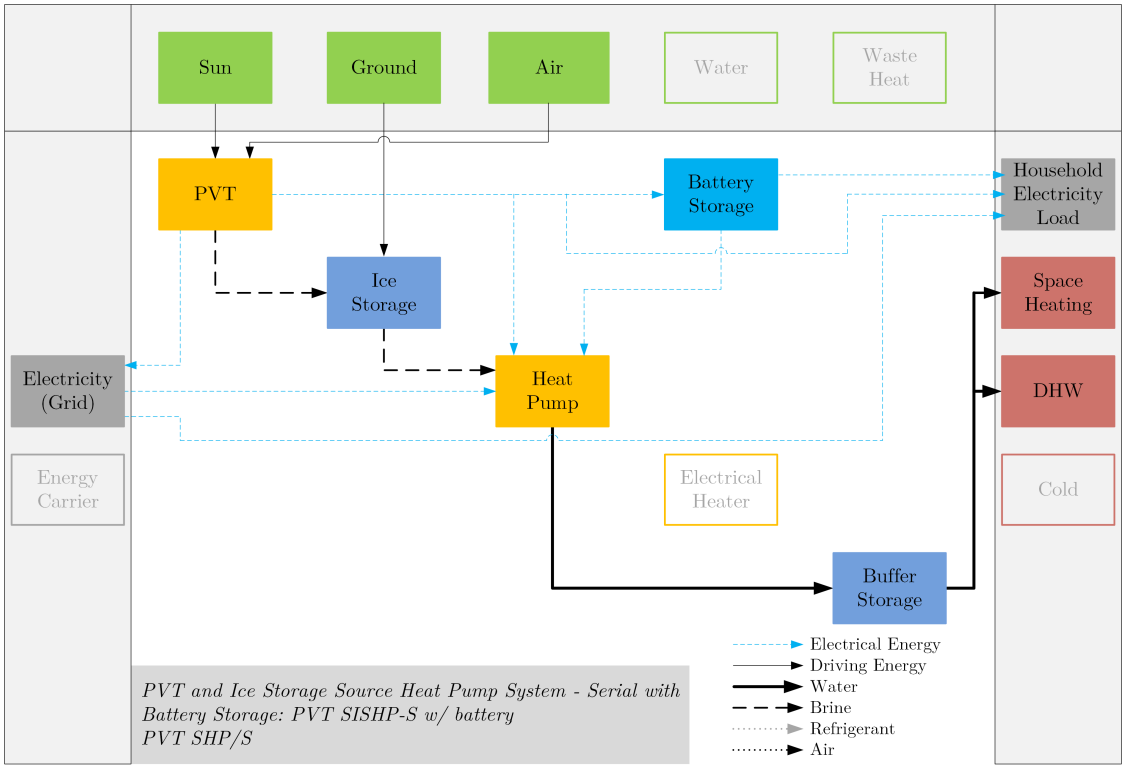

Figure 2.47: Visualization of energy flows in the considered PVT-SISHP-S system with battery storage system.

In addition, the following PV plus PVT and heat pump system concepts will be investigated to use the entire available roof area in smaller sized PVT concepts:

a. Photovoltaic plus parallel photovoltaic-thermal and ground source heat pump systems (PV-PVT-SGSHP-P)

b. Photovoltaic plus parallel photovoltaic-thermal and air source heat pump systems (PV-PVT-SASHP-P)

c. Photovoltaic plus serial photovoltaic-thermal and ice storage source heat pump systems (PV-PVT-SISHP-S)

with or without AC-coupled battery storage system and with PV and PVT self-consumption for the heat pump system as well as the household electricity load. Compared to Figure 2.44, the PV plus PVT and heat pump system only contains a second parallel PV string in addition to the PVT collectors that is connected to the PV inverter with MPPT and hence the system is not shown graphically. Visualizations of the energy flows in the PV plus PVT and heat pump system concepts are given in Figure 2.48, Figure 2.49 and Figure 2.50 for system concepts with battery storage. In system concepts without battery storages, the battery storage is removed and PV as well as PVT is connected directly with the heat pump and the household electricity load.

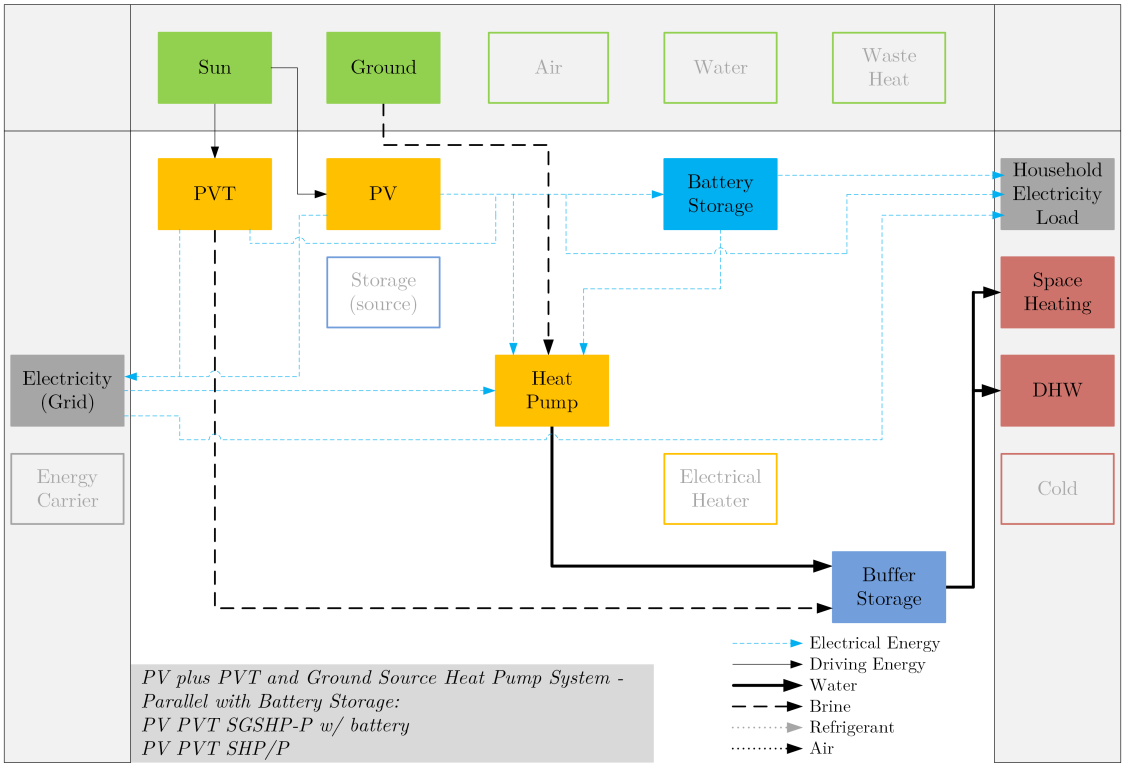

Figure 2.48: Visualization of energy flows in the considered PV-PVT-SGSHP-P system with battery storage system.

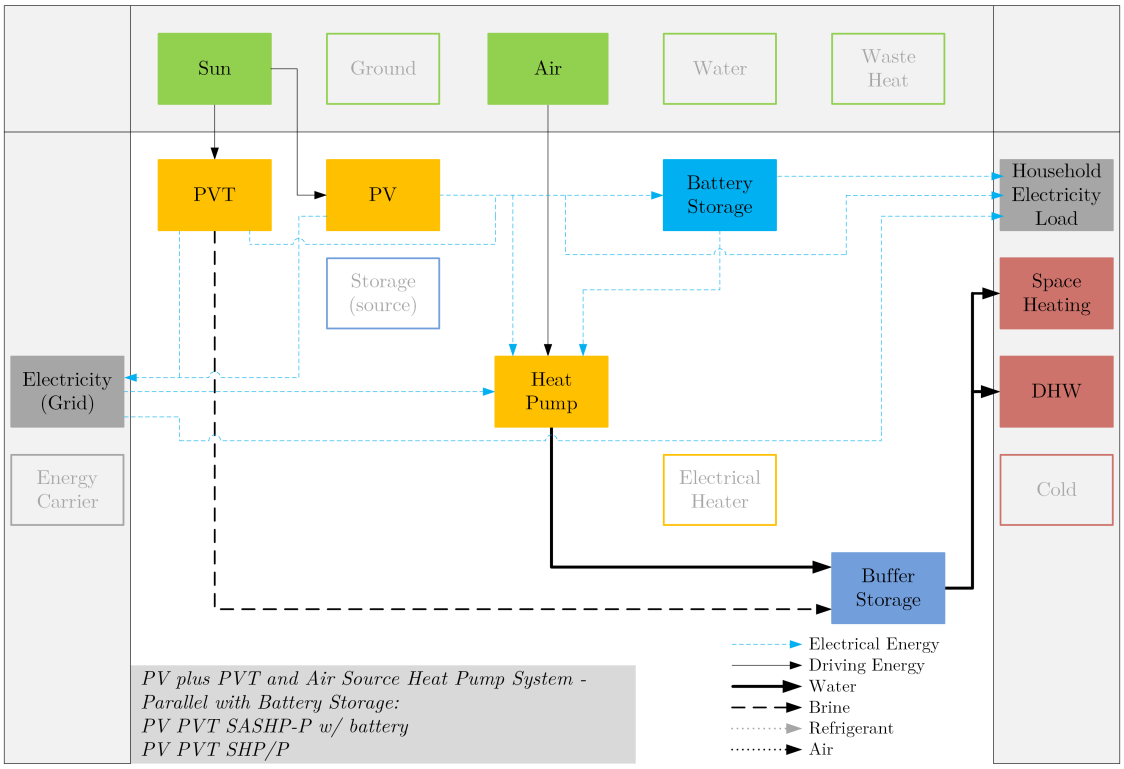

Figure 2.49: Visualization of energy flows in the considered PV-PVT-SASHP-P system with battery storage system.

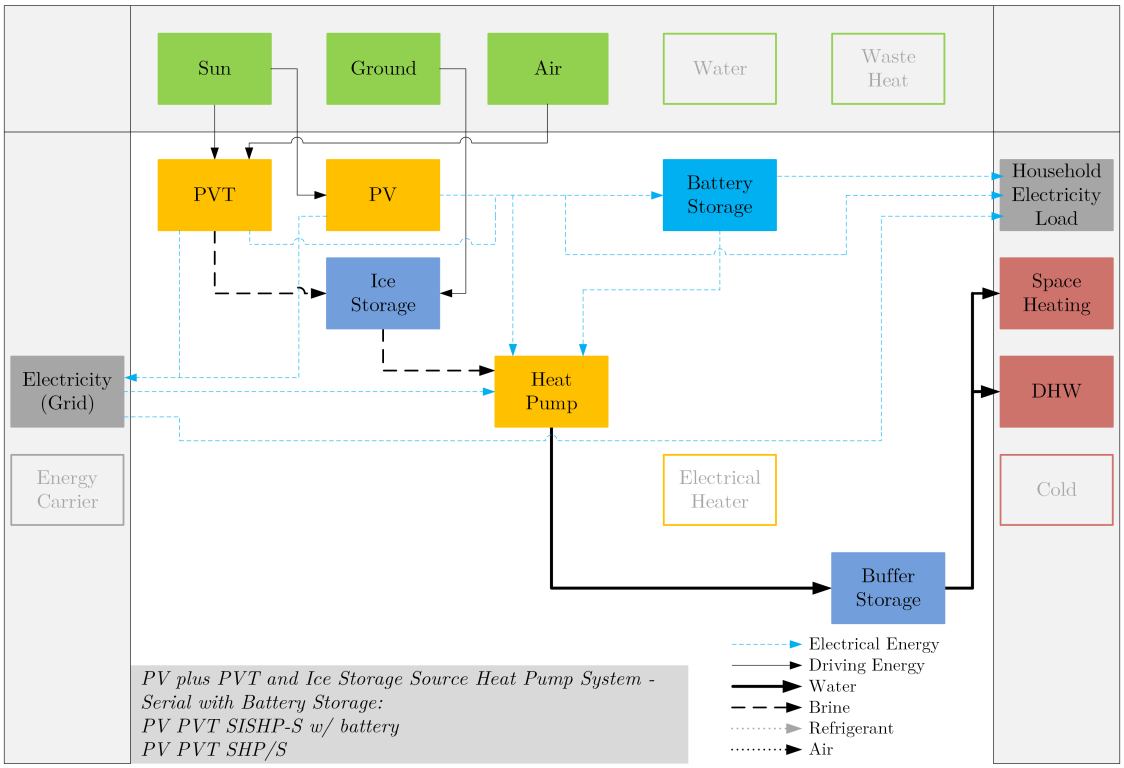

Figure 2.50: Visualization of energy flows in the considered PV-PVT-SISHP-S system with battery storage system.

Furthermore, the use of WISC or covered flat-plate PVT collectors will be analyzed for the described PVT as well as PV plus PVT and heat pump system concepts. Due to its small market relevance and high complexity, further system combinations like PVT plus solar thermal or PV plus PVT plus solar thermal system combinations are not considered in this work to limit the possible system combinations for the following simulation studies.

2.4 Key Performance Indicators of Solar and Heat Pump Systems

The comparison of different system concepts for the energy supply of buildings requires well-defined and uniform KPIs. In a recent systematic review of ASHP systems in combination with solar thermal, PV and PVT, Wang et al. [2020] figured out that there is a lack of standardized indicators to evaluate the system performance and only few papers take into account environmental and economic aspects. As a consequence, this section deals with the definition of KPIs for SHP systems regarding both thermal and electrical energy supply of buildings for the evaluation of performance and efficiency, environmental impact and economic aspects. At this, the definitions of performance indicators from Section 2.1.3 are adapted to SHP systems for its rating in the context of nZEB standards. Furthermore, a procedure for the combined evaluation of economic aspects and environmental impact is presented. The defined equations and figures for SHP systems in the following sections can also be used for the analysis of ASHP and GSHP systems without solar thermal or electrical energy contribution.

2.4.1 Performance and Efficiency

2.4.1.1 Seasonal Performance Factor

The seasonal performance factor (SPF) quantifies the final **energy efficiency for heating applications of a SHP system** and is defined as the ratio of the overall useful heating energy output to the overall driving final energy input for an adopted system boundary over a period of one year [Malenković et al., 2013]. In some cases, SHP systems may not permanently provide the required comfort criteria (domestic hot water tapping temperatures or the room temperature of the building) at all times and thus the useful energy supplied to the rooms or the domestic hot water system is lower or higher than the heating energy demand. Hence, penalty functions are defined as direct electric heating for times in which the system does not reach the defined comfort criteria [Heimrath and Haller, 2007; Weiss, 2003]. In the following definition, the SPF of the overall SHP system with penalties $SPF_{\mathrm{SHP+,pen}}$ indicates the amount of useful energy for space heating $Q_{\mathrm{SH,useful}}$ and domestic hot water preparation $Q_{\mathrm{DHW,useful}}$ divided by the amount of electricity consumption of the overall SHP system including penalties $W_{\mathrm{el,SHP+,pen}}$ for a period of one year [Haller, 2013]:

$$SPF_{\mathrm{SHP+,pen}} = \frac{Q_{\mathrm{SH,useful}} + Q_{\mathrm{DHW,useful}}}{W_{\mathrm{el,SHP+,pen}}} \tag{2.43}$$

with

$$W_{\mathrm{el,SHP+,pen}} = W_{\mathrm{el,SHP+}} + W_{\mathrm{el,SH,pen}} + W_{\mathrm{el,DHW,pen}} \tag{2.44}$$

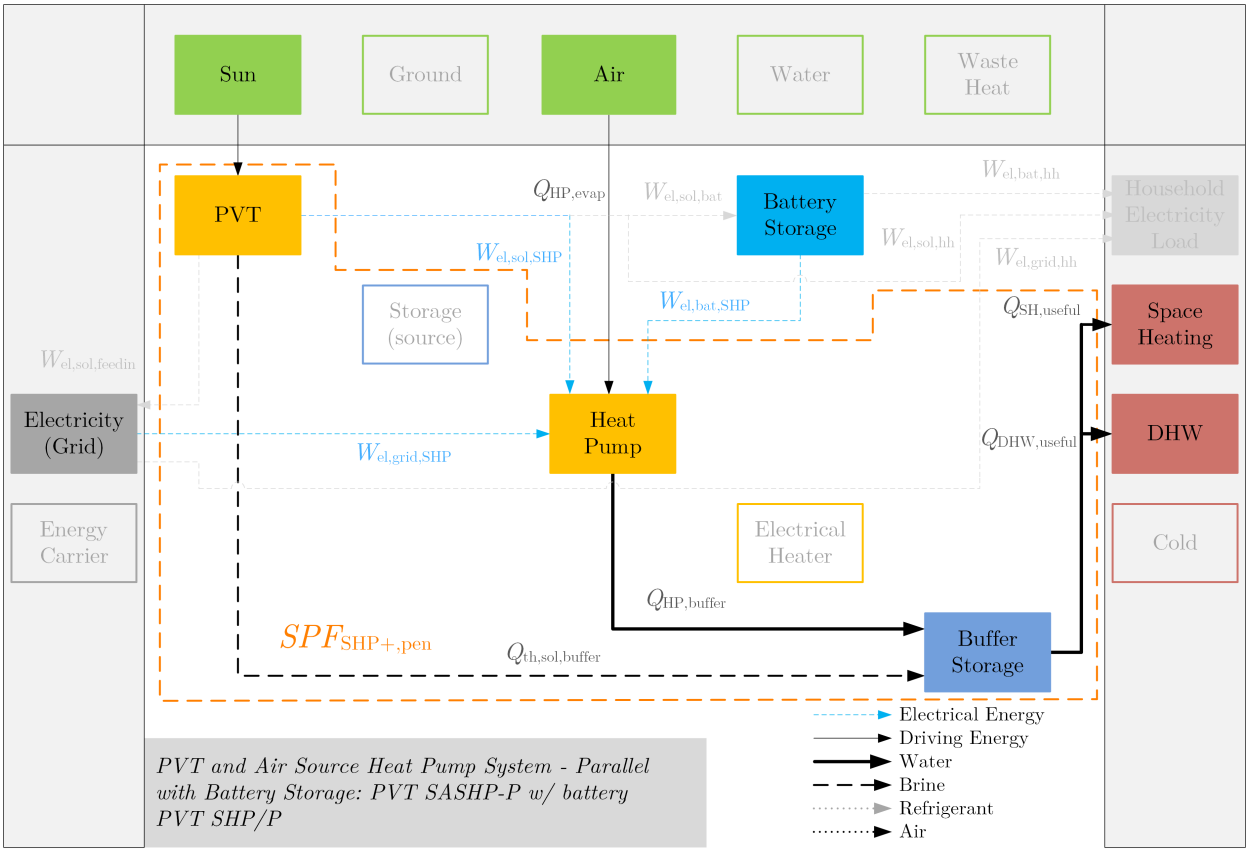

Figure 2.51: System boundary (orange dashed line) for the seasonal performance factor of the overall SHP system with penalties for the example of a PVT SASHP-P system with battery storage.

and

$$W_{\mathrm{el,SHP+}} = W_{\mathrm{el,HP}} + W_{\mathrm{el,SC}} + W_{\mathrm{el,EH}} + W_{\mathrm{el,pu}} + W_{\mathrm{el,ctr}} + W_{\mathrm{el,pu,SH}}, \tag{2.45}$$

where $W_{\mathrm{el,SHP+}}$ is the electricity consumption of the overall SHP system, $W_{\mathrm{el,SH,pen}}$ is the penalty for space heating and $W_{\mathrm{el,DHW,pen}}$ is the penalty for domestic hot water preparation. With the chosen system boundary shown in Figure 2.51 for the example of a PVT SASHP-P system with battery storage, the electricity consumption $W_{\mathrm{el,SHP+}}$ includes all electricity consumptions of the SHP system:

- $W_{\mathrm{el,HP}}$: electricity consumption of the heat pump including e.g. compressor, pumps, controller
- $W_{\mathrm{el,SC}}$: electricity consumption of the solar thermal circuit including e.g. pumps, controller
- $W_{\mathrm{el,EH}}$: electricity consumption of direct electric heating elements which are not included in the heat pump or solar thermal circuit consumption
- $W_{\mathrm{el,pu}}$: electricity consumption of pumps which are not included in the heat pump or solar thermal circuit consumption

- $W_{\mathrm{el,ctr}}$: electricity consumption of additional controllers which are not included in the heat pump or solar thermal circuit consumption

- $W_{\mathrm{el,pu,SH}}$: electricity consumption of circulation pumps for the space heating system.

The electricity consumption of the overall SHP system including penalties $W_{\mathrm{el,SHP+,pen}}$ can also be calculated with:

$$W_{\mathrm{el,SHP+,pen}} = W_{\mathrm{el,grid,SHP}} + W_{\mathrm{el,sol,SHP}} + W_{\mathrm{el,bat,SHP}}, \tag{2.46}$$

where $W_{\mathrm{el,grid,SHP}}$ is the used electrical energy from the grid for the supply of the SHP system, $W_{\mathrm{el,sol,SHP}}$ is the self-consumed solar (PV and PVT) electricity generation of the SHP system and $W_{\mathrm{el,bat,SHP}}$ is the used electrical energy from the battery storage for the supply of the SHP system. This also means that the electrical energy supply of the SHP system includes the covering of penalties. Furthermore, here and in the following, the index *sol* is used for solar electricity generation of both PV and PVT and the solar thermal circuit comprises both thermal circuits with solar thermal collectors and PVT collectors.

The penalty for space heating $W_{\mathrm{el,SH,pen}}$ is defined as:

$$W_{\mathrm{el,SH,pen}} = \int UA_{\mathrm{bui}} \left[\Delta T_{\mathrm{SH,pen}} + \left(\Delta T_{\mathrm{SH,pen}} + 1\right)^2 - 1\right] \mathrm{d}t \tag{2.47}$$

with

$$\Delta T_{\mathrm{SH,pen}} = \max\left\{0, 19.5\,^{\circ}\mathrm{C} - \vartheta_{\mathrm{room}}\right\} \tag{2.48}$$

and the penalty for domestic hot water preparation $W_{\mathrm{el,DHW,pen}}$ as:

$$W_{\mathrm{el,DHW,pen}} = \int 1.5\ \dot{m}_{\mathrm{DHW,loc}}\ c_{p,\mathrm{w}}\ \Delta T_{\mathrm{DHW,pen}}\,\mathrm{d}t \tag{2.49}$$

with

$$\Delta T_{\mathrm{DHW,pen}} = \max\left\{0, \vartheta_{\mathrm{DHW,set}} - \vartheta_{\mathrm{DHW}}\right\}, \tag{2.50}$$

where UA_{bui} is the overall heat loss coefficient of the specific building, $\Delta T_{\mathrm{SH,pen}}$ are the temperature degrees below the defined minimum room temperature of 19.5 °C, $\vartheta_{\mathrm{room}}$ is the actual room temperature, $\dot{m}_{\mathrm{DHW,loc}}$ is the flow rate for hot water tappings at the specific location, $c_{p,\mathrm{w}}$ is the specific heat capacity of water, $\Delta T_{\mathrm{DHW,pen}}$ are the missing temperature degrees for meeting the domestic hot water set temperature $\vartheta_{\mathrm{DHW,set}}$ and ϑ_{DHW} is the actual domestic hot water temperature [Haller, 2013]. As the same SHP system with different implemented control strategies can reach different values for $SPF_{\mathrm{SHP+,pen}}$, the $SPF_{\mathrm{SHP+,pen}}$ can also be used for the **efficiency rating of SHP control strategies for heating applications**.

Furthermore, in SHP systems with self-consumption of electricity generated by PV or PVT, a grid-related SPF of the overall SHP system with penalties $SPF_{\mathrm{SHP+,pen,grid}}$ for a period of one year can be defined as follows:

$$SPF_{\mathrm{SHP+,pen,grid}} = \frac{Q_{\mathrm{SH,useful}} + Q_{\mathrm{DHW,useful}}}{W_{\mathrm{el,grid,SHP}}}. \tag{2.51}$$

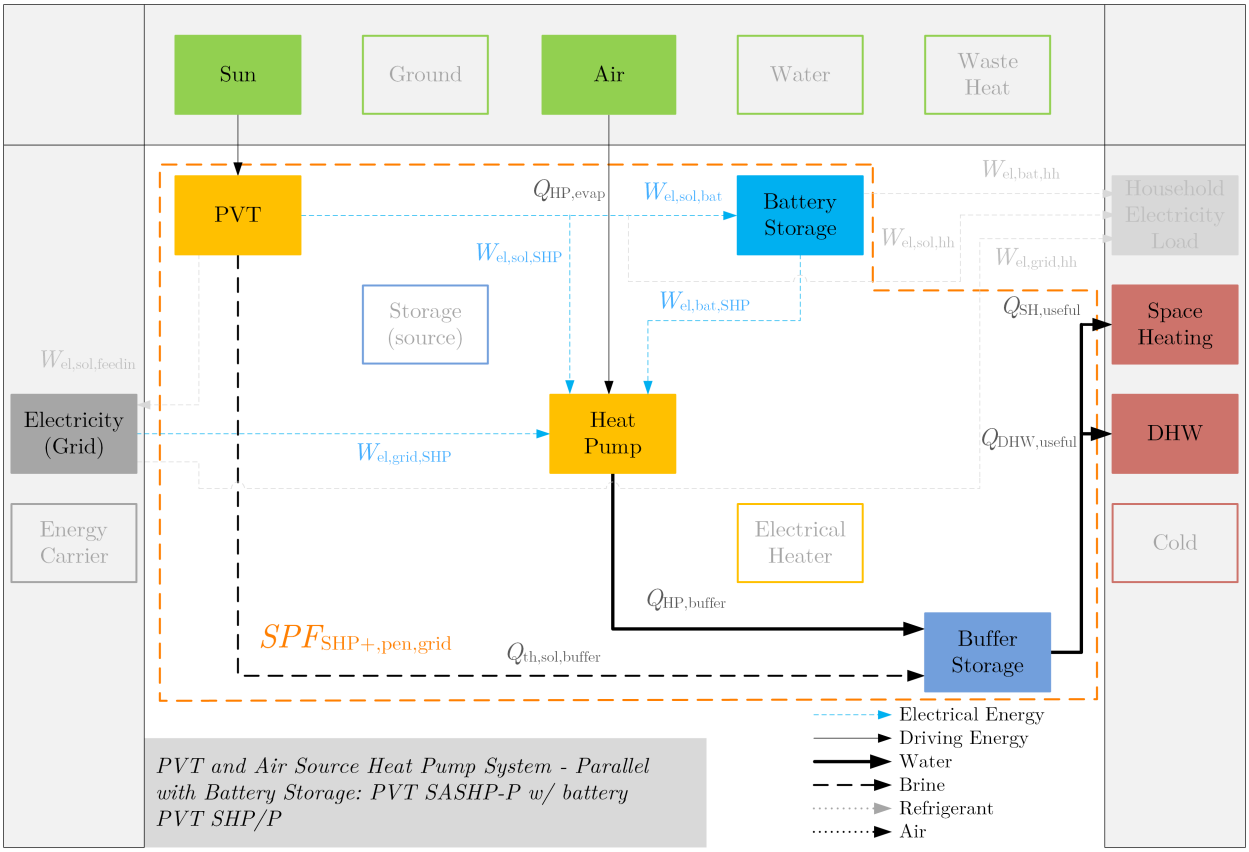

Figure 2.52: System boundary (orange dashed line) for the grid-related seasonal performance factor of the overall SHP system with penalties for the example of a PVT SASHP-P system with battery storage.

The grid-related SPF of the overall SHP system with penalties rewards the self-consumption of solar electricity generated by PV or PVT used for the SHP system in the same way as solar thermal heat provided to the SHP system since the benefit of thermal solar energy supply by solar thermal or PVT collectors is also a reduction of the delivered electricity from the grid. Regarding the system boundary shown in Figure 2.52 for the example of a PVT SASHP-P system with battery storage, the self-consumed solar electricity is included in the inside of the system boundary [Zenhäusern, 2020]. The grid-related SPF of the overall SHP system with penalties offers the possibility to evaluate the system performance for heating applications related to the delivered electricity from the grid regardless of the used solar energy technology and is especially useful to compare solar thermal and heat pump systems with PV or PVT and heat pump systems (and combinations). As a result, it is recommended as KPI for the **efficiency comparison of different SHP concepts for heating applications** and thus the *analysis of the thermal energy supply of a building.*

In addition, the solar grid feed-in electricity $W_{\mathrm{el,sol,feedin}}$ could be taken into account and a net SPF of the overall SHP system with penalties $SPF_{\mathrm{SHP+,pen,net}}$ for a period of one year could be defined with:

$$SPF_{\mathrm{SHP+,pen,net}} = \frac{Q_{\mathrm{SH,useful}} + Q_{\mathrm{DHW,useful}}}{W_{\mathrm{el,grid,SHP}} - W_{\mathrm{el,sol,feedin}}}. \tag{2.52}$$

As the values of this figure can turn negative if the grid feed-in is higher than the delivered electricity, it could no longer be interpreted as a performance factor [Zenhäusern, 2020], and thus it is not useful for SHP system evaluation. Furthermore, the surplus energy fed into the grid is not only related to heating applications and it should only be considered in performance figures for the evaluation of the overall electrical energy supply or the thermal and electrical energy supply of buildings including household electricity load (consumption).

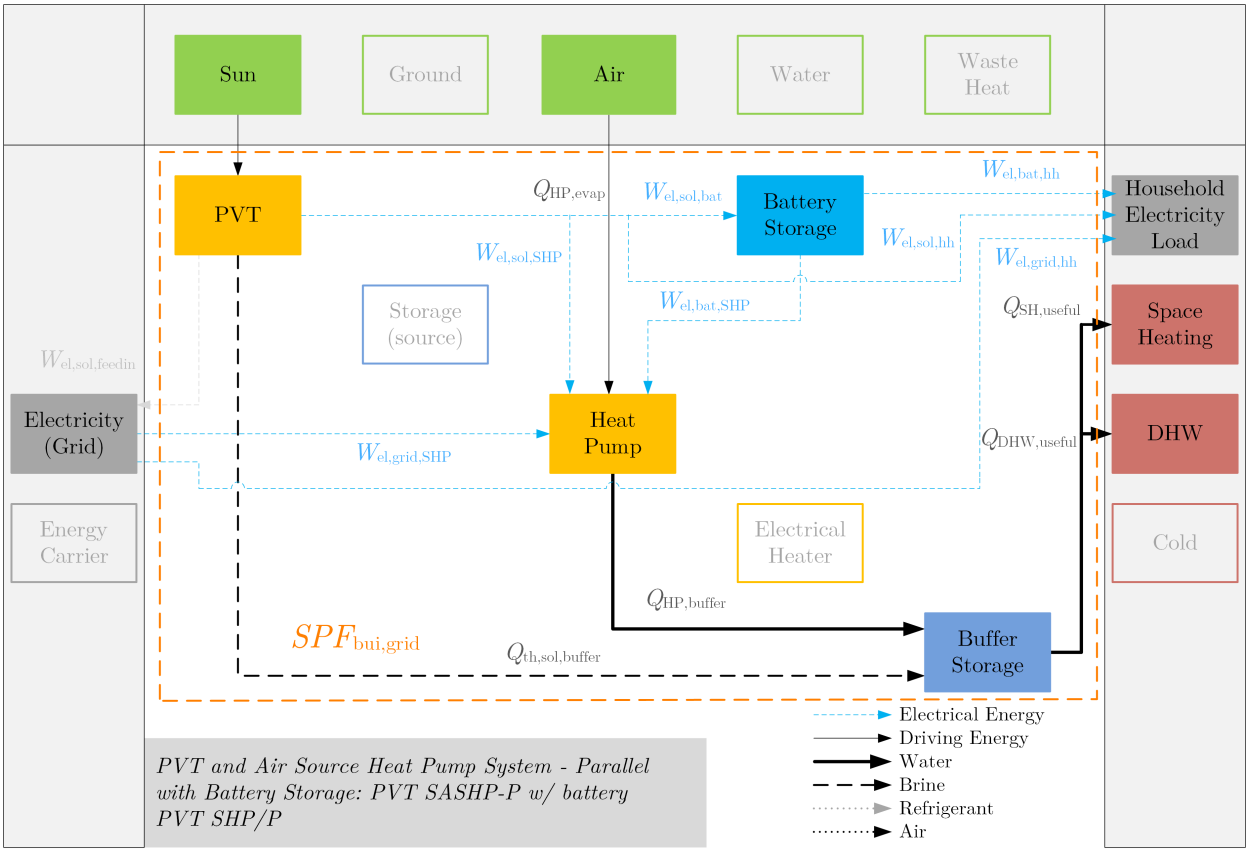

Figure 2.53: System boundary (orange dashed line) for the grid-related seasonal performance factor of the building for the example of a PVT SASHP-P system with battery storage.

For the analysis of the *thermal and electrical energy supply of a building*, the grid-related SPF of the overall SHP system with penalties can be extended by the household electricity load and its grid-related energy supply and a grid-related SPF of the building $SPF_{\mathrm{bui,grid}}$ regarding the **energy efficiency and the solar thermal and electrical energy use of a building** for a period of one year can be introduced as follows (cf. Figure 2.53):

$$SPF_{\mathrm{bui,grid}} = \frac{Q_{\mathrm{SH,useful}} + Q_{\mathrm{DHW,useful}} + W_{\mathrm{el,hh}}}{W_{\mathrm{el,grid,SHP}} + W_{\mathrm{el,grid,hh}}}, \tag{2.53}$$

where $W_{\mathrm{el,grid,hh}}$ is the used electrical energy from the grid to cover the household electricity load. At this, the household electricity demand $W_{\mathrm{el,hh}}$ is equal to the household electricity load and can be calculated with:

$$W_{\mathrm{el,hh}} = W_{\mathrm{el,sol,hh}} + W_{\mathrm{el,bat,hh}} + W_{\mathrm{el,grid,hh}}, \tag{2.54}$$

where $W_{\mathrm{el,sol,hh}}$ is the self-consumed solar electricity generation to cover the household electricity load and $W_{\mathrm{el,bat,hh}}$ is the used electrical energy from the battery storage to cover the household electricity load. As mentioned before for the net SPF of the overall SHP system with penalties, the values of an extended figure considering the solar grid feed-in electricity can turn negative if the grid feed-in is higher than the delivered electricity to the building and thus it could no longer be interpreted as a performance factor and is also not useful for further evaluations. In addition, the definition of a non grid-related SPF of the building is not useful as the useful energy output (household electricity load) is equal to the final energy input for the household electricity supply (used electrical energy from the grid and PV/PVT self-consumption to cover the household electricity load).

For the evaluation of the **performance of the heat pump** itself, the SPF of the heat pump SPF_{HP} indicates the amount of useful energy output of the heat pump Q_{HP} divided by the amount of electricity consumption of the heat pump $W_{\mathrm{el,HP}}$ for a period of one year:

$$SPF_{\mathrm{HP}} = \frac{Q_{\mathrm{HP}}}{W_{\mathrm{el,HP}}}. \tag{2.55}$$

2.4.1.2 Fractional Energy Savings for Heating Applications

For the *comparison of SHP systems or SHP systems with conventional (non-renewable) heating systems*, the fractional energy savings for heating applications, which quantifies the **reduction of the delivered energy for heating applications** achieved by the use of a SHP system instead of a reference SHP or conventional heating system, are often used as performance indicator, usually for a period of one year. The fractional energy savings for heating applications $f_{\mathrm{sav,heating}}$ can be defined as the difference in energy consumption for heating applications of delivered energy between the reference system $E^{\mathrm{ref}}_{\mathrm{del,heating}}$ and the considered SHP system $E^{\mathrm{SHP}}_{\mathrm{del,heating}}$ to the energy consumption for heating applications of delivered energy by the reference system:

$$f_{\mathrm{sav,heating}} = \frac{E^{\mathrm{ref}}_{\mathrm{del,heating}} - E^{\mathrm{SHP}}_{\mathrm{del,heating}}}{E^{\mathrm{ref}}_{\mathrm{del,heating}}}. \tag{2.56}$$

At this, the energy consumption of delivered energy for heating applications by the considered SHP system can be calculated with the used electrical energy from the grid for the supply of the SHP system:

$$E^{\mathrm{SHP}}_{\mathrm{del,heating}} = W_{\mathrm{el,grid,SHP}}. \tag{2.57}$$

If the reference system is a SHP system, the energy consumption of delivered energy for heating applications by the reference system is calculated as described in Equation 2.57 using values of the reference SHP system. For the comparison of SHP systems with conventional heating systems like gas-fired or oil-fired heating systems, the energy consumption of delivered energy for heating applications by a conventional reference heating system can be estimated with:

$$E^{\mathrm{ref}}_{\mathrm{del,heating}} = \frac{Q_{\mathrm{SH}} + Q_{\mathrm{DHW}}}{\eta_{\mathrm{ref}}} + W_{\mathrm{el,grid,ref}}, \tag{2.58}$$

where η_{ref} is the overall efficiency of the conventional reference heating system and $W_{\mathrm{el,grid,ref}}$ is the electrical energy from the grid for the supply of the conventional reference heating system (including pumps for space heating and domestic hot water preparation and additional controllers). At this, the overall efficiency of a gas-fired or oil-fired reference heating system is defined as ratio of useful heating energy output per final energy consumed by the heating system using the net calorific value. Nevertheless, the presented figures are difficult to interpret as the value of electrical energy and fuel energy is not equal.

2.4.1.3 Solar Thermal Fraction

For the evaluation of *thermal solar energy*, the solar thermal fraction $f_{\mathrm{th,sol}}$ is a useful performance figure to specify the share of **heating energy consumption that is covered directly by solar thermal and PVT systems**. It can be described as the ratio of thermal energy provided by solar thermal and PVT systems to the total energy consumption for heating applications in a SHP system, usually for a period of one year. For SHP systems with buffer storage and without direct use of the heat pump or an electric heating device to supply the space heating and domestic hot water systems, the solar thermal fraction can be defined as the amount of solar thermal energy delivered to the buffer storage by solar thermal and PVT collectors with respect to the total energy delivered to the buffer storage:

$$f_{\mathrm{th,sol}} = \frac{Q_{\mathrm{th,sol,buffer}}}{Q_{\mathrm{th,sol,buffer}} + Q_{\mathrm{HP,buffer}} + Q_{\mathrm{EH,buffer}}}, \tag{2.59}$$

where $Q_{\mathrm{th,sol,buffer}}$ is the solar thermal energy delivered to the buffer storage, $Q_{\mathrm{HP,buffer}}$ is the energy delivered to the buffer storage by the heat pump and $Q_{\mathrm{EH,buffer}}$ is the energy delivered to the buffer storage by a direct electric heating element (cf. Figure 2.54). Here and in the following, the index *sol* is used for solar thermal heat generation of both solar thermal collectors and PVT collectors. It is recommended to use the buffer storage as system boundary to consider thermal losses of the buffer storage and the solar thermal circuit in the evaluation of the solar thermal fraction. With this system boundary, thermal losses of the solar thermal circuit reduce the solar thermal energy delivered to the buffer storage and thus reduce the solar thermal fraction. In addition, thermal losses of the buffer storage are assigned to all systems that supply the buffer storage with heat. In contrast, if the SHP system is chosen as system boundary and the solar thermal energy output is related to the useful energy output of the system, the thermal losses of the buffer storage are not considered and thus the solar thermal fraction is higher for high thermal losses of the buffer storage. Furthermore, if the thermal losses of the buffer storage are subtracted from the solar thermal energy output, the losses are only assigned to the solar thermal system.

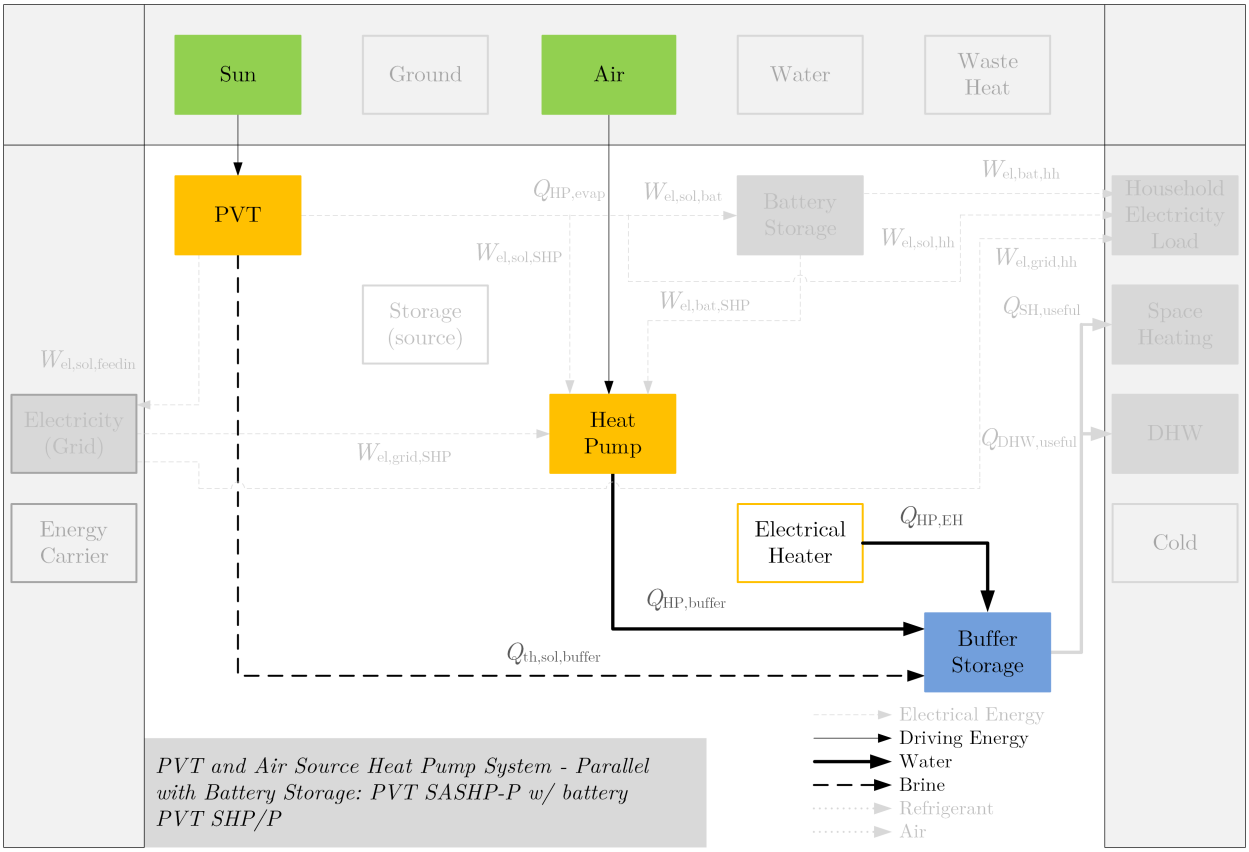

Figure 2.54: Energy flows for the determination of the solar thermal fraction (with optional direct electric heating element) for the example of a PVT SASHP-P system with battery storage.

2.4.1.4 Electrical Self-Sufficiency Rate and Self-Consumption Rate

For the evaluation of *electrical solar energy*, the electrical self-sufficiency rate (SSR) is a useful performance figure to specify the share of **electricity consumption that is covered by PV and PVT systems**. It can be defined as ratio of on-site generated and consumed solar electricity with respect to the electricity consumption of the household, the SHP system or the building (both applications), usually for a period of one year. Within SHP systems without additional energy purchase to the delivered electricity, the SSR of the building provides information on the thermal and electrical energy self-sufficiency of a building, whereas the SSR of the household electricity focus on the electrical self-sufficiency and the SSR of the SHP system focus on the self-sufficiency for heating applications. The SSR of the building SSR_{bui} can be determined as follows (cf. Figure 2.55):

$$SSR_{\mathrm{bui}} = \frac{W_{\mathrm{el,sol,bui}} + W_{\mathrm{el,bat,bui}}}{W_{\mathrm{el,sol,bui}} + W_{\mathrm{el,bat,bui}} + W_{\mathrm{el,grid,bui}}} \tag{2.60}$$

with the self-consumed solar electricity generation of the building

$$W_{\mathrm{el,sol,bui}} = W_{\mathrm{el,sol,SHP}} + W_{\mathrm{el,sol,hh}}, \tag{2.61}$$

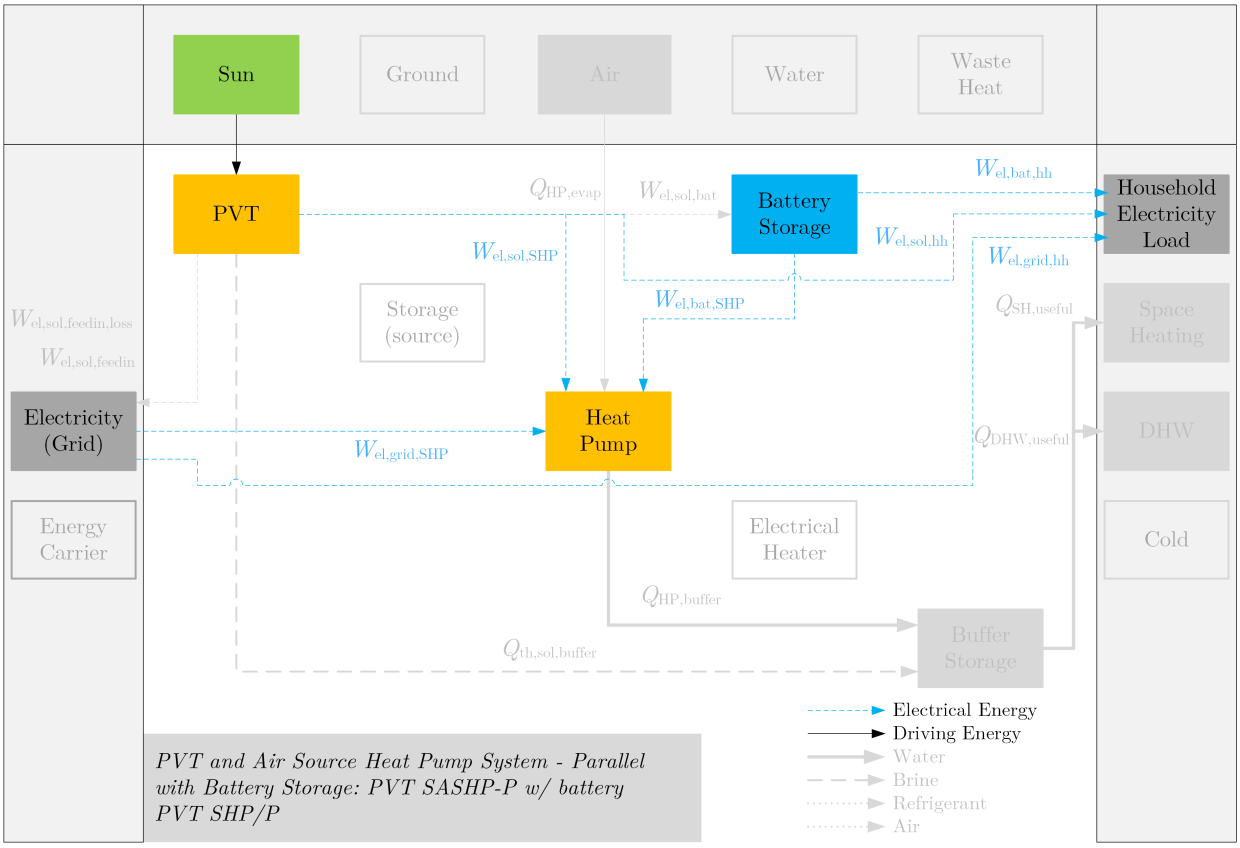

Figure 2.55: Energy flows for the determination of the electrical SSR for the example of a PVT SASHP-P system with battery storage.

the used electrical energy from the battery storage for the supply of the building

$$W_{\mathrm{el,bat,bui}} = W_{\mathrm{el,bat,SHP}} + W_{\mathrm{el,bat,hh}} \tag{2.62}$$

and the used electrical energy from the grid for the supply of the building

$$W_{\mathrm{el,grid,bui}} = W_{\mathrm{el,grid,SHP}} + W_{\mathrm{el,grid,hh}}. \tag{2.63}$$

At this, the solar grid feed-in electricity is not taken into account to avoid suggesting that the building is self-sufficient if it generates more electricity than it consumes but still needs electricity from the grid. Furthermore, battery losses are not included in this SSR definition and thus high battery losses cannot lead to higher SSR values. In addition, the SSR of the household electricity SSR_{hh} can be calculated with:

$$SSR_{\mathrm{hh}} = \frac{W_{\mathrm{el,sol,hh}} + W_{\mathrm{el,bat,hh}}}{W_{\mathrm{el,sol,hh}} + W_{\mathrm{el,bat,hh}} + W_{\mathrm{el,grid,hh}}} \tag{2.64}$$

and the SSR of the SHP system SSR_{SHP} with:

$$SSR_{\mathrm{SHP}} = \frac{W_{\mathrm{el,sol,SHP}} + W_{\mathrm{el,bat,SHP}}}{W_{\mathrm{el,sol,SHP}} + W_{\mathrm{el,bat,SHP}} + W_{\mathrm{el,grid,SHP}}}. \tag{2.65}$$

The SSR of the household electricity can be used for the *analysis of the electrical energy supply of the household* without consideration of the electrical energy usage for heating applications whereas the SSR of the SHP system can be used for the *analysis of the electrical energy supply for heating applications*. In addition, the SSRs are helpful for the **analysis of control strategies of the building energy management system** (BEMS).

The electrical self-consumption rate (SCR) is a performance figure to specify the share of **generated PV and PVT electricity that is consumed on-site**. It can be defined as the ratio of on-site generated and consumed solar electricity with respect to the total on-site solar electricity generation, usually for a period of one year. A distinction must be made, however, between the SCR including or excluding battery losses for the definition of electrical self-consumption.

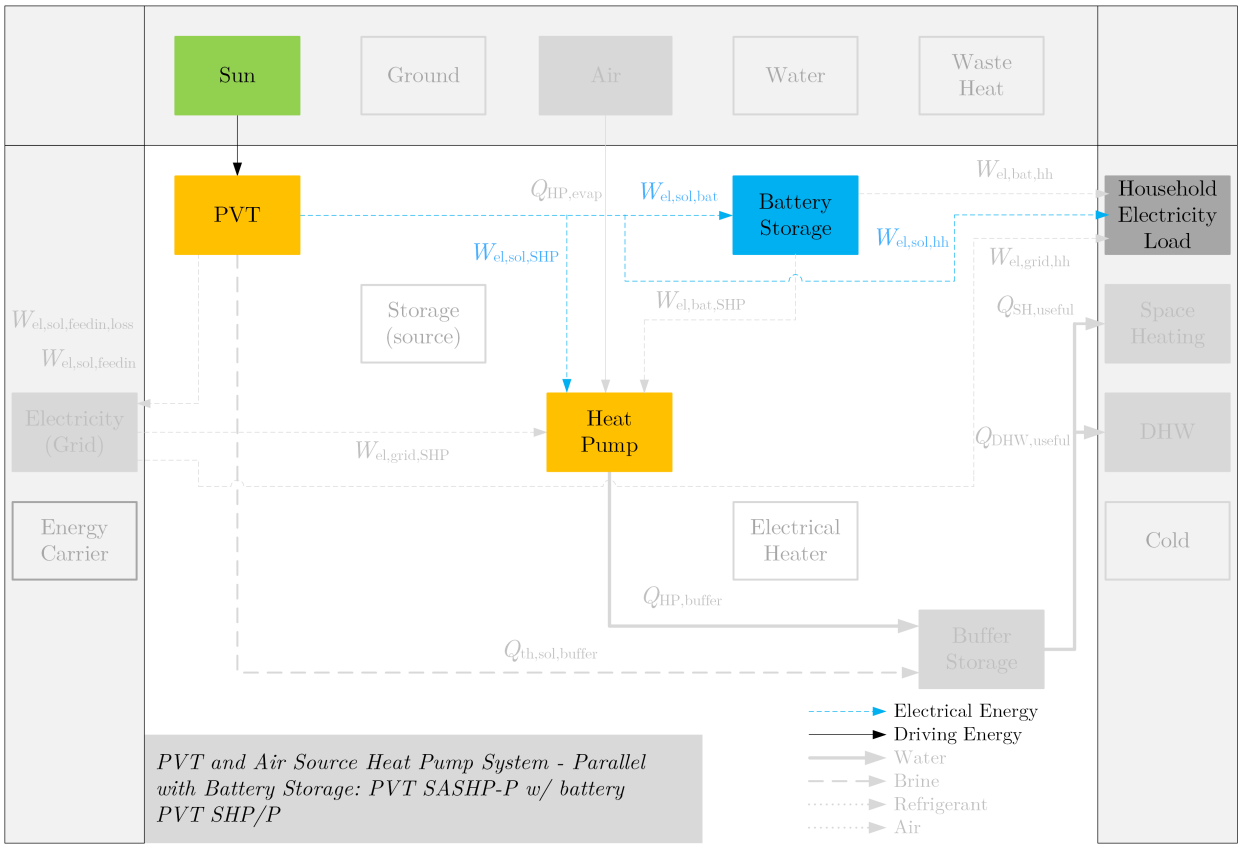

Figure 2.56: Energy flows for the definition of self-consumption for the determination of the SCR including battery losses for the example of a PVT SASHP-P system with battery storage.

The SCR for a building including battery losses $SCR_{\mathrm{bui,bat,loss}}$ can be determined with (cf. Figure 2.56):

$$SCR_{\mathrm{bui,bat,loss}} = \frac{W_{\mathrm{el,sol,SHP}} + W_{\mathrm{el,sol,hh}} + W_{\mathrm{el,sol,bat}}}{W_{\mathrm{el,sol}}}, \tag{2.66}$$

where $W_{\mathrm{el,sol}}$ is the total on-site solar electricity generation (including feed-in losses) and $W_{\mathrm{el,sol,bat}}$ is the self-consumed solar electricity generation for charging the battery storage. For AC-coupled residential PV and PVT battery systems, the AC-sided total on-site solar electricity generation $W_{\mathrm{el,sol,AC}}$ is used for $W_{\mathrm{el,sol}}$ as it represents the useful generated solar

electricity without losses of the solar inverter. It can be calculated with:

$$W_{\text{el,sol,AC}} = W_{\text{el,sol,SHP}} + W_{\text{el,sol,hh}} + W_{\text{el,sol,bat}} + W_{\text{el,sol,feedin}} + W_{\text{el,sol,feedin,loss}}, \tag{2.67}$$

where $W_{\text{el,sol,feedin,loss}}$ are the grid feed-in losses of solar electricity. As battery losses are included in this SCR definition, high battery losses can lead to higher SCR values even if only smaller amounts of the stored electrical energy are used to supply the building. Hence, it is recommended to use the following SCR definitions excluding battery losses, especially for the optimization of control strategies.

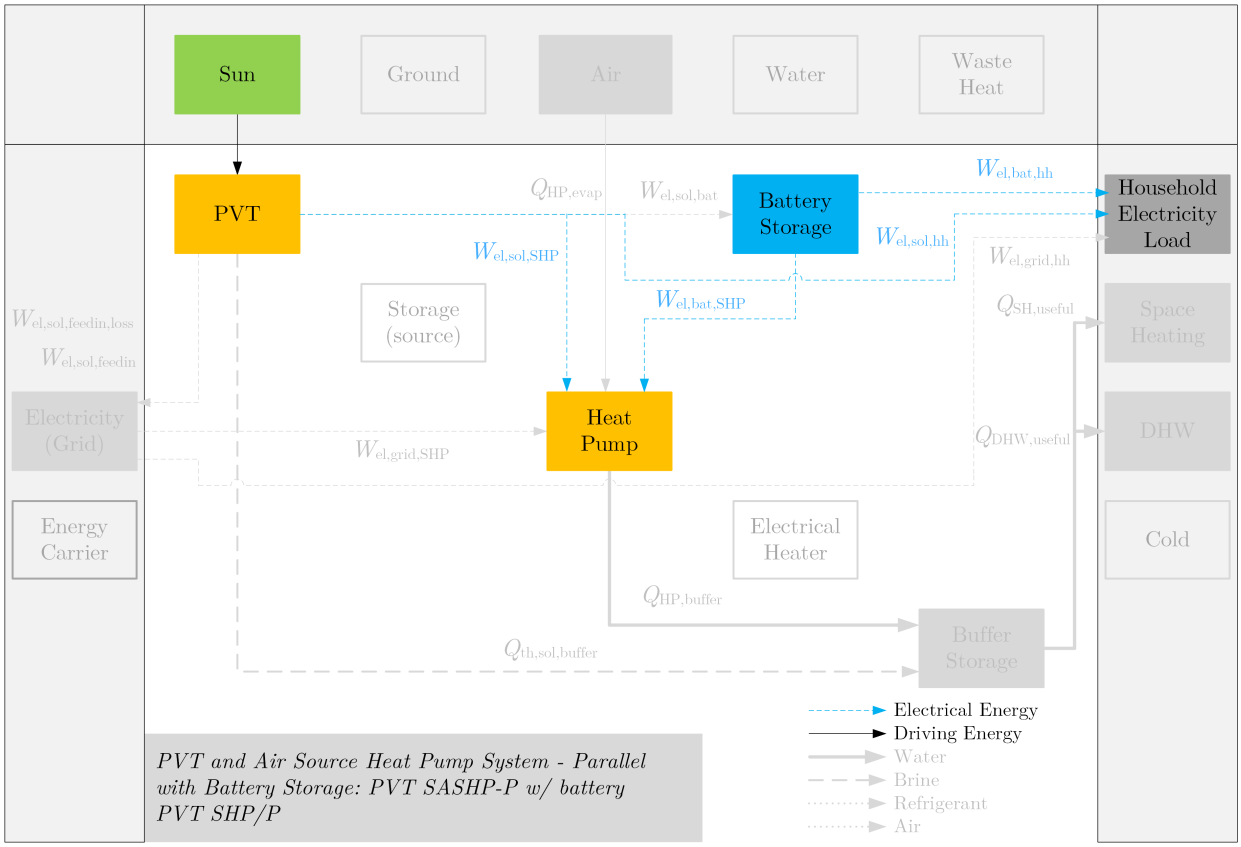

Figure 2.57: Energy flows for the definition of self-consumption for the determination of the SCR excluding battery losses for the example of a PVT SASHP-P system with battery storage.

The SCR for a building excluding battery losses SCR_{bui} can be introduced as (cf. Figure 2.57):

$$SCR_{\text{bui}} = \frac{W_{\text{el,sol,bui}} + W_{\text{el,bat,bui}}}{W_{\text{el,sol}}}. \tag{2.68}$$

In addition, the SCR for the household electricity SCR_{hh} can be calculated with:

$$SCR_{\text{hh}} = \frac{W_{\text{el,sol,hh}} + W_{\text{el,bat,hh}}}{W_{\text{el,sol}}} \tag{2.69}$$

and the SCR for the SHP system SCR_{SHP} with:

$$SCR_{\mathrm{SHP}} = \frac{W_{\mathrm{el,sol,SHP}} + W_{\mathrm{el,bat,SHP}}}{W_{\mathrm{el,sol}}}. \tag{2.70}$$

For AC-coupled residential PV and PVT battery systems, the AC-sided total on-site solar electricity generation $W_{\mathrm{el,sol,AC}}$ is also used for $W_{\mathrm{el,sol}}$ as it represents the useful generated solar electricity without losses of the solar inverter. The SCRs can be used for the *analysis of solar electricity usage* and the **analysis of control strategies of the BEMS**.

2.4.1.5 Specific Solar Yields and Utilization Ratios

For the evaluation of *thermal and electrical solar energy*, the specific solar yields and utilization ratios are additional performance figures to assess the **utilization of the available solar irradiance**. The *solar thermal energy generation* of solar thermal and PVT systems can be quantified by means of the specific solar thermal yield $q_{\mathrm{th,sol}}$ that can be defined in SHP systems as ratio of useful solar thermal energy delivered to the buffer storage $Q_{\mathrm{th,sol,buffer}}$ and the heat source $Q_{\mathrm{th,sol,source}}$ (e.g. the ice storage in SISHP systems) with respect to the gross solar thermal and PVT collector area $A_{\mathrm{th,sol}}$, usually for a period of one year:

$$q_{\mathrm{th,sol}} = \frac{Q_{\mathrm{th,sol,buffer}} + Q_{\mathrm{th,sol,source}}}{A_{\mathrm{th,sol}}}. \tag{2.71}$$

In addition, the *solar electrical energy generation* of PV and PVT systems can be quantified by means of the specific solar electrical yield $w_{\mathrm{el,sol}}$ that can be defined as ratio of on-site solar electricity generation (self-consumed or fed into the grid, without feed-in losses) with respect to the gross PV module and PVT collector area $A_{\mathrm{el,sol}}$, usually for a period of one year:

$$w_{\mathrm{el,sol}} = \frac{W_{\mathrm{el,sol,SHP}} + W_{\mathrm{el,sol,hh}} + W_{\mathrm{el,sol,bat}} + W_{\mathrm{el,sol,feedin}}}{A_{\mathrm{el,sol}}}. \tag{2.72}$$

Within this definition of the specific solar electrical yield, battery losses are included since the thermal losses of the buffer storage or the heat source in the definition of the specific solar thermal yield are also included and thus these values are more consistent. Furthermore, in contrast to the SCR, the specific solar electrical yield focus on the *analysis of the solar electricity generation* and not the solar electricity usage. In addition, the grid feed-in losses are excluded and can be interpreted as a limit for solar electrical energy generation like the maximum buffer storage temperature for storage protection in solar thermal systems.

Following Lämmle [2018], the solar thermal utilization ratio $UR_{\mathrm{th,sol}}$ with respect to the global solar irradiance in the solar module and collector plane G can be defined with:

$$UR_{\mathrm{th,sol}} = \frac{q_{\mathrm{th,sol}}}{\int G \,\mathrm{d}t} \tag{2.73}$$

and the solar electrical utilization ratio $UR_{\mathrm{el,sol}}$ with:

$$UR_{\mathrm{el,sol}} = \frac{w_{\mathrm{el,sol}}}{\int G \,\mathrm{d}t}. \tag{2.74}$$

A combined solar thermal and electrical specific solar yield or utilization ratio is not

recommended in this work as the value of electrical and thermal energy is not equal and thus a combined figure that simply sums up the thermal and electrical energy is difficult to interpret.

2.4.1.6 Net Energy Demand and Net Delivered Energy

The main performance indicator for the *thermal and electrical energy demand of a building* is the net energy demand indicator as defined in Equation 2.3 for a period of one year. Furthermore, the net delivered energy indicator from Section 2.1.2, defined in Equation 2.15, can be used to analyze the **import/export final energy balance of a building** for a period of one year. At this, the net delivered energy from Equation 2.13 can be calculated for a building with SHP system as follows:

$$E^{\mathrm{SHP}}_{\mathrm{bui,del,net}} = E^{\mathrm{SHP}}_{\mathrm{bui,del,el}} - E^{\mathrm{SHP}}_{\mathrm{bui,exp,el}} \tag{2.75}$$

with the delivered electrical energy to the building with SHP system (from the grid)

$$E^{\mathrm{SHP}}_{\mathrm{bui,del,el}} = W_{\mathrm{el,grid,SHP}} + W_{\mathrm{el,grid,hh}} \tag{2.76}$$

and the exported electrical energy of the building with SHP system (to the grid)

$$E^{\mathrm{SHP}}_{\mathrm{bui,exp,el}} = W_{\mathrm{el,sol,feedin}}. \tag{2.77}$$

For a building with conventional gas-fired or oil-fired heating system without PV as reference building, the net delivered energy can be determined as follows:

$$E^{\mathrm{ref}}_{\mathrm{bui,del,net}} = E^{\mathrm{ref}}_{\mathrm{bui,del,fuel}} + E^{\mathrm{ref}}_{\mathrm{bui,del,el}} \tag{2.78}$$

with the delivered fuel energy of the building with reference system

$$E^{\mathrm{ref}}_{\mathrm{bui,del,fuel}} = \frac{Q_{\mathrm{SH}} + Q_{\mathrm{DHW}}}{\eta_{\mathrm{ref}}} \tag{2.79}$$

and the delivered electrical energy to the building with reference system (from the grid)

$$E^{\mathrm{ref}}_{\mathrm{bui,del,el}} = W_{\mathrm{el,grid,ref}} + W_{\mathrm{el,hh}}. \tag{2.80}$$

Nevertheless, it is proposed to use the performance indicators described in Section 2.1.3 and adapted for SHP systems in Section 2.4.2 for the thermal and electrical energy performance rating of a building, especially in the context of nZEBs, and thus it is recommended to analyze the primary energy use and CO_2 emissions instead of the final energy use of a building.

2.4.2 Environmental Impact

The environmental impact analysis of SHP systems and buildings requires further investigations on the usage of natural energy resources and the emission of GHGs. In this context, the primary energy use, the RER and the CO_2 emissions as result of the energy use are of particular importance. For the nZEB rating of a building and the analysis in this work, the described equations in the following are used to calculate the primary energy use and CO_2

emissions indicators as well as the RER based on total primary energy from Section 2.1.3 for a period of one year. In addition, further fractional savings indicators for the comparison of buildings with SHP systems and buildings with a reference heating system are defined in this section.

The total primary energy use of a building from Equation 2.17 is an indicator for the performance of the technical building system and can be calculated for a building with SHP system as follows:

$$E^{\mathrm{SHP}}_{\mathrm{pe,bui,tot}} = E^{\mathrm{SHP}}_{\mathrm{bui,del,el}}\, f_{\mathrm{pe,del,tot,el}} + E^{\mathrm{SHP}}_{\mathrm{bui,ren,self,th}} + E^{\mathrm{SHP}}_{\mathrm{bui,ren,self,el}} \tag{2.81}$$

with the delivered electrical energy to the building with SHP system from Equation 2.76, the thermal self-consumed on-site renewable energy

$$E^{\mathrm{SHP}}_{\mathrm{bui,ren,self,th}} = Q_{\mathrm{HP,evap}} + Q_{\mathrm{th,sol,buffer}} \tag{2.82}$$

and the electrical self-consumed on-site renewable energy

$$E^{\mathrm{SHP}}_{\mathrm{bui,ren,self,el}} = W_{\mathrm{el,sol,SHP}} + W_{\mathrm{el,bat,SHP}} + W_{\mathrm{el,sol,hh}} + W_{\mathrm{el,bat,hh}}, \tag{2.83}$$

where $f_{\mathrm{pe,del,tot,el}}$ is the total primary energy factor for delivered electrical energy from the grid and $Q_{\mathrm{HP,evap}}$ is the heat source energy of the heat pump evaporator (from ambient air, ground or ice storage). For a building with conventional gas-fired or oil-fired heating system without PV as reference building, the total primary energy use can be determined with the delivered fuel energy and electrical energy of the building with reference system from Equation 2.79 and Equation 2.80 as follows:

$$E^{\mathrm{ref}}_{\mathrm{pe,bui,tot}} = E^{\mathrm{ref}}_{\mathrm{bui,del,fuel}}\, f_{\mathrm{pe,del,tot,fuel}} + E^{\mathrm{ref}}_{\mathrm{bui,del,el}}\, f_{\mathrm{pe,del,tot,el}}, \tag{2.84}$$

where $f_{\mathrm{pe,del,tot,fuel}}$ is the total primary energy factor for delivered fuel energy of the reference heating system, e.g. gas or oil.

The non-renewable primary energy use of a building from Equation 2.20 is an indicator for the use of on-site renewable energy sources without compensation by exporting energy and can be calculated for a building with SHP system using the delivered electrical energy to the building with SHP system from Equation 2.76 as follows:

$$E^{\mathrm{SHP}}_{\mathrm{pe,bui,nren}} = E^{\mathrm{SHP}}_{\mathrm{bui,del,el}}\, f_{\mathrm{pe,del,nren,el}}, \tag{2.85}$$

where $f_{\mathrm{pe,del,nren,el}}$ is the non-renewable primary energy factor for delivered electrical energy from the grid, and for a building with conventional gas-fired or oil-fired heating system without PV as reference building using the delivered fuel energy and electrical energy of the building with reference system from Equation 2.79 and Equation 2.80 with:

$$E^{\mathrm{ref}}_{\mathrm{pe,bui,nren}} = E^{\mathrm{ref}}_{\mathrm{bui,del,fuel}}\, f_{\mathrm{pe,del,nren,fuel}} + E^{\mathrm{ref}}_{\mathrm{bui,del,el}}\, f_{\mathrm{pe,del,nren,el}}, \tag{2.86}$$

where $f_{\mathrm{pe,del,fuel,nren}}$ is the non-renewable primary energy factor for delivered fuel energy of the reference heating system, e.g. gas or oil.

Furthermore, the net non-renewable primary energy use of a building from Equation 2.22 considers the compensation by exporting energy and can be calculated for a building with SHP system using the delivered electrical energy to the building with SHP system from Equation 2.76 and the exported electrical energy of the building with SHP system from

Equation 2.77 as follows:

$$E^{\mathrm{SHP}}_{\mathrm{pe,bui,nren,net}} = E^{\mathrm{SHP}}_{\mathrm{bui,del,el}}\, f_{\mathrm{pe,del,nren,el}} - E^{\mathrm{SHP}}_{\mathrm{bui,exp,el}}\, f_{\mathrm{pe,exp,nren,el}}, \tag{2.87}$$

where $f_{\mathrm{pe,exp,nren,el}}$ is the non-renewable primary energy factor for delivered electrical energy from the grid compensated by exported solar electricity which can be set equal to the non-renewable primary energy factor for delivered electrical energy from the grid $f_{\mathrm{pe,exp,nren,el}} = f_{\mathrm{pe,del,nren,el}}$ (substitution value approach). For a building with conventional gas-fired or oil-fired heating system without PV as reference building the net non-renewable primary energy use is equal to the non-renewable primary energy use from Equation 2.86.

For the comparison of a building with SHP system and a building with reference system, the fractional primary energy savings $f_{\mathrm{sav,pe},i}$, which quantifies the reduction of the used primary energy achieved by the use of the SHP system instead of a reference system, can be determined with:

$$f_{\mathrm{sav,pe},i} = 1 - \frac{E^{\mathrm{SHP}}_{\mathrm{pe,bui},i}}{E^{\mathrm{ref}}_{\mathrm{pe,bui},i}}, \tag{2.88}$$

where i can be equal to tot (total), nren (non-renewable) or nren,net (net non-renewable). If the reference system is a SHP system, the considered primary energy use by the building with conventional gas-fired or oil-fired heating system without PV as reference building is replaced by the primary energy use of the building with reference SHP system that is calculated as described for SHP systems using values of the reference SHP system.

The RER based on total primary energy of the building from Equation 2.25 can be calculated for a building with SHP system as follows:

$$RER^{\mathrm{SHP}}_{\mathrm{pe,bui}} = \frac{E^{\mathrm{SHP}}_{\mathrm{bui,ren,th}} + E^{\mathrm{SHP}}_{\mathrm{bui,ren,el}} + E^{\mathrm{SHP}}_{\mathrm{bui,del,el}}\,(f_{\mathrm{pe,del,tot,el}} - f_{\mathrm{pe,del,nren,el}})}{E^{\mathrm{SHP}}_{\mathrm{bui,ren,th}} + E^{\mathrm{SHP}}_{\mathrm{bui,ren,el}} + E^{\mathrm{SHP}}_{\mathrm{bui,del,el}}\, f_{\mathrm{pe,del,tot,el}} - E^{\mathrm{SHP}}_{\mathrm{bui,exp,el}}\, f_{\mathrm{pe,exp,tot,el}}} \tag{2.89}$$

with the thermal renewable energy produced on-site of the building with SHP system (self-consumed)

$$E^{\mathrm{SHP}}_{\mathrm{bui,ren,th}} = Q_{\mathrm{HP,evap}} + Q_{\mathrm{th,sol,buffer}}, \tag{2.90}$$

the electrical renewable energy produced on-site of the building with SHP system (self-consumed or fed into the grid)

$$E^{\mathrm{SHP}}_{\mathrm{bui,ren,el}} = W_{\mathrm{el,sol,SHP}} + W_{\mathrm{el,bat,SHP}} + W_{\mathrm{el,sol,hh}} + W_{\mathrm{el,bat,hh}} + W_{\mathrm{el,sol,feedin}}, \tag{2.91}$$

the delivered electrical energy to the building with SHP system from Equation 2.76 and the exported electrical energy of the building with SHP system from Equation 2.77, where $f_{\mathrm{pe,exp,tot,el}}$ is the total primary energy factor for delivered electrical energy from the grid compensated by exported solar electricity which can be set equal to the total primary energy factor for delivered electrical energy from the grid $f_{\mathrm{pe,exp,tot,el}} = f_{\mathrm{pe,del,tot,el}}$ (substitution value approach).

The CO_2 emissions, expressed in CO_2 equivalent, can be used for the rating of the global warming potential of a building or system. The CO_2 emissions as result of the energy use in the building without compensation by exported energy from Equation 2.26 can be calculated for a building with SHP system using the delivered electrical energy to the building with

SHP system from Equation 2.76 as follows:

$$m^{\mathrm{SHP}}_{\mathrm{CO_2,bui}} = E^{\mathrm{SHP}}_{\mathrm{bui,del,el}}\, f_{\mathrm{CO_2,del,el}}, \tag{2.92}$$

where $f_{\mathrm{CO_2,del,el}}$ is the CO_2 emission coefficient for delivered electrical energy from the grid, and for a building with conventional gas-fired or oil-fired heating system without PV as reference building using the delivered fuel energy and electrical energy of the building with reference system from Equation 2.79 and Equation 2.80 with:

$$m^{\mathrm{ref}}_{\mathrm{CO_2,bui}} = E^{\mathrm{ref}}_{\mathrm{bui,del,fuel}}\, f_{\mathrm{CO_2,del,fuel}} + E^{\mathrm{ref}}_{\mathrm{bui,del,el}}\, f_{\mathrm{CO_2,del,el}}, \tag{2.93}$$

where $f_{\mathrm{CO_2,del,fuel}}$ is the CO_2 emission coefficient for delivered fuel energy of the reference heating system, e.g. gas or oil.

In addition, the net CO_2 emissions of the building with compensation by exported energy from Equation 2.28 can be calculated for a building with SHP system using the delivered electrical energy to the building with SHP system from Equation 2.76 and the exported electrical energy of the building with SHP system from Equation 2.77 with:

$$m^{\mathrm{SHP}}_{\mathrm{CO_2,bui,net}} = E^{\mathrm{SHP}}_{\mathrm{bui,del,el}}\, f_{\mathrm{CO_2,del,el}} - E^{\mathrm{SHP}}_{\mathrm{bui,exp,el}}\, f_{\mathrm{CO_2,exp,el}}, \tag{2.94}$$

where $f_{\mathrm{CO_2,exp,el}}$ is the CO_2 emission coefficient for delivered electrical energy from the grid compensated by exported solar electricity which can be set equal to the CO_2 emission coefficient for delivered electrical energy from the grid $f_{\mathrm{CO_2,exp,el}} = f_{\mathrm{CO_2,del,el}}$ (substitution value approach). For a building with conventional gas-fired or oil-fired heating system without PV as reference building the net CO_2 emissions are equal to the CO_2 emissions from Equation 2.93.

For the comparison of a building with SHP system and a building with reference system, the fractional CO_2 emission savings $f_{\mathrm{sav,CO_2}}$, which quantifies the reduction of CO_2 emissions achieved by the use of the SHP system instead of a reference system, can be determined with:

$$f_{\mathrm{sav,CO_2}} = 1 - \frac{m^{\mathrm{SHP}}_{\mathrm{CO_2,bui}}}{m^{\mathrm{ref}}_{\mathrm{CO_2,bui}}} \tag{2.95}$$

or with compensation by exported energy as net fractional CO_2 emission savings:

$$f_{\mathrm{sav,CO_2,net}} = 1 - \frac{m^{\mathrm{SHP}}_{\mathrm{CO_2,bui,net}}}{m^{\mathrm{ref}}_{\mathrm{CO_2,bui}}}. \tag{2.96}$$

If the reference system is a SHP system, the considered CO_2 emissions by the building with conventional gas-fired or oil-fired heating system without PV as reference building are replaced by the CO_2 emissions of the building with reference SHP system that are calculated as described for SHP systems using values of the reference SHP system.

2.4.3 Economic Efficiency

2.4.3.1 Levelized Cost of Heat

The levelized cost of heat (LCOH) is a standard metric for the economic analysis of heating systems and indicates the sum of heating related costs in relation to the considered energy

amount over the lifetime of a heating system. It is often used to determine the lowest heat generation cost over a certain time period for different technologies [Meyers et al., 2018] and is based on the levelized cost of electricity or energy method, which is a well-known approach in the electrical power sector [Louvet et al., 2018]. In general, the LCOH for a heating system in the residential sector (without tax rate, asset depreciation and residual value) can be calculated with (cf. [Louvet et al., 2018]):

$$LCOH = \frac{I_0 - S_0 + \sum_{t=1}^{T} \frac{O_t + M_t + F_t}{(1+r)^t}}{\sum_{t=1}^{T} \frac{Q_t}{(1+r)^t}}, \tag{2.97}$$

where I_0 is the initial investment, S_0 are subsidies and incentives, O_t are operation costs in year t, M_t are maintenance costs in year t, F_t are fuel costs in year t, r is the discount rate, T is the period of analysis and Q_t is the considered amount of heat in year t.

Furthermore, the LCOH can be calculated with a nominal (including inflation) or real discount rate r. The relation between the nominal discount rate r_{nom} and the real discount rate r_{real} can be expressed with the inflation rate i [Baez and Martínez, 2015]:

$$r_{\text{nom}} = r_{\text{real}}\,(1+i) + i. \tag{2.98}$$

In case of heating systems for single-family buildings, the total system costs are usually paid up front and the real discount rate is set to zero [Louvet et al., 2018]. With this assumption, the nominal discount rate is equal to the inflation rate ($r_{\text{nom}} = i$). As a consequence, LCOH values can be expressed in nominal terms and real terms, depending on the selected discount rate [Louvet et al., 2018]. At this, the cost variables have to be adapted accordingly using constant cash flows for real discount rates and current cash flows for nominal discount rates including inflationary effects [Short et al., 1995]. In addition, it is necessary to adjust all price increase rates in the following for inflation if the cost variables are given in constant cash flows and real discount rates are used [Louvet et al., 2018].

For the comparison of different SHP systems and SHP systems with conventional heating systems, it is useful to set the yearly considered amount of heat to the energy consumption (useful energy for space heating and domestic hot water preparation), which is assumed to be constant over the years, instead of the heat generation. The levelized cost of heat for SHP systems $LCOH^{\text{SHP}}$ without conventional auxiliary heating systems (F_t=0) can then be calculated with:

$$LCOH^{\text{SHP}} = \frac{I_{0,\text{th}}^{\text{SHP}} - S_{0,\text{th}}^{\text{SHP}} + \sum_{t=1}^{T} \frac{O_{t,\text{th}}^{\text{SHP}} + M_{t,\text{th}}^{\text{SHP}}}{(1+r)^t}}{\sum_{t=1}^{T} \frac{Q_{\text{SH,useful}} + Q_{\text{DHW,useful}}}{(1+r)^t}}, \tag{2.99}$$

where $I_{0,\text{th}}^{\text{SHP}}$ is the initial investment for the thermal part of the SHP system, $S_{0,\text{th}}^{\text{SHP}}$ are subsidies and incentives for the thermal part of the SHP system, $O_{t,\text{th}}^{\text{SHP}}$ are operation costs for the thermal part of the SHP system in year t and $M_{t,\text{th}}^{\text{SHP}}$ are maintenance costs for the thermal part of the SHP system in year t. At this, the thermal part of the SHP system comprises costs of system components that are related to heating applications. The IEA SHC Task 54 developed a guideline for LCOH calculations for solar thermal applications [Louvet et al., 2018], which is based on the work of Baez and Martínez [2015]. The definition in Equation 2.99 is similar to the overall levelized cost of heat generated by the solar assisted heating system definition within this guideline, which has to be used to compare a solar

assisted heating system with other heating systems. The operation costs for the thermal part of the SHP system in year t can be calculated with the operation costs for the thermal part of the SHP system in year one $O_{1,\mathrm{th}}^{\mathrm{SHP}}$ and can include an additional electricity price increase rate d_{el}:

$$O_{t,\mathrm{th}}^{\mathrm{SHP}} = O_{1,\mathrm{th}}^{\mathrm{SHP}} \ (1 + d_{\mathrm{el}})^{t-1} . \tag{2.100}$$

The operation costs for the thermal part of the SHP system in year one can be determined with the used electrical energy from the grid for the supply of the SHP system and the electricity price for heating applications in SHP systems $c_{\mathrm{el,SHP}}$ (e.g. a discounted electricity tariff for heat pumps):

$$O_{1,\mathrm{th}}^{\mathrm{SHP}} = W_{\mathrm{el,grid,SHP}} \ c_{\mathrm{el,SHP}}. \tag{2.101}$$

At this, the electrical energy from the grid for the supply of the SHP system is assumed to be constant over the years and thus degradation, e.g. of PV modules, solar thermal and PVT collectors or battery storages, is neglected. The maintenance costs for the thermal part of the SHP system are often calculated by a percentage of the initial investment, e.g. between 1 % and 2 % of the initial investment per year for solar thermal systems [Louvet et al., 2018], and replacements of system components are not considered explicitly.

The LCOH for a conventional reference heating system $LCOH^{\mathrm{ref}}$ without subsidies can be determined in a similar approach including the fuel costs of the system as follows:

$$LCOH^{\mathrm{ref}} = \frac{I_0^{\mathrm{ref}} + \sum_{t=1}^{T} \frac{O_t^{\mathrm{ref}} + M_t^{\mathrm{ref}} + F_t^{\mathrm{ref}}}{(1+r)^t}}{\sum_{t=1}^{T} \frac{Q_{\mathrm{SH}} + Q_{\mathrm{DHW}}}{(1+r)^t}}, \tag{2.102}$$

where I_0^{ref} is the initial investment of the conventional reference heating system, O_t^{ref} are operation costs of the conventional reference heating system in year t, M_t^{ref} are maintenance costs of the conventional reference heating system in year t and F_t^{ref} are fuel costs of the conventional reference heating system in year t. The operation costs of the conventional reference heating system in year t can be calculated with the operation costs of the conventional reference heating in year one O_1^{ref} and can also include an additional electricity price increase rate:

$$O_t^{\mathrm{ref}} = O_1^{\mathrm{ref}} \ (1 + d_{\mathrm{el}})^{t-1} . \tag{2.103}$$

The operation costs of the conventional reference heating system in year one can be determined with the used electrical energy from the grid for the supply of the conventional reference heating system and the electricity price for household electricity $c_{\mathrm{el,hh}}$:

$$O_1^{\mathrm{ref}} = W_{\mathrm{el,grid,ref}} \ c_{\mathrm{el,hh}}. \tag{2.104}$$

The fuel costs of the conventional reference heating system in year t are calculated with the fuel costs of the conventional reference heating system in year one F_1^{ref} and can include an additional fuel price increase rate d_{fuel} (e.g. a gas price increase rate d_{gas} or an oil price increase rate d_{oil}):

$$F_t^{\mathrm{ref}} = F_1^{\mathrm{ref}} \ (1 + d_{\mathrm{fuel}})^{t-1} \tag{2.105}$$

with

$$F_1^{\text{ref}} = \frac{Q_{\text{SH}} + Q_{\text{DHW}}}{\eta_{\text{ref}}} \, c_{\text{fuel}}, \tag{2.106}$$

where c_{fuel} is the fuel price, e.g. the gas price c_{gas} or oil price c_{oil}. The maintenance costs of the conventional reference heating system can also be calculated by a percentage of the initial investment or a fixed value per year.

2.4.3.2 Levelized Cost of Electricity

Following the basic LCOH definition in Equation 2.97, the levelized cost of electricity (LCOE) in the residential sector (without tax rate, asset depreciation and residual value of an electricity generator) adapted from Branker et al. [2011] can be defined with:

$$LCOE = \frac{I_0 - S_0 + \sum_{t=1}^{T} \frac{O_t + M_t + F_t}{(1+r)^t}}{\sum_{t=1}^{T} \frac{W_{\text{el},t}}{(1+r)^t}}, \tag{2.107}$$

where $W_{\text{el},t}$ is the considered amount of electrical energy in year t.

Furthermore, the LCOE for buildings with SHP systems can be defined in a similar manner as the LCOH for SHP systems using the electricity load as reference value instead of the often used electricity generation and considering net electricity consumption costs $C_{t,\text{el,load}}$ (electricity consumption costs minus compensation for electricity fed into the grid). Thus, the load-based levelized cost of electricity can be introduced with:

$$LCOE_{\text{load}} = \frac{I_0 - S_0 + \sum_{t=1}^{T} \frac{O_t + M_t + F_t + C_{t,\text{el,load}}}{(1+r)^t}}{\sum_{t=1}^{T} \frac{W_{\text{el,load},t}}{(1+r)^t}}, \tag{2.108}$$

where $W_{\text{el,load},t}$ is the considered amount of electricity load in year t. As described for the LCOH calculation, LCOE values can be expressed in nominal terms and real terms and all price increase rates in the following have to be adjusted for inflation if the cost variables are given in constant cash flows and real discount rates are used. For the LCOE analysis of single-family buildings, the real discount rate can be set to zero as in the LCOH calculation.

As the used electrical energy from the grid for heating applications is considered in the LCOH calculation, it is useful to relate the LCOE to the household electricity load. Assuming that the household electricity load is constant over the years, the load-based levelized cost of electricity for household applications in buildings with SHP systems $LCOE_{\text{load,hh}}^{\text{SHP}}$ without conventional electricity generators (F_t=0) can be introduced with:

$$LCOE_{\text{load,hh}}^{\text{SHP}} = \frac{I_{0,\text{el}}^{\text{SHP}} - S_{0,\text{el}}^{\text{SHP}} + \sum_{t=1}^{T} \frac{O_{t,\text{el}}^{\text{SHP}} + M_{t,\text{el}}^{\text{SHP}} + C_{t,\text{el,load,hh}}^{\text{SHP}}}{(1+r)^t}}{\sum_{t=1}^{T} \frac{W_{\text{el,hh}}}{(1+r)^t}}, \tag{2.109}$$

where $I_{0,\text{el}}^{\text{SHP}}$ is the initial investment for the electrical part of the SHP system, $S_{0,\text{el}}^{\text{SHP}}$ are subsidies and incentives for the electrical part of the SHP system, $O_{t,\text{el}}^{\text{SHP}}$ are operation costs for the electrical part of the SHP system in year t, $M_{t,\text{el}}^{\text{SHP}}$ are maintenance costs for the electrical part of the SHP system in year t and $C_{t,\text{el,load,hh}}^{\text{SHP}}$ are the net household electricity consumption costs in year t for a building with SHP system. At this, the electrical part of the SHP system comprises costs of system components that are related to the supply of

the household electricity load. The operation and maintenance costs for the electrical part of the SHP system are often calculated by a percentage of the initial investment or a fixed value per year. In this case, replacements of system components are often not considered explicitly. Furthermore, the net household electricity consumption costs in year t for a building with SHP system can be calculated with:

$$C^{\mathrm{SHP}}_{t,\mathrm{el,load,hh}} = C^{\mathrm{SHP}}_{t,\mathrm{el,grid,hh}} - C^{\mathrm{SHP}}_{t,\mathrm{el,feedin}}, \tag{2.110}$$

where $C^{\mathrm{SHP}}_{t,\mathrm{el,grid,hh}}$ are the household electricity consumption costs in year t for a building with SHP system and $C^{\mathrm{SHP}}_{t,\mathrm{el,feedin}}$ is the compensation for electricity fed into the grid in year t for a building with SHP system. The household electricity consumption costs in year t for a building with SHP system can be calculated with the household electricity consumption costs in year one for a building with SHP system $C^{\mathrm{SHP}}_{1,\mathrm{el,grid,hh}}$ and can include an additional electricity price increase rate:

$$C^{\mathrm{SHP}}_{t,\mathrm{el,grid,hh}} = C^{\mathrm{SHP}}_{1,\mathrm{el,grid,hh}} \left(1 + d_{\mathrm{el}}\right)^{t-1}. \tag{2.111}$$

The household electricity consumption costs in year one for a building with SHP system can be determined with the used electrical energy from the grid to cover the household electricity load for a building with SHP system and the electricity price for household electricity:

$$C^{\mathrm{SHP}}_{1,\mathrm{el,grid,hh}} = W_{\mathrm{el,grid,hh}}\ c_{\mathrm{el,hh}}. \tag{2.112}$$

At this, the electrical energy from the grid to cover the household electricity load for a building with SHP system is assumed to be constant over the years and thus degradation, e.g. of PV modules and PVT collectors or battery storages, is neglected. The compensation for electricity fed into the grid in year t for a building with SHP system can be set equal to the compensation for electricity fed into the grid in year one for a building with SHP system $C^{\mathrm{SHP}}_{1,\mathrm{el,feedin}}$ if the feed-in tariff and the grid feed-in electricity are assumed to be constant over the period of analysis. This also means that degradation of system components is neglected. The compensation for electricity fed into the grid in year one for a building with SHP system can then be determined with the grid feed-in electricity by the solar electrical system and the feed-in tariff $c_{\mathrm{el,feedin}}$:

$$C^{\mathrm{SHP}}_{1,\mathrm{el,feedin}} = W_{\mathrm{el,sol,feedin}}\ c_{\mathrm{el,feedin}}. \tag{2.113}$$

For a building with conventional heating system without PV (or a SHP system without PV or PVT) as reference building, the load-based LCOE for household applications can be calculated with the net household electricity consumption costs of the reference building as follows:

$$LCOE^{\mathrm{ref}}_{\mathrm{load,hh}} = \frac{\sum_{t=1}^{T} \frac{C^{\mathrm{ref}}_{t,\mathrm{el,load,hh}}}{(1+r)^t}}{\sum_{t=1}^{T} \frac{W_{\mathrm{el,hh}}}{(1+r)^t}}. \tag{2.114}$$

The net household electricity consumption costs of a reference building with conventional heating system without PV in year t can be calculated with the net household electricity consumption costs in year one $C^{\mathrm{ref}}_{1,\mathrm{el,grid,hh}}$ of a reference building with conventional heating

system without PV and an additional electricity price increase rate as follows:

$$C^{\text{ref}}_{t,\text{el,load,hh}} = C^{\text{ref}}_{1,\text{el,grid,hh}} \left(1 + d_{\text{el}}\right)^{t-1} \tag{2.115}$$

with

$$C^{\text{ref}}_{1,\text{el,grid,hh}} = W_{\text{el,hh}}\ c_{\text{el,hh}}. \tag{2.116}$$

2.4.3.3 Levelized Cost of Energy

Beside of the allocation of the different electricity consumptions to the LCOH and LCOE, it is necessary to divide the costs of PVT collectors, PV modules and battery storage systems in initial investments for the thermal part (heating applications including the electrical energy supply of the SHP system for heating applications) and the electrical part (supply of the household electricity load) of the SHP system. Furthermore, in contrast to the PV and PVT self-consumption that reduces the used electrical energy from the grid for the supply of a SHP system and thus the operation costs for heating applications, the grid feed-in electricity by solar electrical systems is only assigned to the LCOE and the benefit is not apparent in the LCOH analysis. Consequently, it is mandatory to compare the LCOH and LCOE of different buildings in conjunction using the same allocations of costs, especially for buildings with hybrid technologies like PVT.

For the analyses of SHP systems for the thermal and electrical energy supply of buildings, it is thus more useful to evaluate the levelized cost of heat and electricity together as levelized cost of energy (LCOEn) for a building. Following the basic LCOH und LCOE definitions in Equation 2.97 and Equation 2.107, the LCOEn in the residential sector (without tax rate, asset depreciation and residual value) can basically be defined with:

$$LCOEn = \frac{I_0 - S_0 + \sum_{t=1}^{T} \frac{O_t + M_t + F_t}{(1+r)^t}}{\sum_{t=1}^{T} \frac{E_t}{(1+r)^t}}, \tag{2.117}$$

where E_t is the amount of energy in year t. As described for the LCOH and LCOE calculation, LCOEn values can be expressed in nominal terms and real terms and all price increase rates in the following have to be adjusted for inflation if the cost variables are given in constant cash flows and real discount rates are used. In case of systems for the thermal and electrical energy supply of single-family buildings, the real discount rate can be set to zero as described for the LCOH and LCOE calculation.

Regarding the useful energy for the thermal and electrical energy supply of residential buildings and thus following the LCOH and LCOE definitions in Equation 2.99 and Equation 2.109, the levelized cost of heat and electricity for a building with SHP system without conventional auxiliary heating systems (F_t=0) considering the net household electricity consumption costs can be introduced as follows:

$$LCOEn^{\text{SHP}}_{\text{bui}} = \frac{I^{\text{SHP}}_{0,\text{bui}} - S^{\text{SHP}}_{0,\text{bui}} + \sum_{t=1}^{T} \frac{O^{\text{SHP}}_{t,\text{bui}} + M^{\text{SHP}}_{t,\text{bui}} + C^{\text{SHP}}_{t,\text{el,load,hh}}}{(1+r)^t}}{\sum_{t=1}^{T} \frac{Q_{\text{SH,useful}} + Q_{\text{DHW,useful}} + W_{\text{el,hh}}}{(1+r)^t}} \tag{2.118}$$

with

$$I_{0,\mathrm{bui}}^{\mathrm{SHP}} = I_{0,\mathrm{th}}^{\mathrm{SHP}} + I_{0,\mathrm{el}}^{\mathrm{SHP}} \tag{2.119}$$

$$S_{0,\mathrm{bui}}^{\mathrm{SHP}} = S_{0,\mathrm{th}}^{\mathrm{SHP}} + S_{0,\mathrm{el}}^{\mathrm{SHP}} \tag{2.120}$$

$$O_{t,\mathrm{bui}}^{\mathrm{SHP}} = O_{t,\mathrm{th}}^{\mathrm{SHP}} + O_{t,\mathrm{el}}^{\mathrm{SHP}} \tag{2.121}$$

$$M_{t,\mathrm{bui}}^{\mathrm{SHP}} = M_{t,\mathrm{th}}^{\mathrm{SHP}} + M_{t,\mathrm{el}}^{\mathrm{SHP}}. \tag{2.122}$$

The LCOEn for a reference building with conventional heating system without PV and subsidies $LCOEn_{\mathrm{bui}}^{\mathrm{ref}}$ can be determined in a similar approach including the fuel costs of the system and the net household electricity consumption costs as follows:

$$LCOEn_{\mathrm{bui}}^{\mathrm{ref}} = \frac{I_{0,\mathrm{bui}}^{\mathrm{ref}} + \sum_{t=1}^{T} \frac{O_{t,\mathrm{bui}}^{\mathrm{ref}} + M_{t,\mathrm{bui}}^{\mathrm{ref}} + F_{t,\mathrm{bui}}^{\mathrm{ref}} + C_{t,\mathrm{el,load,hh}}^{\mathrm{ref}}}{(1+r)^t}}{\sum_{t=1}^{T} \frac{Q_{\mathrm{SH}} + Q_{\mathrm{DHW}} + W_{\mathrm{el,hh}}}{(1+r)^t}} \tag{2.123}$$

with

$$I_{0,\mathrm{bui}}^{\mathrm{ref}} = I_0^{\mathrm{ref}} \tag{2.124}$$

$$O_{t,\mathrm{bui}}^{\mathrm{ref}} = O_t^{\mathrm{ref}} \tag{2.125}$$

$$M_{t,\mathrm{bui}}^{\mathrm{ref}} = M_t^{\mathrm{ref}} \tag{2.126}$$

$$F_{t,\mathrm{bui}}^{\mathrm{ref}} = F_t^{\mathrm{ref}}. \tag{2.127}$$

2.4.4 Economic Efficiency and Environmental Impact

An approach for linking economic efficiency and environmental impact is the pricing of GHG emissions as established by the German government in 2021 with the purpose of accelerating actions to reach the climate targets in the transport and building sectors. Following the idea of penalizing CO_2 emissions and considering environmental impact costs, the LCOEn from Equation 2.117 can basically be extended by CO_2 emission costs $C_{t,\mathrm{CO_2}}$ over the lifetime:

$$LCOEn_{\mathrm{CO_2}} = \frac{I_0 - S_0 + \sum_{t=1}^{T} \frac{O_t + M_t + F_t + C_{t,\mathrm{CO_2}}}{(1+r)^t}}{\sum_{t=1}^{T} \frac{E_t}{(1+r)^t}}. \tag{2.128}$$

As described in Section 2.4.3.3, LCOEn values can be expressed in nominal terms and real terms and all price increase rates in the following have to be adjusted for inflation if the cost variables are given in constant cash flows and real discount rates are used. In case of systems for single-family buildings, the real discount rate can be set to zero as described for the LCOEn calculation.

The LCOEn including CO_2 emission costs for a building with SHP system without conventional auxiliary heating systems (F_t=0) can then be calculated by the extension of Equa-

tion 2.118 as follows:

$$LCOEn^{\mathrm{SHP}}_{\mathrm{CO_2,bui}} = \frac{I^{\mathrm{SHP}}_{0,\mathrm{bui}} - S^{\mathrm{SHP}}_{0,\mathrm{bui}} + \sum_{t=1}^{T} \frac{O^{\mathrm{SHP}}_{t,\mathrm{bui}} + M^{\mathrm{SHP}}_{t,\mathrm{bui}} + C^{\mathrm{SHP}}_{t,\mathrm{el,load,hh}} + C^{\mathrm{SHP}}_{t,\mathrm{CO_2,bui}}}{(1+r)^t}}{\sum_{t=1}^{T} \frac{Q_{\mathrm{SH,useful}} + Q_{\mathrm{DHW,useful}} + W_{\mathrm{el,hh}}}{(1+r)^t}}, \tag{2.129}$$

where $C^{\mathrm{SHP}}_{t,\mathrm{CO_2,bui}}$ are the CO_2 emission costs for a building with SHP system in year t. The CO_2 emission costs for a building with SHP system in year t can be determined with the CO_2 emission costs for a building with SHP system in year one $C^{\mathrm{SHP}}_{1,\mathrm{CO_2,bui}}$ and an additional carbon price increase rate $d_{\mathrm{CO_2}}$ by:

$$C^{\mathrm{SHP}}_{t,\mathrm{CO_2,bui}} = C^{\mathrm{SHP}}_{1,\mathrm{CO_2,bui}} \left(1 + d_{\mathrm{CO_2}}\right)^{t-1}. \tag{2.130}$$

In addition to the use of a carbon price increase rate, it is possible to calculate the CO_2 emission costs for a building with SHP system individually for each year of the period of analysis with a defined path for the carbon price increase, e.g. as implemented in Germany. The CO_2 emission costs for a building with SHP system in year one can be calculated with the CO_2 emissions without compensation by exported energy for a building with SHP system:

$$C^{\mathrm{SHP}}_{1,\mathrm{CO_2,bui}} = m^{\mathrm{SHP}}_{\mathrm{CO_2,bui}}\, c_{\mathrm{CO_2}} \tag{2.131}$$

or with the CO_2 emissions with compensation by exported energy for a building with SHP system if the compensation of CO_2 emissions by exported solar electricity is considered:

$$C^{\mathrm{SHP}}_{1,\mathrm{CO_2,bui}} = m^{\mathrm{SHP}}_{\mathrm{CO_2,bui,net}}\, c_{\mathrm{CO_2}}, \tag{2.132}$$

where $c_{\mathrm{CO_2}}$ is the carbon price. At this, the CO_2 emissions for a building with SHP system are assumed to be constant over the years and thus degradation, e.g. of solar thermal and PVT collectors, PV modules or battery storages, is neglected. Furthermore, Equation 2.129 has to be calculated using electricity prices that have been adjusted for an included carbon price, e.g. the carbon price by the EU Emission Trading Scheme (ETS). Otherwise, $C^{\mathrm{SHP}}_{1,\mathrm{CO_2,bui}}$ can be assumed to be zero since the CO_2 emission costs are already included in the electricity price.

The LCOEn including CO_2 emission costs for a reference building with conventional heating system without PV and subsidies $LCOEn^{\mathrm{ref}}_{\mathrm{CO_2,bui}}$ can be determined in a similar approach including the fuel costs of the system by the extension of Equation 2.123 as follows:

$$LCOEn^{\mathrm{ref}}_{\mathrm{CO_2,bui}} = \frac{I^{\mathrm{ref}}_{0,\mathrm{bui}} + \sum_{t=1}^{T} \frac{O^{\mathrm{ref}}_{t,\mathrm{bui}} + M^{\mathrm{ref}}_{t,\mathrm{bui}} + F^{\mathrm{ref}}_{t,\mathrm{bui}} + C^{\mathrm{ref}}_{t,\mathrm{el,load,hh}} + C^{\mathrm{ref}}_{t,\mathrm{CO_2,bui}}}{(1+r)^t}}{\sum_{t=1}^{T} \frac{Q_{\mathrm{SH}} + Q_{\mathrm{DHW}} + W_{\mathrm{el,hh}}}{(1+r)^t}}, \tag{2.133}$$

where $C^{\mathrm{ref}}_{t,\mathrm{CO_2,bui}}$ are the CO_2 emission costs for a reference building with conventional heating system in year t. The CO_2 emission costs for a reference building with conventional heating system in year t can be determined with the CO_2 emission costs for a reference building with conventional heating system in year one $C^{\mathrm{ref}}_{1,\mathrm{CO_2,bui},}$ and an additional carbon price increase rate by:

$$C^{\mathrm{ref}}_{t,\mathrm{CO_2,bui}} = C^{\mathrm{ref}}_{1,\mathrm{CO_2,bui}} \left(1 + d_{\mathrm{CO_2}}\right)^{t-1}. \tag{2.134}$$

In addition to the use of a carbon price increase rate, it is also possible to calculate the CO_2 emission costs for a reference building with conventional heating system individually for each year of the period of analysis with a defined path for the carbon price increase. The CO_2 emission costs for a reference building with conventional heating system in year one can be calculated with the CO_2 emissions for a reference building with conventional heating system:

$$C^{\mathrm{ref}}_{1,\mathrm{CO_2,bui}} = m^{\mathrm{ref}}_{\mathrm{CO_2,bui}}\, c_{\mathrm{CO_2}}. \tag{2.135}$$

Furthermore, Equation 2.133 has to be calculated using electricity and fuel prices that have been adjusted for an included carbon price. If the electricity prices are not adjusted for an included carbon price, the CO_2 emission costs as result of delivered electrical energy from the grid of the reference system can be assumed to be zero since the CO_2 emission costs are already included in the electricity price. In this case, the CO_2 emission costs for a reference building with conventional heating system in year one can be calculated with the CO_2 emissions related to the delivered fuel energy of a reference building with conventional heating system:

$$C^{\mathrm{ref}}_{1,\mathrm{CO_2,bui}} = E^{\mathrm{ref}}_{\mathrm{bui,del,fuel}}\, f_{\mathrm{CO_2,del,fuel}}\, c_{\mathrm{CO_2}}. \tag{2.136}$$

2.4.5 Summary

The following table (Table 2.5) gives an overview of the defined KPIs with assignment of its evaluation quantity and usable fields of application. At this, it is marked for which types of SHP systems the considered KPI can be used. KPIs that are not recommended to use in the previous sections are not listed in the summary.

Table 2.5: Overview of key performance indicators for the evaluation of SHP systems.

KPI	Evaluation quantity	Applications		
		Solar thermal and heat pump systems	PV and heat pump systems	PV, solar thermal and heat pump systems
$SPF_{\mathrm{SHP+,pen}}$	Heating efficiency	x	-	-
$SPF_{\mathrm{SHP+,pen,grid}}$	Heating efficiency	x	x	x
$SPF_{\mathrm{bui,grid}}$	Energy efficiency (building)	x	x	x
SPF_{HP}	Heat pump efficiency	x	x	x
$f_{\mathrm{sav,heating}}$	Final energy savings (heating)	x	x	x
$f_{\mathrm{th,sol}}$	Solar thermal energy fraction	x	-	x
SSR_{bui}	Electrical self-sufficiency (building)	-	x	x

Table 2.5: Overview of key performance indicators for the evaluation of SHP systems. *(continued)*

KPI	Evaluation quantity	Applications		
		Solar thermal and heat pump systems	PV and heat pump systems	PV, solar thermal and heat pump systems
SSR_{hh}	Electrical self-sufficiency (household)	-	x	x
SSR_{SHP}	Electrical self-sufficiency (heating)	-	x	x
SCR_{bui}	Solar electricity usage (building)	-	x	x
SCR_{hh}	Solar electricity usage (household)	-	x	x
SCR_{SHP}	Solar electricity usage (heating)	-	x	x
$q_{\mathrm{th,sol}}$	Solar thermal energy generation	x	-	x
$w_{\mathrm{el,sol}}$	Solar electrical energy generation	-	x	x
$UR_{\mathrm{th,sol}}$	Thermal utilization of available solar irradiance	x	-	x
$UR_{\mathrm{el,sol}}$	Electrical utilization of available solar irradiance	-	x	x
EP_{bui}	Net energy demand (building), nZEB rating	x	x	x
$EP^{\mathrm{SHP}}_{\mathrm{bui,del,net}}$	Import/export final energy balance (building)	x	x	x
$EP^{\mathrm{SHP}}_{\mathrm{pe,bui,tot}}$	Total primary energy usage (building), nZEB rating	x	x	x
$EP^{\mathrm{SHP}}_{\mathrm{pe,bui,nren}}$	Non-renewable primary energy usage (building), nZEB rating	x	x	x
$EP^{\mathrm{SHP}}_{\mathrm{pe,bui,nren,net}}$	Non-renewable primary energy usage (building) with compensation (energy export), nZEB rating	x	x	x
$f_{\mathrm{sav,pe,tot}}$	Total primary energy savings (building)	x	x	x
$f_{\mathrm{sav,pe,nren}}$	Non-renewable primary energy savings (building)	x	x	x
$f_{\mathrm{sav,pe,nren,net}}$	Non-renewable primary energy savings (building) with compensation (energy export)	x	x	x
$RER^{\mathrm{SHP}}_{\mathrm{pe,bui}}$	Renewable energy usage (building), nZEB rating	x	x	x

Table 2.5: Overview of key performance indicators for the evaluation of SHP systems. *(continued)*

KPI	Evaluation quantity	Applications		
		Solar thermal and heat pump systems	PV and heat pump systems	PV, solar thermal and heat pump systems
$EP^{\mathrm{SHP}}_{\mathrm{CO_2,bui}}$	CO_2 emissions (building), nZEB rating	x	x	x
$EP^{\mathrm{SHP}}_{\mathrm{CO_2,bui,net}}$	CO_2 emissions (building) with compensation (energy export), nZEB rating	x	x	x
$f_{\mathrm{sav,CO_2}}$	CO_2 emission savings (building)	x	x	x
$f_{\mathrm{sav,CO_2,net}}$	CO_2 emission savings (building) with compensation (energy export)	x	x	x
$LCOH^{\mathrm{SHP}}$	Economic efficiency (heating)	x	x	x
$LCOE^{\mathrm{SHP}}_{\mathrm{load,hh}}$	Economic efficiency (household electricity)	x	x	x
$LCOEn^{\mathrm{SHP}}_{\mathrm{bui}}$	Economic efficiency (energy, building)	x	x	x
$LCOEn^{\mathrm{SHP}}_{\mathrm{CO_2,bui}}$	Economic efficiency and environmental impact (energy, building)	x	x	x

Chapter 3

System Modeling

This chapter presents the modeling of the solar and heat pump systems that are analyzed in this work. Beginning with a general introduction to the model design and simulation in TRNSYS, the used and developed simulation models are described in detail. First, the solar and heat pump component models are presented including a newly developed TRNSYS model for the simulation of photovoltaic-thermal collectors. At this, the parameter identification as well as the validation of the component models are explained in detail. This is followed by the description of the system modeling. Starting with a model overview, the system model is divided in subsystems that can be combined for the simulation of the different solar and heat pump system concepts considered in this work. Within the descriptions of the subsystem models, the boundary conditions (weather data, climate and ground properties), the residential building models and the different parts of the solar and heat pump system itself (e.g. heat pump and heat source circuit, solar thermal circuit or photovoltaic battery system) including the implemented system control strategies are explained.

3.1 Model Design in TRNSYS

TRNSYS is a simulation environment with a modular structure for the simulation of transient systems, especially thermal and electrical energy systems. The used version in this work is TRNSYS 18.02.0000 [TRNSYS, 2020]. Typical TRNSYS applications are simulations of energy systems with renewable energy technologies like solar thermal or PV systems or multizone building simulations including heating, ventilation and air conditioning (HVAC) systems or combined heat and power systems. TRNSYS consists essentially of the following main programs:

- TRNSYS Simulation Studio (visual interface for model design, parameterization and simulation)
- TRNDll (simulation engine) and TRNExe (executable)
- TRNBuild (visual interface for the building simulation input data)

- TRNEdit (editor to create redistributable applications, known as TRNSED applications, or to perform parametric runs).

The source code of the kernel as well as the source code of the component models are delivered with the software, which simplifies the modification of existing models and the development of new individual models in order to fit the user-specific needs. The DLL-based structure of the program allows developers to add component models using different common programming languages like C++ or Fortran (common programming language for TRNSYS models). In addition, TRNSYS can be connected to other programs for pre-/post-processing or for co-simulation with interactive calls during the simulation, e.g. with Matlab/Simulink [Riederer et al., 2009; Engel et al., 2018] or with Modelica tools via Functional Mockup Interface (FMI) [Elsheikh et al., 2013a,b].

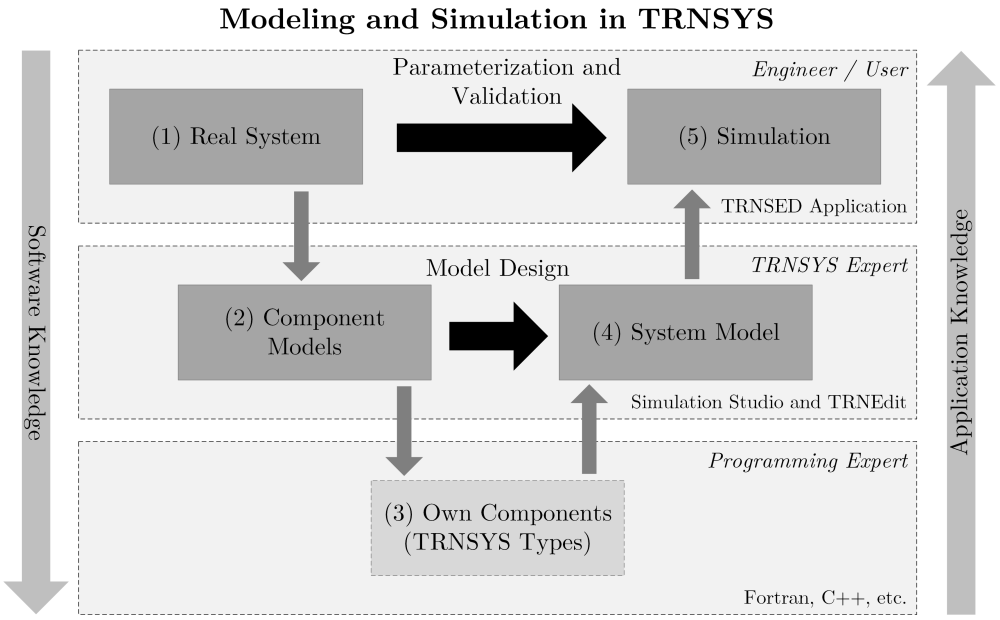

Figure 3.1: TRNSYS model design and simulation procedure.

The general model design and simulation procedure in TRNSYS is shown in Figure 3.1. First, the user starts on an engineering knowledge level with the detailed description of the real system (1). Afterwards, the user has to decide whether the available component models in TRNSYS fulfill the user-specific needs or not (2). Due to the variety of available component models, the user has to be a TRNSYS expert to decide which components fulfill the specific requirements for the later simulation of the system. If the real system can be designed by available models, the user can proceed with the design of the system model in TRNSYS (4). If not, the user has to take a detour via designing detailed models of the missing components and write his own TRNSYS components (*Types*) in a programming language like Fortran (3). Consequently, the user needs to have expert knowledge in developing TRNSYS Types (TRNSYS expert) and in a usable programming language (programming expert). TRNSYS Types typically consist of inputs (variable, e.g. input temperature or mass flow), parameters (fixed, e.g. solar collector area or storage volume) and outputs (e.g. output temperature or mass flow). Depending on the model, the Type can also include external files, like data sheets (e.g. weather data), and derivatives as initial values for the numerical solution of differential equations (cf. Figure 3.2). Now, the user

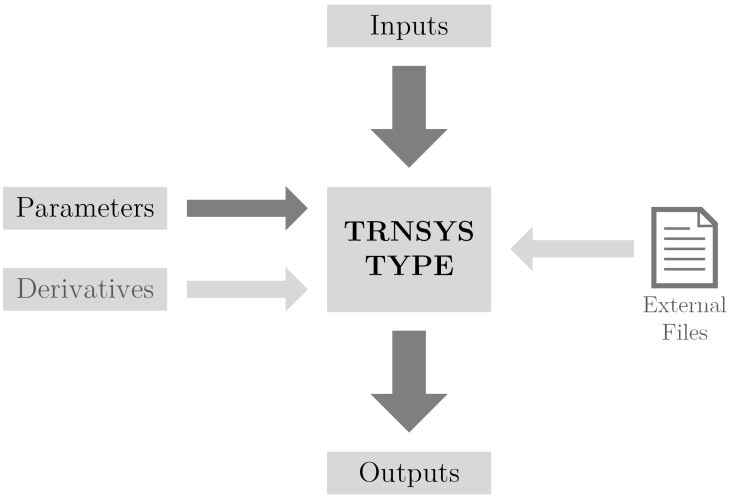

Figure 3.2: TRNSYS Type.

is ready for the design of the system model in the visual interface TRNSYS Simulation Studio (4). The TRNSYS Types are placed by drag & drop and connected to each other. Afterwards, the simulation parameters are defined (usually by standardized, validated parameter sets (literature based), data from manufacturers or parameter identification). After first test simulations, the user has to check whether the simulation results are valid or not, e.g. by comparison with measured data from the real system (quantitative validation) or by plausibility checks, e.g. comparison of the system behavior or energy balances (qualitative validation). Finally, the desired TRNSYS simulation can be performed (5). The simulation project information is saved in a TRNSYS project file and, via starting the simulation, TRNSYS Simulation Studio creates a TRNSYS input file, known as deck file. TRNDll reads all information in the deck file; it is called by TRNExe for the execution of the simulation. In case of building simulations, TRNBuild is used to create different files like a building description file which will be read for the simulation of multizone buildings (Type 56). The results can be printed in external files or visualized in an online plotter.

Alternatively, TRNSYS experts have the possibility to create a TRNSED application with limited possibilities for the parameterization of the models and the simulation itself as a user-friendly framework for end-users like engineers without experience in TRNSYS as shown in Jonas et al. [2017c,a]. In this case, the end-user can bypass steps (2) to (4) and start with the parameterization of the simulation model based on engineering knowledge of the real system (1). Here, the user may perform TRNSYS simulations without any knowledge of modeling or programming in TRNSYS itself. TRNSED applications are redistributable stand-alone applications based on TRNSYS which are executable without the installation of TRNSYS itself. TRNEdit is a specialized editor which can be used for modifying TRNSYS deck files and creating these simplified stand-alone applications as end-user simulation tools without TRNSYS knowledge and license. Within TRNEdit, the TRNSED developer has the possibility to create a graphical user interface (GUI) with multiple tabs, pictures for illustration, links, pull-down menus for parameters or data files, check boxes or radio buttons [TRNSYS, 2020]. At this, the developer can choose which parameters, data sets or simulation options should be provided to the end-user of the simulation tool.

3.2 Solar and Heat Pump Component Models

3.2.1 Brine/Water and Air/Water Heat Pumps

The *performance of a heat pump* can basically be described by a black box model presented in Wetter and Afjei [1997] using biquadratic polynomials for the thermal condenser power:

$$\begin{aligned}\dot{Q}_{\text{cond}} =& bq_1 + bq_2\, T_{\text{n,evap,in}} + bq_3\, T_{\text{n,cond,out}} + bq_4\, T_{\text{n,evap,in}}\, T_{\text{n,cond,out}} \\ &+ bq_5\, T^2_{\text{n,evap,in}} + bq_6\, T^2_{\text{n,cond,out}}\end{aligned} \tag{3.1}$$

and the compressor power of the heat pump:

$$\begin{aligned}P_{\text{el,comp}} =& bp_1 + bp_2\, T_{\text{n,evap,in}} + bp_3\, T_{\text{n,cond,out}} + bp_4\, T_{\text{n,evap,in}}\, T_{\text{n,cond,out}} \\ &+ bp_5\, T^2_{\text{n,evap,in}} + bp_6\, T^2_{\text{n,cond,out}},\end{aligned} \tag{3.2}$$

where $bq_1 - bq_6$ are the condenser model coefficients, $T_{\text{n,evap,in}}$ is the normalized evaporator inlet temperature, $bp_1 - bp_6$ are the compressor model coefficients and $T_{\text{n,cond,out}}$ is the normalized condenser outlet temperature. At this, normalized temperatures are calculated as follows:

$$T_{\text{n},i} = \frac{\vartheta_i\ [^\circ\text{C}]}{273.15} + 1. \tag{3.3}$$

The described model is implemented in TRNSYS Type 401 that is used for the simulation of heat pumps within this work. The model coefficients of the polynomials can be determined using a Microsoft Excel-based fitting tool provided with Type 401. Furthermore, as the described polynomials are only valid for steady-state conditions, Type 401 offers the possibility to model cycling losses (heat-up and cool-down process) using the solution of a first order differential equation (PT1-element). Further details of TRNSYS Type 401 can be found in Wetter and Afjei [1997]. As data basis for the parameterization of the brine/water (BW) and air/water (AW) heat pump models, characteristics of market available heat pumps are used and scaled for the different design heat loads of the residential buildings and the design temperatures of the heat distribution systems. The up and down scaling of the characteristics of the heat pump prevents an influence of the performance of the selected heat pump itself on the performance of the system and thus ensure a better comparability of the simulation results. The determined model coefficients of the polynomials for the basic heat pump sizes are given in Table 3.1 and the main data of the heat pump models with different scales of the condenser power are summarized in Table 3.2.

Within Type 401, the thermal evaporator power is calculated using a steady-state energy balance in a thermodynamic cycle as described by Equation 2.37 with $\dot{W}_{\text{t,comp}} = P_{\text{el,comp}}$:

$$\dot{Q}_{\text{evap}} = \dot{Q}_{\text{cond}} - P_{\text{el,comp}}. \tag{3.4}$$

The heat pump characteristics of manufacturer data are based on condenser power and electrical power measurements for different evaporator inlet and condenser outlet temperatures according to the conditions of EN 14511:2013 [EN 14511, 2013]. In case of air/water heat pumps, the characteristics according to the conditions of EN 14511:2013 are determined with defrosting cycles and the electrical power consumption of the heat pump $P_{\text{el,HP}}$ for the COP calculation considers the power consumption of the evaporator fans. Furthermore,

Table 3.1: Model coefficients of the biquadratic polynomials for the basic heat pump sizes of market available brine/water (BW) and air/water (AW) heat pumps. Performance data for the determination of the model coefficients based on data sheets of Viessmann Vitocal 300-G BW301.B10 [Viessmann, 2017] for BW10 and Viessmann Vitocal 350-A AWHI 351.A10 [Viessmann, 2013] for AW10.

Brine/water BW10					
bq_1	bq_2	bq_3	bq_4	bq_5	bq_6
−267.8168283	43.38881036	387.7521406	−298.3932473	189.0651321	−43.27348465
bp_1	bp_2	bp_3	bp_4	bp_5	bp_6
107.2997351	−76.83835214	−127.7342516	14.36240554	29.27935843	55.05601971
Air/water AW10					
bq_1	bq_2	bq_3	bq_4	bq_5	bq_6
0.450247926	−69.38457583	11.70532773	−87.79855166	114.7072133	39.28456435
bp_1	bp_2	bp_3	bp_4	bp_5	bp_6
−0.401377139	−4.901184335	−10.81683465	7.729934357	−0.304519072	9.457732335

Table 3.2: Key properties of brine/water (BW) and air/water (AW) heat pump models (for brine/water at B0/W35 and for air/water at A7/W35). Performance data based on data sheets of Viessmann Vitocal 300-G BW301.B10 [Viessmann, 2017] for BW10 and Viessmann Vitocal 350-A AWHI 351.A10 [Viessmann, 2013] for AW10.

Model	Nominal condenser power $\dot{Q}_{\mathrm{HP,nom}}$	COP
BW06 (scaled)	6.01 kW	5.01
BW08 (scaled)	8.08 kW	5.01
BW10 (manufacturer)	10.36 kW	5.01
BW13 (scaled)	13.05 kW	5.01
AW06 (scaled)	7.62 kW	4.10
AW10 (manufacturer)	12.70 kW	4.10
AW19 (scaled)	22.86 kW	4.10

the electrical power consumption of a heat pump listed in manufacturer data sheets often contains additional electrical power consumptions of the heat pump like electrical power consumptions of integrated pumps or controllers. Thus, if $P_{\mathrm{el,HP}}$ is used for the fitting of the compressor model coefficients $bp_1 - bp_6$, the thermal evaporator power consumption is underestimated. For air/water heat pumps, this effect can often be neglected as the outlet air on the source side of the heat pump is emitted to the ambient and has no effect on the inlet air temperature. In addition, most data sheets of air/water heat pumps, like those used for the air/water heat pump modeling in this work, does not contain data on the thermal evaporator power or the compressor power for different operating conditions. For brine/water heat pumps, the outlet fluid flows back to the heat source and has a direct impact on the heat source temperature at the inlet of the heat pump. Thus, the power consumption of the compressor $P_{\mathrm{el,comp}}$ has to be calculated for each operating condition of the manufacturers data of the heat pump and has to be used for the fitting of the compressor model coefficients

$bp_1 - bp_6$. The electrical power consumption of a brine/water heat pump in the simulation can then be determined by the use of a correction factor $f_{\text{el,HP}}$ as mean value of the ratio of electrical power consumption of the heat pump to the compressor power of the heat pump for each operating condition i:

$$P_{\text{el,HP}} = P_{\text{el,comp}}\ f_{\text{el,HP}} \tag{3.5}$$

with

$$f_{\text{el,HP}} = \frac{\sum_{i=1}^{n} \frac{P_{\text{el,HP},i}}{P_{\text{el,comp},i}}}{n}. \tag{3.6}$$

A comparison of measured COPs from the data sheets of the manufacturer and simulation results in steady-state conditions of the air/water (based on AW10) and brine/water (based on BW10) heat pumps are shown in Figure 3.3. Furthermore, a summary of further model parameters for the brine/water and air/water heat pump models is given in Table 3.3.

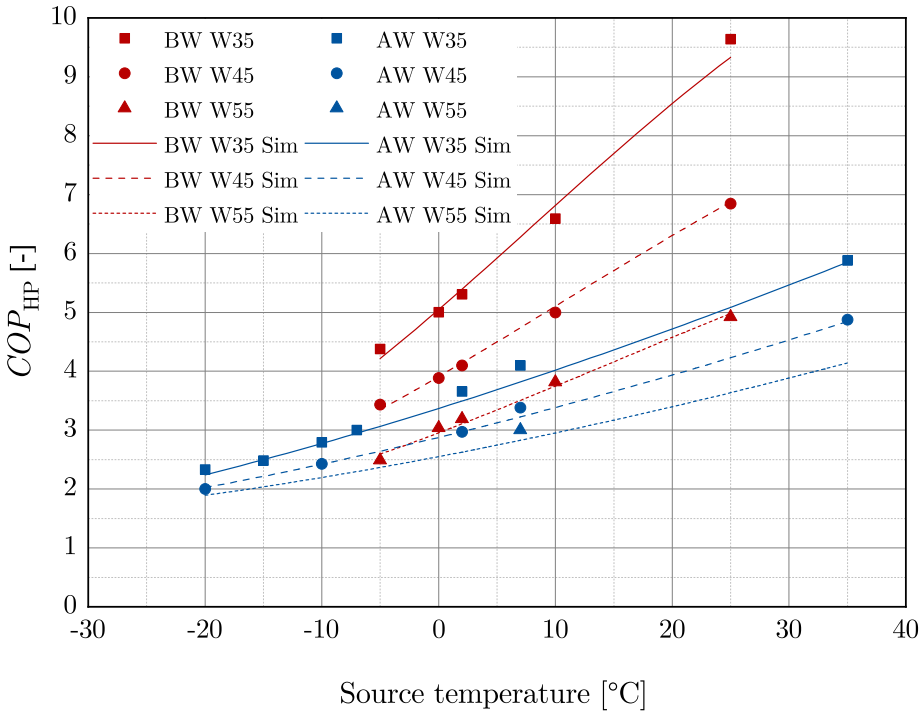

Figure 3.3: Comparison of measured COPs (data points) from data sheets of the manufacturer [Viessmann, 2017, 2013] and COP simulation results (lines) in steady-state conditions for condenser outlet temperatures of 35 °C (W35), 45 °C (W45) and 55 °C (W55) depending on the heat source temperature of the brine/water (BW) or air/water (AW) heat pump.

Table 3.3: Parameters of brine/water and air/water heat pump models.

Parameter	Brine/water	Air/water
Specific heat capacity of evaporator fluid	3.86 kJ/kgK	1 kJ/kgK
Specific heat capacity of condenser fluid	4.19 kJ/kgK	4.19 kJ/kgK
Set point of low-pressure thermostat	−15 °C for GSHP / −13 °C for SISHP [a]	−25 °C [b]
Set point of high-pressure thermostat	66 °C [c]	66 °C [c]
Heat-up constant	30 s [d]	30 s [d]
Cool-down constant	80 s [d]	80 s [d]
$f_{\mathrm{el,HP}}$	1.075	-

[a] Calculated by the minimum evaporator inlet temperature from manufacturer data considering the evaporator design temperature difference (5 K for GSHP, 3 K for SISHP) for determination of the minimum evaporator outlet temperature

[b] Calculated by the minimum evaporator inlet temperature from manufacturer data assuming 5 K as temperature difference for the minimum evaporator outlet temperature; within the following system simulations an external controller is used to switch-off an air/water heat pump and use an electric heating element when the ambient temperature falls below −20 °C

[c] Maximum condenser outlet temperature from manufacturer data plus 1 K hysteresis

[d] Data from Bertram [2015] for a brine/water heat pump, assumed to be equal for air/water heat pumps

3.2.2 Solar Energy

3.2.2.1 Solar Thermal Collectors

The *thermal performance of solar thermal collectors* can be described as one-node thermal model with the effective thermal heat capacity of the collector c_{eff} and the mean fluid temperature T_{m} by the following differential equation, which is an expression of the energy balance of the temperature node T_{m} in Figure 3.4:

$$c_{\mathrm{eff}} \frac{\mathrm{d}T_{\mathrm{m}}}{\mathrm{d}t} = \dot{q}_{\mathrm{rad}} - \dot{q}_{\mathrm{th,loss}} - \dot{q}_{\mathrm{th,sol}}, \tag{3.7}$$

where $\dot{q}_{\mathrm{rad}}$ are the specific radiative energy gains (radiative energy balance), $\dot{q}_{\mathrm{th,loss}}$ the specific thermal losses (or gains) due to heat conduction and convection with the ambient air and $\dot{q}_{\mathrm{th,sol}}$ the specific thermal power output of the solar thermal collector, which is transferred to the fluid. Within this approach all thermal capacities (e.g. fluid, absorber, frame or insulation) are lumped together in the effective thermal heat capacity c_{eff} and it is assumed that the temperature of this node is represented by the fluid temperature [Fischer and Müller-Steinhagen, 2009]. The thermal power output (useful energy gain) can be defined with the mass flow $\dot{m}$, the specific thermal capacity c_p and the outlet T_{out} and inlet temperature T_{in} of the heat transfer fluid relative to the gross solar collector area $A_{\mathrm{th,sol}}$ to:

$$\dot{q}_{\mathrm{th,sol}} = \dot{m}\ c_p\ \left(T_{\mathrm{out}} - T_{\mathrm{in}}\right) / A_{\mathrm{th,sol}}. \tag{3.8}$$

With the assumption that the long wave radiation does not depend on the collector temperature, the specific radiative energy balance can be expressed with the parameters of ISO 9806 as:

$$\dot{q}_{\mathrm{rad}} = \eta_0\ \left(K_{\mathrm{b}}\ G_{\mathrm{b}} + K_{\mathrm{d}}\ G_{\mathrm{d}}\right) + c_4\ \left(E_{\mathrm{L}} - \sigma\ T_{\mathrm{amb}}^4\right) - c_6\ u\ G, \tag{3.9}$$

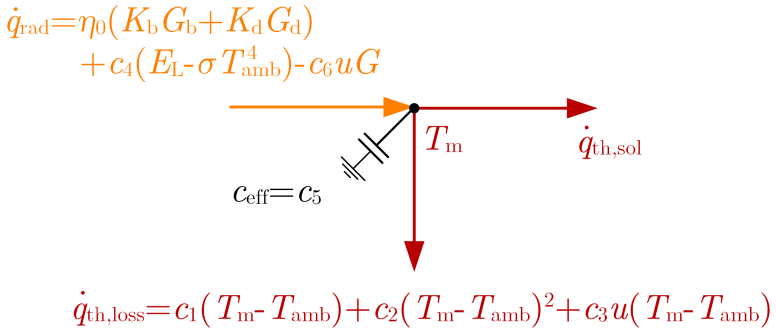

Figure 3.4: One-node model with one thermal capacity of solar thermal collectors.

where η_0 is the zero loss collector efficiency, K_b is the Incidence Angle Modifier (IAM) for beam radiation G_b, K_d is the IAM for diffuse radiation G_d, c_4 is the sky temperature dependence of long wave radiation exchange, E_L is the long wave irradiance, σ is the Stefan-Boltzmann constant, c_6 is the wind speed dependence of the zero loss efficiency, u is the wind speed in the collector plane and G is the global solar irradiance in the collector plane.

Furthermore, the specific thermal losses (or gains) can be expressed with the parameters of ISO 9806 as:

$$\dot{q}_{th,loss} = c_1\ (T_m - T_{amb}) + c_2\ (T_m - T_{amb})^2 + c_3\ u\ (T_m - T_{amb})\,, \tag{3.10}$$

where c_1 is the heat loss coefficient, c_2 is the temperature dependence of the heat loss coefficient and c_3 is the wind speed dependence of the heat loss coefficient.

With Equation 3.9 and Equation 3.10 and the use of coefficient c_5 for the effective thermal capacity c_{eff}, Equation 3.7 can be transformed to the thermal performance model of the quasi-dynamic collector model from ISO 9806:2013 [ISO 9806, 2013]:

$$\begin{aligned}\dot{q}_{th,sol} =& \eta_0\ (K_b\ G_b + K_d\ G_d) - c_1\ (T_m - T_{amb}) - c_2\ (T_m - T_{amb})^2 \\ & - c_3\ u\ (T_m - T_{amb}) + c_4\ \left(E_L - \sigma\ T_{amb}^4\right) - c_5\ \frac{dT_m}{dt} - c_6\ u\ G\end{aligned} \tag{3.11}$$

with

$$K_b = 1 - b_{0,th}\ \left(\frac{1}{\cos(\theta)} - 1\right), \tag{3.12}$$

where $b_{0,th}$ is the constant for the thermal IAM for beam radiation and θ the incidence angle of the beam radiation. Depending on the collector type, some of the coefficients $c_1 - c_6$ can be neglected. In case of glazed collectors tested with artificial wind source at a speed between 2 m/s and 4 m/s, the coefficients c_3, c_4 and c_6 can be set to zero right from the beginning of the parameter identification. In case of unglazed collectors, the use of the full collector model is mandatory excepting the case that c_2 is negative or has no statistical significance. In this case the parameter identification can be applied without c_2 [ISO 9806, 2013].

The quasi-dynamic collector model of ISO 9806:2013 is implemented in TRNSYS Type 832 *Dynamic Collector Model* [Haller et al., 2013b]. For the consideration of ISO 9806:2017 [ISO 9806, 2017], Equation 3.11 has to be extended by the wind speed dependence of long

wave radiation exchange c_7 as well as the radiation losses c_8 and the reduced wind speed $u' = u - 3\,\mathrm{m/s}$ should be used for the modeling. The ISO 9806:2017 model is currently not implemented in TRNSYS Type 832 but could be a good improvement for further development of the TRNSYS Type and its use for solar thermal performance characterization. For this work, it was decided to use the ISO 9806:2013 model without reduced wind speed. In addition to the missing implementation of the current standard in Type 832, this was also done in order to use available parameters for solar thermal collectors and obtain physically more comprehensible results that are comparable with parameters previously determined by other test laboratories if the collector parameters are identified.

Furthermore, Type 832 offers an additional term to Equation 3.11 for the consideration of latent (condensation and sublimation) heat gains $\dot{q}_{\mathrm{lat}}$. For the calculation of condensation gains, two models are implemented which are based on the methods of Perers [2010] and Bertram et al. [2010]. In addition, a frosting mode has been added to both models for the possibility of consideration of sublimation. However, it is noted that there is no validation of the frosting feature and no subsequent melting or increased heat transfer resistance is calculated [Haller et al., 2013b]. In the following simulations, latent heat gains are not considered for FPCs. In contrast, for WISC collectors that are used in SISHP systems operated with low collector temperatures, condensation gains calculated by the method of Bertram et al. [2010] and the frosting mode of Type 832 are switched on. For the FPC models in this work, standard values for selective FPCs from the reference heating system of IEA SHC Task 32 [Heimrath and Haller, 2007] are selected and summarized in Table 3.4. As described before, the parameters c_3, c_4 and c_6 show only an insignificant influence on the collector performance of FPCs and can thus be set to zero.

Table 3.4: Parameters of FPC collector model [Heimrath and Haller, 2007].

Parameter	Value
Zero loss collector efficiency η_0	0.800
Heat loss coefficient c_1	$3.50\,\mathrm{W/m^2K}$
Temperature dependence of the heat loss coefficient c_2	$0.015\,\mathrm{W/m^2K^2}$
Effective thermal capacity c_5	$7\,000\,\mathrm{J/m^2K}$
Constant for the thermal IAM for beam radiation $b_{0,\mathrm{th}}$	0.1800
IAM for diffuse radiation K_{d}	0.90

The parameters of the solar thermal model for the simulation of WISC collectors are identified by comparing and adjusting simulated results in TRNSYS to measured data in steady-state conditions from a manufacturer. In general, identification or determination of model parameters by comparing and adjusting simulated results to measured data is a well-known procedure for different applications, especially in the field of solar thermal systems. An objective (or cost) function is defined to assess the agreement of the model results with the measured data. The model parameters are then adjusted to better fit the measurement by minimization of the objective function. In the field of solar thermal collectors and systems, the most common methods for the minimization process are multiple linear regression (MLR), which has been introduced as extended version by Perers [1997], and a dynamic parameter identification procedure with the fit program DF [Spirkl, 1997] which uses the Levenberg-Marquardt algorithm [Fischer et al., 2012]. Furthermore, newer approaches like Budig et al. [2009] or Almeida et al. [2014] use GenOpt [GenOpt, 2011]

in combination with TRNSYS for the parameter identification. GenOpt is a generic optimization program which is used to minimize an objective function that is evaluated by an external simulation program like TRNSYS. GenOpt includes a library with different local and global one-dimensional and multi-dimensional optimization algorithms, like Particle Swarm Optimization (PSO, meta-heuristic population-based algorithm, stochastic) or Hooke-Jeeves algorithm (GPS-HJ, generalized pattern search method, deterministic). Using these optimization algorithms, a systematic variation of specified parameters is performed in order to minimize the objective function.

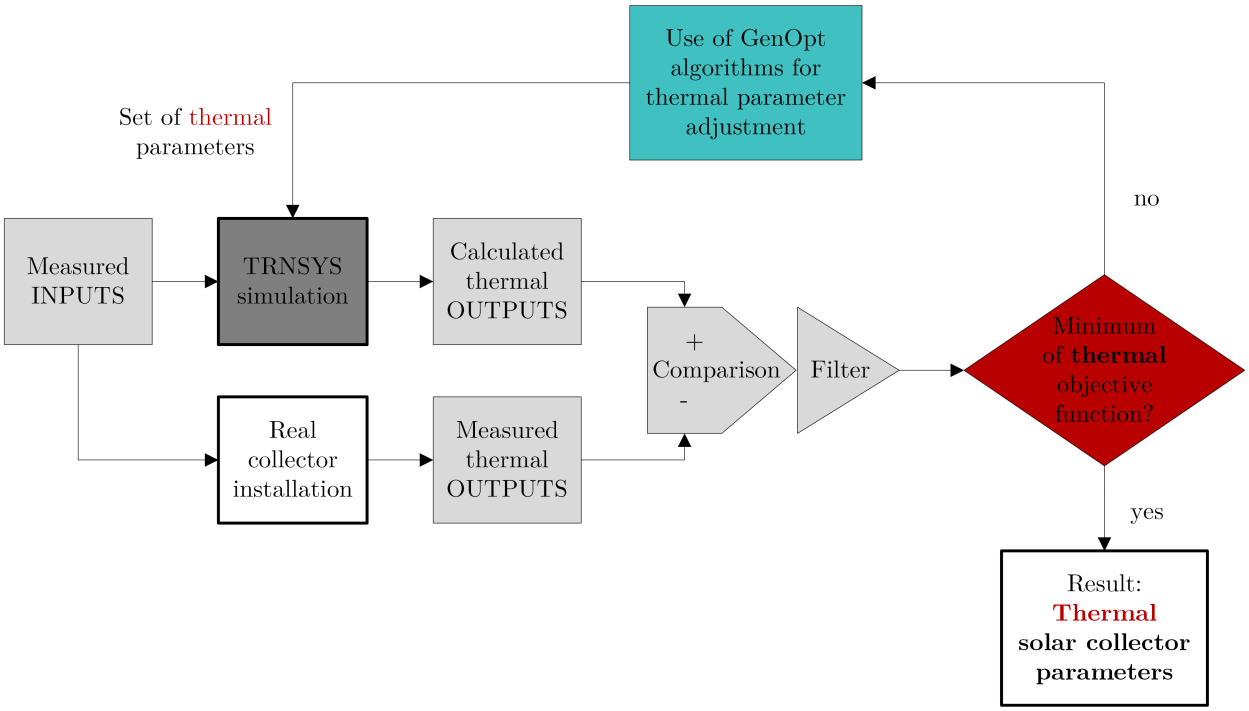

Figure 3.5: Parameter identification procedure for solar thermal collectors.

The parameter identification procedure for the solar thermal collector model using TRNSYS and GenOpt is shown in Figure 3.5. A set of measured values is used as time dependent input for the TRNSYS simulation via a data reader. In this case, as no dynamic measurements were available for the considered WISC collectors, steady-state conditions are used for a time interval of one hour. The available measured and from measurements calculated inputs (E_L, G, θ, T_amb, u, $\dot{m}$, T_in) are then used to simulate the thermal outputs of the TRNSYS model, especially the thermal power output of the solar thermal collector $\dot{Q}_\mathrm{th,sol,sim}$. Subsequently, the calculated thermal outputs are compared via the absolute error with the measured thermal outputs $\dot{Q}_\mathrm{th,sol,meas}$. At this, the results are filtered according to predefined constraints if necessary. This is followed by the calculation of the thermal objective function which has to be minimized. In this iterative procedure, GenOpt is used to systematically vary the thermal collector parameters (η_0, K_d, $b_\mathrm{0,th}$, c_1-c_6) until the minimum of the thermal objective function is reached. For the identification of the WISC collector parameters, the GPS-HJ algorithm and continuous variables with lower and upper bounds are used to adjust the thermal collector parameters. As no dynamic data was available, the effective thermal capacity of the absorber c_5 is set to a fixed value recommend by the manufacturer. The objective function is defined as mean absolute error (MAE) between

simulated and measured thermal power output of the WISC collector:

$$\mathrm{MAE}_{\mathrm{th,sol}} = \frac{1}{n\ \Delta t} \sum_{i=1}^{n} \left(\left| \dot{Q}_{\mathrm{th,sol,sim},i} - \dot{Q}_{\mathrm{th,sol,meas},i} \right| \cdot \Delta t \right). \tag{3.13}$$

The results of the parameter identification are summarized in Table 3.5 and a comparison of measured solar thermal power from the manufacturer and simulations results with the estimated model parameter in steady-state conditions is shown in Figure 3.6.

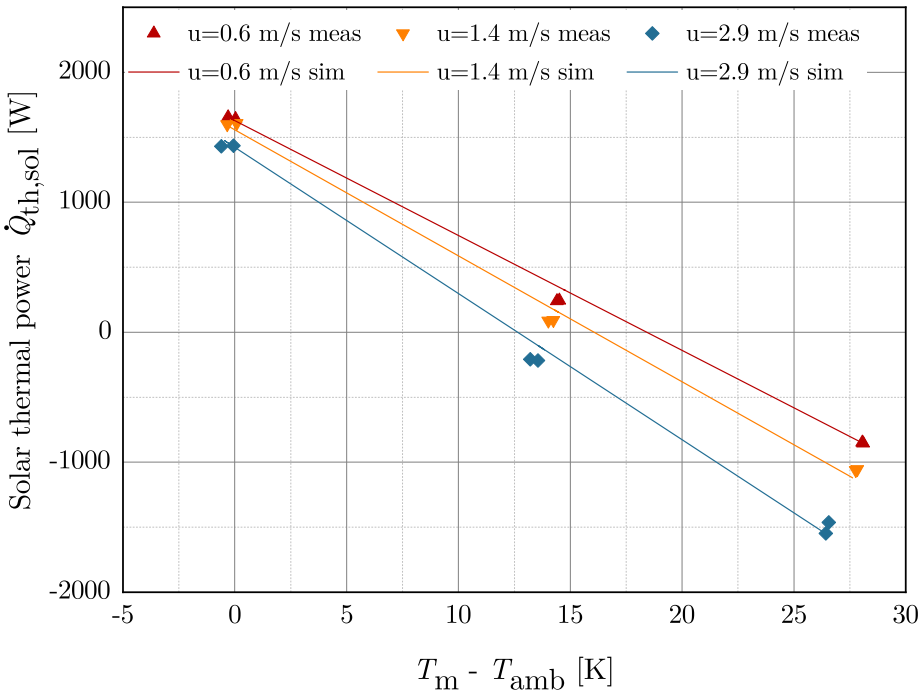

Figure 3.6: Comparison of measured solar thermal power output (data points with two measurements with similar conditions) from the manufacturer and simulation results (lines) for the WISC collector in steady-state conditions for wind speeds of 0.6 m/s, 1.4 m/s and 2.9 m/s and a net irradiance $G'' = 940\,\mathrm{W/m^2}$ depending on the temperature difference between the mean collector temperature T_{m} and the ambient temperature T_{amb}.

Table 3.5: Parameters of WISC collector model.

Parameter	Value
Zero loss collector efficiency η_0	0.699
Heat loss coefficient c_1	$32.79\,\mathrm{W/m^2K}$
Temperature dependence of the heat loss coefficient c_2	$0\,\mathrm{W/m^2K^2}$
Wind speed dependence of the heat loss coefficient c_3	$4.64\,\mathrm{J/m^3K}$
Sky temperature dependence of long wave radiation exchange c_4	0.9338
Effective thermal capacity c_5	$20\,000\,\mathrm{J/m^2K}$
Wind speed dependence of the zero loss efficiency c_6	$0.034\,\mathrm{s/m}$
Constant for the thermal IAM for beam radiation $b_{0,\mathrm{th}}$	0.0327
IAM for diffuse radiation K_d	1.00

3.2.2.2 Photovoltaic Modules

The *electrical performance of PV modules* can be described with a performance model that mostly uses datasheet values of PV modules based on characterization according to standard IEC 61853-1:2011 [IEC 61853-1, 2011]. The overall (or total) electrical efficiency $\eta_{\mathrm{el,sol}}$ of PV modules is calculated with the overall instantaneous performance ratio PR_{tot} as follows:

$$\eta_{\mathrm{el,sol}} = \eta_{\mathrm{el,sol,ref}}\ PR_{\mathrm{tot}}, \tag{3.14}$$

where $\eta_{\mathrm{el,sol,ref}}$ is the electrical efficiency of a PV module at reference conditions (usually standard test conditions (STC)).

The electrical power output of the PV modules $P_{\mathrm{el,sol}}$ is given by:

$$P_{\mathrm{el,sol}} = \eta_{\mathrm{el,sol,ref}}\ PR_{\mathrm{tot}}\ G\ A_{\mathrm{el,sol}} \tag{3.15}$$

and as specific electrical power output by [Lämmle et al., 2017]:

$$p_{\mathrm{el,sol}} = \eta_{\mathrm{el,sol,ref}}\ PR_{\mathrm{tot}}\ G, \tag{3.16}$$

where G is the global solar irradiance in the PV plane and $A_{\mathrm{el,sol}}$ the gross PV area.

The overall instantaneous performance ratio PR_{tot} is calculated with [Lämmle et al., 2017]:

$$PR_{\mathrm{tot}} = PR_{\mathrm{IAM}}\ PR_{\mathrm{T}}\ PR_{\mathrm{G}}. \tag{3.17}$$

At this, the electrical performance model for PV takes the following loss effects (performance ratios PR) into account:

- Loss effects of incidence angle PR_{IAM}
- Loss effects of irradiance PR_{G}
- PV cell temperature dependence of electrical efficiency PR_{T}.

The instantaneous performance ratio due to incidence angle losses PR_{IAM} is calculated

with [Duffie and Beckman, 2013]:

$$PR_{\mathrm{IAM}} = 1 - b_{0,\mathrm{el}} \left(\frac{1}{\cos(\theta)} - 1 \right), \tag{3.18}$$

where $b_{0,\mathrm{el}}$ is the constant for the electrical IAM and θ the incidence angle of beam radiation.

The instantaneous performance ratio due to irradiance losses PR_{G} is calculated with [Heydenreich et al., 2008]:

$$PR_{\mathrm{G}} = a\, G + b \ln(G+1) + c \left[\frac{(\ln(G+\mathrm{e}))^2}{G+1} - 1 \right] \tag{3.19}$$

with the model parameters a in $\mathrm{m^2/W}$, b and c dimensionless, the global solar irradiance in the PV plane G in $\mathrm{W/m^2}$ and the Euler's number e.

The PV cell temperature dependence of the electrical efficiency is calculated with [Skoplaki and Palyvos, 2009]:

$$PR_{\mathrm{T}} = 1 - \beta \left(T_{\mathrm{cell}} - T_{\mathrm{cell,ref}} \right), \tag{3.20}$$

where β is the power temperature coefficient of the PV cells, T_{cell} the temperature of the PV cells and $T_{\mathrm{cell,ref}}$ the PV cell temperature at reference conditions (usually STC conditions).

For PV modules, the temperature of the PV cells $T_{\mathrm{cell,PV}}$ is calculated with [Faiman, 2008]:

$$T_{\mathrm{cell,PV}} = T_{\mathrm{amb}} + \frac{G}{U_0 + U_1\, u}, \tag{3.21}$$

where T_{amb} is the ambient air temperature, U_0 the heat loss coefficient of a PV module, U_1 the wind dependent heat loss coefficient of a PV module and u the wind speed in the PV plane. At this, the PV cell temperature is assumed to be equal to the module temperature and is used for the calculation of the PV cell temperature dependence of the electrical efficiency in Equation 3.20.

Table 3.6: Parameters of PV module model.

Parameter	Value
Electrical efficiency at STC conditions $\eta_{\mathrm{el,sol,ref}}$	0.1497
Power temperature coefficient β	0.386 %/K
Heat loss coefficient U_0	30.02 $\mathrm{W/m^2K}$
Wind dependent heat loss coefficient U_1	6.28 $\mathrm{Ws/m^3K}$
Constant for electrical IAM $b_{0,\mathrm{el}}$	0.041
Model parameter a for irradiance dependence	−0.00008411 $\mathrm{m^2/W}$
Model parameter b for irradiance dependence	−0.03388
Model parameter c for irradiance dependence	−1.367

For the implementation of the described PV model in TRNSYS, a new TRNSYS Type (Type 835) was programmed within this work and published in Jonas [2019a]. The model has different modes and is also used for the electrical modeling of PVT collectors (see Section 3.2.2.3). The electrical parameters of the simulated PV modules are summarized in

Table 3.6 and are set equal to the electrical parameters of the PVT collectors from Section 3.2.2.3 to achieve comparable results without influences of the electrical power characteristics of different PV module types. At this, U_0 and U_1 determined by Koehl et al. [2011] are used as values for a crystalline PV module.

3.2.2.3 Photovoltaic-Thermal Collectors

The thermal performance of PVT collectors is currently tested according to ISO 9806 and the electrical performance according to different IEC standards (depending on the module types). At this, the thermal performance characterization of PVT collectors shall take place with simultaneous thermal and electrical generation under MPP conditions. As the instantaneous thermal and electrical power is interlinked [Hofmann et al., 2010], it is important to further develop performance models specifically for the characterization of PVT collectors.

For the electrical performance modeling of PVT collectors, a variety of modeling approaches exist, like those presented in Chow [2003]; Perers et al. [2012]; Helmers and Kramer [2013]; Bilbao and Sproul [2015]; Zenhäusern et al. [2015]. At this, the electrical performance modeling is mostly based on the work of Florschuetz [1979], who extended the Hottel-Whillier-Bliss equation and coupled the PV cell and fluid temperature node by a heat transfer coefficient. All proposed performance models have their specific strengths and weaknesses but there is currently no standardized modeling and testing approach [Lämmle, 2018]. In this context, the main objective of the previously published work in Jonas et al. [2019] was the development and validation of a novel PVT collector performance model based on existing modeling approaches using mainly standardized model parameters, which can be implemented in common simulation tools like TRNSYS and used for system simulations. Furthermore, the performance model may form the basis for future PVT collector performance testing, certification and standardization schemes.

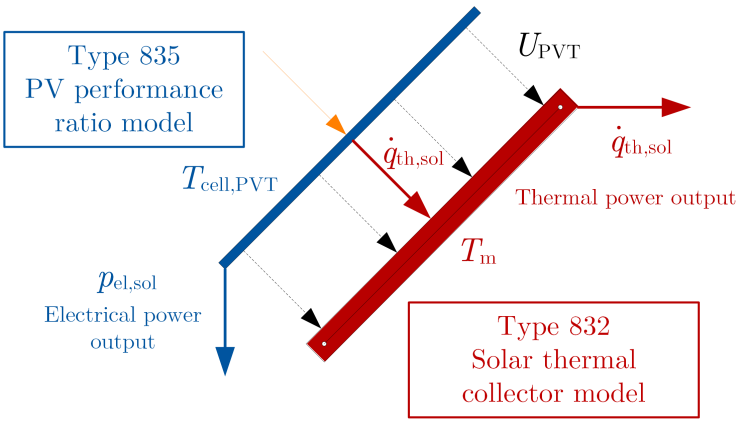

Figure 3.7: Coupled PVT model with electrical and thermal performance model.

The main concept of the proposed model was the development of a *PVT performance* model, which connects the quasi-dynamic thermal collector model of ISO 9806 described in Section 3.2.2.1 with the PV performance model described in Section 3.2.2.2 via a two-node model approach with internal heat transfer coefficient U_{PVT} (see Figure 3.7). The numerical description is based on the work of Lämmle et al. [2017] and Jonas et al. [2018]. The PV performance model implemented in TRNSYS Type 835 can be connected to the ISO 9806 implementation in TRNSYS Type 832 for a combined PVT performance model in TRNSYS. In addition, TRNSYS Type 835 can be coupled to other existing models of solar

thermal collectors or absorbers for the calculation of the electrical power output of PVT collectors or, as described before, can be used as PV performance model with internal PV cell temperature calculation.

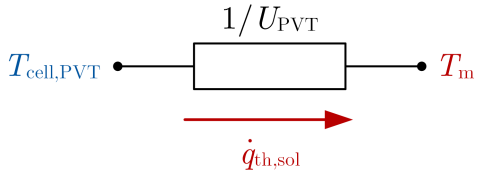

Figure 3.8: Equivalent thermal network of the two-node PVT model between temperature nodes T_{m} and $T_{\mathrm{cell,PVT}}$ interlinked by U_{PVT}.

The major difference between the electrical performance calculation of PV modules and PVT collectors in this approach results from the PV cell temperature calculation. Instead of the described PV cell temperature calculation in Section 3.2.2.2 for PV modules, the PV cell temperature of PVT collectors $T_{\mathrm{cell,PVT}}$ is calculated via an equivalent thermal network with the internal heat transfer coefficient U_{PVT}, which connects the PV cell temperature to the mean fluid temperature T_{m} of the PVT collector (cf. Figure 3.8). In this case, the PV cell temperature of a PVT collector is calculated as second thermal node without capacitance via the equivalent thermal network as follows [Lämmle et al., 2017]:

$$T_{\mathrm{cell,PVT}} = T_{\mathrm{m}} + \frac{\dot{q}_{\mathrm{th,sol}}}{U_{\mathrm{PVT}}}, \tag{3.22}$$

where $\dot{q}_{\mathrm{th,sol}}$ is the specific thermal power output of the PVT collector calculated via the ISO 9806 quasi-dynamic collector model from Equation 3.11 and T_{m} the mean fluid temperature as average of inlet and outlet temperature T_{in} and T_{out}. This approach was introduced as *two-node model with one thermal capacity* in Jonas et al. [2019]. The PV cell temperature

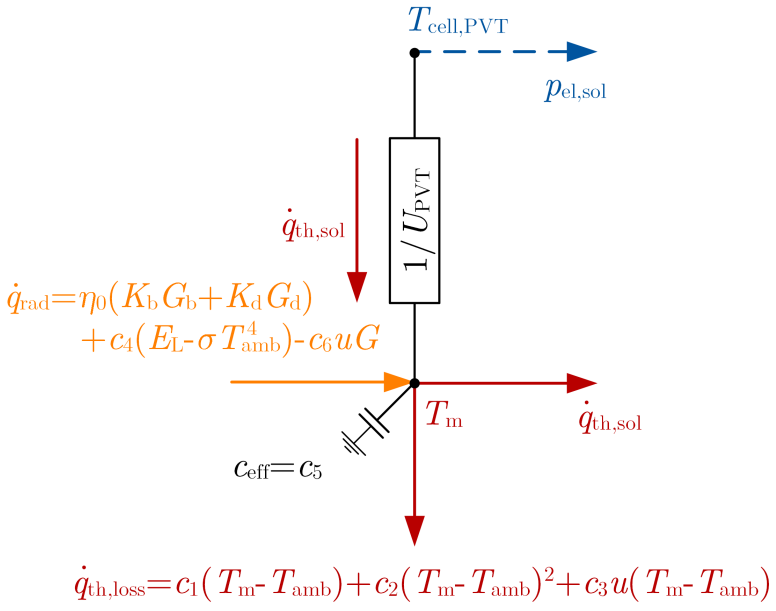

Figure 3.9: Two-node model with one thermal capacity of PVT collectors.

of the PVT collector is then used for the calculation of the PV cell temperature dependence of the electrical efficiency in Equation 3.20 and the specific electrical power output $p_{\mathrm{el,sol}}$ in Equation 3.16 (cf. Figure 3.9). For the calculation of the thermal and electrical power output of PVT collectors, the gross PVT collector area is used as gross solar collector area and gross PV area. Regarding the thermal modeling, condensation and frosting is not considered for PVT collectors in the following simulations. In addition to the introduced solar thermal and PV model parameters, the model requires the parameter U_{PVT} for the explicit calculation of the PV cell temperature of PVT collectors. As the electrical mode of operation has a significant impact on the thermal efficiency, it is important that the thermal performance coefficients for the thermal power output calculation of PVT collectors are determined in MPP mode [Lämmle, 2018]. The constant parameter U_{PVT} is characterized by parameter identification during quasi-dynamic or steady-state performance measurements according to ISO 9806. Alternatively, U_{PVT} can be obtained numerically from the collector efficiency factor F', by dark-measurements with surface temperature measurements, or via finite element methods [Lämmle, 2018].

As alternative to the proposed approach, a second approach was introduced in Jonas et al. [2019] as *two-node model with two thermal capacities* that considers the thermal capacitances for each separate node of the mean fluid temperature T_{m} and the mean absorber temperature T_{abs}. For solar thermal collectors, it is known as *two-node model* [Fischer and Müller-Steinhagen, 2009; Theis et al., 2009]. Nevertheless, as figured out in Jonas et al. [2019], using two thermal capacities instead of one does not achieve a consistent improvement of the model accuracy and both models achieve a good agreement between simulation and test. On the contrary, the use of the standardized model with one thermal capacity from ISO 9806 leads to a better comparability with solar thermal collectors and an easier interpretation of the model parameters. As a consequence, the two-node model with one thermal capacity is recommended as standard model for PVT collectors and is used for the system simulation in this work. Regarding the electrical performance modeling, a comparison of the described electrical performance model with a four-parameter (single diode) PV model, presented in Jonas et al. [2018], figured out that the implementation of a four-parameter PV model has no noticeable advantages for the simulation of the electrical power output in case of the analyzed PVT collectors and operating conditions. Hence, further investigations with a four-parameter PV model are not subject of this work and the proposed electrical performance model is used for the system simulation in this work.

The thermal and electrical parameters for the simulation of WISC and covered flat-plate PVT collectors in this work are based on the parameter identification of a WISC and a covered flat-plate PVT collector by experimental measurements previously published in Jonas et al. [2019]. In the following, parts of the experimental measurements, the parameter identification procedure and the model validation presented in Jonas et al. [2019] and used for this work are explained in detail. This is followed by the summary of the PVT collector parameters for the system simulation in this work.

The experimental measurements were realized on an outdoor test bench in Saarbrücken, Germany at the Laboratory for Solar Energy Systems of the University of Applied Sciences htw saar (Figure 3.10). The two different PVT collectors were installed on a test roof and monitored under dynamic outdoor conditions during MPP operation:

- WISC PVT collector with rear collector cover and thermal insulation material on the back of the PVT absorber
- Covered flat-plate PVT collector with front glazing, rear collector cover and no thermal

insulation material on the back of the PVT absorber.

Figure 3.10: Outdoor testbench with the investigated PVT collectors [Jonas et al., 2019].

For PVT collectors, the standard measurements of the thermal performance of solar thermal collectors according to ISO 9806:2017 are extended by the relevant electrical values and were measured continuously. A systematic scheme of the measurement set-up including the main measured values used for the performance characterization of the PVT collectors is shown in Figure 3.11.

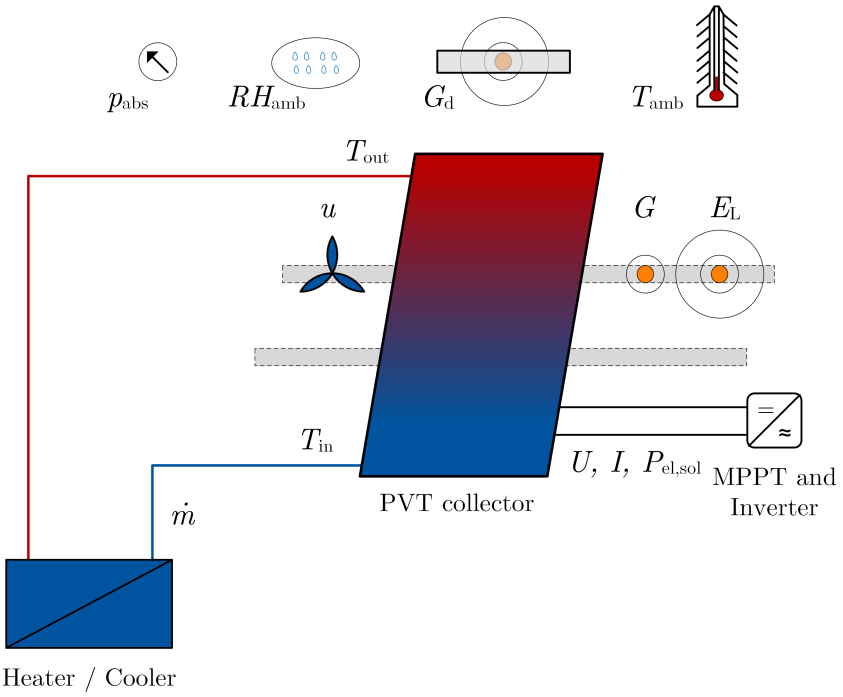

Figure 3.11: Measurement scheme of the outdoor testbench. Adapted from Jonas et al. [2019].

ISO 9806:2017 defines the following typical days that have to be included in the measurement datasets for thermal performance characterization of solar collectors:

- Day type 1: η_0-conditions, mostly clear sky conditions
- Day type 2: elevated operating temperature or η_0-conditions, partly cloudy conditions including broken cloud and clear sky conditions
- Day type 3: mean operating temperature conditions including clear sky conditions
- Day type 4: high operating temperature conditions including clear sky conditions.

For a better representation of the thermal behavior of the PVT collectors over the entire operating temperature range, two different temperature differences of the mean collector temperature to the ambient ($T_\mathrm{m} - T_\mathrm{amb}$) were measured for day type 3 for both PVT collectors. Furthermore, it was possible to operate the covered flat-plate PVT collector with a higher temperature difference to the ambient, due to the lower thermal losses in comparison to the WISC PVT collector. Hence, in case of the covered flat-plate PVT collector, a second temperature difference to the ambient was measured for day type 4. The assignment of the measurements to the different operating temperatures of the PVT collectors is summarized in Table 3.7.

Table 3.7: Performed measurements over the operating temperature range of the PVT collectors.

Day type	1	2	3a	3b	4a	4b
$T_\mathrm{m} - T_\mathrm{amb}$	0 K	0 K or higher	10 K	15 K	20 K	30 K
WISC PVT	x	x	x	x	x	-
Covered flat-plate PVT	x	x	x	x	x	x

For the identification of the model parameters for the WISC and covered flat-plate PVT collectors, the measured test data were evaluated and usable test sequences were separated. For each day type and each type of PVT collector, one test sequence was chosen and the test sequences were combined to one data set. Within the combined test sequences, a Boolean value was defined for each time step as indicator whether the time step should be considered for the parameter identification or not. The objective of this process was the filtering of start-up sequences between the test sequences of different day types and the exclusion of invalid data, e.g. if something was changed in the test bench or measured values were outside a reliable or usable range. To remove unsuitable data, the datasets were filtered to a set of constraints ($G < 100\,\mathrm{W/m^2}$; $\dot{q}_\mathrm{th,sol}, p_\mathrm{el,sol} < 0\,\mathrm{W/m^2}$; $p_\mathrm{el,sol}, G_\mathrm{d} > G$; $T_\mathrm{m} < (T_\mathrm{amb} - 3\,\mathrm{K})$) considering the requirements of each day type. Data points at which at least one of the constraints was violated were disregarded for the calculation of the objective function for the parameter identification process. In addition, it was necessary to remove data points manually, e.g. malfunctions of the MPP tracker, and to exclude these data generously from the calculation of the objective function to ensure that the effects of the failure were balanced out again.

The parameter identification procedure is nearly the same as described for solar thermal collectors in Section 3.2.2.1 with an extension for the electrical parameters that are needed

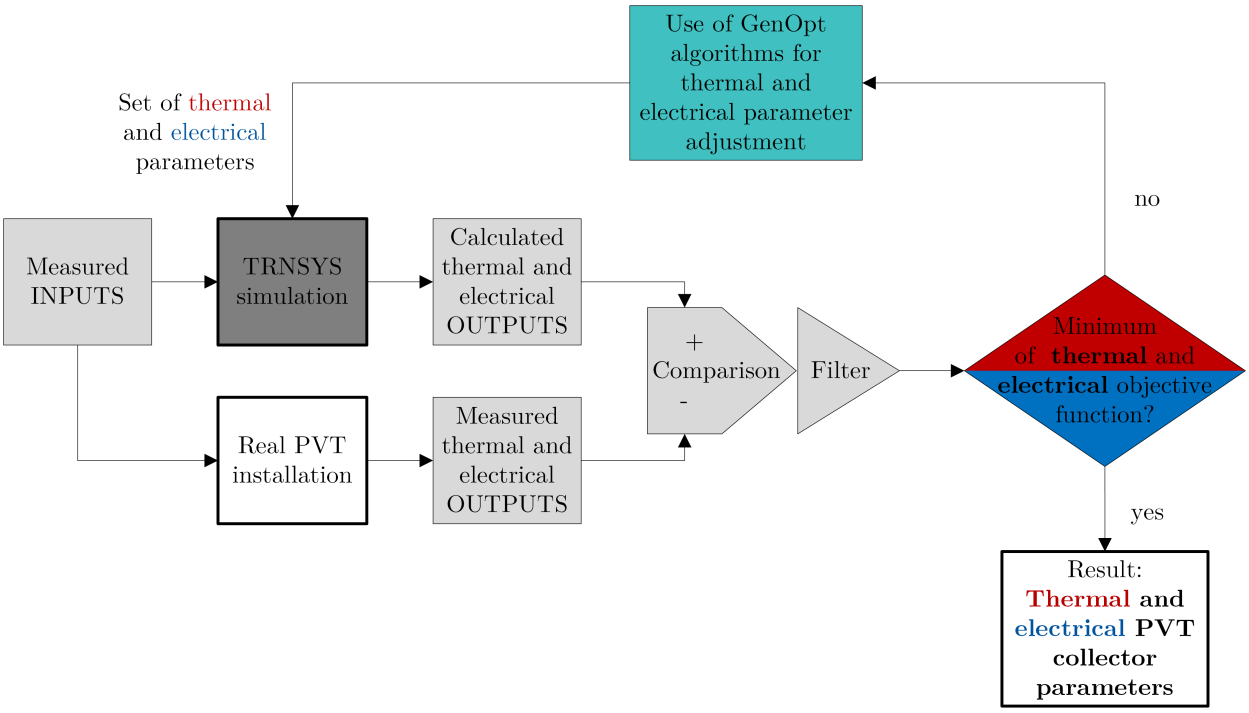

Figure 3.12: Parameter identification procedure for PVT collectors.

for PVT collectors. The approach with combined thermal and electrical parameter identification procedure for the PVT collector model using TRNSYS and GenOpt is shown in Figure 3.12. A set of measured values is used as time dependent input for the TRNSYS simulation via a data reader. The measured inputs (E_L, G, G_d, θ, T_amb, RH_amb, p_abs, u, $\dot{m}$, T_in) are then used to simulate the thermal and electrical outputs of the TRNSYS model, especially the thermal $\dot{Q}_\mathrm{th,sol,sim}$ and the electrical $P_\mathrm{el,sol,sim}$ power output of the PVT collector. Subsequently, the calculated outputs are compared with the corresponding measured thermal $\dot{Q}_\mathrm{th,sol,meas}$ and electrical $P_\mathrm{el,sol,meas}$ outputs via the absolute error and filtered according to the constraints described before. This is followed by the calculation of the combined thermal and electrical objective function which has to be minimized. In this iterative procedure, GenOpt is used to systematically vary the thermal (η_0, K_d, $b_\mathrm{0,th}$, c_1-c_6) as well as the electrical ($\eta_\mathrm{el,sol,ref}$, β, $b_\mathrm{0,el}$, a, b, c) PVT collector parameters and the parameter U_PVT simultaneously until the minimum of the combined thermal and electrical objective function is reached. At this, the GPS-HJ algorithm and continuous variables with lower and upper bounds are used to adjust the mentioned parameters. The used combined thermal and electrical objective function is defined as the sum of the MAE of the thermal and electrical power as follows:

$$\mathrm{MAE}_\mathrm{th+el,sol} = \frac{\sum_{i=1}^{n} \left(\left| \dot{Q}_\mathrm{th,sol,sim,}i - \dot{Q}_\mathrm{th,sol,meas,}i \right| \cdot \Delta t + \left| P_\mathrm{el,sol,sim,}i - P_\mathrm{el,sol,meas,}i \right| \cdot \Delta t \right)}{n\ \Delta t}. \quad (3.23)$$

For further analysis of the model accuracy, the MAE of the thermal power output (Equation 3.13), the MAE of the electrical power output and the corresponding normalized root

mean square errors (nRMSEs) can be used and defined as follows:

$$\mathrm{MAE}_{\mathrm{el,sol}} = \frac{1}{n\ \Delta t}\ \sum_{i=1}^{n} \left(\left|P_{\mathrm{el,sol,sim},i} - P_{\mathrm{el,sol,meas},i}\right| \cdot \Delta t\right) \tag{3.24}$$

$$\mathrm{nRMSE}_{\mathrm{th,sol}} = \mathrm{RMSE}_{\mathrm{th,sol}}\ /\ \left[\frac{1}{n\ \Delta t}\ \sum_{i=1}^{n} \left(\dot{Q}_{\mathrm{th,sol,meas},i} \cdot \Delta t\right)\right] \tag{3.25}$$

$$\mathrm{nRMSE}_{\mathrm{el,sol}} = \mathrm{RMSE}_{\mathrm{el,sol}}\ /\ \left[\frac{1}{n\ \Delta t}\ \sum_{i=1}^{n} \left(P_{\mathrm{el,sol,meas},i} \cdot \Delta t\right)\right] \tag{3.26}$$

with the root mean square errors (RMSEs):

$$\mathrm{RMSE}_{\mathrm{th,sol}} = \sqrt{\frac{\sum\limits_{i=1}^{n} \left[\left(\dot{Q}_{\mathrm{th,sol,sim},i} - \dot{Q}_{\mathrm{th,sol,meas},i}\right)^2 \cdot \Delta t\right]}{n\ \Delta t}} \tag{3.27}$$

and

$$\mathrm{RMSE}_{\mathrm{el,sol}} = \sqrt{\frac{\sum\limits_{i=1}^{n} \left[\left(P_{\mathrm{el,sol,sim},i} - P_{\mathrm{el,sol,meas},i}\right)^2 \cdot \Delta t\right]}{n\ \Delta t}}. \tag{3.28}$$

The results of the parameter identification for the WISC PVT collector and the covered flat-plate PVT collector using the described approach are summarized in Table 3.8. The

Table 3.8: Results of the PVT model parameter identification.

Parameter	WISC PVT	Covered flat-plate PVT
Zero loss collector efficiency η_0	0.532	0.595
Heat loss coefficient c_1	8.018 W/m^{2}K	6.023 W/m^{2}K
Temperature dependence of the heat loss coefficient c_2	0.029 W/m^{2}K^2	0.034 W/m^{2}K^2
Wind speed dependence of the heat loss coefficient c_3	1.7175 J/m^{3}K	0.0140 J/m^{3}K
Sky temperature dependence of long wave radiation exchange c_4	0.303	0.213
Effective thermal capacity c_5	37 925 J/m^{2}K	17 031 J/m^{2}K
Wind speed dependence of the zero loss efficiency c_6	0.031 s/m	0.006 s/m
Constant for the thermal IAM for beam radiation $b_{0,\mathrm{th}}$	0.019	0.085
IAM for diffuse radiation K_{d}	0.920	0.905
Internal heat transfer coefficient from PV cell to fluid U_{PVT}	46.08 W/m^{2}K	33.10 W/m^{2}K
Electrical efficiency at STC conditions $\eta_{\mathrm{el,sol,ref}}$	0.1497	0.1376
Power temperature coefficient β	0.386 %/K	0.474 %/K
Constant for electrical IAM $b_{0,\mathrm{el}}$	0.041	0.130
Model parameter a for irradiance dependence	−0.00008411 m^2/W	0.00004785 m^2/W
Model parameter b for irradiance dependence	−0.03388	−0.04900
Model parameter c for irradiance dependence	−1.367	−1.332

MAE_{th} is 13.84 W for the WISC PVT collector and 9.34 W for the covered flat-plate PVT collector. The MAE_{el} reaches values of 2.36 W for the WISC PVT collector and 2.28 W for the covered flat-plate PVT collector.

The presented approach was introduced as *one-step approach with combined thermal and electrical parameter identification procedure (combined fit)* in Jonas et al. [2019]. As alternative to the proposed approach, a second approach was introduced in Jonas et al. [2019] as *two-step approach with separated thermal and electrical parameter identification procedure (separated fit)* in which the thermal parameters are identified in a first step and are used as fixed parameters for the electrical parameter identification including U_{PVT} in a second step using the corresponding thermal or electrical MAE. Nevertheless, as figured out in Jonas et al. [2019], the results of the combined fit are nearly the same as those of the separated approach and due to lower effort and time demand the combined fit (one-step approach) is preferable and thus it is used and presented in this work.

Instead of the described parameter identification of all electrical model parameters, the electrical parameters $\eta_{el,ref}$ and β can be obtained from the datasheets of PV modules. Furthermore, the irradiance-dependent parameters a, b and c can be determined by a parameter identification of Equation 3.19 based on performance measurements according to standard IEC 61853-1:2011. Since measurement data regarding this standard is rarely provided by manufacturers, literature data, e.g. from Lämmle et al. [2017], can be used as assumption for the modeling of the irradiance behavior. In addition, the IAM parameter $b_{0,el}$ can either be identified by the described parameter identification procedures or assumed to be equal to the thermal IAM $b_{0,th}$. Nevertheless, the results in Jonas et al. [2019] show that the parameter identification of all electrical parameters leads to an improvement of the electrical model accuracy. As a consequence, the fit of all electrical parameters is preferable over the parameterization with data sheet values or standard values from literature. Furthermore, this leads to the advantage that the parameterization is independent from the availability of manufacturer data which is often not provided with the required details. In conclusion, for the parameter identification of PVT collectors a one-step approach with combined simultaneous fit of all thermal and electrical parameters was identified as the most suitable method using the MAEs as objective function and the Hooke-Jeeves optimization algorithm in GenOpt [Jonas et al., 2019].

For the validation of the TRNSYS model and the parameter identification procedure, the PVT collectors were simulated with measurement data sets that are different to the data used for the parameter identification and the simulation results were compared with the measured values. The dynamic behavior of the thermal and electrical power output of the WISC and covered flat-plate PVT collectors as well as the main solar irradiance data are shown in Figure 3.13 and Figure 3.14 for validation sequence 1 (mostly clear sky, day type 1), in Figure 3.15 and Figure 3.16 for validation sequence 2 (partly cloudy, day type 2) and in Figure 3.17 and Figure 3.18 for validation sequence 3 (mean operating temperature conditions including clear sky, day type 3b).

In case of day type 1, the simulated dynamic behavior shows a good agreement to the measured values of the thermal and electrical power output of the PVT collectors, which is also expressed in a small $nRMSE_{th,sol}$ of 1.95 % for the WISC PVT collector and 1.17 % for the covered flat-plate PVT collector. The $nRMSE_{el,sol}$ amounts to 0.90 % for the WISC PVT collector and 1.94 % for the covered flat-plate PVT collector. Regarding the ratio of the difference between the simulated and measured thermal ($\Delta Q_{th,sol}$) or electrical ($\Delta W_{el,sol}$) energy generation related to the measured thermal ($Q_{th,sol,meas}$) or electrical ($W_{el,sol,meas}$) energy, the modeled energy production over the period is also in a good accuracy with

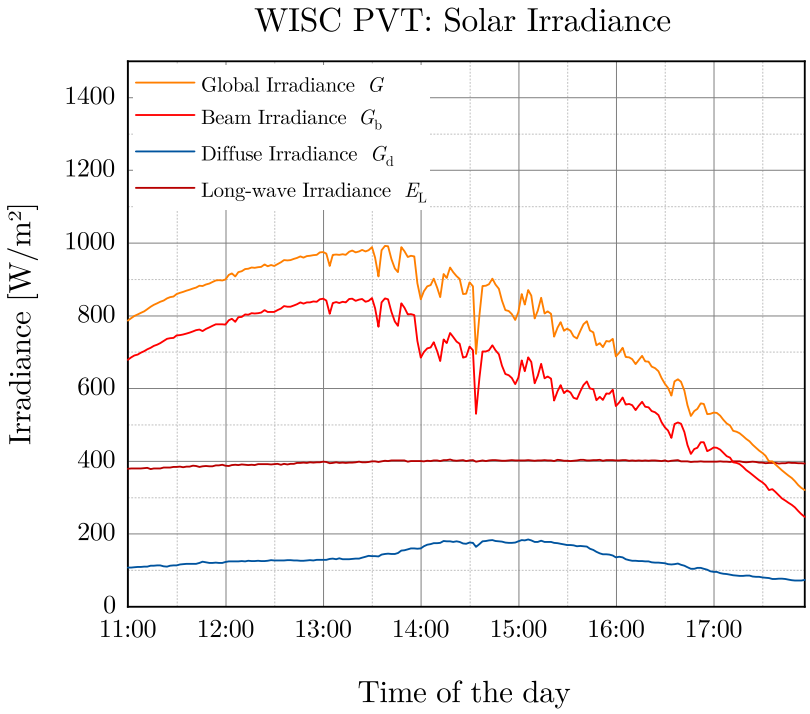

(a) Main solar irradiance data

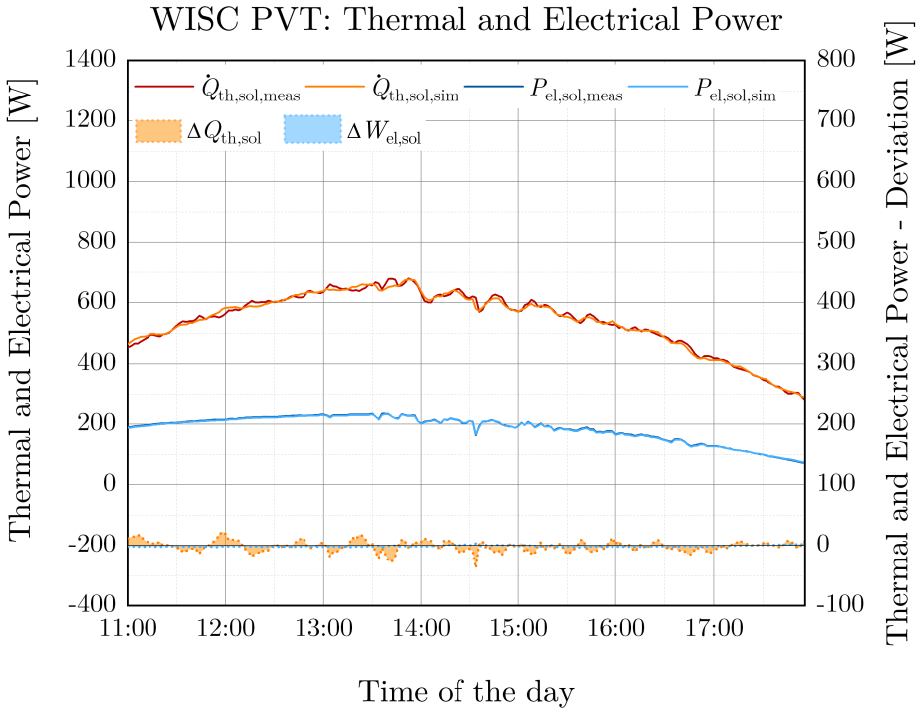

(b) Thermal and electrical power output and deviation

Figure 3.13: WISC PVT collector model validation - mostly clear sky (day type 1).

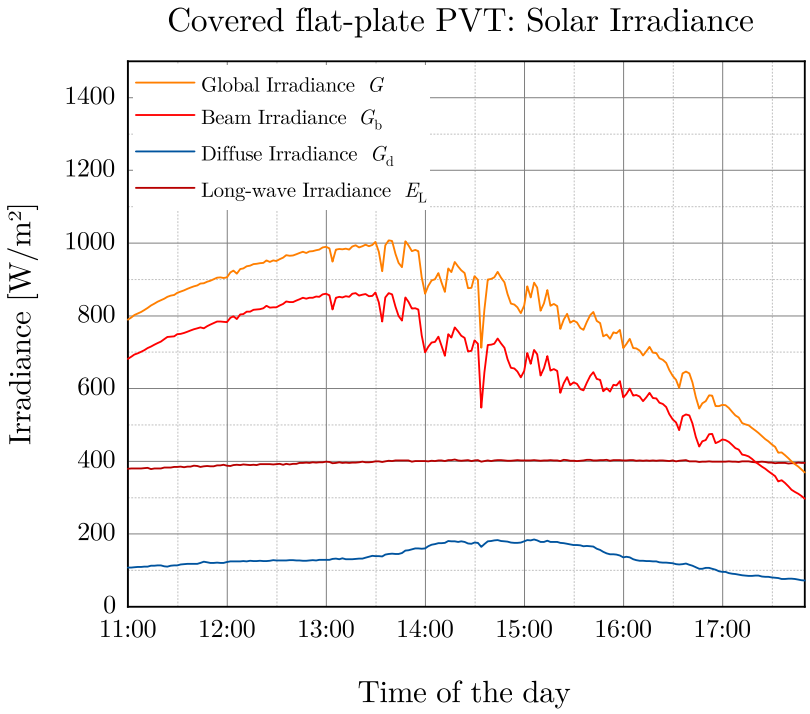

(a) Main solar irradiance data

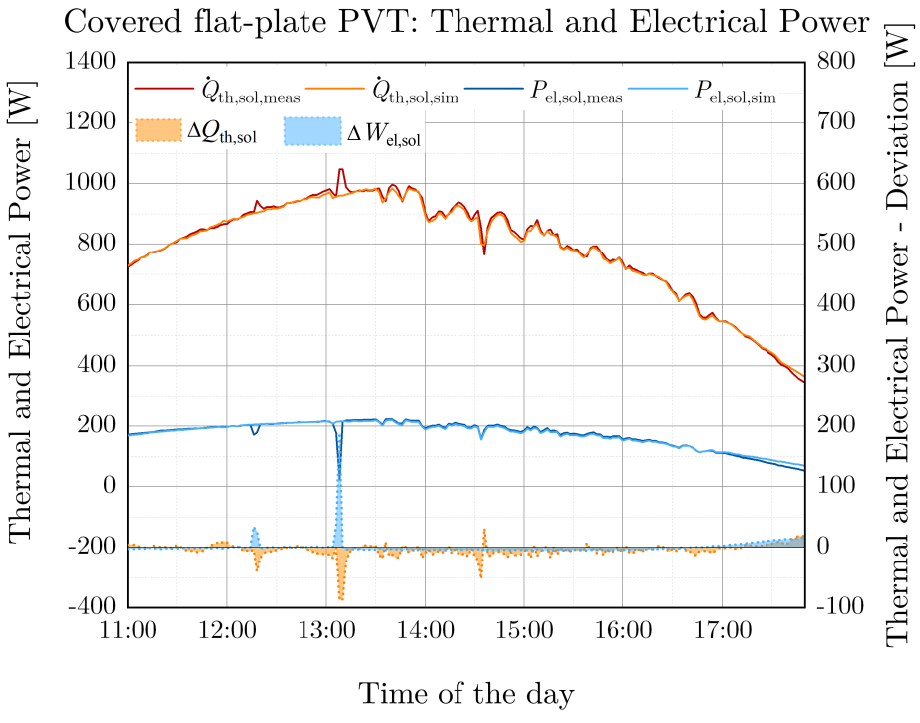

(b) Thermal and electrical power output and deviation

Figure 3.14: Covered flat-plate PVT collector model validation - mostly clear sky (day type 1).

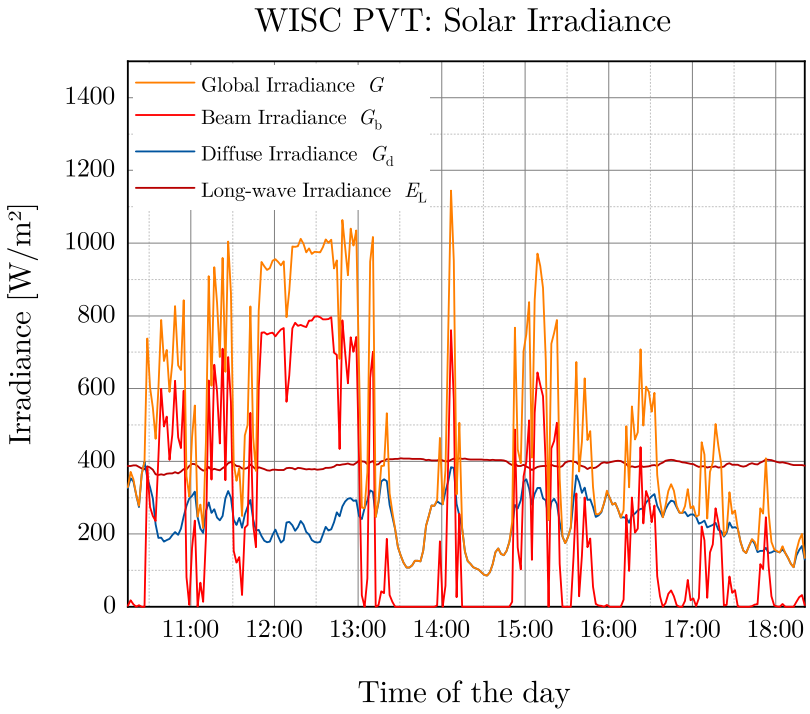

(a) Main solar irradiance data

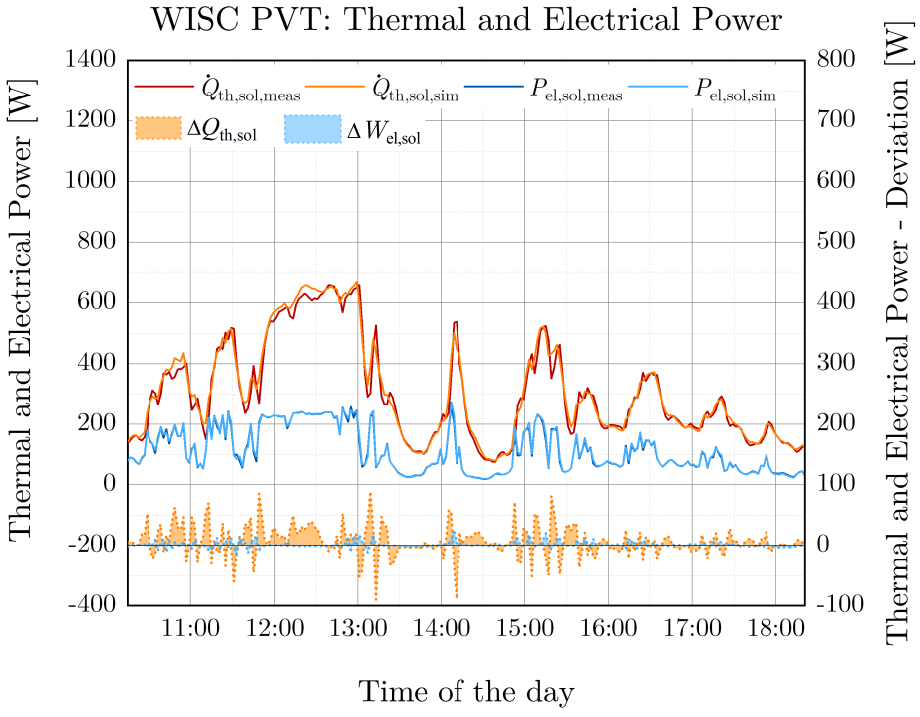

(b) Thermal and electrical power output and deviation

Figure 3.15: WISC PVT collector model validation - partly cloudy (day type 2).

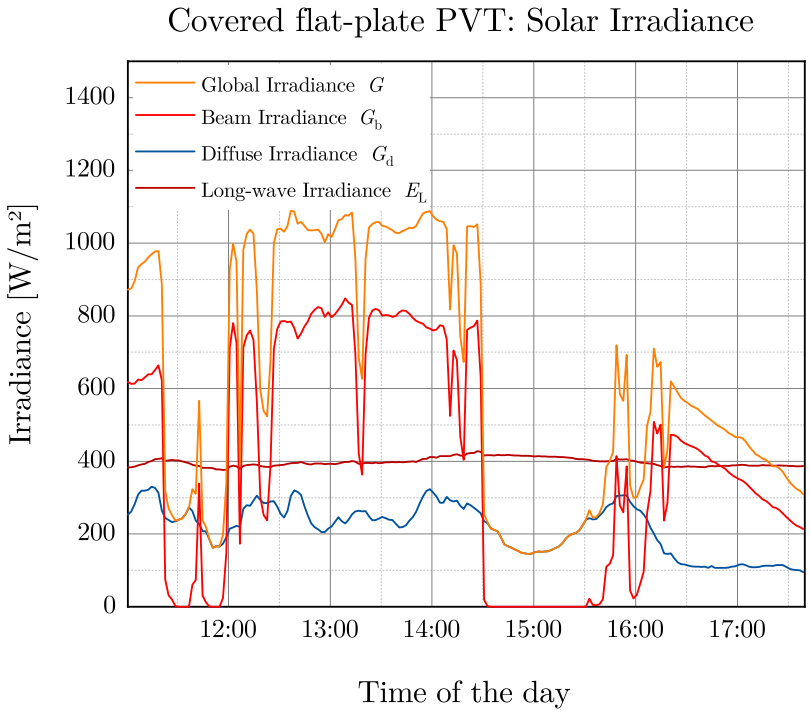

(a) Main solar irradiance data

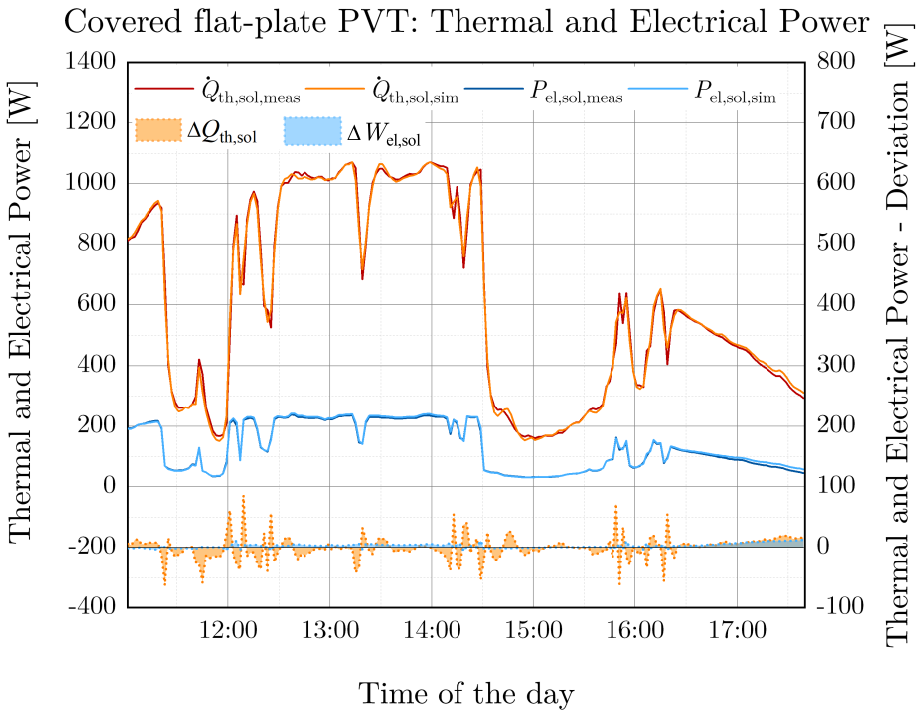

(b) Thermal and electrical power output and deviation

Figure 3.16: Covered flat-plate PVT collector model validation - partly cloudy (day type 2).

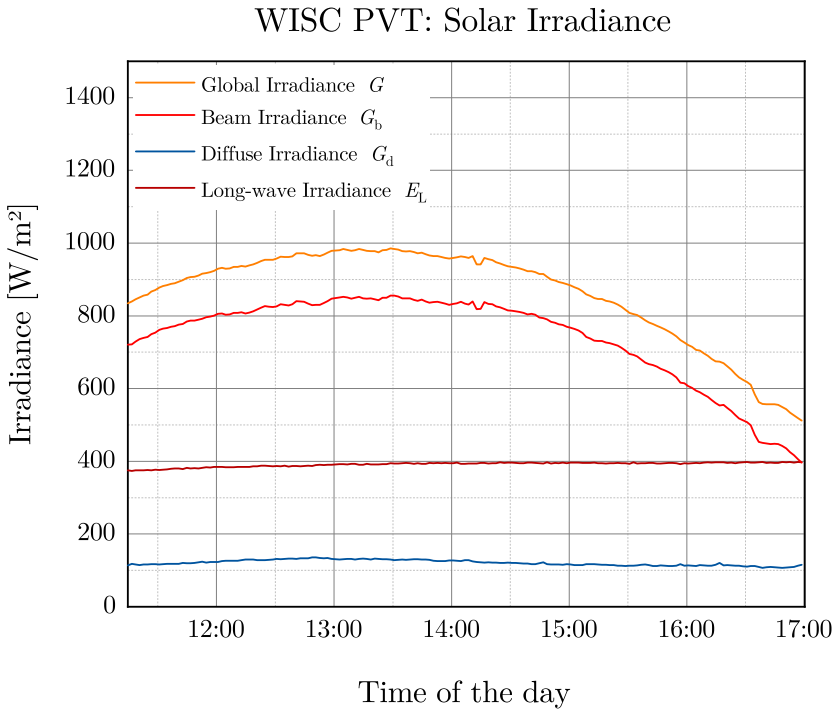

(a) Main solar irradiance data

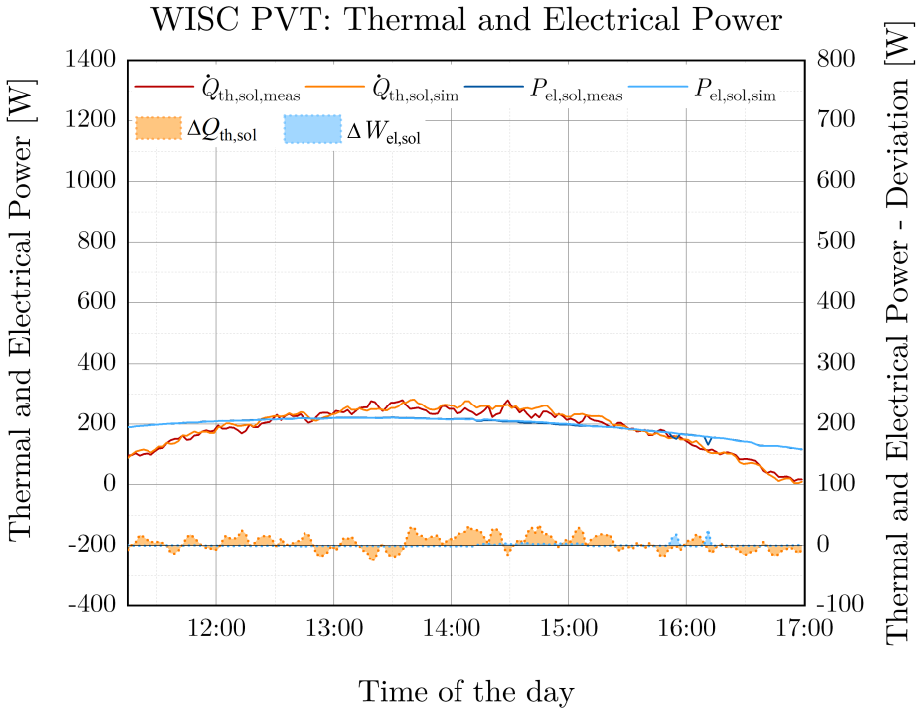

(b) Thermal and electrical power output and deviation

Figure 3.17: WISC PVT collector model validation - mean operating temperature, clear sky (day type 3b).

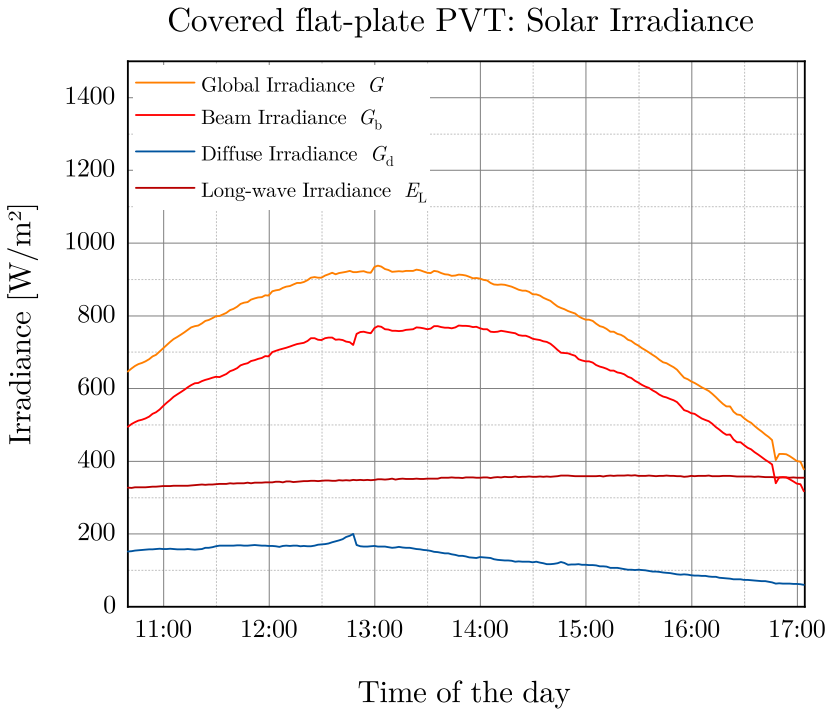

(a) Main solar irradiance data

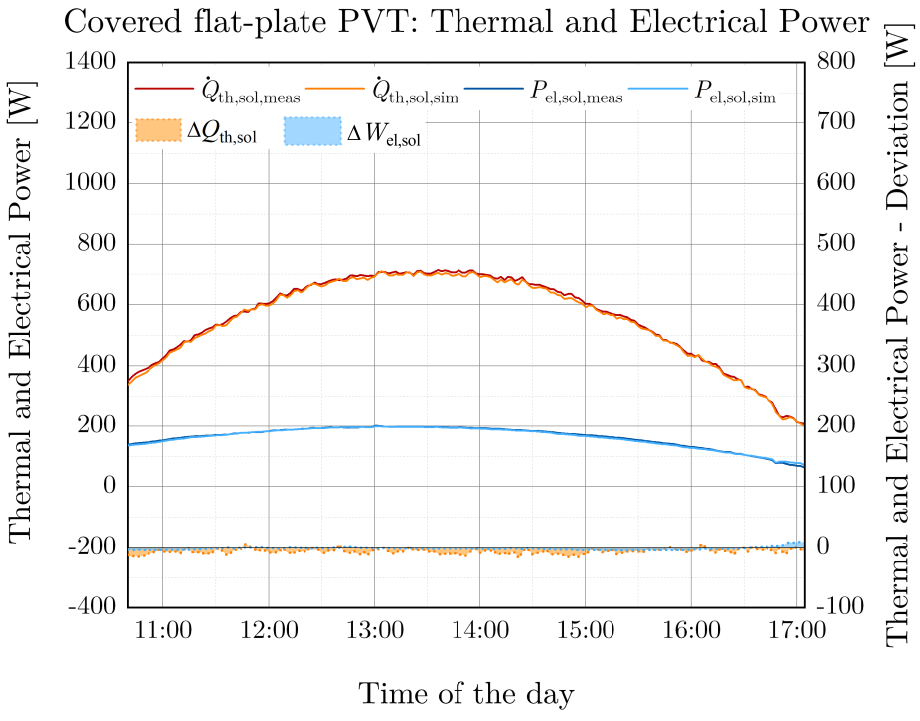

(b) Thermal and electrical power output and deviation

Figure 3.18: Covered flat-plate PVT collector model validation - mean operating temperature, clear sky (day type 3b).

a $\Delta Q_{\mathrm{th,sol}}/Q_{\mathrm{th,sol,meas}}$-ratio of $-0.24\,\%$ for the WISC PVT collector and $-0.55\,\%$ for the covered flat-plate PVT collector and a $\Delta W_{\mathrm{el,sol}}/W_{\mathrm{el,sol,meas}}$-ratio of $-0.64\,\%$ for the WISC PVT collector and $+0.31\,\%$ for the covered flat-plate PVT collector.

The dynamic behavior of the solar radiation for day type 2 results in higher differences between the measured and simulated results with a $\mathrm{nRMSE}_{\mathrm{th,sol}}$ of $9.10\,\%$ for the WISC PVT collector and $3.55\,\%$ for the covered flat-plate PVT collector as well as a $\mathrm{nRMSE}_{\mathrm{el,sol}}$ of $5.34\,\%$ for the WISC PVT collector and $3.85\,\%$ for the covered flat-plate PVT collector. The higher value for $\mathrm{nRMSE}_{\mathrm{th,sol}}$ of the WISC PVT collector for this day with considerable dynamic behavior may be a result of the significantly higher thermal capacity in comparison to the covered flat-plate PVT collector. In case of the covered flat-plate PVT collector, the result is additionally negatively affected by malfunctions of the MPP tracking at 12:15 PM and 13:10 PM which leads to an increase of $\mathrm{nRMSE}_{\mathrm{th,sol}}$ and $\mathrm{nRMSE}_{\mathrm{el,sol}}$. However, the modeled energy production over the period is still in a good accuracy with a $\Delta Q_{\mathrm{th,sol}}/Q_{\mathrm{th,sol,meas}}$-ratio of $+2.24\,\%$ for the WISC PVT collector and $-0.06\,\%$ for the covered flat-plate PVT collector and a $\Delta W_{\mathrm{el,sol}}/W_{\mathrm{el,sol,meas}}$-ratio of $+1.32\,\%$ for the WISC PVT collector and $+2.10\,\%$ for the covered flat-plate PVT collector.

For day type 3b, the behavior shows a good agreement to the measurements, except the thermal behavior of the WISC PVT collector with a high $\mathrm{nRMSE}_{\mathrm{th,sol}}$ of $18.57\,\%$. This large relative deviation may be a result of the increasing measurement uncertainty due to the low thermal power output of the WISC PVT collector and high wind speeds in the collector plane during the measurements. The $\mathrm{nRMSE}_{\mathrm{th,sol}}$ of $1.32\,\%$ for the covered flat-plate PVT collector shows a better agreement. The $\mathrm{nRMSE}_{\mathrm{el,sol}}$ of $0.66\,\%$ for the WISC PVT collector and $0.52\,\%$ for the covered flat-plate PVT collector show a high model accuracy. Despite the high $\mathrm{nRMSE}_{\mathrm{th,sol}}$, the modeled energy production over the period achieves a good accuracy with a $\Delta Q_{\mathrm{th,sol}}/Q_{\mathrm{th,sol,meas}}$-ratio of $+2.37\,\%$ for the WISC PVT collector and $-1.04\,\%$ for the covered flat-plate PVT collector and a $\Delta W_{\mathrm{el,sol}}/W_{\mathrm{el,sol,meas}}$-ratio of $+0.22\,\%$ for the WISC PVT collector and $-0.78\,\%$ for the covered flat-plate PVT collector.

In general, the electrical results show a better fit of the dynamic behavior than the thermal results, which is expressed in smaller values of $\mathrm{nRMSE}_{\mathrm{el,sol}}$. Due to its lower thermal capacity, the covered flat-plate PVT collector achieves a more accurate description of the dynamic behavior than the WISC PVT collector. This emphasizes the importance of an accurate parameter identification of the thermal capacity of PVT collectors. Nevertheless, the results show a very good agreement of the modeled energy production in all investigated cases and the proposed PVT collector model can be considered validated. Furthermore, it can be concluded that the presented PVT model and its TRNSYS implementation in Type 835 in combination with Type 832, as well as the proposed parameter identification procedure, are suitable for modeling the electrical and thermal performance of PVT collectors and that the model could be used as standardized PVT model for PVT collectors in the future.

For the system simulation, the electrical parameters from the WISC PVT collector are used for both PVT collectors and the thermal parameters are adapted from the covered flat-plate PVT collector for the simulation of a covered flat-plate PVT collector with the same electrical performance behavior. This procedure results in the PVT model parameters summarized in Table 3.9.

Table 3.9: Parameters of PVT models for system simulations.

Parameter	WISC PVT	Covered flat-plate PVT
Zero loss collector efficiency η_0	0.532	0.595
Heat loss coefficient c_1	$8.018\,\mathrm{W/m^2K}$	$6.023\,\mathrm{W/m^2K}$
Temperature dependence of the heat loss coefficient c_2	$0.029\,\mathrm{W/m^2K^2}$	$0.034\,\mathrm{W/m^2K^2}$
Wind speed dependence of the heat loss coefficient c_3	$1.7175\,\mathrm{J/m^3K}$	$0.0140\,\mathrm{J/m^3K}$
Sky temperature dependence of long wave radiation exchange c_4	0.303	0.213
Effective thermal capacity c_5	$37\,925\,\mathrm{J/m^2K}$	$17\,031\,\mathrm{J/m^2K}$
Wind speed dependence of the zero loss efficiency c_6	$0.031\,\mathrm{s/m}$	$0.006\,\mathrm{s/m}$
Constant for the thermal IAM for beam radiation $b_{0,\mathrm{th}}$	0.019	0.085
IAM for diffuse radiation K_d	0.920	0.905
Internal heat transfer coefficient from PV cell to fluid U_PVT	$46.08\,\mathrm{W/m^2K}$	$33.10\,\mathrm{W/m^2K}$
Electrical efficiency at STC conditions $\eta_\mathrm{el,sol,ref}$	0.1497	0.1497
Power temperature coefficient β	$0.386\,\%/\mathrm{K}$	$0.386\,\%/\mathrm{K}$
Constant for electrical IAM $b_{0,\mathrm{el}}$	0.041	0.041
Model parameter a for irradiance dependence	$-0.00008411\,\mathrm{m^2/W}$	$-0.00008411\,\mathrm{m^2/W}$
Model parameter b for irradiance dependence	-0.03388	-0.03388
Model parameter c for irradiance dependence	-1.367	-1.367

3.3 System Model

3.3.1 Model Overview and Subsystems

A simplified overview of the *system model* for the simulation of SHP systems for the energy supply of residential buildings in TRNSYS and its main components is illustrated in Figure 3.19. For a better structure and a higher level of modularity the TRNSYS model is divided in the following subsystems:

- Reference System and Buffer Storage
- Heat Pump and Heat Source Circuit
- Parallel Solar Thermal Circuit
- Photovoltaic Battery System
- Solar Thermal and Heat Pump (STHP) System Control
- Building Energy Management System (BEMS) Control.

The subsystems can be combined for the different simulation studies of SHP systems and can be connected via TRNSYS equation blocks. The equation blocks are used as inputs and outputs of the subsystems and are connected via variables (cf. [Kuethe et al., 2008]), whereas some inputs are directly connected to the TRNSYS Types via the defined variables. Additionally, the equation blocks are used for the definition of required calculations and the

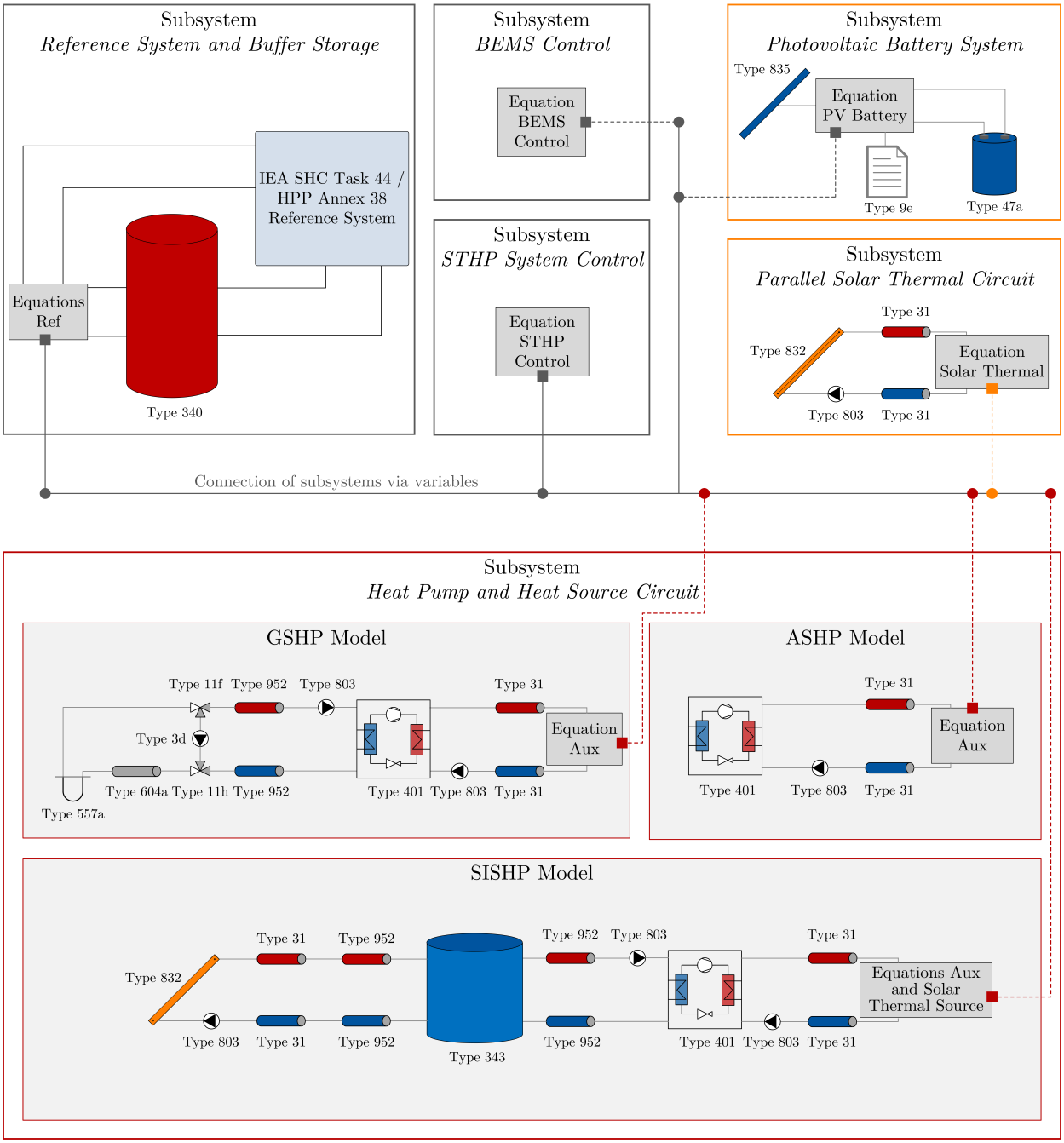

Figure 3.19: TRNSYS system model with subsystems.

definition of variables which are used as parameters in the TRNSYS Types. Furthermore, some main model parameters and settings are defined in the control card of the TRNSYS Simulation Studio as equations or constants. An assignment of the subsystems to the different heat pump and SHP system concepts described in Section 2.2.1.3 and Section 2.3 is given in Table 3.10.

Every system model consists of the main subsystems *Reference System and Buffer Storage*, *Heat Pump and Heat Source Circuit* (GSHP, ASHP or SISHP model) and *STHP System Control*. Furthermore, the simulation models of systems with parallel integration of a solar thermal circuit contain the subsystem *Parallel Solar Thermal Circuit*. In case of SHP systems with PV or PVT integration, the subsystems *Photovoltaic Battery System* and

Table 3.10: Assignment of subsystem models to different SHP system models.

	Reference System and Buffer Storage	Heat Pump and Heat Source Circuit			Parallel Solar Thermal Circuit	PV Battery System	STHP System Control	BEMS Control
		GSHP	ASHP	SISHP				
GSHP	x	x	-	-	-	-	x	-
ASHP	x	-	x	-	-	-	x	-
SGSHP-P	x	x	-	-	x	-	x	-
SASHP-P	x	-	x	-	x	-	x	-
SISHP-S	x	-	-	x	-	-	x	-
SISHP-S,P	x	-	-	x	x	-	x	-
PV-GSHP	x	x	-	-	-	x	x	x
PV-ASHP	x	-	x	-	-	x	x	x
PV-SGSHP-P	x	x	-	-	x	x	x	x
PV-SASHP-P	x	-	x	-	x	x	x	x
PV-SISHP-S	x	-	-	x	-	x	x	x
PV-SISHP-S,P	x	-	-	x	x	x	x	x
PVT-SGSHP-P	x	x	-	-	x	x	x	x
PVT-SASHP-P	x	-	x	-	x	x	x	x
PVT-SISHP-S	x	-	-	x	-	x	x	x
PV-PVT-SGSHP-P	x	x	-	-	x	x	x	x
PV-PVT-SASHP-P	x	-	x	-	x	x	x	x
PV-PVT-SISHP-S	x	-	-	x	-	x	x	x

BEMS Control are additionally part of the system model. The individual subsystem models for the different simulation cases and systems differ especially in terms of parameterization and in case of SHP systems with parallel solar thermal circuit in an implemented control strategy for the solar circuit in the subsystem *STHP System Control* and the use of an internal heat exchanger in the buffer storage tank model. In case of SHP systems with PVT integration, the subsystem *Photovoltaic Battery System* and the thermal part of the PVT collector in the subsystems *Heat Pump and Heat Source Circuit* or *Parallel Solar Thermal Circuit* are linked via the described two-node model approach with internal heat transfer coefficient in Section 3.2.2.3. The used simulation models of the main system components are summarized in Table 3.11.

The participants of IEA SHC Task 44 / HPP Annex 38 (in the following referred to as *T44A38*) defined a reference framework for system simulations of solar thermal and heat pump systems which is implemented in detail in the simulation environment TRNSYS. The objective of the reference framework is to achieve a better comparability of simulation results performed by different researchers. In addition to general boundary conditions like weather data files, climate and ground properties (Section 3.3.2.1), the reference framework contains the definition of thermal loads for space heating (building model) and domestic hot water preparation in residential buildings (Section 3.3.2.2). Furthermore, the participants defined

Table 3.11: Used TRNSYS models of the main system components.

Component	TRNSYS model
Weather data reading and processing	Type 109 [TRNSYS, 2020]
Building	Type 56 [TRNSYS, 2020]
FPC/WISC collectors and thermal part of PVT collectors	Type 832 [Haller et al., 2013b]
PV modules and electrical part of PVT collectors	Type 835 [Jonas, 2019a]
Compressor heat pump	Type 401 [Wetter and Afjei, 1997]
BHE	Type 557a [TESS, 2014]
Buried ice storage tank	Type 343 [Hornberger, 2006]
Buffer storage tank	Type 340 [Drück, 2006]
Battery storage	Type 47a [TRNSYS, 2020]
Single speed pump	Type 3d [TRNSYS, 2020]
Variable speed pump	Type 803 [Heimrath and Haller, 2007]
Pipe	Type 31 [TRNSYS, 2020]
Bi-directional noded pipe	Type 604a [TESS, 2014]
Buried noded pipe	Type 952 [TESS, 2014]
Flow diverter	Type 11f [TRNSYS, 2020]
Tee-piece	Type 11h [TRNSYS, 2020]
Data reader for load profiles (e.g. DHW, electrical load)	Type 9c, Type 9e [TRNSYS, 2020]

additional boundary conditions within the framework, especially for the simulation of solar thermal components or ground heat exchangers. The reference framework and the boundary conditions are also used for the simulations in this work and are included in the subsystem *Reference System and Buffer Storage*. Detailed information on the reference framework can be found in Hadorn [2015]; Haller et al. [2013a]; Dott et al. [2013].

Apart from the subsystem *Reference System and Buffer Storage*, all TRNSYS subsystem models were compiled with some minor modifications in a model library for TRNSYS and are published as SHP-SimLib on GitHub [Jonas, 2023a]. Furthermore, a TRNSYS-based stand-alone tool (TRNSED application) for the simulation of ASHP, GSHP, SASHP-P and SGSHP-P systems using older versions of the presented subsystem models was presented in Jonas et al. [2017c,a] as SHP-SimFrame. Due to its greater flexibility, the subsystems are published as model library and the development of a stand-alone tool was not pursued. In addition, first results of system simulations using older versions of the subsystem models were published in Jonas et al. [2017b,d]; Jonas and Frey [2018]. In the following sections, the modeling of the subsystems of the system model are described in detail.

3.3.2 Reference System and Buffer Storage

The subsystem *Reference System and Buffer Storage* includes the T44A38 reference system, the multiport-store model Type 340 and especially the equation blocks *Ref Basic* and *Ref Storage* as connection to the other subsystems, cf. Figure 3.19 and Figure 3.20. In the following sections, the main properties of the reference system including the residential building and the heat loads for space heating and domestic hot water are described. In addition, the main properties of the buffer storage model are summarized.

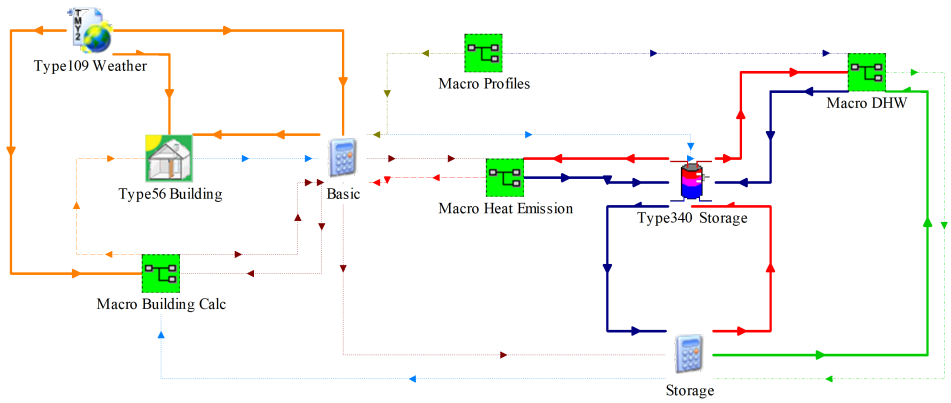

Figure 3.20: TRNSYS subsystem *Reference System and Buffer Storage*.

3.3.2.1 Weather Data, Climate and Ground Properties

The T44A38 reference framework contains, inter alia, weather data of three different locations which represents warm (Athens), moderate (Strasbourg) and cold (Helsinki) climates [Haller et al., 2013a; Meteonorm, 2009]. Table 3.12 shows the key climate values for the locations containing altitude h, design ambient temperature for the heating system $\vartheta_{\mathrm{amb,D}}$, annual average ambient temperature $\bar{\vartheta}_{\mathrm{amb}}$ and total yearly irradiation on a 45 degree sloped south facing plane $I_{\mathrm{tot,45,S}}$. For the simulation of ground coupling losses of the building and the ground heat exchangers, a heat conductivity of the ground of 2 W/mK, a density of 2 500 kg/m^3, a specific heat capacity of the ground of 800 J/kgK and a geothermal gradient of the ground of 0.025 K/m are used [Haller et al., 2013a]. Further information and details on the weather data, climates and ground properties can be found in Haller et al. [2013a].

Table 3.12: Key climate values for Athens, Strasbourg and Helsinki [Haller et al., 2013a; Meteonorm, 2009].

	h [m]	$\vartheta_{\mathrm{amb,D}}$ [°C]	$\bar{\vartheta}_{\mathrm{amb}}$ [°C]	$I_{\mathrm{tot,45,S}}$ [kWh/m^{2}a]
Athens	15	−1	18.4	1 708
Strasbourg	150	−10	11.0	1 227
Helsinki	53	−19	5.6	1 177

3.3.2.2 Residential Building, Heat Distribution System and Domestic Hot Water Preparation

Within the T44A38 reference framework, detailed residential building models and hot water draw off profiles are defined. This includes detailed TRNSYS models which are also used for this work. In general, three residential buildings, representing single-family houses (SFH) with the same geometries and different energy demands, are defined to consider different building types within the simulations. A simplified sketch of the building and its geometry is shown in Figure 3.21. The defined buildings correspond to specific heat loads for space heating of approximately 15 kWh/m^{2}a (SFH15), 45 kWh/m^{2}a (SFH45) and 100 kWh/m^{2}a (SFH100) for the climate of Strasbourg (in relation to the useful floor area of 140 m^2). SFH15 represents a new building with very high energy standard, SFH45 is oriented at

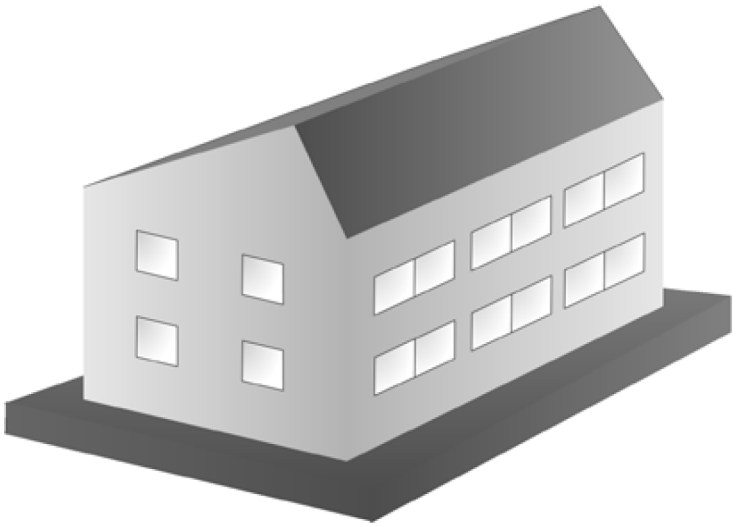

Figure 3.21: Sketch of the residential building (showing south and west facades) defined by IEA SHC Task 44 / HPP Annex 38 and modeled in TRNSYS [Dott et al., 2013].

current legal requirements or represents a renovated building with good thermal quality of the building envelope and SFH100 represents a non-renovated existing building [Dott et al., 2013]. The monthly heat loads for space heating of the different buildings for the climates of Athens, Strasbourg and Helsinki are shown in Figure 3.22. The annual heat loads for space heating Q_{SH} and domestic hot water preparation Q_{DHW} for the different locations and buildings are summarized in Table 3.13 and a comparison of the shares of the annual heat loads and the annual household electricity loads from Section 3.3.5 in the net energy demand of the different buildings for the considered locations is given in Appendix A. Furthermore, Table 3.13 contains the UA-values of the different buildings UA_{bui}, the design heat loads for space heating $\dot{Q}_{\mathrm{SH}}$, the design supply $\vartheta_{\mathrm{SH,in}}$ and return temperatures $\vartheta_{\mathrm{SH,out}}$ of the heat distribution system as well as the heating season limit ϑ_{HS}. SFH15 and SFH45 use floor heating systems, whereas SFH100 is supplied by radiator heating systems, resulting in higher design supply and return temperatures of the heat distribution systems of SFH100. The hot water draw off profiles correspond to an average draw off of 140 l/d with a draw off temperature of 45 °C and are equivalent to an energy consumption for domestic hot water preparation of 5.845 kWh/d with a cold water temperature of 10 °C [Haller et al., 2013a]. Further information and detailed descriptions of the used building models including control of the space heating system and details on the hot water draw off profiles can be found in Dott et al. [2013] and Haller et al. [2013a].

The calculation of the electricity consumption of the space heating circuit pump $P_{\mathrm{el,pu,SH}}$ is based on the following equation [Weiss, 2003]:

$$P_{\mathrm{el,pu,SH}} = 90\,\mathrm{W} + 0.2 \cdot 10^{-3} \cdot \dot{Q}_{\mathrm{HP,nom}}, \tag{3.29}$$

where $\dot{Q}_{\mathrm{HP,nom}}$ is the nominal condenser power of the heat pump in W. Currently, high-efficiency pumps with maximal power consumptions of 25 W or 40 W are used for the supply of distribution systems for space heating. Therefore, the calculation of the electricity con-

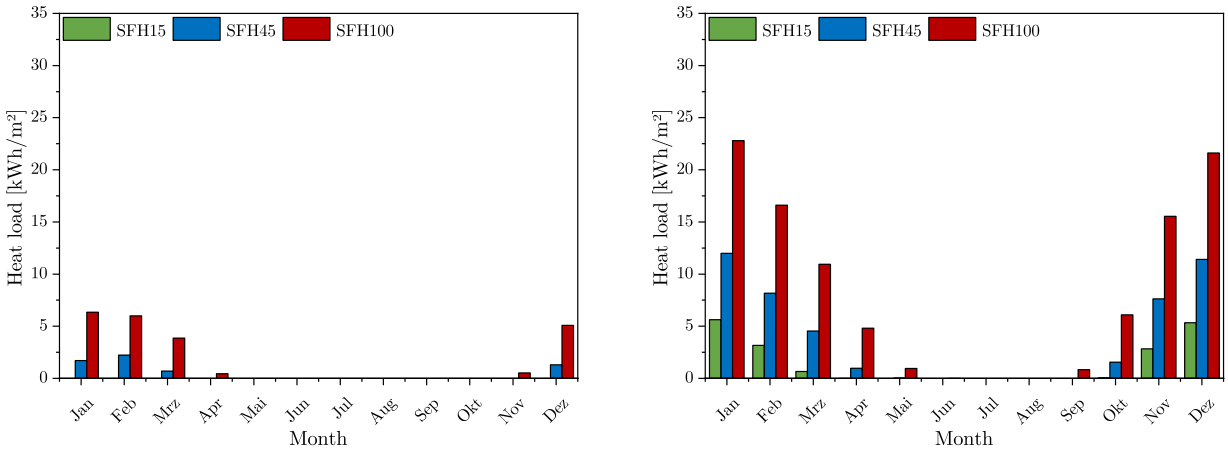

(a) Athens **(b)** Strasbourg

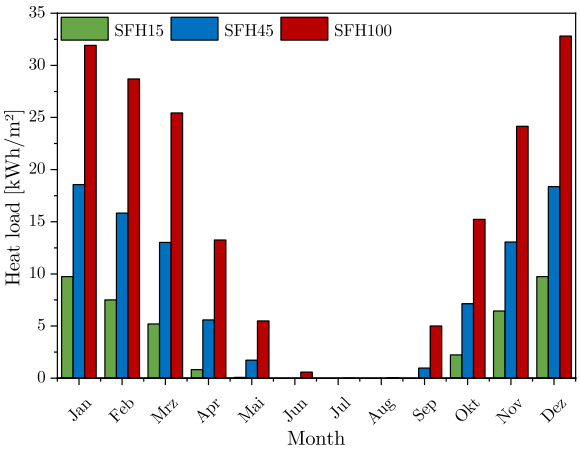

(c) Helsinki

Figure 3.22: Monthly heat loads for space heating for different locations and buildings.

Table 3.13: Key values of heating demand for space heating and domestic hot water consumptions and design parameters of the heating system for different locations and buildings [Dott et al., 2013; Haller, 2013].

Location	Building	Q_{SH} [kWh/a]	Q_{DHW} [kWh/a]	UA_{bui} [W/K]	$\dot{Q}_{SH}$ [W]	$\vartheta_{SH,in}$ [°C]	$\vartheta_{SH,out}$ [°C]	ϑ_{HS} [°C]
Athens	SFH15	-	1 648	97	-	-	-	12 °C
	SFH45	832	1 648	168	1 310	35 °C	30 °C	14 °C
	SFH100	3 115	1 648	290	3 382	55 °C	45 °C	15 °C
Strasbourg	SFH15	2 474	2 076	97	1 792	35 °C	30 °C	12 °C
	SFH45	6 476	2 076	168	4 072	35 °C	30 °C	14 °C
	SFH100	14 031	2 076	290	7 337	55 °C	45 °C	15 °C
Helsinki	SFH15	5 846	2 398	97	3 097	35 °C	30 °C	12 °C
	SFH45	13 197	2 398	168	6 315	40 °C	35 °C	14 °C
	SFH100	25 565	2 398	290	10 931	60 °C	50 °C	15 °C

sumption of the space heating circuit pump is reduced to:

$$P_{\mathrm{el,pu,SH}} = 25\,\mathrm{W} + 0.2 \cdot 10^{-3} \cdot \dot{Q}_{\mathrm{HP,nom}}. \tag{3.30}$$

The electricity consumption of the domestic hot water circuit pump $P_{\mathrm{el,pu,DHW}}$ is calculated with [Weiss, 2003]:

$$P_{\mathrm{el,pu,DHW}} = 49.4\,\mathrm{W} \cdot \mathrm{e}^{(0.0083 \cdot 10^{-3}\mathrm{W}^{-1} \cdot \dot{Q}_{\mathrm{HP,nom}})}. \tag{3.31}$$

The electricity consumption of additional controllers to the heat pump controller $P_{\mathrm{el,ctr}}$, e.g. controller for space heating, is assumed to be 10 W.

3.3.2.3 Buffer Storage Tank

The volume of the buffer storage tank (combi-storage) varies in the different simulation cases between 500 l and 2 000 l. The heat transfer rate from the buffer storage to the environment is calculated for every storage volume by the calculation method described in Heimrath and Haller [2007] with a thermal conductivity of the storage insulation of 0.042 W/mK and an insulation thickness of 0.15 m without user specified factor for correction of the heat loss coefficient. The relative heights of the buffer storage tank in- and outlets and temperature sensors are fixed for every simulation and are summarized in Table 3.14. At this, the connections of the additional solar thermal heat exchanger and temperature sensors for storage protection and solar thermal circuit charging are only used for models with parallel solar thermal circuit (models with subsystem *Parallel Solar Thermal Circuit*). For these systems, the heat transfer rates of the internal heat exchanger $UA_{\mathrm{HX,SC}}$ are calculated dependent on the gross FPC or PVT collector area $A_{\mathrm{th,sol}}$ in m^2 with the following equation [Heimrath and Haller, 2007]:

$$UA_{\mathrm{HX,SC}} = 88.561\,\mathrm{W/m^2} \cdot A_{\mathrm{th,sol}} + 328.19\,\mathrm{W}. \tag{3.32}$$

Table 3.14: Relative heights of the in- and outlets and temperature sensors of the buffer storage tank model.

Parameter	Value [-]
Inlet from / Outlet to heat pump for domestic hot water preparation	0.95 / 0.75
Inlet from / Outlet to heat pump for space heating	0.55 / 0.25
Inlet from / Outlet to space heating circuit	0.25 / 0.55
Inlet from / Outlet to domestic hot water circuit	0.00 / 1.00
Inlet / Outlet for additional solar thermal heat exchanger	0.26 / 0.00
Temperature sensor for domestic hot water preparation ($\vartheta_{\mathrm{buffer,DHW}}$)	0.85
Temperature sensor for space heating ($\vartheta_{\mathrm{buffer,SH}}$)	0.55
Temperature sensor for storage protection ($\vartheta_{\mathrm{buffer,prot}}$)	0.91
Temperature sensor for solar thermal circuit charging ($\vartheta_{\mathrm{buffer,SC}}$)	0.26

3.3.3 Heat Pump and Heat Source Circuit

In the following sections, the *Heat Pump and Heat Source Circuit* subsystems for the different heat sources and system concepts are described in detail. The assignments of the heat pumps from Section 3.2.1 to the different locations and buildings are summarized in Table 3.15. In general, the heat pump sizes are designed for monovalent system operation using the design heat load of the considered building at the design ambient air temperature of the specific location and the corresponding heating power of the heat pump at design supply temperature conditions from Table 3.13. For air/water heat pump systems, the design ambient air temperatures from Table 3.12 are used as reference values for the design source temperatures, whereas for brine/water heat pump systems in GSHP systems a source temperature of 0 °C and in SISHP systems a source temperature of −5 °C is used for the calculation of the heating power at design supply temperature conditions. Due to the low ambient air temperatures in Helsinki and the operating limits of air/water heat pumps, air/water heat pumps are switched-off by an external controller when the ambient air temperature of Helsinki in the simulation falls below −20 °C and an electric heating element is used to heat up the buffer storage at a relative height of 0.40. Thus, systems with air/water heat pumps in Helsinki are designed for monoenergetic system operation with a bivalence point at −20 °C (bivalent alternative). Regarding the design heat loads for Helsinki in Table 3.13 and considering typical sizes of direct electric heating elements, the nominal heating power of the electric heating element is set to 6 kW for SFH15, 9 kW for SFH45 and 12 kW for SFH100. As the design heat load for space heating of SFH15 in Athens is zero (cf. Table 3.13), it is not considered in Table 3.15 and in the following investigations.

Table 3.15: Assignment of brine/water (BW) and air/water (AW) heat pump models for different locations and buildings.

Location	Building	Air/water heat pump	Brine/water heat pump
Athens	SFH45	AW06	BW06
	SFH100	AW06	BW06
Strasbourg	SFH15	AW06	BW06
	SFH45	AW06	BW06
	SFH100	AW10	BW10
Helsinki	SFH15	AW06	BW06
	SFH45	AW10	BW08
	SFH100	AW19	BW13

3.3.3.1 Ground Source Heat Pump Circuit

The subsystem *Heat Pump and Heat Source Circuit* for GSHP systems includes the components for the heat source circuit with ground heat exchanger, the brine/water heat pump, the pump for buffer storage charging, the pipes from the heat pump to the buffer storage and the equation block *Aux*, cf. Figure 3.23.

The heat source circuit consists of the vertical BHE, the heat source circulation pump, buried pipes and an additional circuit with adiabatic pre-pipe in front of the input of the BHE. The adiabatic pre-pipe is used for a better representation of the short-term behavior of the BHE in the simulation due to missing short term heat capacity effects of Type 557. More

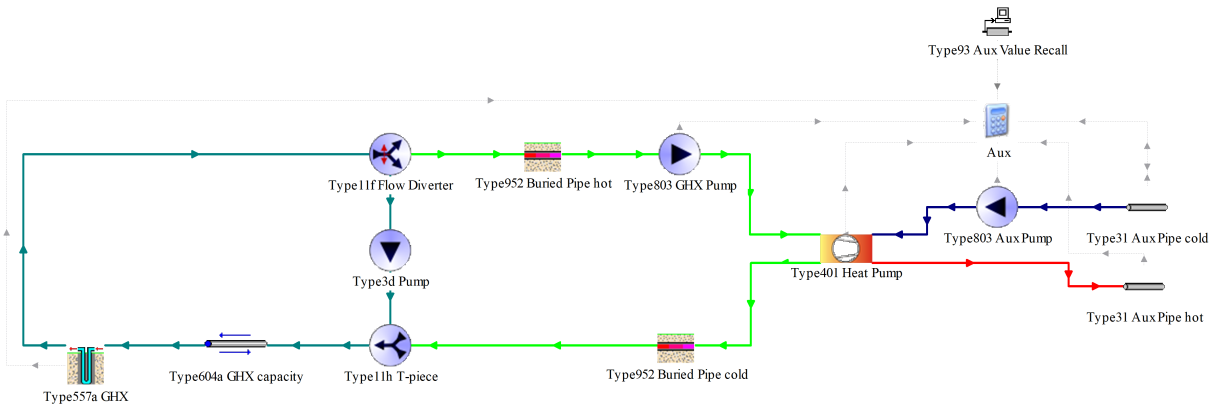

Figure 3.23: TRNSYS subsystem *Heat Pump and Heat Source Circuit* for GSHP systems.

information on the pre-pipe concept, the model validation and parameterization rules can be found in Pärisch et al. [2015] and Bertram [2015]. According to the boundary conditions of T44A38, the BHEs are simulated as double-U pipes. The main properties of the BHEs are summarized in Table 3.16 and the assignment of the number and length of BHEs to the different locations and buildings is given in Table 3.17.

According to ZHAW IFM [2021], the electricity consumption of BHE heat source circulation pumps should not excess 0.5 W per meter BHE length. Hence, the electricity consumption of the BHE heat source circulation pump $P_{\mathrm{el,pu,BHE}}$ is assumed to be:

$$P_{\mathrm{el,pu,BHE}} = 0.5\,\mathrm{W/m} \cdot n_{\mathrm{BHE}}\, l_{\mathrm{BHE}}, \tag{3.33}$$

where n_{BHE} is the number of BHEs and l_{BHE} the BHE length. The electricity consumption of the auxiliary storage charging pump from the heat pump to the buffer storage $P_{\mathrm{el,pu,buffer}}$ is assumed to be 30 W. The mass flow rates through the condenser and evaporator of the heat pump are calculated for a nominal temperature difference of 5 K for the condenser and 5 K for the evaporator by the nominal condenser and evaporator power of the used heat pump at B0/W35.

Table 3.16: BHE and heat carrier fluid properties [Haller et al., 2013a].

Parameter	Value
BHEs	
Borehole diameter	0.18 m
Inner diameter of pipes	0.026 m
Heat conductivity of the filling material	2 W/mK
Density of the filling material	2 000 kg/m^3
Specific heat capacity of the filling material	1.65 kJ/kgK
Heat carrier fluid (brine)	
Specific heat capacity of the brine	3.86 kJ/kgK
Density of the brine	1 035 kg/m^3
Heat conductivity of the brine	0.449 W/mK
Kinematic viscosity of the brine	6.5×10^{-6} m^2/s

Table 3.17: Assignment of number and length of BHEs for different locations and buildings (cf. [Haller et al., 2013a]).

Location	Building	Number and length of BHEs
Athens	SFH45	49 m [a]
	SFH100	49 m [a]
Strasbourg	SFH15	49 m
	SFH45	84 m
	SFH100	2 × 90 m
Helsinki	SFH15	75 m
	SFH45	2 × 95 m
	SFH100	4 × 95 m

[a] For SFH45 and SFH100 in Athens, the BHE lengths of SFH15 in Strasbourg from Haller et al. [2013a] are used as assumption due to the low energy demands in Athens.

3.3.3.2 Air Source Heat Pump Circuit

The subsystem *Heat Pump and Heat Source Circuit* for ASHP systems includes the air/water heat pump, the pump for buffer storage charging, the pipes from the heat pump to the storage and the equation block *Aux*, cf. Figure 3.24. The electricity consumption of the auxiliary storage charging pump from the heat pump to the buffer storage $P_{\mathrm{el,pu,buffer}}$ is assumed to be 30 W. The mass flow rate through the condenser of the heat pump is calculated for a nominal temperature difference of 5 K for the condenser by the nominal condenser power of the used heat pump at A7/W35.

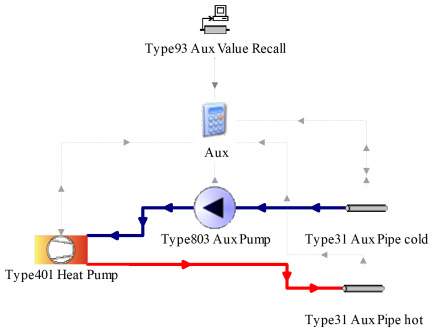

Figure 3.24: TRNSYS subsystem *Heat Pump and Heat Source Circuit* for ASHP systems.

3.3.3.3 Ice Storage Source Heat Pump Circuit

The subsystem *Heat Pump and Heat Source Circuit* for SISHP systems includes the components for the heat source circuit with ice storage, the brine/water heat pump, the pump for buffer storage charging, the pipes from the heat pump to the buffer storage and the equation block *Aux*, cf. Figure 3.25.

The heat source circuit consists of the buried ice storage tank model, the heat source circulation pump to the heat pump, buried pipes and an additional solar thermal source circuit. The solar thermal source circuit includes WISC collectors or the thermal part of PVT collectors (depending on the considered SHP system concept), the solar source circuit

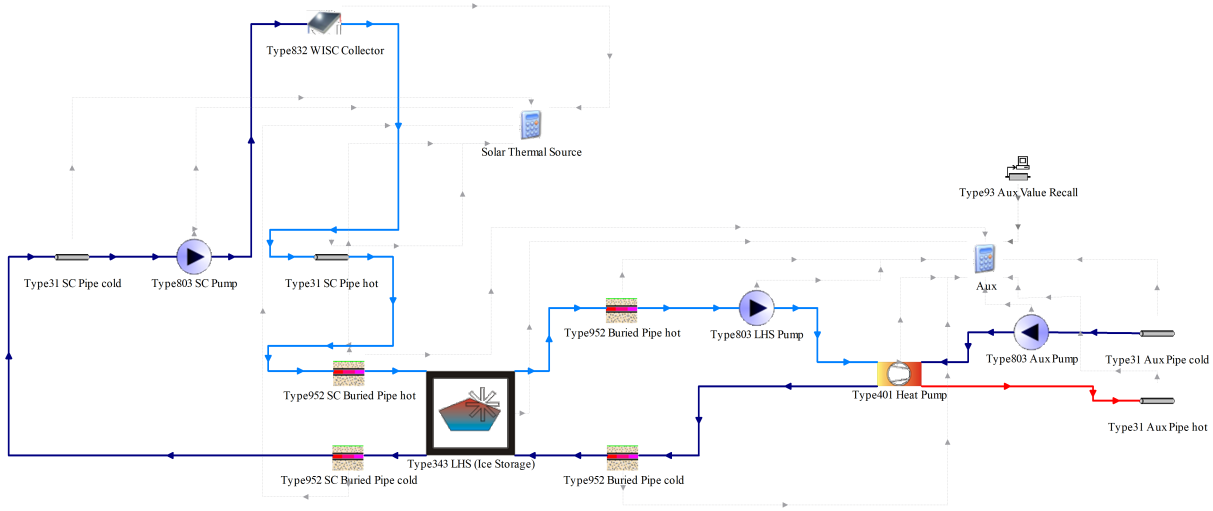

Figure 3.25: TRNSYS subsystem *Heat Pump and Heat Source Circuit* for SISHP systems.

pump, pipes from the solar collectors to the ice storage tank for ice storage charging and the equation block *Solar Thermal Source*. The main properties of the ice storage model are summarized in Table 3.18.

Table 3.18: Main properties of the ice storage model.

Parameter	Value
Ice storage volume	10 m^3
Inner diameter of the ice storage	2.5 m^2
Depth of top of the ice storage below ground surface	0.9 m
Volumetric thermal heat capacity of the storage material (water, 0 °C)	4 217 kJ/m^3K
Heat conductivity of liquid water	idealized [a]
Heat conductivity of frozen water (ice)	2.25 W/mK
Volumetric thermal heat capacity of the local soil	2 000 kJ/m^3K
Heat conductivity of the local soil	2 W/mK
Number of heat exchangers cycles	2 [b]
Specific heat capacity of the brine in heat exchanger pipe coils	3.86 kJ/kgK

[a] The ice storage is simulated with two zones and idealized heat transfer between those two zones due to limitations of the heat exchanger modeling possibilities with TRNSYS Type 343.

[b] Details on the heat exchanger modeling are restricted due to a confidentiality agreement with the manufacturer.

The electricity consumption of the solar source circuit pump for the ice storage charging $P_{el,pu,SC,ice}$ is calculated depending on the gross WISC or PVT collector area $A_{th,sol,ice}$ with [Weiss, 2003]:

$$P_{el,pu,SC,ice} = 44.6\,W \cdot e^{(0.0181\,m^{-2} \cdot A_{th,sol,ice})}. \quad (3.34)$$

The electricity consumption of the heat source circulation pump from the ice storage to the heat pump $P_{el,pu,ice}$ is assumed to be 40 W and the electricity consumption of the auxiliary storage charging pump from the heat pump to the buffer storage $P_{el,pu,buffer}$ is assumed to be 30 W. The mass flow rates through the condenser and evaporator of the heat pump

are calculated for a nominal temperature difference of 5 K for the condenser and 3 K for the evaporator by the nominal condenser and evaporator power of the used heat pump at B0/W35. The mass flow rate of the solar source circuit is set to 100 kg/h per m^2 collector area for WISC collectors and 75 kg/h per m^2 collector area for PVT collectors as result of a parameter study. According to the boundary conditions for solar thermal system simulations of T44A38, the WISC and PVT collectors are simulated with a collector tilt of 45° oriented towards south (azimuth of 0°) and the wind speed on the collector plane is taken as half of the meteorological wind speed from the climate data [Haller et al., 2013a]. The key parameters of the WISC and PVT collectors for the simulations are summarized in Table 3.5 and Table 3.9.

3.3.4 Parallel Solar Thermal Circuit

The subsystem *Parallel Solar Thermal Circuit* consists of the FPCs or the thermal part of the PVT collectors (depending on the considered SHP system concept), the solar circuit pump, the pipes from the solar collectors to the storage and the equation block *Solar Thermal*, cf. Figure 3.26.

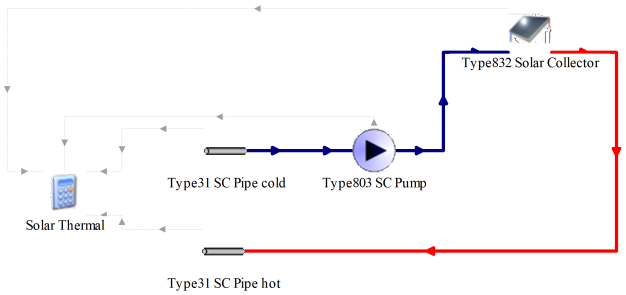

Figure 3.26: TRNSYS subsystem *Parallel Solar Thermal Circuit*.

The electricity consumption of the solar circuit pump $P_{\mathrm{el,pu,SC}}$ is calculated depending on the gross FPC or PVT collector area $A_{\mathrm{th,sol}}$ with [Weiss, 2003]:

$$P_{\mathrm{el,pu,SC}} = 44.6\,\mathrm{W} \cdot \mathrm{e}^{(0.0181\,\mathrm{m}^{-2} \cdot A_{\mathrm{th,sol}})}. \tag{3.35}$$

The mass flow rate of the solar thermal circuit is set to 35 kg/h per m^2 collector area for FPCs and 50 kg/h per m^2 collector area for PVT collectors as result of a parameter study. According to the boundary conditions for solar thermal system simulations of T44A38, the FPCs and PVT collectors are simulated with a collector tilt of 45° oriented towards south (azimuth of 0°) and for the PVT collectors the wind speed on the collector plane is taken as half of the meteorological wind speed from the climate data [Haller et al., 2013a]. In case of the used FPC models, the wind speed has no influence as the wind speed dependence parameters of the quasi-dynamic collector model are set to zero for the considered glazed collectors (cf. Section 3.2.2.1). For the frost protected brine in the solar thermal circuit a specific heat capacity of 3.816 kJ/kgK is used. The key parameters of the FPCs and PVT collectors for the simulations are summarized in Table 3.4 and Table 3.9.

3.3.5 Photovoltaic Battery System

The subsystem *Photovoltaic Battery System* consists of the PV modules or the electrical part of the PVT collectors (depending on the considered SHP system concept) modeled with TRNSYS Type 835, the battery storage, the data reader for the residential electrical load profiles and the equation block *PV Battery*, cf. Figure 3.27.

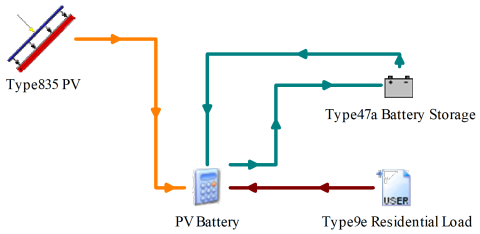

Figure 3.27: TRNSYS subsystem *Photovoltaic Battery System*.

The residential electrical loads (household electricity loads) are based on the reference load profiles of VDI 4655:2008 [VDI 4655, 2008]. The dynamic electrical load profile for Strasbourg was generated by the determination of typical days according to VDI 4655 from the used weather data file for Strasbourg (Section 3.3.2.1) and by scaling the resulting electrical loads to a reference household electricity load of 4 200 kWh/a for a single-family household in Strasbourg. The scaled electrical loads for the typical days are then used for the generation of dynamic electrical load profiles for Athens and Helsinki by composition of typical days over the year of the considered location from the weather data files, resulting in a household electricity load of 3 837 kWh/a for a single-family household in Athens and 4 415 kWh/a for a single-family household in Helsinki. A comparison of the shares of the household electricity loads and the annual heat loads from Section 3.3.2.2 in the net energy demand of the different buildings for the considered locations is given in Appendix A. The main properties of the components of the PV battery system model are summarized in Table 3.19. Degradation effects of PV cells or the battery storage are not considered as the evaluation period of the system simulations in this work is basically one year and advanced control strategies to minimize battery storage degradation are not considered in this work. The battery size varies in the different simulation cases between 5 kWh and 15 kWh for systems with battery storage and is zero for systems without battery storage. In case of systems with PV modules and PVT collectors, a second instance of TRNSYS Type 835 is added to the subsystem *Photovoltaic Battery System* and the resulting electrical power outputs of the PV modules and PVT collectors are summed up. Furthermore, the boundary conditions for solar thermal system simulations of T44A38 are adapted for solar electrical systems. Hence, the PV modules and PVT collectors are simulated with a module or collector tilt of 45° oriented towards south (azimuth of 0°) and the wind speed on the module or collector plane is taken as half of the meteorological wind speed from the climate data [Haller et al., 2013a]. The key parameters of the PV modules and PVT collectors for the simulations are summarized in Table 3.6 and Table 3.9.

Table 3.19: Main properties of the components of the PV battery system model.

Parameter	Value
PV inverter efficiency DC to AC	0.960 [SMA, 2015]
Battery inverter efficiency AC to DC (charging)	0.988 [a] [Weniger et al., 2019]
Battery inverter efficiency DC to AC (discharging)	0.987 [b] [Weniger et al., 2019]
Battery charging and discharging efficiency	0.949 [Weniger et al., 2019]
High limit of fractional state of charge ($FSOC^{\max}$)	0.90 [Akasol, 2014]
Low limit of fractional state of charge ($FSOC^{\min}$)	0.05 [Akasol, 2014]

[a] Calculated by total conversion efficiency from AC to battery divided by battery charging and discharging efficiency.

[b] Calculated by total conversion efficiency from battery to AC divided by battery charging and discharging efficiency.

3.3.6 Solar Thermal and Heat Pump System Control

In general, the subsystem *Solar Thermal and Heat Pump (STHP) System Control* includes a combination of differential controllers (Type 2b) and the equation block *STHP Control*. Due to the simplicity of the models, the specific STHP system control subsystems for different SHP system concepts are not shown graphically, but the different controllers and control tasks (depending on the considered SHP system concept) are explained in the following sections.

3.3.6.1 Buffer Storage Charging by the Heat Pump

The charging of the buffer storage by the heat pump is included in all SHP system concepts and is designed as rule-based controller (RBC) shown in Figure 3.28. In general, the charging of the buffer storage by the heat pump depends on the current values of the buffer storage temperatures and the set point temperatures for space heating and domestic hot water preparation with priority on domestic hot water preparation. To protect the heat pump and avoid frequent starting of the heat pump, a minimum runtime $t^{\min}_{\mathrm{HP,on}}$ of 15 min and a minimum pause-time $t^{\min}_{\mathrm{HP,off}}$ of 15 min for the heat pump are implemented in the RBC. The buffer storage charging for domestic hot water depends on the value of the upper buffer storage temperature sensor for domestic hot water preparation $\vartheta_{\mathrm{buffer,DHW}}$ and is turned on if the temperature falls below 53 °C ($\vartheta_{\mathrm{DHW,on}}$) until it rises above 55 °C ($\vartheta_{\mathrm{DHW,off}}$). The set point calculation of the supply temperature for space heating ($\vartheta_{\mathrm{SH,set}}$) depends especially on the current ambient temperature and the design heat load of the considered building and location and is described in Dott et al. [2013]. The buffer storage charging for space heating is turned on if the temperature difference between the temperature sensor for space heating $\vartheta_{\mathrm{buffer,SH}}$ and the set point for the supply temperature for space heating $\vartheta_{\mathrm{SH,set}}$ falls below 0 K ($\Delta T_{\mathrm{SH,on}}$) until the temperature difference is higher than 3 K ($\Delta T_{\mathrm{SH,off}}$). Furthermore, if the buffer storage charging for space heating or domestic hot water turns off but the minimum run-time of the heat pump is not reached, the buffer storage charging for the SH zone is switched on for the remaining runtime.

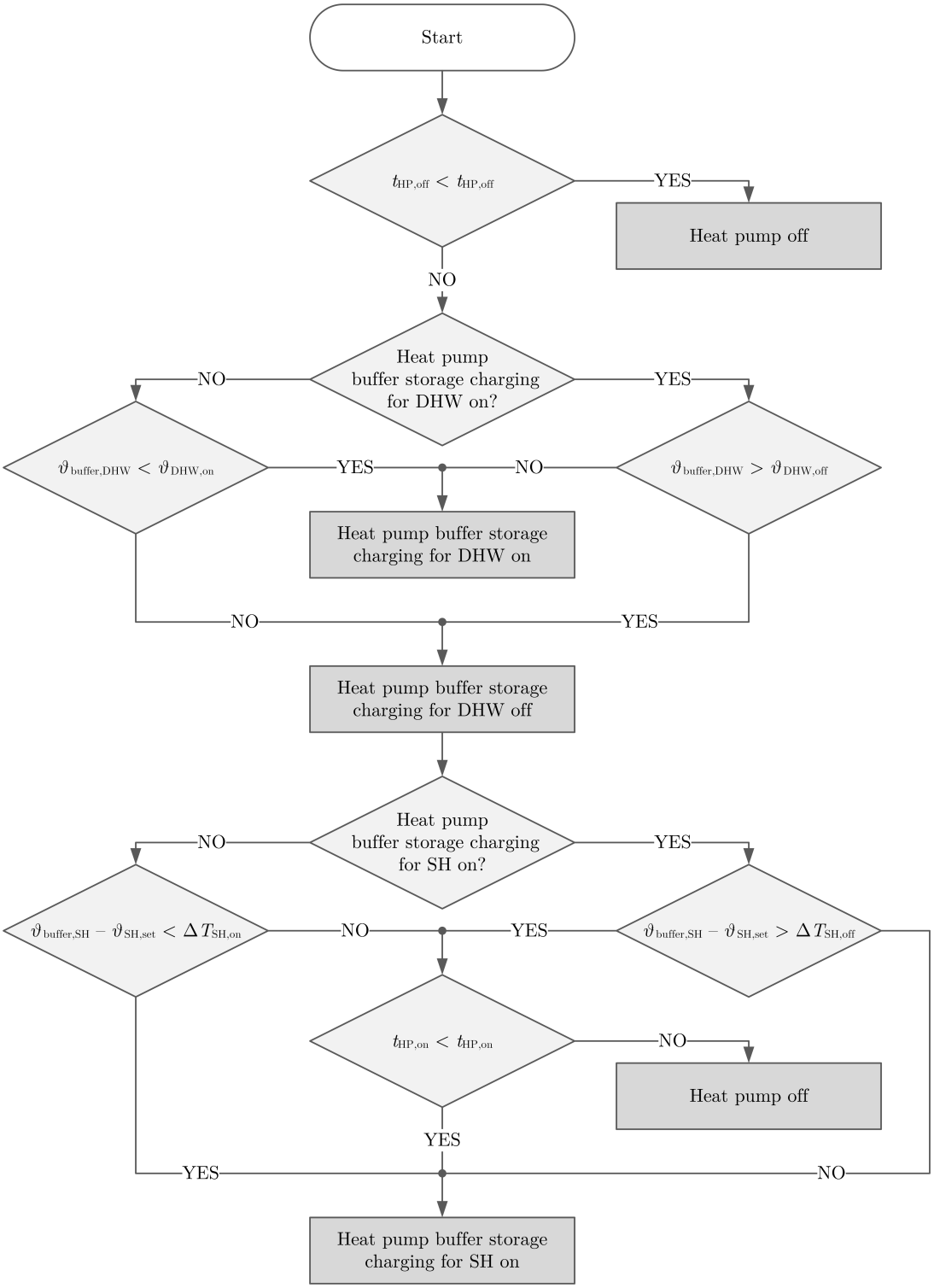

Figure 3.28: RBC for buffer storage charging by the heat pump.

3.3.6.2 Buffer Storage Charging by the Solar Thermal Circuit

The flowchart of the RBC for buffer storage charging by the solar thermal circuit in SHP systems with parallel solar thermal circuit is shown in Figure 3.29. The solar circuit is basically switched on if the temperature difference between the supply temperature of the FPC or PVT collectors ϑ_{sol} and the buffer storage temperature sensor for solar thermal

circuit charging $\vartheta_{\text{buffer,SC}}$ is equal or higher than 5 K ($\Delta T_{\text{sol,on}}$) and will remain switched on until the temperature difference falls below 2 K ($\Delta T_{\text{sol,off}}$). For storage protection, a maximum storage temperature of 80 °C ($\vartheta^{\text{max}}_{\text{buffer}}$) is defined for the buffer storage temperature sensor for storage protection $\vartheta_{\text{buffer,prot}}$ (storage protection mode). Furthermore, a high limit cut-out for the FPC or PVT collector temperature is defined in the controller to avoid damage of the components in the solar circuit if the supply temperature of the FPC or PVT collectors ϑ_{sol} reaches 130 °C ($\vartheta^{\text{max}}_{\text{sol,on}}$). In this case (solar circuit protection mode), the solar circuit pump is turned off until the supply temperature falls below 120 °C ($\vartheta^{\text{max}}_{\text{sol,off}}$).

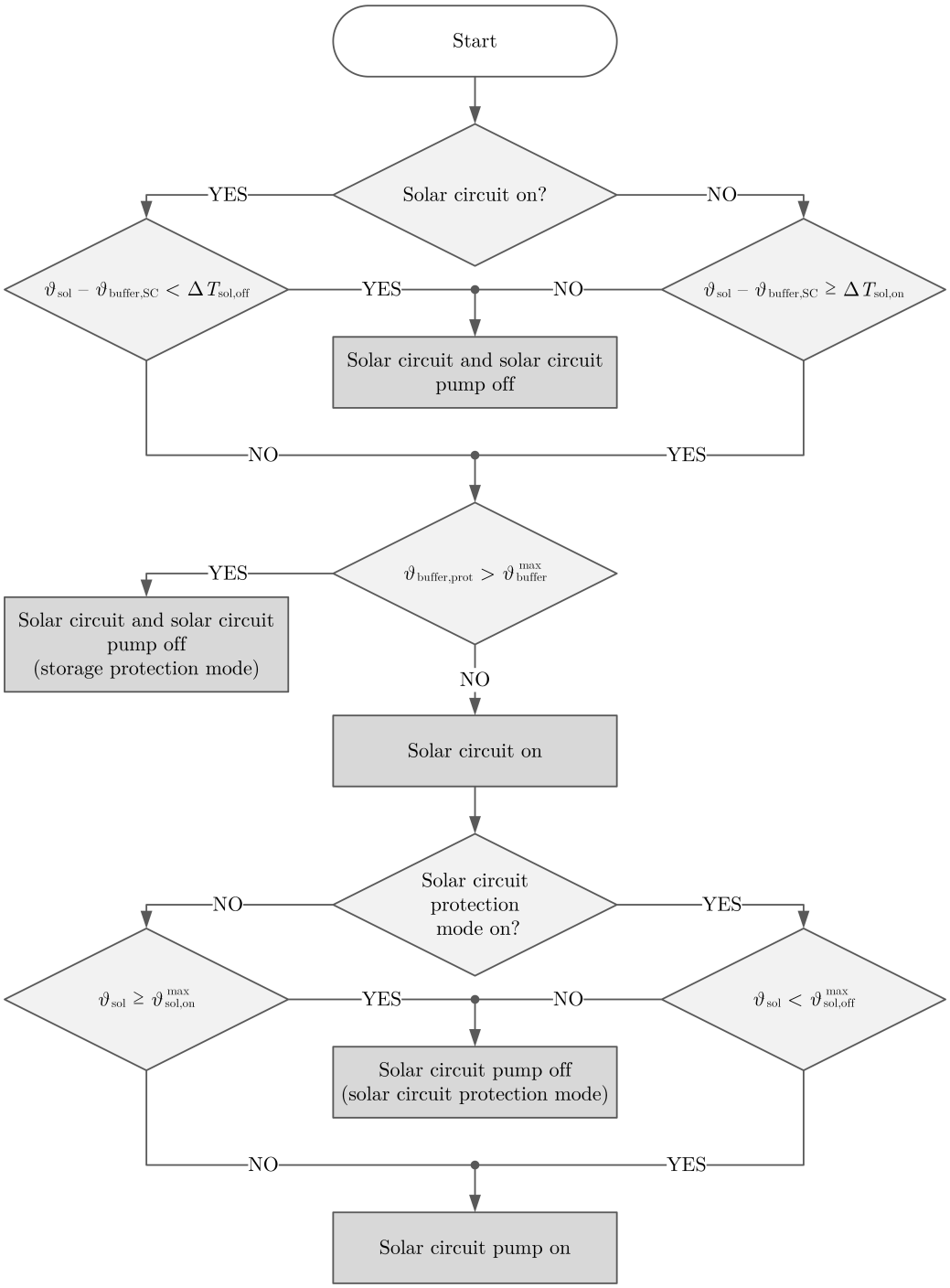

Figure 3.29: RBC for buffer storage charging by the solar thermal circuit.

3.3.6.3 Ice Storage Charging by the Solar Thermal Source Circuit

The flowchart of the RBC for ice storage charging by the solar thermal source circuit in SISHP systems is shown in Figure 3.30. The solar source circuit pump for ice storage charging by the WISC or PVT collectors is switched on if:

- the difference between the supply temperature of the WISC or PVT collectors $\vartheta_{\mathrm{sol,ice}}$ and the ice storage temperature ϑ_{ice} is equal or higher than 3 K ($\Delta T_{\mathrm{sol,ice,on}}$) and
- the supply temperature of the WISC or PVT collectors $\vartheta_{\mathrm{sol,ice}}$ is equal or higher than −9 °C ($\vartheta^{\mathrm{min}}_{\mathrm{sol,ice,on}}$) and
- the ice storage temperature ϑ_{ice} is below 14 °C ($\vartheta^{\mathrm{max}}_{\mathrm{ice,off}}$).

If the solar source circuit pump is switched on, it will remain switched on until:

- the temperature difference between the supply temperature of the WISC or PVT collectors collectors $\vartheta_{\mathrm{sol,ice}}$ and the ice storage temperature ϑ_{ice} falls below 1 K ($\Delta T_{\mathrm{sol,ice,off}}$) or

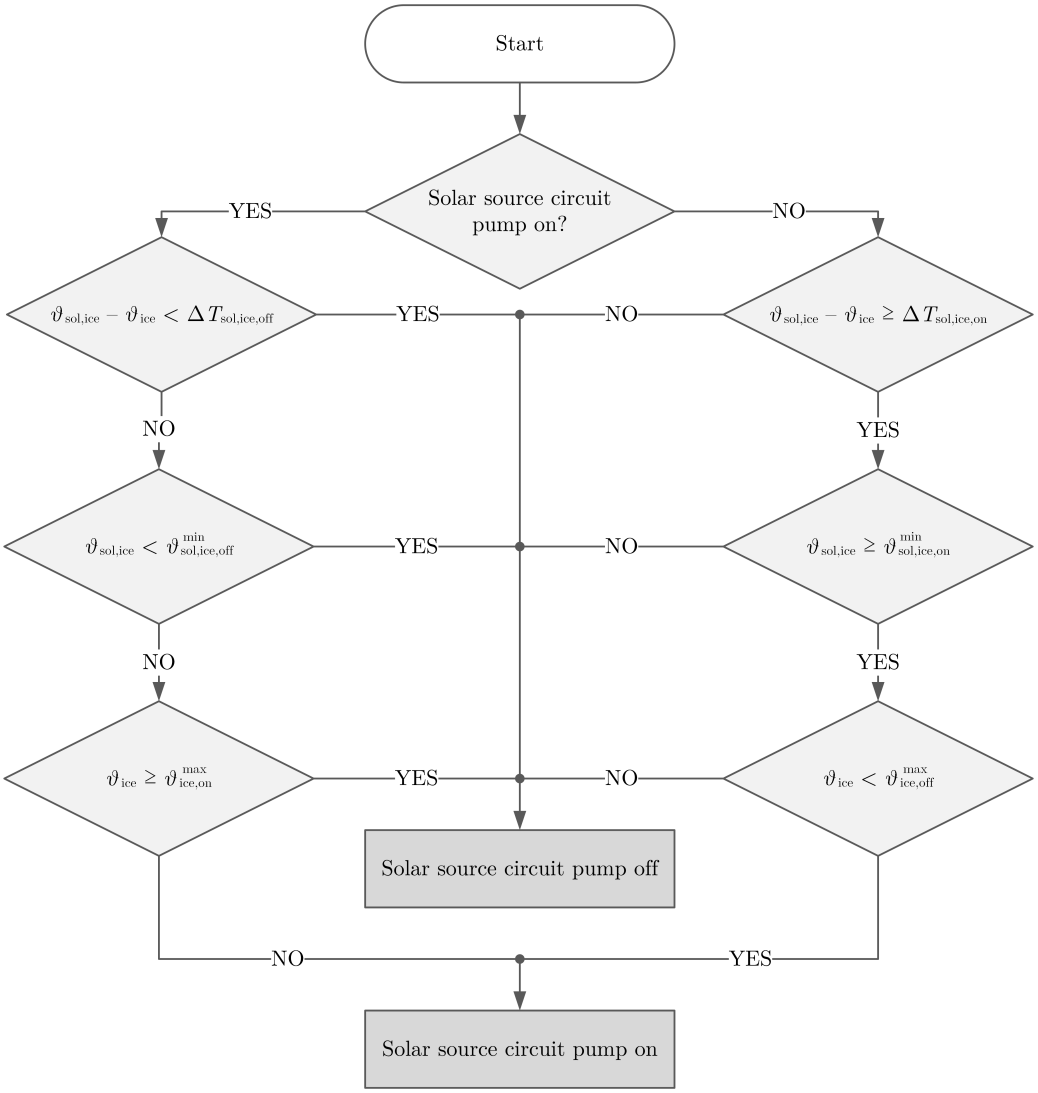

Figure 3.30: RBC for ice storage charging by the solar thermal source circuit.

- the supply temperature of the WISC or PVT collectors $\vartheta_{\mathrm{sol,ice}}$ falls below $-10\,^{\circ}\mathrm{C}$ ($\vartheta^{\mathrm{min}}_{\mathrm{sol,ice,off}}$) or
- the ice storage temperature ϑ_{ice} reaches $15\,^{\circ}\mathrm{C}$ ($\vartheta^{\mathrm{max}}_{\mathrm{ice,on}}$).

3.3.7 Building Energy Management System Control

In general, the subsystem *Building Energy Management System (BEMS) Control* includes a combination of differential controllers (Type 2b) and the equation block *BEMS Control*. Due to the simplicity of the models, the BEMS control subsystem is not shown graphically, but the controller and control tasks are explained in the following. The flowchart of the RBC of the BEMS for the usage of solar power generated by PV or PVT as well as the battery storage charging and discharging in SHP systems with PV battery system is shown in Figure 3.31. In general, the generated solar power is self-consumed by the household and the SHP system with priority on covering the household electricity load. If the solar power generation exceeds the household electricity and SHP system loads, the excess solar power is used for charging the battery storage until the fractional state of charge (FSOC) reaches its high limit ($FSOC^{\mathrm{max}}$). If the battery storage is fully charged, the excess solar power is fed into the grid. In times without solar power generation or excess solar power, the battery storage is discharged if the FSOC is higher than its low limit ($FSOC^{\mathrm{min}}$) or the (additional) required electricity is delivered by the grid. The described priority on household electricity usage of self-consumed solar electricity is chosen as heat pump tariffs are often more favorable than electricity tariffs for household electricity and thus this leads to a higher

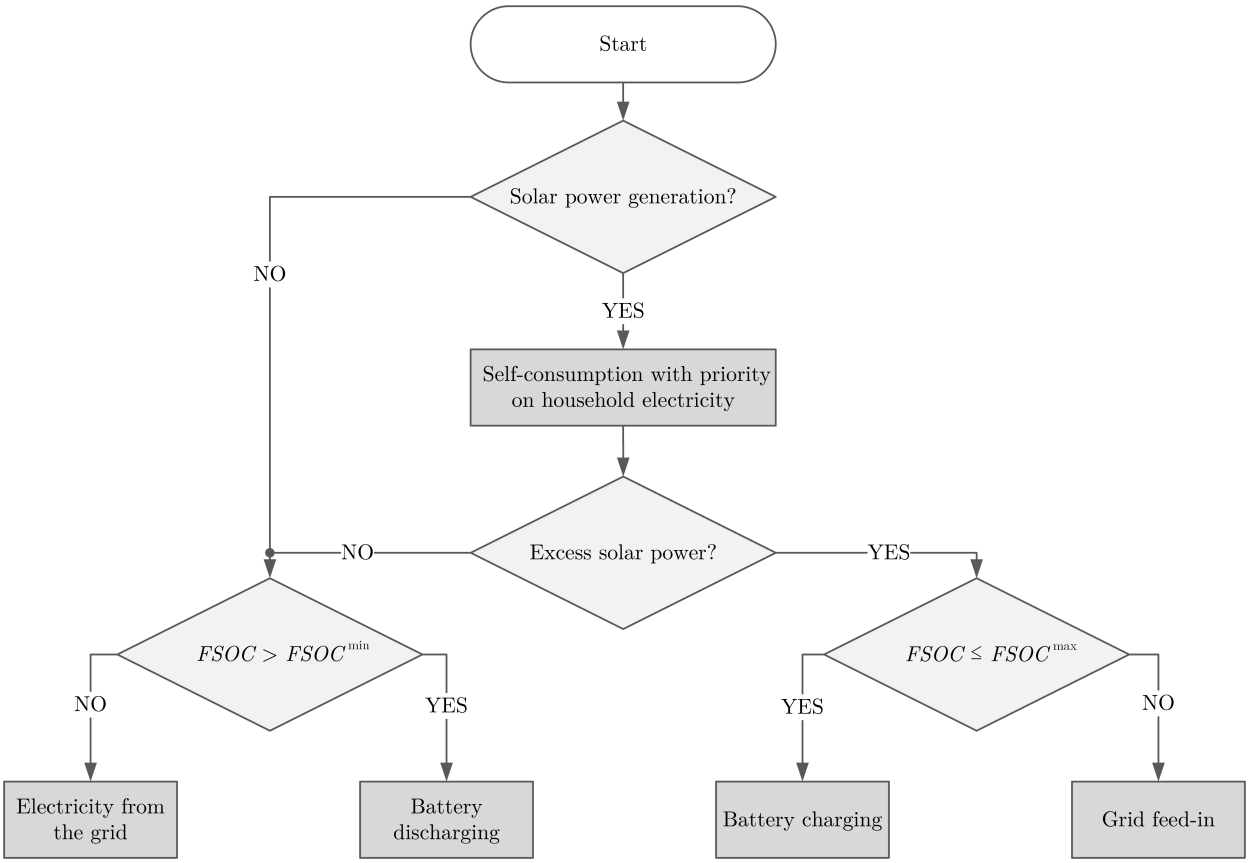

Figure 3.31: RBC of the building energy management system.

reduction of energy costs by self-consumption of solar electricity. In systems without battery storage, the generated solar power is self-consumed by the household and the SHP system with priority on household electricity and excess solar power is fed into the grid. In times without solar power generation or excess solar power, the (additional) required electricity is delivered by the grid. Due to different national regulations, a feed-in limit for excess solar power or shut-off times of the heat pump by utilities are not considered in this work.

Chapter 4

System Design

This chapter presents the general analysis and evaluation of system design and performance for the considered solar and heat pump systems and applications in this work. Beginning with a general introduction to the performed simulations and boundary conditions, the system design analysis is presented in detail. First, the performance and efficiency of different solar and heat pump system concepts regarding different building types and locations is evaluated. This is followed by the analysis of the environmental impact with focus on the CO_2 emissions for the rating of the global warming potential of the different buildings and systems. Furthermore, a basic analysis of economic efficiency is presented in this chapter. Finally, the results are summarized and discussed.

4.1 Overview of System Simulations

The presented system simulations in the following were performed with TRNSYS 18.02.0000 [TRNSYS, 2020] using the system models described in Section 3.3. Even if building simulations are often performed with hourly time steps, system simulations coupling the building and the energy supply system require higher time step resolutions. Poppi et al. [2018] reported that larger time steps within SHP system simulations will suggest a greater supply of PV generation to the loads and that several studies had identified significant errors in the PV self-consumption for time steps greater than five minutes. Hence, for the system simulations in this work, a time step of two minutes was used as compromise between accuracy and computational time. Furthermore, to minimize the influence of initial values, the simulations were performed for two years whereas the second year is used for the evaluation of the system simulations.

In general, all heat pump and SHP system concepts described in Section 2.2.1.3 and Section 2.3 were taken into account for the performed system simulations. Nevertheless, not all combinations of system concepts and locations or buildings are feasible or worthwhile for simulation and further analysis. As a result, SFH15 was excluded for the climate of Athens due to the missing energy demand for space heating. Furthermore, due to the low annual

heat loads for space heating of SFH45 and SFH100 and high ambient air temperatures in Athens, SISHP systems were not considered in the investigations for Athens. In case of Helsinki, the simulations showed that the ice storage volume had to be set higher than 30 m^3 for SFH45 and SFH100, which corresponds to an installation of more than three market available ice storages with a size of 10 m^3 for a single-family house, and thus only SFH15 was considered for the analysis of SISHP systems in Helsinki. An assignment of the simulated heat pump and SHP system concepts depending on the location and building type is given in Table 4.1.

Table 4.1: Assignment of simulated heat pump and SHP system concepts to locations and building types.

	Athens		Strasbourg			Helsinki		
	SFH45	SFH100	SFH15	SFH45	SFH100	SFH15	SFH45	SFH100
ASHP	x	x	x	x	x	x	x	x
GSHP	x	x	x	x	x	x	x	x
SASHP-P	x	x	x	x	x	x	x	x
SGSHP-P	x	x	x	x	x	x	x	x
SISHP-S	-	-	x	x	x	x	-	-
SISHP-S,P	-	-	x	x	x	x	-	-
PV-ASHP	x	x	x	x	x	x	x	x
PV-GSHP	x	x	x	x	x	x	x	x
PV-SASHP-P	x	x	x	x	x	x	x	x
PV-SGSHP-P	x	x	x	x	x	x	x	x
PV-SISHP-S	-	-	x	x	x	x	-	-
PV-SISHP-S,P	-	-	x	x	- [a]	x	-	-
PVT-SASHP-P	x	x	x	x	x	x	x	x
PVT-SGSHP-P	x	x	x	x	x	x	x	x
PVT-SISHP-S	-	-	x	x	x	x	-	-
PV-PVT-SASHP-P	x	x	x	x	x	x	x	x
PV-PVT-SGSHP-P	x	x	x	x	x	x	x	x
PV-PVT-SISHP-S	-	-	x	x	- [a]	x	-	-

[a] This combination was not possible due to the limited roof area and the minimum required serial WISC or PVT collector area for the supply of ice storages from Table 4.4.

The assignment of ice storage volumes to different locations and buildings is given in Table 4.2 and results from performed system simulations with variation of the ice storage volume. At this, the minimum required ice storage volumes to avoid a total freezing of the ice storage were chosen as ice storage design volumes. Beside of the system design purpose, this is a consequence of the limitations of TRNSYS Type 343 that does not allow for the operation below 0 °C. Nevertheless, it is a reasonable choice for the ice storage design due to the decreasing efficiency of the heat pump with decreasing source temperature. Furthermore, the ice storage volumes were adjusted by means of the height of the ice storage instead of adding a second ice storage model as only one instance of TRNSYS Type 343 can be used in a system model. The sizing varied in steps of 10 m^3 as typical size of market available ice storages.

Table 4.2: Assignment of ice storage volumes to different locations and building types.

Location	Building	Ice storage volume
Strasbourg	SFH15	$10\,m^3$
	SFH45	$10\,m^3$ for WISC collectors, $20\,m^3$ for PVT collectors
	SFH100	$20\,m^3$ for WISC collectors, $30\,m^3$ for PVT collectors
Helsinki	SFH15	$30\,m^3$

Regarding the further system design, the simulations were performed with variations of PV module, solar thermal (WISC or FPC) and PVT (WISC or covered flat-plate) collector areas in $5\,m^2$ steps for a maximum available roof area of $25\,m^2$. If two or more solar technologies are combined within a SHP system concept, only combinations with a total used roof area of $25\,m^2$ were considered to limit the number of simulation cases to be carried out. Furthermore, the battery storage size was varied between 5 kWh and 15 kWh for typical applications in residential buildings. A summary of the parameter variations including the used step size is given in Table 4.3. Regarding system concepts with ice storage, not all possible combinations of PV module, solar thermal and PVT collector areas could be evaluated as some simulations aborted when the ice storage was totally frozen. This results in a minimum required serial WISC or PVT collector area for the supply of the ice storage that is summarized for different locations and buildings depending on the used solar technology in Table 4.4.

Table 4.3: Parameter variations within the performed system simulations.

Parameter	Values	Parameter	Values
A_{WISC}	$5\,m^2$, $10\,m^2$, $15\,m^2$, $20\,m^2$, $25\,m^2$	$A_{\mathrm{PVT,WISC}}$ [a]	$5\,m^2$, $10\,m^2$, $15\,m^2$, $20\,m^2$, $25\,m^2$
A_{FPC}	$5\,m^2$, $10\,m^2$, $15\,m^2$, $20\,m^2$, $25\,m^2$	$A_{\mathrm{PVT,covered}}$ [a]	$5\,m^2$, $10\,m^2$, $15\,m^2$, $20\,m^2$, $25\,m^2$
A_{PV} [a]	$5\,m^2$, $10\,m^2$, $15\,m^2$, $20\,m^2$, $25\,m^2$	C_{bat} [b]	0 kWh, 5 kWh, 10 kWh, 15 kWh

[a] By using the same electrical model parameters, the nominal electrical power of PV modules and PVT collectors depending on the module/collector area is identical. At this, $5\,m^2$, $10\,m^2$, $15\,m^2$, $20\,m^2$ and $25\,m^2$ correspond to nominal electrical powers of 0.75 kWp, 1.50 kWp, 2.25 kWp, 2.99 kWp and 3.74 kWp.

[b] The battery storage capacities are nominal values without consideration of $FSOC^{\min}$ and $FSOC^{\max}$.

Table 4.4: Minimum required serial WISC or PVT collector area for the supply of ice storages depending on location and building type.

Location	Building	$A^{\min}_{\mathrm{WISC}}$ [a]	$A^{\min}_{\mathrm{PVT,WISC}}$	$A^{\min}_{\mathrm{PVT,covered}}$
Strasbourg	SFH15	$5\,m^2$	$5\,m^2$	$5\,m^2$
	SFH45	$15\,m^2$	$10\,m^2$	$10\,m^2$
	SFH100	$20\,m^2$	$25\,m^2$	$25\,m^2$
Helsinki	SFH15	$15\,m^2$	$25\,m^2$	$15\,m^2$

[a] In some simulation cases of SISHP-S,P systems, the required serial WISC collector area for the supply of the ice storage was lower due to the shorter annual operating time of the heat pump. These cases were excluded from the evaluation as the heat source circuit of the heat pump should not be undersized.

With regard to the parallel integration of FPC or PVT collectors, the buffer storage design was analyzed for Strasbourg by a parametric study for SGSHP-P and SASHP-P

system concepts considering the building types SFH15, SFH45 and SFH100. For both SHP system concepts and each building, the FPC collector size was varied between 5 m² and 25 m² in 5 m² steps and for each collector area the buffer storage size was varied by 1 000 l, 1 500 l and 2 000 l. By evaluating earlier simulation results, a minimum of 1 000 l was chosen in order to extend the heat pump runtime and to avoid too frequent on and off switching of the heat pump. Buffer storage volumes larger than 2 000 l are usually not used in single-family houses and are thus not considered within this work. As a result of the parametric study, a previously used design rule of 100 l buffer storage volume per m² FPC collector area can be verified to reach the highest $SPF_{\mathrm{SHP+,pen}}$ on the average of the evaluated SHP systems with a buffer storage size between 1 000 l and 2 000 l (cf. Figure 4.1a). Regarding the same boundary conditions (building, location, SHP concept) for covered flat-plate PVT collectors, the yearly solar thermal yield with a collector area of 25 m² is in the range of FPC systems with a collector area between 5 m² and 10 m². For WISC collectors, the yearly solar thermal yield is even lower. Following the design rules verified for FPC collectors, this indicates that the buffer storage volume for PVT collectors should be 1 000 l which could be verified by simulation (cf. Figure 4.1b). As a consequence, the buffer storage is sized with 1 000 l for SHP systems with PVT collectors. These design rules are only recommended for the evaluated SHP concepts and for FPC or PVT collector sizes between 5 m² and 25 m². An assignment of the buffer storage size to the FPC or PVT collector area used in parallel within SHP system concepts is given in Table 4.5. In system concepts without parallel FPC or PVT integration, the buffer storage size is set to the defined size of 1 000 l for the heat pump operation.

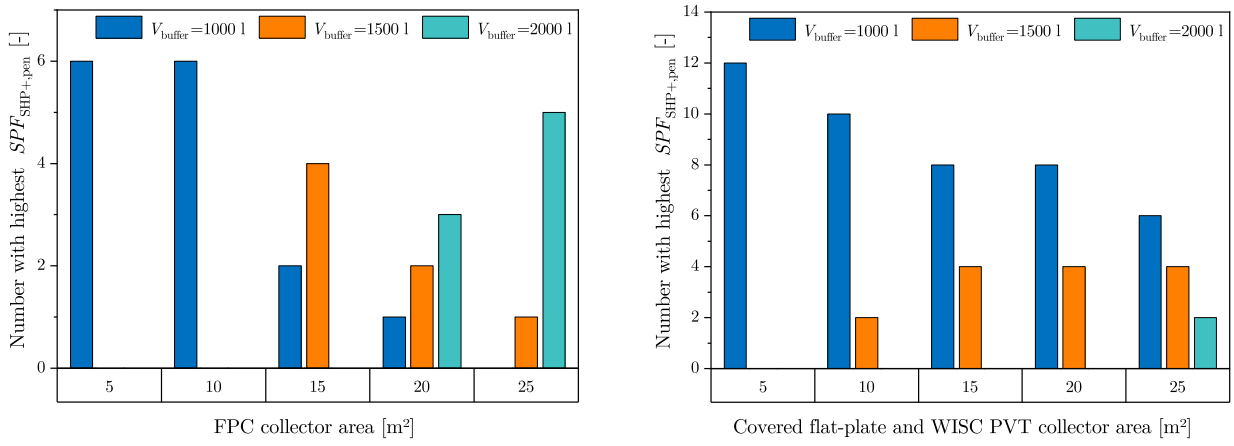

(a) FPC **(b)** PVT

Figure 4.1: Number of simulation cases with highest $SPF_{\mathrm{SHP+,pen}}$ depending on the solar collector area and buffer storage size for different solar collector technologies.

In summary, a total of 2 074 simulations were evaluated for the following analyses within this chapter. Thus, some restriction had to be made to minimize the possible simulation cases like the described predefinition of the buffer storage sizes or the complete covering of the available roof area with solar collectors or PV modules for simulation cases with more than one solar technology. Furthermore, the multitude of simulation results requires a restriction of the evaluated KPIs within this work focusing on a selection of main performance figures. Nevertheless, summaries of the results of the performed simulations considering most defined KPIs within Section 2.4 are published as SHP-SimResults on GitHub [Jonas, 2023b] and

Table 4.5: Assignment of buffer storage volumes to different solar collector technologies depending on the solar collector area.

Collector type	Collector area	Buffer storage volume
FPC collectors	$5\,m^2$, $10\,m^2$	1 000 l
	$15\,m^2$	1 500 l
	$20\,m^2$, $25\,m^2$	2 000 l
Covered flat-plate and WISC PVT collectors	$5\,m^2$ – $25\,m^2$	1 000 l

can be used for further research and evaluation. In the following sections, the results are presented as box-and-whisker diagrams using lines (whiskers) for results outside the lower quartile (25th percentile, median of the lower half of the results) and the upper quartile (75th percentile, median of the upper half of the results). Outliers that are outside the 1.5 interquartile range (IQR) are shown as separate data points beyond the whiskers. The IQR describes the distance between the lower and the upper quartiles, whereas 1.5 IQR means a distance of 1.5 times the IQR below the lower and above the upper quartiles [Dekking et al., 2005]. In addition, the results of WISC and covered flat-plate PVT collectors are summarized in system concepts with PVT collectors and are not divided as it is part of the comparison and analysis in Section 5.1.2.

4.2 Performance and Efficiency

This section presents the *performance and efficiency evaluation* of the considered SHP systems in this work. The objective of this evaluation is the comparison of SHP system concepts for a wide range of boundary conditions in order to identify suitable applications with focus on the general system design and to determine the efficiency benefits of different SHP system concepts. The SPF is chosen as main KPI, whereas:

- the grid-related SPF of the overall system with penalties $SPF_{\mathrm{SHP+,pen,grid}}$ is used for the heating efficiency comparison and
- the grid-related SPF of the building $SPF_{\mathrm{bui,grid}}$ is used for the energy efficiency comparison regarding the thermal and electrical energy supply of the building.

Furthermore, additional KPIs are used to justify the results of the analysis and to draw conclusions. In the following, the SFH45 building in Strasbourg is used as base case as it represents current legal requirements or renovated buildings with good thermal quality of the building envelope in moderate climates. Starting with the base case, the influence of different building types on the results is analyzed using SFH15 for new buildings with very high energy standard and SFH100 for non-renovated existing buildings. This is followed by the assessment of the influence of cold (Helsinki) and warm (Athens) climates on the performance and efficiency evaluation.

4.2.1 Base Case: Strasbourg SFH45

An overview of the range of grid-related SPFs of the overall system with penalties for the different heat pump and SHP system concepts in Strasbourg for SFH45 is shown in

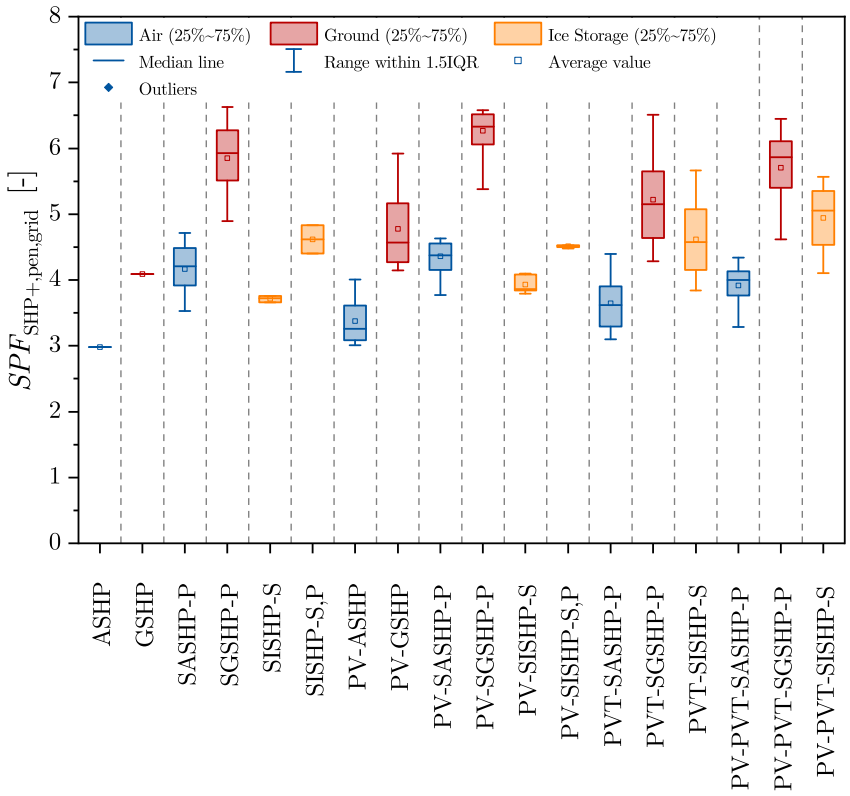

Figure 4.2: Grid-related SPF of the overall system with penalties for different heat pump and SHP system concepts in Strasbourg for SFH45.

Figure 4.2. For systems with ASHP, the SPF is in the range of 2.99 (ASHP) and 4.72 (SASHP-P), for systems with GSHP in the range of 4.09 (GSHP) and 6.62 (SGSHP-P) and for SISHP systems in the range of 3.66 (SISHP-S) and 5.67 (PVT-SISHP-S). Basically, the simulation results show that the heating efficiency can significantly be increased by adding solar technologies and that the different system concepts compete with each other. In general, the SPF increases with increasing FPC/PVT collector or PV module area. Furthermore, in case of systems with PV or PVT and battery storage, the SPF increases with increasing battery storage capacity. Both effects can be explained by higher amounts of solar energy that can be used for the supply of the SHP system. Comparing different concepts, systems with parallel solar thermal (FPC, PVT) circuit achieve the highest SPFs in terms of heating efficiency with regard to ASHP and GSHP systems. At this, systems with FPCs reach slightly higher SPF values than systems with PVT collectors. In contrast, systems with PVT collectors reach the highest SPFs for system concepts with ice storage. The SPFs of PV and heat pump systems are lower on average than those of systems with solar thermal integration (FPC, PVT) and PV and heat pump systems can only compete with these concepts if a battery storage is used. It should be noted that this is, at least in part, an effect of the used control strategy with priority on household electricity usage of self-consumed solar electricity. This is also illustrated by SCR values for the SHP system between 3 % and 18 %, whereas the SCR values for household electricity are in the range of 32 % and 89 % for the investigated PV and heat pump system concepts. Furthermore, general improvements by combining PV with system concepts with parallel FPC or PVT collectors cannot be observed with regard to the heating efficiency in comparison to the corresponding solar thermal or PVT and heat pump systems.

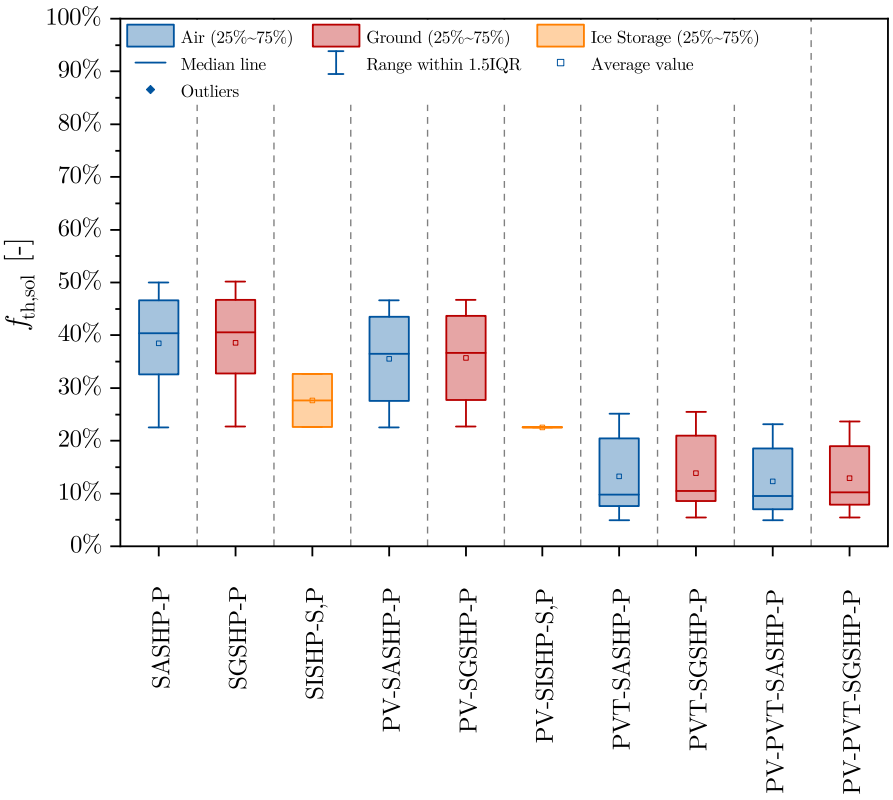

Figure 4.3: Solar thermal fractions for different SHP system concepts in Strasbourg for SFH45.

Regarding system concepts with ASHP or GSHP, the relative increase of the SPF by adding parallel solar thermal circuits in comparison to the corresponding system without solar integration varies between 18 % and 62 % for systems with FPC reaching solar thermal fractions between 23 % and 50 %, whereas the relative increase of the SPF for systems with PVT varies between 4 % and 59 % reaching solar thermal fractions between 5 % and 26 % (cf. Figure 4.3). The relatively high increases of the SPF for systems with PVT with lower solar thermal fractions in comparison to systems with FPC point out that systems with PVT benefit from the use of solar electricity for the supply of the SHP system in combination with the solar thermal yields. In case of systems with PV, the SPF increases between 1 % and 10 % for systems without battery storage and between 3 % and 45 % for systems with battery storage in comparison to the corresponding ASHP or GSHP system (cf. Figure 4.4). For systems with PV, the relative increase of the SPF in comparison to the corresponding PV and heat pump system without battery storage varies between 2 % and 17 % for a battery storage size of 5 kWh and between 2 % and 32 % for a battery storage size of 15 kWh depending on the heat pump technology and the PV module area. For systems with PVT, the relative increase of the SPF in comparison to the corresponding PVT and heat pump system without battery storage varies between 1 % and 15 % for a battery storage size of 5 kWh and between 1 % and 28 % for a battery storage size of 15 kWh depending on the heat pump technology, the PVT collector technology and the PVT collector area. At this, the improvement of the SPF by adding a battery storage increases with increasing PV module or PVT collector area as a result of higher amounts of generated solar electrical energy that can be stored in the battery storage. In addition, it can be observed that the improvement of the SPF by adding a battery storage is higher for systems with GSHP. The reason for this is the generally lower

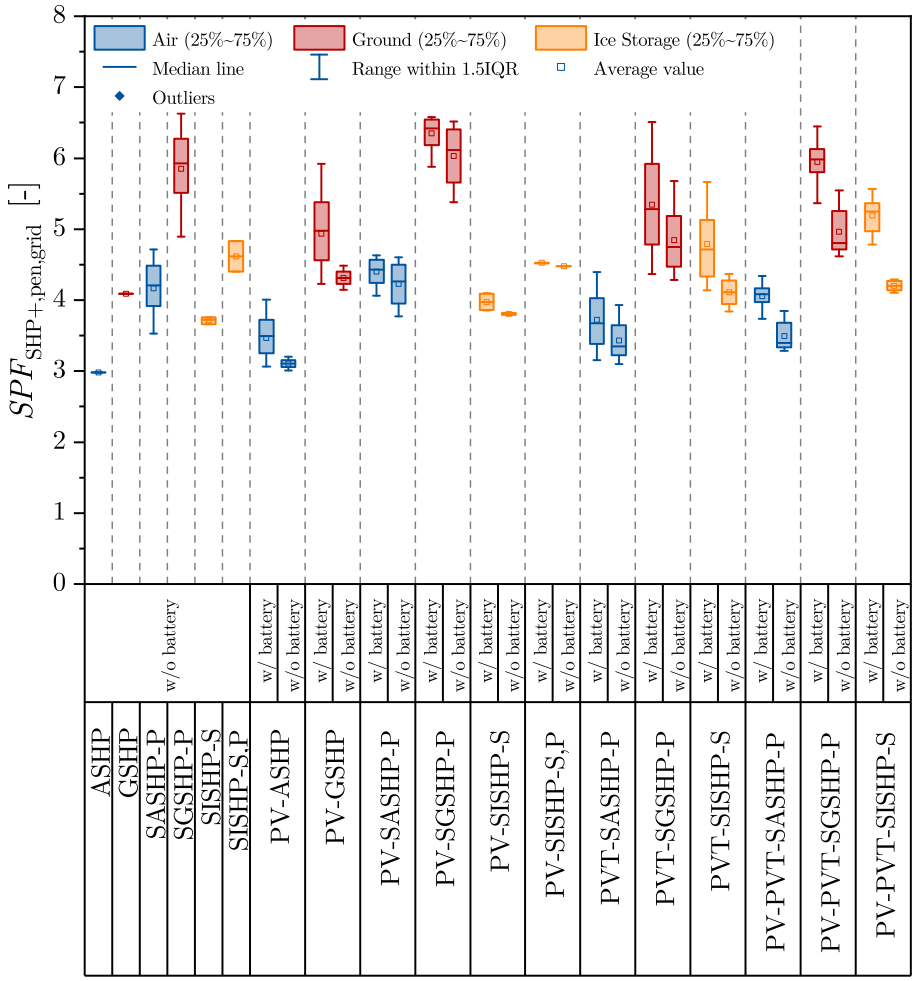

Figure 4.4: Grid-related SPF of the overall system with penalties for different heat pump and SHP system concepts with and without battery storage in Strasbourg for SFH45.

electricity consumption of the GSHP system in comparison to the ASHP system and thus higher relative increases of the SPF for covering similar amounts of electricity for the supply of the SHP system by solar energy. Furthermore, systems with GSHP achieve higher values of SPF than systems with ASHP for the combination with the same solar technology which can also be explained by the better performance of the GSHP system in comparison to the ASHP system in general for SFH45 in Strasbourg. Nevertheless, in some cases, SASHP-P, PV-SASHP-P, PVT-SASHP-P as well as PV-PVT-SASHP-P systems can reach the same or even higher values of SPF than GSHP systems without integration of solar technologies. In contrast, PV-ASHP systems cannot reach the performance of GSHP systems with regard to the heating efficiency.

Regarding system concepts with ice storage, SISHP-S systems achieve SPF values in the range of 3.66 to 3.76 and thus higher values than ASHP systems without integration of solar technologies. If a parallel solar thermal circuit with FPC is added to SISHP-S systems, the SPF can be increased between 18 % and 32 % reaching solar thermal fractions between 23 % and 33 % (cf. Figure 4.3). As a result, SISHP-S,P systems achieve SPF values between 4.40 and 4.83 which are higher than those of GSHP systems without integration of solar technologies. In case of PV-SISHP-S systems, the benefit of adding PV modules

with regard to the heating efficiency is lower than the improvement by adding the same FPC area. Nevertheless, the SPF can be improved by 2 % to 4 % for systems without battery storage and by 4 % to 12 % for systems with battery storage in comparison to the corresponding SISHP-S system (cf. Figure 4.4). In order to correctly assess these results, it should be mentioned that the additional PV module or FPC area is limited to 10 m^2 due to the limited available roof area and the minimum required WISC collector area for the supply of the ice storage. With regard to the heating efficiency, PVT-SISHP-S systems reach the highest SPFs of all system concepts with ice storage. At this, the relative increase by replacing WISC collectors with PVT collectors with the same collector area achieves values up to 16 % for systems without battery storage and up to 51 % for systems with battery storage (cf. Figure 4.4). On the one hand, the increase of the SPF can be influenced, at least in part, by the larger ice storage volume in case of systems with PVT which leads to lower maximum degrees of icing between 38 % and 59 % for PVT-SISHP-S systems in comparison to between 66 % and 84 % for SISHP-S systems with the same collector area. This is also reflected in a smaller minimum required PVT collector area in comparison to the minimum required WISC collector area. On the other hand, a reason for the increase is the additional solar electrical yield that can be used for the supply of the SHP system in comparison to systems with serial WISC collectors as figured out in the last paragraph for the parallel integration of PVT collectors. To sum up, these results illustrate that especially PVT-SISHP-S systems reaching high SPFs between 3.84 and 5.67 can compete with SHP systems with ASHP or GSHP with regard to the heating efficiency.

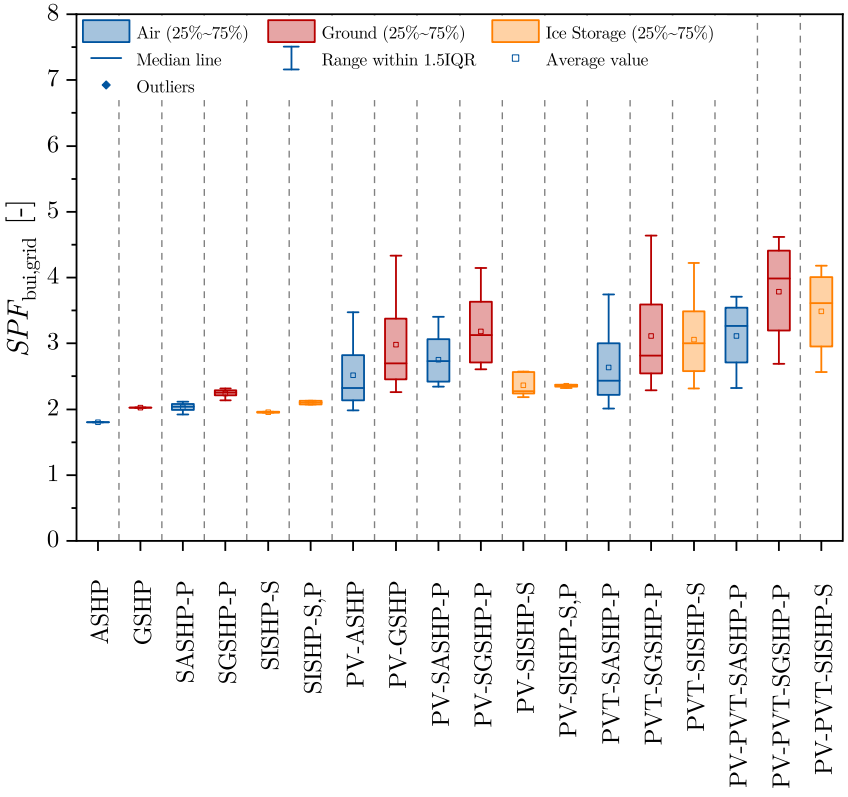

Figure 4.5: Grid-related SPF of the building for different heat pump and SHP system concepts in Strasbourg for SFH45.

An overview of the range of grid-related SPFs of the building for the different heat pump and SHP system concepts in Strasbourg for SFH45 is shown in Figure 4.5. For systems

with ASHP, the SPF is in the range of 1.80 (ASHP) and 3.74 (PVT-SASHP-P), for systems with GSHP in the range of 2.02 (GSHP) and 4.64 (PVT-SGSHP-P) and for SISHP systems in the range of 1.95 (SISHP-S) and 4.22 (PVT-SISHP-S). Basically, the simulation results show that the energy efficiency can only significantly be increased by adding PV modules (for systems with ASHP and GSHP) or PVT collectors (for all system concepts), especially in combination with a battery storage. As previously observed for the heating efficiency, the SPF of the building also increases with increasing FPC/PVT collector or PV module area and with increasing battery storage capacity for systems with PV or PVT and battery storage. Both effects result from higher amounts of solar energy that can be used for the supply of the building. Comparing different concepts, in contrast to the heating efficiency, solar thermal and heat pump concepts achieve the lowest maximum SPF values beside systems without solar technology integration, whereas systems with PVT collectors reach the highest SPFs in terms of energy efficiency. At this, PV and heat pump systems achieve slightly lower SPF values than systems with PVT collectors in case of systems with ASHP and GSHP. Regarding systems with ice storage, system concepts with PVT collectors reach by far the best results. Furthermore, the SPF of system concepts with parallel FPCs can be increased by the combination with PV, whereas general improvements by combining PV with system concepts with PVT collectors cannot be observed with regard to the energy efficiency in comparison to the corresponding PVT and heat pump systems. Depending on the battery storage size (especially for low battery storage sizes or systems without battery storage), some combinations of parallel FPCs and PV modules achieve even slightly higher SPFs than the corresponding systems with PV. Nevertheless, the maximum SPFs of PV-SASHP-P, PV-SGSHP-P and PV-SISHP-S,P systems are slightly lower than those of the corresponding systems with PV modules instead of parallel FPCs. In general, the results illustrate the benefit of on-site generated solar electrical energy, which can be used to cover both SHP and household electricity consumption and, as a result, the improvement of the energy efficiency with regard to the thermal and electrical energy supply of a building. This also results in high SSRs of the building reaching values up to 53 % for systems with PV and up to 54 % for systems with PVT (cf. Figure 4.6). At this, systems without battery storage achieve values between 9 % and 24 % for systems with PV and between 10 % and 25 % for systems with PVT.

Regarding system concepts with ASHP or GSHP, the relative increase of the SPF by adding parallel solar thermal circuits in comparison to the corresponding system without solar integration reaches only values between 6 % and 17 % for systems with FPC, whereas the relative increase of the SPF for systems with PVT varies between 12 % and 130 %. The significantly higher increases of the SPF for systems with PVT with lower solar thermal fractions in comparison to systems with FPC point out that systems with PVT benefit primarily from the use of solar electricity with regard to the thermal and electrical supply of a building. At this, major benefits for the specific solar electrical yield of PVT collectors in comparison to PV modules cannot be observed. The specific solar electrical yield is hardly improved or even decreases for some of the investigated cases (cf. Figure 4.7). The high impact of self-consumed solar electrical energy on the energy efficiency is also reflected in high SPF values for systems with PV. At this, the SPF increases between 10 % and 31 % for systems without battery storage and between 13 % and 115 % for systems with battery storage in comparison to the corresponding ASHP or GSHP system (cf. Figure 4.8). In addition, this illustrates the high impact of battery storages on the energy efficiency of a building. For systems with PV, the relative increase of the SPF in comparison to the corresponding PV and heat pump system without battery storage varies between 2 % and 30 %

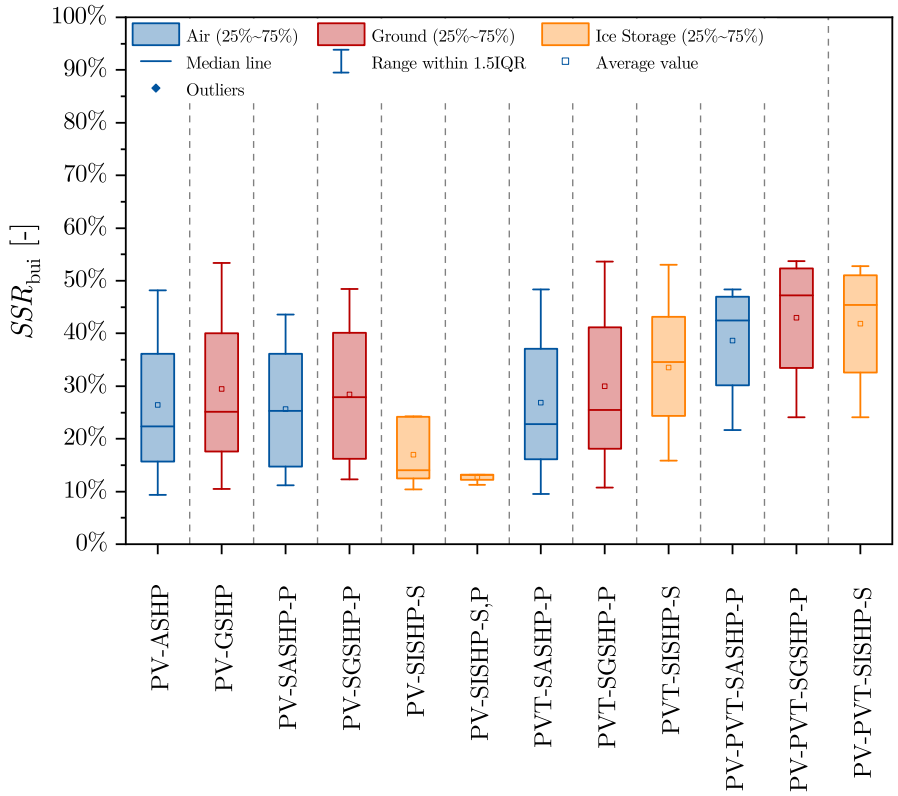

Figure 4.6: SSR of the building for different SHP system concepts in Strasbourg for SFH45.

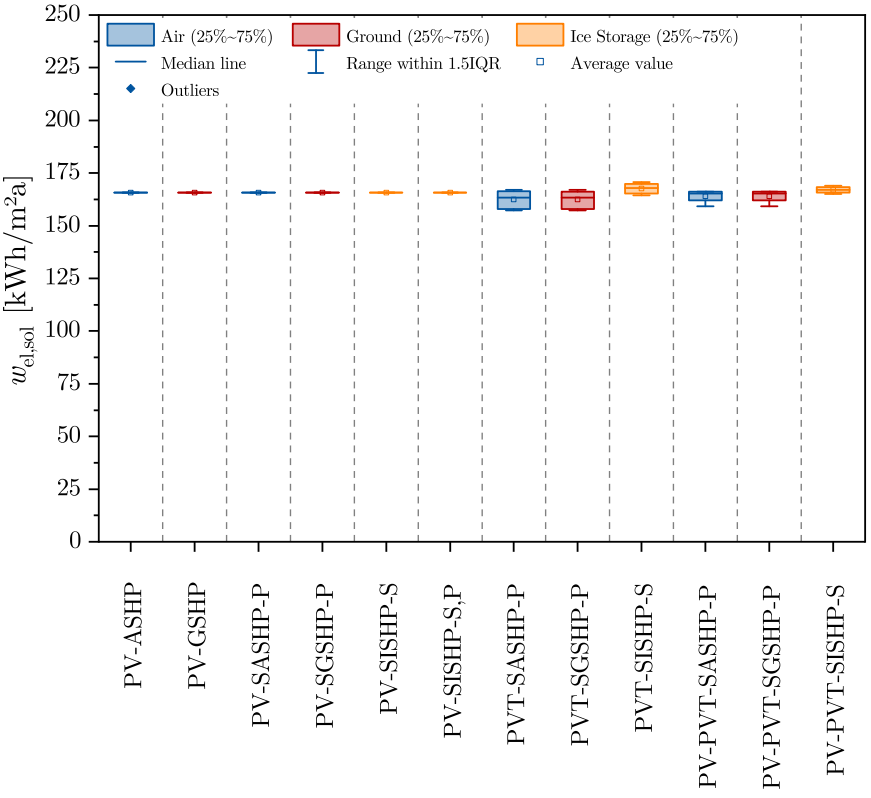

Figure 4.7: Specific solar electrical yields for different SHP system concepts in Strasbourg for SFH45.

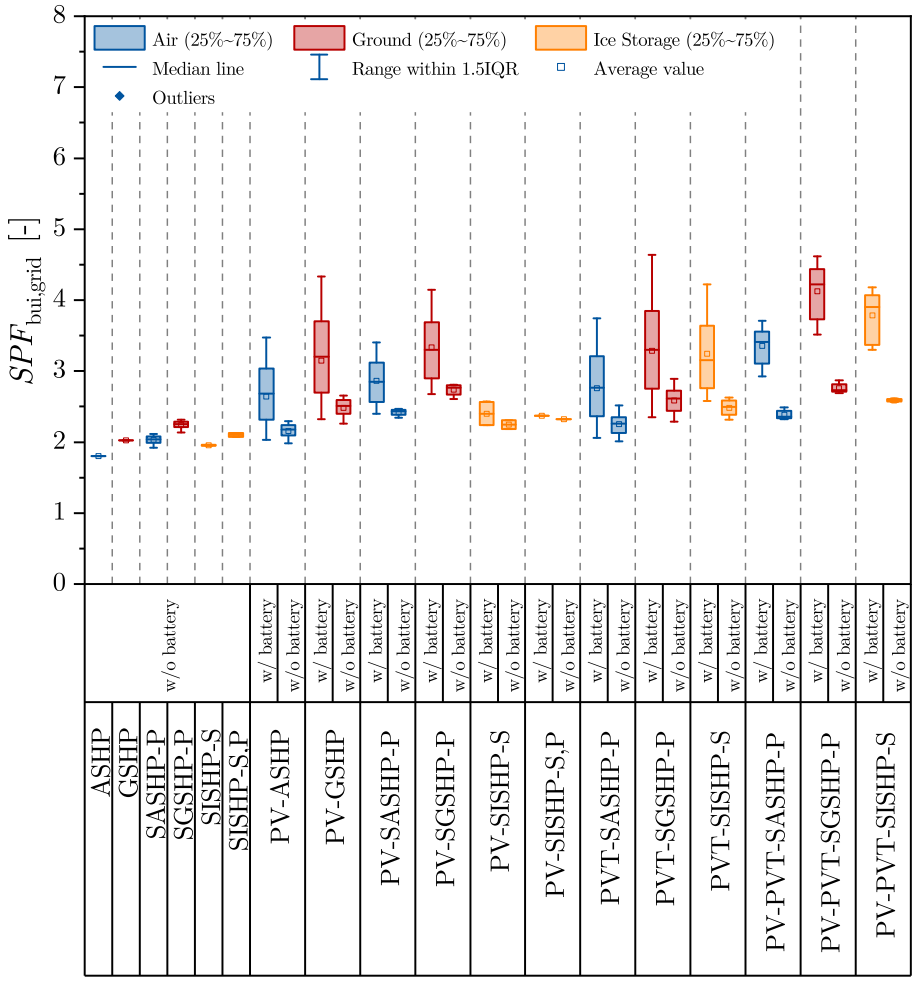

Figure 4.8: Grid-related SPF of the building for different heat pump and SHP system concepts with and without battery storage in Strasbourg for SFH45.

for a battery storage size of 5 kWh and between 2 % and 63 % for a battery storage size of 15 kWh depending on the heat pump technology and the PV module area. For systems with PVT, the relative increase of the SPF in comparison to the corresponding PVT and heat pump system without battery storage varies between 2 % and 33 % for a battery storage size of 5 kWh and between 2 % and 63 % for a battery storage size of 15 kWh depending on the heat pump technology, the PVT collector technology and the PVT collector area. As previously observed for the heating efficiency, the improvement of the SPF by adding a battery storage increases with increasing PV module or PVT collector area due to the higher amounts of generated solar electrical energy that can be stored in the battery storage. Moreover, it can also be observed that the improvement of the SPF by adding a battery storage is higher for systems with GSHP. As explained before, the reason for this is the generally lower electricity consumption of the GSHP system in comparison to the ASHP system and thus higher relative increases of the SPF for covering similar amounts of electricity for the supply of the building by solar energy. In addition, systems with GSHP achieve higher values of SPF and SSR than systems with ASHP for the combination with the same solar technology which can also be explained by the better performance of the GSHP system in comparison to the ASHP system in general for SFH45 in Strasbourg. However, in contrast to the results for the heating efficiency, ASHP systems with PV or PVT can compete

with GSHP systems with the same solar technology depending on the used PV module or PVT collector area and battery storage capacity. Furthermore, in most cases, PV-ASHP, PV-SASHP-P, PVT-SASHP-P as well as PV-PVT-SASHP-P systems can reach the same or higher values of SPF than GSHP systems without integration of solar technologies or SGSHP-P systems, especially for system concepts with battery storage.

Regarding system concepts with ice storage, SISHP-S systems achieve SPF values of the building in the range of 1.95 to 1.96 and thus higher values than ASHP systems without integration of solar technologies. If a parallel solar thermal circuit with FPC is added to SISHP-S systems, the SPF can only be increased between 6 % and 9 %. As a result, SISHP-S,P systems achieve SPF values of 2.07 to 2.13 which are slightly higher than those of GSHP systems without integration of solar technologies. In case of PV-SISHP-S systems, the benefit of adding PV modules with regard to the energy efficiency is higher than the improvement by adding the same FPC area. At this, the SPF can be improved by 12 % to 19 % for systems without battery storage and by 14 % to 32 % for systems with battery storage in comparison to the corresponding SISHP-S system (cf. Figure 4.8). As mentioned before, it should be noted that the additional PV module or FPC area is limited to 10 m^2 due to the limited available roof area and the minimum required WISC collector area for the supply of the ice storage. With regard to the energy efficiency, PVT-SISHP-S systems reach the highest SPFs of all system concepts with ice storage. At this, the relative increase by replacing WISC collectors with PVT collectors with the same collector area achieves values up to 34 % for systems without battery storage and up to 115 % for systems with battery storage (cf. Figure 4.8). As figured out for the heating efficiency, the increase of the SPF can be influenced, at least in part, by the larger ice storage volume in case of systems with PVT. Nevertheless, the main reason for the increase of the energy efficiency is the additional solar electrical yield that can be used for the supply of the building in comparison to systems with serial WISC collectors as figured out in the last paragraph for the parallel integration of PVT collectors. Especially for SISHP concepts, in which the PVT collectors replace the required WISC collectors, the results illustrate the benefit of combined generation of heat and electricity by PVT collectors for limited roof areas as the SISHP-S concept requires a minimum WISC collector area of 15 m^2 and thus the additional PV or FPC area is limited to 10 m^2. This disadvantage can be compensated by the use of PVT collectors and thus a replacement of the WISC collectors using the entire roof area for the generation of both heat and electricity. Due to the lower operating temperatures, the specific solar electrical yields of PVT collectors in SISHP systems are slightly higher than those of system concepts with parallel PVT integration, but, as observed before, the solar specific electrical yields cannot be significantly increased in comparison to PV modules (cf. Figure 4.7). Nevertheless, to sum up, these results illustrate that especially PVT-SISHP-S systems reaching high SPFs between 2.32 and 4.22 can compete with SHP systems with ASHP or GSHP with regard to the energy efficiency.

4.2.2 Influence of Building Type

Overviews of the range of grid-related SPFs of the overall system with penalties for the different heat pump and SHP system concepts in Strasbourg for SFH15 and SFH100 are shown in Figure 4.9 and Figure 4.10. Regarding the results for SFH15 (cf. Figure 4.9), the SPF for systems with ASHP is in the range of 2.51 (ASHP) and 4.87 (SASHP-P, PV-SASHP-P), for systems with GSHP in the range of 3.21 (GSHP) and 6.44 (PV-SGSHP-P) and for SISHP systems in the range of 2.94 (SISHP-S) and 5.45 (PV-SISHP-S,P). Basically, the results

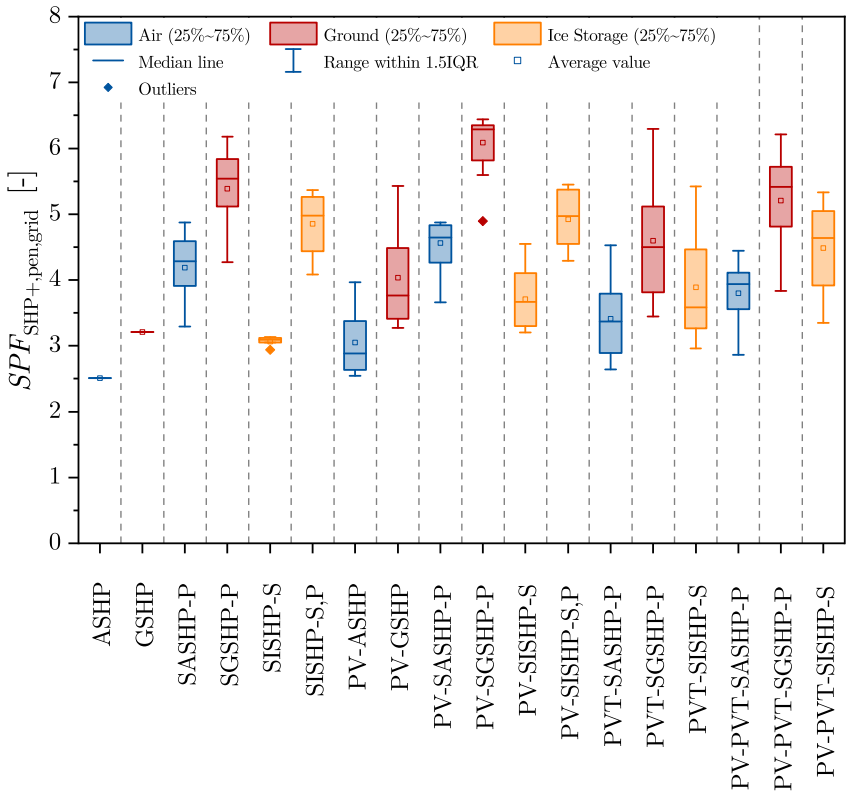

Figure 4.9: Grid-related SPF of the overall system with penalties for different heat pump and SHP system concepts in Strasbourg for SFH15.

show that the minimum values of SPF for new buildings with very high energetic quality and a high fraction of energy demand for domestic hot water preparation (46 %) are lower in comparison to the SFH45 building. The lower values of SPF show the impact of energy demands at high temperature level for domestic hot water preparation and as a result a lower performance of the heat pump. Additionally, the energy demand for space heating occurs predominantly in winter season with lower ambient/source temperatures, especially in case of systems with ASHP, and the heat pump runs with a lower performance. Furthermore, the main findings for the SFH45 building in Strasbourg can be confirmed for SFH15 with regard to the heating efficiency. Nevertheless, there are some differences that will be discussed in the following. Comparing different concepts, the results are more diverse. In contrast to the SFH45 building, PV plus parallel solar thermal and heat pump systems achieve the same or slightly higher SPFs than systems with parallel solar thermal (FPC, PVT) circuit with regard to system concepts with ASHP and GSHP and even slightly higher SPFs than systems with serial PVT collectors with regard to system concepts with ice storage. At this, it has to be noted that the improvement in comparison to the corresponding system with parallel solar thermal (FPC, PVT) circuit or serial PVT collectors with the maximum SPF is not higher than 4 % and 1 %, respectively, and the minimum required WISC collector area in case of SISHP-S systems for SFH15 in Strasbourg is only 5 m^2. In addition, general improvements by combining PV with system concepts with PVT collectors cannot be observed with regard to the heating efficiency in comparison to the corresponding PVT and heat pump systems. Regarding systems with ice storage, in contrast to SFH45, the ice storage volume is the same for systems with WISC and PVT collectors. In this case, general improvements of the maximum degrees of icing by the use of PVT collectors in comparison

to WISC collectors cannot be observed, even if in some cases for SFH15 the maximum degrees of icing can be reduced by the use of PVT collectors. Furthermore, in case of systems with GSHP, PVT-SGSHP-P systems reach higher SPFs than SGSHP-P systems. Moreover, as observed for SFH45, the SPFs of PV and heat pump systems are lower on average than those of systems with solar thermal integration (FPC, PVT) and PV and heat pump systems can only compete with these concepts if a battery storage is used. In contrast to SFH45, PV-ASHP systems can reach the performance of GSHP systems with regard to the heating efficiency and all SHP concepts with ASHP can achieve the same or even higher values of SPF than GSHP systems without integration of solar technologies. This suggests that the benefit of GSHPs is lower for buildings with low energy demand.

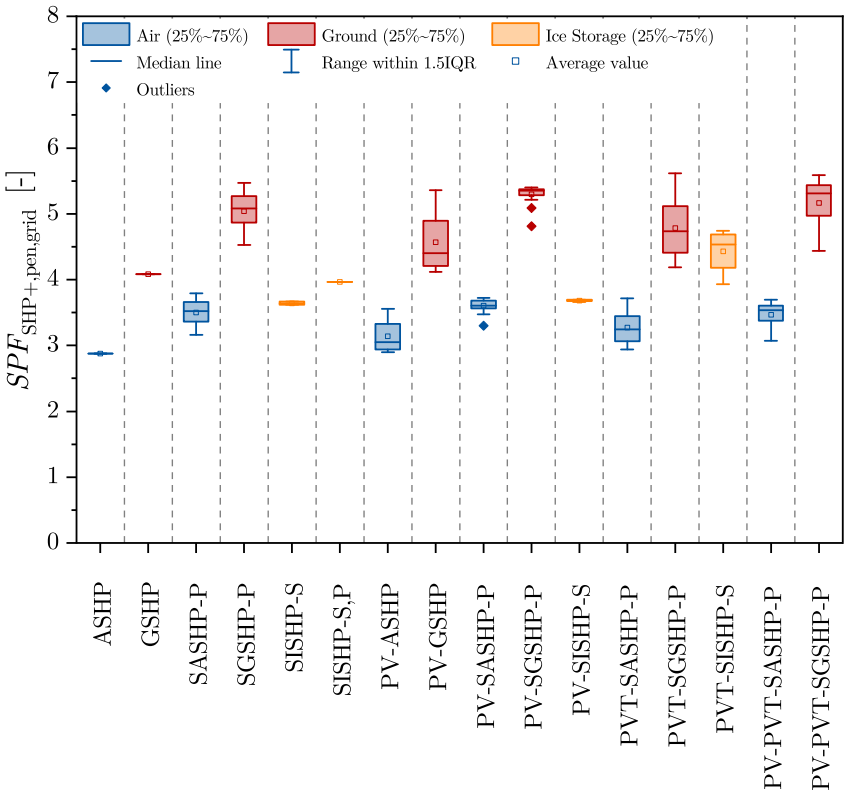

Figure 4.10: Grid-related SPF of the overall system with penalties for different heat pump and SHP system concepts in Strasbourg for SFH100.

Regarding the range of grid-related SPFs of the overall system with penalties for SFH100 (cf. Figure 4.10), the SPF for systems with ASHP is in the range of 2.88 (ASHP) and 3.79 (SASHP-P), for systems with GSHP in the range of 4.09 (GSHP) and 5.62 (PVT-SGSHP-P) and for SISHP systems in the range of 3.62 (SISHP-S) and 4.74 (PVT-SISHP-S). Basically, the results show that the minimum SPFs in case of non-renovated existing buildings are the same or lower in comparison to the SFH45 building. The lower values of SPF show in particular the impact of energy demands for space heating at a higher temperature level as the supply temperatures of 55 °C for SFH100 are higher than those for SFH15 and SFH45. This leads to a lower performance of the heat pump due to the higher temperature differences between heat source and heat sink. Furthermore, the main findings for the SFH45 building in Strasbourg can be confirmed for SFH100 with regard to the heating efficiency. As figured out for SFH15, there are also some differences for SFH100 that will be discussed in the following. Comparing different concepts, the results vary slightly in comparison to SFH15

and SFH45. As observed for SFH45, systems with parallel solar thermal (FPC, PVT) circuit achieve the highest SPFs in terms of heating efficiency with regard to system concepts with ASHP and GSHP. At this, systems with FPCs reach slightly higher SPF values than systems with PVT collectors for systems with ASHP, whereas, in contrast to SFH45, systems with PVT achieve slightly higher SPF values for systems with GSHP. Furthermore, systems with PVT collectors reach the highest SPFs for system concepts with ice storage. At this, it has to be noted that the minimum required WISC collector area in case of SISHP-S systems for SFH100 in Strasbourg is $20\,m^2$ and the improvement by the use of PVT collectors in comparison to the corresponding system with WISC collectors is up to 29 %, although improvements of the maximum degrees of icing for systems with PVT and larger ice storage volume in comparison to systems with WISC collectors cannot be observed. This is also reflected in a larger minimum required PVT collector area in comparison to the minimum required WISC collector area. As observed for SFH15 and SFH45, the SPFs of PV and heat pump systems are lower on average than those of systems with solar thermal integration (FPC, PVT) and PV and heat pump systems can only compete with these concepts if a battery storage is used. Due to the high minimum required WISC collector area for SISHP-S systems, the benefit of adding PV modules to the SISHP-S system concept is only up to 2 % and, thus, PV-SISHP-S systems can especially not compete with PVT-SISHP-S systems. Furthermore, general improvements by combining PV with system concepts with parallel FPC or PVT collectors cannot be observed with regard to the heating efficiency in comparison to the corresponding solar thermal or PVT and heat pump systems. In contrast to SFH15 and SFH45, SHP concepts with ASHP cannot reach the performance of GSHP systems without integration of solar technologies regarding the heating efficiency for SFH100. This confirms that the benefit of GSHPs is lower for buildings with low energy demand or, in other words, the benefit of GSHPs is higher for buildings with high heating energy demand. The reasons for the lower SPFs of systems with ASHP than those of systems with GSHP are especially high amounts of energy demand for space heating in the cold season with low ambient temperatures and minimal solar irradiation. In these periods with low electrical or thermal solar energy yields, the low ambient temperatures lead to low performance of the ASHP itself, which cannot be compensated by large PV module or FPC/PVT collector areas in case of SFH100.

Overviews of the range of grid-related SPFs of the building for the different heat pump and SHP system concepts in Strasbourg for SFH15 and SFH100 are shown in Figure 4.11 and Figure 4.12. Regarding the results for SFH15 (cf. Figure 4.11), the SPF for systems with ASHP is in the range of 1.45 (ASHP) and 3.61 (PVT-SASHP-P), for systems with GSHP in the range of 1.55 (GSHP) and 4.13 (PVT-SGSHP-P) and for SISHP systems in the range of 1.52 (SISHP-S) and 3.81 (PVT-SISHP-S). As observed for the heating efficiency, the results show that the minimum SPFs in case of new buildings with very high energetic quality are lower in comparison to the SFH45 building. The lower minimum values suggest that the impact of energy demands at high temperature level for domestic hot water preparation and thus a lower performance of the heat pump on the SPF for the heating efficiency is the same for the energy efficiency. However, in addition to the identified effects of higher fractions of energy demand for domestic hot water preparation at high temperature level on the heating efficiency, the lower fraction of heating energy demand on the net energy demand of the building in comparison to SFH45 influences the results with regard to the energy efficiency. Furthermore, the main findings for the SFH45 building in Strasbourg can be confirmed for SFH15 with regard to the energy efficiency. At this, there are only some minor differences with regard to systems with ice storage. Comparing different concepts,

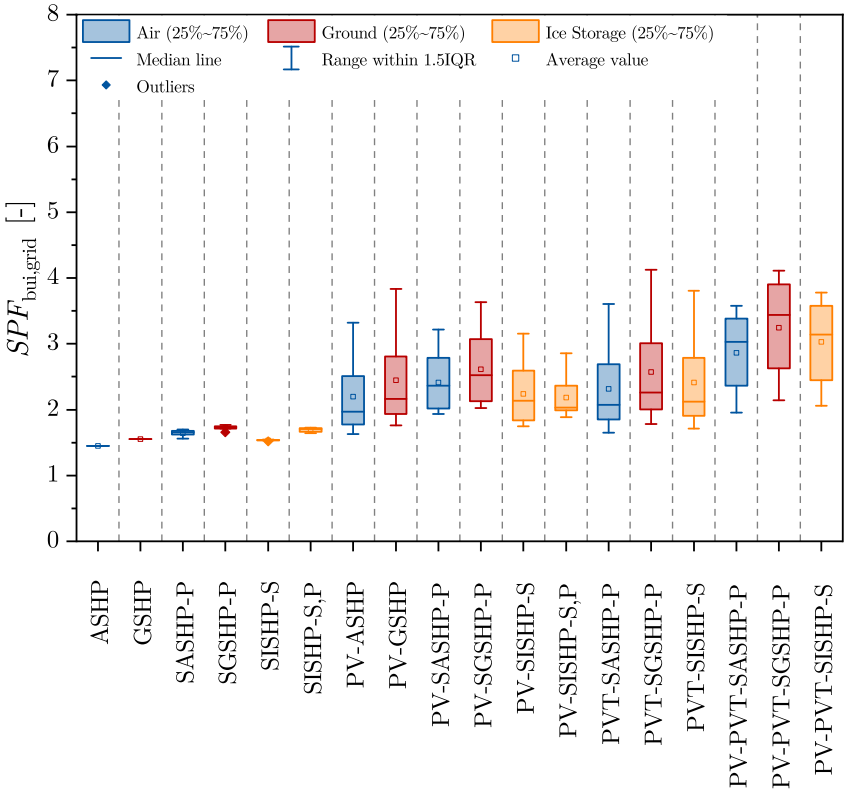

Figure 4.11: Grid-related SPF of the building for different heat pump and SHP system concepts in Strasbourg for SFH15.

the simulation results confirm that the energy efficiency can only significantly be increased by adding PV modules or PVT collectors, especially in combination with a battery storage. The SSRs of the building reach values up to 60 % for systems with PV as well as PVT. At this, systems without battery storage achieve values between 11 % and 26 % for systems with PV and between 11 % and 28 % for systems with PVT. In contrast to SFH45, the SPF can also significantly be increased by adding PV modules to system concepts with ice storage due to the lower minimum required WISC collector area of 5 m^2 and, thus, the larger available roof area for PV modules. Nevertheless, system concepts with PVT collectors reach the best results for systems with ice storage.

Regarding the range of grid-related SPFs of the building for SFH100 (cf. Figure 4.12), the SPF for systems with ASHP is in the range of 2.05 (ASHP) and 3.38 (PVT-SASHP-P), for systems with GSHP in the range of 2.46 (GSHP) and 4.52 (PVT-SGSHP-P) and for SISHP systems in the range of 2.32 (SISHP-S) and 3.95 (PVT-SISHP-S). In contrast to the heating efficiency, the results show that the minimum SPFs in case of non-renovated existing buildings are higher in comparison to the SFH45 building. This disproves the conclusion previously assumed for SFH15 that the impact of a lower performance of the heat pump on the heating efficiency is the same for the energy efficiency comparing different building types. In particular, the higher minimum values of SPF show how higher fractions of heating energy demand on the net energy demand of the building influence the results with regard to the energy efficiency and can counteract the identified effects on the heating efficiency for the energy efficiency. Thus, a lower performance of the heat pump does not generally lead to lower SPFs for the energy efficiency comparing different buildings. Furthermore, the main findings for the SFH45 building in Strasbourg can be confirmed for SFH100 with

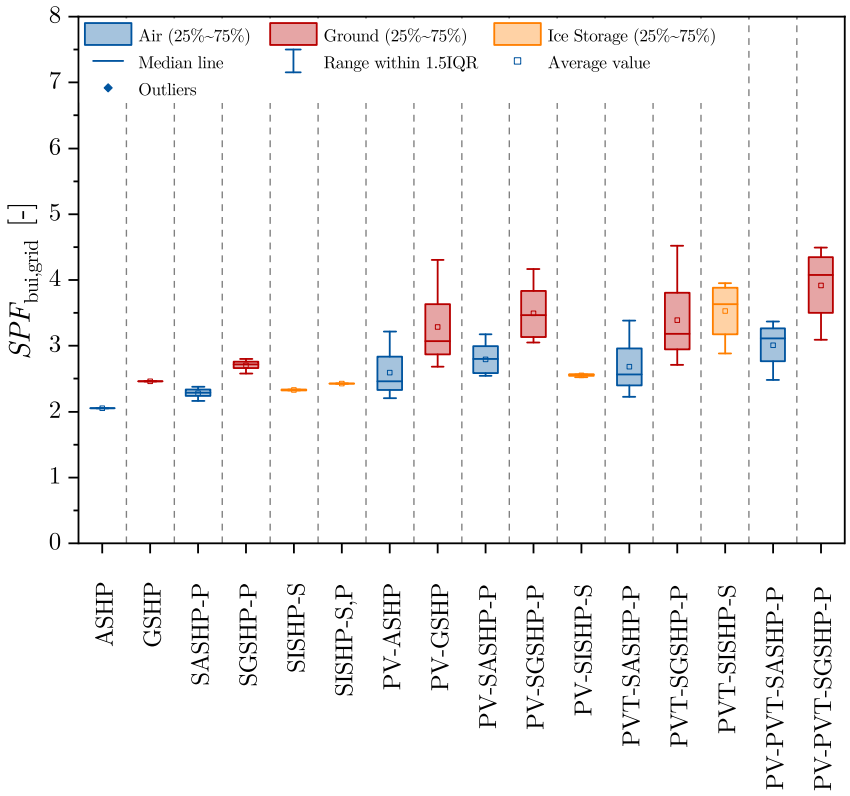

Figure 4.12: Grid-related SPF of the building for different heat pump and SHP system concepts in Strasbourg for SFH100.

regard to the energy efficiency. Comparing different concepts, the simulation results confirm that the energy efficiency can only significantly be increased by adding PV modules (only for systems with ASHP and GSHP in case of SFH100) or PVT collectors (for all system concepts), especially in combination with a battery storage. The SSRs of the building reach values up to 43 % for systems with PV as well as PVT. At this, systems without battery storage achieve values between 7 % and 20 % for systems with PV as well as PVT.

Comparing system concepts with ASHP and GSHP with regard to the energy efficiency for the SFH15 and SFH100 building, in most cases and in contrast to the heating efficiency for SFH100, PV-ASHP, PV-SASHP-P, PVT-SASHP-P and PV-PVT-SASHP-P systems can reach the same or higher values of SPF than GSHP systems without integration of solar technologies or SGSHP-P systems, especially for system concepts with battery storage. As observed for SFH45, ASHP systems with PV or PVT can even compete with GSHP systems with the same solar technology depending on the used PV module or PVT collector area and battery storage capacity. At this, the differences in energy efficiency between systems with GSHP and ASHP are significantly higher for SFH100 in comparison to SFH15. This also reflects the higher benefit of GSHPs for buildings with high heating energy demand as figured out for the heating efficiency. In addition, as observed for SFH45, solar thermal and heat pump concepts achieve the lowest maximum SPF values beside systems without solar technology integration, whereas systems with PVT collectors reach the highest SPFs for SFH15 and SFH100. Regarding systems with ice storage, especially PVT-SISHP-S systems reaching high SPFs between 1.71 and 3.81 for SFH15 and between 2.89 and 3.95 for SFH100 can compete with SHP systems with ASHP or GSHP with regard to the energy efficiency. As observed for SFH45, the SPF of system concepts with parallel FPCs can be

increased by the combination with PV, whereas general improvements by combining PV with system concepts with PVT collectors cannot be observed with regard to the energy efficiency in comparison to the corresponding PVT and heat pump systems. Depending on the battery storage size (especially for low battery storage sizes or systems without battery storage), some combinations of parallel FPCs and PV modules achieve even slightly higher SPFs than the corresponding systems with PV. Nevertheless, the maximum SPFs of PV-SASHP-P, PV-SGSHP-P and PV-SISHP-S,P systems are also slightly lower than those of the corresponding systems with PV modules instead of parallel FPCs.

4.2.3 Influence of Climate

4.2.3.1 Warm Climates

Regarding warm climates, overviews of the range of grid-related SPFs of the overall system with penalties for the different heat pump and SHP system concepts in Athens for SFH45 and SFH100 are shown in Figure 4.13 and Figure 4.14. With regard to the results for SFH45 (cf. Figure 4.13), the SPF for systems with ASHP is in the range of 2.16 (ASHP) and 11.26 (PV-SASHP-P) and for systems with GSHP in the range of 2.59 (GSHP) and 13.83 (PVT-SGSHP-P). Basically, the results show that the minimum values of SPF for SFH45 in Athens with a very high fraction of energy demand for domestic hot water preparation (66 %) are lower in comparison to the SFH45 building in Strasbourg, whereas the maximum values of SPF are significantly higher. The lower minimum values of SPF illustrate the impact of energy demands at high temperature level for domestic hot water

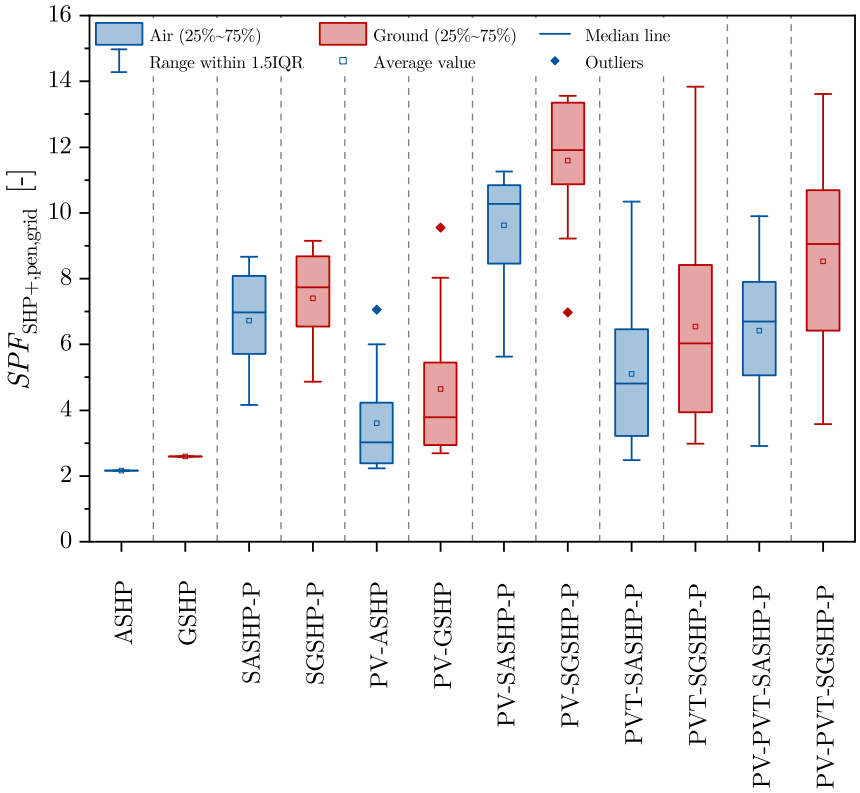

Figure 4.13: Grid-related SPF of the overall system with penalties for different heat pump and SHP system concepts in Athens for SFH45.

preparation and as a result a lower performance of the heat pump. In addition, the higher maximum values of SPF show the impact of higher total yearly irradiation and higher annual average ambient temperature, and as a result higher specific solar electrical yields and lower heating energy demands reaching higher SSRs and solar thermal fractions. Furthermore, the main findings for the SFH45 building in Strasbourg can be confirmed for SFH45 in Athens with regard to the heating efficiency. Nevertheless, there are some differences that will be discussed in the following. Comparing different concepts, the results are more diverse. In contrast to the SFH45 building in Strasbourg, PV plus parallel solar thermal and heat pump systems achieve higher SPFs than systems with parallel FPC collectors with regard to system concepts with ASHP and GSHP. In addition, general improvements by combining PV with system concepts with PVT collectors cannot be observed with regard to the heating efficiency in comparison to the corresponding PVT and heat pump systems. Furthermore, in case of systems with GSHP, PVT-SGSHP-P systems reach higher SPFs than PV-SGSHP-P and especially SGSHP-P systems. Depending on the battery storage size, PV-GSHP systems can even achieve higher maximum values of SPF than SGSHP-P systems. In case of systems with ASHP, as observed for SFH45 in Strasbourg, the SPFs of PV-ASHP systems are lower on average than those of systems with solar thermal integration (FPC, PVT), whereas PVT-SASHP-P systems reach higher SPFs than concepts with FPC. Furthermore, PV-SASHP-P systems achieve higher maximum SPFs than PVT-SASHP-P systems. As observed before, PV and heat pump systems can only compete with concepts with solar thermal integration (FPC, PVT) if a battery storage is used. In contrast to SFH45 in Strasbourg, all SHP concepts with ASHP can achieve the same or even higher values of SPF than GSHP systems without integration of solar technologies. This points out that the benefit of GSHPs is lower for buildings in warm climates.

Regarding the range of grid-related SPFs of the overall system with penalties for SFH100 in Athens (cf. Figure 4.14), the SPF for systems with ASHP is in the range of 2.51 (ASHP) and 7.03 (PV-SASHP-P) and for systems with GSHP in the range of 2.95 (GSHP) and 8.39 (PV-SGSHP-P). Basically, the results show that the minimum values of SPF for SFH100 in Athens with relatively high fraction of energy demand for domestic hot water preparation (35 %) are lower in comparison to the SFH100 building in Strasbourg, but higher in comparison to the SFH45 building in Athens. Furthermore, the maximum values of SPF are significantly higher in comparison to the SFH100 building in Strasbourg. The lower minimum values of SPF in comparison to the SFH100 building in Strasbourg and higher minimum values in comparison to the SFH45 building in Athens confirm the impact of energy demands at high temperature level for domestic hot water preparation on the SPF. In contrast to SFH100 in moderate climates, for warm climates with lower energy demands for space heating the increase of the SPF by lower fractions of domestic hot water preparation predominates the decreasing effects on the SPF by higher supply temperatures for space heating. In addition, the higher maximum values of SPF in comparison to the SFH100 building in Strasbourg confirm the impact of higher total yearly irradiation and higher annual average ambient temperature on the SPF. Furthermore, the findings for the SFH45 building in Athens can be confirmed for SFH100 in Athens with regard to the heating efficiency. Nevertheless, there are some differences that will be discussed in the following. Comparing different concepts, the results vary slightly in comparison to SFH45 in Athens. In contrast to SFH45, PV plus parallel solar thermal and heat pump systems achieve higher SPFs than all systems with parallel solar thermal (FPC, PVT) circuit, even with PVT collectors, with regard to system concepts with ASHP and GSHP. In addition, as observed before, general improvements by combining PV with system concepts with PVT

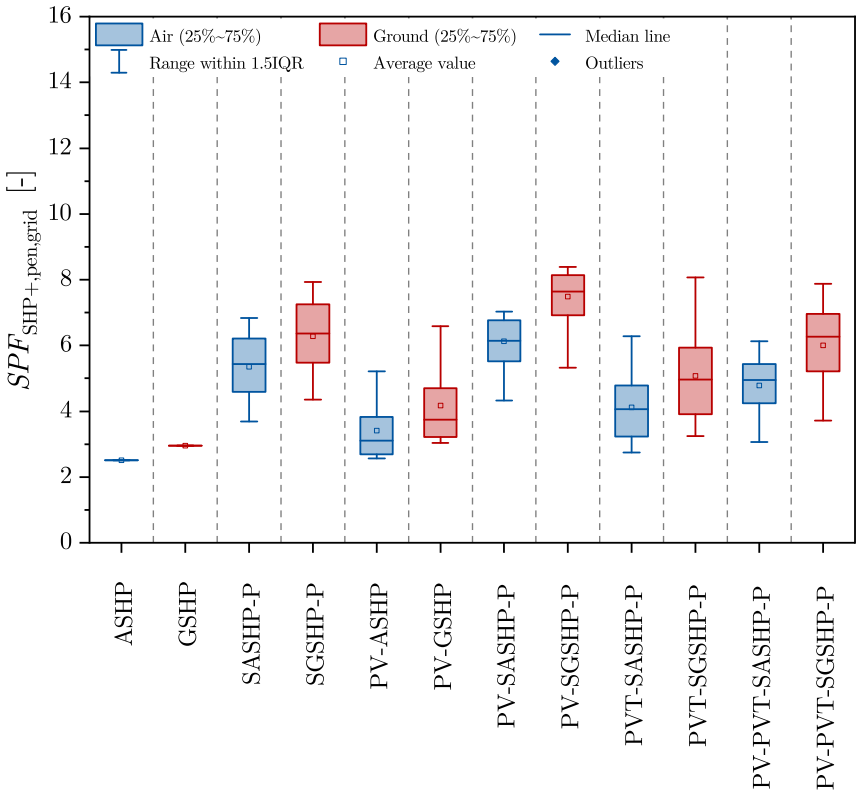

Figure 4.14: Grid-related SPF of the overall system with penalties for different heat pump and SHP system concepts in Athens for SFH100.

collectors cannot be observed. Furthermore, in case of systems with GSHP, PVT-SGSHP-P systems reach higher SPFs than SGSHP-P systems, whereas, in contrast to SFH45 in Athens, SASHP-P reach higher SPFs than PVT-SASHP-P systems. As observed for buildings in Strasbourg, the SPFs of PV and heat pump systems are lower on average than those of systems with solar thermal integration (FPC, PVT) and PV and heat pump systems can only compete with these concepts if a battery storage is used. In contrast to SFH100 in Strasbourg, all SHP concepts with ASHP can achieve the same or even higher values of SPF than GSHP systems without integration of solar technologies. This confirms that the benefit of GSHPs is lower for buildings in warm climates.

Overviews of the range of grid-related SPFs of the building for the different heat pump and SHP system concepts in Athens for SFH45 and SFH100 are shown in Figure 4.15 and Figure 4.16. Regarding the results for SFH45 (cf. Figure 4.15), the SPF for systems with ASHP is in the range of 1.26 (ASHP) and 8.62 (PVT-SASHP-P) and for systems with GSHP in the range of 1.31 (GSHP) and 9.61 (PVT-SGSHP-P). As observed for the heating efficiency, the results basically show that the maximum values of SPF for SFH45 in Athens are significantly higher in comparison to the SFH45 building in Strasbourg. The higher maximum values of SPF suggest that the impact of higher total yearly irradiation and higher annual average ambient temperature on the SPF for the heating efficiency is the same for the energy efficiency. In addition, the lower fraction of heating energy demand on the net energy demand of the building in comparison to the SFH45 building in Strasbourg influences the results with regard to the energy efficiency. Comparing different concepts, the simulation results confirm that the energy efficiency can only significantly be increased by adding PV modules or PVT collectors, especially in combination with a battery storage.

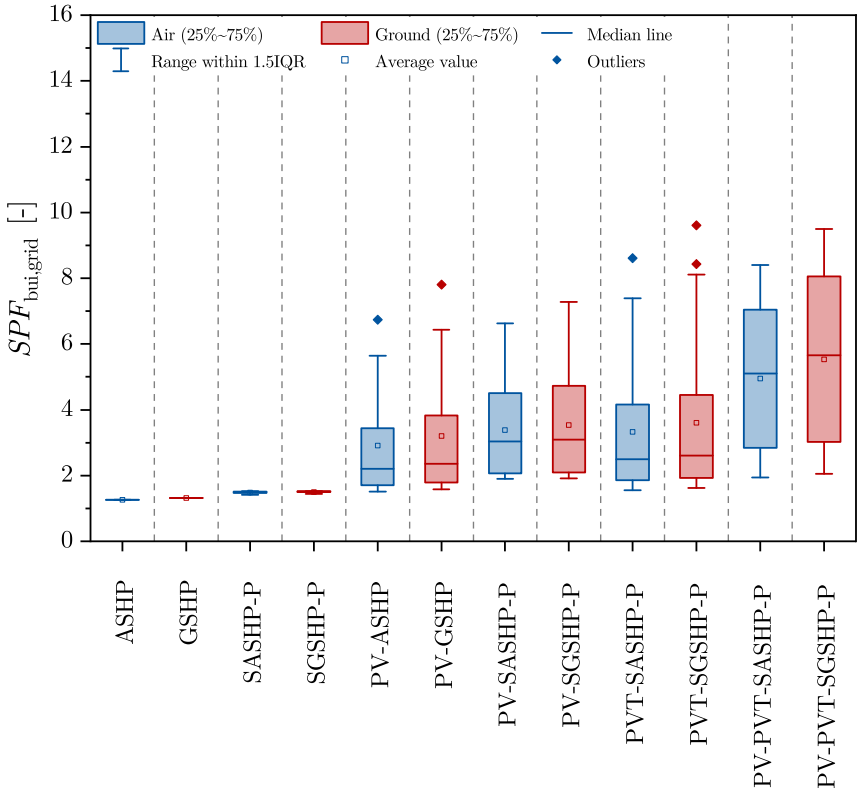

Figure 4.15: Grid-related SPF of the building for different heat pump and SHP system concepts in Athens for SFH45.

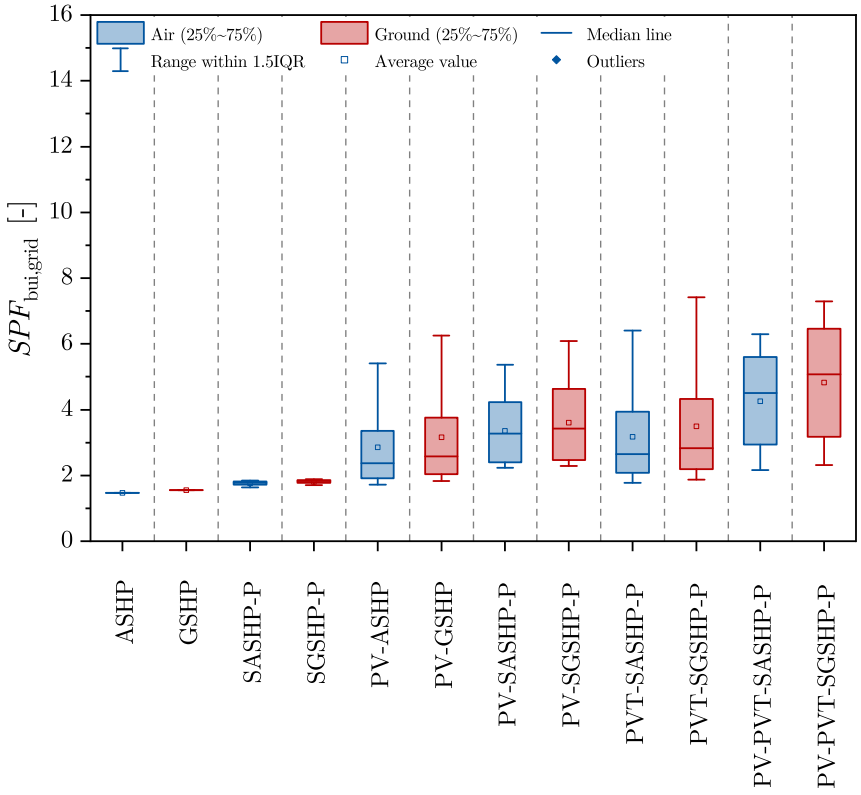

Figure 4.16: Grid-related SPF of the building for different heat pump and SHP system concepts in Athens for SFH100.

The SSRs of the building reach values up to 83 % for systems with PV and up to 85 % for systems with PVT. At this, systems without battery storage achieve values between 16 % and 34 % for systems with PV and between 17 % and 37 % for systems with PVT.

Regarding the grid-related SPFs of the building for SFH100 in Athens (cf. Figure 4.16), the SPF for systems with ASHP is in the range of 1.47 (ASHP) and 6.41 (PVT-SASHP-P) and for systems with GSHP in the range of 1.55 (GSHP) and 7.41 (PVT-SGSHP-P). As observed for SFH15, the maximum values of SPF are significantly higher in comparison to the SFH100 building in Strasbourg. The higher maximum values of SPF confirm the impact of higher total yearly irradiation and higher annual average ambient temperature on the SPF, even for the energy efficiency. As mentioned before for the SFH45 building in Athens, the lower fraction of heating energy demand on the net energy demand of the building in comparison to the SFH100 building in Strasbourg influences the results with regard to the energy efficiency. Comparing different concepts, the simulation results also confirm that the energy efficiency can only significantly be increased by adding PV modules or PVT collectors, especially in combination with a battery storage. The SSRs of the building reach values up to 75 % for systems with PV and up to 77 % for systems with PVT. At this, systems without battery storage achieve values between 15 % and 32 % for systems with PV and between 15 % and 34 % for systems with PVT.

In general, the main findings for Strasbourg can be confirmed for SFH45 and SFH100 in Athens with regard to the energy efficiency. Comparing system concepts with ASHP and GSHP with regard to the energy efficiency for the SFH45 and SFH100 building in Athens, all SHP concepts with ASHP can reach the same or higher values of SPF than GSHP systems without integration of solar technologies or SGSHP-P systems, especially for system concepts with battery storage. As observed for Strasbourg, ASHP systems with PV or PVT can compete with GSHP systems with the same solar technology depending on the used PV module or PVT collector area and battery storage capacity. In addition, solar thermal and heat pump concepts achieve also the lowest maximum SPF values beside systems without solar technology integration, whereas systems with PVT collectors reach the highest SPFs for SFH45 and SFH100 in Athens. At this, the improvement by the use of PVT collectors instead of PV raises slightly in comparison to Strasbourg. As observed for Strasbourg, the SPF of system concepts with parallel FPCs can be increased by the combination with PV, whereas general improvements by combining PV with system concepts with PVT collectors cannot be observed with regard to the energy efficiency in comparison to the corresponding PVT and heat pump systems. Depending on the battery storage size (especially for low battery storage sizes or systems without battery storage), some combinations of parallel FPCs and PV modules achieve even slightly higher SPFs than the corresponding systems with PV. Nevertheless, the maximum SPFs of PV-SASHP-P and PV-SGSHP-P systems are also slightly lower than those of the corresponding systems with PV modules instead of parallel FPCs.

4.2.3.2 Cold Climates

Regarding cold climates, overviews of the range of grid-related SPFs of the overall system with penalties for the different heat pump and SHP system concepts in Helsinki for SFH15, SFH45 and SFH100 are shown in Figure 4.17, Figure 4.18 and Figure 4.19. With regard to the results for SFH15 (cf. Figure 4.17), the SPF for systems with ASHP is in the range of 2.54 (ASHP) and 3.45 (SASHP-P), for systems with GSHP in the range of 3.94 (GSHP) and 5.74 (PVT-SGSHP-P) and for SISHP systems in the range of 3.62 (SISHP-S) and 5.16

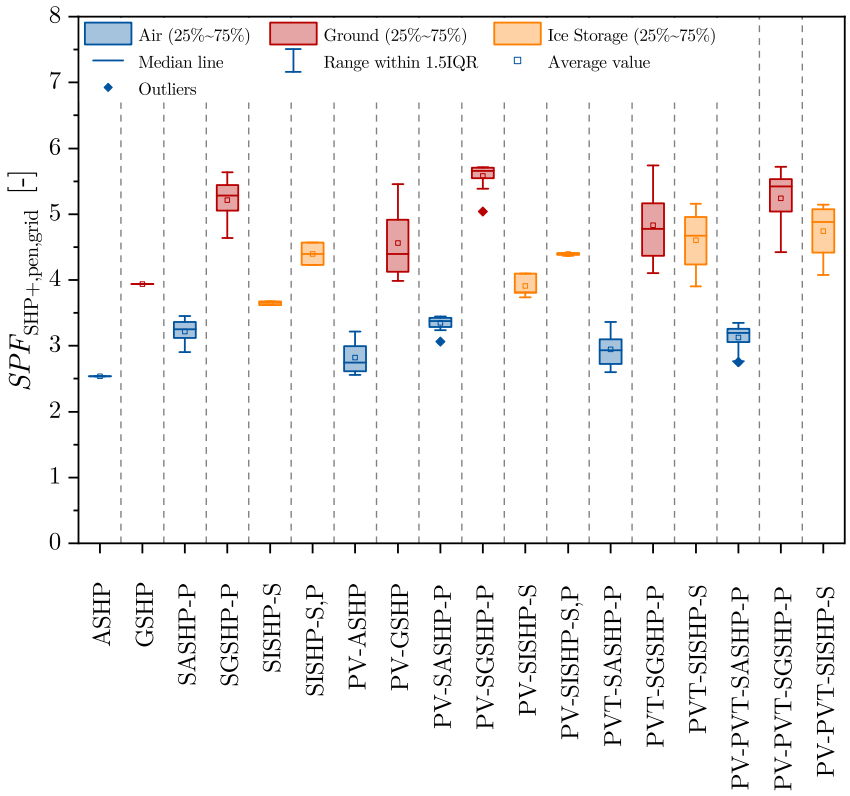

Figure 4.17: Grid-related SPF of the overall system with penalties for different heat pump and SHP system concepts in Helsinki for SFH15.

(PVT-SISHP-S). Basically, the results show that the minimum values of SPF for SFH15 in Helsinki with a lower fraction of energy demand for domestic hot water preparation (29 %) in comparison to the SFH15 building in Strasbourg are nearly the same (for systems with ASHP) or higher (for systems with GSHP or SISHP) in comparison to the SFH15 building in Strasbourg, whereas the maximum values of SPF are lower for all system concepts, especially for system concepts with ASHP. On the one hand, the higher minimum value of SPF for systems with GSHP illustrates the impact of energy demands at high temperature level for domestic hot water preparation and as a result a better performance of the heat pump for lower fractions of energy demand for domestic hot water preparation. On the other hand, in case of systems with ASHP, the lower performance of the heat pump due to lower ambient temperatures and the use of an electric heating element when the ambient air temperature falls below −20 °C counteract this effect and thus the minimum value of SPF for ASHP systems is nearly the same for SFH15 in Helsinki and Strasbourg. In addition, the lower maximum values of SPF show especially the impact of lower annual average ambient temperatures and slightly lower total yearly irradiation, and as a result lower specific solar electrical yields and higher heating energy demands reaching lower SSRs and solar thermal fractions. Furthermore, the main findings for the SFH15 building in Strasbourg can be confirmed for SFH15 in Helsinki with regard to the heating efficiency. Nevertheless, there are some differences that will be discussed in the following. Comparing different concepts, the results vary in comparison to SFH15 in Strasbourg. In contrast to the SFH15 building in Strasbourg, general improvements by combining PV with system concepts with parallel FPC collectors cannot be observed. At this, only some combinations of PV-SGSHP-P systems achieve slightly higher (around 1 %) SPFs than the corresponding systems with

FPC, whereas PVT-SGSHP-P systems reach higher SPFs than PV-SGSHP-P and SGSHP-P systems. Furthermore, even if PV-SASHP-P systems achieve slightly higher maximum SPFs than PVT-SASHP-P systems, SASHP-P systems reach the highest SPFs. As observed for SFH15 in Strasbourg, general improvements by combining PV with system concepts with PVT collectors cannot be observed with regard to the heating efficiency in comparison to the corresponding PVT and heat pump systems. With regard to system concepts with ice storage, PVT-SISHP-S reach the highest SPFs. At this, it has to be noted that the minimum required WISC collector area in case of SISHP-S systems for SFH15 in Helsinki is 15 m^2 and the improvement by the use of PVT collectors in comparison to the corresponding system with WISC collectors is up to 40 %. Furthermore, in some cases the maximum degrees of icing can be reduced by the use of PVT collectors, but general improvements of the maximum degrees of icing by the use of PVT collectors in comparison to the use of WISC collectors for the same ice storage volume in case of SFH15 in Helsinki cannot be observed. Even if the benefit of adding PV modules to the SISHP-S system concept is up to 13 %, PV-SISHP-S systems can especially not compete with PVT-SISHP-S systems and the benefit of adding PV modules is lower than the improvement by adding the same FPC area. As observed for SFH15 in Strasbourg, the SPFs of PV and heat pump systems are lower on average than those of systems with solar thermal integration (FPC, PVT) and PV and heat pump systems can only compete with these concepts if a battery storage is used. In contrast to SFH15 in Strasbourg, SHP system concepts with ASHP cannot reach the performance of GSHP systems without integration of solar technologies. This illustrates that the benefit of GSHPs is higher for buildings in cold climates with high heating energy demand and low annual average ambient temperature. Furthermore, SHP system concepts with ASHP cannot achieve the performance of systems with ice storage.

Regarding the results for SFH45 (cf. Figure 4.18), the SPF for systems with ASHP is in the range of 2.76 (ASHP) and 3.42 (SASHP-P) and for systems with GSHP in the range of 4.71 (GSHP) and 6.19 (PVT-SGSHP-P, PV-PVT-SGSHP-P). Basically, the results show that the minimum values of SPF for SFH45 in Helsinki with a low fraction of energy demand for domestic hot water preparation (15 %) are higher in comparison to the SFH15 building in Helsinki. As observed before, the higher minimum values of SPF illustrate the impact of energy demands at high temperature level for domestic hot water preparation and as a result a better performance of the heat pump for lower fractions of energy demand for domestic hot water preparation. This can be confirmed by a higher minimum SPF for systems with GSHP in comparison to the SFH45 building in Strasbourg. As observed for SFH15, in case of systems with ASHP the lower performance of the heat pump due to lower ambient temperatures and the use of an electric heating element counteract this effect and thus the minimum value of SPF for ASHP systems is lower for SFH45 in Helsinki in comparison to the SFH45 building in Strasbourg. In addition, the maximum values of SPF are lower in comparison to the SFH45 building in Strasbourg, which confirms the impact of lower annual average ambient temperatures and slightly lower total yearly irradiation on the heating efficiency. Furthermore, the findings for the SFH15 building in Helsinki can be confirmed for SFH45 in Helsinki with regard to the heating efficiency. Nevertheless, there are some differences that will be discussed in the following. Comparing different concepts, the results vary slightly in comparison to SFH15 in Helsinki. In contrast to SFH15, PV-SGSHP-P systems cannot achieve higher SPFs than the corresponding systems with FPC. As observed for SFH15 and in contrast to SFH45 in Strasbourg, PVT-SGSHP-P systems reach higher SPFs than SGSHP-P systems, whereas SASHP-P systems achieve higher SPFs than PVT-SASHP-P systems. At this, PV-PVT-SGSHP-P systems achieve

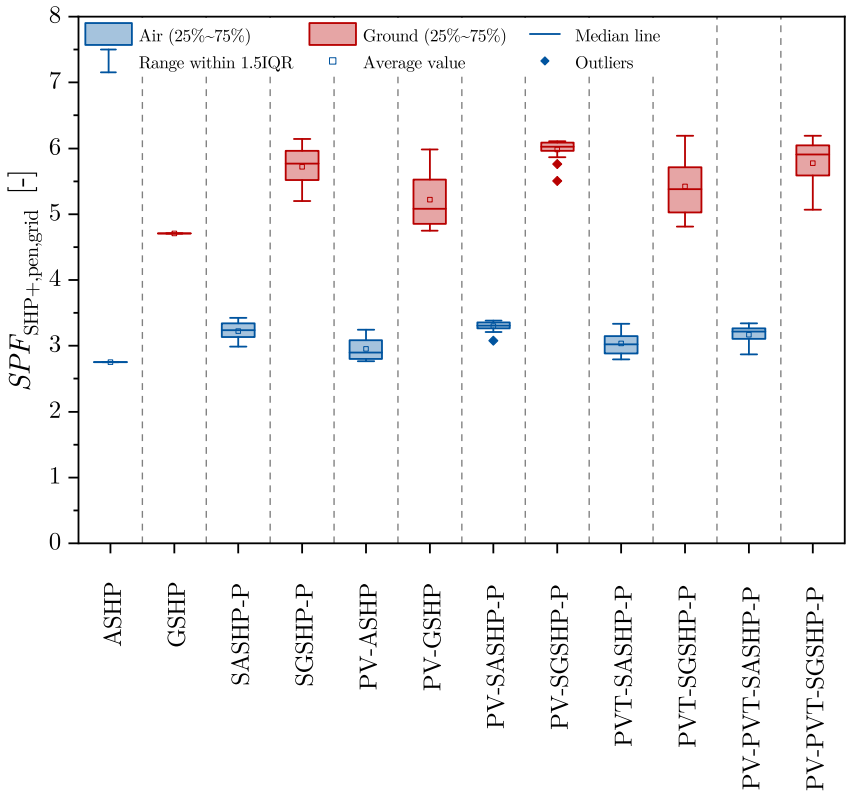

Figure 4.18: Grid-related SPF of the overall system with penalties for different heat pump and SHP system concepts in Helsinki for SFH45.

the same maximum SPFs as PVT-SGSHP-P systems. Nevertheless, general improvements by combining PV with system concepts with parallel FPC or PVT collectors cannot be observed with regard to the heating efficiency. As observed for buildings in Strasbourg and SFH15 in Helsinki, the SPFs of PV and heat pump systems are lower on average than those of systems with solar thermal integration (FPC, PVT) and PV and heat pump systems can only compete with these concepts if a battery storage is used. In contrast to SFH45 in Strasbourg, SHP system concepts with ASHP cannot reach the performance of GSHP systems without integration of solar technologies. This points out that the benefit of GSHPs is higher for buildings in cold climates with high heating energy demand and low annual average ambient temperature.

Regarding the range of grid-related SPFs of the overall system with penalties for SFH100 in Helsinki (cf. Figure 4.19), the SPF for systems with ASHP is in the range of 2.58 (ASHP) and 2.96 (SASHP-P) and for systems with GSHP in the range of 4.12 (GSHP) and 4.99 (PVT-SGSHP-P). Basically, the results show that the values of SPF for SFH100 in Helsinki with a very low fraction of energy demand for domestic hot water preparation (9 %) are lower in comparison to the SFH45 building in Helsinki. As observed for SFH100 in Strasbourg, the lower values of SPF show in particular the impact of energy demands for space heating at a higher temperature level as the supply temperatures of 60 °C for SFH100 are significantly higher than those for SFH45 (40 °C) in Helsinki. This leads to a lower performance of the heat pump due to the higher temperature differences between heat source and heat sink. In comparison to the SFH100 building in Strasbourg, the minimum SPF is lower for systems with ASHP and only slightly higher for systems with GSHP. As figured out before, the lower minimum SPF, and thus the lower performance of the heat pump, in case of systems with

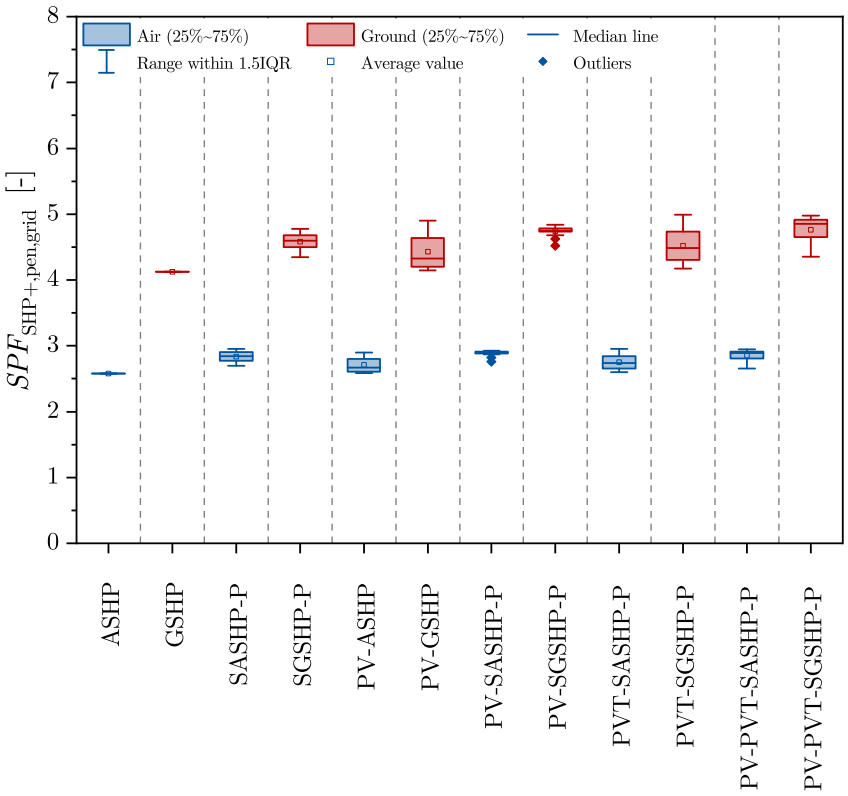

Figure 4.19: Grid-related SPF of the overall system with penalties for different heat pump and SHP system concepts in Helsinki for SFH100.

ASHP is mainly caused by the lower ambient temperatures and the use of an electric heating element, but also by slightly higher supply temperatures for space heating in Helsinki. The higher supply temperatures for space heating also influence the minimum SPF for systems with GSHP which is just slightly higher in comparison to the SFH100 building in Strasbourg. In addition, the maximum values of SPF are lower in comparison to the SFH100 building in Strasbourg, which confirms the impact of lower annual average ambient temperatures and slightly lower total yearly irradiation on the heating efficiency. Furthermore, the findings for the SFH15 and SFH45 building in Helsinki can be confirmed for SFH100 with regard to the heating efficiency. Nevertheless, there are some differences that will be discussed in the following. Comparing different concepts, the results vary slightly in comparison to SFH15 and SFH45 in Helsinki. As observed for SFH15 and in contrast to SFH45 in Helsinki and SFH100 in Strasbourg, some combinations of PV-SGSHP-P systems achieve slightly higher (around 1 %) SPFs than the corresponding systems with FPC, whereas PVT-SGSHP-P systems also reach higher SPFs than PV-SGSHP-P and SGSHP-P systems. In contrast to SFH15 and SFH45 in Helsinki and SFH100 in Strasbourg, PV-GSHP systems can achieve higher maximum values of SPF than SGSHP-P systems, depending on the battery storage size. In case of systems with ASHP, as observed for Strasbourg and SFH15 and SFH45 in Helsinki, the SPFs of PV-ASHP systems are slightly lower on average than those of systems with solar thermal integration (FPC, PVT) and SASHP-P systems achieve higher SPFs than PVT-SASHP-P systems. Furthermore, general improvements by combining PV with system concepts with parallel FPC or PVT collectors cannot be observed with regard to the heating efficiency and PV and heat pump systems can only compete with concepts with solar thermal integration (FPC, PVT) if a battery storage is used. As observed before

for buildings in Helsinki and for SFH100 in Strasbourg, SHP system concepts with ASHP cannot reach the performance of GSHP systems without integration of solar technologies which confirms the higher benefit of GSHPs for buildings in cold climates with high heating energy demand and low annual average ambient temperature.

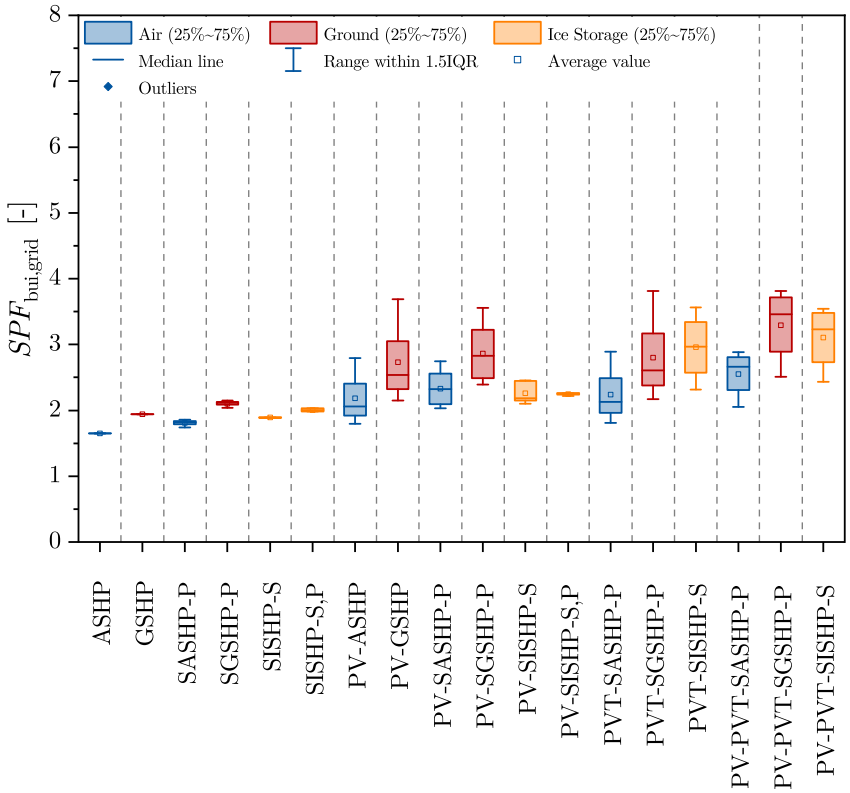

Figure 4.20: Grid-related SPF of the building for different heat pump and SHP system concepts in Helsinki for SFH15.

Overviews of the range of grid-related SPFs of the building for the different heat pump and SHP system concepts in Helsinki for SFH15, SFH45 and SFH100 are shown in Figure 4.20, Figure 4.21 and Figure 4.22. Regarding the results for SFH15 (cf. Figure 4.20), the SPF for systems with ASHP is in the range of 1.65 (ASHP) and 2.89 (PVT-SASHP-P, PV-PVT-SASHP-P), for systems with GSHP in the range of 1.94 (GSHP) and 3.82 (PVT-SGSHP-P) and for SISHP systems in the range of 1.89 (SISHP-S) and 3.56 (PVT-SISHP-S). As observed for the heating efficiency, the results show basically that the maximum values of SPF for SFH15 in Helsinki are lower in comparison to the SFH15 building in Strasbourg, especially for system concepts with ASHP. The lower maximum values of SPF suggest that the impact of lower annual average ambient temperatures and slightly lower total yearly irradiation on the SPF for the heating efficiency is the same for the energy efficiency. In addition, the higher fraction of heating energy demand on the net energy demand of the building in comparison to the SFH15 building in Strasbourg influences the results with regard to the energy efficiency. Comparing different concepts, the simulation results show that the energy efficiency can only significantly be increased by adding PV modules (only for systems with ASHP and GSHP in case of SFH15 in Helsinki) or PVT collectors (for all system concepts), especially in combination with a battery storage. The SSRs of the building reach values up to 47 % for systems with PV as well as PVT. At this,

systems without battery storage achieve values between 8 % and 22 % for systems with PV and between 8 % and 23 % for systems with PVT.

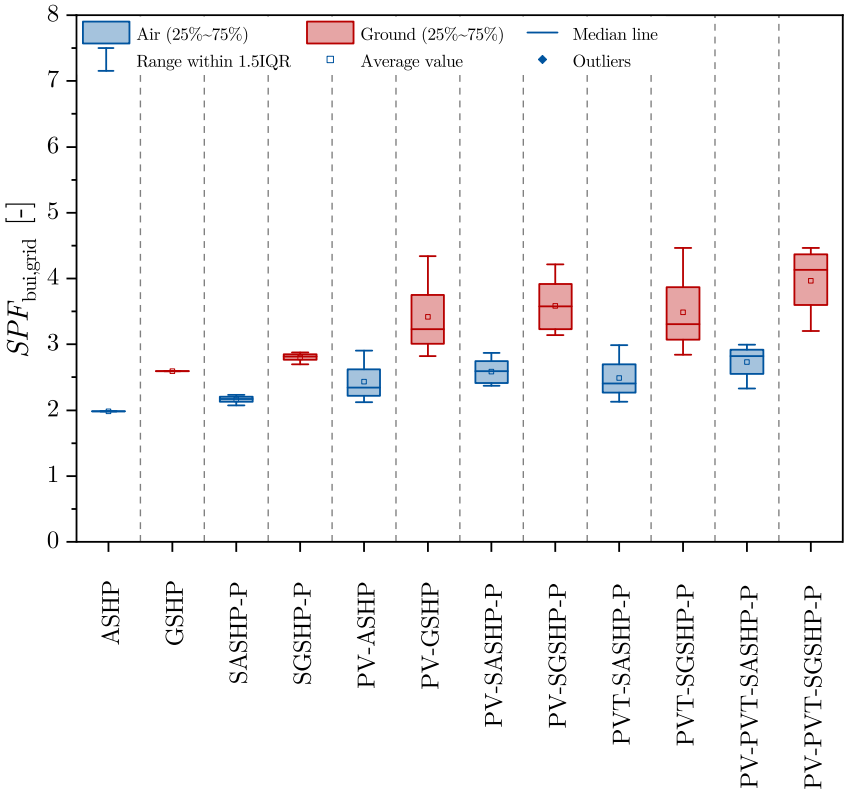

Figure 4.21: Grid-related SPF of the building for different heat pump and SHP system concepts in Helsinki for SFH45.

Regarding the grid-related SPFs of the building for SFH45 in Helsinki (cf. Figure 4.21), the SPF for systems with ASHP is in the range of 1.99 (ASHP) and 2.99 (PVT-SASHP-P, PV-PVT-SASHP-P) and for systems with GSHP in the range of 2.59 (GSHP) and 4.47 (PVT-SGSHP-P). As observed for SFH15, the maximum values of SPF are lower in comparison to the SFH45 building in Strasbourg, especially for system concepts with ASHP. The lower maximum values of SPF confirm the impact of lower annual average ambient temperatures and slightly lower total yearly irradiation on the SPF, even for the energy efficiency. As mentioned before for the SFH15 building in Helsinki, the higher fraction of heating energy demand on the net energy demand of the building in comparison to the SFH45 building in Strasbourg influences the results with regard to the energy efficiency. Comparing different concepts, the simulation results confirm that the energy efficiency can only significantly be increased by adding PV modules or PVT collectors, especially in combination with a battery storage. The SSRs of the building reach values up to 40 % for systems with PV as well as PVT. At this, systems without battery storage achieve values between 6 % and 19 % for systems with PV as well as PVT.

Regarding the grid-related SPFs of the building for SFH100 in Helsinki (cf. Figure 4.22), the SPF for systems with ASHP is in the range of 2.12 (ASHP) and 2.76 (PVT-SASHP-P) and for systems with GSHP in the range of 2.88 (GSHP) and 4.14 (PVT-SGSHP-P). As observed for SFH15 and SFH100, the maximum values of SPF are lower in comparison to the SFH100 building in Strasbourg, especially for system concepts with ASHP. The

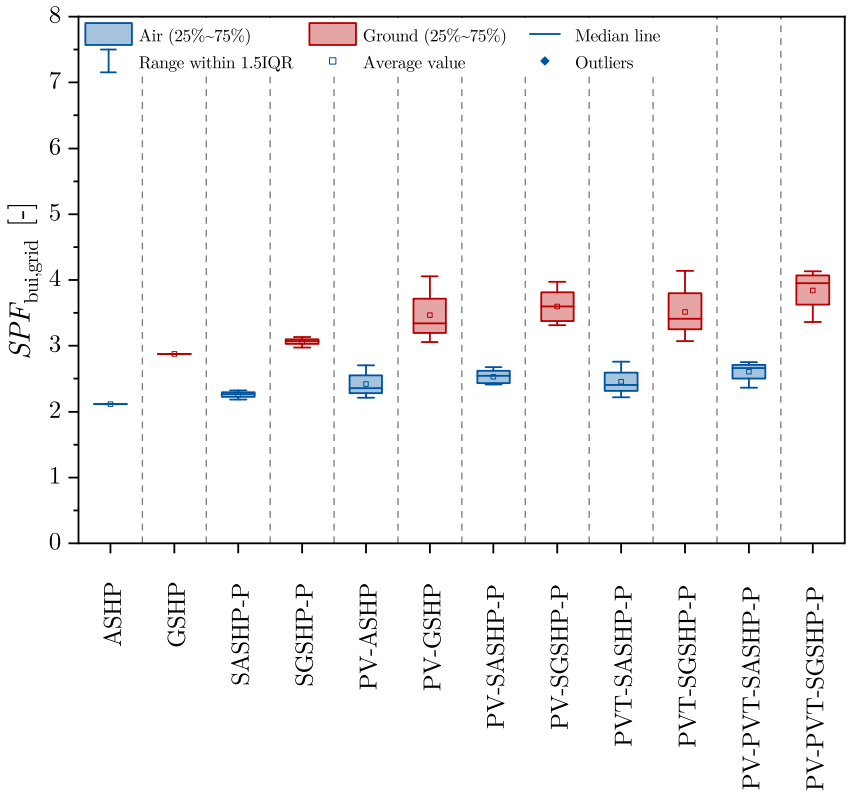

Figure 4.22: Grid-related SPF of the building for different heat pump and SHP system concepts in Helsinki for SFH100.

lower maximum values of SPF also confirm the impact of lower annual average ambient temperatures and slightly lower total yearly irradiation on the SPF for the energy efficiency. As mentioned before for the SFH15 and SFH45 building in Helsinki, the higher fraction of heating energy demand on the net energy demand of the building in comparison to the SFH100 building in Strasbourg influences the results with regard to the energy efficiency. Comparing different concepts, the simulation results also confirm that the energy efficiency can only significantly be increased by adding PV modules or PVT collectors, especially in combination with a battery storage. The SSRs of the building reach values up to 29 % for systems with PV as well as PVT. At this, systems without battery storage achieve values between 4 % and 14 % for systems with PV as well as PVT.

In general, the main findings for Strasbourg can be confirmed for SFH15, SFH45 and SFH100 in Helsinki with regard to the energy efficiency. Comparing system concepts with ASHP and GSHP with regard to the energy efficiency, PV-ASHP, PV-SASHP-P, PVT-SASHP-P and PV-PVT-SASHP-P systems can reach higher values of SPF than GSHP systems without integration of solar technologies or SGSHP-P systems, especially for system concepts with battery storage, for SFH15 in Helsinki. In case of SFH45 in Helsinki, PV-ASHP, PV-SASHP-P, PVT-SASHP-P and PV-PVT-SASHP-P systems can reach nearly the same or slightly higher values of SPF than GSHP systems without integration of solar technologies or SGSHP-P systems, whereas SHP system concepts with ASHP cannot achieve the performance of GSHP systems without integration of solar technologies for SFH100 in Helsinki. In contrast to Strasbourg, ASHP systems with PV or PVT can compete with GSHP systems with the same solar technology depending on the used PV module or PVT collector area and battery storage capacity for SFH15, but can hardly (SFH45)

or not (SFH100) compete with GSHP systems with the same solar technology for SFH45 and SFH100. Thus, the results show the higher benefit of GSHPs for buildings in cold climates with high heating energy demand and low annual average ambient temperature, even for the energy efficiency. In addition, as observed for Strasbourg, solar thermal and heat pump concepts achieve the lowest maximum SPF values beside systems without solar technology integration, whereas systems with PVT collectors reach the highest SPFs for all building types in Helsinki. Regarding systems with ice storage for SFH15, especially PVT-SISHP-S systems reaching high SPFs between 2.31 and 3.56 can compete with SHP systems with ASHP or GSHP with regard to the energy efficiency. In case of SFH15 and SFH45, PV-PVT-SASHP-P systems achieve the same maximum SPFs as PVT-SASHP-P systems. Nevertheless, general improvements by combining PV with system concepts with PVT collectors cannot be observed with regard to the energy efficiency in comparison to the corresponding PVT and heat pump systems. Furthermore, the improvement by the use of PVT collectors instead of PV decreases slightly in comparison to Strasbourg for systems with ASHP and GSHP. As observed for Strasbourg, the SPF of system concepts with parallel FPCs can be increased by the combination with PV. Depending on the battery storage size (especially for low battery storage sizes or systems without battery storage), some combinations of parallel FPCs and PV modules achieve even slightly higher SPFs than the corresponding systems with PV. Nevertheless, the maximum SPFs of PV-SASHP-P, PV-SGSHP-P and PV-SISHP-S,P (SFH15) systems are also slightly lower than those of the corresponding systems with PV modules instead of parallel FPCs.

4.2.4 Summary

The following general conclusions on the heating and energy efficiency can be given for the climates of Strasbourg, Athens and Helsinki:

- The SPF increases with increasing FPC/PVT collector or PV module area.
- Battery storages have a major impact on the heating and especially the energy efficiency of a building in systems with PV or PVT. At this, the SPF increases with increasing battery storage capacity and the improvement of the SPF by adding a battery storage increases with increasing PV module or PVT collector area.
- Major benefits for the specific electrical solar yield of PVT collectors in comparison to PV modules cannot be observed. The specific solar electrical yield is slightly improved for some cases (especially in SISHP systems), but even decreases for some of the investigated systems (especially with parallel PVT integration).
- Heat pump and SHP systems with GSHP reach higher SPFs in comparison with corresponding system concepts with ASHP or ice storage.
- SISHP-S systems achieve higher SPF values than ASHP systems without integration of solar technologies and SISHP-S,P systems achieve even higher SPFs than those of GSHP systems without integration of solar technologies for SFH15 and SFH45. At this, the benefit of adding FPCs in SISHP systems with minimum required WISC collector area is higher than the improvement by adding the same WISC collector area. PVT-SISHP-S systems reach the highest SPFs of all system concepts with ice storage (with exception of the heating efficiency for SFH15 in moderate climates),

reach higher SPFs than all system concepts with ASHP and can even compete with systems with GSHP.

- The maximum achieved SPFs of SHP system concepts increase for locations with higher total yearly irradiation and higher annual average ambient temperature as a result of higher specific solar electrical yields and lower heating energy demands reaching higher SSRs and solar thermal fractions.

Regarding the heating efficiency, the following conclusions can be given for the climates of Strasbourg, Athens and Helsinki:

- The heating efficiency can significantly be increased by the use of solar technologies. The SPFs of systems with PV are lower on average than those of systems with solar thermal integration (FPC, PVT) and PV and heat pump systems can only compete with these concepts if a battery storage is used.

- The minimum achieved SPFs for the heating efficiency of heat pump and SHP system concepts decrease for high fractions of energy demand for domestic hot water preparation at high temperature level and energy demands for space heating with high supply temperatures as a result of a lower performance of the heat pump. At this, the lower performance of the heat pump for space heating with high supply temperatures as well as the lower performance of ASHP systems and the use of an electric heating element in cold climates with lower ambient temperatures counteract the effect of higher heating efficiency for lower fractions of energy demand for domestic hot water preparation.

- Systems with PVT benefit from the use of solar electricity for the supply of the SHP system in combination with the solar thermal yields.

- In case of SHP systems with ASHP, systems with parallel FPC reach higher SPFs than concepts with PVT or especially PV in moderate and cold climates and for SFH100 in warm climates, whereas PVT-SASHP-P systems reach higher SPFs than systems with parallel FPC or especially PV for SFH45 in warm climates. In case of SHP systems with GSHP, systems with parallel FPC reach also higher SPFs than concepts with PVT or especially PV for SFH45 in moderate climates, whereas PVT-SGSHP-P systems reach higher SPFs than concepts with parallel FPC or especially PV in warm and cold climates and for SFH15 and SFH100 in moderate climates. For SFH45 in warm climates and SFH100 in cold climates, GSHP systems with PV can even achieve higher maximum SPFs than systems with parallel FPCs, depending on the battery storage size.

- SASHP-P, PV-SASHP-P, PVT-SASHP-P and PV-PVT-SASHP-P systems can reach the same or even higher values of SPF than GSHP systems without integration of solar technologies in warm climates and for SFH15 and SFH45 in moderate climates, whereas PV-ASHP systems only reach the performance of GSHP systems in warm climates and for SFH15 in moderate climates. In case of cold climates and SFH100 in moderate climates, SHP concepts with ASHP cannot reach the performance of GSHP systems without integration of solar technologies. This reflects especially the higher benefit of GSHPs for buildings with high heating energy demand and locations with low annual average ambient temperature. Furthermore, ASHP systems can hardly compete with GSHP systems with the same solar technology in moderate climates and

cannot compete with GSHP systems with the same solar technology in cold climates. In addition, SHP system concepts with ASHP cannot achieve the performance of systems with ice storage for SFH15 in cold climates.

- In case of SISHP systems, the benefit of adding PV modules is lower than the improvement by adding the same FPC area, but system concepts with PVT reach the highest SPFs for SFH45 and SFH100 in moderate climates and SFH15 in cold climates. In case of SFH15, PV-SISHP-S,P reach slightly (1 %) higher SPFs than systems with PVT collectors.

- General improvements by combining PV with system concepts with parallel FPC or PVT collectors cannot be observed. In case of SFH100 in warm climates and SFH15 in moderate climates, PV plus parallel solar thermal and heat pump systems achieve the same or slightly higher SPFs than systems with parallel solar thermal (FPC, PVT) circuit with regard to system concepts with ASHP and GSHP and even slightly higher SPFs than systems with serial PVT collectors with regard to system concepts with ice storage. In case of SFH45 in warm climates, PV-SASHP-P achieve higher SPFs than ASHP systems with parallel solar thermal (FPC, PVT) circuit, whereas PVT-SGSHP-P achieve the highest SPFs even if PV-SGSHP-P reach significantly higher SPFs than SGSHP-P systems. In case of SFH15 and SFH100 in cold climates, PV-SGSHP-P systems achieve slightly higher (around 1 %) SPFs than the corresponding systems with FPC, whereas PVT-SGSHP-P systems reach higher SPFs than PV-SGSHP-P and SGSHP-P systems.

The results illustrate that there are some general findings, but the system concepts compete with each other and have to be compared for the considered use case to identify the best system concept with regard to the heating efficiency. Regarding the energy efficiency, the following conclusions can be given for the climates of Strasbourg, Athens and Helsinki:

- The energy efficiency can only significantly be increased by adding PV modules (for systems with ASHP and GSHP and in case of SFH15 in moderate climates for systems with ice storage) or PVT collectors (for all system concepts), especially in combination with a battery storage. Heat pump as well as solar thermal and heat pump systems cannot compete with system concepts with PV or PVT integration, especially with battery storage. Furthermore, systems with PV reach higher values of SPF than systems with the same parallel FPC area, even without battery storage. This illustrates the benefit of on-site generated solar electrical energy, which can be used to cover both SHP and household electricity consumption.

- The SSRs of the building decrease for buildings with high energy demand and locations with lower total yearly irradiation and lower annual average ambient temperature, and are higher for systems with GSHP in comparison to systems with ASHP. At this, the SSRs of the building reach values up to 60 % (SFH15), 54 % (SFH45) and 43 % (SFH100) in Strasbourg, up to 85 % (SFH45) and 77 % (SFH100) in Athens and up to 47 % (SFH15), 40 % (SFH45) and 29 % (SFH100) in Helsinki.

- The SPF of system concepts with parallel FPCs can be increased by the combination with PV, whereas general improvements by combining PV with system concepts with PVT collectors cannot be observed. Depending on the battery storage size (especially

for low battery storage sizes or systems without battery storage), some combinations of parallel FPCs and PV modules achieve even slightly higher SPFs than the corresponding systems with PV. Nevertheless, the maximum SPFs of PV-SASHP-P, PV-SGSHP-P and PV-SISHP-S,P systems are slightly lower than those of the corresponding systems with PV modules instead of parallel FPCs.

- Systems with PVT benefit primarily from the use of solar electricity with regard to the thermal and electrical supply of a building. Especially for SISHP concepts, in which the PVT collectors replace the required WISC collectors, the results illustrate the benefit of combined generation of heat and electricity by PVT collectors for limited roof areas.

- Systems with PVT collectors achieve the highest SPFs. At this, PV and heat pump systems reach (slightly) lower SPF values than systems with PVT collectors in case of systems with ASHP and GSHP, whereas system concepts with PVT collectors reach by far the best results for systems with ice storage, especially for SFH45 and SFH100 in moderate climates and SFH15 in cold climates. For systems with ASHP and GSHP, the improvement by the use of PVT collectors instead of PV increases slightly for warm climates and decreases slightly for cold climates in comparison to moderate climates.

- With the exception of SFH45 and SFH100 in cold climates, PV-ASHP, PV-SASHP-P, PVT-SASHP-P and PV-PVT-SASHP-P systems can reach higher values of SPF than GSHP systems without integration of solar technologies or SGSHP-P systems, especially for system concepts with battery storage. In case of SFH45 in cold climates, PV-ASHP, PV-SASHP-P, PVT-SASHP-P and PV-PVT-SASHP-P systems can reach nearly the same or slightly higher values of SPF than GSHP systems without integration of solar technologies or SGSHP-P systems, whereas SHP system concepts with ASHP cannot achieve the performance of GSHP systems without integration of solar technologies for SFH100 in cold climates. In contrast to the results for the heating efficiency, ASHP systems with PV or PVT can even compete with GSHP systems with the same solar technology in warm and moderate climates and for SFH15 in cold climates, depending on the used PV module or PVT collector area and battery storage capacity. However, ASHP systems with PV or PVT can hardly (SFH45) or not (SFH100) compete with GSHP systems with the same solar technology for SFH45 and SFH100 in cold climates. Furthermore, for moderate climates it can be observed that the differences in energy efficiency between systems with GSHP and ASHP are significantly higher for SFH100 in comparison to SFH15. Thus, the results also reflect the higher benefit of GSHPs for buildings with high heating energy demand and locations with low annual average ambient temperature, even for the energy efficiency.

- The fraction of heating energy demand on the net energy demand of the building influences the results with regard to the energy efficiency and can counteract identified effects on the heating efficiency for the energy efficiency. Thus, a lower performance of the heat pump does not generally lead to lower SPFs for the energy efficiency comparing different buildings.

With regard to the comparison of different SHP concepts with PV, PVT or solar thermal collectors, the efficiency analysis shows especially the importance to use the introduced grid-related SPF of the building $SPF_{\mathrm{bui,grid}}$ to assess the energy efficiency regarding the thermal and electrical energy supply of a building.

4.3 Environmental Impact

This section presents the *environmental impact evaluation* of the considered SHP systems in this work. The objective of this evaluation is the comparison of SHP system concepts for a wide range of boundary conditions in order to identify the environmental benefits of different SHP system concepts. At this, it is useful to compare SHP systems with a reference building with conventional heating system to figure out the environmental benefits of SHP system concepts for the energy supply of residential buildings. Within this work, the reference building is equipped with a conventional gas-fired heating system. The delivered fuel energy of the reference building is calculated by Equation 2.79 for each location and building type using an overall efficiency of $\eta_{\mathrm{ref,gas}} = 0.9$. The delivered electrical energy to the reference building (from the grid) is calculated by Equation 2.80 for each location and building type. At this, the electrical energy from the grid for the supply of the conventional gas-fired heating system is assumed to be equal to the electricity consumption of pumps which are not included in the heat pump consumption $W_{\mathrm{el,pu}}$, the electricity consumption of additional controllers which are not included in the heat pump consumption $W_{\mathrm{el,ctr}}$ and the electricity consumption of circulation pumps for the space heating system $W_{\mathrm{el,pu,SH}}$ of the ASHP system for the considered location and building.

The CO_2 emissions are chosen as main KPI for the rating of the environmental impact as result of the energy use in a building, whereas:

- the CO_2 emissions indicator of the building $EP_{\mathrm{CO_2,bui}}$ is used for the CO_2 emissions comparison without compensation by exported energy and
- the net CO_2 emissions indicator of the building $EP_{\mathrm{CO_2,bui,net}}$ is used for the CO_2 emissions comparison with compensation by exported energy.

Furthermore, additional KPIs are used for further analysis of the results. As described in Section 4.2, the SFH45 building in Strasbourg is used as base case. The evaluation of the base case is followed by the analysis of the influence of different building types and climates on the results. The used CO_2 emission coefficients for the environmental impact calculations are summarized in Table 4.6.

Table 4.6: CO_2 emission coefficients for environmental impact calculations based on ISO 52000-1:2017 [ISO 52000-1, 2017].

Parameter	Value	Parameter	Value
$f_{\mathrm{CO_2,del,el}}$	420 g CO_2eq/kWh	$f_{\mathrm{CO_2,del,gas}}$	220 g CO_2eq/kWh
$f_{\mathrm{CO_2,exp,el}}$	420 g CO_2eq/kWh		

4.3.1 Base Case: Strasbourg SFH45

An overview of the range of CO_2 emissions indicators of the building for the different heat pump and SHP system concepts in Strasbourg for SFH45 is shown in Figure 4.23. For systems with ASHP, the CO_2 emissions of the building are in the range of 10.17 kg CO_2eq/m^{2}a (PVT-SASHP-P) and 21.13 kg CO_2eq/m^{2}a (ASHP), for systems with GSHP in the range of 8.20 kg CO_2eq/m^{2}a (PVT-SGSHP-P) and 18.82 kg CO_2eq/m^{2}a (GSHP) and for SISHP systems in the range of 9.01 kg CO_2eq/m^{2}a (PVT-SISHP-S) and 19.55 kg CO_2eq/m^{2}a (SISHP-S).

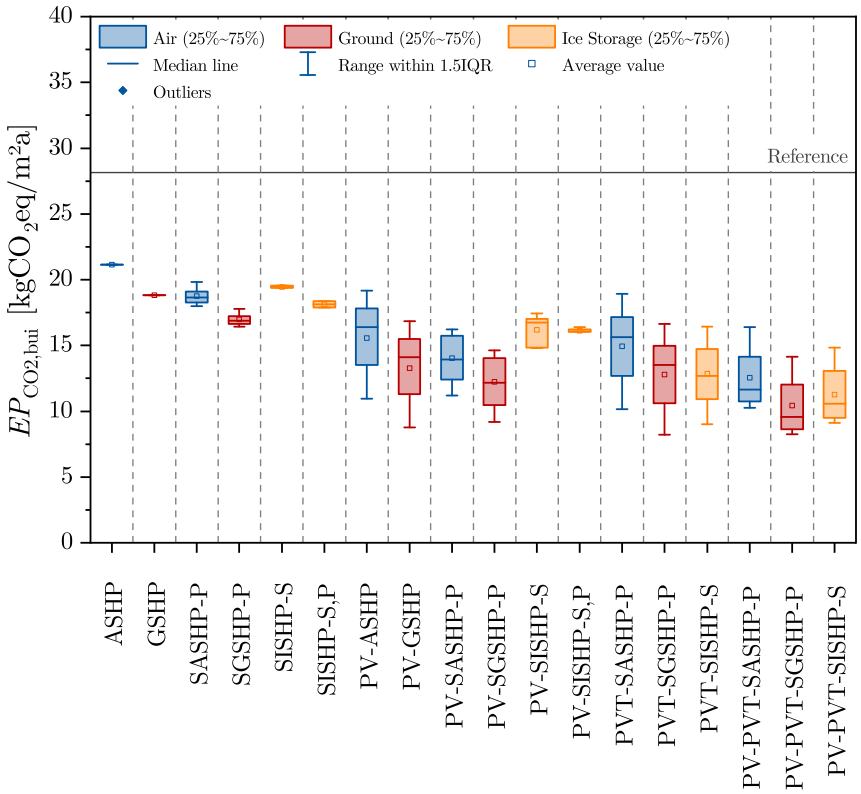

Figure 4.23: CO_2 emissions indicators of the building for different heat pump and SHP system concepts in Strasbourg for SFH45.

For comparison, the value of the reference building with conventional heating system is 28.14 kg CO_2eq/m^{2}a and, thus, all heat pump and SHP system concepts achieve lower CO_2 emissions indicators of the building than the reference building reaching fractional CO_2 emission savings up to 71 %. Basically, the simulation results show that the CO_2 emissions indicators of the building can be decreased by adding solar technologies and that the different system concepts compete with each other. At this, the CO_2 emissions indicators can only significantly be decreased by adding PV modules (for systems with ASHP and GSHP) or PVT collectors (for all system concepts), especially in combination with a battery storage (cf. Figure 4.24). This also points out that systems with PVT benefit primarily from the use of solar electricity with regard to the reduction of CO_2 emissions of a building. In general, the CO_2 emissions decrease with increasing FPC/PVT collector or PV module area and, in case of systems with battery storage, the CO_2 emissions decrease with increasing battery storage capacity. Both effects result from higher amounts of solar energy that can be used for the supply of the building and thus a reduction of delivered electrical energy to the building. The reduction of CO_2 emissions by adding a battery storage increases with increasing PV module or PVT collector area due to the higher amounts of generated solar electrical energy that can be stored in the battery storage. At this, the CO_2 emissions can be reduced by up to 39 % using battery storages in comparison to the corresponding system without battery storage. Comparing different concepts, solar thermal and heat pump concepts achieve the highest minimum CO_2 emissions indicator values beside systems without solar technology integration, whereas systems with PVT collectors reach the lowest CO_2 emissions indicators. At this, PV and heat pump systems achieve slightly higher CO_2 emissions indicators than systems with PVT collectors in case of systems with ASHP and GSHP. Regarding

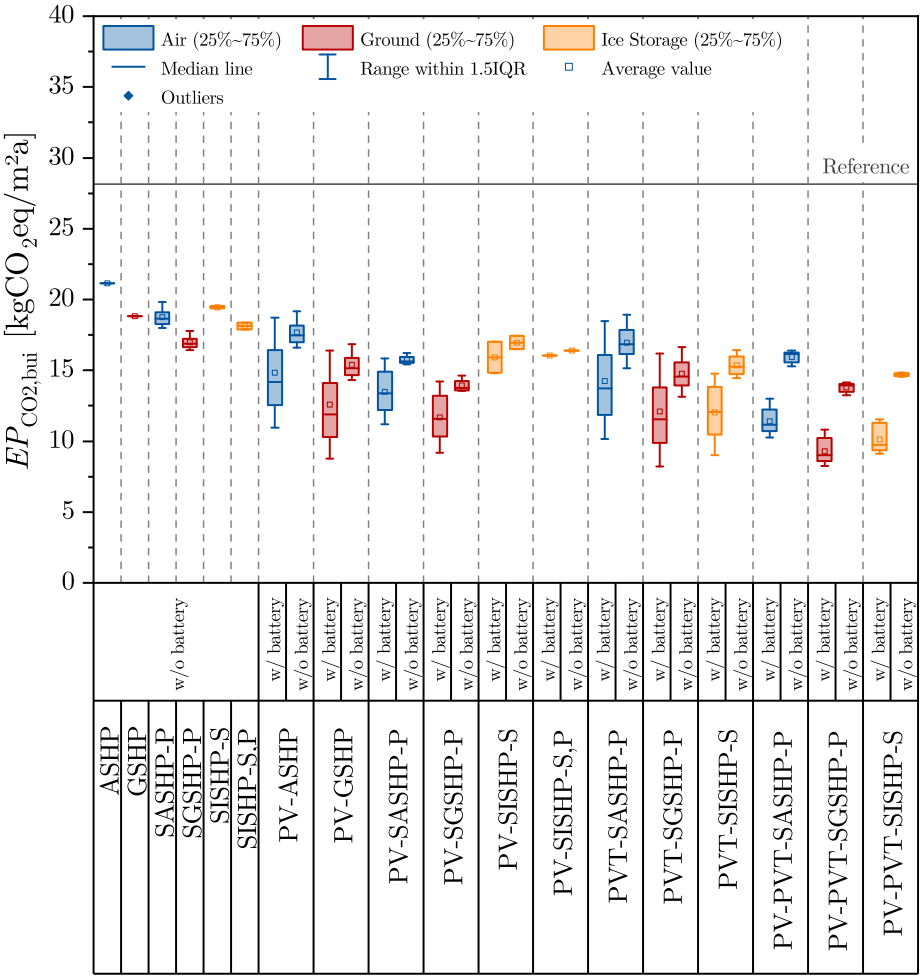

Figure 4.24: CO_2 emissions indicators of the building for different heat pump and SHP system concepts with and without battery storage in Strasbourg for SFH45.

systems with ice storage, system concepts with PVT collectors reach by far the best results. Furthermore, the CO_2 emissions of system concepts with parallel FPCs can be decreased by the combination with PV, whereas general improvements by combining PV with system concepts with PVT collectors cannot be observed with regard to the CO_2 emissions indicators in comparison to the corresponding PVT and heat pump systems. Depending on the battery storage size (especially for low battery storage sizes or systems without battery storage), some combinations of parallel FPCs and PV modules achieve even slightly lower CO_2 emissions indicators than the corresponding systems with PV. Nevertheless, the minimum CO_2 emissions of PV-SASHP-P, PV-SGSHP-P and PV-SISHP-S,P systems are slightly higher than those of the corresponding systems with PV modules instead of parallel FPCs. In general, the results illustrate the benefit of on-site generated solar electrical energy, which can be used to cover both SHP and household electricity consumption and, as a result, the reduction of the CO_2 emissions of a building.

Comparing system concepts with ASHP and GSHP with regard to the CO_2 emissions indicators of the building, ASHP systems with PV or PVT can compete with GSHP systems with the same solar technology depending on the used PV module or PVT collector area and battery storage capacity. Furthermore, in most cases, PV-ASHP, PV-SASHP-P, PVT-SASHP-P as well as PV-PVT-SASHP-P systems can reach the same or lower CO_2

emissions than GSHP systems without integration of solar technologies or SGSHP-P systems, especially for system concepts with battery storage. Regarding systems with ice storage, especially PVT-SISHP-S systems reaching low CO_2 emissions indicators between 9.01 kg CO_2eq/m^{2}a and 16.43 kg CO_2eq/m^{2}a can compete with SHP systems with ASHP or GSHP. In case of PV-SISHP-S systems, the benefit of adding PV modules with regard to the reduction of CO_2 emissions is higher than the improvement by adding the same FPC area, but the values of PVT-SISHP-S systems cannot be reached due to the limited available additional PV module area of 10 m^2 as result of the minimum required WISC collector area for the supply of the ice storage. At this, the main reason for the high reduction of CO_2 emissions in case of PVT-SISHP-S systems is the additional solar electrical yield that can be used for the supply of the building in comparison to systems with serial WISC collectors. Especially for SISHP concepts, in which the PVT collectors replace the required WISC collectors, the results illustrate the benefit of combined generation of heat and electricity by PVT collectors for limited roof areas. At this, the limited additional PV or FPC area can be compensated by the use of PVT collectors using the entire roof area for the generation of both heat and electricity.

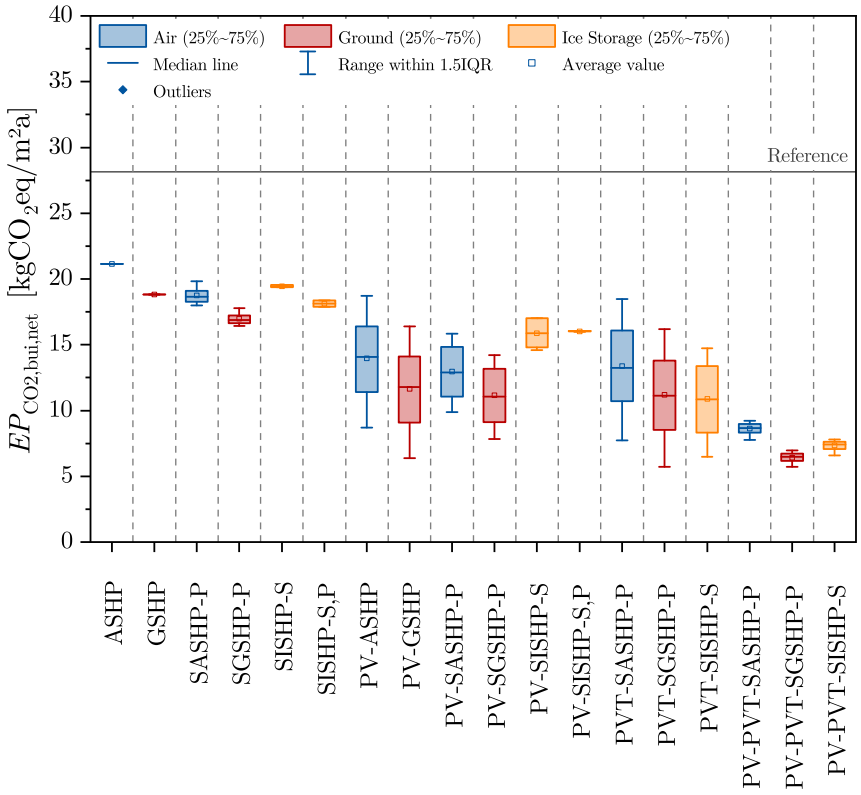

Figure 4.25: Net CO_2 emissions indicators of the building for different heat pump and SHP system concepts in Strasbourg for SFH45.

An overview of the range of net CO_2 emissions indicators of the building for the different heat pump and SHP system concepts in Strasbourg for SFH45 is shown in Figure 4.25. In comparison to the CO_2 emissions indicators, the net CO_2 emissions indicators for systems with PV or PVT are slightly lower due to the additional compensation by exported energy. Furthermore, the main differences between CO_2 emissions indicators and net CO_2 emissions indicators are the negative effects of battery storages on the net CO_2 emissions indicators due to the battery losses (cf. Figure 4.26) and, thus, the missing exported solar electricity

for the compensation of CO_2 emissions for delivered electrical energy from the grid. As a result, the net CO_2 emissions decrease with increasing FPC/PVT collector or PV module area, but increase with increasing battery storage capacity.

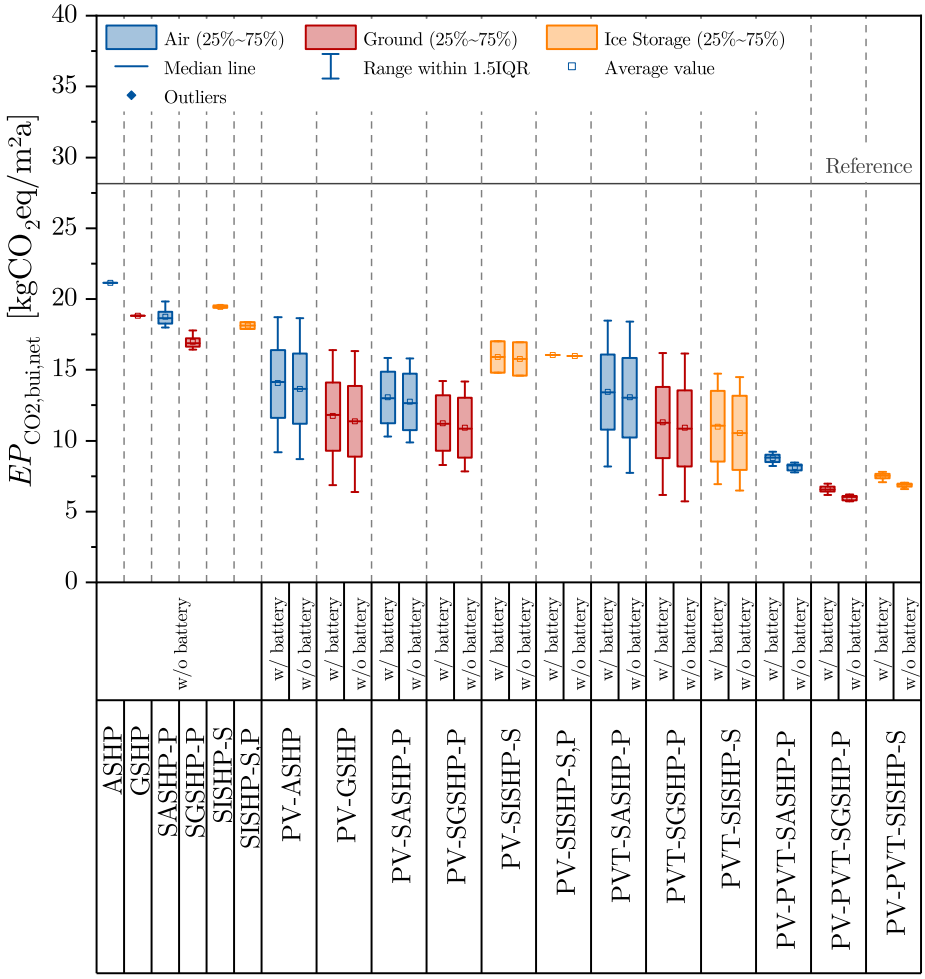

Figure 4.26: Net CO_2 emissions indicators of the building for different heat pump and SHP system concepts with and without battery storage in Strasbourg for SFH45.

4.3.2 Influence of Building Type

Overviews of the range of CO_2 emissions indicators of the building for the different heat pump and SHP system concepts in Strasbourg for SFH15 and SFH100 are shown in Figure 4.27 and Figure 4.28. Regarding the CO_2 emissions for SFH15 (cf. Figure 4.27), the CO_2 emissions indicators of the building for systems with ASHP are in the range of 7.23 kg CO_2eq/m^{2}a (PVT-SASHP-P) and 17.97 kg CO_2eq/m^{2}a (ASHP), for systems with GSHP in the range of 6.32 kg CO_2eq/m^{2}a (PVT-SGSHP-P) and 16.80 kg CO_2eq/m^{2}a (GSHP) and for SISHP systems in the range of 6.85 kg CO_2eq/m^{2}a (PVT-SISHP-S) and 17.18 kg CO_2eq/m^{2}a (SISHP-S). For comparison, the value of the reference building with conventional heating system is 21.07 kg CO_2eq/m^{2}a and, thus, all heat pump and SHP system concepts achieve lower CO_2 emissions indicators of the building than the reference building reaching fractional CO_2 emission savings up to 70 %. Basically, the results show

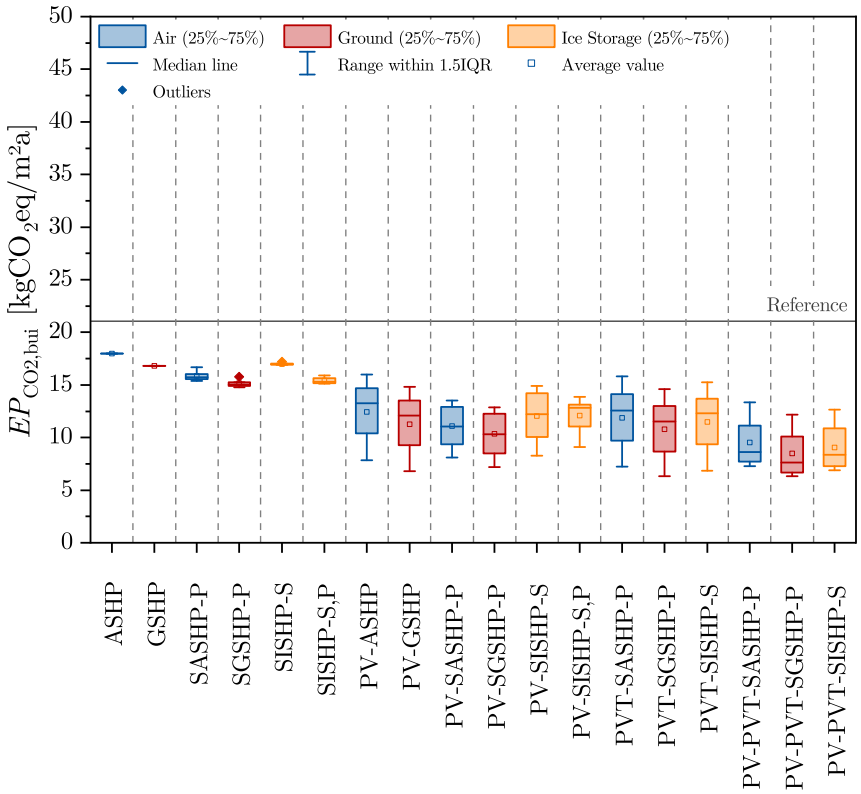

Figure 4.27: CO_2 emissions indicators of the building for different heat pump and SHP system concepts in Strasbourg for SFH15.

that the minimum CO_2 emissions indicators in case of new buildings with very high energetic quality are lower in comparison to the SFH45 building. Nevertheless, the maximum CO_2 emissions indicators of heat pump and SHP system concepts for SFH15 are higher than the minimum CO_2 emissions indicators for SFH45 and thus, depending on the SHP system design, renovated buildings can partially achieve lower CO_2 emissions than new buildings with very high energetic quality. Furthermore, the main findings for the SFH45 building in Strasbourg can be confirmed for SFH15 with regard to the environmental impact. At this, there are only some minor differences with regard to systems with ice storage. Comparing different concepts, the simulation results confirm that the CO_2 emissions indicators can only significantly be decreased by adding PV modules or PVT collectors, especially in combination with a battery storage. At this, the CO_2 emissions can be reduced by up to 45 % using battery storages in comparison to the corresponding system without battery storage. In contrast to SFH45, the CO_2 emissions can also significantly be decreased by adding PV modules to system concepts with ice storage due to the lower minimum required WISC collector area of 5 m^2 and, thus, the larger available roof area for PV modules. Nevertheless, system concepts with PVT collectors reach the best results for systems with ice storage.

Regarding the CO_2 emissions for SFH100 (cf. Figure 4.28), the CO_2 emissions indicators of the building for systems with ASHP are in the range of 17.44 kg CO_2eq/m^{2}a (PVT-SASHP-P) and 28.72 kg CO_2eq/m^{2}a (ASHP), for systems with GSHP in the range of 13.06 kg CO_2eq/m^{2}a (PVT-SGSHP-P) and 23.95 kg CO_2eq/m^{2}a (GSHP) and for SISHP systems in the range of 14.93 kg CO_2eq/m^{2}a (PVT-SISHP-S) and 25.43 kg CO_2eq/m^{2}a (SISHP-S). For comparison, the value of the reference building with conventional heating system is 41.44 kg CO_2eq/m^{2}a and, thus, all heat pump and SHP system concepts achieve

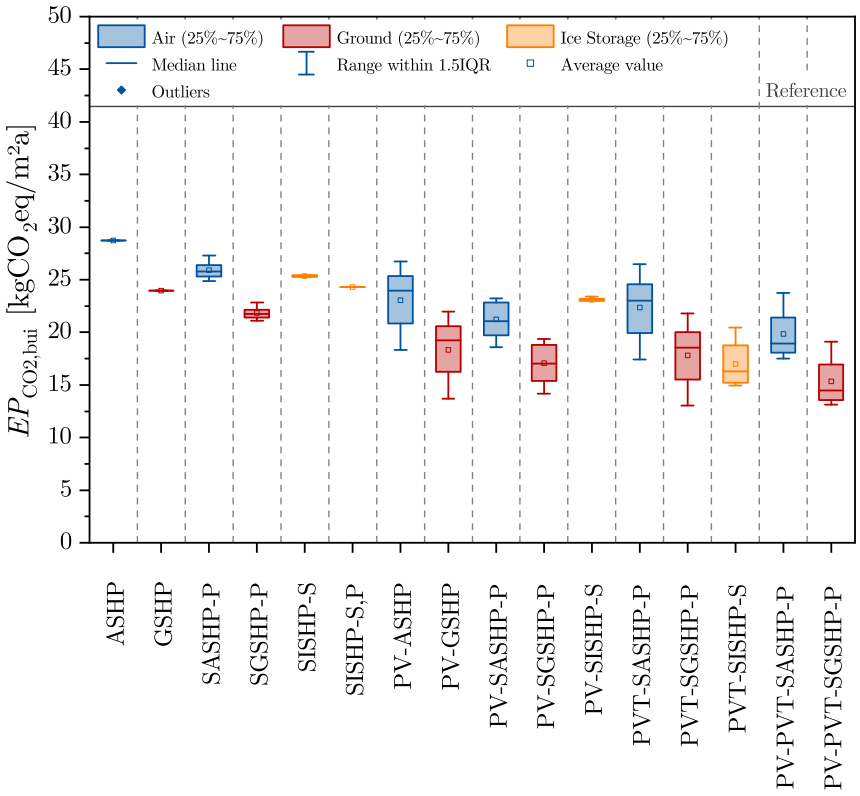

Figure 4.28: CO_2 emissions indicators of the building for different heat pump and SHP system concepts in Strasbourg for SFH100.

lower CO_2 emissions indicators of the building than the reference building reaching fractional CO_2 emission savings up to 68 %. Basically, the results show that the minimum CO_2 emissions indicators in case of non-renovated existing buildings are higher in comparison to the SFH15 and SFH45 building. Nevertheless, the maximum CO_2 emissions indicators of heat pump and SHP system concepts for SFH45 are higher than the minimum CO_2 emissions indicators for SFH100 and thus, depending on the SHP system design, non-renovated existing buildings can partially achieve lower CO_2 emissions than renovated buildings. In case of moderate climates, the minimum CO_2 emissions indicators for SFH100 are also lower than the maximum CO_2 emissions indicators of heat pump and SHP system concepts for SFH15 and thus, depending on the SHP system design, in some cases non-renovated existing buildings can even achieve lower CO_2 emissions than new buildings with very high energetic quality. Furthermore, the main findings for the SFH45 building in Strasbourg can be confirmed for SFH100 with regard to the environmental impact. Comparing different concepts, the simulation results confirm that the CO_2 emissions indicators can only significantly be decreased by adding PV modules (only for systems with ASHP and GSHP in case of SFH100) or PVT collectors (for all system concepts), especially in combination with a battery storage. At this, the CO_2 emissions can be reduced by up to 29 % using battery storages in comparison to the corresponding system without battery storage.

Comparing system concepts with ASHP and GSHP with regard to the CO_2 emissions for the SFH15 and SFH100 building, in most cases, PV-ASHP, PV-SASHP-P, PVT-SASHP-P and PV-PVT-SASHP-P systems can reach the same or lower CO_2 emissions indicators than GSHP systems without integration of solar technologies or SGSHP-P systems, especially for system concepts with battery storage. As observed for SFH45, ASHP systems with PV

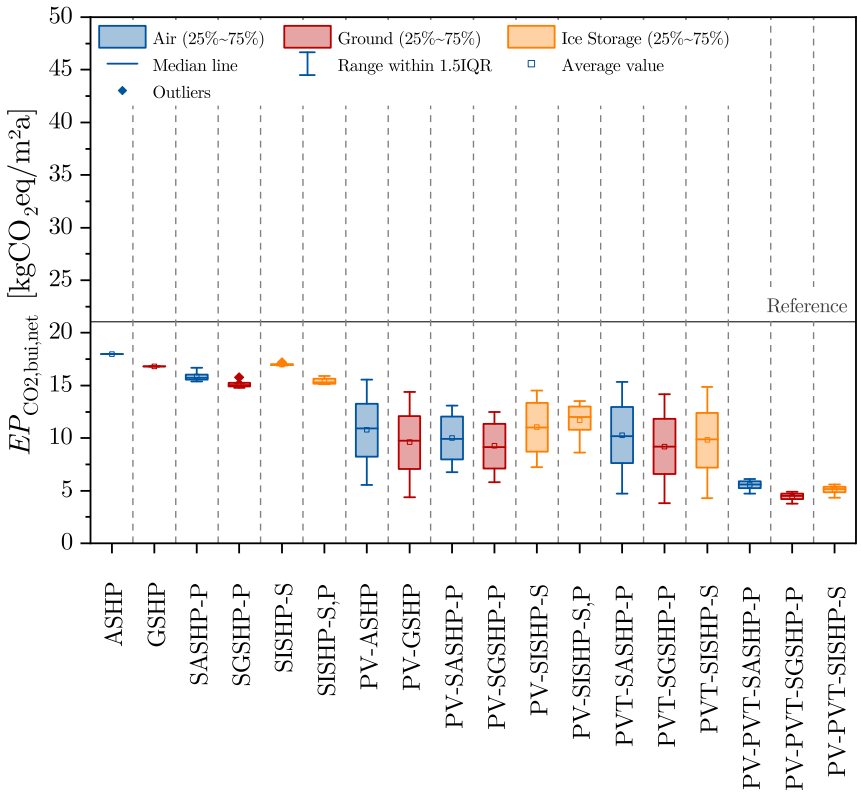

Figure 4.29: Net CO_2 emissions indicators of the building for different heat pump and SHP system concepts in Strasbourg for SFH15.

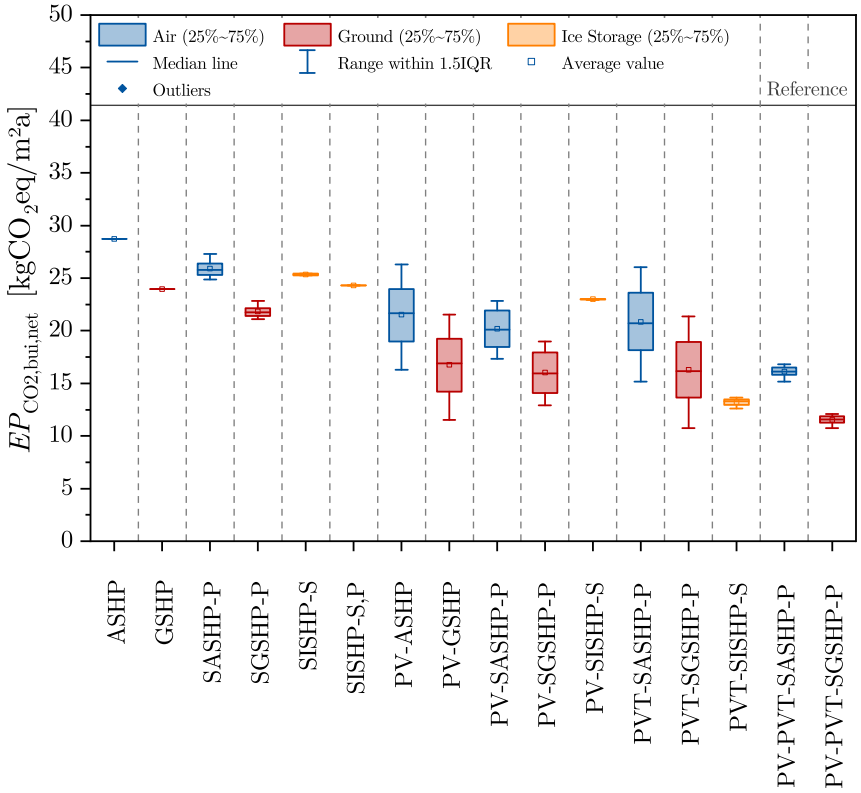

Figure 4.30: Net CO_2 emissions indicators of the building for different heat pump and SHP system concepts in Strasbourg for SFH100.

or PVT can even compete with GSHP systems with the same solar technology depending on the used PV module or PVT collector area and battery storage capacity. At this, the differences in CO_2 emissions indicators between systems with GSHP and ASHP are significantly higher for SFH100 in comparison to SFH15. This reflects the higher benefit of GSHPs for buildings with high heating energy demand as figured out for the efficiency evaluation. In addition, as observed for SFH45, solar thermal and heat pump concepts achieve the highest minimum CO_2 emissions indicator values beside systems without solar technology integration, whereas systems with PVT collectors reach the lowest CO_2 emissions indicators for SFH15 and SFH100. Depending on the building type, system concept, battery storage size and PV/PVT area, the CO_2 emissions reductions are up to 12 % for ASHP or GSHP systems with PVT in comparison to the corresponding systems with PV in Strasbourg. Regarding systems with ice storage, especially PVT-SISHP-S systems reaching low CO_2 emissions indicators between 6.85 kg CO_2eq/m^{2}a and 15.25 kg CO_2eq/m^{2}a for SFH15 and between 14.93 kg CO_2eq/m^{2}a and 20.44 kg CO_2eq/m^{2}a for SFH100 can compete with SHP systems with ASHP or GSHP with regard to the environmental impact. As observed for SFH45, the CO_2 emissions of system concepts with parallel FPCs can be decreased by the combination with PV, whereas general improvements by combining PV with system concepts with PVT collectors cannot be observed with regard to the CO_2 emissions indicators in comparison to the corresponding PVT and heat pump systems. Depending on the battery storage size (especially for low battery storage sizes or systems without battery storage), some combinations of parallel FPCs and PV modules achieve even slightly lower CO_2 emissions indicators than the corresponding systems with PV. Nevertheless, the minimum CO_2 emissions of PV-SASHP-P, PV-SGSHP-P and PV-SISHP-S,P systems are slightly higher than those of the corresponding systems with PV modules instead of parallel FPCs.

An overview of the range of net CO_2 emissions indicators of the building for the different heat pump and SHP system concepts in Strasbourg for SFH15 is shown in Figure 4.29 and for SFH100 in Figure 4.30. As observed for SFH45, in comparison to the CO_2 emissions indicators, the net CO_2 emissions indicators for systems with PV or PVT are slightly lower due to the additional compensation by exported energy. Furthermore, it can be confirmed that the main differences between CO_2 emissions indicators and net CO_2 emissions indicators are the negative effects of battery storages on the net CO_2 emissions indicators due to the battery losses and, as described before, the missing exported solar electricity for the compensation of CO_2 emissions for delivered electrical energy from the grid. As a result, the net CO_2 emissions decrease with increasing FPC/PVT collector or PV module area, but increase with increasing battery storage capacity for all building types in Strasbourg.

4.3.3 Influence of Climate

4.3.3.1 Warm Climates

Regarding warm climates, overviews of the range of CO_2 emissions indicators of the building for the different heat pump and SHP system concepts in Athens for SFH45 and SFH100 are shown in Figure 4.31 and Figure 4.32. With regard to the CO_2 emissions for SFH45 in Athens (cf. Figure 4.31), the CO_2 emissions indicators of the building for systems with ASHP are in the range of 2.19 kg CO_2eq/m^{2}a (PVT-SASHP-P) and 14.90 kg CO_2eq/m^{2}a (ASHP) and for systems with GSHP in the range of 1.96 kg CO_2eq/m^{2}a (PVT-SGSHP-P) and 14.34 kg CO_2eq/m^{2}a (GSHP). For comparison, the value of the reference building with conventional heating system is 16.24 kg CO_2eq/m^{2}a and, thus, all heat pump and SHP sys-

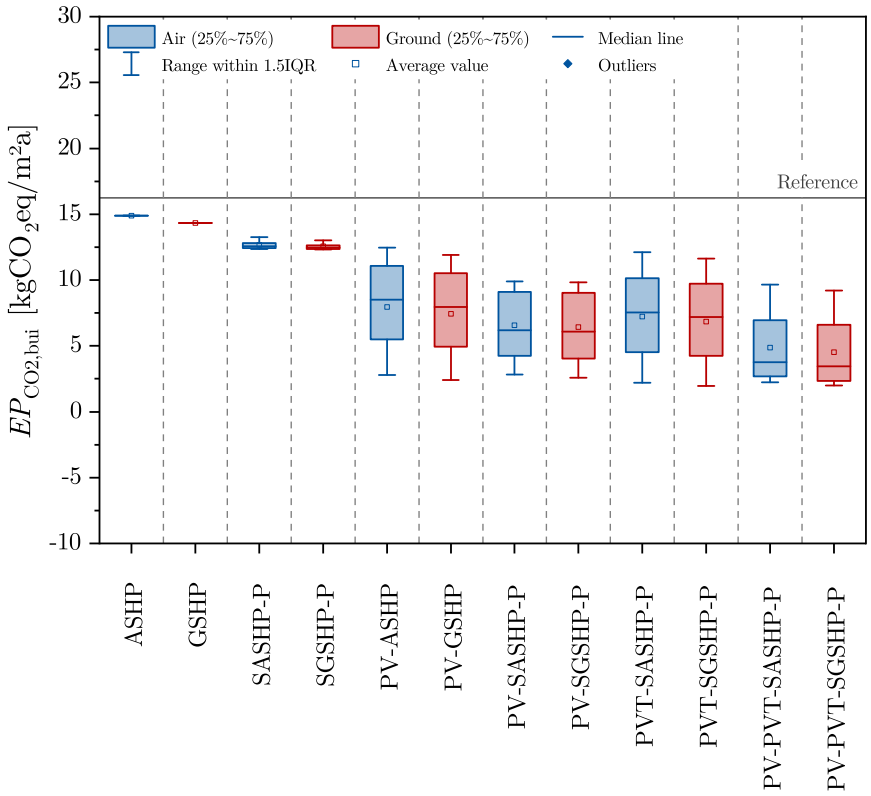

Figure 4.31: CO_2 emissions indicators of the building for different heat pump and SHP system concepts in Athens for SFH45.

tem concepts achieve lower CO_2 emissions indicators of the building than the reference building reaching fractional CO_2 emission savings up to 88 %. Basically, the results show that the minimum and maximum CO_2 emissions indicators in Athens are significantly lower in comparison to the SFH45 building in Strasbourg. The lower CO_2 emissions show the impact of higher total yearly irradiation and higher annual average ambient temperature on the CO_2 emissions indicators and as a result higher specific solar electrical yields, lower heating energy demands and slightly lower household electricity demands causing less CO_2 emissions. Comparing different concepts, the simulation results confirm that the CO_2 emissions indicators can only significantly be decreased by adding PV modules or PVT collectors, especially in combination with a battery storage. At this, the CO_2 emissions can be reduced by up to 76 % using battery storages in comparison to the corresponding system without battery storage.

Regarding the CO_2 emissions for SFH100 in Athens (cf. Figure 4.32), the CO_2 emissions indicators of the building for systems with ASHP are in the range of 3.87 kg CO_2eq/m^{2}a (PVT-SASHP-P) and 16.81 kg CO_2eq/m^{2}a (ASHP) and for systems with GSHP in the range of 3.34 kg CO_2eq/m^{2}a (PVT-SGSHP-P) and 16.01 kg CO_2eq/m^{2}a (GSHP). For comparison, the value of the reference building with conventional heating system is 20.33 kg CO_2eq/m^{2}a and, thus, all heat pump and SHP system concepts achieve lower CO_2 emissions indicators of the building than the reference building reaching fractional CO_2 emission savings up to 84 %. Basically, the results show that the minimum and maximum CO_2 emissions indicators for SFH100 in Athens are significantly lower in comparison to the SFH100 building in Strasbourg, but higher in comparison to the SFH45 building in Athens. As observed for Strasbourg, the maximum CO_2 emissions indicators of heat pump and SHP system concepts

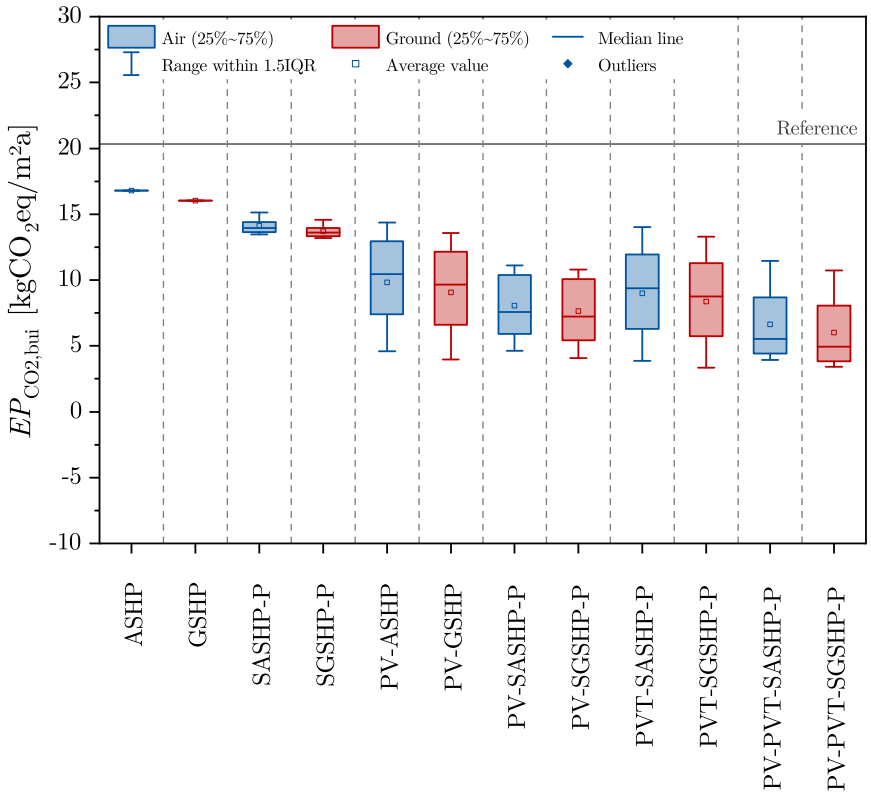

Figure 4.32: CO_2 emissions indicators of the building for different heat pump and SHP system concepts in Athens for SFH100.

for SFH45 in Athens are higher than the minimum CO_2 emissions indicators for SFH100 in Athens and thus, depending on the SHP system design, non-renovated existing buildings can also achieve lower CO_2 emissions than renovated buildings in warm climates. In addition, the lower CO_2 emissions in comparison to the SFH100 building in Strasbourg confirm the impact of higher total yearly irradiation and higher annual average ambient temperature on the CO_2 emissions indicators. Comparing different concepts, the simulation results also confirm that the CO_2 emissions indicators can only significantly be decreased by adding PV modules or PVT collectors, especially in combination with a battery storage. At this, the CO_2 emissions can be reduced by up to 65 % using battery storages in comparison to the corresponding system without battery storage.

In general, the main findings for Strasbourg can be confirmed for SFH45 and SFH100 in Athens with regard to the environmental impact. Comparing system concepts with ASHP and GSHP with regard to the CO_2 emissions for the SFH45 and SFH100 building in Athens, all SHP concepts with ASHP can reach the same or lower CO_2 emissions indicators than GSHP systems without integration of solar technologies or SGSHP-P systems, especially for system concepts with battery storage. As observed for Strasbourg, ASHP systems with PV or PVT can compete with GSHP systems with the same solar technology depending on the used PV module or PVT collector area and battery storage capacity. At this, the differences in CO_2 emissions indicators between systems with GSHP and ASHP are significantly lower for Athens in comparison to Strasbourg. This reflects the lower benefit of GSHPs for buildings in warm climates as figured out for the efficiency evaluation. In addition, solar thermal and heat pump concepts achieve also the highest minimum CO_2 emissions indicator values beside systems without solar technology integration, whereas systems with PVT

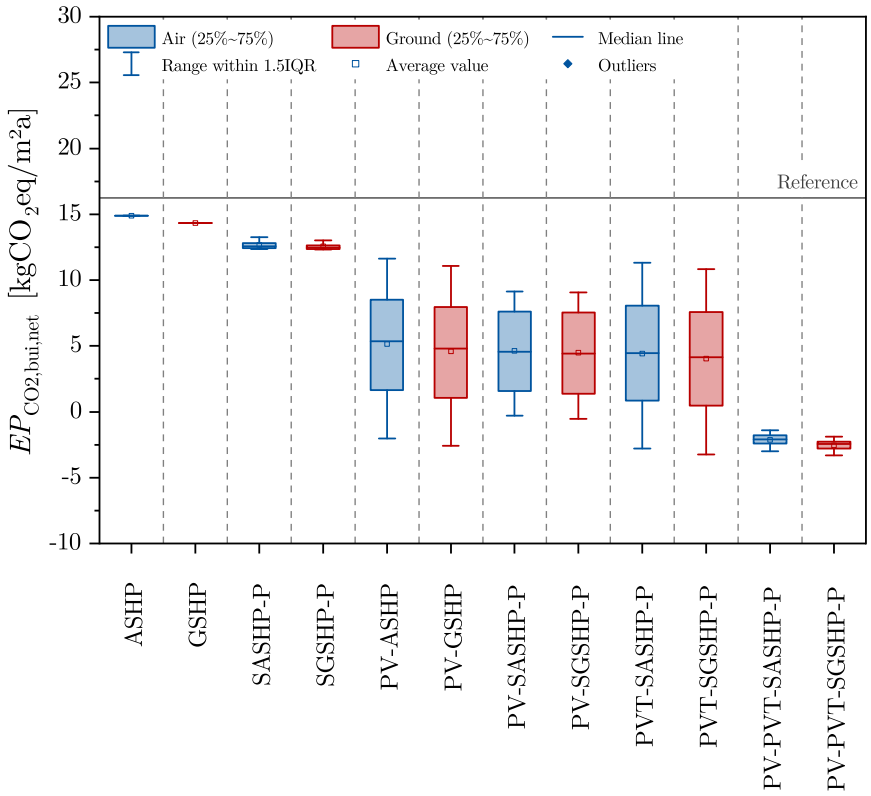

Figure 4.33: Net CO_2 emissions indicators of the building for different heat pump and SHP system concepts in Athens for SFH45.

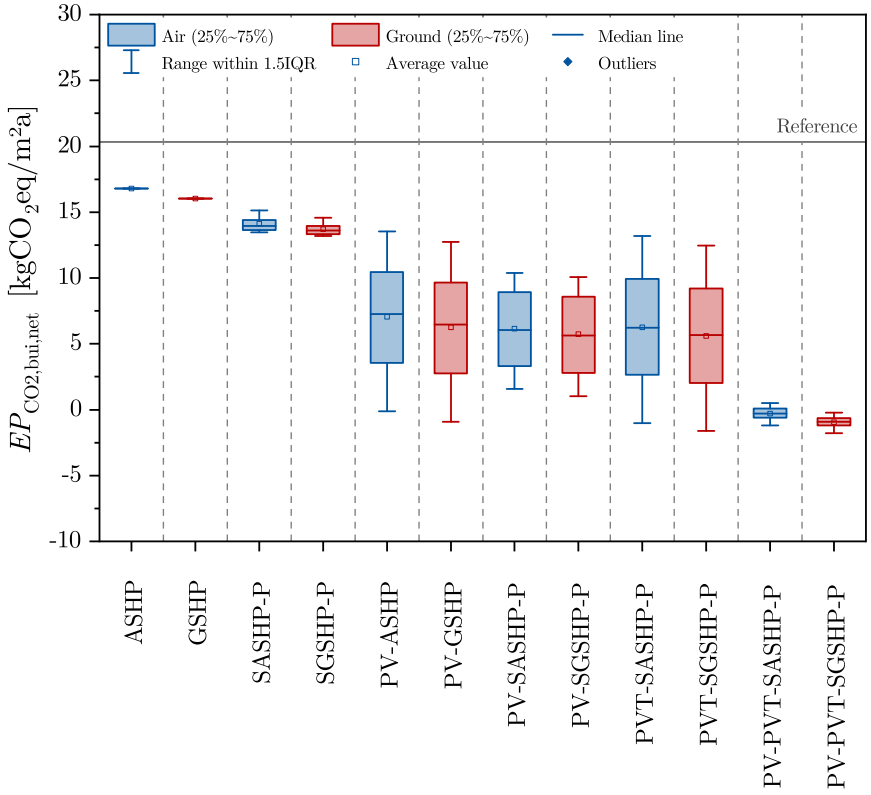

Figure 4.34: Net CO_2 emissions indicators of the building for different heat pump and SHP system concepts in Athens for SFH100.

collectors reach the lowest CO_2 emissions indicators for SFH45 and SFH100 in Athens. At this, the improvement by the use of PVT collectors instead of PV increases in comparison to Strasbourg reaching CO_2 emissions reductions up to 26 % depending on the building type, system concept, battery storage size and PV/PVT area. As observed for Strasbourg, the CO_2 emissions of system concepts with parallel FPCs can be decreased by the combination with PV, whereas general improvements by combining PV with system concepts with PVT collectors cannot be observed with regard to the CO_2 emissions indicators in comparison to the corresponding PVT and heat pump systems. Depending on the battery storage size (especially for low battery storage sizes or systems without battery storage), some combinations of parallel FPCs and PV modules achieve even slightly lower CO_2 emissions indicators than the corresponding systems with PV. Nevertheless, the minimum CO_2 emissions of PV-SASHP-P and PV-SGSHP-P systems are also slightly higher than those of the corresponding systems with PV modules instead of parallel FPCs.

An overview of the range of net CO_2 emissions indicators of the building for the different heat pump and SHP system concepts in Athens for SFH45 is shown in Figure 4.33 and for SFH100 in Figure 4.34. As observed for Strasbourg, the net CO_2 emissions indicators for systems with PV or PVT are slightly lower than the CO_2 emissions indicators due to the additional compensation by exported energy. In comparison to Strasbourg, the minimum and maximum net CO_2 emissions indicators in Athens are significantly lower reaching values below zero. Furthermore, it can be confirmed that the main differences between CO_2 emissions indicators and net CO_2 emissions indicators are the negative effects of battery storages on the net CO_2 emissions indicators due to the battery losses and, as described for Strasbourg, the missing exported solar electricity for the compensation of CO_2 emissions for delivered electrical energy from the grid. As a result, the net CO_2 emissions decrease with increasing FPC/PVT collector or PV module area, but increase with increasing battery storage capacity for all building types in Athens.

4.3.3.2 Cold Climates

Regarding cold climates, overviews of the range of CO_2 emissions indicators of the building for the different heat pump and SHP system concepts in Helsinki for SFH15, SFH45 and SFH100 are shown in Figure 4.35, Figure 4.36 and Figure 4.37. With regard to the CO_2 emissions for SFH15 in Helsinki (cf. Figure 4.35), the CO_2 emissions indicators of the building for systems with ASHP are in the range of 13.05 kg CO_2eq/m^{2}a (PVT-SASHP-P) and 22.91 kg CO_2eq/m^{2}a (ASHP), for systems with GSHP in the range of 9.89 kg CO_2eq/m^{2}a (PVT-SGSHP-P) and 19.47 kg CO_2eq/m^{2}a (GSHP) and for SISHP systems in the range of 10.60 kg CO_2eq/m^{2}a (PVT-SISHP-S) and 20.02 kg CO_2eq/m^{2}a (SISHP-S). For comparison, the value of the reference building with conventional heating system is 28.27 kg CO_2eq/m^{2}a and, thus, all heat pump and SHP system concepts achieve lower CO_2 emissions indicators of the building than the reference building reaching fractional CO_2 emission savings up to 65 %. Basically, the results show that the minimum and maximum CO_2 emissions indicators in Helsinki are significantly higher in comparison to the SFH15 building in Strasbourg, especially for systems with ASHP. The higher CO_2 emissions show the impact of lower annual average ambient temperatures and slightly lower total yearly irradiation on the CO_2 emissions indicators and as a result lower specific solar electrical yields, higher heating energy demands and slightly higher household electricity demands causing more CO_2 emissions. Comparing different concepts, the simulation results show that the CO_2 emissions indicators can only significantly be decreased by adding PV modules (only for systems with ASHP and

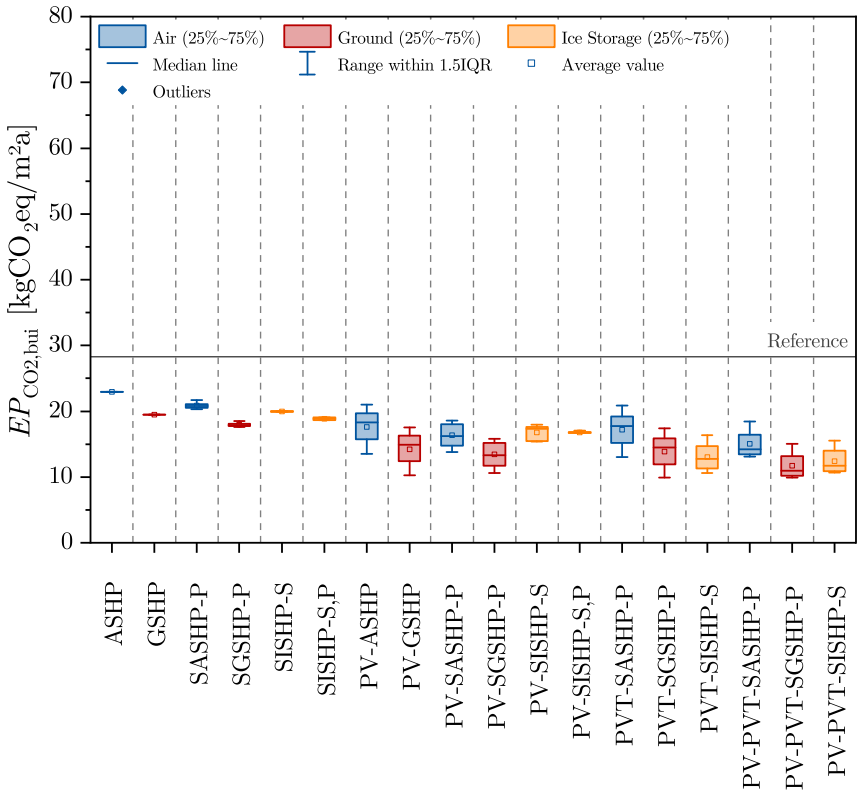

Figure 4.35: CO_2 emissions indicators of the building for different heat pump and SHP system concepts in Helsinki for SFH15.

GSHP in case of SFH15 in Helsinki) or PVT collectors (for all system concepts), especially in combination with a battery storage. At this, the CO_2 emissions can be reduced by up to 33 % using battery storages in comparison to the corresponding system without battery storage.

Regarding the CO_2 emissions for SFH45 in Helsinki (cf. Figure 4.36), the CO_2 emissions indicators of the building for systems with ASHP are in the range of 20.05 kg CO_2eq/m^{2}a (PV-PVT-SASHP-P) and 30.21 kg CO_2eq/m^{2}a (ASHP), whereas the CO_2 emissions indicators of the building for systems with GSHP are in the range of 13.43 kg CO_2eq/m^{2}a (PVT-SGSHP-P) and 23.18 kg CO_2eq/m^{2}a (GSHP). For comparison, the value of the reference building with conventional heating system is 41.19 kg CO_2eq/m^{2}a and, thus, all heat pump and SHP system concepts achieve lower CO_2 emissions indicators of the building than the reference building reaching fractional CO_2 emission savings up to 67 %. Basically, the results show that the minimum and maximum CO_2 emissions indicators for SFH45 in Helsinki are significantly higher in comparison to the SFH45 building in Strasbourg and the SFH15 building in Helsinki, especially for systems with ASHP. As observed for Strasbourg, the maximum CO_2 emissions indicators of heat pump and SHP system concepts for SFH15 in Helsinki are higher than the minimum CO_2 emissions indicators for SFH45 in Helsinki, especially for systems with GSHP, and thus, depending on the SHP system design, renovated buildings can partially achieve lower CO_2 emissions than new buildings with very high energetic quality, even in cold climates. In addition, the higher CO_2 emissions in comparison to the SFH45 building in Strasbourg confirm the impact of lower annual average ambient temperatures and slightly lower total yearly irradiation on the CO_2 emissions indicators. Comparing different concepts, the simulation results confirm that the CO_2 emissions indica-

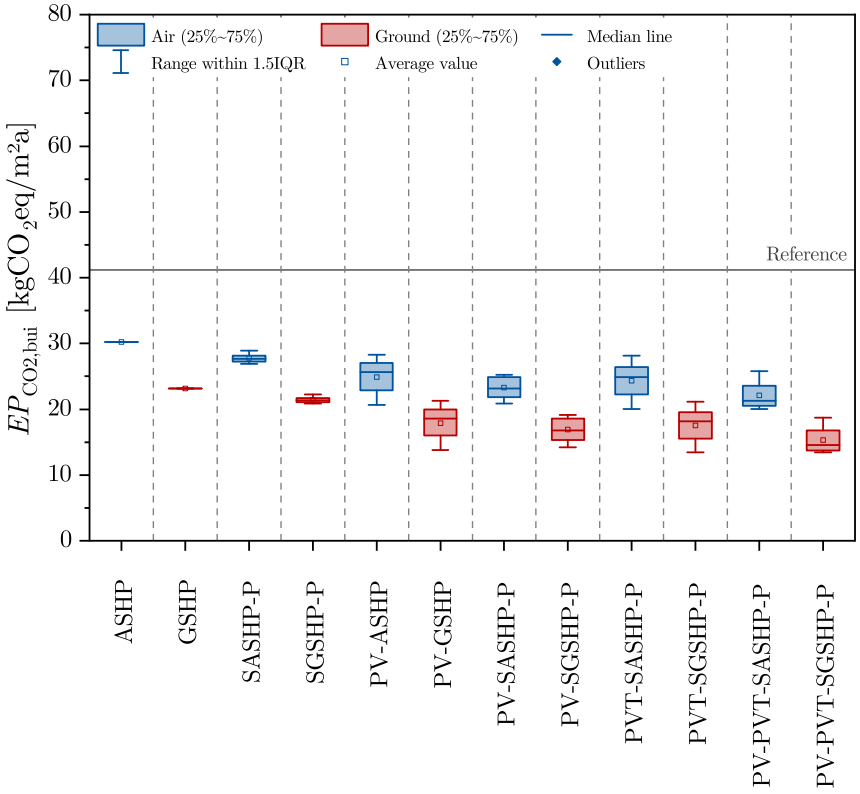

Figure 4.36: CO_2 emissions indicators of the building for different heat pump and SHP system concepts in Helsinki for SFH45.

tors can only significantly be decreased by adding PV modules or PVT collectors, especially in combination with a battery storage. At this, the CO_2 emissions can be reduced by up to 27 % using battery storages in comparison to the corresponding system without battery storage.

Regarding the CO_2 emissions for SFH100 in Helsinki (cf. Figure 4.37), the CO_2 emissions indicators of the building for systems with ASHP are in the range of 34.65 kg CO_2eq/m^{2}a (PVT-SASHP-P) and 45.17 kg CO_2eq/m^{2}a (ASHP) and for systems with GSHP in the range of 23.10 kg CO_2eq/m^{2}a (PVT-SGSHP-P) and 33.21 kg CO_2eq/m^{2}a (GSHP). For comparison, the value of the reference building with conventional heating system is 62.89 kg CO_2eq/m^{2}a and, thus, all heat pump and SHP system concepts achieve lower CO_2 emissions indicators of the building than the reference building reaching fractional CO_2 emission savings up to 63 %. Basically, the results show that the minimum and maximum CO_2 emissions indicators for SFH100 in Helsinki are significantly higher in comparison to the SFH100 building in Strasbourg and the SFH15 and SFH45 building in Helsinki, especially for systems with ASHP. In contrast to Strasbourg, the maximum CO_2 emissions indicators of heat pump and SHP system concepts for SFH45 in Helsinki are lower in case of systems with ASHP or only slightly higher (0.08 kg CO_2eq/m^{2}a) in case of systems with GSHP than the minimum CO_2 emissions indicators for SFH100 and thus, non-renovated existing buildings cannot (or hardly) achieve lower CO_2 emissions than renovated buildings (or even new buildings with lower CO_2 emissions) in cold climates (for the same heat source). In addition, the higher CO_2 emissions in comparison to the SFH100 building in Strasbourg also confirm the impact of lower annual average ambient temperatures and slightly lower total yearly irradiation on the CO_2 emissions indicators. Comparing different concepts, the simulation results also

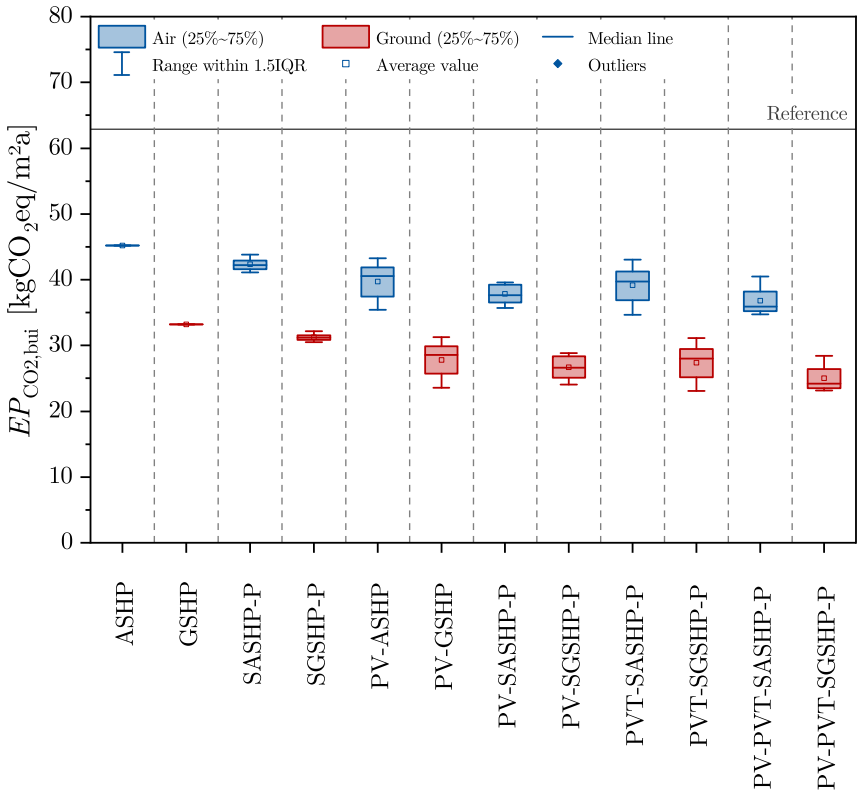

Figure 4.37: CO_2 emissions indicators of the building for different heat pump and SHP system concepts in Helsinki for SFH100.

confirm that the CO_2 emissions indicators can only significantly be decreased by adding PV modules or PVT collectors, especially in combination with a battery storage. At this, the CO_2 emissions can be reduced by up to 17 % using battery storages in comparison to the corresponding system without battery storage.

In general, the main findings for Strasbourg can be confirmed for SFH15, SFH45 and SFH100 in Helsinki with regard to the environmental impact. Comparing system concepts with ASHP and GSHP with regard to the CO_2 emissions, PV-ASHP, PV-SASHP-P, PVT-SASHP-P and PV-PVT-SASHP-P systems can reach the same or lower CO_2 emissions indicators than GSHP systems without integration of solar technologies or SGSHP-P systems, especially for system concepts with battery storage, for SFH15 in Helsinki. In case of SFH45 in Helsinki, PV-ASHP, PV-SASHP-P, PVT-SASHP-P and PV-PVT-SASHP-P systems can reach nearly the same or slightly lower CO_2 emissions indicators than GSHP systems without integration of solar technologies or SGSHP-P systems, whereas all SHP system concepts with ASHP achieve higher CO_2 emissions than systems with GSHP for SFH100 in Helsinki. In contrast to Strasbourg, ASHP systems with PV or PVT can compete with GSHP systems with the same solar technology depending on the used PV module or PVT collector area and battery storage capacity for SFH15, but can hardly (SFH45) or not (SFH100) compete with GSHP systems with the same solar technology for SFH45 and SFH100. Thus, the results show the higher benefit of GSHPs for buildings in cold climates with high heating energy demand and low annual average ambient temperature, even for the environmental impact. In addition, as observed for Strasbourg, solar thermal and heat pump concepts achieve also the highest minimum CO_2 emissions indicator values beside systems without solar technology integration, whereas systems with PVT collectors reach

the lowest CO_2 emissions indicators for all building types in Helsinki. In case of SFH45, PV-PVT-SASHP-P systems achieve slightly lower CO_2 emissions than PVT-SASHP-P systems, but only 0.01 kg CO_2eq/m^{2}a. Nevertheless, general improvements by combining PV with system concepts with PVT collectors cannot be observed with regard to the environmental impact in comparison to the corresponding PVT and heat pump systems. Furthermore, the improvement by the use of PVT collectors instead of PV decreases in comparison to Strasbourg for systems with ASHP and GSHP reaching CO_2 emissions reductions up to 6 % depending on the building type, system concept, battery storage size and PV/PVT area. Regarding systems with ice storage for SFH15, especially PVT-SISHP-S systems reaching low CO_2 emissions indicators between 10.60 kg CO_2eq/m^{2}a and 16.33 kg CO_2eq/m^{2}a can compete with SHP systems with ASHP or GSHP with regard to the environmental impact. As observed for Strasbourg, the CO_2 emissions of system concepts with parallel FPCs can be decreased by the combination with PV. Depending on the battery storage size (especially for low battery storage sizes or systems without battery storage), some combinations of parallel FPCs and PV modules achieve even slightly lower CO_2 emissions indicators than the corresponding systems with PV. Nevertheless, the minimum CO_2 emissions of PV-SASHP-P, PV-SGSHP-P and PV-SISHP-S,P (SFH15) systems are also slightly higher than those of the corresponding systems with PV modules instead of parallel FPCs.

An overview of the range of net CO_2 emissions indicators of the building for the different heat pump and SHP system concepts in Helsinki for SFH15 is shown in Figure 4.38, for SFH45 in Figure 4.39 and for SFH100 in Figure 4.40. As observed for Strasbourg, the net CO_2 emissions indicators for systems with PV or PVT are slightly lower than the CO_2

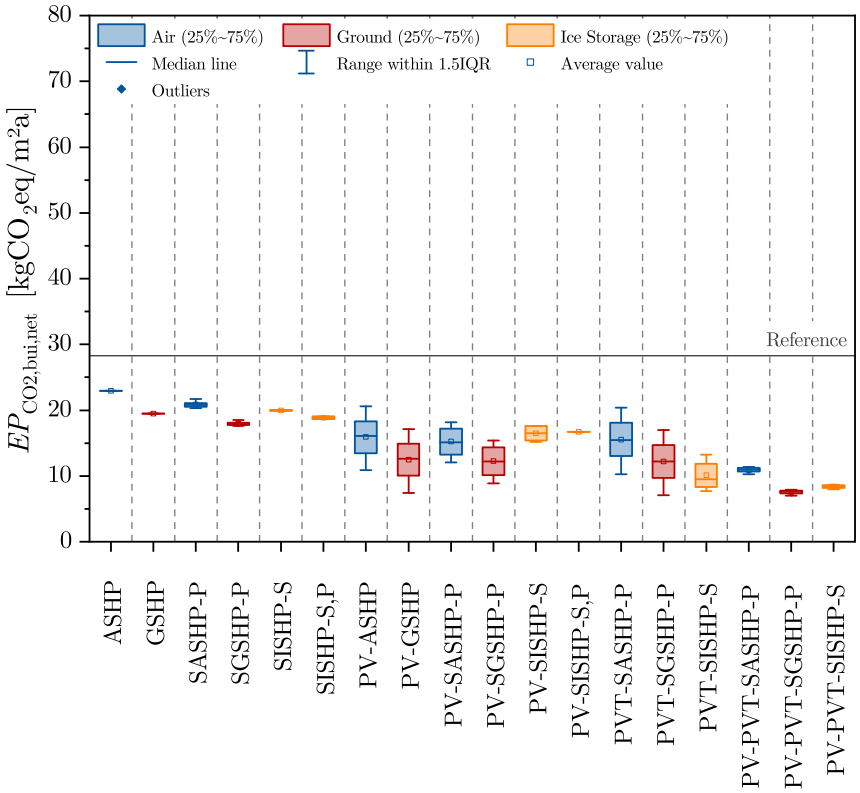

Figure 4.38: Net CO_2 emissions indicators of the building for different heat pump and SHP system concepts in Helsinki for SFH15.

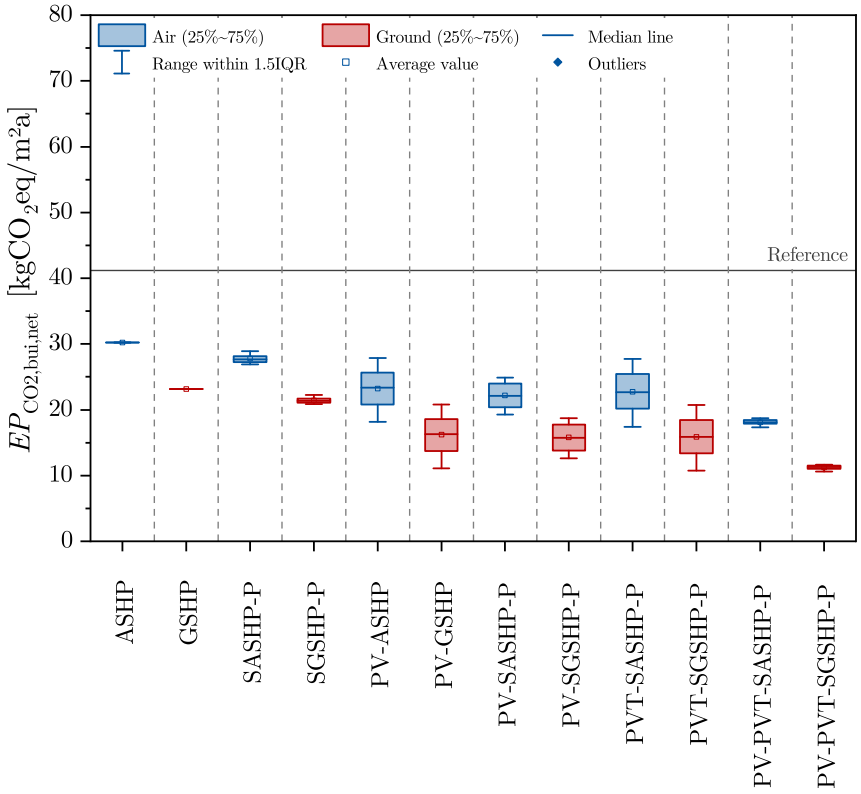

Figure 4.39: Net CO_2 emissions indicators of the building for different heat pump and SHP system concepts in Helsinki for SFH45.

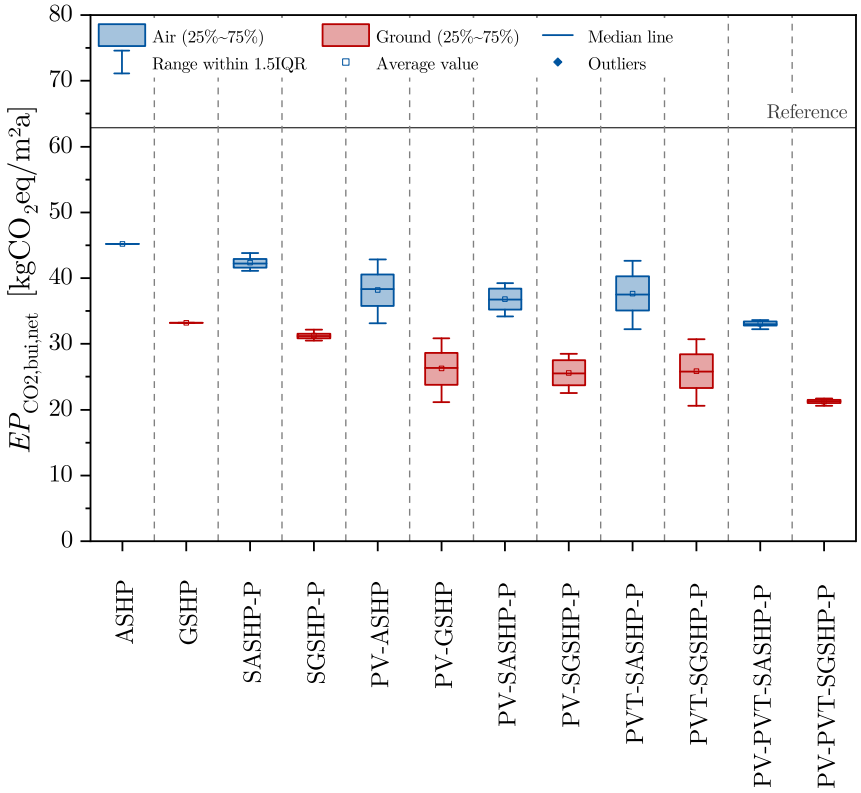

Figure 4.40: Net CO_2 emissions indicators of the building for different heat pump and SHP system concepts in Helsinki for SFH100.

emissions indicators due to the additional compensation by exported energy. In comparison to Strasbourg, the minimum and maximum net CO_2 emissions indicators in Helsinki are significantly higher. Furthermore, it can be confirmed that the main differences between CO_2 emissions indicators and net CO_2 emissions indicators are the negative effects of battery storages on the net CO_2 emissions indicators due to the battery losses and, as described for Strasbourg, the missing exported solar electricity for the compensation of CO_2 emissions for delivered electrical energy from the grid. As a result, the net CO_2 emissions decrease with increasing FPC/PVT collector or PV module area, but increase with increasing battery storage capacity for all building types in Helsinki.

4.3.4 Summary

The following general conclusions on the environmental impact can be given for the climates of Strasbourg, Athens and Helsinki:

- All heat pump and SHP system concepts achieve lower CO_2 emissions indicators of the building than the reference buildings with conventional gas-fired heating system reaching fractional CO_2 emission savings up to 88 %. At this, the fractional CO_2 emission savings decrease for locations with lower total yearly irradiation and lower annual average ambient temperature.

- The CO_2 emissions indicators can only significantly be decreased by adding PV modules (for systems with ASHP and GSHP and in case of SFH15 in moderate climates for systems with ice storage) or PVT collectors (for all system concepts), especially in combination with a battery storage. Heat pump as well as solar thermal and heat pump systems cannot compete with system concepts with PV or PVT integration, especially with battery storage. Furthermore, systems with PV reach lower CO_2 emissions than systems with the same parallel FPC area, even without battery storage. This illustrates the benefit of on-site generated solar electrical energy, which can be used to cover both SHP and household electricity consumption.

- The CO_2 emissions decrease with increasing FPC/PVT collector or PV module area.

- Battery storages have a major impact on the environmental impact of a building in systems with PV or PVT, especially with regard to the CO_2 emissions indicators. At this, the CO_2 emissions decrease with increasing battery storage capacity and the reduction of CO_2 emissions by adding a battery storage increases with increasing PV module or PVT collector area, whereas the net CO_2 emissions increase with increasing battery storage capacity due to the battery losses and the missing exported solar electricity for the compensation of CO_2 emissions for delivered electrical energy from the grid. The reductions of CO_2 emissions by the use of battery storages in comparison to the corresponding systems without battery storage are up to 45 % (SFH15), 39 % (SFH45) and 29 % (SFH100) in moderate climates, up to 76 % (SFH45) and 65 % (SFH100) in warm climates and up to 33 % (SFH15), 27 % (SFH45) and 17 % (SFH100) in cold climates.

- The net CO_2 emissions indicators for systems with PV or PVT are slightly lower than the CO_2 emissions indicators due to the additional compensation by exported energy.

- Heat pump and SHP systems with GSHP reach lower CO_2 emissions in comparison with corresponding system concepts with ASHP or ice storage.

- SISHP-S systems achieve lower CO_2 emissions than ASHP systems without integration of solar technologies and SISHP-S,P systems achieve even lower CO_2 emissions than those of GSHP systems without integration of solar technologies for SFH15 and SFH45. PVT-SISHP-S systems reach the lowest CO_2 emissions of all system concepts with ice storage, reach lower CO_2 emissions than all system concepts with ASHP and can even compete with systems with GSHP.

- The minimum and maximum CO_2 emissions indicators of the building increase for locations with lower total yearly irradiation and lower annual average ambient temperature.

- The CO_2 emissions of system concepts with parallel FPCs can be decreased by the combination with PV, whereas general improvements by combining PV with system concepts with PVT collectors cannot be observed with regard to the CO_2 emissions indicators in comparison to the corresponding PVT and heat pump systems. Depending on the battery storage size (especially for low battery storage sizes or systems without battery storage), some combinations of parallel FPCs and PV modules achieve even slightly lower CO_2 emissions indicators than the corresponding systems with PV. Nevertheless, the minimum CO_2 emissions of PV-SASHP-P, PV-SGSHP-P and PV-SISHP-S,P systems are slightly higher than those of the corresponding systems with PV modules instead of parallel FPCs.

- Systems with PVT benefit primarily from the use of solar electricity with regard to the reduction of CO_2 emissions of a building. Especially for SISHP concepts, in which the PVT collectors replace the required WISC collectors, the results illustrate the benefit of combined generation of heat and electricity by PVT collectors for limited roof areas.

- Systems with PVT collectors achieve the lowest CO_2 emissions indicators. At this, PV and heat pump systems achieve (slightly) higher CO_2 emissions indicators than systems with PVT collectors in case of systems with ASHP and GSHP, whereas system concepts with PVT collectors reach by far the best results for systems with ice storage, especially for SFH45 and SFH100 in moderate climates and SFH15 in cold climates. For systems with ASHP and GSHP, the improvement by the use of PVT collectors instead of PV increases for warm climates and decreases for cold climates in comparison to moderate climates. Depending on the building type, system concept, battery storage size and PV/PVT area, the CO_2 emissions of systems with ASHP or GSHP can be decreased by up to 12 % in moderate climates, up to 26 % in warm climates and up to 6 % in cold climates for systems with PVT in comparison to the corresponding systems with PV.

- With the exception of SFH45 and SFH100 in cold climates, PV-ASHP, PV-SASHP-P, PVT-SASHP-P and PV-PVT-SASHP-P systems can reach the same or lower CO_2 emissions than GSHP systems without integration of solar technologies or SGSHP-P systems, especially for system concepts with battery storage. In case of SFH45 in cold climates, PV-ASHP, PV-SASHP-P, PVT-SASHP-P and PV-PVT-SASHP-P systems can reach nearly the same or slightly lower CO_2 emissions indicators than GSHP systems without integration of solar technologies or SGSHP-P systems, whereas all

SHP system concepts with ASHP achieve higher CO_2 emissions than systems with GSHP for SFH100 in cold climates. ASHP systems with PV or PVT can even compete with GSHP systems with the same solar technology in warm and moderate climates and for SFH15 in cold climates, depending on the used PV module or PVT collector area and battery storage capacity. However, ASHP systems with PV or PVT can hardly (SFH45) or not (SFH100) compete with GSHP systems with the same solar technology for SFH45 and SFH100 in cold climates. Regarding warm climates, the differences in CO_2 emissions indicators between systems with GSHP and ASHP are significantly lower in comparison to moderate climates. Furthermore, for moderate climates it can be observed that the differences in CO_2 emissions indicators between systems with GSHP and ASHP are significantly higher for SFH100 in comparison to SFH15. Thus, the results also reflect the higher benefit of GSHPs for buildings with high heating energy demand and locations with low annual average ambient temperature, even for the environmental impact.

- The minimum CO_2 emissions indicators of SFH100 are higher in comparison to the SFH15 and SFH45 building and the minimum CO_2 emissions indicators of SFH15 are lower in comparison to the SFH45 building. Nevertheless, depending on the SHP system design, renovated buildings can partially achieve lower CO_2 emissions than new buildings with very high energetic quality for moderate and cold climates and non-renovated existing buildings can partially achieve lower CO_2 emissions than renovated buildings for moderate climates and warm climates and can even achieve lower CO_2 emissions than new buildings with very high energetic quality in some cases for moderate climates. In contrast, non-renovated existing buildings cannot (or hardly for systems with GSHP) achieve lower CO_2 emissions than renovated buildings (or even new buildings with lower CO_2 emissions) in cold climates (for the same heat source).

The results illustrate that there are some general findings, but the system concepts compete with each other and have to be compared for the considered use case to identify the best system concept with regard to the environmental impact. With regard to the comparison of different SHP concepts with or without battery storage, the environmental impact analysis shows especially the importance to use the CO_2 emissions indicators instead of the net CO_2 emissions indicators to assess the local environmental impact of a building without compensation by exported energy.

4.4 Economic Efficiency

This section presents the *economic efficiency evaluation* of the considered SHP systems in this work. The objective of this evaluation is the comparison of SHP system concepts for a wide range of boundary conditions in order to identify economically efficient SHP system solutions for the energy supply of residential buildings. At this, it is useful to compare SHP systems with a reference building with conventional gas-fired heating system as described for the environmental impact evaluation in Section 4.3. The LCOEn is chosen as main KPI for the rating of the economic efficiency of the thermal and electrical energy supply of a building, whereas:

- the levelized cost of heat and electricity for a building with SHP system without conventional auxiliary heating systems (F_t=0) considering the net household electricity

consumption costs $LCOEn_{\text{bui}}^{\text{SHP}}$ is used for the comparison of different heat pump and SHP system concepts and

- the levelized cost of heat and electricity for a building with conventional heating system without PV and subsidies $LCOEn_{\text{bui}}^{\text{ref}}$ including the fuel costs of the system and the net household electricity consumption costs is used as reference value.

As described in Section 4.2, the SFH45 building in Strasbourg is used as base case. The evaluation of the base case is followed by the analysis of the influence of different building types and climates on the results. The general boundary conditions for the economic efficiency comparisons of SHP systems within this section are summarized in Table 4.7. For a better international comparability, subsidies are not considered and all prices are net values excluding VAT. Furthermore, the real discount rate is set to zero for single-family buildings as described in Section 2.4.3 and inflation as well as price increase rates are assumed to be zero. As described in Section 3.3.7, shut-off times of the heat pump by utilities are not considered in this work and therefore electricity tariffs for heat pumps are not taken into account for the economic efficiency evaluations.

Table 4.7: Boundary conditions for economic efficiency calculations (all costs are net values excluding VAT).

Parameter	Value	Parameter	Value
$c_{\text{el,SHP}}$	0.1853 €/kWh [Eurostat, 2021a]	$S_{0,\text{th}}^{\text{SHP}}$	0 € (no subsidies)
$c_{\text{el,hh}}$	0.1853 €/kWh [Eurostat, 2021a]	$M_{t,\text{th}}^{\text{SHP}}$	$1\,\% \cdot I_{0,\text{th}}^{\text{SHP}}$
d_{el}	0 %	M_{t}^{ref}	$1\,\% \cdot I_{0}^{\text{ref}}$
$c_{\text{el,feedin}}$	0.0703 €/kWh [a]	$S_{0,\text{el}}^{\text{SHP}}$	0 € (no subsidies)
c_{gas}	0.0410 €/kWh [Eurostat, 2021b]	$O_{t,\text{el}}^{\text{SHP}}$	$0.5\,\% \cdot I_{0,\text{el}}^{\text{SHP}}$
d_{gas}	0 %	$M_{t,\text{el}}^{\text{SHP}}$	$0.5\,\% \cdot I_{0,\text{el}}^{\text{SHP}}$
r	0 %	T	20 a

[a] Based on the feed-in tariff for PV systems in Germany on November 1st, 2021 [Bundesnetzagentur, 2021].

The initial investment costs of SHP systems are divided into investment costs related to the thermal ($I_{0,\text{th}}^{\text{SHP}}$) and electrical part ($I_{0,\text{el}}^{\text{SHP}}$) of the SHP system including different system components based on the considered SHP system. Table 4.9 contains cost function definitions for the investment costs of different system components based on market available products, offers from installers, online stores and additional assumptions, e.g. for installation costs. More details on the constituent elements of the cost functions are summarized in Appendix B. The assignment of the cost functions to different heat pump and SHP system concepts is given in Table 4.8. Furthermore, the initial investment costs of conventional gas-fired heating systems as reference heating systems are calculated with:

$$I_0^{\text{ref}} = I_{0,\text{ref,gas}} + I_{0,\text{buffer}}, \tag{4.1}$$

where $I_{0,\text{ref,gas}}$ are the initial investment costs of the reference gas-fired boilers and $I_{0,\text{buffer}}$ are the initial investment costs of buffer storages including DHW heat exchanger. At this, the buffer storage volumes are assumed to be 500 l for the reference heating systems.

Table 4.8: Assignment of cost functions to different SHP system concepts.

	$I_{0,\mathrm{th}}^{\mathrm{SHP}}$									$I_{0,\mathrm{el}}^{\mathrm{SHP}}$		
	$I_{0,\mathrm{HP,BW}}$	$I_{0,\mathrm{HP,AW}}$	$I_{0,\mathrm{BHE}}$	$I_{0,\mathrm{ice}}$	$I_{0,\mathrm{buffer}}$	$I_{0,\mathrm{WISC}}$	$I_{0,\mathrm{FPC}}$	$I_{0,\mathrm{PVT}}$ [a]	$I_{0,\mathrm{parallel}}$	$I_{0,\mathrm{PV}}$	$I_{0,\mathrm{PVT}}$ [a]	$I_{0,\mathrm{bat}}$
ASHP	-	x	-	-	x	-	-	-	-	-	-	-
GSHP	x	-	x	-	x	-	-	-	-	-	-	-
SASHP-P	-	x	-	-	x	-	x	-	x	-	-	-
SGSHP-P	x	-	x	-	x	-	x	-	x	-	-	-
SISHP-S	x	-	-	x	x	x	-	-	-	-	-	-
SISHP-S,P	x	-	-	x	x	x	x	-	x	-	-	-
PV-ASHP	-	x	-	-	x	-	-	-	-	x	-	x [c]
PV-GSHP	x	-	x	-	x	-	-	-	-	x	-	x [c]
PV-SASHP-P	-	x	-	-	x	-	x	-	x	x	-	x [c]
PV-SGSHP-P	x	-	x	-	x	-	x	-	x	x	-	x [c]
PV-SISHP-S	x	-	-	x	x	x	-	-	-	x	-	x [c]
PV-SISHP-S,P	x	-	-	x	x	x	x	-	x	x	-	x [c]
PVT-SASHP-P	-	x	-	-	x	-	-	50 % [b]	x	-	50 % [b]	x [c]
PVT-SGSHP-P	x	-	x	-	x	-	-	50 % [b]	x	-	50 % [b]	x [c]
PVT-SISHP-S	x	-	-	x	x	-	-	50 % [b]	-	-	50 % [b]	x [c]
PV-PVT-SASHP-P	-	x	-	-	x	-	-	50 % [b]	x	x	50 % [b]	x [c]
PV-PVT-SGSHP-P	x	-	x	-	x	-	-	50 % [b]	x	x	50 % [b]	x [c]
PV-PVT-SISHP-S	x	-	-	x	x	-	-	50 % [b]	-	x	50 % [b]	x [c]

[a] Depending on the considered PVT technology, $I_{0,\mathrm{PVT}}$ is equal to $I_{0,\mathrm{PVT,WISC}}$ or $I_{0,\mathrm{PVT,covered}}$.

[b] The costs of PVT collectors are divided equally into thermal and electrical system costs.

[c] The costs of battery storages are only considered if the analyzed system concept includes a battery storage.

Table 4.9: Cost functions of investment costs for different system components based on market prices and assumptions in Appendix B (all costs are net values excluding VAT).

Component/System	Cost function [a]
Brine/water heat pumps	$I_{0,\mathrm{HP,BW}} = 12\,634\,€ + 224.81\,€/\mathrm{kW} \cdot \dot{Q}_{\mathrm{HP,nom}}$
Air/water heat pumps	$I_{0,\mathrm{HP,AW}} = 13\,216\,€ + 331.80\,€/\mathrm{kW} \cdot \dot{Q}_{\mathrm{HP,nom}}$
Reference gas-fired boilers	$I_{0,\mathrm{ref,gas}} = 9\,908\,€ + 32.14\,€/\mathrm{kW} \cdot \dot{Q}_{\mathrm{ref,nom}}$ [b]
BHEs	$I_{0,\mathrm{BHE}} = 1\,580\,€ + 53.50\,€/\mathrm{m} \cdot n_{\mathrm{BHE}}\, l_{\mathrm{BHE}}$
Ice storages	$I_{0,\mathrm{ice}} = 5\,991\,€ + 561.80\,€/\mathrm{m}^3 \cdot V_{\mathrm{ice}}$
Buffer storages including DHW heat exchanger	$I_{0,\mathrm{buffer}} = 2\,583\,€ + 584.46\,€/\mathrm{m}^3 \cdot V_{\mathrm{buffer}}$
WISC collectors	$I_{0,\mathrm{WISC}} = 282\,€ + 352.59\,€/\mathrm{m}^2 \cdot A_{\mathrm{WISC}}$
FPC collectors	$I_{0,\mathrm{FPC}} = 263\,€ + 300.83\,€/\mathrm{m}^2 \cdot A_{\mathrm{FPC}}$
WISC PVT collectors	$I_{0,\mathrm{PVT,WISC}} = 1\,721\,€ + 472.64\,€/\mathrm{m}^2 \cdot A_{\mathrm{PVT,WISC}}$
Covered flat-plate PVT collectors	$I_{0,\mathrm{PVT,covered}} = 1\,721\,€ + 642.36\,€/\mathrm{m}^2 \cdot A_{\mathrm{PVT,covered}}$
Parallel integration of FPC and PVT collectors	$I_{0,\mathrm{parallel}} = 3\,820\,€$
PV	$I_{0,\mathrm{PV}} = 1\,632\,€ + 171.69\,€/\mathrm{m}^2 \cdot A_{\mathrm{PV}}$
Battery Storages	$I_{0,\mathrm{bat}} = 3\,842\,€ + 363.21\,€/\mathrm{kWh} \cdot C_{\mathrm{bat}}$

[a] Component and system costs include hydraulic and electrical components, accessories, installation and additional costs like earthwork or approvals. For details see Appendix B.

[b] The nominal heating power of the reference gas-fired boiler $\dot{Q}_{\mathrm{ref,nom}}$ is set to the design heat load for space heating from Table 3.13 of the considered location and building with a minimum value of 11 kW assumed for the minimum size of a market-available gas-fired boiler.

4.4.1 Base Case: Strasbourg SFH45

An overview of the range of LCOEn values for the SFH45 building with different heat pump and SHP system concepts in Strasbourg is shown in Figure 4.41. For systems with ASHP, the LCOEn is in the range of 0.1837 €/kWh (PV-ASHP) and 0.2820 €/kWh (PVT-SASHP-P), for systems with GSHP in the range of 0.1930 €/kWh (PV-GSHP) and 0.2927 €/kWh (PVT-SGSHP-P) and for SISHP systems in the range of 0.2551 €/kWh (PV-SISHP-S) and 0.3320 €/kWh (PVT-SISHP-S). For comparison, the value of the reference building with conventional heating system is 0.1636 €/kWh and, thus, all heat pump and SHP system concepts achieve higher LCOEn values than the reference building. At this, systems with ASHP achieve the lowest LCOEn values, whereas systems with GSHP achieve slightly higher values and systems with ice storage achieve by far the highest LCOEn values. These results illustrate that the higher initial investment costs for systems with GSHP and especially systems with ice storage cannot be compensated by the reduction of delivered electrical energy to the building due to the higher energy efficiency of the systems in comparison to the corresponding systems with ASHP. Comparing different system concepts with regard to the used solar technologies, the simulation results show that the LCOEn can only be decreased in some cases by adding PV modules in comparison to heat pump systems without

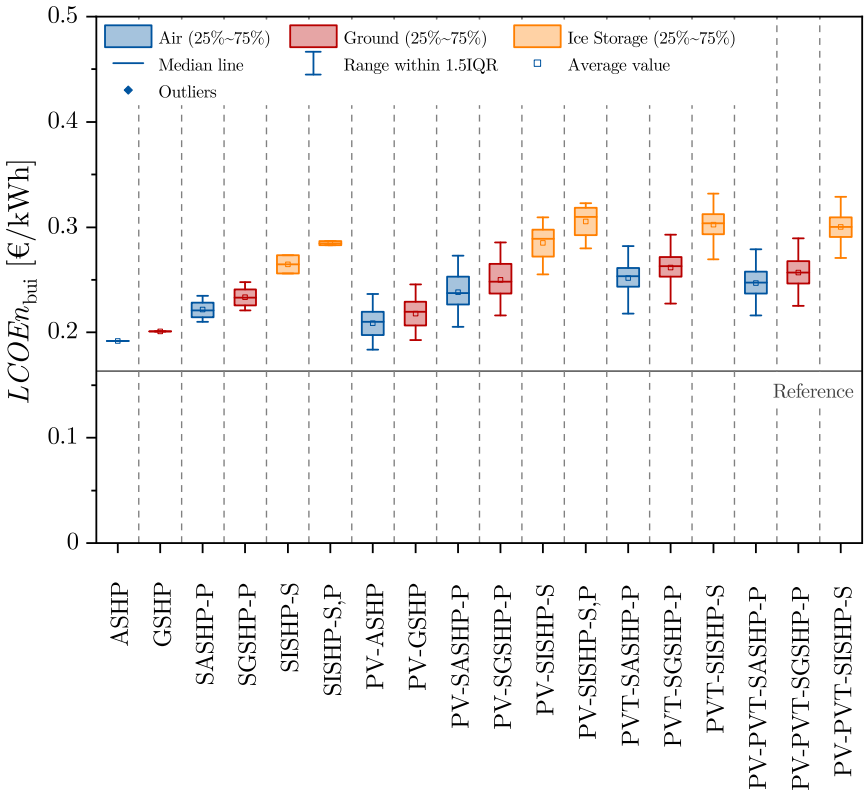

Figure 4.41: LCOEn for the SFH45 building with different heat pump and SHP system concepts in Strasbourg.

solar technologies. All other SHP system concepts reach higher LCOEn values than heat pump systems without solar technologies. PVT and heat pump concepts achieve the highest LCOEn values, whereas PV and heat pump systems and PV-SISHP-S systems in case of systems with ice storage achieve the lowest LCOEn values. At this, solar thermal and heat pump systems achieve lower minimum LCOEn values than PVT and heat pump systems. In addition, the LCOEn values are higher for SHP system concepts with battery storage in comparison to the same SHP system concept without battery storage (cf. Figure 4.42). At this, the LCOEn increases with increasing battery storage capacity. This means that the higher initial investment costs for battery storages cannot be compensated by the reduction of delivered electrical energy to the building due to the higher self-sufficiency by the use of battery storages. Moreover, in case of solar thermal and heat pump systems, the LCOEn increases with increasing FPC area in case of systems with GSHP and ASHP and with increasing WISC collector area in case of SISHP-S systems, whereas the LCOEn of PV and heat pump system concepts decreases with increasing PV module area. Furthermore, in case of SISHP-S,P systems, the LCOEn decreases with increasing FPC area. Depending on the used PV module area and battery storage capacity, the LCOEn values of solar thermal and heat pump systems can be decreased by the combination with PV, but the LCOEn also increases for some cases, especially with high battery storage capacities. In case of PVT and heat pump systems, the results are more diverse. In most cases, the LCOEn increases with increasing PVT collector area, but in some cases with battery storage the LCOEn first decreases slightly with increasing PVT collector area and then increases for larger PVT areas. Depending on the used PV module area, the LCOEn of PVT and heat pump system concepts can also slightly be decreased by the combination with PV. At this,

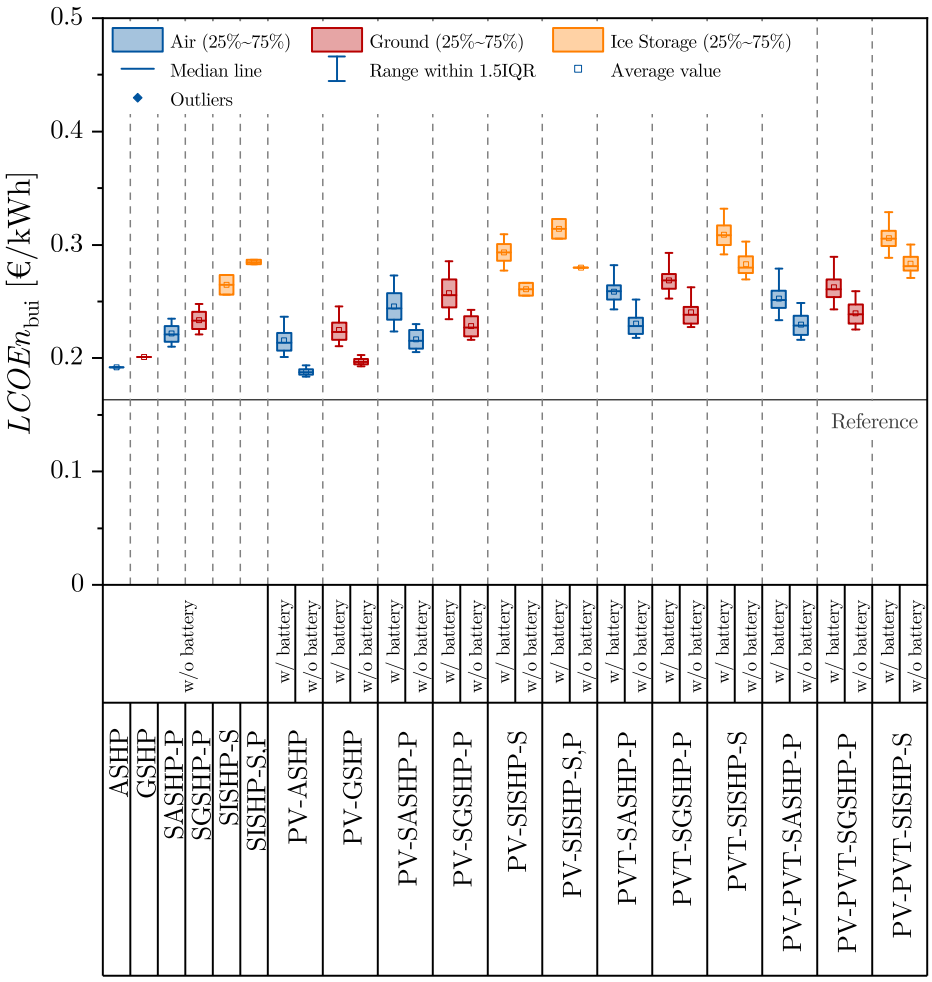

Figure 4.42: LCOEn for the SFH45 building with different heat pump and SHP system concepts with and without battery storage in Strasbourg.

and in case of PV plus solar thermal and heat pump system concepts, the LCOEn decreases with increasing PV module area which illustrates the better economic efficiency of PV in comparison to solar thermal or PVT collectors in case of SFH45 in moderate climates.

4.4.2 Influence of Building Type

Overviews of the range of LCOEn values for the SFH15 and SFH100 building with different heat pump and SHP system concepts in Strasbourg are shown in Figure 4.43 and Figure 4.44. Regarding the LCOEn values for SFH15 (cf. Figure 4.43), the LCOEn for systems with ASHP is in the range of 0.2460 €/kWh (PV-ASHP) and 0.3903 €/kWh (PVT-SASHP-P), for systems with GSHP in the range of 0.2545 €/kWh (PV-GSHP) and 0.4006 €/kWh (PVT-SGSHP-P) and for SISHP systems in the range of 0.3243 €/kWh (PV-SISHP-S) and 0.4528 €/kWh (PV-SISHP-S,P). For comparison, the value of the reference building with conventional heating system is 0.2191 €/kWh and, thus, all heat pump and SHP system concepts achieve higher LCOEn values than the reference building. Basically, the results show that the LCOEn values in case of new buildings with lower heating energy demand are higher in comparison to the SFH45 building. These results reflect especially the higher ratio of costs to the useful energy for the thermal and electrical energy supply of the building

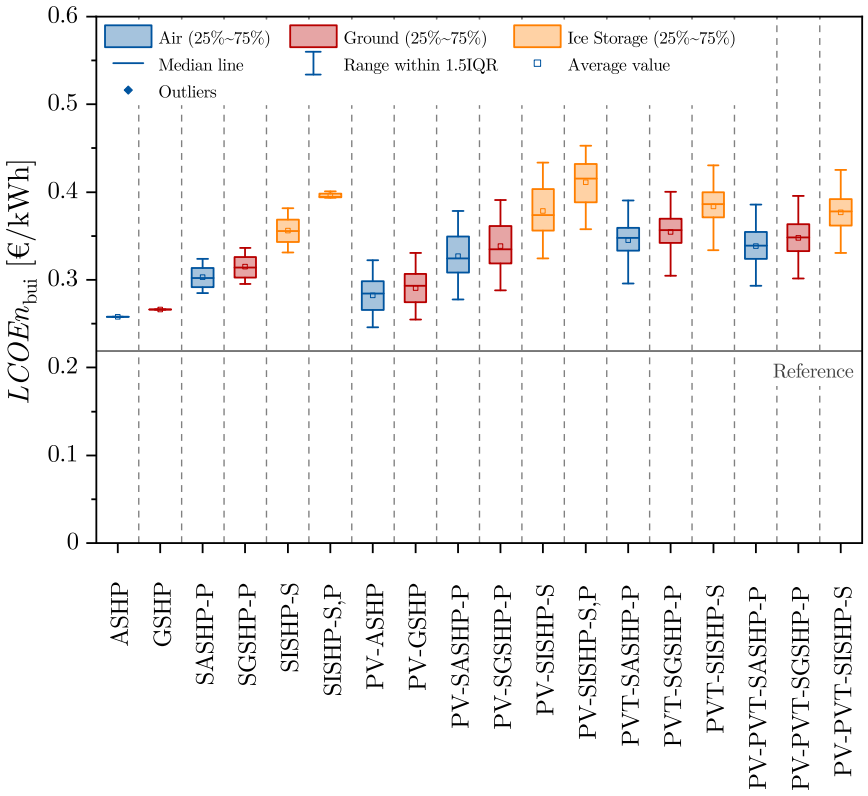

Figure 4.43: LCOEn for the SFH15 building with different heat pump and SHP system concepts in Strasbourg.

due to the lower energy demand. Comparing different system concepts, systems with ASHP achieve the lowest LCOEn values, whereas systems with GSHP achieve slightly higher values and systems with ice storage achieve by far the highest LCOEn values. These results confirm that the higher initial investment costs for systems with GSHP and especially systems with ice storage cannot be compensated by the reduction of delivered electrical energy to the building due to the higher energy efficiency of the systems in comparison to the corresponding systems with ASHP for SFH15 in Strasbourg. Furthermore, the main findings for the SFH45 building in Strasbourg can be confirmed for SFH15 with regard to the economic efficiency. At this, there are only some minor differences with regard to systems with ice storage. In contrast to SFH45, the LCOEn values of PV-SISHP-S,P systems are higher in comparison to PVT-SISHP-S systems. At this, it should be noted that PV-SISHP-S,P and PVT-SISHP-S systems have the same ice storage volume of 10 m^3 and thus the same investment costs for the ice storage in case of SFH15, whereas PVT-SISHP-S systems require a larger ice storage volume than PV-SISHP-S,P systems in case of SFH45. Comparing different system concepts with regard to the used solar technologies, the simulation results confirm that the LCOEn can only be decreased in some cases by adding PV modules in comparison to heat pump systems without solar technologies. All other SHP system concepts reach higher LCOEn values than heat pump systems without solar technologies. Furthermore, the results confirm that the higher initial investment costs for battery storages cannot be compensated by the reduction of delivered electrical energy to the building due to the higher self-sufficiency by the use of battery storages and that the economic efficiency of PV is better in comparison to solar thermal or PVT collectors in case of SFH15 in moderate climates.

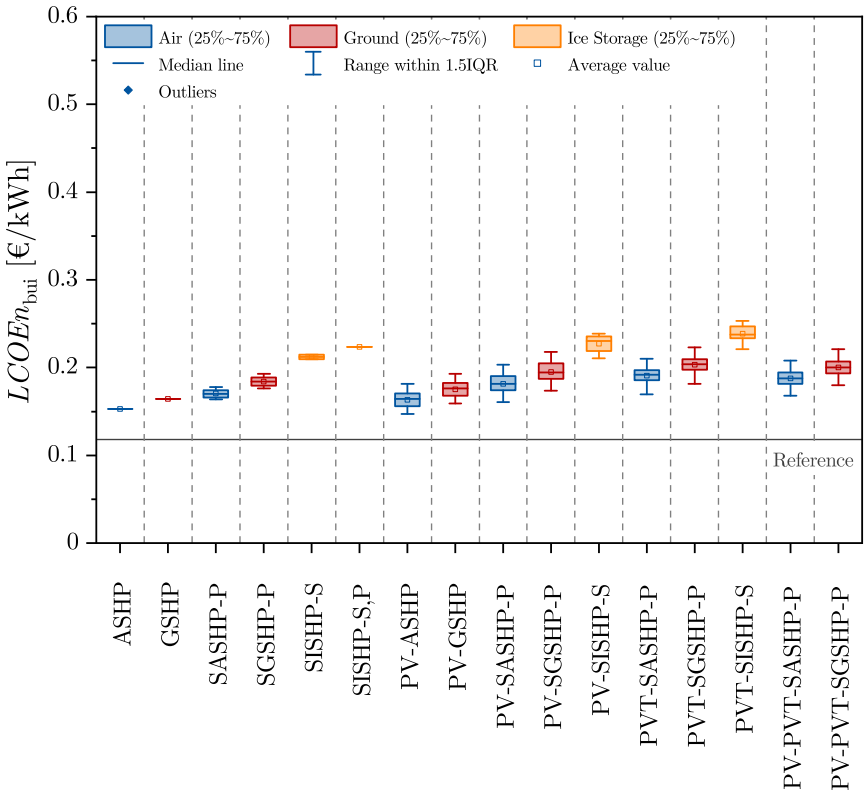

Figure 4.44: LCOEn for the SFH100 building with different heat pump and SHP system concepts in Strasbourg.

Regarding the LCOEn values for SFH100 (cf. Figure 4.44), the LCOEn for systems with ASHP is in the range of 0.1471 €/kWh (PV-ASHP) and 0.2099 €/kWh (PVT-SASHP-P), for systems with GSHP in the range of 0.1589 €/kWh (PV-GSHP) and 0.2229 €/kWh (PVT-SGSHP-P) and for SISHP systems in the range of 0.2096 €/kWh (SISHP-S) and 0.2530 €/kWh (PVT-SISHP-S). For comparison, the value of the reference building with conventional heating system is 0.1183 €/kWh and, thus, all heat pump and SHP system concepts achieve higher LCOEn values than the reference building. Basically, the results show that the LCOEn values in case of non-renovated existing buildings with higher heating energy demand are lower in comparison to the SFH45 building. This result reflects especially the lower ratio of costs to the useful energy for the thermal and electrical energy supply of the building due to the higher energy demand. Comparing different system concepts, systems with ASHP achieve the lowest LCOEn values, whereas systems with GSHP achieve slightly higher values and systems with ice storage achieve by far the highest LCOEn values. These results confirm that the higher initial investment costs for systems with GSHP and especially systems with ice storage cannot be compensated by the reduction of delivered electrical energy to the building due to the higher energy efficiency of the systems in comparison to the corresponding systems with ASHP even for SFH100 in Strasbourg with high energy demand. Furthermore, the main findings for the SFH45 building in Strasbourg can be confirmed for SFH100 with regard to the economic efficiency. At this, there are only some minor differences with regard to systems with ice storage. In contrast to SFH45, the LCOEn values of SISHP-S systems are lower in comparison to PV-SISHP-S systems. This result can be explained by the smaller available roof area for PV modules and, thus, smaller possible PV installations with relatively high area specific investment costs. Com-

paring different system concepts with regard to the used solar technologies, the simulation results also confirm that the LCOEn can only be decreased in some cases by adding PV modules in comparison to heat pump systems without solar technologies. All other SHP system concepts reach higher LCOEn values than heat pump systems without solar technologies. Furthermore, the results also confirm that the higher initial investment costs for battery storages cannot be compensated by the reduction of delivered electrical energy to the building due to the higher self-sufficiency by the use of battery storages and that the economic efficiency of PV is better in comparison to solar thermal or PVT collectors in case of SFH100 in moderate climates with the aforementioned exception of SISHP systems due to the small available roof area for PV modules.

4.4.3 Influence of Climate

4.4.3.1 Warm Climates

Overviews of the range of LCOEn values for the SFH45 and SFH100 building with different heat pump and SHP system concepts in Athens are shown in Figure 4.45 and Figure 4.46. Regarding the LCOEn values for SFH45 (cf. Figure 4.45), the LCOEn for systems with ASHP is in the range of 0.2909 €/kWh (PV-ASHP) and 0.4853 €/kWh (PV-SASHP-P) and for systems with GSHP in the range of 0.3086 €/kWh (PV-GSHP) and 0.5080 €/kWh (PV-SGSHP-P). For comparison, the value of the reference building with conventional heating system is 0.2781 €/kWh and, thus, all heat pump and SHP system concepts achieve higher LCOEn values than the reference building in case of SFH45 in Athens. Regarding the LCOEn values for SFH100 (cf. Figure 4.46), the LCOEn for systems with ASHP is in the range of 0.2347 €/kWh (PV-ASHP) and 0.3790 €/kWh (PVT-SASHP-P) and for systems with GSHP in the range of 0.2463 €/kWh (PV-GSHP) and 0.3933 €/kWh (PV-SGSHP-P). For comparison, the value of the reference building with conventional heating system is 0.2159 €/kWh and, thus, all heat pump and SHP system concepts achieve also higher LCOEn values than the reference building in case of SFH100 in Athens. Basically, the results show that the LCOEn values in Athens are significantly higher in comparison to the SFH45 and SFH100 building in Strasbourg. These results reflect especially the higher ratio of costs to the useful energy for the thermal and electrical energy supply of the building due to the lower energy demand as result of higher annual average ambient temperature and higher total yearly irradiation in Athens. Comparing different system concepts, systems with ASHP achieve the lowest LCOEn values, whereas systems with GSHP achieve slightly higher values. These results confirm that the higher initial investment costs for systems with GSHP cannot be compensated by the reduction of delivered electrical energy to the building due to the higher energy efficiency of the systems in comparison to the corresponding systems with ASHP for SFH45 and SFH100 in Athens. Furthermore, the main findings for the SFH45 and SFH100 building in Strasbourg can be confirmed for SFH45 and SFH100 in Athens with regard to the economic efficiency. Comparing different system concepts with regard to the used solar technologies, the simulation results confirm that the LCOEn can only be decreased in some cases by adding PV modules in comparison to heat pump systems without solar technologies. In contrast to Strasbourg, the LCOEn even decreases for some case of PV and heat pump systems with battery storage in comparison to the corresponding heat pump system without solar technologies. All other SHP system concepts reach higher LCOEn values than heat pump systems without solar technologies. Some minor differences can be observed with regard to systems with PVT. In contrast to Strasbourg, PV plus so-

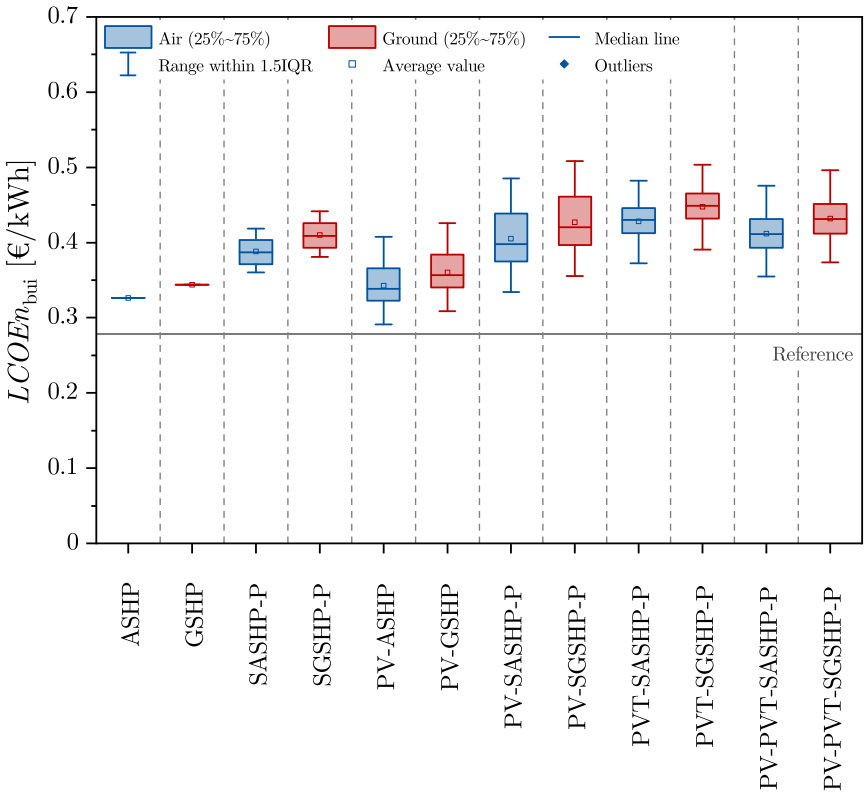

Figure 4.45: LCOEn for the SFH45 building with different heat pump and SHP system concepts in Athens.

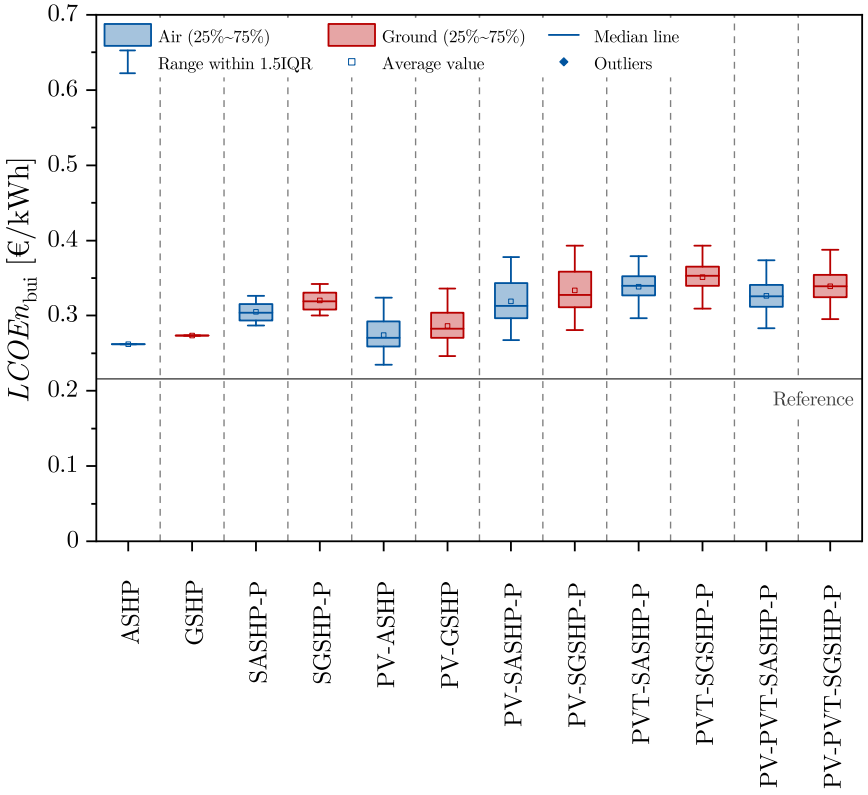

Figure 4.46: LCOEn for the SFH100 building with different heat pump and SHP system concepts in Athens.

lar thermal and heat pump systems achieve the highest LCOEn values with exception of PVT-SASHP-P in case of SFH100 in Athens. Furthermore, the results confirm that the higher initial investment costs for battery storages cannot be compensated by the reduction of delivered electrical energy to the building due to the higher self-sufficiency by the use of battery storages and that the economic efficiency of PV is better in comparison to solar thermal or PVT collectors in case of SFH45 and SFH100 in warm climates.

4.4.3.2 Cold Climates

Overviews of the range of LCOEn values for the SFH15, SFH45 and SFH100 building with different heat pump and SHP system concepts in Helsinki are shown in Figure 4.47, Figure 4.48 and Figure 4.49. Regarding the LCOEn values for SFH15 (cf. Figure 4.47), the LCOEn for systems with ASHP is in the range of 0.1950 €/kWh (PV-ASHP) and 0.2974 €/kWh (PVT-SASHP-P), for systems with GSHP in the range of 0.1967 €/kWh (PV-GSHP) and 0.3001 €/kWh (PVT-SGSHP-P) and for SISHP systems in the range of 0.3133 €/kWh (PV-SISHP-S) and 0.3820 €/kWh (PV-SISHP-S,P). For comparison, the value of the reference building with conventional heating system is 0.1671 €/kWh and, thus, all heat pump and SHP system concepts achieve higher LCOEn values than the reference building in case of SFH15 in Helsinki. Regarding the LCOEn values for SFH45 (cf. Figure 4.48), the LCOEn for systems with ASHP is in the range of 0.1504 €/kWh (PV-ASHP) and 0.2141 €/kWh (PVT-SASHP-P) and for systems with GSHP in the range of 0.1549 €/kWh (PV-GSHP) and 0.2197 €/kWh (PVT-SGSHP-P). For comparison, the value of the reference building with conventional heating system is 0.1210 €/kWh and,

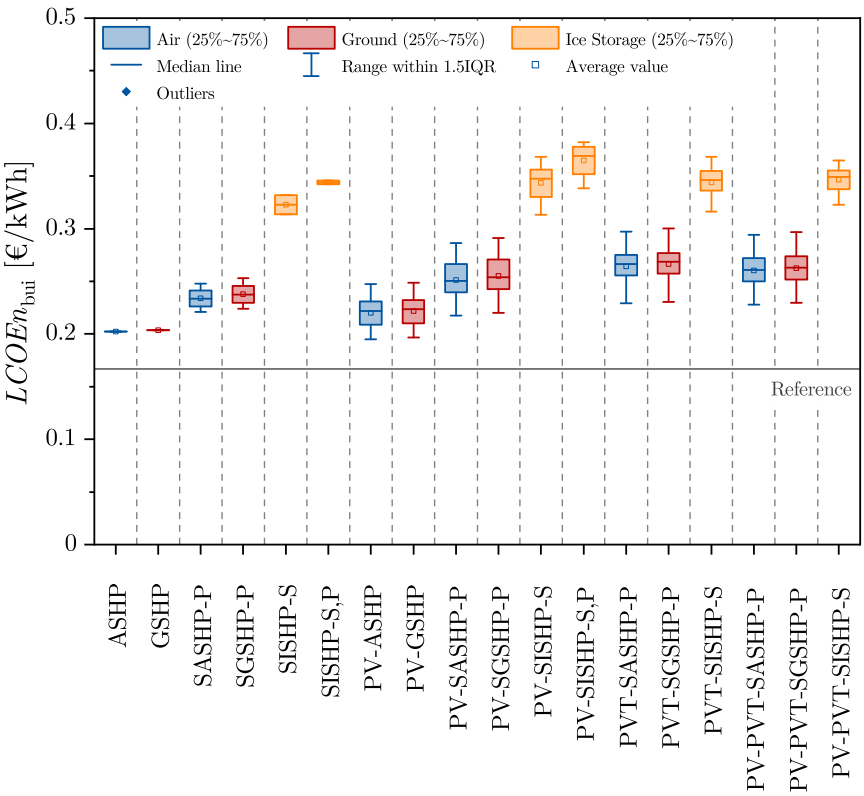

Figure 4.47: LCOEn for the SFH15 building with different heat pump and SHP system concepts in Helsinki.

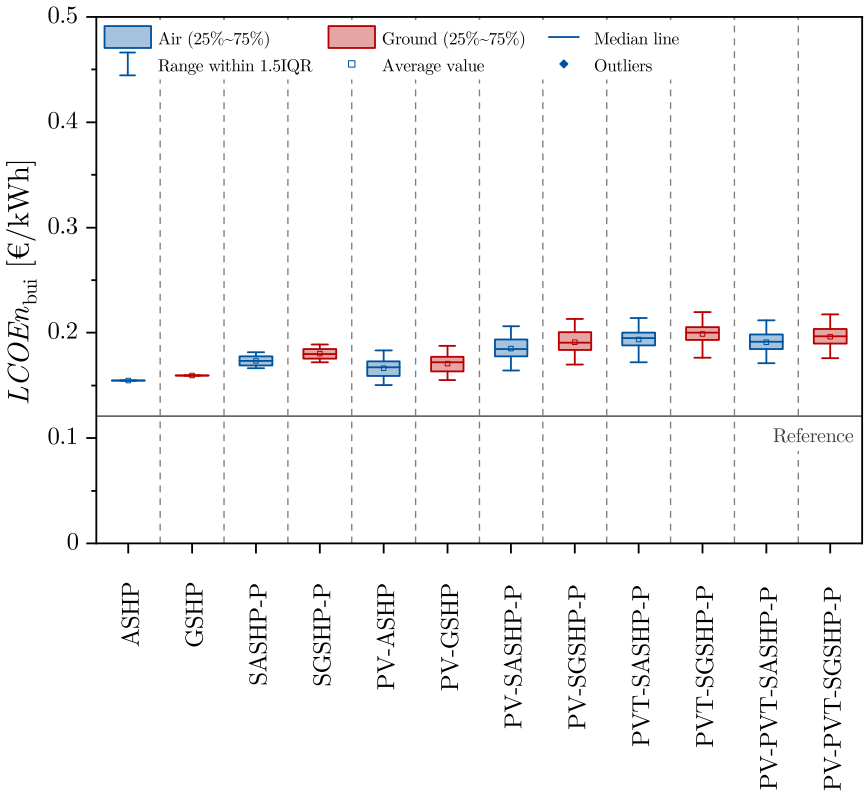

Figure 4.48: LCOEn for the SFH45 building with different heat pump and SHP system concepts in Helsinki.

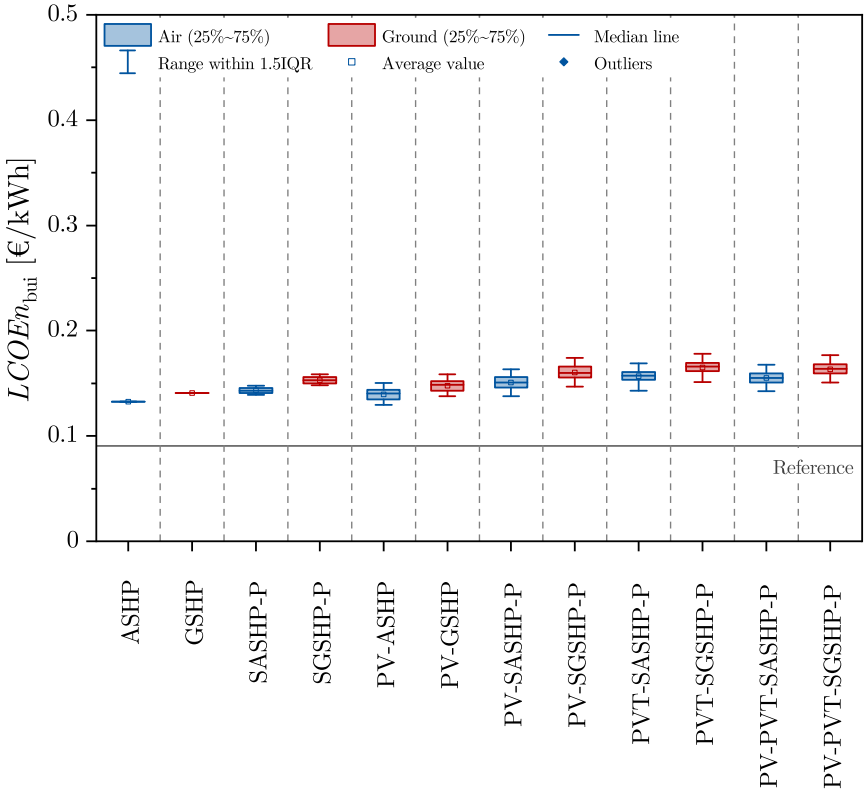

Figure 4.49: LCOEn for the SFH100 building with different heat pump and SHP system concepts in Helsinki.

thus, all heat pump and SHP system concepts achieve higher LCOEn values than the reference building in case of SFH45 in Helsinki. Regarding the LCOEn values for SFH100 (cf. Figure 4.49), the LCOEn for systems with ASHP is in the range of 0.1295 €/kWh (PV-ASHP) and 0.1692 €/kWh (PVT-SASHP-P) and for systems with GSHP in the range of 0.1376 €/kWh (PV-GSHP) and 0.1781 €/kWh (PVT-SGSHP-P). For comparison, the value of the reference building with conventional heating system is 0.0906 €/kWh and, thus, all heat pump and SHP system concepts achieve also higher LCOEn values than the reference building in case of SFH100 in Helsinki. Basically, the results show that the LCOEn values in Helsinki are significantly lower in comparison to the SFH15, SFH45 and SFH100 building in Strasbourg. These results reflect especially the lower ratio of costs to the useful energy for the thermal and electrical energy supply of the building due to the higher energy demand as result of lower annual average ambient temperature and slightly lower total yearly irradiation in Helsinki. Comparing different system concepts, systems with ASHP achieve the lowest LCOEn values, whereas systems with GSHP achieve slightly higher values and in case of SFH15 in Helsinki systems with ice storage achieve by far the highest LCOEn values. These results confirm that the higher initial investment costs for systems with GSHP, and especially systems with ice storage in case of SFH15, cannot be compensated by the reduction of delivered electrical energy to the building due to the higher energy efficiency of the systems in comparison to the corresponding systems with ASHP, even in cold climates. Furthermore, the main findings for Strasbourg can be confirmed for the evaluated building types in Helsinki with regard to the economic efficiency. As observed for SFH15 in Strasbourg, the LCOEn values of PV-SISHP-S,P systems are higher in comparison to PVT-SISHP-S systems for SFH15 in Helsinki. At this, PV-SISHP-S,P and PVT-SISHP-S systems have also the same ice storage volume (30 m^3 in case of SFH15 in Helsinki). Comparing different system concepts with regard to the used solar technologies, the simulation results confirm that the LCOEn can only be decreased in some cases by adding PV modules in comparison to heat pump systems without solar technologies. All other SHP system concepts reach higher LCOEn values than heat pump systems without solar technologies. Furthermore, the results confirm that the higher initial investment costs for battery storages cannot be compensated by the reduction of delivered electrical energy to the building due to the higher self-sufficiency by the use of battery storages and that the economic efficiency of PV is better in comparison to solar thermal or PVT collectors, even in cold climates.

4.4.4 Summary

The following general conclusions on the economic efficiency can be given for the climates of Strasbourg, Athens and Helsinki:

- All heat pump and SHP system concepts achieve higher LCOEn values than the reference buildings with conventional gas-fired heating system. At this, systems with ASHP achieve the lowest LCOEn values, whereas systems with GSHP achieve slightly higher values and systems with ice storage achieve by far the highest LCOEn values. The results illustrate that the higher initial investment costs for systems with GSHP and especially systems with ice storage cannot be compensated by the reduction of delivered electrical energy to the building due to the higher energy efficiency of the systems in comparison to the corresponding systems with ASHP.
- The LCOEn of heat pump systems can only be decreased in some cases by adding PV modules in comparison to heat pump systems without solar technologies. For warm

climates, the LCOEn even decreases for some case of PV and heat pump systems with battery storage in comparison to the corresponding heat pump system without solar technologies. All other SHP system concepts reach higher LCOEn values than heat pump systems without solar technologies.

- PV and heat pump systems and PV-SISHP-S systems achieve the lowest LCOEn values, except for systems with ice storage in case of SFH100 in moderate climates. At this, the LCOEn values of SISHP-S systems are lower in comparison to PV-SISHP-S systems for SFH100 in moderate climates due to the smaller available roof area for PV modules resulting in relatively high area specific investment costs for PV installations. Furthermore, solar thermal and heat pump systems achieve lower minimum LCOEn values than PVT and heat pump systems.

- PVT and heat pump concepts achieve the highest LCOEn values for moderate and cold climates, except for systems with ice storage in case of SFH15. At this, the LCOEn values of PV-SISHP-S,P systems are higher in comparison to PVT-SISHP-S systems for SFH15 with the same ice storage volumes for PV-SISHP-S,P and PVT-SISHP-S systems. In case of warm climates, PV plus solar thermal and heat pump systems achieve the highest LCOEn values with exception of PVT-SASHP-P for SFH100.

- The LCOEn values are higher for SHP system concepts with battery storage in comparison to the same SHP system concept without battery storage and the LCOEn increases with increasing battery storage capacity. This means that the higher initial investment costs for battery storages cannot be compensated by the reduction of delivered electrical energy to the building due to the higher self-sufficiency by the use of battery storages. Nevertheless, depending on the used PV module area and battery storage capacity, the economic efficiency of PV and heat pump systems with battery storage is partially higher than for the corresponding solar thermal and heat pump systems with the same parallel FPC collector area.

- The LCOEn increases with increasing FPC area in case of systems with GSHP and ASHP and with increasing WISC collector area in case of SISHP-S systems, whereas the LCOEn of PV and heat pump system concepts decreases with increasing PV module area. In case of SISHP-S,P systems, the LCOEn decreases with increasing FPC area. In case of PVT and heat pump systems, the results are more diverse. In most cases, the LCOEn increases with increasing PVT collector area, but in some cases with battery storage the LCOEn first decreases slightly with increasing PVT collector area and then increases for larger PVT areas.

- The LCOEn values decrease for locations with lower total yearly irradiation and lower annual average ambient temperature and buildings with higher heating energy demand. These results reflect especially the lower ratio of costs to the useful energy for the thermal and electrical energy supply of the building for higher energy demands.

- Depending on the used PV module area and battery storage capacity, the LCOEn values of solar thermal and heat pump systems and PVT and heat pump systems can be decreased by the combination with PV, but the LCOEn also increases for some cases by the combination with PV. Nevertheless, the LCOEn of PV plus solar thermal or PV plus PVT and heat pump systems decreases with increasing PV module area which illustrates the better economic efficiency of PV in comparison to solar thermal

or PVT collectors with exception of SISHP systems in case of SFH100 in moderate climates due to the small available roof area for PV modules.

For the used boundary conditions, the results especially illustrate that all heat pump and SHP system concepts achieve higher LCOEn values than the reference buildings and only PV and heat pump systems can compete with heat pump systems without solar technologies. Nevertheless, the economic efficiency analysis is limited to the used boundary conditions, which are currently very uncertain and variable and cannot be predicted for the future. The comparison with the reference building is influenced in particular by electricity and gas prices and subsidies for renewable technologies. Furthermore, in case of significant changes in the boundary conditions and especially cost reductions or subsidies for a specific technology, the SHP system concepts have to be compared again for the considered use case to identify the best system concept in terms of economic efficiency using boundary conditions valid for the period under consideration.

4.5 Summary and Discussion

In general, the presented system evaluation illustrates that the efficiency and environmental impact of heat pump systems can be improved by the use of solar technologies (PV, PVT and solar thermal energy) and battery storage systems (for systems with PV or PVT). At this, the benefits increase with increasing collector and module area as well as increasing battery storage size (with exception of net CO_2 emissions). These results especially confirm some main findings for the efficiency of solar thermal and heat pump systems by several authors mentioned in Section 2.3.1 and can thus be assigned to SHP systems in general. In addition, it can be confirmed for SHP systems with PV and/or PVT that the self-consumption increases for all considered climates by the use of battery storages as concluded for PV-ASHP systems by Bee [2019]. The SSRs of the building decrease for buildings with high energy demand and locations with lower total yearly irradiation and lower annual average ambient temperature reaching values up to 60 % (SFH15), 54 % (SFH45) and 43 % (SFH100) in moderate climates, up to 85 % (SFH45) and 77 % (SFH100) in warm climates and up to 47 % (SFH15), 40 % (SFH45) and 29 % (SFH100) in cold climates. In comparison to reference buildings with conventional gas-fired heating system, all heat pump and SHP system concepts achieve lower CO_2 emission indicators of the building with CO_2 emission savings up to 71 % in moderate climates, up to 88 % in warm climates and up to 67 % in cold climates. In contrast, all heat pump and SHP system concepts achieve higher LCOEn values than the reference buildings.

Comparing different *solar technologies*, systems with PVT achieve the lowest CO_2 emissions indicators with PV and heat pump systems achieving (slightly) higher CO_2 emissions indicators for systems with ASHP and GSHP, while system concepts with PVT collectors achieve by far the best results for systems with ice storage. Depending on the building type, system concept, battery storage size and PV/PVT area, the CO_2 emissions of systems with ASHP or GSHP can be decreased by up to 12 % in moderate climates, up to 26 % in warm climates and up to 6 % in cold climates for systems with PVT in comparison to the corresponding systems with PV. Although systems with parallel FPC integration achieve good results in terms of heating efficiency (especially compared to systems with PV), systems with PV and PVT have major advantages in terms of energy efficiency and reducing CO_2 emissions. As a result, the CO_2 emissions can only significantly be decreased by adding

PV modules (for systems with ASHP and GSHP and in case of SFH15 in moderate climates for systems with ice storage) or PVT collectors (for all system concepts), especially in combination with a battery storage. This illustrates the benefit of on-site generated solar electrical energy, which can be used to cover both the electricity consumption of the heating system and household electricity consumption. Systems with PVT benefit additionally from the combined generation of heat and electricity (especially for concepts with ice storage in which the PVT collectors replace the required WISC collectors), but with regard to the energy efficiency and reduction of the CO_2 emissions of a building especially from the use of solar electricity. The results generally confirm that PVT and heat pump systems have the highest solar energy utilization and most energy production in comparison to solar thermal or PV and heat pump systems observed by Wang et al. [2020] for SHP systems with ASHP. Even if major benefits for the specific solar electrical yield of PVT collectors compared to PV modules cannot be observed, the specific solar electrical yield is slightly improved for some cases, especially in SISHP systems as reported by Dott et al. [2012] for serial system concepts, but even decreases for some of the investigated systems (especially with parallel PVT integration). This result may be due to the construction of the analyzed PVT collectors and a contrary result could be observed for other PVT collector designs. Regarding systems with PV and PVT, on the one hand, battery storages have a major influence on the efficiency and environmental impact and are necessary to reach low CO_2 emission indicators. At this, the CO_2 emissions can be reduced by up to 45 % (SFH15), 39 % (SFH45) and 29 % (SFH100) in moderate climates, up to 76 % (SFH45) and 65 % (SFH100) in warm climates and up to 33 % (SFH15), 27 % (SFH45) and 17 % (SFH100) in cold climates using battery storages in comparison to the corresponding systems without battery storage. On the other hand, the LCOEn values of SHP system concepts with battery storage are higher compared to the same SHP system concept without battery storage and increase with increasing battery storage capacity. This means that the higher initial investment costs for battery storage systems cannot be compensated by the higher self-sufficiency by the use of battery storage systems. Nevertheless, depending on the used PV module area and battery storage capacity, the economic efficiency of PV and heat pump systems with battery storage is partially higher than for the corresponding solar thermal and heat pump systems with the same parallel FPC collector area. Furthermore, general improvements by the combination of PV with system concepts with parallel FPC collectors cannot be observed with regard to the heating efficiency. The energy efficiency and CO_2 emissions of system concepts with parallel FPCs can be improved by combining them with PV. Depending on the battery storage size (especially for low battery storage sizes or systems without battery storage), some combinations of parallel FPCs and PV modules achieve even slightly better results than the corresponding systems with PV, but the systems do not achieve the maximum energy efficiency values or minimum CO_2 emissions of the corresponding systems with PV modules instead of parallel FPCs. Furthermore, general improvements by combining PV with system concepts with PVT cannot be observed. Regarding the economic efficiency, systems with PV achieve better results compared to systems with PVT and parallel FPCs, which confirms the findings by Wang et al. [2020] for SHP systems with ASHP and by Thygesen and Karlsson [2013] for the comparison of GSHP systems with PV and FPC. Furthermore, the results point out that for the used boundary conditions only PV and heat pump systems can compete economically with heat pump systems without solar technologies.

With regard to the *heat source*, heat pump and SHP systems with GSHP achieve better efficiency values and lower CO_2 emissions compared to corresponding system concepts with ASHP or ice storage and show their benefits especially for buildings with high heating

energy demands and locations with low annual average ambient temperature. SHP systems with ice storage achieve higher efficiency values and lower CO_2 emissions than systems with ASHP without integration of solar technologies and can compete with systems with ASHP and GSHP, especially in combination with PVT collectors. This result is similar to the findings of Haller et al. [2014a] for the heating efficiency of solar only systems with regard to solar thermal and heat pump systems. Depending on the system concept, SHP systems with ASHP can compete with systems with GSHP (especially without the use of solar technologies), in moderate and warm climates, while in cold climates the efficiency of GSHP systems cannot be achieved by systems with ASHP. Nevertheless, with the exception of non-renovated existing buildings in cold climates, SHP systems with ASHP can partially achieve lower CO_2 emissions than systems with GSHP without integration of solar technologies. Regarding the economic efficiency, systems with ASHP achieve the lowest values, while systems with GSHP achieve slightly higher values and systems with ice storage achieve by far the highest values. The results of the economic efficiency analysis thus illustrate that the higher initial investment costs for systems with GSHP and in particular systems with ice storage cannot be compensated by the higher energy efficiency of the systems compared to the corresponding systems with ASHP.

Regarding different *locations*, the fractional CO_2 savings basically decrease and the CO_2 emission indicators of the buildings increase for locations with lower total yearly irradiation and lower annual average ambient temperature. Furthermore, the maximum SPFs increase for locations with higher total yearly irradiation and higher annual average ambient temperature, in particular due to higher specific solar electrical yields and lower heating energy demands, achieving higher SSRs and solar thermal fractions. Regarding different *building types*, the heating efficiency of heat pump and SHP system concepts decreases for high fractions of energy demand for domestic hot water preparation at high temperature level and energy demands for space heating with high supply temperatures as a result of a lower efficiency of the heat pump. At this, the lower efficiency of the heat pump for space heating with high supply temperatures as well as the lower efficiency of ASHP systems and the use of an electric heating element in cold climates with lower ambient temperatures counteract the effect of higher heating efficiency for lower fractions of energy demand for domestic hot water preparation. With regard to the environmental impact, depending on the SHP system design, renovated buildings can partially achieve lower CO_2 emissions than new buildings with very high energy quality (for moderate and cold climates). In addition, non-renovated existing buildings achieve partially lower CO_2 emissions than renovated buildings (for moderate and warm climates) and even new buildings with very high energy quality (in some cases for moderate climates). In cold climates, however, non-renovated existing buildings cannot (or hardly for systems with GSHP) achieve lower CO_2 emissions than renovated buildings (or even new buildings) for SHP systems with the same heat source. Nevertheless, the results point out that the use of SHP systems can partially compensate a lower quality of the building envelope with regard to the environmental impact. In addition, when comparing different buildings, it should be mentioned that higher efficiency does not generally lead to lower CO_2 emission indicators, since the energy demands of the building types differ. Regarding the economic efficiency, the LCOEn values decrease for locations with lower total yearly irradiation and lower annual average ambient temperature and buildings with higher heating energy demand which reflects especially the lower ratio of costs to useful energy for higher energy demands. Consequently, LCOEn values related to useful energy should only be compared for the same building type and location.

To sum up, the evaluated system concepts compete with each other and should be com-

pared for the use case under consideration in order to identify the best system concept in terms of efficiency, environmental impact and economic efficiency. In most cases, a good compromise of environmental impact and economic efficiency is given by PV-ASHP system concepts in moderate and warm climates and PV-GSHP system concepts in cold climates. Even if the economic efficiency analysis is limited to the used boundary conditions, the results point out the need for cost reductions, especially for battery storages and PVT collectors, and subsidies to enhance the economic efficiency of SHP system concepts with low CO_2 emissions or other governmental regulations. Thus, Section 5.3 presents a case study with consideration of subsidies and carbon prices.

Chapter 5

Case Studies

This chapter presents case studies on different topics with regard to the considered solar and heat pump systems and applications in this work for the moderate climate of Strasbourg. Beginning with case studies on the solar and battery storage design in terms of detailed system sizing with focus on efficiency, CO_2 emissions and economic efficiency, the influence of the use of different photovoltaic-thermal collector technologies depending on the application (serial or parallel system concept) regarding efficiency and CO_2 emissions are presented. This is followed by a case study on the assessment of nearly zero energy building rating for new buildings with solar and heat pump system to figure out which system concepts should be used to fulfill the requirements of a nearly zero energy building. Finally, a case study on the influence of subsidies and carbon prices on the economic efficiency is evaluated in this chapter.

5.1 Solar and Battery Storage System Design

This section presents detailed *solar and battery storage system design evaluations*. The objective of this section is to provide insights to the detailed system design including:

- the detailed system sizing for the example of a PV-ASHP system to show the influence of PV system size and battery storage capacity on efficiency, CO_2 emissions and economic efficiency and
- the comparison of WISC and covered flat-plate PVT collectors for different applications (serial or parallel system concept) in SHP systems to figure out its influence on efficiency and CO_2 emissions.

For the following evaluations, the SFH45 building in Strasbourg is used as use case as it represents current legal requirements or renovated buildings with good thermal quality of the building envelope in moderate climates. The PV-ASHP system is chosen as use case for the detailed system sizing as it offers a good compromise of environmental impact and economic efficiency in moderate climates as figured out in the last chapter and it represents the typical

installed SHP system in moderate climates. At this, the SFH45 building in Strasbourg with PV-ASHP system has an electricity consumption of the overall SHP system including penalties of 2 845 kWh/a (40 %) and a household electricity consumption of 4 200 kWh/a (60 %).

5.1.1 Influence of PV System and Battery Storage Sizing on Efficiency, Environmental Impact and Economic Efficiency

Overviews of self-sufficiency (SSR_{bui}) and self-consumption (SCR_{bui}) of the building for the PV-ASHP system in Strasbourg for SFH45 depending on PV system and battery storage size are shown as contour plots in Figure 5.1. At this, the SSRs reach values up to 48 % and the SCR up to 98 %. Basically, the results show that the self-sufficiency increases with increasing battery storage capacity and PV system size, whereas the self-consumption increases with increasing battery storage capacity and decreasing PV system size. For a maximum SSR, the battery storage capacity and PV system size should be as large as possible within the considered range. For a maximum SCR, a high ratio of battery storage capacity to PV system size should be used to maximize the self-consumption of generated solar electrical energy and avoid high grid feed-in of solar electrical energy. Regarding the SSR of the building, the increase of SSR decreases for a larger sizing of the PV system in case of systems without battery storage or with small battery storage sizes as result of higher amounts of generated excess solar electrical energy that cannot be used for the supply of the building. Furthermore, the effect of higher battery storage sizes on the SSR is lower or even does not lead to an increase of the SSR for small PV system sizes. This is also reflected in high SCR values that can hardly be improved by higher battery storage sizes for small PV system sizes. At this, the SSR and SCR tends to reach a maximum at a ratio of battery storage capacity to PV system size of around 5 kWh/1 kWp. A moderate increase of SSR can be achieved up to a ratio of battery storage capacity to PV system size of around 2.5 kWh/1 kWp.

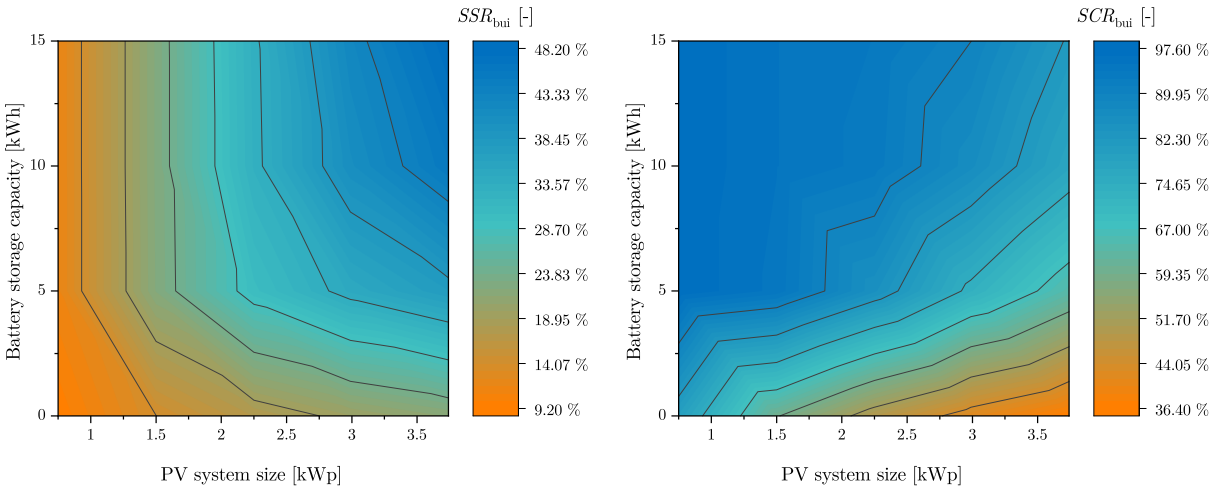

(a) SSR_{bui} **(b)** SCR_{bui}

Figure 5.1: SSR and SCR of the building for the PV-ASHP system in Strasbourg for SFH45 depending on PV system and battery storage size.

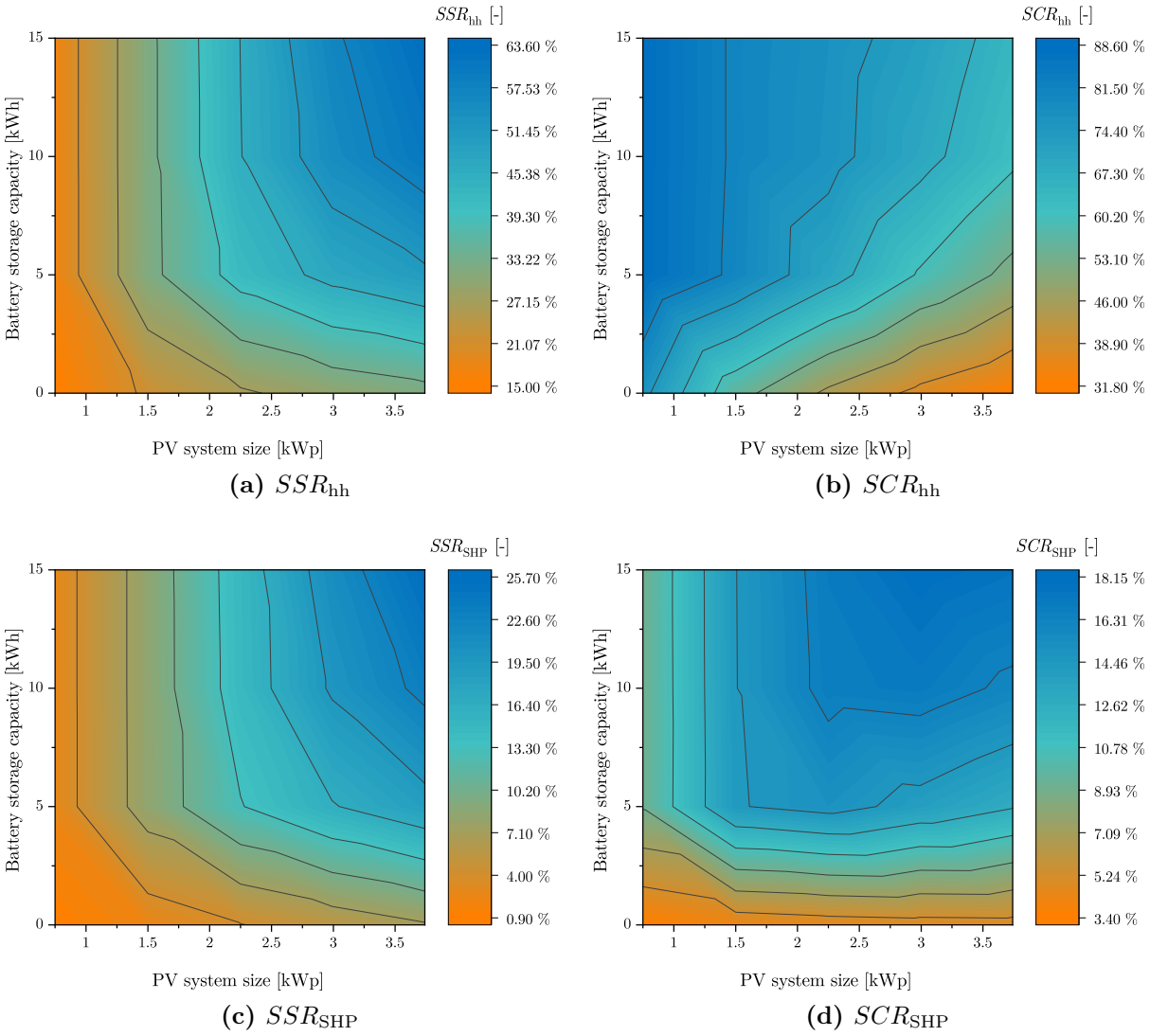

(a) SSR_{hh} **(b)** SCR_{hh}

(c) SSR_{SHP} **(d)** SCR_{SHP}

Figure 5.2: SSR and SCR of the household electricity and the SHP system for the PV-ASHP system in Strasbourg for SFH45 depending on PV system and battery storage size.

Overviews of SSR and SCR with distinction between household electricity and SHP system usage for the PV-ASHP system in Strasbourg for SFH45 depending on PV system and battery storage size are shown in Figure 5.2. For the shown example of a PV-ASHP system, the SSRs of the SHP system reach values up to 26 % with a battery storage capacity of 15 kWh and up to 7 % without battery storage, whereas the SSRs of the household electricity reach values up to 63 % with a battery storage capacity of 15 kWh and up to 31 % without battery storage. As observed before, the self-sufficiency increases with increasing battery storage capacity and PV system size. At this, the relative increase for the self-sufficiency by the use of battery storages is higher for the SHP system than for the household electricity, whereas the absolute increase is higher for the household electricity. With regard to the SCR, the self-consumption increases with increasing battery storage capacity and decreasing PV system size for the household electricity, but shows a different behavior for the SHP system. The SCR of the SHP system also increases with increasing battery storage capacity, but

increases initially for increasing PV system sizes until it decreases for larger PV system sizes in case of systems with battery storage. On the one hand, this shows especially the effect of the implemented priority on household electricity usage of self-consumed solar electricity. For small PV system sizes, the largest part of solar electrical energy is used for the household electricity and only a low proportion of solar electrical energy can be used for the SHP system. With increasing PV system size, the amount of excess solar electrical energy that can be used for the SHP system increases and leads to higher proportions of solar electrical energy that can be used for the SHP system on the self-consumption of solar electrical energy for the building. For larger PV system sizes with battery storage, higher amounts of solar electrical energy cannot be used for the supply of the building and are fed into the grid and thus the SCRs of the building, the household electricity and the SHP system decrease. On the other hand, the described results for the SCR of the SHP system could be at least in parts a result of the different dynamic behavior (seasonal and time of the day dependent) of electricity consumption for household and SHP system application.

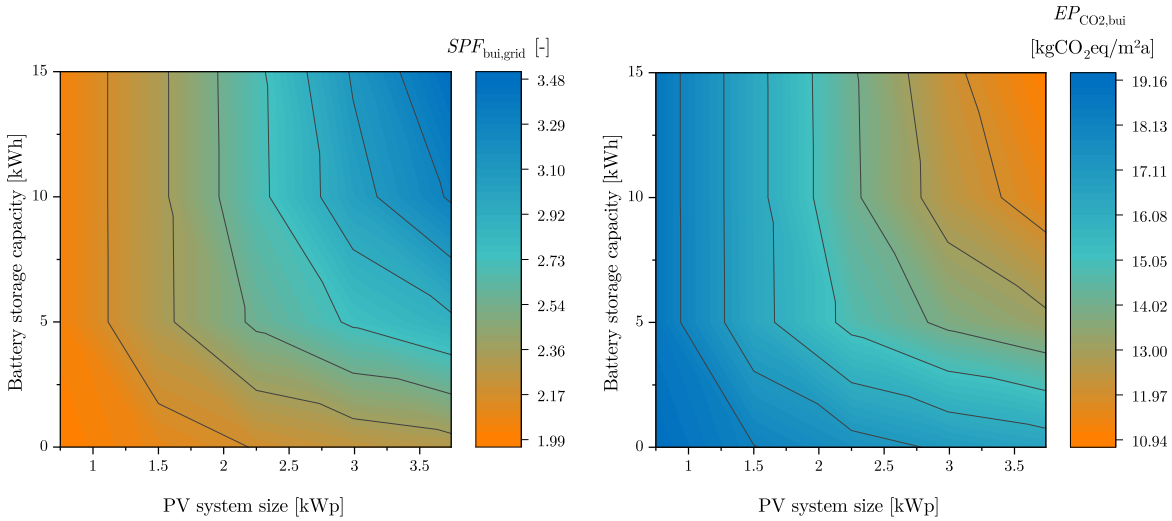

(a) $SPF_{\mathrm{bui,grid}}$ **(b)** $EP_{\mathrm{CO_2,bui}}$

Figure 5.3: Grid-related SPF of the building and CO_2 emissions indicators of the building for the PV-ASHP system in Strasbourg for SFH45 depending on PV system and battery storage size.

Overviews of grid-related SPF of the building and CO_2 emissions indicators of the building for the PV-ASHP system in Strasbourg for SFH45 depending on PV system and battery storage size are shown in Figure 5.3. For the shown example of a PV-ASHP system, the grid-related SPF of the building reach values up to 3.47 with a battery storage capacity of 15 kWh and up to 2.29 without battery storage. The CO_2 emissions indicators of the building reach minimum values of 10.96 kg CO_2eq/m^{2}a with a battery storage capacity of 15 kWh and of 16.59 kg CO_2eq/m^{2}a without battery storage. As observed for the self-sufficiency, the SPF increases with increasing battery storage capacity and PV system size. In contrast, the CO_2 emissions indicators decrease with increasing battery storage capacity and PV system size, but this means on the other hand that the CO_2 emissions reductions increase with increasing battery storage capacity and PV system size. For a maximum SPF and minimum CO_2 emissions indicator, the battery storage capacity and PV system size should be as large as possible within the considered range. As observed for the self-sufficiency, the increase of

SPF and the decrease of the CO_2 emissions also decrease for a larger sizing of the PV system in case of systems without battery storage or with small battery storage sizes as result of higher amounts of generated excess solar electrical energy that cannot be used for the supply of the building. Furthermore, the effect of higher battery storage sizes on the SPF and CO_2 emissions is also lower or even does not lead to an increase of the SPF or decrease of CO_2 emissions for small PV system sizes. Thus, the results especially illustrate the correlation between SSR, grid-related SPF and CO_2 emissions indicators of the building and shows that higher SSRs lead to higher grid-related SPFs and lower CO_2 emissions indicators of the building. At this, the grid-related SPF and CO_2 emissions indicators of the building also tend to reach a maximum at a ratio of battery storage capacity to PV system size of around 5 kWh/1 kWp with a moderate increase up to a ratio of battery storage capacity to PV system size of around 2.5 kWh/1 kWp.

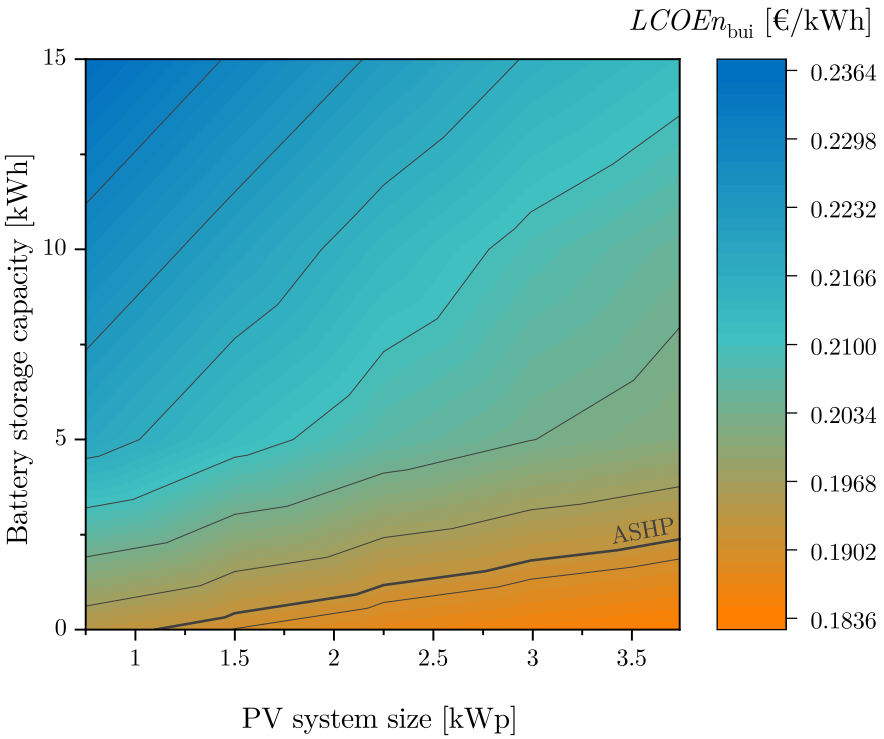

Figure 5.4: LCOEn for the SFH45 building with PV-ASHP system in Strasbourg depending on PV system and battery storage size.

An overview of LCOEn values for the SFH45 building with PV-ASHP system in Strasbourg depending on PV system and battery storage size is shown in Figure 5.4. For the shown example of a PV-ASHP system, the LCOEn reaches minimum values of 0.2121 €/kWh with a battery storage capacity of 15 kWh and of 0.1837 €/kWh without battery storage. The LCOEn decreases with increasing PV system size and decreasing battery storage capacity. At this, the LCOEn falls below the values of an ASHP system without PV for PV system sizes larger than around 1.1 kWp for systems without battery storage. In addition, the contour plot suggests that a good ratio of battery storage capacity to PV system size to achieve LCOEn values below the values of an ASHP is around 0.5 kWh/1 kWp. For a minimum LCOEn, a system without battery storage should be used and the PV system size should be as large as possible within the considered range. In comparison to the efficiency and environmental impact results, a direct correlation between SSR, grid-related

SPF and CO_2 emissions indicators of the building and LCOEn cannot be observed. Thus, higher SSRs and grid-related SPFs or lower CO_2 emissions indicators of the building do not necessarily lead to lower LCOEn values. Nevertheless, for a given battery storage size, the LCOEn decreases with increasing PV system size which correlates to higher SSRs and grid-related SPFs and lower CO_2 emissions indicators of the building. Consequently, the economic efficiency does not generally counteract the system efficiency or environmental impact. Lower LCOEn values can also be achieved by systems with higher SSRs and grid-related SPFs and lower CO_2 emissions indicators, but it depends especially on the costs of system components like PV system or battery storage and the used boundary conditions for the economic efficiency calculation. Furthermore, the results show that higher SCRs of the building do not lead to lower LCOEn values, even not for a given battery storage size. To sum up, the system design especially depends on the objective as the system design with highest efficiency and lowest environmental impact is not equal to the system design with the highest economic efficiency (for the used boundary conditions).

5.1.2 Influence of PVT Collector Technology on Efficiency and Environmental Impact

Comparisons of the grid-related SPF of the overall system with penalties and the grid-related SPF of the building of PVT and heat pump systems with WISC and covered flat-plate PVT collectors for the example of the SFH45 building in Strasbourg are shown in Figure 5.5. Regarding the parallel integration of PVT collectors, the results mainly illustrate that system concepts with covered flat-plate PVT collectors achieve higher SPFs in terms of heating and energy efficiency than those with WISC PVT collectors, for the considered PVT collector constructions in this work. With regard to the serial integration of PVT collectors in system

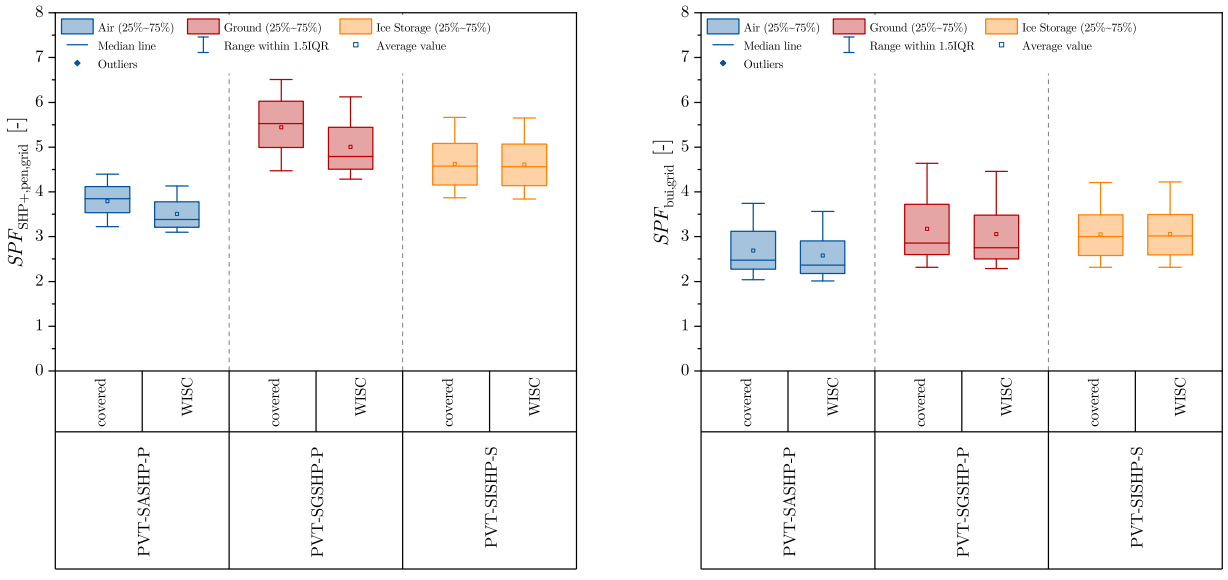

(a) $SPF_{\mathrm{SHP+,pen,grid}}$ **(b)** $SPF_{\mathrm{bui,grid}}$

Figure 5.5: Grid-related SPF of the overall system with penalties and grid-related SPF of the building for different PVT and heat pump system concepts in Strasbourg for SFH45.

concepts with ice storage, there are no consistent results or significant improvements for the SPFs of systems with WISC or covered flat-plate PVT collectors.

Furthermore, the differences in the constructions of the analyzed PVT collectors are particularly evident with regard to specific solar thermal and electrical yields (cf. Figure 5.6). On the one hand, the specific solar thermal yields of systems with parallel integration are significantly higher for covered flat-plate PVT collectors leading to higher solar thermal fractions between 11 % and 26 %. In comparison, systems with parallel integration of WISC PVT collectors achieve solar thermal fractions between 5 % and 10 %. In contrast, the specific solar thermal yields of system concepts with ice storage and serial PVT integration show only small differences between WISC and covered flat-plate PVT collectors with slightly higher range of the results for WISC PVT collectors. On the other hand, the specific solar electrical yields are higher for all PVT and heat pump concepts with WISC PVT collectors. Thus, in case of systems with parallel PVT integration, the lower specific solar electrical yields of covered flat-plate PVT collectors counteracts the higher specific solar thermal yields in comparison to WISC PVT collectors. At this, the thermal improvement of covered flat-plate PVT collectors predominates the lower electrical performance which is shown in higher SPFs for PVT and heat pump systems with parallel integration of covered flat-plate PVT collectors.

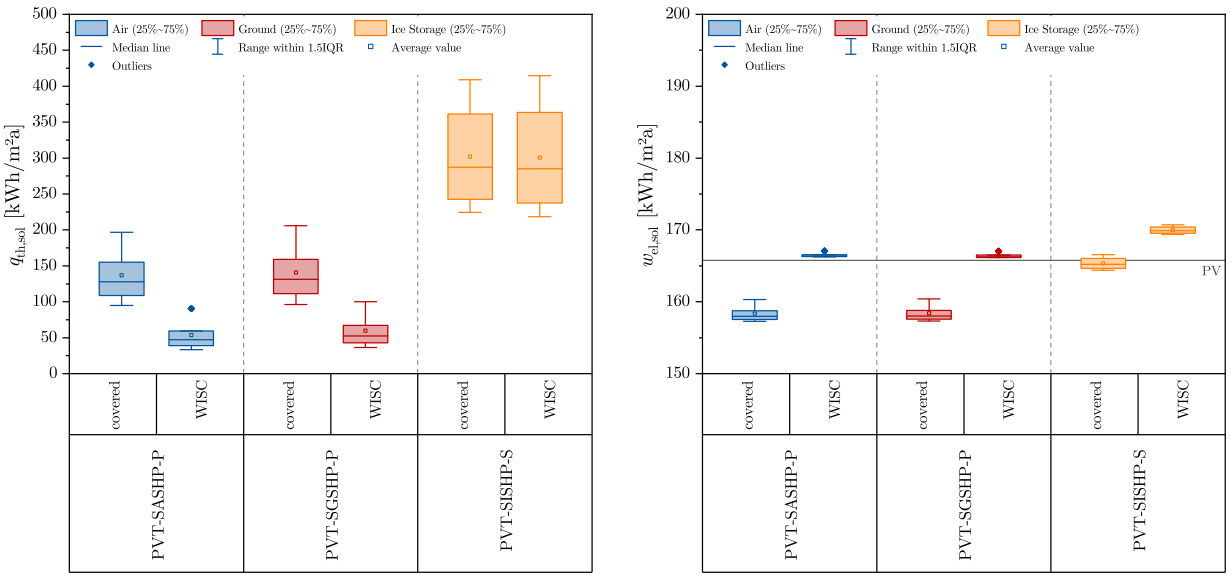

(a) $q_{\mathrm{th,sol}}$ **(b)** $w_{\mathrm{el,sol}}$

Figure 5.6: Specific solar thermal yields and specific solar electrical yields for different PVT and heat pump system concepts in Strasbourg for SFH45.

As figured out in Chapter 4, major benefits for the specific electrical solar yield of PVT collectors in comparison to PV modules cannot be observed. In case of systems with parallel PVT integration, the specific solar electrical yields are lower for covered flat-plate PVT collectors (up to 5 %) and slightly higher (less than 1 %) for WISC PVT collectors in comparison to systems with PV with the identical electrical model parameters. In case of system concepts with ice storage and serial PVT integration, the specific solar electrical yields for WISC PVT collectors are slightly higher (up to 3 %) than the specific solar electrical yields of PV modules. In contrast, the results for systems with covered flat-plate PVT collectors are not consistent. In case of 10 m^2 covered flat-plate PVT collector area, the specific solar

electrical yields are slightly higher (less than 1 %), whereas the specific solar electrical yields are slightly lower (less than 1 %) than the specific solar electrical yields of PV modules for larger PVT collector areas. On the one hand, the results reflect the performance increase of PV cells due to the cooling effect by lower operating temperatures of WISC PVT collectors (for all system concepts) and in some cases of covered flat-plate PVT collectors (for serial operation in system concepts with ice storage). Due to the lower operating temperatures in the heat source circuit of the heat pump, the effect is higher for serial operation in system concepts with ice storage which leads to higher specific solar electrical yields of PVT collectors in PVT-SISHP-S systems in comparison to system concepts with parallel PVT integration. On the other hand, the results illustrate that the higher operating temperatures reached by covered flat-plate PVT collectors, especially in systems with parallel PVT integration, can lead to increasing PV cell temperatures and thus to lower specific solar electrical yields in comparison to PV modules. Thus, the results confirm the findings from Chapter 4 and give more insights with regard to the benefits for the specific electrical solar yield of different PVT collector constructions in comparison to PV modules. As mentioned before, a contrary result could be observed for other PVT collector designs. As the considered covered flat-plate PVT collectors in this work are not equipped with a backside thermal insulation, the results should be verified, for example, for other covered flat-plate PVT collector constructions.

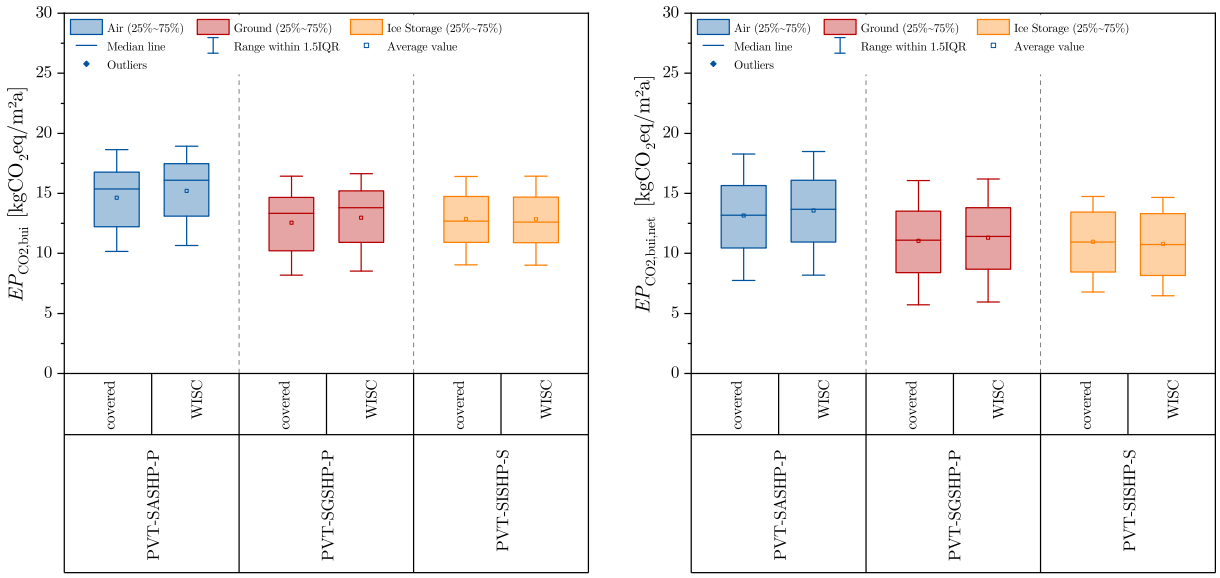

(a) $EP_{\mathrm{CO_2,bui}}$ **(b)** $EP_{\mathrm{CO_2,bui,net}}$

Figure 5.7: CO_2 emissions and net CO_2 emissions indicators of the building for different PVT and heat pump system concepts in Strasbourg for SFH45.

With regard to the CO_2 emissions indicators shown in Figure 5.7, the results for the SPFs can be confirmed in case of parallel integration of PVT collectors resulting in lower CO_2 emissions for covered flat-plate PVT collectors than for WISC PVT collectors. In contrast to the SPFs, slight improvements for the net CO_2 emissions indicators in case of serial integration of WISC PVT collectors can be observed compared to covered flat-plate PVT collectors, whereas the comparison show no consistent results for the CO_2 emissions indicators without compensation by exported energy. At this, the slight improvements for

the net CO_2 emissions indicators reflect especially the higher specific solar electrical yields of WISC PVT collectors.

In summary, the results point out that in system concepts with parallel integration of PVT collectors especially covered flat-plate PVT collectors should be used due to the higher thermal performance in comparison to WISC PVT collectors that leads to higher SPFs and lower CO_2 emissions, even if the electrical performance is lower in comparison to WISC PVT collectors and decreases in comparison to PV modules. In contrast, in case of system concepts with serial integration of PVT collectors, WISC PVT collectors show slightly better results in terms of CO_2 emissions if the exported energy is taken into account.

5.2 Assessment of nZEB Rating of Buildings with SHP System

This section presents a case study on the *assessment of nZEB rating* of new buildings with SHP system. The objective of this section is to figure out which system concept should be used to fulfill the requirements of a nearly zero energy building using the proposed nZEB rating procedure from Section 2.1.3. For the following evaluations, the SFH15 building in Strasbourg is used as use case as it represents new buildings with very high energy standard. As described in Section 2.1.3, it is assumed that the SFH15 building fulfill the requirements for the net energy demand with regard to the nZEB definition. Moreover, the SFH45 building does not fulfill the nZEB requirements due to its high total primary energy use with regard to the considered SHP systems in this work. As before, the PV-ASHP system is chosen as use case to give insights into the nZEB rating depending on the detailed system sizing. Furthermore, the reference building with conventional gas-fired heating system described for the environmental impact evaluation in Section 4.3 is used to calculate reference values for the different KPIs. The used primary energy factors for the nZEB ratings are summarized in Table 5.1. With regard to the results of SHP system concepts with combinations of two or more solar technologies, it should be noted in the following that, as described in Chapter 4, only combinations with a total used roof area of $25\,m^2$ were considered to limit the number of simulation cases to be carried out. This especially results in lower maximum achieved primary energy use indicators for PV plus PVT and heat pump systems in comparison to PV or PVT and heat pump systems. Furthermore, it has to be noted that the thermal evaporator power consumption of air/water heat pumps is underestimated as described in Section 3.2.1 due to missing data within manufacturer data sheets. Hence, the thermal self-consumed on-site renewable energy used for the calculation of the total primary energy use of a building and the thermal renewable energy produced on-site used for the calculation of the RER based on total primary energy of the building are also underestimated in the following for system concepts with ASHP. Nevertheless, it can be

Table 5.1: Primary energy factors for nZEB calculations based on ISO 52000-1:2017 [ISO 52000-1, 2017].

Parameter	Value	Parameter	Value
$f_{pe,del,tot,el}$	2.5	$f_{pe,del,nren,el}$	2.3
$f_{pe,exp,tot,el}$	2.5	$f_{pe,exp,nren,el}$	2.3
$f_{pe,del,tot,gas}$	1.1	$f_{pe,del,nren,gas}$	1.1

assumed that similar simplifications have to be made within other calculation tools that are used to determine these values according to national regulations due to the missing data provided by the manufacturers.

As mentioned in Section 2.1.3, in contrast to the calculations within this work, the presented numerical benchmarks in Table 2.1 do not mandatory take appliances into account and thus have to be increased and adapted by the energy use for appliances. Although the household electricity consumption of 4 200 kWh/a in Strasbourg includes the energy use for lighting, it is used as energy use for appliances to simplify the following adaptions. With this assumption, the additional energy use for appliances in moderate climates can be calculated by the household electricity consumption of 4 200 kWh/a for an useful floor area of 140 m^2 resulting in an additional energy use for appliances of 30 kWh/m^2a. Assuming that 50 % of the additional energy use has to be covered by on-site self-consumed renewable energy, the additional total primary energy use for the maximum total primary energy use indicator can be calculated with:

$$\Delta EP^{\max}_{\mathrm{pe,bui,tot}} = \Delta E_{\mathrm{bui,del,el}}\ f_{\mathrm{pe,del,tot,el}} + \Delta E_{\mathrm{bui,ren,self,el}} \tag{5.1}$$

with $\Delta E_{\mathrm{bui,del,el}} = 15\,\mathrm{kWh/m^2a}$ (50 %) and $\Delta E_{\mathrm{bui,ren,self,el}} = 15\,\mathrm{kWh/m^2a}$ (50 %) resulting in $\Delta EP^{\max}_{\mathrm{pe,bui,tot}} = 52.5\,\mathrm{kWh_{pe}/m^2a}$. The additional non-renewable primary energy use for the maximum non-renewable primary energy use indicator can then be calculated with:

$$\Delta EP^{\max}_{\mathrm{pe,bui,nren}} = \Delta E_{\mathrm{bui,del,el}}\ f_{\mathrm{pe,del,nren,el}} \tag{5.2}$$

resulting in $\Delta EP^{\max}_{\mathrm{pe,bui,nren}} = 34.5\,\mathrm{kWh_{pe}/m^2a}$. Using the proposed rule that a maximum of 50 % of the difference between maximum total primary energy use and maximum net non-renewable primary energy use can be compensated by exporting energy (see Section 2.1.3), Equation 2.24 can be used to calculate the additional net non-renewable primary energy use for the maximum net non-renewable primary energy use indicator:

$$\Delta EP^{\max}_{\mathrm{pe,bui,nren}} = \Delta EP^{\max}_{\mathrm{pe,bui,nren,net}} + 0.5\ \left(\Delta EP^{\max}_{\mathrm{pe,bui,tot}} - \Delta EP^{\max}_{\mathrm{pe,bui,nren,net}}\right) \tag{5.3}$$

by solving the equation for $\Delta EP^{\max}_{\mathrm{pe,bui,nren,net}}$:

$$\Delta EP^{\max}_{\mathrm{pe,bui,nren,net}} = 2\ \Delta EP^{\max}_{\mathrm{pe,bui,nren}} - \Delta EP^{\max}_{\mathrm{pe,bui,tot}} \tag{5.4}$$

resulting in $\Delta EP^{\max}_{\mathrm{pe,bui,nren,net}} = 16.5\,\mathrm{kWh_{pe}/m^2a}$. The proposed increased maximum values for the total primary energy use indicator, the non-renewable primary energy use indicator and the net non-renewable primary energy use indicator to achieve the nZEB standard with consideration of appliances are summarized in Table 5.2 for moderate climates, whereas the

Table 5.2: Proposed numerical benchmarks for nZEB primary energy use of single-family houses in moderate (oceanic) climate including appliances adapted and extended from European Commission [2016].

	Maximum values in $\mathrm{kWh_{pe}/m^2a}$
$EP^{\max}_{\mathrm{pe,bui,tot}}$	102.5 – 117.5
$EP^{\max}_{\mathrm{pe,bui,nren}}$	67 – 82
$EP^{\max}_{\mathrm{pe,bui,nren,net}}$	31.5 – 46.5

highest values are used as maximum for the following evaluations.

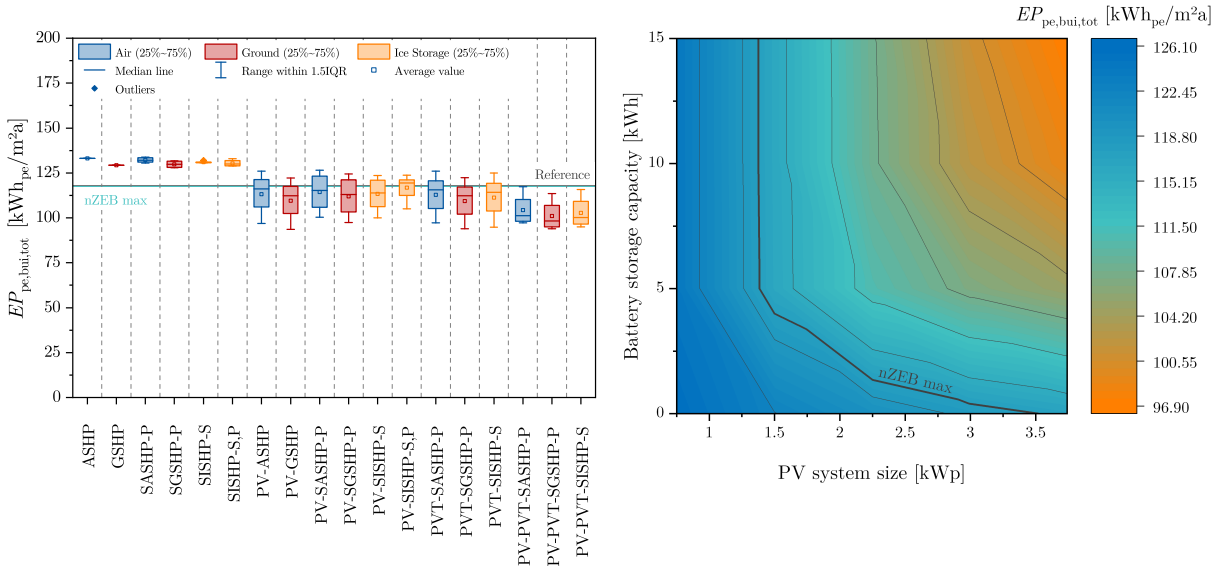

(a) Overview **(b)** PV-ASHP

Figure 5.8: Total primary energy use indicators of the building for different heat pump and SHP system concepts in Strasbourg for SFH15.

An overview of the range of calculated total primary energy use indicators of the SFH15 building for the different heat pump and SHP system concepts in Strasbourg is shown in Figure 5.8a. For systems with ASHP, the total primary energy use indicators of the building are in the range of 96.91 kWh$_{pe}$/m²a (PV-ASHP) and 133.74 kWh$_{pe}$/m²a (SASHP-P), for systems with GSHP in the range of 93.52 kWh$_{pe}$/m²a (PV-GSHP) and 131.74 kWh$_{pe}$/m²a (SGSHP-P) and for SISHP systems in the range of 94.74 kWh$_{pe}$/m²a (PVT-SISHP-S) and 132.85 kWh$_{pe}$/m²a (SISHP-S,P). For comparison, the value of the reference building with conventional heating system is 117.85 kWh$_{pe}$/m²a and is thus slightly higher than the maximum value to achieve nZEB standard. Basically, the simulation results show that the total primary energy use indicators of the building can be decreased in most cases by adding solar technologies and that the different system concepts compete with each other. For solar thermal and heat pump systems with parallel FPC integration, the total primary energy use indicators are in some cases higher than for the corresponding heat pump or SHP system concepts without FPC integration, which is a result of higher buffer storage losses due to higher buffer storage temperatures and partly higher buffer storage sizes within SHP concepts with parallel FPC integration. Furthermore, the total primary energy use indicators can only significantly be decreased to fulfill the nZEB requirements by adding PV modules or PVT collectors, especially in combination with a battery storage. Depending on the system concept, the required PV module or PVT collector area to fulfill the nZEB requirements is between 15 m² (2.25 kWp) and 25 m² (3.74 kWp) for system concepts without battery storage and can be reduced to 10 m² (1.50 kWp) for systems with battery storage capacities of 15 kWh. The total primary energy use indicators decrease with increasing battery storage capacity and PV/PVT system size. This is also shown for the example of a PV-ASHP system by the total primary energy use indicators of the building depending on PV system and battery storage size in Figure 5.8b. For a minimum total primary energy use indicator, the battery storage capacity and PV system size should be as large as possible

within the considered range. As observed for the CO_2 emissions indicators, the decrease of the total primary energy use indicator decreases for a larger sizing of the PV system in case of systems without battery storage or with small battery storage sizes as result of higher amounts of generated excess solar electrical energy that cannot be used for the supply of the building. Furthermore, the effect of higher battery storage sizes on the total primary energy use indicator is also lower or even does not lead to a decrease of the total primary energy use indicator for small PV system sizes. At this, the total primary energy use indicators of the building tend to reach a maximum at a ratio of battery storage capacity to PV system size of around 5 kWh/1 kWp with a moderate increase up to a ratio of battery storage capacity to PV system size of around 2.5 kWh/1 kWp.

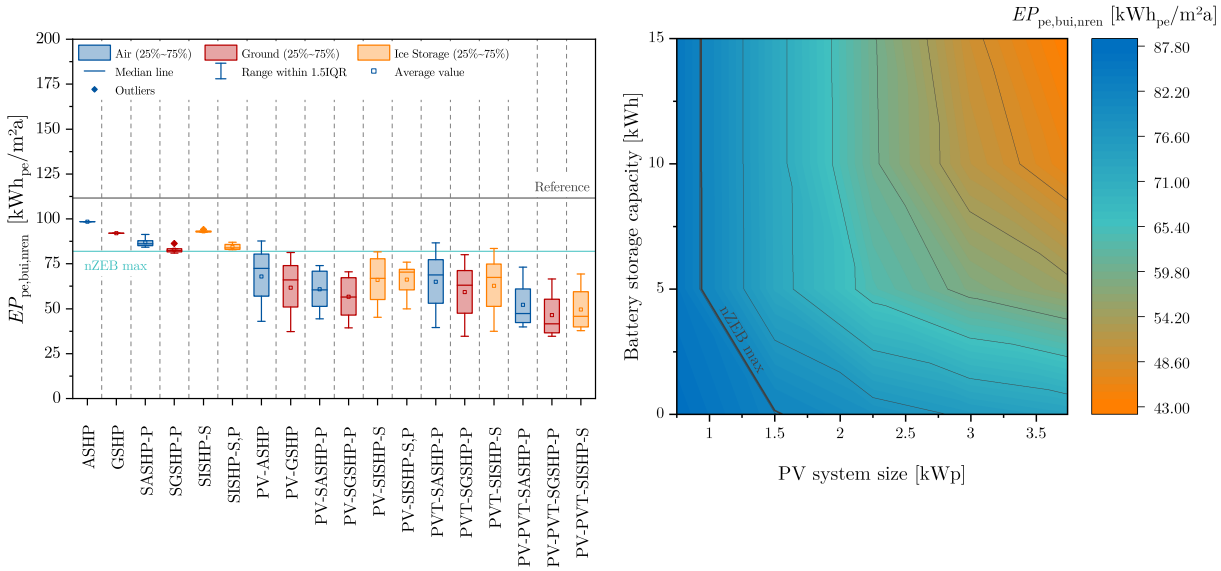

(a) Overview **(b)** PV-ASHP

Figure 5.9: Non-renewable primary energy use indicators of the building for different heat pump and SHP system concepts in Strasbourg for SFH15.

An overview of the range of non-renewable primary energy use indicators of the SFH15 building for the different heat pump and SHP system concepts in Strasbourg is shown in Figure 5.9a. The non-renewable primary energy use indicators for systems with ASHP are in the range of 39.59 kWh$_{pe}$/m^{2}a (PVT-SASHP-P) and 98.40 kWh$_{pe}$/m^{2}a (ASHP), for systems with GSHP in the range of 34.61 kWh$_{pe}$/m^{2}a (PVT-SGSHP-P) and 91.99 kWh$_{pe}$/m^{2}a (GSHP) and for SISHP systems in the range of 37.52 kWh$_{pe}$/m^{2}a (PVT-SISHP-S) and 94.09 kWh$_{pe}$/m^{2}a (SISHP-S). For comparison, the value of the reference building with conventional heating system is 111.60 kWh$_{pe}$/m^{2}a and is thus significantly higher than the maximum value to achieve nZEB standard. Basically, the simulation results show that the non-renewable primary energy use indicators of the building can be decreased by adding solar technologies and that the different system concepts compete with each other. In contrast to the total primary energy use indicators, solar thermal and heat pump systems with parallel FPC integration reach lower non-renewable primary energy use indicators than the corresponding heat pump or SHP system concepts without FPC integration. Nevertheless, the non-renewable primary energy use indicators can only significantly be decreased by adding PV modules or PVT collectors, especially in combination with a battery storage, even if SGSHP-P systems with a minimum FPC area of 20 m^2 fulfill the nZEB requirements.

Depending on the system concept, the required PV module or PVT collector area to fulfill the nZEB requirements is between 5 m² (0.75 kWp) and 15 m² (2.25 kWp) for system concepts without battery storage and can be reduced to between 5 m² (0.75 kWp) and 10 m² (1.50 kWp) for systems with battery storage capacities of 15 kWh. As observed for the total primary energy use indicators, the non-renewable primary energy use indicators decrease with increasing battery storage capacity and PV/PVT system size. This is also shown for the example of a PV-ASHP system by the non-renewable primary energy use indicators of the building depending on PV system and battery storage size in Figure 5.9b. For a minimum non-renewable primary energy use indicator, the battery storage capacity and PV system size should also be as large as possible within the considered range. Furthermore, the decrease of the non-renewable primary energy use indicator also decreases for a larger sizing of the PV system in case of systems without battery storage or with small battery storage sizes and the effect of higher battery storage sizes on the non-renewable primary energy use indicator is also lower or even does not lead to a decrease of the non-renewable primary energy use indicator for small PV system sizes. At this, the non-renewable primary energy use indicators of the building also tend to reach a maximum at a ratio of battery storage capacity to PV system size of around 5 kWh/1 kWp with a moderate increase up to a ratio of battery storage capacity to PV system size of around 2.5 kWh/1 kWp.

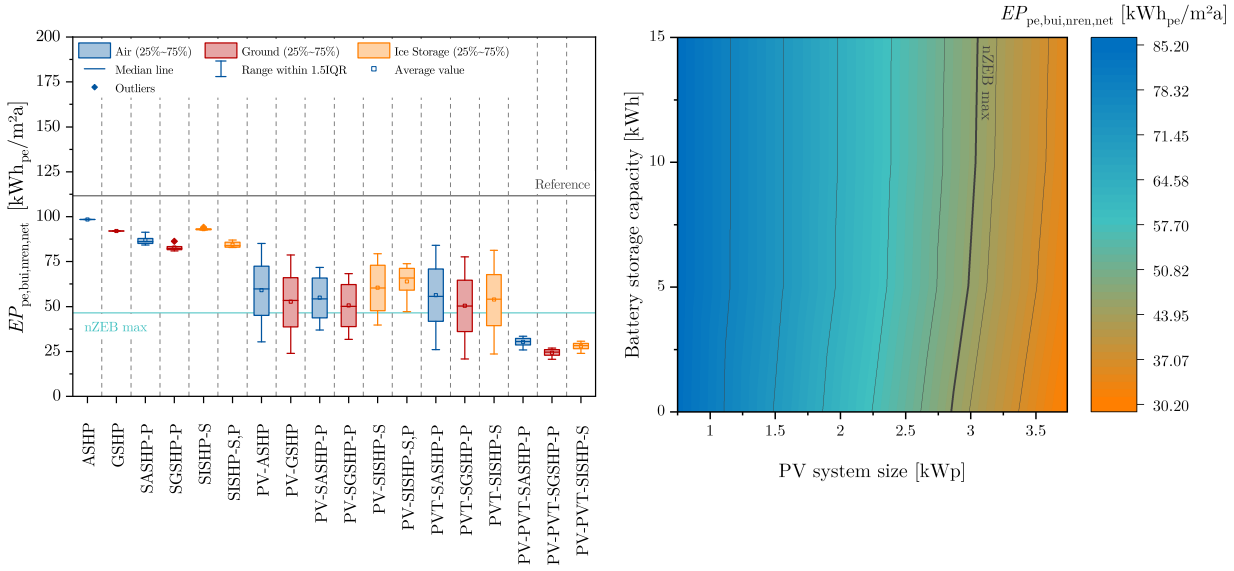

(a) Overview **(b)** PV-ASHP

Figure 5.10: Net non-renewable primary energy use indicators of the building for different heat pump and SHP system concepts in Strasbourg for SFH15.

An overview of the range of net non-renewable primary energy use indicators of the SFH15 building for the different heat pump and SHP system concepts in Strasbourg is shown in Figure 5.10a. For systems with ASHP, the net non-renewable primary energy use indicators are in the range of 25.88 kWh$_{pe}$/m²a (PV-PVT-SASHP-P) and 98.40 kWh$_{pe}$/m²a (ASHP), for systems with GSHP in the range of 20.56 kWh$_{pe}$/m²a (PV-PVT-SGSHP-P) and 91.99 kWh$_{pe}$/m²a (GSHP) and for SISHP systems in the range of 23.53 kWh$_{pe}$/m²a (PVT-SISHP-S) and 94.09 kWh$_{pe}$/m²a (SISHP-S). For comparison, the value of the reference building with conventional heating system is 111.60 kWh$_{pe}$/m²a and is thus significantly higher than the maximum value to achieve nZEB standard. Basically, the simulation re-

sults show that the net non-renewable primary energy use indicators of the building can also be decreased by adding solar technologies and that the different system concepts compete with each other. As observed for the non-renewable primary energy use indicators, solar thermal and heat pump systems with parallel FPC integration reach lower net non-renewable primary energy use indicators than the corresponding heat pump or SHP system concepts without FPC integration. Nevertheless, the net non-renewable primary energy use indicators can only significantly be decreased by adding PV modules or PVT collectors. Beside of heat pump systems without solar technology integration and solar thermal and heat pump systems also PV-SISHP-S,P systems cannot fulfill the nZEB requirements with regard to the net non-renewable primary energy use indicators. Depending on the system concept, the required PV module or PVT collector area to fulfill the nZEB requirements is between 15 m^2 (2.25 kWp) and 20 m^2 (2.99 kWp) for system concepts without battery storage and increases for systems with battery storage to between 15 m^2 (2.25 kWp) and 25 m^2 (3.74 kWp) for battery storage capacities of 15 kWh. As observed for the net CO_2 emissions indicators, a main difference between non-renewable primary energy use indicators and net non-renewable primary energy use indicators is the negative effect of battery storages on the net non-renewable primary energy use indicators due to the battery losses and, thus, the missing exported solar electricity for the compensation of non-renewable primary energy use for delivered electrical energy from the grid. As a result, the net non-renewable primary energy use indicators of the building decrease with increasing PV/PVT system size, but increase with increasing battery storage capacity. This is also shown for the example of a PV-ASHP system by the net non-renewable primary energy use indicators of the building depending on PV system and battery storage size in Figure 5.10b. For a minimum net non-renewable primary energy use indicator, the PV system size should be as large as possible within the considered range and the use of battery storage systems should be avoided.

Merging all results, only SHP systems with PV or PVT can fulfill the complete nZEB rating requirements (no exceeding of one of the maximum values). At this, a minimum PV module or PVT collector area between 15 m^2 (2.25 kWp) and 25 m^2 (3.74 kWp) is required, depending on the system concept, whereas PV-SISHP-S,P systems cannot fulfill the nZEB rating requirements. A summary of the results with regard to the complete nZEB rating is given in Table 5.3. Beside of the results for PV-ASHP and PVT-SASHP-P systems, differences between the minimum required PV module and minimum required PVT collector area to fulfill the complete nZEB rating cannot be observed, comparing PV and heat pump systems and PV-SISHP-S systems with PVT and heat pump systems. In case of PV plus solar thermal and heat pump systems with ASHP or GSHP, the minimum required PV module area can partially be reduced by the use of FPC collectors in comparison to the corresponding PV and heat pump systems. As described before, SHP systems with combinations of PV and PVT are equipped with a combined PV module and PVT collector area of 25 m^2 and are thus not considered in Table 5.3 as the minimum PV module and PVT collector area cannot be determined within the performed simulations. Nevertheless, it can be assumed that the minimum required PV module and PVT collector area is in the range of the minimum required PV module or PVT collector area of the corresponding PV or PVT and heat pump system. In case of PV-ASHP systems with battery storage, it can be observed for battery storage sizes larger than 5 kWh that the higher battery storage losses lead to higher minimum required PV module areas due to the exceeding of the nZEB requirements with regard to the net non-renewable primary energy use indicators. In contrast, in case of PV-ASHP systems without battery storage the total primary energy use indicators are the limiting values that lead to a minimum required PV module area of 25 m^2 (3.74 kWp).

Table 5.3: Overview of results and minimum required PV or PVT area to fulfill complete nZEB rating requirements for different heat pump and SHP system concepts in Strasbourg for SFH15.

	Minimum required PV or PVT area (system size)	
	System concepts without battery storage	System concepts with battery storage
ASHP	not fulfilled	not fulfilled
GSHP	not fulfilled	not fulfilled
SASHP-P	not fulfilled	not fulfilled
SGSHP-P	not fulfilled	not fulfilled
SISHP-S	not fulfilled	not fulfilled
SISHP-S,P	not fulfilled	not fulfilled
PV-ASHP	25 m^2 (3.74 kWp)	20 m^2 (2.99 kWp) for a battery storage capacity of 5 kWh, else 25 m^2 (3.74 kWp)
PV-GSHP	20 m^2 (2.99 kWp)	20 m^2 (2.99 kWp)
PV-SASHP-P	20 m^2 (2.99 kWp)	20 m^2 (2.99 kWp)
PV-SGSHP-P	15 m^2 (2.25 kWp)	15 m^2 (2.25 kWp)
PV-SISHP-S	20 m^2 (2.99 kWp)	20 m^2 (2.99 kWp)
PV-SISHP-S,P	not fulfilled	not fulfilled
PVT-SASHP-P	25 m^2 (3.74 kWp) for WISC PVT collectors / 20 m^2 (2.99 kWp) for covered flat-plate PVT collectors	20 m^2 (2.99 kWp)
PVT-SGSHP-P	20 m^2 (2.99 kWp)	20 m^2 (2.99 kWp)
PVT-SISHP-S	20 m^2 (2.99 kWp)	20 m^2 (2.99 kWp)

In addition to the mandatory KPIs for the nZEB rating, an overview of the range of RER based on total primary energy of the SFH15 building for the different heat pump and SHP system concepts in Strasbourg is shown in Figure 5.11. The RERs for system concepts with ASHP are in the range of 26 % (ASHP) and 75 % (PVT-SASHP-P, PV-PVT-SASHP-P), for systems with GSHP in the range of 29 % (GSHP) and 80 % (PVT-SGSHP-P, PV-PVT-SGSHP-P) and for SISHP systems in the range of 29 % (SISHP-S) and 77 % (PVT-SISHP-S, PV-PVT-SISHP-S). Basically, the simulation results show that the RER based on total primary energy of the building can be increased by adding solar technologies and that the different system concepts compete with each other. As observed for the decrease of primary energy, the RER can only significantly be increased by adding PV modules or PVT collectors. At this, the RER increases with increasing PV/PVT system size, but decreases due to battery losses with increasing battery storage capacity as observed for the net non-renewable primary energy use indicators as result of missing compensation of delivered primary energy by exported primary energy. With regard to the proposed nZEB rating procedure, the numerical benchmarks for the nZEB primary energy use lead to minimum RERs of SFH15 buildings that fulfill the nZEB requirements of 54 % for systems with ASHP, 56 % for systems with GSHP and 56 % for SISHP systems. With regard to CO_2 emissions, the CO_2 emissions indicators of SFH15 buildings that fulfill the nZEB requirements in moderate climates reach maximum values of 13.52 kg CO_2eq/m^2a for systems with ASHP, 12.70 kg CO_2eq/m^2a for systems with GSHP and 12.95 kg CO_2eq/m^2a for SISHP systems. This corresponds to minimum fractional CO_2 emission savings of 36 % compared

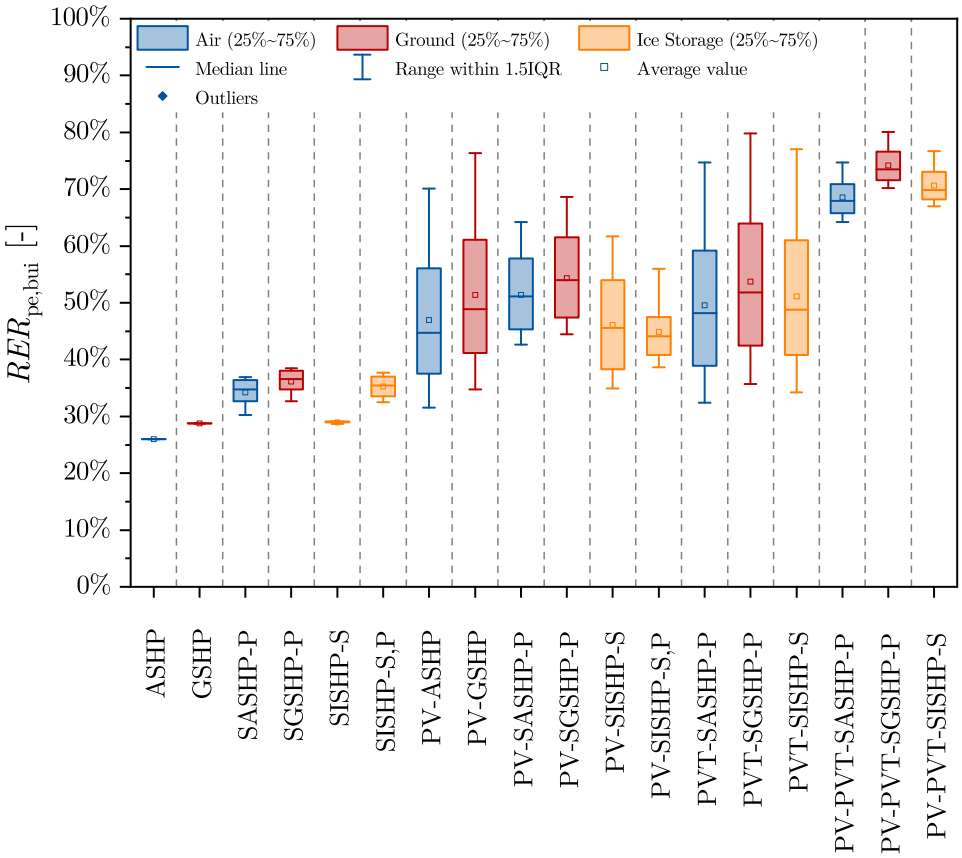

Figure 5.11: RER based on total primary energy of the building for different heat pump and SHP system concepts in Strasbourg for SFH15.

to the reference building with conventional heating system. Furthermore, the maximum net CO_2 emissions indicators of SFH15 buildings that fulfill the nZEB requirements in moderate climates are 8.46 kg CO_2eq/m^{2}a for systems with ASHP, 8.24 kg CO_2eq/m^{2}a for systems with GSHP and 7.88 kg CO_2eq/m^{2}a for SISHP systems. This corresponds to minimum net fractional CO_2 emission savings of 60 % compared to the reference building with conventional heating system. At this, the maximum CO_2 emissions indicators are achieved by system concepts without battery storage, whereas the maximum net CO_2 emissions indicators are achieved by system concepts with battery storage. In summary, the results point out that the integration of PV modules or PVT collectors is essential not only to fulfill the requirements of a nZEB, but also to achieve high RER values and low CO_2 emissions as required by the EPBD.

5.3 Influence of Subsidies and Carbon Prices on the Economic Efficiency

This section presents a case study on the *influence of subsidies and carbon prices on the economic efficiency* of SHP systems. For the following evaluations, the SFH45 building in Strasbourg is used as use case as it represents current legal requirements or renovated buildings with good thermal quality of the building envelope in moderate climates. As before, the PV-ASHP system is chosen to figure out the influence of subsidies and carbon

Table 5.4: Boundary conditions for economic efficiency calculations including CO_2 emission costs (all costs are net values excluding VAT).

Parameter	Value	Parameter	Value
$c_{\mathrm{el,SHP}}$	0.1643 €/kWh [a]	$c_{\mathrm{CO_2}}$	50 €/t CO_2eq [b]
$c_{\mathrm{el,hh}}$	0.1643 €/kWh [a]	$d_{\mathrm{CO_2}}$	20 %
c_{gas}	0.0410 €/kWh	$c_{\mathrm{CO_2,max}}$	180 €/t CO_2eq [c]

[a] Values from Table 4.7 are adjusted for an included carbon price by the EU ETS of $c_{\mathrm{CO_2}} = 50$ €/t CO_2eq from May 2021 [PV Magazine, 2021] with $f_{\mathrm{CO_2,del,el}} = 420$ g CO_2eq/kWh [ISO 52000-1, 2017].

[b] Based on a carbon price by the EU ETS of $c_{\mathrm{CO_2}} = 50$ €/t CO_2eq from May 2021 [PV Magazine, 2021].

[c] Based on a carbon price increase path to 180 €/t CO_2eq until 2030 presented by Kemmler et al. [2020].

prices on the detailed system sizing. Furthermore, the reference building with conventional gas-fired heating system described for the environmental impact evaluation in Section 4.3 is also used to calculate reference values. The LCOEn is chosen as main KPI for the rating of the economic efficiency of the thermal and electrical energy supply of a building, whereas a distinction is made between:

- the levelized cost of heat and electricity for a building $LCOEn_{\mathrm{bui}}$ and
- the levelized cost of heat and electricity for a building including CO_2 emission costs $LCOEn_{\mathrm{CO_2,bui}}$.

The CO_2 emission costs are calculated without compensation by exported energy using carbon prices. Furthermore, the calculations based on the boundary conditions and initial investment costs described in Section 4.4, whereas in case of electricity prices the values from Table 4.7 are adjusted for an included carbon price. The adjusted values are summarized in Table 5.4 with additional values for the calculation of LCOEn values with CO_2 emission costs. Similar to the conditions for building renovations with heat pumps or SHP systems in Germany, the amount of subsidies is assumed to be 35 % of the investment costs related to the heat pump system or the thermal part of the SHP system including different system components depending on the considered heat pump or SHP system:

$$S_{0,\mathrm{th}}^{\mathrm{SHP}} = 35\,\% \cdot I_{0,\mathrm{th}}^{\mathrm{SHP}}. \tag{5.5}$$

Beginning with the base case without subsidies and carbon prices from Section 4.4.1, the following use cases are analyzed in this section:

- Economic efficiency with consideration of carbon prices
- Economic efficiency with consideration of subsidies
- Economic efficiency with consideration of carbon prices and subsidies.

An overview of the range of LCOEn values for the SFH45 building with different heat pump and SHP system concepts in Strasbourg is shown in Figure 5.12a. The LCOEn reaches minimum values of 0.1837 €/kWh for systems with ASHP (PV-ASHP), 0.1930 €/kWh for systems with GSHP (PV-GSHP) and 0.2551 €/kWh for SISHP systems (PV-SISHP-S). For comparison, the value of the reference building with conventional heating system is 0.1636 €/kWh and, thus, all heat pump and SHP system concepts achieve higher LCOEn

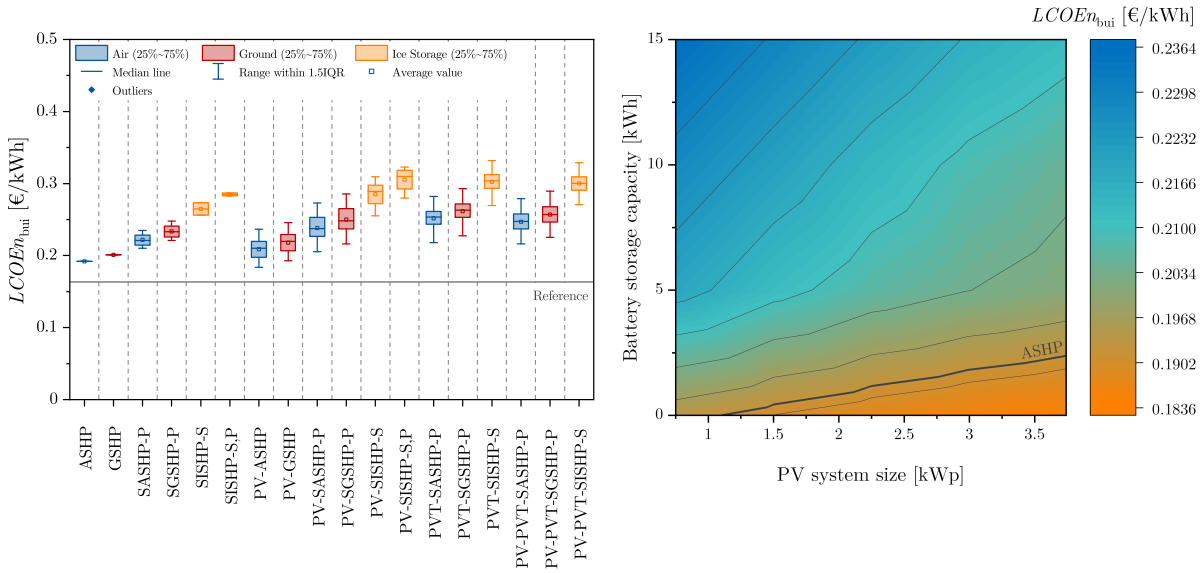

(a) Overview **(b)** PV-ASHP

Figure 5.12: LCOEn for the SFH45 building with different heat pump and SHP system concepts in Strasbourg.

values than the reference building. At this, the lower LCOEn values of systems with ASHP in comparison with systems with GSHP or ice storage illustrate that the higher initial investment costs of these systems cannot be compensated by the reduction of delivered electrical energy to the building due to the higher energy efficiency of these systems. Furthermore, the LCOEn can only be decreased in some cases by adding PV modules in comparison to heat pump systems without solar technologies. PVT and heat pump system concepts achieve the highest LCOEn values, whereas PV and heat pump systems and PV-SISHP-S systems in case of systems with ice storage achieve the lowest LCOEn values. At this, solar thermal and heat pump systems achieve lower minimum LCOEn values than PVT and heat pump systems. In addition, the higher initial investment costs for battery storages cannot be compensated by the reduction of delivered electrical energy to the building due to higher self-sufficiency which is shown by increasing LCOEn values with increasing battery storage capacity. For the shown example of a PV-ASHP system (Figure 5.12b), the LCOEn reaches minimum values of 0.2121 €/kWh with a battery storage capacity of 15 kWh and 0.1837 €/kWh without battery storage. At this, the LCOEn decreases with increasing PV system size and decreasing battery storage capacity and falls below the values of an ASHP system without PV for PV system sizes larger than around 1.1 kWp in case of systems without battery storage. In addition, the contour plot suggests that a good ratio of battery storage capacity to PV system size to achieve LCOEn values below the values of an ASHP is around 0.5 kWh/1 kWp. For a minimum LCOEn, a system without battery storage should be used and the PV system size should be as large as possible within the considered range.

An overview of the range of LCOEn values including CO_2 emission costs for the SFH45 building with different heat pump and SHP system concepts in Strasbourg is shown in Figure 5.13a. The LCOEn values increase compared to the values without CO_2 emission costs reaching minimum values of 0.2019 €/kWh for systems with ASHP (PV-ASHP), 0.2087 €/kWh for systems with GSHP (PV-GSHP) and 0.2731 €/kWh for SISHP systems (PV-SISHP-S). For comparison, the value of the reference building with conventional heat-

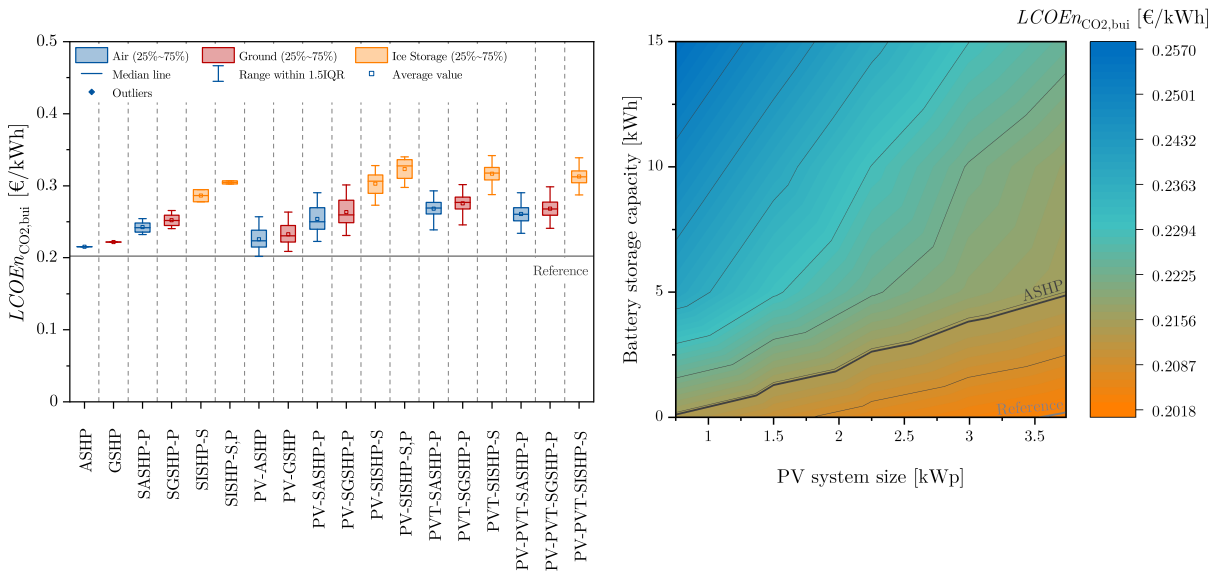

(a) Overview **(b)** PV-ASHP

Figure 5.13: LCOEn including CO_2 emission costs (without compensation by exported energy) for the SFH45 building with different heat pump and SHP system concepts in Strasbourg.

ing system is 0.2025 €/kWh. Even if all heat pump and SHP system concepts beside of PV-ASHP systems achieve higher LCOEn values than the reference building, the consideration of carbon prices leads to an increase of the economic efficiency of heat pump and SHP systems in comparison to the reference building. Moreover, the higher initial investment costs for systems with GSHP can also not be compensated by the higher energy efficiency of the systems in comparison to the corresponding systems with ASHP, but the difference between the LCOEn values decreases by consideration of carbon prices. Furthermore, the main findings from the LCOEn evaluation without CO_2 emission costs for the SFH45 building in Strasbourg can be confirmed. For the shown example of a PV-ASHP system (Figure 5.13b), the LCOEn reaches minimum values of 0.2241 €/kWh with a battery storage capacity of 15 kWh and 0.2019 €/kWh without battery storage. At this, the LCOEn also decreases with increasing PV system size and decreasing battery storage capacity and falls below the values of an ASHP system without PV for all PV system sizes in case of systems without battery storage. In addition, the contour plot suggests that a good ratio of battery storage capacity to PV system size to achieve LCOEn values below the values of an ASHP is around 1 kWh/1 kWp. Furthermore, it can be observed that the LCOEn of the reference building can be reached by PV-ASHP systems without battery storage with large PV system sizes around 3.5 kWp. For a minimum LCOEn including CO_2 emission costs, a system without battery storage should be used and the PV system size should be as large as possible within the considered range.

An overview of the range of LCOEn values with consideration of subsidies for the SFH45 building with different heat pump and SHP system concepts in Strasbourg is shown in Figure 5.14a. The LCOEn values decrease compared to the values without subsidies reaching minimum values of 0.1576 €/kWh for systems with ASHP (PV-ASHP), 0.1609 €/kWh for systems with GSHP (PV-GSHP) and 0.2077 €/kWh for SISHP systems (PV-SISHP-S). For comparison, the value of the reference building with conventional heating system is un-

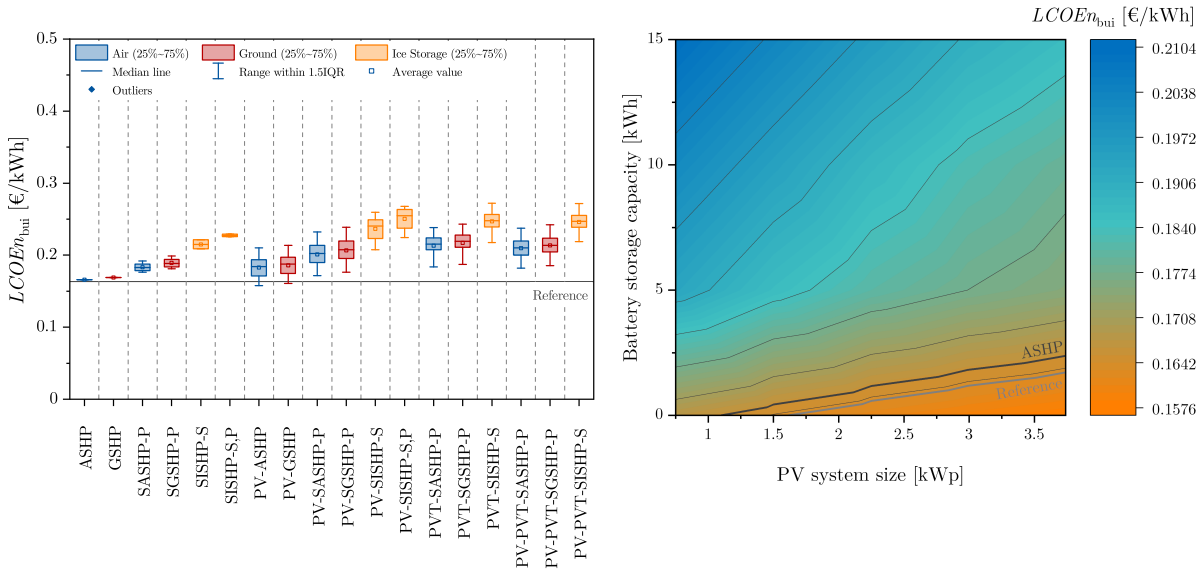

(a) Overview **(b)** PV-ASHP

Figure 5.14: LCOEn with subsidies for the SFH45 building with different heat pump and SHP system concepts in Strasbourg.

changed at 0.1636 €/kWh. In contrast to the evaluations without consideration of subsidies, PV-GSHP as well as PV-ASHP systems achieve lower minimum LCOEn values than the reference building, whereas all other heat pump and SHP system concepts achieve higher LCOEn values than the reference building. Nevertheless, the consideration of subsidies leads to an increase of the economic efficiency of heat pump and SHP systems in comparison to the reference building. Even if the higher initial investment costs for systems with GSHP can also not be compensated by the higher energy efficiency of the systems in comparison to the corresponding systems with ASHP, the difference between the LCOEn values decreases by consideration of subsidies. Furthermore, the main findings from the LCOEn evaluation without subsidies for the SFH45 building in Strasbourg can be confirmed. For the shown example of a PV-ASHP system (Figure 5.14b), the LCOEn reaches minimum values of 0.1860 €/kWh with a battery storage capacity of 15 kWh and 0.1576 €/kWh without battery storage. At this, the LCOEn also decreases with increasing PV system size and decreasing battery storage capacity and falls below the values of an ASHP system without PV for PV system sizes larger than around 1.1 kWp in case of systems without battery storage. In addition, the contour plot suggests that a good ratio of battery storage capacity to PV system size to achieve LCOEn values below the values of an ASHP is around 0.5 kWh/1 kWp. Furthermore, it can be observed that the LCOEn of the reference building can be reached by PV-ASHP systems without battery storage with PV system sizes around 1.6 kWp. For a minimum LCOEn including subsidies, a system without battery storage should be used and the PV system size should be as large as possible within the considered range.

An overview of the range of LCOEn values including CO_2 emission costs with consideration of subsidies for the SFH45 building with different heat pump and SHP system concepts in Strasbourg is shown in Figure 5.15a. The LCOEn values decrease compared to the evaluations without subsidies, but increase compared to the values with subsidies without consideration of CO_2 emission costs. The LCOEn reaches minimum values of 0.1758 €/kWh for systems with ASHP (PV-ASHP), 0.1766 €/kWh for systems with GSHP (PV-GSHP)

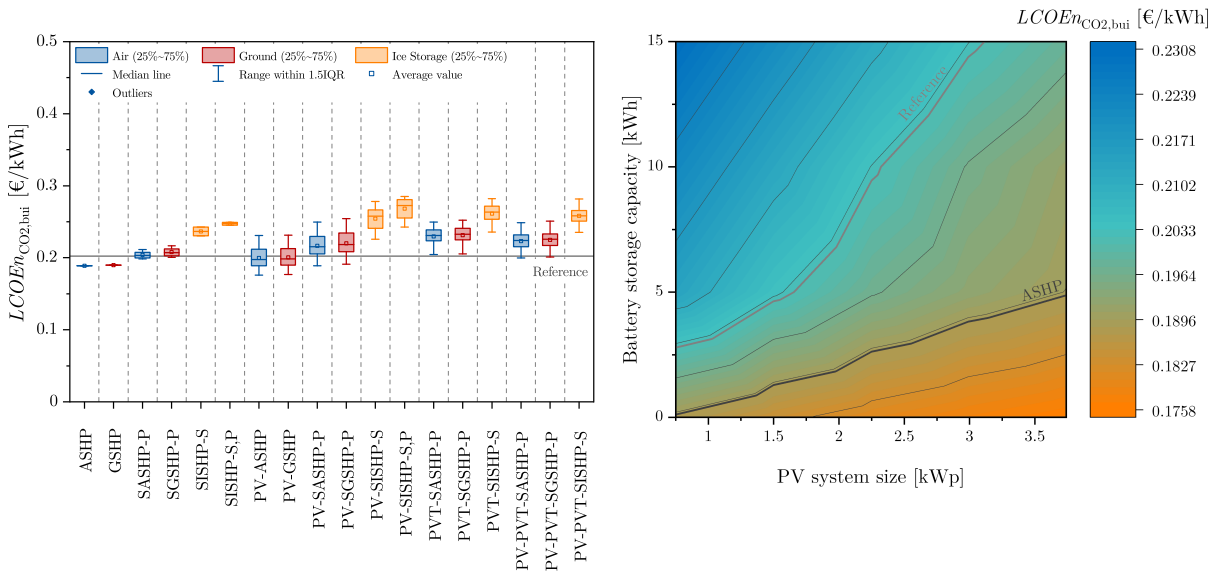

(a) Overview **(b)** PV-ASHP

Figure 5.15: LCOEn including CO_2 emission costs (without compensation by exported energy) with subsidies for the SFH45 building with different heat pump and SHP system concepts in Strasbourg.

and 0.2258 €/kWh for SISHP systems (PV-SISHP-S). For comparison, the value of the reference building with conventional heating system is 0.2025 €/kWh. In contrast to the previous use cases, all heat pump and SHP system concepts achieve lower minimum LCOEn values than the reference building with exception of PVT and heat pump systems and system concepts with ice storage. Hence, the consideration of carbon prices and subsidies leads to the highest economic efficiency of heat pump and SHP systems in comparison to the reference building. At this, solar thermal and heat pump systems can only reach the LCOEn values of the reference building for small FPC areas which illustrates that the higher initial investment costs for larger FPC areas cannot be compensated by the higher energy efficiency. In contrast, the higher initial investment costs for systems with GSHP can nearly be compensated by the higher energy efficiency of the systems in comparison to the corresponding systems with ASHP and the LCOEn values are only slightly higher for systems with GSHP. Moreover, the LCOEn can be decreased in some cases of PV and heat pump systems as well as PV-SASHP-P systems in comparison to heat pump systems without solar technologies. Furthermore, PV plus solar thermal and heat pump systems with parallel FPC integration achieve the highest LCOEn values, whereas PV and heat pump systems and PV-SISHP-S systems in case of systems with ice storage achieve the lowest LCOEn values. At this, PVT-SASHP-P and PV-SASHP-P reach the same maximum LCOEn values. Consequently, the results show that the higher energy efficiency of PVT and heat pump systems can partially compensate the higher initial investment costs in comparison to PV plus solar thermal and heat pumps systems if both carbon prices and subsidies are taken into account. Further findings from the LCOEn evaluation without subsidies for the SFH45 building in Strasbourg can be confirmed. For the shown example of a PV-ASHP system (Figure 5.15b), the LCOEn reaches minimum values of 0.1980 €/kWh with a battery storage capacity of 15 kWh and 0.1758 €/kWh without battery storage. At this, the LCOEn also decreases with increasing PV system size and decreasing battery storage capacity and falls

below the values of an ASHP system without PV for all PV system sizes in case of systems without battery storage. In addition, the contour plot suggests that a good ratio of battery storage capacity to PV system size to achieve LCOEn values below the values of an ASHP is around 1 kWh/1 kWp. Furthermore, it can be observed that the LCOEn of the reference building can be undershot by PV-ASHP systems without battery storage for all PV system sizes. In contrast to the previous use cases, even PV-ASHP systems with battery storage can reach the LCOEn values of the reference building, whereas the counter plot suggests that a good ratio of battery storage capacity to PV system size to achieve LCOEn values below the values of the reference building is around 3 kWh/1 kWp. Nevertheless, for a minimum LCOEn including CO_2 emission costs and subsidies, a system without battery storage should be used and the PV system size should be as large as possible within the considered range.

Even if the economic efficiency analysis is limited to the used boundary conditions, the results point out that the consideration of carbon prices benefits more efficient systems with less CO_2 emissions which is shown in an increasing economic efficiency of buildings with SHP systems in comparison to buildings with heat pumps or conventional gas-fired heating system. This results e.g. in a better economic efficiency of PV-ASHP systems without battery storage in comparison to ASHP systems. Moreover, subsidies significantly support the economic efficiency of heat pump and SHP systems and can lead in combination with carbon prices to an economic competitiveness of most SHP system concepts in comparison to the reference system recognizing the reduction of CO_2 emissions. Furthermore, the results point out the need for cost reductions, especially for battery storages, ice storages and PVT collectors. At this, PVT and heat pump systems or systems with ice storage cannot compete economically with other SHP systems or reach the economic efficiency of buildings with conventional gas-fired heating system. Nevertheless, as mentioned before, the economic efficiency analysis depends on the used boundary conditions, which are currently very uncertain and variable and cannot be predicted for the future.

Chapter 6

Conclusions and Outlook

Future building design requires the efficient and smart energy supply of residential buildings with high amounts of renewable energies and low CO_2 emissions. Solar and heat pump (SHP) systems are one of the most, or even perhaps the most, promising concepts to meet this challenge. This work addresses main issues on the modeling and simulation of SHP systems and the evaluation of SHP system concepts with regard to efficiency, environmental impact and economic aspects for different climates and types of single-family houses. The objective was further to close the gap of widely ranged and comparable studies with special focus on both thermal and electrical energy supply of buildings by SHP systems. The contributions of this work can be summarized in three main parts by the used methodological approach of model-based system analysis: *theoretical and conceptual work*, *modeling* and *system analysis*.

In the first part of this thesis, the reader was introduced to the basics of solar and heat pump technologies as well as SHP systems with special focus on the energy supply of buildings. First, the necessary background information on the technologies, its functioning and classification to understand the research work were given. The EU Energy Performance of Buildings Directive (EPBD) introduced nearly zero energy buildings (nZEB) as standard for all new buildings by 2021. Therefore, an extended rating procedure for the evaluation of the nZEB standard was adapted for its application on the whole thermal and electrical energy supply of buildings with SHP system, whereas new numerical benchmarks including appliances were proposed in the last part of this work. Furthermore, a methodology to describe the composition of SHP systems with special attention on the interaction of thermal and electrical system component parts by block diagrams was developed and applied for the description of the considered SHP systems in this work. It can be stated that the developed method serves its purpose as it was accepted by the research community and had been used for the representation of photovoltaic-thermal (PVT) systems within the International Energy Agency Solar Heating and Cooling Programme Task 60. Due to the lack of appropriate standardized performance indicators, detailed formulations of key performance indicators (KPIs) were presented with introduction of new KPIs, e.g. a seasonal performance figure of the whole building including the thermal and electrical energy supply to evaluate the energy efficiency of SHP systems or the levelized cost of heat and electricity

together as levelized cost of energy (LCOEn) including a modification for the consideration of environmental impact costs within economic efficiency evaluations. Furthermore, this part presented an overview for which application and evaluation quantity the different KPIs can be used. Hence, this thesis provides an overview of methods for the description and evaluation of SHP systems for the energy supply of residential buildings.

The second part mainly focuses on the modeling of SHP systems within the simulation environment TRNSYS [TRNSYS, 2020]. On the one hand, this part gave the reader detailed insights to the modeling of SHP systems and its components like heat pumps and heat source circuits, energy storages or solar thermal collectors by existing models. On the other hand, a new model for PVT collectors based on existing modeling approaches was implemented in TRNSYS. The model connects the quasi-dynamic thermal collector model of ISO 9806 with a photovoltaic (PV) performance model via a two-node model approach with internal heat transfer coefficient. The model was validated using a new developed parameter identification procedure for TRNSYS with GenOpt and measurements of real PVT collectors. The presented approach was introduced as *one-step approach with combined thermal and electrical parameter identification procedure (combined fit)*. The PVT performance model may form the basis for future PVT collector performance testing, certification and standardization schemes. In addition, this work has shown how SHP systems can be modeled and connected to building models by a modeling approach based on subsystems in TRNSYS. The composition of the component models to SHP subsystem models were wrapped up in a model library for TRNSYS called SHP-SimLib which is published and freely available. Finally, this part gave insights to the rule-based control of SHP systems. Thus, a valuable contribution was made to the modeling of SHP systems that offers further simulation possibilities by other works.

The last part of this thesis includes the *system analysis* based on the developed models and can be divided in two main contributions starting with the *system design analysis* regarding performance and efficiency, environmental impact and economic aspects and ending up with *case studies* to discuss the potential of SHP systems and special topics by detailed analyses of use cases, as, unfortunately, the wide range of this work did not allow a detailed analysis of each simulation case.

In general, the *system design analysis* illustrates that the use of solar technologies and battery storages improves the *efficiency and environmental impact* of heat pump systems reaching CO_2 emission savings up to 71 % in comparison to reference buildings with conventional gas-fired heating system in moderate climates. Although systems with parallel flat-plate collector (FPC) integration achieve good results in terms of heating efficiency, systems with PV and PVT have major advantages in terms of energy efficiency and reducing CO_2 emissions with (slightly) better results for systems with PVT. Even if systems with PVT benefit from the combined generation of heat and electricity, especially for system concepts with ice storage in which the necessary solar thermal collectors are replaced, the on-site generated solar electrical energy, used to cover both the electricity consumption of the heating system and the household electricity consumption, has the greatest impact on the energy efficiency and reduction of CO_2 emissions of a building. At this, major benefits for the specific solar electrical yield of PVT collectors compared to PV modules cannot be observed and the advantage of PVT systems is less the cooling of PV cells, but the better utilization of limited roof areas. Furthermore, battery storages have a major influence on the efficiency and environmental impact for systems with PV and PVT and are necessary to reach low CO_2 emission indicators without compensation by exported energy. At this, the CO_2 emissions can be reduced by up to 45 % in moderate climates due to the increasing

self-consumption reaching self-sufficiency values of the building up to 60 %. Major benefits by the combination of different solar technologies cannot be observed. With regard to the heat source, SHP systems with ground source heat pump (GSHP) achieve the highest efficiency and lowest CO_2 emissions and show their benefits especially for buildings with high heating energy demands and locations with low annual average ambient temperature. SHP systems with ice storage achieve higher efficiency values and lower CO_2 emissions than systems with air source heat pump (ASHP) without integration of solar technologies and can compete with systems with ASHP and GSHP, especially in combination with PVT collectors. Depending on the system concept, SHP systems with ASHP can compete with systems with GSHP in moderate and warm climates, while in cold climates the efficiency of GSHP systems cannot be achieved by systems with ASHP. Regarding different building types, the results point out that the use of SHP systems can partially compensate a lower quality of the building envelope with regard to the environmental impact. In addition, when comparing different buildings, it should be mentioned that higher efficiency does not generally lead to lower CO_2 emission indicators, since the energy demands of the building types differ. Regarding the *economic efficiency* in terms of LCOEn, systems with ASHP achieve the lowest values (i.e. the best results), while systems with GSHP achieve slightly higher values and systems with ice storage achieve by far the highest values. Nevertheless, SHP system concepts are not profitable in comparison with the reference systems if carbon prices or subsidies are not considered. Furthermore, the results point out that for the used boundary conditions only PV and heat pump systems can compete economically with heat pump systems without solar technologies. Moreover, the results of the economic efficiency analysis illustrate that the higher initial investment costs for systems with GSHP and in particular systems with ice storage cannot be compensated by the higher energy efficiency of the systems compared to the corresponding systems with ASHP. In addition, the higher initial investment costs for battery storage systems cannot be compensated by the higher self-sufficiency. Nevertheless, depending on the PV and battery storage size, the economic efficiency of PV and heat pump systems with battery storage is partially higher than for the corresponding solar thermal and heat pump systems with the same parallel FPC collector area. In most cases, a good compromise of environmental impact and economic efficiency is given by PV-ASHP system concepts in moderate and warm climates and PV-GSHP system concepts in cold climates.

Regarding the *case studies*, a detailed solar and battery storage design analysis shows the correlation of different KPIs of the building and mainly illustrates that even if the economic efficiency does not generally counteract the efficiency or environmental impact, the system design with highest efficiency and lowest environmental impact is not equal to the system design with the highest economic efficiency (for the used boundary conditions). Thus, the system design especially depends on the objective. A high self-sufficiency reached by large battery storage and PV system sizing leads to high efficiency and low CO_2 emissions of the building, whereas for a maximum economic efficiency a system without battery storage should be used and the PV system size should be as large as possible within the considered range. With regard to different PVT collector technologies, it can be recommended to use covered flat-plate PVT collectors in system concepts with parallel integration, while wind and/or infrared sensitive PVT collectors show slightly better results in terms of CO_2 emissions for system concepts with serial integration if the exported energy is taken into account. Nevertheless, the results should be verified for other PVT collector constructions. A case study on nZEBs in moderate climates points out that even new buildings with very high energy standard need PV/PVT systems with a minimum module/collector area

of between 15 m² (2.25 kWp) and 25 m² (3.74 kWp) to fulfill the nZEB requirements which raises the question of whether current legal regulations in different countries comply with the EPBD. An extended economic efficiency analysis − limited to the used boundary conditions that are currently very uncertain and cannot be predicted for the future − demonstrates that even if the consideration of carbon prices benefits more efficient systems with less CO_2 emissions, subsidies significantly support the economic efficiency of heat pump and SHP systems and can lead in combination with carbon prices to an economic competitiveness of most SHP system concepts in comparison to the reference system recognizing the reduction of CO_2 emissions. Furthermore, the results point out the need for cost reductions, especially for battery storages, ice storages and PVT collectors. In summary, the system investigations in this work illustrate that SHP systems with PV or PVT are an essential technology for buildings to fulfill the requirements of a nZEB and to achieve high renewable energy ratios and low CO_2 emissions as required by the EPBD. SHP systems will further support the linking of heat and electricity in future energy systems providing decentralized thermal and electrical energy storage capacities and energy flexibility to buildings.

As a continuation of this work, the developed model libraries and achieved results will allow for further investigations that are described in the following. First of all, future work could address the *enhancement of the model library* SHP-SimLib. Here, the most important extensions are the integration of electric vehicles and cooling systems (e.g. with reversible heat pumps) for a better representation of future building requirements. With regard to electric vehicles, it would be interesting to analyze aspects like the increasing possibilities of solar electricity self-consumption, bidirectional charging or the influence of day- and night-charging scenarios. This is directly linked to the *development and analysis of control strategies* by the use of SHP-SimLib, e.g. with focus on the smartness and flexibility of buildings with SHP systems. Beside the system design, the system control and grid integration of SHP systems are current and future research objects. Nevertheless, operation in a smart grid not necessarily increase the efficiency of the individual systems and different objectives like reducing operating cost and maximizing system efficiency or PV self-consumption can be conflicting [Fischer, 2017]. Thus, future work should investigate the smart control of SHP systems, e.g. by the use of the Smart Grid-Ready interface and advanced control methods like model predictive control, from a household investors and distribution network operators perspective. At this, the developed models have already been enhanced and used for first studies in this research direction. Furthermore, *adaptions of the model libraries* would allow investigations of multi-family houses, office buildings or even district heating and cooling systems. In addition, the model libraries could be used for the *improvement and development of system components and new system approaches* including hardware-in-the-loop investigations. The influence of other PVT collector constructions or more efficient variable speed heat pumps on the results are further research questions that could not be answered by this work. For urban areas with limited space or structural restrictions, the serial integration of PVT collectors directly coupled to a heat pump without ice storage is an example for an interesting new system approach. Finally, the *further analysis of SHP systems* using the developed models, e.g. the application of multi-objective optimization for the system design, the analysis of the influence of feed-in limit for excess solar power or shut-off times of the heat pump (heat pump tariffs) or the influence of other roof constructions with larger PV system sizes, could give more insights to SHP systems. In addition, a limitation of this work is the consideration of different user behavior and its influence on the results, which could be analyzed by the developed models. The published results could also be used to investigate research topics that could not be addressed within

the scope of this work, namely: multi-criteria evaluation/assessment with different multi-criteria decision-making techniques, life cycle assessment or economic efficiency analysis with changing boundary conditions. In summary, this work not only makes a contribution to the model-based analysis of SHP systems, it also provides the basis for further work in this research area.

List of Figures

List of Tables

Bibliography

Akasol, 2014. Bedienung & Installation. neeoQube 48 V. Akasol GmbH.

Almeida, P., Carvalho, M. J., Amorim, R., Mendes, J. F., Lopes, V., 2014. Dynamic testing of systems - Use of TRNSYS as an approach for parameter identification. Solar Energy 104, 60–70.

Baez, M. J., Martínez, T. L., 2015. Technical Report on the Elaboration of a Cost Estimation Methodology. Work Package 3 - Estimating RHC energy costs. Deliverable number D.3.1. Creara, Madrid, Spain.

Battaglia, M., Haberl, R., Bamberger, E., Haller, M., 2017. Increased self-consumption and grid flexibility of PV and heat pump systems with thermal and electrical storage. 11th International Renewable Energy Storage Conference, IRES 2017, 14-16 March 2017, Düsseldorf, Germany. Energy Procedia 135, 358–366.

Bee, E., 2019. Heat pump and photovoltaic systems in residential applications. Performance, potential, and control of the system. Ph.D. thesis, University of Trento, Italy.

Bee, E., Prada, A., Baggio, P., Psimopoulos, E., 2019. Air-source heat pump and photovoltaic systems for residential heating and cooling: Potential of self-consumption in different European climates. Building Simulation 12 (3), 453–463.

Bellos, E., Tzivanidis, C., Moschos, K., Antonopoulos, K. A., 2016. Energetic and financial evaluation of solar assisted heat pump space heating systems. Energy Conversion and Management 120, 306–319.

Bertram, E., 2015. Heat Pump Systems with Vertical Ground Heat Exchanger and Uncovered Solar Thermal Collectors. Ph.D. thesis, Leibniz Universität Hannover, Germany.

Bertram, E., Glembin, J., Scheuren, J., Rockendorf, G., 2010. Condensation Heat Gains on Unglazed Solar Collectors in Heat Pump Systems. In: Proceedings of the 8th ISES EuroSun Conference (EuroSun 2010). Graz, Austria.

Bilbao, J. I., Sproul, A. B., 2015. Detailed PVT-water model for transient analysis using RC networks. Solar Energy 115, 680–693.

Bonin, J., 2015. Heat Pump Planning Handbook. Routledge, New York, USA.

Branker, K., Pathak, M. J. M., Pearce, J. M., 2011. A review of solar photovoltaic levelized cost of electricity. Renewable and Sustainable Energy Reviews 15, 4470–4482.

Budig, C., Orozaliev, J., de Keizer, A. C., Kusyy, O., K., V., 2009. Collector parameter identification methods and their uncertainties. In: Proceedings of the ISES Solar World Congress 2009 (SWC 2009). Johannesburg, South Africa.

Bundesnetzagentur, 2021. Zahlen, Daten und Informationen zum EEG. Accessed 10 November 2021.
URL https://www.bundesnetzagentur.de/DE/Sachgebiete/ElektrizitaetundGas/Unternehmen_Institutionen/ErneuerbareEnergien/ZahlenDatenInformationen/start.html

Carbonell, D., Haller, M. Y., Frank, E., 2014a. Potential benefit of combining heat pumps with solar thermal for heating and domestic hot water preparation. 2013 ISES Solar World Congress. Energy Procedia 57, 2656–2665.

Carbonell, D., Haller, M. Y., Philippen, D., Frank, E., 2014b. Simulations of combined solar thermal and heat pump systems for domestic hot water and space heating. SHC 2013, International Conference on Solar Heating and Cooling for Buildings and Industry September 23-25, 2013, Freiburg, Germany. Energy Procedia 48, 524–534.

Chow, T. T., 2003. Performance analysis of photovoltaic-thermal collector by explicit dynamic model. Solar Energy 75, 143–152.

Chua, K. J., Chou, S. K., Yang, W. M., 2010. Advances in heat pump systems: A review. Applied Energy 87, 3611–3624.

D'Agostino, D., Mazzarella, L., 2019. What is a Nearly zero energy building? Overview, implementation and comparison of definitions. Journal of Building Engineering 21, 200–212.

Dekking, F. M., Kraaikamp, C., Lopuhaä, H. P., Meester, L. E., 2005. A Modern Introduction to Probability and Statistics. Understanding Why and How. Springer, London, England.

Dott, R., Genkinger, A., Afjei, T., 2012. System evaluation of combined solar & heat pump systems. SHC 2012. Energy Procedia 30, 562–570.

Dott, R., Haller, M. Y., Ruschenburg, J., Ochs, F., Bony, J., 2013. The Reference Framework for System Simulations of the IEA SHC Task 44 / HPP Annex 38. Part B: Building and Space Heat Load. Report C1 Part B, Final Revised Edition. International Energy Agency, Solar Heating and Cooling Programme.

Drück, H., 2006. TRNSYS Type 340 MULTIPORT Store-Model. Institut für Thermodynamik und Wärmetechnik (ITW), Universität Stuttgart, Stuttgart, Germany.

Duffie, J. A., Beckman, W. A., 2013. Solar Engineering of Thermal Processes, Fourth Edition. John Wiley & Sons, New Jersey, USA.

Duffie, J. A., Beckman, W. A., Blair, N., 2020. Solar Engineering of Thermal Processes, Photovoltaics and Wind, Fifth Edition. John Wiley & Sons, New Jersey, USA.

EHPA, 2021. Heat pump sales overview. European Heat Pump Association, accessed 03 March 2021.
URL http://www.stats.ehpa.org/hp_sales/story_sales/

Eicker, U., 2003. Solar Technologies for Buildings. John Wiley & Sons, Chichester, England.

Elsheikh, A., Awais, M. U., Widl, E., Palensky, P., 2013a. Modelica-enabled rapid prototyping of cyber-physical energy systems via the functional mockup interface. In: Proceedings of the 2013 IEEE Workshop on Modeling and Simulation of Cyber-Physical Energy Systems (MSCPES 2013). Kuala Lumpur, Malaysia.

Elsheikh, A., Widl, E., Palensky, P., Dubisch, F., Brychta, M., Basciotti, D., Müller, W., 2013b. Modelica-enabled rapid prototyping via TRNSYS. In: Proceedings of the 13th International IBPSA Building Simulation Conference (BS 2013). Chambéry, France, pp. 3291–3298.

EN 14511, 2013. EN 14511:2013 Air conditioners, liquid chilling packages and heat pumps with electrically driven compressors for space heating and cooling. European Committee for Standardization (CEN), Brussels, Belgium.

Engel, G., Chakkaravarthy, A. S., Schweiger, G., 2018. Co-simulation Between Trnsys and Simulink Based on Type155. In: Cerone, A., Roveri, M. (Eds.), Software Engineering and Formal Methods. Vol. 10729 of Lecture Notes in Computer Science. Springer, Cham, Switzerland, pp. 315–329.

European Commission, 2013. Progress by Member States towards Nearly Zero-Energy Buildings. Report from the Comission to the European Parliament and the Council.

European Commission, 2016. Commission recommendation (EU) 2016/1318 of 29 July 2016 on guidelines for the promotion of nearly zero-energy buildings and best practices to ensure that, by 2020, all new buildings are nearly zero-energy buildings.

European Commission, 2019. EU climate action. Accessed 16 January 2019.
URL https://ec.europa.eu/clima/citizens/eu_en

European Commission, 2020a. 2050 long-term strategy. Accessed 27 November 2020.
URL https://ec.europa.eu/clima/policies/strategies/2050_en#tab-0-0

European Commission, 2020b. Energy performance of buildings directive. Accessed 27 November 2020.
URL https://ec.europa.eu/energy/topics/energy-efficiency/energy-efficient-buildings/energy-performance-buildings-directive_en

European Commission, 2021a. 2030 climate & energy framework. Accessed 23 April 2021.
URL https://ec.europa.eu/clima/policies/strategies/2030_en#tab-0-0

European Commission, 2021b. Communication from the Commission to the European Parliament, the Council, the European Economic and Social Committee and the Committee of the Regions Empty 'Fit for 55': delivering the EU's 2030 Climate Target on the way to climate neutrality.

European Commission, 2021c. European Green Deal: Commission proposes transformation of EU economy and society to meet climate ambitions. Accessed 04 September 2022.
URL https://ec.europa.eu/commission/presscorner/detail/en/IP_21_3541

European Environment Agency, 2021. EU achieves 20-20-20 climate targets, 55 % emissions cut by 2030 reachable with more efforts and policies. Accessed 04 September 2022. URL https://www.eea.europa.eu/highlights/eu-achieves-20-20-20

European Parliament, 2010. Directive 2010/31/EU of the European Parliament and of the Council of 19 May 2010 on the energy performance of buildings.

European Parliament, 2018. Directive 2018/844/EU of the European Parliament and of the Council of 30 May 2018 amending Directive 2010/31/EU on the energy performance of buildings and Directive 2012/27/EU on energy efficiency.

Eurostat, 2020a. Energy consumption in households. Accessed 27 November 2020. URL https://ec.europa.eu/eurostat/statistics-explained/index.php?title=Energy_consumption_in_households

Eurostat, 2020b. Europe 2020 headline indicators. Accessed 27 November 2020. URL https://ec.europa.eu/eurostat/statistics-explained/index.php?title=Europe_2020_headline_indicators#Energy_efficiency.2C_greenhouse_gas_emissions_and_share_of_renewable_energy_in_gross_final_energy_consumption

Eurostat, 2021a. Electricity price statistics. Accessed 10 November 2021. URL https://ec.europa.eu/eurostat/statistics-explained/index.php?title=Electricity_price_statistics#Electricity_prices_for_household_consumers

Eurostat, 2021b. Natural gas price statistics. Accessed 10 November 2021. URL https://ec.europa.eu/eurostat/statistics-explained/index.php?title=Natural_gas_price_statistics#Natural_gas_prices_for_household_consumers

Facci, A. L., Krastev, V. K., Falcucci, G., Ubertini, S., 2019. Smart integration of photovoltaic production, heat pump and thermal energy storage in residential applications. Solar Energy 192, 133–143.

Faiman, D., 2008. Assessing the outdoor operating temperature of photovoltaic modules. Progress in Photovoltaics: Research and Applications 16, 307–315.

Faßnacht, T., 2015. Moderne Regelungsansätze für Solarsysteme mit integrierter Wärmepumpe und Gebäudeheizung. Ph.D. thesis, Universität Stuttgart, Germany.

Fischer, D., 2017. Integrating Heat Pumps into Smart Grids. Ph.D. thesis, KTH Royal Institute of Technology, Stockholm, Sweden.

Fischer, S., Frey, P., Drück, H., 2012. A comparison between state-of-the-art and neural network modelling of solar collectors. Solar Energy 86, 3268–3277.

Fischer, S., Müller-Steinhagen, H., 2009. Collector efficiency testing - the 2-node collector model ready for implementation in european standard EN 12975. In: Proceedings of the ISES Solar World Congress 2009 (SWC 2009). Johannesburg, South Africa.

Florschuetz, L. W., 1979. Extension of the Hottel-Whillier model to the analysis of combined photovoltaic/thermal flat plate collectors. Solar Energy 22 (4), 361–366.

Frank, E., Haller, M. Y., Herkel, S., Ruschenburg, J., 2010. Systematic Classification of Combined Solar Thermal and Heat Pump Systems. In: Proceedings of the 8th ISES EuroSun Conference (EuroSun 2010). Graz, Austria.

Fraunhofer ISE, 2020. Photovoltaics Report, 16 September 2020 Edition. Fraunhofer Institute for Solar Energy Systems ISE, Freiburg, Germany, accessed 17 March 2021. URL https://www.ise.fraunhofer.de/content/dam/ise/de/documents/publications/studies/Photovoltaics-Report.pdf

Freeman, T. L., Mitchell, J. W., Audit, T. E., 1979. Performance of combined solar-heat pump systems. Solar Energy 22 (2), 125–135.

GenOpt, 2011. Generic Optimization Program. Version 3.1.0. Lawrence Berkeley National Laboratory, Berkeley, USA.

Goffin, P., 2014. Evaluation of control strategies for lowEx residential buildings. Ph.D. thesis, ETH Zurich, Switzerland.

Graulich, K., Bauknecht, D., Heinemann, C., Hilbert, I., Vogel, M., Seifried, D., Albert-Seifried, S., 2018. Einsatz und Wirtschaftlichkeit von Photovoltaik-Batteriespeichern in Kombination mit Stromsparen. Öko-Institut e.V., Freiburg, Germany.

Hadorn, J.-C. (Ed.), 2015. Solar and Heat Pump Systems for Residential Buildings. Wilhelm Ernst & Sohn, Berlin, Germany.

Haller, M. Y., 2013. System Simulation Reports for the IEA SHC Task 44 / HPP Annex 38. Report C3, Final Draft Edition. International Energy Agency, Solar Heating and Cooling Programme.

Haller, M. Y., Carbonell, D., Mojic, I., Winteler, C., Bertram, E., Bunea, M., Lerch, W., Ochs, F., 2014a. Solar and heat pump systems - Summary of simulation results of the IEA SHC Task 44 / HPP Annex 38. In: Proceedings of the 11th IEA Heat Pump Conference. Montreal, Canada.

Haller, M. Y., Dott, R., Ruschenburg, J., Ochs, F., Bony, J., 2013a. The Reference Framework for System Simulations of the IEA SHC Task 44 / HPP Annex 38. Part A: General Boundary Conditions. Report C1 Part A, Final Revised Edition. International Energy Agency, Solar Heating and Cooling Programme.

Haller, M. Y., Haberl, R., Mojic, I., Frank, E., 2014b. Hydraulic integration and control of heat pump and combi-storage: Same components, big differences. SHC 2013, International Conference on Solar Heating and Cooling for Buildings and Industry September 23-25, 2013, Freiburg, Germany. Energy Procedia 48, 571–580.

Haller, M. Y., Perers, B., Bales, C., Paavilainen, J., Dalibard, A., Fischer, S., Bertram, E., 2013b. TRNSYS Type 832 v5.01 Dynamic Collector Model. SPF Institut für Solartechnik, Hochschule für Technik HSR, Rapperswil, Switzerland.

Heimrath, R., Haller, M. Y., 2007. The Reference Heating System, the Template Solar System of Task 32. A Report of IEA Solar Heating and Cooling programme - Task 32 Advanced storage concepts for solar and low energy buildings. Report A2 of Subtask A. International Energy Agency, Solar Heating and Cooling Programme.

Helmers, H., Kramer, K., 2013. Multi-linear performance model for hybrid (c)PVT solar collectors. Solar Energy 92, 313–322.

Heydenreich, W., Müller, B., Reise, C., 2008. Describing the world with three parameters: a new approach to PV module power modelling. In: Proceedings of the 23rd European Photovoltaic Solar Energy Conference and Exhibition (23rd EUPVSEC). Valencia, Spain.

Hofmann, P., Dupeyrat, P., Kramer, K., Hermann, M., Stryi-Hipp, G., 2010. Measurements and benchmark of PV-T collectors according to EN 12975 and development of a standardized measurement procedure. In: Proceedings of the 8th ISES EuroSun Conference (EuroSun 2010). Graz, Austria.

Hornberger, M., 2006. ICEPIT. Simulation program for vertically stratified storage bed for heat and cold storage.

IEA, 2013. Modernising Building Energy Codes to Secure our Global Energy Future. International Energy Agency.

IEA, 2019. Energy in Buildings and Communities Programme Annex 67 Energy Flexible Buildings. Summary Report. International Energy Agency.

IEA, 2021. Net Zero by 2050. A Roadmap for the Global Energy Sector. Revised version, October 2021 (4th revision). International Energy Agency.

IEA HPC, 2010. Retrofit Heat Pumps for Buildings. Final Report of IEA Heat Pump Programme Annex 30. International Energy Agency, Heat Pump Centre.

IEC 61853-1, 2011. IEC 61853-1:2011 Photovoltaic (PV) module performance testing and energy rating. Part 1: Irradiance and temperature performance measurements and power rating. International Electrotechnical Commission.

IPCC, 2018. Global warming of 1.5 °C. An IPCC Special Report on the impacts of global warming of 1.5 °C above pre-industrial levels and related global greenhouse gas emission pathways, in the context of strengthening the global response to the threat of climate change, sustainable development, and efforts to eradicate poverty. Summary for Policymakers. Intergovernmental Panel on Climate Change, Switzerland.

IRENA, 2021. Query Tool. Renewable Electricity Capacity and Generation Statistics, July 2020. International Renewable Energy Agency, accessed 18 March 2021.
URL `https://www.irena.org/Statistics/Download-Data`

ISO 52000-1, 2017. ISO 52000-1:2017 Energy performance of buildings - Overarching EPB assessment - Part 1: General framework and procedures. International Organization for Standardization.

ISO 9806, 2013. ISO 9806:2013 Solar energy - Solar thermal collectors - Test methods. International Organization for Standardization.

ISO 9806, 2017. ISO 9806:2017 Solar energy - Solar thermal collectors - Test methods. International Organization for Standardization.

Jonas, D., 2019a. TRNSYS Type 835. PV model for the coupling with solar thermal absorber and collector models as PVT model. Version 3.4.
URL https://github.com/DnJns/TRNSYS_Type835_PVT/

Jonas, D., 2019b. Visualization of energy flows in PVT systems. A visualization scheme for the uniform representation of combined electrical and thermal energy flows in PVT systems. Report D4, SHC Task 60. International Energy Agency, Solar Heating and Cooling Programme.

Jonas, D., 2023a. SHP-SimLib. A library of solar and heat pump subsystem simulation models in TRNSYS. Version 1.0.
URL https://github.com/DnJns/SHP-SimLib/

Jonas, D., 2023b. SHP-SimResults. A library of solar and heat pump system simulation results. Version 1.0.
URL https://github.com/DnJns/SHP-SimResults/

Jonas, D., Felgner, F., Frey, G., Theis, D., 2017a. A User-friendly Simulation Framework for the Analysis of Solar Thermal and Heat Pump Systems using TRNSYS. In: Proceedings of the 8th IEEE International Renewable Energy Congress (IREC 2017). Amman, Jordan.

Jonas, D., Frey, G., 2018. Model-based Analysis of the Performance and the Environmental Impact of Solar Thermal and Heat Pump Systems. In: Proceedings of the 9th IEEE International Renewable Energy Congress (IREC 2018). Hammamet, Tunisia.

Jonas, D., Frey, G., Theis, D., 2017b. Simulation and performance analysis of combined parallel solar thermal and ground or air source heat pump systems. Solar Energy 150, 500–511.

Jonas, D., Lämmle, M., Theis, D., Schneider, S., Frey, G., 2019. Performance modeling of PVT collectors: Implementation, validation and parameter identification approach using TRNSYS. Solar Energy 193, 51–64.

Jonas, D., Theis, D., Felgner, F., Frey, G., 2017c. A TRNSYS-Based Simulation Framework for the Analysis of Solar Thermal and Heat Pump Systems. Applied Solar Energy 53 (2), 126–137.

Jonas, D., Theis, D., Frey, G., 2018. Implementation and Experimental Validation of a Photovoltaic-Thermal (PVT) Collector Model in TRNSYS. In: Proceedings of the 12th ISES International Conference on Solar Energy for Buildings and Industry (EuroSun 2018). Rapperswil, Switzerland.

Jonas, D., Theis, D., Meiers, J., Frey, G., 2017d. Model-based Analysis of Solar Thermal and Heat Pump Systems using TRNSYS. In: Proceedings of the 2017 ISES Solar World Congress (SWC 2017) / International Conference on Solar Heating and Cooling for Buildings and Industry (SHC 2017). Abu Dhabi, UAE.

Kabir, E., Kumar, P., Kumar, S., Adelodun, A. A., Kim, K.-H., 2018. Solar energy: Potential and future prospects. Renewable and Sustainable Energy Reviews 82, 894–900.

Kalogirou, S., 2014. Solar energy engineering. Processes and Systems, Second Edition. Elsevier / Academic Press, USA.

Kalogirou, S. A., 2004. Solar thermal collectors and applications. Progress in Energy and Combustion Science 30, 231–295.

Kemmler, A., Kirchner, A., Auf der Maur, A., Ess, F., Kreidelmeyer, S., Piégsa, A., Spillmann, T., Wünsch, M., Ziegenhagen, I., 2020. Energiewirtschaftliche Projektionen und Folgeabschätzungen 2030/2050. Dokumentation von Referenzszenario und Szenario mit Klimaschutzprogramm 2030. Prognos AG.

Kjellsson, E., 2009. Solar Collectors Combined with Ground-Source Heat Pumps in Dwellings. Analyses of System Performance. Ph.D. thesis, Lund University, Sweden.

Koehl, M., Heck, M., Wiesmeier, S., Wirth, J., 2011. Modeling of the nominal operating cell temperature based on outdoor weathering. Solar Energy Materials & Solar Cells 95, 1638–1646.

Kuethe, S., Wilhelms, C., Zass, K., Heinzen, R., Vajen, K., Jordan, U., 2008. Modelling complex systems with TRNSYS SIMULATION STUDIO. In: Proceedings of the 7th ISES EuroSun Conference (EuroSun 2008). Lisbon, Portugal.

Kurnitski, J. (Ed.), 2013a. Cost Optimal and Nearly Zero-Energy Buildings (nZEB). Definition, Calculation Principles and Case Studies. Springer, London, England.

Kurnitski, J., 2013b. Technical definitions for nearly zero energy buildings. REHVA European HVAC Journal 2013 (3), 22–28.

Kurnitski, J., Allard, F., Braham, D., Goeders, G., Heiselberg, P., Jagemar, L., Kosonen, R., Lebrun, J., Mazzarella, L., Railio, J., Seppänen, O., Schmidt, M., Virta, M., 2011a. How to define nearly zero energy buildings nZEB - REHVA proposal for uniformed national implementation of EPBD recast. REHVA European HVAC Journal 2011 (3), 6–12.

Kurnitski, J., Saari, A., Kalamees, T., Vuolle, M., Niemelä, J., Tark, T., 2011b. Cost optimal and nerly zero (nZEB) energy performance calculations for residential buildings with REHVA definition for nZEB national implementation. Energy and Buildings 43, 3279–3288.

Lämmle, M., 2018. Thermal management of PVT collectors. Development and modelling of highly efficient glazed, flat plate PVT collectors with low-emissivity coatings and overheating protection. Ph.D. thesis, Albert-Ludwigs-Universität, Freiburg im Breisgau, Germany.

Lämmle, M., 2020a. Map of PVT collector technologies and PVT applications per operating temperature. Accessed 26 March 2021.
URL `https://commons.wikimedia.org/w/index.php?curid=87526793`

Lämmle, M., 2020b. Utilization of the electromagnetic solar spectrum by a PVT collector, indicating the solar spectrum AM1.5, optical losses, thermal losses, thermal gains, and electrical gains. Accessed 26 March 2021.
URL `https://commons.wikimedia.org/w/index.php?curid=87526248`

Lämmle, M., Herrando, M., Ryan, G., 2020. Basic concepts of PVT collector technologies, applications and markets. Report D5, SHC Task 60. International Energy Agency, Solar Heating and Cooling Programme.

Lämmle, M., Oliva, A., Hermann, M., Kramer, K., Kramer, W., 2017. PVT collector technologies in solar thermal systems: A systematic assessment of electrical and thermal yields with the novel characteristic temperature approach. Solar Energy 100, 34–42.

Lerch, W., Heinz, A., Heimrath, R., 2015. Direct use of solar energy as heat source for a heat pump in comparison to a conventional parallel solar air heat pump system. Energy and Buildings 100, 867–879.

Louvet, Y., Fischer, S., Furbo, S., Giovannetti, F., Köhl, M., Mauthner, F., Mugnier, D., Philippen, D., Veynandt, F., 2018. Guideline for levelized cost of heat (LCOH) calculations for solar thermal applications. Info Sheet A01, SHC Task 54, Revised 10.04.2018 Edition. International Energy Agency, Solar Heating and Cooling Programme.

Luque, A., Hegedus, S. (Eds.), 2011. Handbook of Photovoltaic Science and Engineering, Second Edition. John Wiley & Sons, Chichester, United Kingdom.

Malenković, I., Pärisch, P., Eicher, S., Bony, J., Hartl, M., 2013. Definition of Main System Boundaries and Performance Figures for Reporting on SHP Systems. Deliverable B1, Final Edition. International Energy Agency, Solar Heating and Cooling Programme.

Marguerite, C., Geyer, R., Hangartner, D., Lindahl, M., Pedersen, S. V., 2019. IEA Heat Pumping Technologies Annex 47 Heat Pumps in District Heating and Cooling Systems Task 3: Review of concepts and solutions of heat pump integration. International Energy Agency, Technology Collaboration Programme on Heat Pumping Technologies.

Martorana, F., Bonomolo, M., Leone, G., Monteleone, F., Zizzo, G., Beccali, M., 2021. Solar-assisted heat pumps systems for domestic hot water production in small energy communities. Solar Energy 217, 113–133.

Meteonorm, 2009. Global Meteorological Database for Engineers, Planners and Education. Software and Data on CD-ROM, Version 6.1.0.9. Meteotest, Bern, Switzerland.

Meyers, S., Schmitt, B., Vajen, K., 2018. Renewable process heat from solar thermal and photovoltaics: The development and application of a universal methodology to determine the more economical technology. Applied Energy 212, 1537–1552.

Parida, B., Iniyan, S., Goic, R., 2011. A review of solar photovoltaic technologies. Renewable and Sustainable Energy Reviews 15, 1625–1636.

Pärisch, P., Mercker, O., Oberdorfer, P., Bertram, E., Tepe, R., Rockendorf, G., 2015. Short-term experiments with borehole heat exchangers and model validation in TRNSYS. Renewable Energy 74, 471–477.

Perers, B., 1997. An improved dynamic solar collector test method for determination of non-linear optical and thermal characteristics with multiple regression. Solar Energy 59, 163–178.

Perers, B., Kovacs, P., Olsson, M., Persson, M., Pettersson, U., 2012. A tool for standardized collector performance calculations including PVT. SHC 2012. Energy Procedia 30, 1354–1364.

Perers, P., 2010. An improved dynamic solar collector model including condensation and asymmetric incidence angle modifiers. In: Proceedings of the 8th ISES EuroSun Conference (EuroSun 2010). Graz, Austria.

Poppi, S., 2017. Solar heat pump systems for heating applications. Ph.D. thesis, KTH Royal Institute of Technology, Stockholm, Sweden.

Poppi, S., Bales, C., 2014. Influence of hydraulics and control of thermal storage in solar assisted heat pump combisystems. SHC 2013, International Conference on Solar Heating and Cooling for Buildings and Industry September 23-25, 2013, Freiburg, Germany. Energy Procedia 48, 946–955.

Poppi, S., Bales, C., Haller, M. Y., Heinz, A., 2016. Influence of boundary conditions and component size on electricity demand in solar thermal and heat pump combisystems. Applied Energy 162, 1062–1073.

Poppi, S., Sommerfeldt, N., Bales, C., Madani, H., Lundqvist, P., 2018. Techno-economic review of solar heat pump systems for residential heating applications. Renewable and Sustainable Energy Reviews 81, 22–32.

PV Magazine, 2021. EU carbon price running at level not expected until next year. Accessed 10 November 2021.
URL `https://www.pv-magazine.com/2021/05/13/eu-carbon-price-running-at-level-not-expected-until-next-year/`

Ramschak, T. (Ed.), 2020. Existing PVT systems and solutions. Report A1, SHC Task 60. International Energy Agency, Solar Heating and Cooling Programme.

Riederer, P., Keilholz, W., Ducreux, V., 2009. Coupling of TRNSYS with Simulink - A method to automatically export and use TRNSYS models within Simulink and vice versa. In: Proceedings of the 11th International IBPSA Building Simulation Conference (BS 2009). Glasgow, Scotland, pp. 1628–1633.

Ritter, V., 2012. Optimizing the combination of active and passive building components in refurbishment projects to allow for net-zero emission architecture. Ph.D. thesis, ETH Zurich, Switzerland.

Ruschenburg, J., Herkel, S., Henning, H.-M., 2013. A statistical analysis on market-available solar thermal heat pump systems. Solar Energy 95, 79–89.

Sarbu, I., Sebarchievici, C., 2014. General review of ground-source heat pump systems for heating and cooling of buildings. Energy and Buildings 70, 441–454.

Sartori, I., Napolitano, A., Voss, K., 2012. Net zero energy buildings: A consistent definition framework. Energy and Buildings 48, 220–232.

Short, W., Packey, D. J., Holt, T., 1995. A Manual for the Economic Evaluation of Energy Efficiency and Renewable Energy Technologies. National Renewable Energy Laboratory, Golden, Colorado, USA.

Skoplaki, E., Palyvos, J., 2009. On the temperature dependence of photovoltaic module electrical performance: A review of efficiency/power correlations. Solar Energy 83, 614–624.

SMA, 2015. Sunny Boy 3000TL / 3600TL / 4000TL / 5000TL mit Reactive Power Control. Data sheet. SMA Solar Technology AG.

Solar Heat Europe, 2019. Solar Thermal Markets in Europe. Trends and Market Statistics 2018. Summary (November 2019). Solar Heat Europe / ESTIF.

Solar Heat Europe, 2020. Solar Thermal Markets in Europe. Trends and Market Statistics 2019. Summary (December 2020). Solar Heat Europe / ESTIF.

Solar Heat Europe, 2021. Solar Thermal Markets in Europe 2015. Solar Heat Europe / ESTIF, accessed 15 March 2021.
URL http://solarheateurope.eu/publications/market-statistics/interactive-statistic/

SolarPower Europe, 2020. European Market Outlook For Residential Battery Storage 2020-2024.

Sommerfeldt, N., Madani, H., 2018. A Techno-Economic Comparison between PV and PVT Integrated Ground Source Heat Pumps for Multi-Family Houses. In: Proceedings of the 12th ISES International Conference on Solar Energy for Buildings and Industry (EuroSun 2018). Rapperswil, Switzerland.

Sommerfeldt, N., Madani, H., 2019. In-depth techno-economic analysis of PV/Thermal plus ground source heat pump systems for multi-family houses in a heating dominated climate. Solar Energy 190, 44–62.

Spirkl, W., 1997. Dynamic System Testing Program Manual. Version 2.7. InSitu Scientific Software.

Sporn, P., Ambrose, E. R., 1955. The heat pump and solar energy. In: Proceedings of the World Symposium on Applied Solar Energy. Phoenix, USA.

TESS, 2014. TESS Component Library, Version 17. Thermal Energy System Specialists, LLC, Madison, Wisconsion, USA.

Theis, D., Bischoff, T., Scheidhauer, T., 2009. Implementation of the 2 nodes model for the collector performance characterisation. In: Proceedings of the 4th European Solar Thermal Energy Conference (ESTEC 2009). Munich, Germany.

Thirugnanasambandam, M., Iniyan, S., Goic, R., 2010. A review of solar thermal technologies. Renewable and Sustainable Energy Reviews 14, 312–322.

Thür, A., Calabrese, T., Streicher, W., 2018. Smart grid and PV driven ground heat pump as thermal battery in small buildings for optimized electricity consumption. Solar Energy 174, 273–285.

Thygesen, R., 2016. Low energy buildings equipped with heat pumps for high self-consumption of photovoltaic electricity. Ph.D. thesis, Mälardalen University, Sweden.

Thygesen, R., Karlsson, B., 2013. Economic and energy analysis of three solar assisted heat pump systems in near zero energy buildings. Energy and Buildings 66, 77–87.

Thygesen, R., Karlsson, B., 2014. Simulation and analysis of a solar assisted heat pump system with two different storage types for high levels of PV electricity self-consumption. Solar Energy 103, 19–27.

Trinkl, C., 2006. A domestic solar/heat pump heating system incorporating latent and stratified thermal storage. Ph.D. thesis, De Montfort University, Leicester, United Kingdom.

TRNSYS, 2020. TRNSYS - a Transient System Simulation Program, Version 18.02.0000. Solar Energy Laboratory, University of Wisconsin, Madison, Wisconsin, USA.

United Nations, 2015. Paris Agreement.

VDI 4655, 2008. VDI 4655:2008 Reference load profiles of single-family and multi-family houses for the use of CHP systems. Verein Deutscher Ingenieure.

Viessmann, 2013. Planungsanleitung VITOCAL. Luft/Wasser-Wärmepumpen. Viessmann Werke GmbH & Co KG.

Viessmann, 2017. Planungsanleitung VITOCAL. Sole/Wasser- und Wasser/Wasser-Wärmepumpen. Viessmann Werke GmbH & Co KG.

Von Appen, J., 2018. Sizing and operation of residential photovoltaic systems in combination with battery storage systems and heat pumps. Ph.D. thesis, Kassel University, Germany.

Von Appen, J., Braun, M., 2019. Sizing and improved grid integration of residential PV systems with heat pumps and battery storage systems. IEEE Transactions on Energy Conversion 34 (1), 562–571.

Voss, K., Sartori, I., Lolloni, R., 2012. Nearly-zero, Net zero and Plus Energy Buildings - How definition & regulations affect the solutions. REHVA European HVAC Journal 2012 (6), 23–27.

Wang, X., Xia, L., Bales, C., Zhang, X., Copertaro, B., Pan, S., Wu, J., 2020. A systematic review of recent air source heat pump (ASHP) systems assisted by solar thermal, photovoltaic and photovoltaic/thermal sources. Renewable Energy 146, 2472–2487.

Weiss, W. (Ed.), 2003. Solar Heating Systems for Houses. A Design Handbook for solar combisystems. Routledge, New York, USA.

Weiss, W., Spörk-Dür, M., 2020. Solar Heat Worldwide. Global Market Development and Trends in 2019. Detailed Market Data 2018. International Energy Agency, Solar Heating and Cooling Programme.

Weniger, J., Orth, N., Böhme, N., Quaschning, V., 2019. Stromspeicher-Inspektion 2019: Speicher im Test. In: pv magazine Webinar.
URL `https://pvspeicher.htw-berlin.de/wp-content/uploads/WENIGER-2019-Stromspeicher-Inspektion-2019-Speicher-im-Test.pdf`

Weniger, J., Tjaden, T., Bergner, J., Quaschning, V., 2016. Sizing of Battery Converters for Residential PV Storage Systems. 10th International Renewable Energy Storage Conference, IRES 2016, 15-17 March 2016, Düsseldorf, Germany. Energy Procedia 99, 3–10.

Weniger, J., Tjaden, T., Quaschning, V., 2014. Sizing of residential PV battery systems. 8th International Renewable Energy Storage Conference and Exhibition, IRES 2013. Energy Procedia 46, 78–87.

Wetter, M., Afjei, T., 1997. TRNSYS Type 401 Compressor heat pump including frost and cycle losses. Zentralschweizerisches Technikum Luzern, Horw, Switzerland.

Winteler, C., Dott, R., Afjei, T., Hafner, B., 2014. Heat pump, solar energy and ice storage systems - modelling and seasonal performance. In: Proceedings of the 11th IEA Heat Pump Conference. Montréal, Canada.

Zenhäusern, D., 2020. Key Performance Indicators for PVT Systems. Report D1, SHC Task 60. International Energy Agency, Solar Heating and Cooling Programme.

Zenhäusern, D., Bohren, A., Rommel, M., Dittmann, S., 2015. Thermische und elektrische Charakterisierung von unabgedeckten PVT-Kollektoren. In: Tagungsband zum 25. Symposium Thermische Solarenergie. Bad Staffelstein, Germany.

ZHAW IFM, 2021. Optimierung von Erdwärmesonden. Umwälzpumpe optimieren. Institut für Facility Management (IFM), Zürcher Hochschule für Angewandte Wissenschaften (ZHAW), accessed 02 August 2021.
URL `http://www.erdsondenoptimierung.ch/index.php?id=268892&mode=1`

Zirngibl, J., 2014. Nearly Zero Energy Buildings (nZEB) in the CEN draft standard. REHVA European HVAC Journal 2014 (3), 10–13.

Zondag, H. A., 2008. Flat-plate PV-Thermal collectors and systems: A review. Renewable and Sustainable Energy Reviews 12, 891–959.

Appendix A

Appendix: Annual Energy Demands

Athens

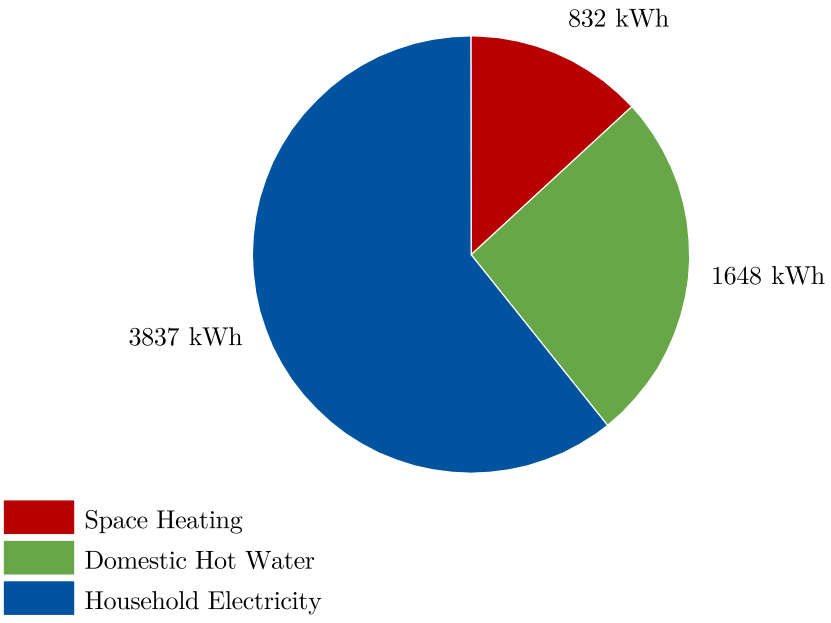

Figure A.1: Annual energy demands for SFH45 in Athens.

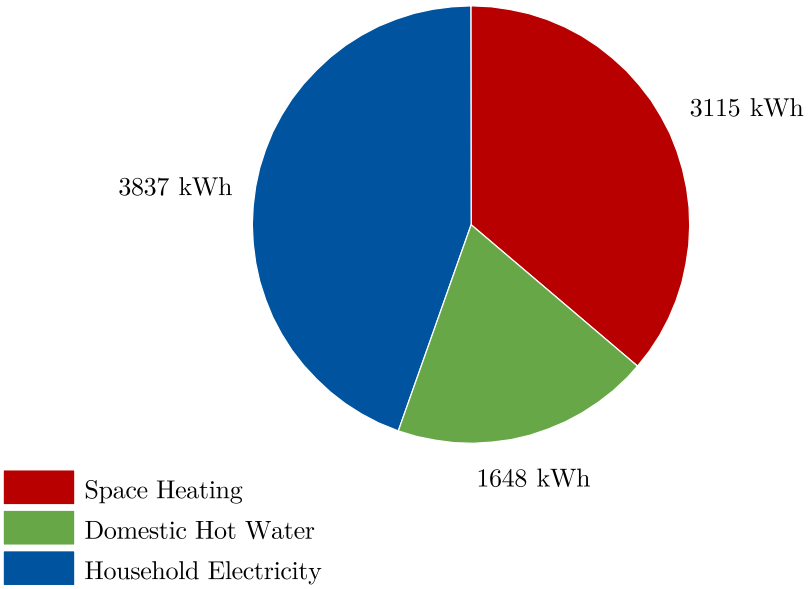

Figure A.2: Annual energy demands for SFH100 in Athens.

Strasbourg

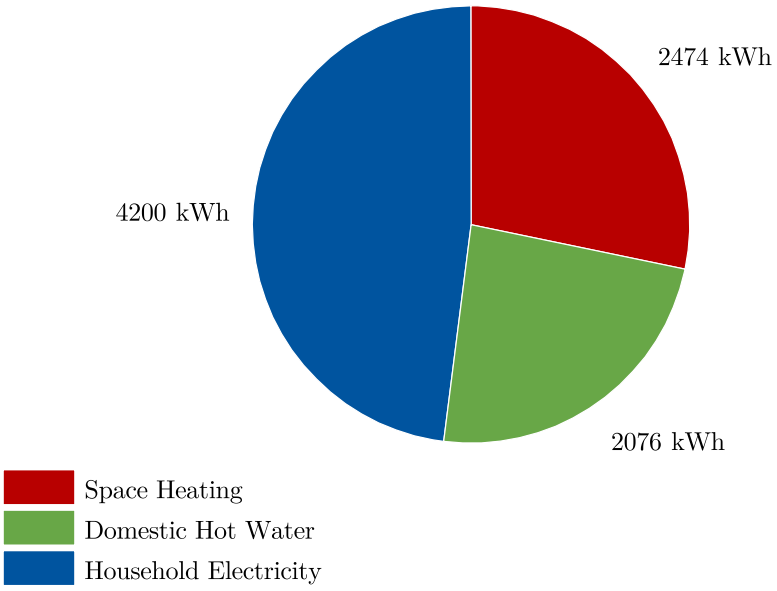

Figure A.3: Annual energy demands for SFH15 in Strasbourg.

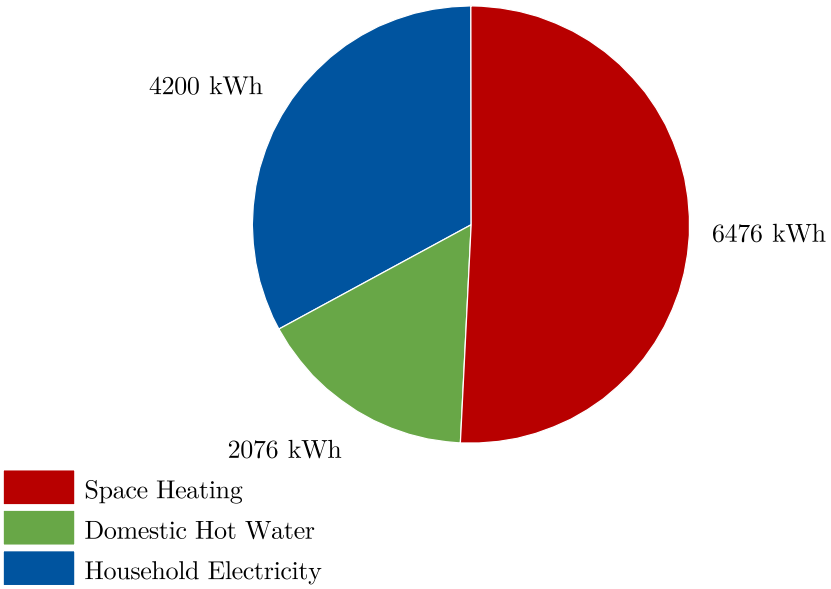

Figure A.4: Annual energy demands for SFH45 in Strasbourg.

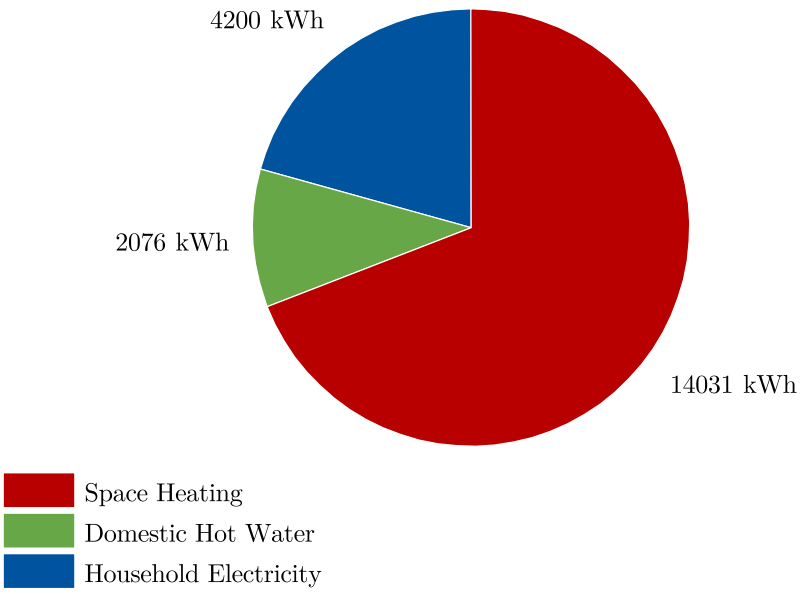

Figure A.5: Annual energy demands for SFH100 in Strasbourg.

Helsinki

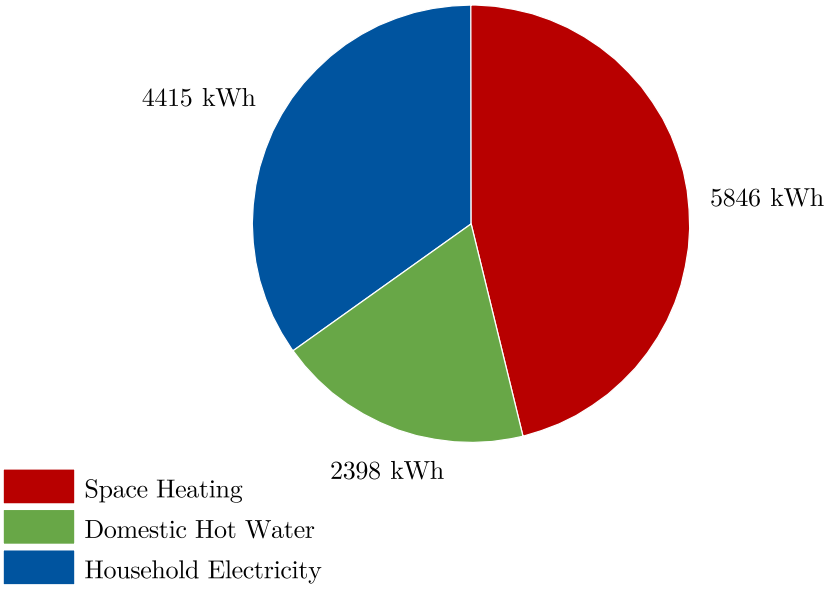

Figure A.6: Annual energy demands for SFH15 in Helsinki.

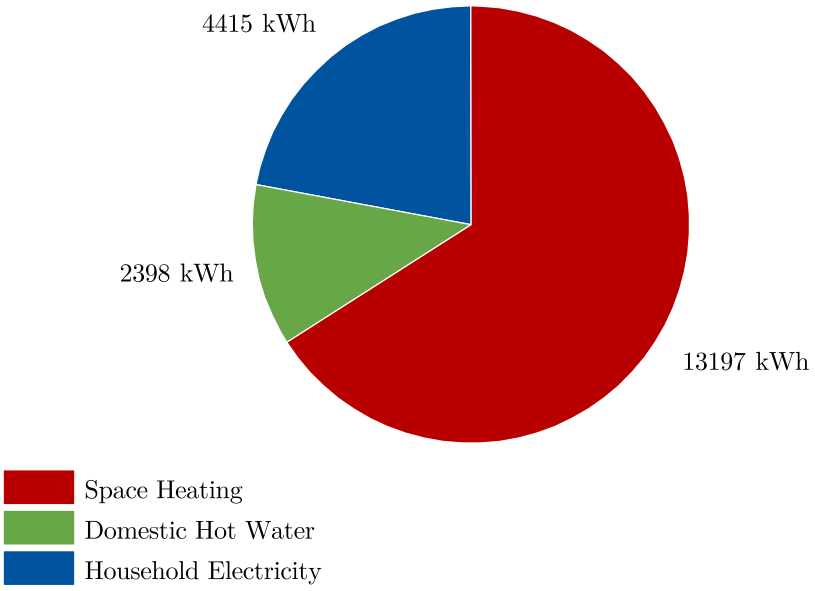

Figure A.7: Annual energy demands for SFH45 in Helsinki.

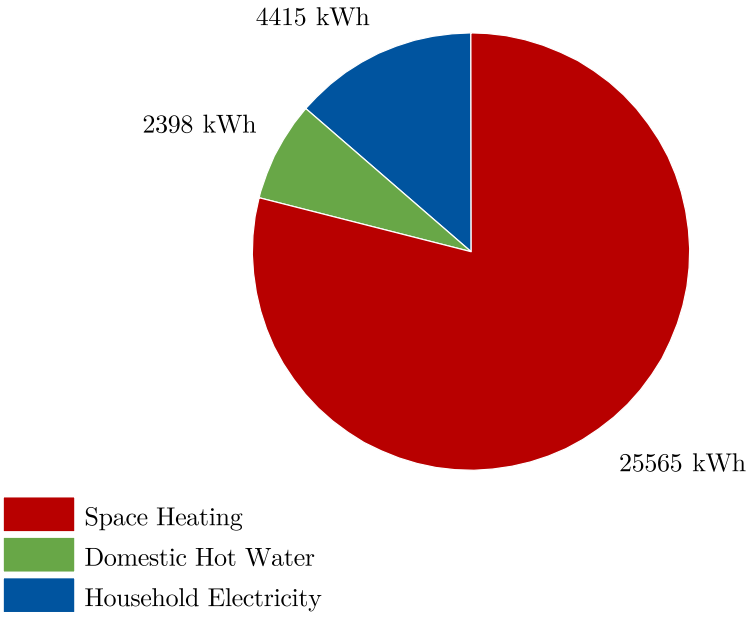

Figure A.8: Annual energy demands for SFH100 in Helsinki.

Appendix B

Appendix: Costs of System Components

All prices and costs of the system components in the following are net values excluding VAT based on market available products, offers from installers, online stores and additional assumptions, e.g. for installation costs.

Table B.1: Air/water heat pump costs.

Power of condenser (A7/W35)	[kW]	12.70	16.70	20.60
Heat pump	[€]	9 888.82	11 140.92	12 510.67
Hydraulic and electrical components, accessories and installation	[€]	7 565.71	7 565.71	7 565.71
Sum	[€]	17 454.53	18 706.63	20 076.38

Table B.2: Brine/water heat pump costs.

Power of condenser (B0/W35)	[kW]	5.69	7.64	10.36	12.99
Heat pump	[€]	6 308.66	6 914.54	7 244.47	8 052.35
Hydraulic and electrical components, accessories and installation	[€]	7 565.71	7 565.71	7 565.71	7 565.71
Sum	[€]	13 874.36	14 480.24	14 810.18	15 618.06

Table B.3: Reference gas-fired boiler costs.

Nominal heating power	[kW]	11	19
Gas boiler and flue gas system	[€]	4 757.57	5 014.71
Hydraulic and electrical components, accessories and installation	[€]	5 503.71	5 503.71
Sum	[€]	10 261.27	10 518.42

Table B.4: Borehole heat exchanger costs.

Borehole heat exchanger length	[m]	49	75	84	180	190	380
Borehole heat exchangers including hydraulic components, accessories, installation, earthworks and approvals	[€]	4 472.17	5 554.30	5 928.88	11 176.53	11 592.73	22 004.79
Sum	[€]	4 472.17	5 554.30	5 928.88	11 176.53	11 592.73	22 004.79

Table B.5: Ice storage costs.

Ice storage volume	$[m^3]$	10	20
Ice storage including hydraulic and electrical components, accessories, installation and earthworks	[€]	8 597.31	14 150.91
Hydraulic and electrical components for solar source circuit integration	[€]	3 011.19	3 075.59
Sum	[€]	11 608.50	17 226.50

Table B.6: Buffer storage costs including DHW heat exchanger.

Buffer storage volume	$[m^3]$	0.5	1.0	1.5	2.0
Buffer storage including hydraulic components, accessories and DHW heat exchanger	[€]	2 843.42	3 242.27	3 402.70	3 764.05
Sum	[€]	2 843.42	3 242.27	3 402.70	3 764.05

Table B.7: WISC collector costs.

WISC collector area	$[m^2]$	5	10	15	20	25
WISC collectors including roof fixation, roof installation and accessories	[€]	2 044.83	3 807.76	5 570.69	7 333.62	9 096.55
Sum	[€]	2 044.83	3 807.76	5 570.69	7 333.62	9 096.55

Table B.8: FPC collector costs.

FPC collector area	[m²]	5	10	15	20	25
FPC collectors including roof fixation, roof installation and accessories	[€]	1 768.16	3 270.93	4 774.30	6 280.19	7 784.39
Sum	[€]	1 768.16	3 270.93	4 774.30	6 280.19	7 784.39

Table B.9: WISC PVT collector costs.

WISC PVT collector area	[m²]	5	10	15	20	25
PVT collectors including roof fixation, roof installation and accessories	[€]	2 426.70	4 563.74	6 700.78	8 837.82	10 974.86
Electrical components, inverter and installation	[€]	1 688.75	1 824.14	2 135.99	2 338.61	2 562.23
Sum	[€]	4 115.45	6 387.88	8 836.78	11 176.43	13 537.09

Table B.10: Covered flat-plate PVT collector costs.

Covered flat-plate PVT collector area	[m²]	5	10	15	20	25
PVT collectors including roof fixation, roof installation and accessories	[€]	3 275.33	6 260.99	9 246.65	12 232.32	15 217.98
Electrical components, inverter and installation	[€]	1 688.75	1 824.14	2 135.99	2 338.61	2 562.23
Sum	[€]	4 964.08	8 085.13	11 382.65	14 570.92	17 780.21

Table B.11: Parallel integration of FPC and PVT collector costs.

Hydraulic and electrical components, accessories and installation	[€]	3 819.90
Sum	[€]	3 819.90

Table B.12: PV costs.

PV module area	[m²]	5	10	15	20	25
PV modules including roof fixation, roof installation and accessories	[€]	832.30	1 464.59	2 096.89	2 729.18	3 361.48
Electrical components, inverter and installation	[€]	1 688.75	1 824.14	2 135.99	2 338.61	2 562.23
Sum	[€]	2 521.04	3 288.73	4 232.88	5 067.79	5 923.71

Table B.13: Battery storage costs.

Battery storage capacity	[kWh]	5	10	15
Battery storages including electrical components, inverter, installation and accessories	[€]	5 556.36	7 677.51	9 188.47
Sum	[€]	5 556.36	7 677.51	9 188.47

Appendix C

Appendix: List of Publications

The following publications have been published during the progress of this work. Parts of the content in this thesis have been presented and published in these publications.

Journal papers in the context of this PhD thesis (reverse chronological)

Usman, M., **Jonas, D.**, Frey, G., 2022. A methodology for multi-criteria assessment of renewable integrated energy supply options and alternative HVAC systems in a household. Energy and Buildings 273, Article 112397.

Jonas, D., Lämmle, M., Theis, D., Schneider, S., Frey, G., 2019. Performance modeling of PVT collectors: Implementation, validation and parameter identification approach using TRNSYS. Solar Energy 193, 51–64.

Jonas, D., Frey, G., Theis, D., 2017. Simulation and performance analysis of combined parallel solar thermal and ground or air source heat pump systems. Solar Energy 150, 500–511.

Jonas, D., Theis, D., Felgner, F., Frey, G., 2017. A TRNSYS-Based Simulation Framework for the Analysis of Solar Thermal and Heat Pump Systems. Applied Solar Energy 53 (2), 126–137.

Conference papers in the context of this PhD thesis (reverse chronological)

Ortleb, M., Meiers, J., **Jonas, D.**, Frey, G., 2022. Operation strategies using the Smart Grid Ready interface in solar heat pump systems. In: Proceedings of the 1st IEEE Industrial Electronics Society Annual On-Line Conference (ONCON). Received ONCON2022 Best Paper Prize.

Meiers, J., El Jeddab, A., Theis, D., **Jonas, D.**, Frey, G., Deissenroth-Uhrig, M., 2022. Hardware-in-the-loop integration of PVT models using Internet of Things-enabled communication. In: Proceedings of the ISES and IEA SHC International Conference on Solar Energy for Buildings and Industry (EuroSun2022). Kassel, Germany.

Jonas, D., Theis, D., Frey, G., 2018. Implementation and Experimental Validation of a Photovoltaic-Thermal (PVT) Collector Model in TRNSYS. In: Proceedings of the 12th ISES International Conference on Solar Energy for Buildings and Industry (EuroSun 2018). Rapperswil, Switzerland.

Meiers, J., **Jonas, D.**, Bernat, M., Frey, G., 2018. Modellbasierte Analyse von Photovoltaiksystemen mit Batteriespeichern zur Deckung des Strombedarfs von Gebäuden. 19. Leitkongress der Mess- und Automatisierungstechnik (AUTOMATION 2018), Seamless Convergence of Automation & IT, Baden-Baden, 03. und 04. Juli 2018. VDI-Berichte 2330, 921–932.

Theis, D., **Jonas, D.**, El Jeddab, A., Schneider, S., Rückert, F., Frey, G., 2018. Solare Wärmepumpensysteme mit PVT-Kollektoren und Stromspeicher auf dem HiL-Prüfstand. In: Tagungsband zum Symposium Solarthermie 2018. Bad Staffelstein, Germany.

Jonas, D., Frey, G., 2018. Model-based Analysis of the Performance and the Environmental Impact of Solar Thermal and Heat Pump Systems. In: Proceedings of the 9th IEEE International Renewable Energy Congress (IREC 2018). Hammamet, Tunisia.

Jonas, D., Theis, D., Meiers, J., Frey, G., 2017. Model-based Analysis of Solar Thermal and Heat Pump Systems using TRNSYS. In: Proceedings of the 2017 ISES Solar World Congress (SWC 2017) / International Conference on Solar Heating and Cooling for Buildings and Industry (SHC 2017). Abu Dhabi, UAE.

Jonas, D., Felgner, F., Frey, G., Theis, D., 2017. A User-friendly Simulation Framework for the Analysis of Solar Thermal and Heat Pump Systems using TRNSYS. In: Proceedings of the 8th IEEE International Renewable Energy Congress (IREC 2017). Amman, Jordan.

Contributions to research reports in the context of this PhD thesis (reverse chronological)

Jonas, D. in Zenhäusern, D., 2020. Key Performance Indicators for PVT Systems. Report D1, SHC Task 60. International Energy Agency, Solar Heating and Cooling Programme.

Jonas, D. in Kramer, K., 2020. Status Quo of PVT Characterization. Report B1, SHC Task 60. International Energy Agency, Solar Heating and Cooling Programme.

Jonas, D. in Sanz, A., 2020. Numerical simulation tools for PVT collectors and systems. Report C1, SHC Task 60. International Energy Agency, Solar Heating and Cooling Programme.

Jonas, D. in Lämmle, M., Herrando, M., Ryan, G., 2020. Basic concepts of PVT collector technologies, applications and markets. Report D5, SHC Task 60. International Energy Agency, Solar Heating and Cooling Programme.

Jonas, D., 2019. Visualization of energy flows in PVT systems. A visualization scheme for the uniform representation of combined electrical and thermal energy flows in PVT systems. Report D4, SHC Task 60. International Energy Agency, Solar Heating and Cooling Programme.